

# Manual Hydraulic Structures

February 2016

Faculty of Civil Engineering and  
Geosciences

ir. W.F. Molenaar  
ing. M.Z. Voorendt



Artikelnummer 06917290051

## PREFACE TO THE 2016 EDITION

This manual is the result of group work and origins in Dutch lecture notes that have been used since long time. Amongst the employees of the Hydraulic Engineering Department that contributed to this work are dr.ir. S. van Baars, ir.K.G.Bezuijen, ir.G.P.Bourguignon, prof.ir.A.Glerum, dr.ir.P.A.Kolkman, ir. H.K.T. Kuijper, ir. H.G. Voortman and prof.drs.ir. J.K. Vrijling. The latest years, this manual has been clarified, revised and expanded by ir. W.F. Molenaar and ing. M.Z. Voorendt. We have received much feedback from students and got good input from our student-assistants, which is highly appreciated and has been taken into account for this new edition.

In the 2016 edition, some minor corrections were made throughout the Manual, most noticeably the equation for the spring stiffness of a combined system in Section 29.2. Section 11.1 has been updated with more generic weir discharge equations. Furthermore, serviceability requirements have been added to the chapter on wave-overtopping (Chapter 17) and the Blum theory for laterally loaded piles has been better explained in Chapter 44. The largest change is the addition of Chapter 49, about the determination of the height of flood defences.

Wilfred Molenaar and Mark Voorendt,  
Delft, February 2016

## READER TO THIS MANUAL

Isn't it a challenge to design a hydraulic structure? To make a first sketch or hand calculation; think about and decide how to construct the structure in, under, above or next to water? For sure, it is not easy to keep the bigger picture in mind, while, at the same time, too many details have to be dealt with as well. Indeed, the design of hydraulic structures may be complicated, not because it requires a lot of 'rocket science' but all the more because the facts and the theories of many civil engineering disciplines have to be used.

The idea behind the Manual was to have only those things together that are needed for a first conceptual design of a hydraulic structure. Nothing more than a small collection of formulas, data, graphs, etc., just from the relevant civil engineering fields. But throughout the years, the number of formulas grew and for educational reasons, more and more bits of explanatory text and many calculation examples were included.

It has become a bit of a challenge to find fast what is needed in the Manual. Of course an effort has been made to keep it as accessible as possible by splitting it in 4 parts, General, Loads, Materials, (Temporary) Structures, dealing with more or less similar subjects and of course by providing an extensive Table of Content. Do use the 4-part structure and the Table of Content to find faster what is needed.

For sure work will continue on the Manual, because new materials are being introduced, better ways to calculate loads etc.. Suggestions, comments to improve this Manual will be appreciated. What could, maybe should have been added already is an elaborate treatise on safety and how to apply the right partial (safety) factors in hydraulic engineering.

Since work on the Manual is not finished, it is best to consider it as a toolbox. The available tool in the box might not be the perfect tool for the job, but it will be something to push design of the hydraulic structure a bit further. Select what is needed using a good understanding of basic physical laws.

The Manual is officially part of the lecture notes for the course "Hydraulic Structures 1" at Delft University of Technology (course code CTB3355 / CIE3330). Rumour has it, that the Manual is of service for design work in many other university courses as well as in real engineering life situations. Not bad for a toolbox!

*Picture on the front cover: Haringvliet discharge sluices (picture by Mark Voorendt, 2014)*

# Manual Hydraulic Structures

---

## Table of contents

### Part I: General

<b>1.</b>	<b>STANDARDS AND GUIDELINES.....</b>	<b>1</b>
1.1	Standards.....	1
1.2	Guidelines.....	3
<b>2.</b>	<b>SAFETY OF STRUCTURES.....</b>	<b>4</b>
2.1	Introductory definitions.....	4
2.2	Failure of structures.....	4
2.3	The need for safety factors.....	5
2.4	Deterministic design (level 0).....	6
2.5	Semi-probabilistic design (level I).....	6
2.6	Probabilistic design (levels II and III).....	15
2.7	Literature.....	18
<b>3.</b>	<b>STRUCTURAL MECHANICS.....</b>	<b>19</b>
3.1	Moment and deflection formulas.....	19
3.2	Second moments of area and properties of plane figures.....	25
3.3	Natural oscillation frequencies.....	29
<b>4.</b>	<b>SOME HELPFUL COMPUTER PROGRAMS.....</b>	<b>30</b>
<b>5.</b>	<b>UNITS AND CONVENTIONS.....</b>	<b>31</b>
5.1	Units.....	31
5.2	Conventions.....	33
<b>6.</b>	<b>DUTCH TRANSLATION OF HYDRAULIC STRUCTURES KEYWORDS.....</b>	<b>34</b>

---

## Part II: Loads

<b>7.</b>	<b>WEIGHT .....</b>	<b>41</b>
7.1	General.....	41
7.2	Design .....	41
<b>8.</b>	<b>WIND .....</b>	<b>42</b>
8.1	Theory .....	42
8.2	(Preliminary) design of structures .....	44
8.3	Wind load on vessels .....	54
8.4	Literature .....	55
<b>9.</b>	<b>HYDROSTATIC PRESSURE .....</b>	<b>56</b>
9.1	Theory .....	56
9.2	Water pressure on gates.....	57
<b>10.</b>	<b>WATER, FLOW, WATER LEVELS .....</b>	<b>62</b>
10.1	River: discharge and water level .....	62
10.2	Flow in open water ways .....	62
10.3	Flow through and along structures .....	63
<b>11.</b>	<b>WATER, FLOW, WALL.....</b>	<b>65</b>
11.1	Conservation of momentum .....	65
11.2	Potential flow and pressure distribution.....	70
11.3	Literature.....	71
<b>12.</b>	<b>WATER, FLOW, SLENDER STRUCTURES.....</b>	<b>72</b>
12.1	Drag and lift forces.....	72
12.2	Drag and lift forces, static part.....	72
12.3	Drag and lift forces, dynamic part (vibrations).....	75
<b>13.</b>	<b>WATER, TIDE AND WIND SET-UP .....</b>	<b>77</b>
13.1	Astronomical tide .....	77
13.2	Wind set-up.....	79
13.3	Storm surge .....	80
13.4	Other influences.....	82
<b>14.</b>	<b>WATER, WAVES, THEORY.....</b>	<b>83</b>
14.1	Translation waves.....	83
14.2	Wind waves .....	84
<b>15.</b>	<b>WATER, WAVES, WAVE HEIGHTS.....</b>	<b>89</b>
15.1	Estimate of wave height and period if no measurements are available .....	89
15.2	The design wave height.....	90
15.3	Literature.....	92
<b>16.</b>	<b>WATER, WAVES, SHALLOWS + BREAKING .....</b>	<b>93</b>
16.1	Shallows: refraction .....	93

16.2	Shallows: shoaling .....	95
16.3	Shallows: breaking .....	96
16.4	Obstacle: reflection .....	98
16.5	Obstacle: diffraction .....	98
<b>17.</b>	<b>WATER, WAVES, RUN-UP + OVERTOPPING .....</b>	<b>100</b>
17.1	Wave run-up .....	100
17.2	Wave overtopping .....	103
17.3	Literature .....	107
<b>18.</b>	<b>WATER, WAVES, WALL, NON-BREAKING .....</b>	<b>108</b>
18.1	Rule of thumb .....	108
18.2	Linear theory .....	108
18.3	Sainflou .....	109
18.4	Rundgren .....	110
18.5	Goda .....	110
<b>19.</b>	<b>WATER, WAVES, WALL, BREAKING .....</b>	<b>112</b>
19.1	Introduction .....	112
19.2	Minikin .....	112
19.3	CERC 1984 .....	113
19.4	Goda-Takahashi .....	114
19.5	Comparison .....	115
<b>20.</b>	<b>WATER, WAVES, SLENDER STRUCTURE, NON-BREAKING .....</b>	<b>118</b>
20.1	Theory .....	118
20.2	(Preliminary) design .....	119
20.3	$C_D$ coefficient (SPM) .....	120
20.4	$K_D$ coefficient .....	121
20.5	$K_I$ coefficient .....	122
20.6	$S_D$ coefficient .....	123
20.7	$S_I$ coefficient .....	124
<b>21.</b>	<b>WATER, WAVES, SLENDER STRUCTURE, BREAKING .....</b>	<b>125</b>
<b>22.</b>	<b>ICE .....</b>	<b>126</b>
22.1	Thermal expansion .....	126
22.2	Ice accumulation .....	126
22.3	Collision .....	127
22.4	Ice attachment .....	127
22.5	Design rules .....	128
22.6	Literature .....	130
<b>23.</b>	<b>TEMPERATURE .....</b>	<b>131</b>
23.1	General .....	131
23.2	Unobstructed thermal deformation .....	132
23.3	Restrained thermal deformation .....	134
<b>24.</b>	<b>SOIL - LOADING AND STRESSES .....</b>	<b>137</b>
24.1	Vertical soil stress .....	137
24.2	Horizontal soil stress .....	141
<b>25.</b>	<b>SOIL, SETTLEMENT .....</b>	<b>149</b>

<b>26.</b>	<b>SOIL, EARTHQUAKE .....</b>	<b>151</b>
26.1	General .....	151
26.2	Richter scale .....	151
26.3	Design.....	153
<b>27.</b>	<b>SOIL, GROUNDWATER .....</b>	<b>156</b>
27.1	Groundwater pressure .....	156
27.2	Groundwater flow.....	157
27.3	Drainage .....	159
27.4	Influences on strength .....	159
27.5	Influence on stiffness.....	160
<b>28.</b>	<b>SHIPPING, HYDRAULIC ASPECTS.....</b>	<b>161</b>
<b>29.</b>	<b>SHIPPING, BERTHING .....</b>	<b>162</b>
29.1	Introduction .....	162
29.2	Theory.....	162
29.3	Design.....	163
<b>30.</b>	<b>SHIPPING - MOORING FORCES .....</b>	<b>168</b>
30.1	Theory.....	168
30.2	Preliminary design .....	168

---

## Part III: Materials

<b>31.</b>	<b>SOIL - PROPERTIES .....</b>	<b>171</b>
31.1	Stiffness and strength .....	171
31.2	Soil investigation.....	171
31.3	Determination soil type .....	172
31.4	Determination of soil parameters from laboratory tests.....	173
31.5	Determination of soil parameters from cone penetration tests.....	173
31.6	Determination of soil parameters with the Eurocode table.....	176
31.7	Soil parameters and models.....	178
31.8	Literature.....	180
<b>32.</b>	<b>SOIL - STRENGTH .....</b>	<b>181</b>
32.1	Soil strength schematization (Mohr-Coulomb) .....	181
32.2	Vertical bearing capacity (Prandtl & Brinch Hansen) .....	182
32.3	Horizontal bearing capacity (resistance against sliding) .....	186
32.4	Stability of slopes (Fellenius and Bishop).....	187
<b>33.</b>	<b>SOIL - STIFFNESS .....</b>	<b>191</b>
33.1	Spring schematisation .....	191
33.2	Modulus of subgrade reaction .....	193
33.3	Vertical modulus of subgrade reaction (using Flamant).....	193
33.4	Horizontal modulus of subgrade reaction for (sheet piling) walls.....	194
33.5	Horizontal modulus of subgrade reactions for piles .....	195
<b>34.</b>	<b>SOIL - SETTLEMENT .....</b>	<b>197</b>
34.1	Consolidation .....	197
34.2	Primary settlement and creep.....	199
34.3	Soil relaxation .....	201
34.4	Literature.....	202
<b>35.</b>	<b>CONCRETE.....</b>	<b>203</b>
35.1	Properties of concrete .....	203
35.2	Properties of reinforcement steel.....	204
35.3	Properties of prestressed steel.....	205
35.4	Concrete cover .....	206
35.5	Reinforced and prestressed concrete.....	208
35.6	Stiffness of the concrete structure .....	217
35.7	Literature.....	221
<b>36.</b>	<b>STEEL .....</b>	<b>222</b>
36.1	General .....	222
36.2	Strength .....	224
36.3	Stability .....	228
36.4	Welded connections .....	231
36.5	Bolt connections .....	238
36.6	Fatigue.....	245
36.7	Literature.....	248

---

## Part IV: (temporary) structures

<b>37.</b>	<b>STABILITY OF STRUCTURES ON SHALLOW FOUNDATIONS .....</b>	<b>251</b>
37.1	Horizontal stability.....	251
37.2	Rotational stability.....	252
37.3	Vertical stability.....	253
37.4	Piping (internal backward erosion) .....	254
37.5	Scour protection.....	257
37.6	References .....	260
<b>38.</b>	<b>STABILITY OF FLOATING ELEMENTS.....</b>	<b>261</b>
38.1	Static stability.....	261
38.2	Dynamic stability.....	269
38.3	References .....	273
<b>39.</b>	<b>SOIL RETAINING STRUCTURES .....</b>	<b>274</b>
39.1	Sheet piling.....	275
39.2	Combi-walls .....	296
39.3	Diaphragm walls .....	299
39.4	References .....	306
<b>40.</b>	<b>STRUTS AND WALES.....</b>	<b>307</b>
40.1	Struts .....	307
40.2	Wales.....	310
40.3	References .....	318
<b>41.</b>	<b>ANCHORS.....</b>	<b>319</b>
41.1	General .....	319
41.2	Extreme tensile force.....	321
41.3	Strength of a tie rod .....	325
41.4	Total stability.....	325
41.5	References .....	327
<b>42.</b>	<b>COMPRESSION PILES .....</b>	<b>328</b>
42.1	Strength, general .....	328
42.2	Strength, Prandtl and Meyerhof.....	328
42.3	Strength, Koppejan (NEN 6743).....	331
42.4	Stiffness.....	335
<b>43.</b>	<b>TENSION PILES .....</b>	<b>337</b>
43.1	Strength, general .....	338
43.2	Strength, CUR-report 2001-4 .....	339
43.3	Clump criterion.....	345
43.4	Edge piles.....	346
43.5	Stiffness .....	346
43.6	References .....	349

<b>44.</b>	<b>LATERALLY LOADED PILES .....</b>	<b>350</b>
<b>45.</b>	<b>PILE GROUPS .....</b>	<b>353</b>
<b>46.</b>	<b>UNDERWATER CONCRETE FLOOR .....</b>	<b>356</b>
46.1	General .....	356
46.2	Limit states.....	356
46.3	2-D Arch effect.....	357
46.4	3-D Dome effect.....	358
46.5	Transfer of forces to piles .....	359
<b>47.</b>	<b>DEWATERING .....</b>	<b>361</b>
47.1	General.....	361
47.2	Design.....	364
<b>48.</b>	<b>GATES .....</b>	<b>371</b>
48.1	Flat gate.....	371
48.2	Mitre gate.....	373
48.3	Water pressure on radial gates .....	375
48.4	Water pressure on sector gates .....	378
48.5	Water pressure on arcs .....	379
<b>49.</b>	<b>THE HEIGHT OF FLOOD DEFENCES .....</b>	<b>380</b>
49.1	Design philosophy of flood defences.....	380
49.2	Determination of the retaining height of a flood defence.....	380
49.3	Literature.....	387



# Manual Hydraulic Structures

---

## **Part I: General**



# 1. Standards and guidelines

Standards, or 'codes', are statutory documents that have to be dealt with by force of law. In the structural engineering field, they are often material specific, or structure type specific. For instance, demands regarding the reference period and probability of failure of large hydraulic engineering projects can deviate from general standards. This means that, for instance, the partial safety factors (load and material factors) given in these standards cannot be applied. And also, generally, characteristic values or load factors for typical hydraulic engineering loads, such as waves and current, are not specified in standards. The reason for this is obvious, as the statistics of waves and currents differ from one location to another and therefore cannot be generalised in a norm. Moreover, calculation rules regarding deviating reference periods are lacking in most standards and it is not specified how to deal with different acceptable probabilities of failure.

This is the reason why more specific guidelines, design handbooks and recommendations have been published and can be prescribed by the client. For probabilities of failure that deviate from the standards, one has to resort to probabilistic calculation techniques to determine the design values of the load and strength. For this, reference is made to course CIE4130 'Probabilistic design'.

## 1.1 Standards

The old Dutch TGB-standards ("Technische Grondslagen voor Bouwconstructies") were officially withdrawn per 31 March 2010. They were replaced by the Eurocodes, which have a similar structure as the TGB's. This manual sometimes still refers to the TGB-standards, which could be considered as outdated, however, for this course this is not a major problem because it deals with main principles in the first place.

### **Eurocodes**

The basic Eurocode, EN 1990, describes the basic principles and load combinations. The loads for the design of buildings and other structures are elaborated in the ten parts of EN 1991. Material properties follow in EN 1992 (concrete), EN 1993 (steel), EN 1994 (steel-concrete), EN 1995 (timber), EN 1996 (masonry), EN 1997 (soil) and EN 1999 (aluminium). EN 1998 should be used for the design of structures for earthquake resistance. In addition to the general European standards, obligatory national supplements have been issued.

Below follows a list of Eurocodes. These codes are available (free for our students!) from the website of the library of Delft University of Technology (accessible from within Delft campus): <http://www.library.tudelft.nl/>, or more directly from: <http://connect.nen.nl/>.

### **EN 1990 – Eurocode: Basis of structural design**

#### **EN 1991 – Eurocode 1: Actions on structures**

- EN 1991-1-1 Densities, self-weight and imposed loads
- EN 1991-1-2 Actions on structures exposed to fire
- EN 1991-1-3 Snow loads
- EN 1991-1-4 Wind loads
- EN 1991-1-5 Thermal actions
- EN 1991-1-6 Actions during execution
- EN 1991-1-7 Accidental loads due to impact and explosions
- EN 1991-2 Traffic loads on bridges
- EN 1991-3 Actions induced by cranes and machinery
- EN 1991-4 Actions in silos and tanks

#### **EN 1992 – Eurocode 2: Design of concrete structures**

- EN 1992-1-1 Common rules for buildings and civil engineering structures
- EN 1992-1-2 Structural fire design
- EN 1992-2 Bridges
- EN 1992-3 Liquid retaining and containment structures

**EN 1993 – Eurocode 3: Design of steel structures**

- EN 1993-1-1 General rules and rules for buildings
- EN 1993-1-2 Structural fire design
- EN 1993-1-3 Cold formed thin gauge members and sheeting
- EN 1993-1-4 Structures in stainless steel
- EN 1993-1-5 Strength and stability of planar plated structures without transverse loading
- EN 1993-1-6 Strength and stability of shell structures
- EN 1993-1-7 Strength and stability of plate structures loaded transversally
- EN 1993-1-8 Design of joints
- EN 1993-1-9 Fatigue strength
- EN 1993-1-10 Fracture toughness assessment
- EN 1993-1-11 Design of structures with tension components made of steel
- EN 1993-1-12 Use of high strength steels
- EN 1993-2 Bridges
- EN 1993-3-1 Towers, masts and chimneys – towers and masts
- EN 1993-3-2 Towers, masts and chimneys – chimneys
- EN 1993-4-1 Silos, tanks and pipelines – silos
- EN 1993-4-2 Silos, tanks and pipelines – tanks
- EN 1993-4-3 Silos, tanks and pipelines – pipelines
- EN 1993-5 Piling
- EN 1993-6 Crane supporting structures

**EN 1994 – Eurocode 4: Design of composite steel and concrete structures**

- EN 1994-1-1 General – common rules
- EN 1994-1-2 Structural fire design
- EN 1994-2 Bridges

**EN 1995 – Eurocode 5: Design of timber structures**

- EN 1995-1-1 General rules and rules for buildings
- EN 1995-1-2 Structural fire design
- EN 1995-2 Bridges

**EN 1996 – Eurocode 6: Design of masonry structures**

- EN 1996-1-1 Rules for reinforced and un-reinforced masonry
- EN 1996-1-2 Structural fire design
- EN 1996-2 Selection and execution of masonry
- EN 1996-3 Simplified calculation methods and simple rules for masonry structures

**EN 1997 – Eurocode 7: Geotechnical design**

- EN 1997-1 General rules
- EN 1997-2 Ground investigation and testing

**EN 1998 – Eurocode 8: Design of structures for earthquake resistance**

- EN 1998-1 General rules, seismic actions and rules for buildings
- EN 1998-2 Bridges
- EN 1998-3 Strengthening and repair of buildings
- EN 1998-4 Silos, tanks and pipelines
- EN 1998-5 Foundations, retaining structures and geotechnical aspects
- EN 1998-6 Towers, masts and chimneys

**EN 1999 – Eurocode 9: Design of aluminium structures**

- EN 1999-1-1 Common rules
- EN 1999-1-2 Structural fire design
- EN 1999-1-3 Structures subjected to fatigue
- EN 1999-1-4 Trapezoidal sheeting
- EN 1999-1-5 Shell structures

**Other standards**

Some commonly used standards:

- Nederlands Normalisatie instituut: NEN 6702 Belastingen en vervormingen (TGB 1990)
- Nederlands Normalisatie instituut: NEN 6740 Geotechniek, Basiseisen en belastingen
- Nederlands Normalisatie instituut: NEN 6743 Geotechniek, Drukpalen
- Nederlands Normalisatie instituut : NEN 6720 Voorschriften beton (VBC 1995)
- Nederlands Normalisatie instituut, NEN 6008: "Steel for the reinforcement of concrete", july 2008.
- Nederlands Normalisatie instituut, NEN-EN 10080: "Steel for the reinforcement of concrete – Weldable Reinforcing steel - General", juni 2005.
- Nederlands Normalisatie instituut, NEN-EN 10138-1 Draft: "Prestressing steels – Part 1 to 4, september 2000.

**1.2 Guidelines**

- Empfehlungen des Arbeitsausschusses "Ufereinfassungen" Häfen und Wasserstraßen EAU 2012. Arbeitsausschusses "Ufereinfassungen" Hamburg; Deutsche Gesellschaft für Geotechnik, Essen, Germany.
- Handbook Quay Walls, second edition. SBRCURnet, Municipality Rotterdam, Port of Rotterdam. Published by CRC Press/Balkema, the Netherlands, ISBN: 978-1-138-00023-0 (eBook: ISBN 978-1-315-77831-0), 2014.
- Handboek damwandconstructies, SBRCURnet-publicatie 166, 6e druk, Stichting CURNET, Gouda, 2012.
- Hydraulische randvoorwaarden 2006 voor het toetsen van primaire waterkeringen. Technische Adviescommissie voor de Waterkeringen.
- Ontwerp van Schutsluizen (2 delen). Ministerie van Verkeer en Waterstaat, Rijkswaterstaat, Bouwdienst.
- Prediction of wind and current loads on VLCC's, second edition. Oil Companies International Marine Forum: Witherby & Co Ltd., London, 1994.
- Richtlijn Vaarwegen RVW 2011. Ministerie van Verkeer en Waterstaat, Rijkswaterstaat Adviesdienst Verkeer en Vervoer. Rotterdam, december 2011.
- Wave Overtopping of Sea Defences and Related Structures: Assessment Manual ("European Overtopping Manual"). EurOtop 2007.
- Coastal Engineering Manual. US Army Corps of Engineers; Coastal and Hydraulics Laboratory, 2006, United States.

Other useful guidelines and technical reports are produced by the 'Technische Adviescommissie voor de Waterkeringen' which has been succeeded by the 'Expertise Netwerk Waterveiligheid' ([www.enwinfo.nl](http://www.enwinfo.nl)).

Many guidelines and other documents related to hydraulic engineering can be found at [www.kennisbank-waterbouw.nl](http://www.kennisbank-waterbouw.nl).

## 2. Safety of structures

major revision: February 2015

### 2.1 Introductory definitions

*Safety* is defined in the ISO-code 8402 as 'a state in which the risk of harm to people or material damage is limited to an acceptable level. This means that safety is complementary to risk.

*Risk* in engineering is often quantified as the product of the probability of failure and the consequences of failure. *Probability* is the likelihood of an event and its *consequences* are quantified as the direct or total economic damage, or the loss of life, given that the hazardous event occurs.

What risk is considered *acceptable* is usually determined using three criteria:

- Individual risk: the probability that an individual, continuously residing at a certain place during a year, will perish due to an undesired event;
- Societal risk (group risk): the probability that a (large) number of individuals perishes due to an undesired event. This is considered a measure for societal disruption;
- Economic optimum: the investments in reducing the failure probability should balance the prevented loss of economic value.

The risk level that is considered acceptable is subjective and depends, amongst others, on the extent of voluntariness of exposure to the threat, the recognisability of the threat and social advantages of opposing the risk.

*Reliability* is the probability of a structure or system performing its required function adequately for a specified period of time under stated conditions (Reeve, 2010). In other words: reliability is the probability of non-failure.

### 2.2 Failure of structures

To determine the dimensions of structural elements of a civil engineering work, one needs to know the expected loads and material characteristics. One also needs structural design rules. Nearly all design rules are derived from failure modes and describe a certain limit state.

A failure mechanism (*faalmechanisme*) is a description of the way in which a structure is no longer able to fulfil its function. Not being able to fulfil a function can relate to persistent, transient, accidental or seismic situations. Failure is permanent if a structure *collapses*.

Limit states (*grenstoestanden*) are conditions just before failure. Several limit state types can be distinguished. Eurocode gives the following overview of limit states:

- Serviceability limit state (SLS, *bruikbaarheidsgrenstoestand*), indicating disruption of normal use
- Ultimate limit state (ULS, *uiterste grenstoestand*), indicating collapse of all or part of the structure
  - Loss of static equilibrium of the structure or any part of it, considered as a rigid body (EQU).
  - Internal failure of the structure or structural elements, including footings, piles, basement walls, etc., in which the strength of construction materials or excessive deformation of the structure governs (STR)
  - Failure or excessive deformation of the ground in which the strengths of soil or rock are significant in providing resistance (GEO)
  - Fatigue failure of the structure or structural elements (FAT)

Instead of FAT, Eurocode 7 (Geotechnical Design) mentions:

- Loss of equilibrium due to uplift by water pressure (buoyancy) or other vertical actions (UPL)
- Hydraulic heave, internal erosion and piping caused by hydraulic gradients (HYD).

An example of an ultimate limit state of a breakwater (*golfbreker*) is the toppling of the breakwater as a result of the collapse of its foundation. Due to its collapse, the breakwater can no longer fulfil its function. An example of the serviceability limit state is the overtopping of a large number of waves over the breakwater, in which case there is no guarantee of calm water behind the breakwater.

Sometimes also a damage limit state is distinguished, indicating unacceptable damage but no immediate failure. However, the damage limit state is often included in the ultimate limit state.

During the design process one must take both the ultimate limit state and the serviceability limit state into account. In this case, the ultimate limit state refers to the stability, strength and stiffness of the structure and the subsoil whilst the serviceability limit state is defined by serviceability requirements for the geometry of the design. (In the ultimate limit state, stiffness is of importance when deformation induces 'collapse' of the structure or structural element.)

In general, a structure does not collapse if its loading (solicitation) can be resisted:

$$S < R$$

where:  $S$  = the load (**S**olicitation)  
 $R$  = the resistance to failure (**R**esistance), or the strength

The type of solicitation and resistance depends on the regarding failure mechanism. It could be a force if a horizontal or vertical equilibrium is checked or a turning moment if a rotational equilibrium is considered. If the water retaining height of a flood defence has to be determined, loading and resistance are expressed as an elevation above reference level (m above NAP in the Netherlands).

For example, in case of the serviceability limit state of a breakwater, the resistance is defined as the maximum allowed wave height in the harbour and the solicitation is the occurring wave height in the harbour basin, which is influenced by the geometry of the structure.

In modern standards like the Eurocodes, this is often expressed as a dimensionless unity-check:

$$S / R < 1$$

The relation between solicitation and resistance can also be expressed as a limit state function (*grenstoestandsfunctie*). The general form of a limit state function is:

$$Z = R - S$$

If  $Z < 0$  the structure will fail according to the given mode.

## 2.3 The need for safety factors

In practice, several kinds of uncertainties have to be taken into account while making an engineering design. There are four main categories of uncertainties:

1. physical or inherent uncertainties;
2. statistical uncertainties;
3. modelling uncertainties;
4. human error.

*Physical uncertainties* consist of randomness or variations in nature. Variables can differ in time (water level, for example), or in space (dike height). These uncertainties are mainly caused by a lack of data of loading or strength. *Statistical uncertainties* occur if the distribution function of the possible values for loading or strength is not exactly known, or if the parameters of the distribution function are determined with a limited number of data. *Modelling uncertainties* consist of imperfectness of the models, or failure modes, describing natural phenomena. This can be caused by a lack of knowledge of these processes, or of over-simplification. Financial uncertainties (like construction costs and damage costs) are comprised in this category of modelling uncertainties. Finally, *human error* often forms a big threat to the reliability of a structure.

All these uncertainties can be taken into account by introducing a safety margin between loading and strength. There are various calculation techniques available to incorporate this margin in a structural design. These techniques are classified according to the following levels:

- Level 0: deterministic design;
- Level I: semi-probabilistic design;
- Level II: simplified probabilistic design;
- Level III: full probabilistic design.

These methods are briefly explained in the following sections.

## 2.4 Deterministic design (level 0)

Based on experience, or engineering judgement, overall safety factors ( $\gamma$ ) were applied to create a margin between loading and strength. In general, a structure is considered safe, if:

$$S \cdot \gamma < R, \text{ where } \gamma > 1,0 [-]$$

In the Netherlands, the crest height of flood defences used to be based on the highest observed water level (often the water level that caused most recent flood), plus a freeboard ( $fb$ , *waakhoogte*) of 0,5 to 1,0 metres to account for wave overtopping and uncertainties:

$$S + fb < R, \text{ where } 0,5 \text{ m} \leq fb \leq 1,0 \text{ m}$$

The estimation of these overall safety factors was not based on a quantification of the uncertainties, so it was very difficult to determine the extent of over-design (or under-design) relative to some desired level of safety. This can be overcome by using (semi-) probabilistic techniques, which is explained in the following sections.

## 2.5 Semi-probabilistic design (level I)

### 2.5.1 Theory

In semi-probabilistic design methods, load and strength variables are treated as stochastics, which means that their possible values are distributed around a mean value  $\mu$  (Figure 2-1). The characteristic value of the strength  $R_k$  is the value that is exceeded by 95% of the samples. The characteristic value of the load  $S_k$  is the value that is exceeded by only 5% (in other words: the single tails represent 5% of the possible values).

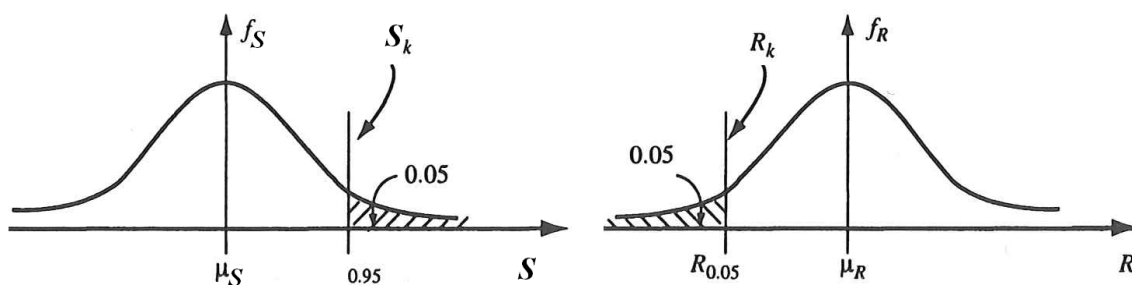


Figure 2-1 Characteristic values for load and strength

The idea is that, by assuming 95% of the upper limit of the load and by multiplying this with a load factor, a design value is acquired with a small probability of exceedance. The failure probability then is very low, especially when these characteristic values are multiplied by partial safety factors.

The characteristic values deviate from the mean values depending on the 'width' of the distribution, which can be expressed as a function of the standard deviation:

$$R_k = \mu_R - k \cdot \sigma_R \quad \text{and} \quad S_k = \mu_S + k \cdot \sigma_S$$

- where:  $\mu$  = mean value of strength  $\mu_R$  or load  $\mu_S$   
 $\sigma$  = standard deviation of strength  $\sigma_R$  or load  $\sigma_S$   
 $(\sigma = \sqrt{\frac{1}{N} \sum_{i=1}^N (x_i - \mu)^2}$  or  $\sigma = \sqrt{\frac{1}{N-1} \sum_{i=1}^N (x_i - \mu)^2}$  for a limited number of samples)  
 $k$  = multiplication constant for the standard deviation to obtain the 5% / 95% value;  
 $k = 0,645$  for a normal distribution

These characteristic values of strength and loading are used to obtain the representative values that are needed to evaluate the limit states (SLS or ULS).

In hydraulic engineering, for the estimation of water loads (water levels), characteristic values are used with a low probability of exceedance during a year, like 1/1250 or 1/10 000. This is based on statistics of measurements, like explained in section 13.3.

Every load has four representative values:

- **the characteristic value** (the main representative value), which is found using statistic methods on a preferably large number of samples, as described above.
- **the combination value**  
 If the loads are time-dependent, it is too conservative to add up the representative values of all loads and to multiply them all by the same partial safety coefficient. After all, the maximum values of the loads do not necessarily all act on the structure at the same time. This can be overcome by using the Turkstra rule for the variable loads. According to Turkstra, one load is considered dominant in every combination of loads. In that case, only averages of the other loads should be taken into account. The Eurocodes don't work with averages of variable loads, but contain reduction factors for load combinations (see the following section on load combinations).
- **the frequent value**  
 The frequent value is chosen in such a way that it can only be exceeded during a short period. It is mainly used in the serviceability limit state and in extreme ultimate limit state.
- **the quasi-permanent value**  
 It is permissible that quasi-permanent values are exceeded during long periods of time. These values could be considered as time-averaged values. They are used for long-term effects in SLS, accidental combinations and seismic design in ULS.

These representative values can be obtained by multiplying the characteristic values by the combination factor  $\psi_0$ , frequent factor  $\psi_1$ , or quasi-permanent factor  $\psi_2$  (see the following section for their values according to the Eurocodes).

The representative values for material properties are mostly the same as the characteristic values, anyway in the Eurocodes. In some foreign codes the representative material factors could differ from the characteristic values.

When determining the dimensions of the design in a limit state check, the required strength has to have a design value larger than the design value of the load. These design values are related to the representative values through partial safety factors:

$$R_d \geq S_d \Leftrightarrow \frac{R_{rep}}{\gamma_R} \geq \gamma_S S_{rep}$$

- in which:  $R_{rep}$  = representative value for the strength  
 $S_{rep}$  = representative value for the load  
 $\gamma_R$  = partial safety factor for the strength (material factor) =  $\gamma_M$   
 $\gamma_S$  = partial safety factor for the load (load factor) =  $\gamma_g, \gamma_q, \gamma_R$   
 $R_d$  = design value of the strength  
 $S_d$  = design value of the load

For the estimation of water levels, needed to estimate hydrostatic loads and water retaining heights, a statistical approach based on the extrapolation of water level measurements can be used, see Section 13.3.

## 2.5.2 Load combinations

The steps that have to be followed to obtain a design value needed for a design calculation of a load are:

1. Estimate the types of the load (permanent, variable or accidental);
2. Discern all realistic loads;
3. Estimate the partial load factors (see below) for all relevant combinations of loads;
4. Combine the loads in such a way that the most critical circumstances are obtained.

In case of a load combination with only one variable load, the magnitude of this load is obtained by multiplying with the concerning partial load factor. If more than one variable loads are combined, the main variable load should be distinguished from other, possibly simultaneously occurring, loads. A simultaneously occurring load is always considered as a combination value.

### Fundamental load combinations

For fundamental load combinations, the Eurocode distinguishes permanent and variable loads. Loads from pre-stressing are treated as a separate permanent load and the main variable load is treated apart from other variable loads.

The design value of the load effect  $E_d$  (combined loads) for persistent and transient load combinations (fundamental combinations) should, according to Eurocode 0, be calculated as:

$$E_d = E \left\{ \sum_{j \geq 1}^n \gamma_{G,j} \cdot G_{k,j} + \gamma_p \cdot P + \gamma_{Q,1} \cdot Q_{k,1} + \sum_{i > 1}^n \gamma_{Q,i} \cdot \psi_{0,i} \cdot Q_{k,i} \right\}$$

For the STR and GEO limit states, the most unfavourable of the following equations should be used:

$$E_d = E \left\{ \sum_{j \geq 1}^n \gamma_{G,j} \cdot G_{k,j} + \gamma_p \cdot P + \gamma_{Q,1} \cdot \psi_{0,1} \cdot Q_{k,1} + \sum_{i > 1}^n \gamma_{Q,i} \cdot \psi_{0,i} \cdot Q_{k,i} \right\}$$

$$E_d = E \left\{ \sum_{j \geq 1}^n \xi_j \cdot \gamma_{G,j} \cdot G_{k,j} + \gamma_p \cdot P + \gamma_{Q,1} \cdot Q_{k,1} + \sum_{i > 1}^n \gamma_{Q,i} \cdot \psi_{0,i} \cdot Q_{k,i} \right\}$$

where:

- $E\{\dots\}$  = the combination of the permanent, pre-stressing and variable loads
- $G_{k,j}$  = characteristic value of permanent load  $j$
- $\gamma_{G,j}$  = partial factor for permanent load  $j$
- $\xi_j$  = reduction factor for unfavourable permanent load  $j$
- $P$  = representative value for the pre-stressing load
- $\gamma_p$  = partial factor for the pre-stressing load
- $Q_{k,1}$  = characteristic value of the main variable load
- $\gamma_{Q,1}$  = partial factor for the main variable load
- $\psi_{0,1}$  = combination reduction factor for the main variable load
- $Q_{k,i}$  = characteristic value of variable load  $i$
- $\gamma_{Q,i}$  = partial factor for variable load  $i$
- $\psi_{0,i}$  = combination reduction factor for variable load  $i$

It should be judged by the structural engineer what possible loads are useful to combine. The national annexes to Eurocode 0 give tables with values for the reduction factors  $\gamma$ ,  $\psi$  and  $\xi$ , depending on failure state, load type and type of building.

**Load combinations for accidental design situations**

In case of combined loads for accidental design situations (fire or impact), the design value of the load effect  $E_d$  should be calculated as:

$$E_d = E \left\{ \sum_{j \geq 1} G_{k,j} + P + A_d + (\psi_{1,1} \text{ or } \psi_{2,1}) \cdot Q_{k,1} + \sum_{i > 1} \psi_{2,i} Q_{k,i} \right\}$$

The choice between  $\psi_{1,1} Q_{k,1}$  or  $\psi_{2,1} Q_{k,1}$  should be related to the relevant accidental design situation (impact, fire or survival after an accidental event or situation).

**Load combinations for seismic design situations**

The design value of the load effect  $E_d$  during earthquake situations should be calculated as:

$$E_d = E \left\{ \sum_{j \geq 1} G_{k,j} + P + A_{Ed} + \sum_{i \geq 1} \psi_{2,i} Q_{k,i} \right\}$$

**Reduction factors for the combination of loads**

Eurocode 0 recommends values for the load combination factor  $\psi$ . This factor is either 1, or  $\psi_1$ ,  $\psi_2$  or  $\psi_3$  as indicated in Table 2-1.

Action	$\psi_0$	$\psi_1$	$\psi_2$
Imposed loads in buildings, category (see EN 1991-1-1)			
Category A : domestic, residential areas	0,7	0,5	0,3
Category B : office areas	0,7	0,5	0,3
Category C : congregation areas	0,7	0,7	0,6
Category D : shopping areas	0,7	0,7	0,6
Category E : storage areas	1,0	0,9	0,8
Category F : traffic area, vehicle weight $\leq 30\text{kN}$	0,7	0,7	0,6
Category G : traffic area, $30\text{kN} < \text{vehicle weight} \leq 160\text{kN}$	0,7	0,5	0,3
Category H : roofs	0	0	0
Snow loads on buildings (see EN 1991-1-3)*			
Finland, Iceland, Norway, Sweden	0,70	0,50	0,20
Remainder of CEN Member States, for sites located at altitude $H > 1000$ m a.s.l.	0,70	0,50	0,20
Remainder of CEN Member States, for sites located at altitude $H \leq 1000$ m a.s.l.	0,50	0,20	0
Wind loads on buildings (see EN 1991-1-4)	0,6	0,2	0
Temperature (non-fire) in buildings (see EN 1991-1-5)	0,6	0,5	0
NOTE The $\psi$ values may be set by the National annex. * For countries not mentioned below, see relevant local conditions.			

Table 2-1 Factor for the combination of loads for buildings (Eurocode 0)  
Note: values mentioned in national annexes to Eurocode 0 may differ from this table

### 2.5.3 Partial load factors

Eurocode 0 gives design values of actions in persistent and transient design situations in ultimate limit state. Static equilibrium (EQU) for building structures should be verified using Table 2-2. The design of structural members (STR), not involving geotechnical actions should be verified with help of Table 2-3.

For the design of structural members like footings, piles and basement walls (STR), involving geotechnical actions and the resistance of the soil, verification should be done using one of the following three approaches:

- Design values from Table 2-4 are applied in separate calculations and Table 2-3 is used for geotechnical loads as well as for other actions on/from the structure. The dimensioning of foundations is carried out with the values mentioned in Table 2-4 and the structural resistance with Table 2-3.
- Table 2-3 is used for both the geotechnical loads as well as for other loads on or from the structure.
- Table 2-4 is used for geotechnical loads and Table 2-3 is simultaneously used for partial factors to other actions on/from the structure.

Persistent and transient design situations	Permanent actions		Leading variable action (*)	Accompanying variable actions	
	Unfavourable	Favourable		Main (if any)	Others
(Eq. 6.10)	$\gamma_{Gj,sup} G_{kj,sup}$	$\gamma_{Gj,inf} G_{kj,inf}$	$\gamma_{Q,1} Q_{k,1}$		$\gamma_{Q,i} \psi_{0,i} Q_{k,i}$

(\*) Variable actions are those considered in Table A1.1

NOTE 1 The  $\gamma$  values may be set by the National annex. The recommended set of values for  $\gamma$  are :

$\gamma_{Gj,sup} = 1,10$   
 $\gamma_{Gj,inf} = 0,90$   
 $\gamma_{Q,1} = 1,50$  where unfavourable (0 where favourable)  
 $\gamma_{Q,i} = 1,50$  where unfavourable (0 where favourable)

NOTE 2 In cases where the verification of static equilibrium also involves the resistance of structural members, as an alternative to two separate verifications based on Tables A1.2(A) and A1.2(B), a combined verification, based on Table A1.2(A), may be adopted, if allowed by the National annex, with the following set of recommended values. The recommended values may be altered by the National annex.

$\gamma_{Gj,sup} = 1,35$   
 $\gamma_{Gj,inf} = 1,15$   
 $\gamma_{Q,1} = 1,50$  where unfavourable (0 where favourable)  
 $\gamma_{Q,i} = 1,50$  where unfavourable (0 where favourable)

provided that applying  $\gamma_{Gj,inf} = 1,00$  both to the favourable part and to the unfavourable part of permanent actions does not give a more unfavourable effect.

Table 2-2 Partial factors for loads in EQU ultimate limit states (Eurocode 0)  
 Note: values mentioned in national annexes to Eurocode 0 may differ from this table

Persistent and transient design situations	Permanent actions		Leading variable action	Accompanying variable actions (*)	
	Unfavourable	Favourable		Main (if any)	Others
(Eq. 6.10)	$\gamma_{Gj,sup} G_{kj,sup}$	$\gamma_{Gj,inf} G_{kj,inf}$	$\gamma_{Q,1} Q_{k,1}$		$\gamma_{Q,i} \psi_{0,i} Q_{k,i}$
(Eq. 6.10a)	$\gamma_{Gj,sup} G_{kj,sup}$	$\gamma_{Gj,inf} G_{kj,inf}$		$\gamma_{Q,1} \psi_{0,1} Q_{k,1}$	$\gamma_{Q,i} \psi_{0,i} Q_{k,i}$
(Eq. 6.10b)	$\xi \gamma_{Gj,sup} G_{kj,sup}$	$\gamma_{Gj,inf} G_{kj,inf}$	$\gamma_{Q,1} Q_{k,1}$		$\gamma_{Q,i} \psi_{0,i} Q_{k,i}$

(\*) Variable actions are those considered in Table A1.1

NOTE 1 The choice between 6.10, or 6.10a and 6.10b will be in the National annex. In case of 6.10a and 6.10b, the National annex may in addition modify 6.10a to include permanent actions only.

NOTE 2 The  $\gamma$  and  $\xi$  values may be set by the National annex. The following values for  $\gamma$  and  $\xi$  are recommended when using expressions 6.10, or 6.10a and 6.10b.  
 $\gamma_{Gj,sup} = 1,35$   
 $\gamma_{Gj,inf} = 1,00$   
 $\gamma_{Q,1} = 1,50$  where unfavourable (0 where favourable)  
 $\gamma_{Q,i} = 1,50$  where unfavourable (0 where favourable)  
 $\xi = 0,85$  (so that  $\xi \gamma_{Gj,sup} = 0,85 \times 1,35 \cong 1,15$ ).  
 See also EN 1991 to EN 1999 for  $\gamma$  values to be used for imposed deformations.

NOTE 3 The characteristic values of all permanent actions from one source are multiplied by  $\gamma_{G,sup}$  if the total resulting action effect is unfavourable and  $\gamma_{G,inf}$  if the total resulting action effect is favourable. For example, all actions originating from the self weight of the structure may be considered as coming from one source ; this also applies if different materials are involved.

NOTE 4 For particular verifications, the values for  $\gamma_G$  and  $\gamma_Q$  may be subdivided into  $\gamma_{G_e}$  and  $\gamma_{G_s}$  and the model uncertainty factor  $\gamma_{Sd}$ . A value of  $\gamma_{Sd}$  in the range 1,05 to 1,15 can be used in most common cases and can be modified in the National annex.

Table 2-3 Partial factors for loads in STR/GEO ultimate limit states (Eurocode 0)  
 Note: values mentioned in national annexes to Eurocode 0 may differ from this table.

Persistent and transient design situation	Permanent actions		Leading variable action (*)	Accompanying variable actions (*)	
	Unfavourable	Favourable		Main (if any)	Others
(Eq. 6.10)	$\gamma_{Gj,sup} G_{kj,sup}$	$\gamma_{Gj,inf} G_{kj,inf}$	$\gamma_{Q,1} Q_{k,1}$		$\gamma_{Q,i} \psi_{0,i} Q_{k,i}$

(\*) Variable actions are those considered in Table A1.1

NOTE The  $\gamma$  values may be set by the National annex. The recommended set of values for  $\gamma$  are :  
 $\gamma_{Gj,sup} = 1,00$   
 $\gamma_{Gj,inf} = 1,00$   
 $\gamma_{Q,1} = 1,30$  where unfavourable (0 where favourable)  
 $\gamma_{Q,i} = 1,30$  where unfavourable (0 where favourable)

Table 2-4 Partial factors for non-geotechnical loads on structural members in STR/GEO ultimate limit states (Eurocode 0)  
 Note: values mentioned in national annexes to Eurocode 0 may differ from this table

**Design values of load combinations in accidental and seismic design situations**

For an overview of design values of combinations of accidental and seismic loads, see Table 2-5. The partial factors for loads for the ultimate limit states in the accidental and seismic design situations should be 1,0. Values for  $\psi$  are given in Table 2-1.

Design situation	Permanent actions		Leading accidental or seismic action	Accompanying variable actions (**)	
	Unfavourable	Favourable		Main (if any)	Others
Accidental (*) (Eq. 6.11a/b)	$G_{kj,sup}$	$G_{kj,inf}$	$A_d$	$\psi_{11}$ or $\psi_{21} Q_{k1}$	$\psi_{2,i} Q_{k,i}$
Seismic (Eq. 6.12a/b)	$G_{kj,sup}$	$G_{kj,inf}$	$\gamma A_{Ek}$ or $A_{Ed}$	$\psi_{2,i} Q_{k,i}$	

(\*) In the case of accidental design situations, the main variable action may be taken with its frequent or, as in seismic combinations of actions, its quasi-permanent values. The choice will be in the National annex, depending on the accidental action under consideration. See also EN 1991-1-2.

(\*\*) Variable actions are those considered in Table A1.1.

Table 2-5 Design values of loads for use in accidental and seismic combinations of loads (Eurocode 0)  
Note: values mentioned in national annexes to Eurocode 0 may differ from this table

### Partial load factors for serviceability limit states

For serviceability limit states the partial factors for loads  $\gamma_s$  should be equal to 1,0, except if differently specified in EN 1991 to EN 1999. See Table 2-6.

Combination	Permanent actions $G_d$		Variable actions $Q_d$	
	Unfavourable	Favourable	Leading	Others
Characteristic	$G_{kj,sup}$	$G_{kj,inf}$	$Q_{k,1}$	$\psi_{0,i} Q_{k,i}$
Frequent	$G_{kj,sup}$	$G_{kj,inf}$	$\psi_{1,1} Q_{k,1}$	$\psi_{2,i} Q_{k,i}$
Quasi-permanent	$G_{kj,sup}$	$G_{kj,inf}$	$\psi_{2,1} Q_{k,1}$	$\psi_{2,i} Q_{k,i}$

Table 2-6 Design values of loads for use in load combinations for SLS (Eurocode 0)  
Note: values mentioned in national annexes to Eurocode 0 may differ from this table

## 2.5.4 Partial material factors

### Concrete

Partial factors for plain, reinforced, or prestressed concrete in ultimate limit states,  $\gamma_c$  and  $\gamma_s$  should be used as indicated in Table 2-7.

Design situations	$\gamma_c$ for concrete	$\gamma_s$ for reinforcing steel	$\gamma_s$ for prestressing steel
Persistent & Transient	1,5	1,15	1,15
Accidental	1,2	1,0	1,0

Table 2-7 Material factors for structures in plain, reinforced or prestressed concrete in ULS (Eurocode 2)  
Note: values mentioned in national annexes to Eurocode 2 may differ from this table

The partial factor  $\gamma_c$  should be multiplied by a factor  $k_f$  (recommended value is 1,1) for the calculation of the design resistance of cast-in-place piles without permanent casing.

### Steel

For steel structures, partial factors as indicated in Table 2-8 should be used.

type of material resistance	partial material factor $\gamma_m$
resistance of cross-sections of all steel classes	1,0
resistance of members to instability assessed by member checks	1,0
resistance of cross-sections in tension to fracture	1,25
resistance of various joints	see Eurocode 1993-1-8

Table 2-8 Partial material factors for steel structures in ULS (Eurocode 3)  
Note: values mentioned in national annexes to Eurocode 3 may differ from this table

**Soil**

For soil parameters the following partial factors ( $\gamma_M$ ) shall be applied for the verification of equilibrium limit state (EQU), when including minor shearing resistances:

soil parameter	symbol	value
angle of internal friction <sup>1)</sup>	$\gamma_{\phi'}$	1,25
effective cohesion	$\gamma_{c'}$	1,25
undrained shear strength	$\gamma_{cu}$	1,4
prism compressive strength	$\gamma_{qu}$	1,4
specific weight	$\gamma_{\gamma}$	1,0
<sup>1)</sup> This factor relates to $\tan\phi'$		

Table 2-9 Partial factors for soil properties for equilibrium state verification (EQU) (Eurocode 7)  
Note: values mentioned in national annexes to Eurocode 7 may differ from this table

For the verification of structural (STR) and geotechnical (GEO) limit states set *M1* or set *M2* of the partial factors on soil parameters ( $\gamma_M$ ) shall be applied as given in Table 2-10. The most unfavourable set *M1* or *M2* shall be used.

Soil parameter	Symbol	Set	
		<i>M1</i>	<i>M2</i>
Angle of shearing resistance <sup>a</sup>	$\gamma_{\phi'}$	1,0	1,25
Effective cohesion	$\gamma_{c'}$	1,0	1,25
Undrained shear strength	$\gamma_{cu}$	1,0	1,4
Unconfined strength	$\gamma_{qu}$	1,0	1,4
Weight density	$\gamma_{\gamma}$	1,0	1,0
<sup>a</sup> This factor is applied to $\tan\phi'$			

Table 2-10 Partial factors for soil properties For the verification of structural (STR) and geotechnical (GEO) limit states verification (Eurocode 7)  
Note: values mentioned in national annexes to Eurocode 7 may differ from this table

For spread foundations and verifications of structural (STR) and geotechnical (GEO) limit states, set *R1*, *R2* or *R3* of the following partial factors on resistance ( $\gamma_R$ ) shall be applied:  $\gamma_{R,v}$  on bearing resistance and  $\gamma_{R,h}$  on sliding resistance, see Table 2-11.

Resistance	Symbol	Set		
		<i>R1</i>	<i>R2</i>	<i>R3</i>
Bearing	$\gamma_{R,v}$	1,0	1,4	1,0
Sliding	$\gamma_{R,h}$	1,0	1,1	1,0

Table 2-11 Partial resistance factors ( $\gamma_R$ ) for spread foundations (Eurocode 7)  
Note: values mentioned in national annexes to Eurocode 7 may differ from this table

Partial resistance factors for various types of piles are given in Table 2-12, Table 2-13 and Table 2-14

Resistance	Symbol	Set			
		R1	R2	R3	R4
Base	$\gamma_b$	1,0	1,1	1,0	1,3
Shaft (compression)	$\gamma_s$	1,0	1,1	1,0	1,3
Total/combined (compression)	$\gamma_t$	1,0	1,1	1,0	1,3
Shaft in tension	$\gamma_{s,t}$	1,25	1,15	1,1	1,6

Table 2-12 Partial resistance factors ( $\gamma_R$ ) for driven piles (Eurocode 7)  
Note: values mentioned in national annexes to Eurocode 7 may differ from this table

Resistance	Symbol	Set			
		R1	R2	R3	R4
Base	$\gamma_b$	1,25	1,1	1,0	1,6
Shaft (compression)	$\gamma_s$	1,0	1,1	1,0	1,3
Total/combined (compression)	$\gamma_t$	1,15	1,1	1,0	1,5
Shaft in tension	$\gamma_{s,t}$	1,25	1,15	1,1	1,6

Table 2-13 Partial resistance factors ( $\gamma_R$ ) for bored piles (Eurocode 7)  
Note: values mentioned in national annexes to Eurocode 7 may differ from this table

Resistance	Symbol	Set			
		R1	R2	R3	R4
Base	$\gamma_b$	1,1	1,1	1,0	1,45
Shaft (compression)	$\gamma_s$	1,0	1,1	1,0	1,3
Total/combined (compression)	$\gamma_t$	1,1	1,1	1,0	1,4
Shaft in tension	$\gamma_{s,t}$	1,25	1,15	1,1	1,6

Table 2-14 Partial resistance factors ( $\gamma_R$ ) for continuous flight auger (CFA) piles (Eurocode 7)  
Note: values mentioned in national annexes to Eurocode 7 may differ from this table

For retaining structures and verifications of structural (STR) and geotechnical (GEO) limit states, set R1, R2 or R3 of the partial factors on resistance ( $\gamma_R$ ) shall be applied as mentioned in Table 2-15 :  $\gamma_{R,v}$  on bearing capacity,  $\gamma_{R,h}$  on sliding resistance and  $\gamma_{R,e}$  on earth resistance.

Resistance	Symbol	Set			
		R1	R2	R3	R4
Temporary	$\gamma_{a,t}$	1,1	1,1	1,0	1,1
Permanent	$\gamma_{a,p}$	1,1	1,1	1,0	1,1

Table 2-15 Partial resistance factors ( $\gamma_R$ ) for retaining structures (Eurocode 7)  
Note: values mentioned in national annexes to Eurocode 7 may differ from this table

For slopes and overall stability and verifications of structural (STR) and geotechnical (GEO) limit states a partial factor on ground resistance ( $\gamma_{R,e}$ ) shall be applied. The recommended value for the three sets R1, R2 and R3 is given in Table 2-16.

Resistance	Symbol	Set		
		R1	R2	R3
Earth resistance	$\gamma_{R,e}$	1,0	1,1	1,0

Table 2-16 Partial resistance factors ( $\gamma_R$ ) for slopes and overall stability (Eurocode 7)  
 Note: values mentioned in national annexes to Eurocode 7 may differ from this table

Eurocode 7 also gives partial material factors for the verification of the uplift limit state and hydraulic heave limit state. Furthermore, partial specific load factors are given for the geotechnical limit states mentioned above.

**Important note.** This chapter shows a selection of load and material factors from the General Eurocodes. Therefore, for design calculations in engineering practice, one is advised to consult the complete text of the Eurocode standards, including the relevant national annex.

## 2.6 Probabilistic design (levels II and III)

Both level II and level III calculations are probabilistic design methods. Level II methods are simplifications of full probabilistic design methods, level III. The full probabilistic design, level III, is explained first in this Manual (Section 2.6.1) and then the simplified methods, level II (Section 2.6.2).

### 2.6.1 Full probabilistic design (level III)

Level III-methods are full probabilistic approaches in which the probability density functions of all stochastic variables are described and included in the analysis. A probability density function is a function that describes the relative likelihood for a random variable to take on a given value. Figure 2-2 shows the probability density functions of the loading  $f_S(S)$  and strength  $f_R(R)$  as well as the resulting probability density function of the limit state  $f_Z(Z)$ . The failure probability  $p_f$  is represented by the area where  $Z < 0$  (the small grey area).

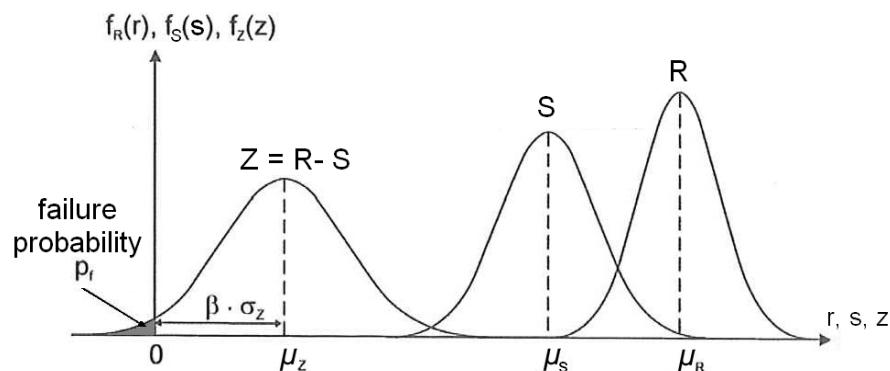


Figure 2-2 Probability density distributions of loading and strength, plus corresponding limit state function

A 'wide' distribution around the average limit state value  $\mu_Z$  implies a large uncertainty, while a 'tight' distribution indicates a high certainty. The 'wideness' of the distribution should be judged relative to its mean value to obtain a good impression of the reliability. A useful expression for judging the reliability of a structure is the reliability index  $\beta$ , which is related to the mean value and the standard deviation of the limit state distribution:

$$\beta = \frac{\mu_Z}{\sigma_Z}$$

where:  $\beta$  = reliability index  
 $\mu_Z$  = mean value of the limit state density function ( $\mu_Z = \mu_R - \mu_S$ )  
 $\sigma_Z$  = standard deviation of the limit state density function ( $\sigma_Z = \sqrt{\sigma_R^2 + \sigma_S^2}$ )

It can be seen in Figure 2-2 that  $\mu_Z = \beta \cdot \sigma_Z$ .

The influence of the distribution of the load or resistance on the distribution of the limit state function is usually expressed by the influence coefficient (*invloedscoëfficiënt*):

$$\alpha_R = -\frac{\sigma_R}{\sigma_Z} \quad \text{and} \quad \alpha_S = \frac{\sigma_S}{\sigma_Z}$$

where:  $\alpha$  = influence coefficient for the strength ( $\alpha_R$ ) or load ( $\alpha_S$ )  
 $\sigma$  = standard deviation of the strength ( $\sigma_R$ ), load ( $\sigma_S$ ), or limit state function ( $\sigma_Z$ )

Level III and level II calculations can be used to calculate the partial factors used in level I calculations, if the reliability index  $\beta$  and influence coefficient  $\alpha$  are known:

$$\gamma_R = \frac{1 + k_R \cdot V_R}{1 + \alpha_R \cdot \beta \cdot V_R} \quad \text{and} \quad \gamma_S = \frac{1 + k_S \cdot V_S}{1 + \alpha_S \cdot \beta \cdot V_S}$$

where:  $k$  = factor indicating the limit of the representative value of strength ( $k_R$ ) or load ( $k_S$ )  
 $V$  = coefficient of variation for strength ( $V_R = \sigma_R/\mu_R$ ) or load ( $V_S = \sigma_S/\mu_S$ )

For the calculation of partial factors for building codes for steel and concrete structures it is usual to adopt  $k_R = 1.64$  and  $k_S = 0$ , but other values may also be chosen. The value of the reliability index  $\beta$  used for the determination of the partial factors depends on the severity of consequences (in Eurocode 0 indicated by consequence classes) and the reference period (life time) of the structure. Values of influence coefficients used for the determination of partial factors are based on calculations of failure probabilities for a number of reference cases.

The relation between the stochastic variables of loading and strength can be mathematically described and the probability of exceedance can be calculated for the considered limit state. The probability of failure  $p_f$  is the probability that the loading exceeds the resistance:

$$p_f = P(R < S) = P(Z < 0)$$

If loading and strength are independent, the failure probability can be calculated using:

$$p_f = \iint_{r < s} f_R(r) f_S(s) dr ds$$

where:  $f_R(R)$  = probability density function of strength  
 $f_S(S)$  = probability density function of load

The product of  $f_R(r)$  and  $f_S(s)$  is the joint probability function  $f_{RS}(r,s)$ :

$$f_R(r) f_S(s) = f_{RS}(r,s)$$

Figure 2-3 shows such a joint density function  $f_{R,S}$ , including the  $Z = 0$  line.

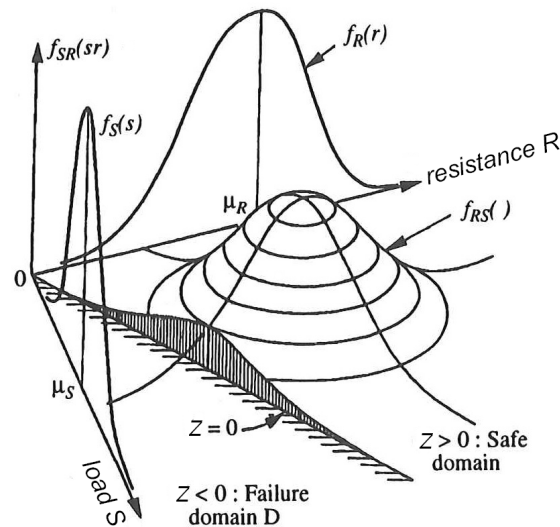


Figure 2-3 Joint density function (Melchers, 1999)

The failure probability can therefore be expressed as a function of the joint density function:

$$p_f = \int_{-\infty}^r \int_{-\infty}^s f_{R,S}(r,s) dr ds$$

If more than one failure mode or more than one structural element is considered, the failure probability can be formulated as an  $n$ -fold integral. For independent variables  $x_i$  this looks like:

$$p_f = \iint_{Z(x)<0} \dots \int \prod_{i=1}^n f_{x_i}(x_i) dx_i$$

Solving this kind of integrals is a tough task, especially if  $n$  exceeds 5. However, in some cases with not too low failure probabilities, the integral can be solved with help of a Monte Carlo simulation. However, the difficulty of applying probabilistic techniques is that it requires a detailed knowledge of each variable and the relationship between these variables.

### 2.6.2 Simplified probabilistic design (level II)

Because of the drawbacks of a full deterministic design, methods have been developed to approximate the distribution functions of loading and strength. As a simplification, the limit state function is linearized and for most methods all parameters are considered to be independent and the probability density functions of loading and strength are replaced by normal distributions (also called Gaussian distributions):

$$f(x) = \frac{1}{\sigma_x \sqrt{2\pi}} \cdot e^{-\frac{(x-\mu_x)^2}{2\sigma_x^2}}, \text{ where } x \text{ can represent load (s) or strength (r).}$$

Depending on the order of approximation, first-order risk methods (FORMs) or second-order risk methods (SORMs) can be used.

These methods and more backgrounds on probabilistic design are treated in the lecture notes CIE4130 'Probability in Civil Engineering'. These probabilistic methods can be used to derive the partial safety factors needed for a semi-probabilistic design, as prescribed in many building standards like the Eurocodes (see also Section 2.5).

## **2.7 Literature**

CUR/TAW report 141 (1990) Probabilistic design of flood defences. Gouda, CUR.

CUR report 190 (1997) Probability in Civil Engineering, Part 1 (Lecture notes CIE4130). Gouda, CUR

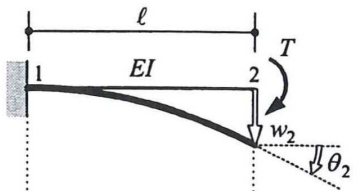
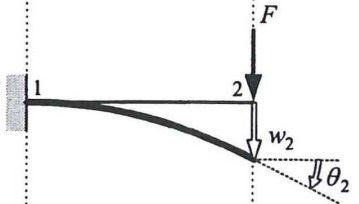
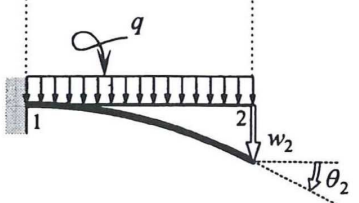
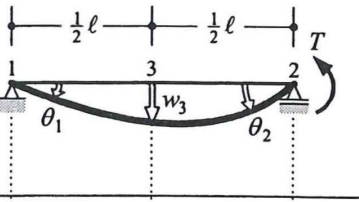
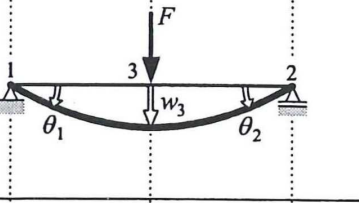
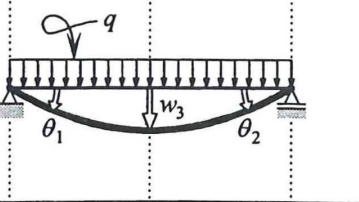
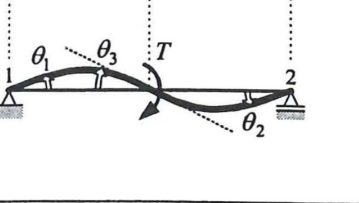
Dominic Reeve (2010) Risk and reliability: coastal and hydraulic engineering. Abingdon, Spon Press.

Robert E. Melchers (1999) Structural reliability analysis prediction. Chichester, John Wiley & Sons.

### 3. Structural Mechanics

#### 3.1 Moment and deflection formulas

The 'moment and deflection formulas' (*vergeetmenietjes*) consist of a set of equations of rotation angles and deflections for standard load situations on supported and fixed beams.

(1)		$\theta_2 = \frac{Tl}{EI}; \quad w_2 = \frac{Tl^2}{2EI}$
(2)		$\theta_2 = \frac{Fl^2}{2EI}; \quad w_2 = \frac{Fl^3}{3EI}$
(3)		$\theta_2 = \frac{ql^3}{6EI}; \quad w_2 = \frac{ql^4}{8EI}$
(4)		$\theta_1 = \frac{1}{6} \frac{Tl}{EI}; \quad \theta_2 = \frac{1}{3} \frac{Tl}{EI}; \quad w_3 = \frac{1}{16} \frac{Tl^2}{EI}$
(5)		$\theta_1 = \theta_2 = \frac{1}{16} \frac{Fl^2}{EI}; \quad w_3 = \frac{1}{48} \frac{Fl^3}{EI}$
(6)		$\theta_1 = \theta_2 = \frac{1}{24} \frac{ql^3}{EI}; \quad w_3 = \frac{5}{384} \frac{ql^4}{EI}$
(a)		$\theta_1 = \theta_2 = \frac{1}{24} \frac{Tl}{EI}; \quad \theta_3 = \frac{1}{12} \frac{Tl}{EI}; \quad w_3 = 0$

cantilevering beam

simply supported beam (statically determinate)

statically indeterminate beam (one fixed end and one simple support)	(7)		$\theta_2 = \frac{1}{4} \frac{Tl}{EI}; \quad w_3 = \frac{1}{32} \frac{Tl^2}{EI}$ $M_1 = \frac{1}{2} T; \quad V_1 = V_2 = \frac{3}{2} \frac{T}{l}$
	(8)		$\theta_2 = \frac{1}{32} \frac{Fl^2}{EI}; \quad w_3 = \frac{7}{768} \frac{Fl^3}{EI}$ $M_1 = \frac{3}{16} Fl; \quad V_1 = \frac{11}{16} F; \quad V_2 = \frac{5}{16} F$
	(9)		$\theta_2 = \frac{1}{48} \frac{ql^3}{EI}; \quad w_3 = \frac{1}{192} \frac{ql^4}{EI}$ $M_1 = \frac{1}{8} ql^2; \quad V_1 = \frac{5}{8} ql; \quad V_2 = \frac{3}{8} ql$
statically indeterminate beam (two fixed ends)	(10)		$w_3 = \frac{1}{192} \frac{Fl^3}{EI}$ $M_1 = M_2 = \frac{1}{8} Fl; \quad V_1 = V_2 = \frac{1}{2} F$
	(11)		$w_3 = \frac{1}{384} \frac{ql^4}{EI}$ $M_1 = M_2 = \frac{1}{12} ql^2; \quad V_1 = V_2 = \frac{1}{2} ql$
	(b)		$\theta_3 = \frac{1}{16} \frac{Tl}{EI}; \quad w_3 = 0$ $M_1 = M_2 = \frac{1}{4} T; \quad V_1 = V_2 = \frac{3}{2} \frac{T}{l}$

Some formulae for prismatic beams with bending stiffness  $EI$ .

$T$ ,  $F$  and  $q$  represent the load by a couple, force and uniformly distributed load respectively.

$M_i$  and  $V_i$  represent the bending moment and shear force on the end  $i$  of the beam, due to the support reactions.

(c)		$\theta_1 = \frac{Fab(\ell + b)}{6EI\ell} = \frac{F\ell^2}{6EI} \left( 2\frac{a}{\ell} - 3\frac{a^2}{\ell^2} + \frac{a^3}{\ell^3} \right)$ $\theta_2 = \frac{Fab(\ell + a)}{6EI\ell} = \frac{F\ell^2}{6EI} \left( \frac{a}{\ell} - \frac{a^3}{\ell^3} \right)$
(d)		$M_1 = \frac{Fb(\ell^2 - b^2)}{2\ell^2} = F\ell \left( \frac{a}{\ell} - \frac{3a^2}{2\ell^2} + \frac{1a^3}{2\ell^3} \right)$ $V_1 = \frac{Fb(3\ell^2 - b^2)}{2\ell^3} = F \left( 1 - \frac{3a^2}{2\ell^2} + \frac{1a^3}{2\ell^3} \right)$ $V_2 = \frac{Fa^2(3\ell - a)}{2\ell^3} = F \left( \frac{3a^2}{2\ell^2} - \frac{1a^3}{2\ell^3} \right)$ $\theta_2 = \frac{Fa^2b}{4EI\ell} = \frac{F\ell^2}{4EI} \left( \frac{a^2}{\ell^2} - \frac{a^3}{\ell^3} \right)$
(e)		$M_1 = \frac{Fab^2}{\ell^2} = F\ell \left( \frac{a}{\ell} - 2\frac{a^2}{\ell^2} + \frac{a^3}{\ell^3} \right)$ $V_1 = \frac{Fb^2(\ell + 2a)}{\ell^3} = F \left( 1 - 3\frac{a^2}{\ell^2} + 2\frac{a^3}{\ell^3} \right)$ $M_2 = \frac{Fa^2b}{\ell^2} = F\ell \left( \frac{a^2}{\ell^2} - \frac{a^3}{\ell^3} \right)$ $V_2 = \frac{Fa^2(\ell + 2b)}{\ell^3} = F\ell \left( 3\frac{a^2}{\ell^2} - 2\frac{a^3}{\ell^3} \right)$
(f)		$M_1 = \frac{3EI}{\ell^2} w^0; \quad V_1 = V_2 = \frac{3EI}{\ell^3} w^0$ $\theta_2 = \frac{3}{2} \frac{w^0}{\ell}$ $\theta_3 = \frac{9}{8} \frac{w^0}{\ell}; \quad w_3 = \frac{5}{16} w^0$
(g)		$M_1 = M_2 = \frac{6EI}{\ell^2} w^0; \quad V_1 = V_2 = \frac{12EI}{\ell^3} w^0$ $\theta_3 = \frac{3}{2} \frac{w^0}{\ell}; \quad w_3 = \frac{1}{2} w^0$

support reactions and rotations at the beam ends

displacements

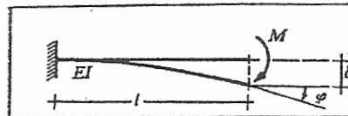
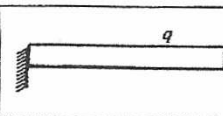
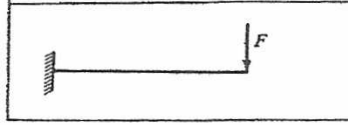
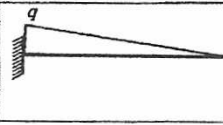
Table 3-1 Moment and deflection formulas (from: Hartsuijker / Welleman: Engineering Mechanics, Volume 2)

	$A_{\text{vert}} = \frac{11}{16} F$ $B_{\text{vert}} = \frac{5}{16} F$	$M_A = \frac{3}{16} Fl$ $\varphi_B = \frac{Fl^2}{32EI}$	$\delta_C = \frac{7Fl^3}{768EI}$
	$A_{\text{vert}} = \frac{F \cdot b(3l^2 - b^2)}{2l^3}$ $B_{\text{vert}} = \frac{F \cdot a^2(2l + b)}{2l^3}$	$M_A = \frac{F \cdot b \cdot (l^2 - b^2)}{2l^2}$ $\varphi_B = \frac{Fa^2b}{4lEI}$	$a \leq b \quad \delta_C = \frac{F \cdot a^2 \cdot (9b - 2a)}{96EI}$ $a \geq b \quad \delta_C = \frac{F \cdot b \cdot (3l^2 - 5b^2)}{96EI}$
	$A_{\text{vert}} = \frac{4}{10} ql$ $B_{\text{vert}} = \frac{1}{10} ql$	$M_A = \frac{1}{15} ql^2$ $\varphi_B = \frac{ql^3}{120EI}$	$\delta_C = \frac{9ql^4}{3840EI}$
	$A_{\text{vert}} = \frac{5}{8} ql$ $B_{\text{vert}} = \frac{3}{8} ql$	$M_A = \frac{1}{8} ql^2$ $\varphi_B = \frac{ql^3}{48EI}$	$\delta_C = \frac{ql^4}{192EI}$
	$A_{\text{vert}} = \frac{21}{64} ql$ $B_{\text{vert}} = \frac{11}{64} ql$	$M_A = \frac{5}{64} ql^2$ $\varphi_B = \frac{5ql^3}{384EI}$	$\delta_C = \frac{ql^4}{290EI}$
	$A_{\text{vert}} = \frac{q(5l^3 - 4al^2 - 2a^2l + a^3)}{8l^2}$ $B_{\text{vert}} = q(l - a) - A_{\text{vert}}$	$M_A = \frac{q(l^3 - 2a^2l + a^2)}{8l}$ $\varphi_B = \frac{q(l^3 - 2a^2l + a^3)}{48EI}$	$\delta_C = \frac{q(10l^4 - 10a^2l^2 - 15a^3l + 16a^4)}{1920EI}$
	$A_{\text{vert}} = \frac{3M(l^2 - b^2)}{2l^3} \uparrow$ $B_{\text{vert}} = \frac{3M(l^2 - b^2)}{2l^3} \downarrow$	$M_A = \frac{M(3b^2 - l^2)}{2l^2} \zeta$ $\varphi_B = \frac{M \cdot a(a - 2b)}{4lEI}$	$a \leq b \quad \delta_C = \frac{M \cdot a \cdot (6b - 5a)}{32EI} \uparrow$ $a \geq b \quad \delta_C = \frac{M(l^2 - 5b^2)}{32EI} \downarrow$
	$A_{\text{vert}} = \frac{3}{2} \frac{M}{l} \uparrow$ $B_{\text{vert}} = \frac{3}{2} \frac{M}{l} \downarrow$	$M_A = \frac{1}{2} M \zeta$ $\varphi_B = \frac{Ml}{4EI}$	$\delta_C = \frac{Ml^2}{32EI}$
	$A_{\text{vert}} = \frac{3EI\delta}{l^3} \downarrow$ $B_{\text{vert}} = \frac{3EI\delta}{l^3} \uparrow$	$M_A = \frac{3EI\delta}{l^2} \zeta$ $\varphi_B = \frac{3}{2} \frac{\delta}{l}$	$\delta_C = \frac{5}{16} \delta \uparrow$

Table 3-2 Singular statically indeterminate beams (Ir.E.O.E van Rotterdam: Sterkteleer 2 toegepaste mechanica)

	$A_{\text{vert}} = \frac{1}{2} F \uparrow$ $B_{\text{vert}} = \frac{1}{2} F \uparrow$	$M_A = \frac{1}{8} Fl \curvearrowright$ $M_B = \frac{1}{8} Fl \curvearrowleft$	$\delta_C = \frac{Fl^3}{192EI} \downarrow$
	$A_{\text{vert}} = \frac{Fb^2(3a + b)}{l^3}$ $B_{\text{vert}} = \frac{Fa^2(a + 3b)}{l^3}$	$M_A = \frac{Fab^2}{l^2}$ $M_B = \frac{Fa^2b}{l^2}$	$a \leq b$ $\delta_C = \frac{Fa^2(3b - a)}{48EI}$
	$A_{\text{vert}} = \frac{7}{20} ql$ $B_{\text{vert}} = \frac{3}{20} ql$	$M_A = \frac{1}{20} ql^2$ $M_B = \frac{1}{30} ql^2$	$\delta_C = \frac{ql^4}{768EI}$
	$A_{\text{vert}} = \frac{1}{2} ql$ $B_{\text{vert}} = \frac{1}{2} ql$	$M_A = \frac{1}{12} ql^2$ $M_B = \frac{1}{12} ql^2$	$\delta_C = \frac{ql^4}{384EI}$
	$A_{\text{vert}} = \frac{1}{4} ql$ $B_{\text{vert}} = \frac{1}{4} ql$	$M_A = \frac{5}{96} ql^2$ $M_B = \frac{5}{96} ql^2$	$\delta_C = \frac{7ql^4}{3840EI}$
	$A_{\text{vert}} = \frac{q(l - a)}{2}$ $B_{\text{vert}} = \frac{q(l - a)}{2}$	$M_A = \frac{q(l^3 - 2a^2l + a^3)}{12l}$ $M_B = \frac{q(l^3 - 2a^2l + a^3)}{12l}$	$\delta_C = \frac{q(5l^4 - 20a^3l + 16a^4)}{1920EI}$
	$A_{\text{vert}} = \frac{6Mab}{l^3} \uparrow$ $B_{\text{vert}} = \frac{6Mab}{l^3} \downarrow$	$M_A = \frac{Mb(b - 2a)}{l^2} \curvearrowright$ $M_B = \frac{Ma(2b - a)}{l^2} \curvearrowleft$	$\delta_C = \frac{Ma(b - a)}{8EI} \uparrow$
	$A_{\text{vert}} = \frac{12EI\delta}{l^3} \downarrow$ $B_{\text{vert}} = \frac{12EI\delta}{l^3} \uparrow$	$M_A = \frac{6EI\delta}{l^2} \curvearrowright$ $M_B = \frac{6EI\delta}{l^2} \curvearrowleft$	$\delta_C = \frac{1}{2} \delta \uparrow$

Table 3-3 Twofold statically indeterminate beams (Ir.E.O.E van Rotterdam: Sterkteleer 2 toegepaste mechanica)  
(Point C is in the middle of the beam)

	$\varphi = \frac{Ml}{EI}$	$\delta = \frac{Ml^2}{2EI}$		$\varphi = \frac{ql^3}{6EI}$	$\delta = \frac{ql^4}{8EI}$
	$\varphi = \frac{Fl^2}{2EI}$	$\delta = \frac{Fl^3}{3EI}$		$\varphi = \frac{ql^3}{24EI}$	$\delta = \frac{ql^4}{30EI}$

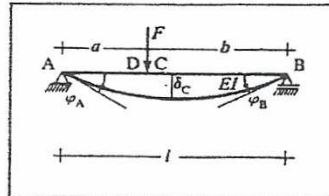
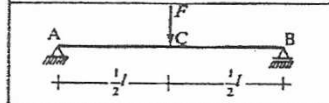
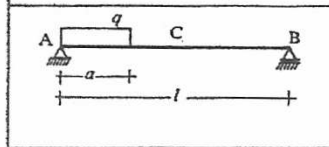
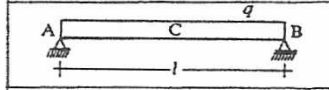
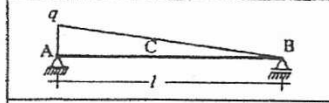
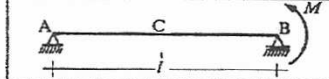
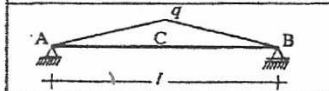
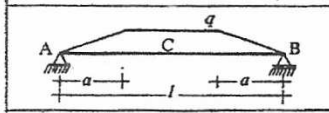
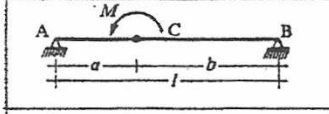
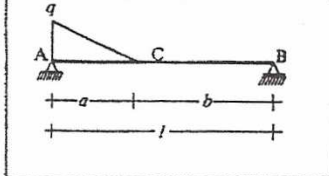
	$\varphi_A = \frac{Fab(l+b)}{6EI}$	$\varphi_B = \frac{Fab(l+a)}{6EI}$	$\delta_D = \frac{Fa^2b^2}{3EI}$
			als $a \leq b$ $\delta_C \approx \delta_{max} = \frac{Fa(3l^2 - 4a^2)}{48EI}$
	$\varphi_A = \varphi_B = \frac{Fl^2}{16EI}$		$\delta_C = \delta_{max} = \frac{Fl^3}{48EI}$
	$\varphi_A = \frac{qa^2(2l-a)^2}{24EI}$	$\varphi_B = \frac{qa^2(2l^2-a^2)}{24EI}$	als $a \leq \frac{1}{2}l$ $\delta_C \approx \delta_{max} = \frac{qa^2(3l^2-2a^2)}{96EI}$
	$\varphi_A = \varphi_B = \frac{ql^3}{24EI}$		$\delta_C = \delta_{max} = \frac{5ql^4}{384EI}$
	$\varphi_A = \frac{ql^3}{45EI}$	$\varphi_B = \frac{7 \cdot ql^3}{360EI}$	$\delta_C = \delta_{max} = \frac{1}{2} \cdot \frac{5ql^4}{384EI}$
	$\varphi_A = \frac{Ml}{6EI}$	$\varphi_B = \frac{Ml}{3EI}$	$\delta_C \approx \delta_{max} = \frac{Ml^2}{16EI}$
	$\varphi_A = \varphi_B = \frac{5ql^3}{192EI}$		$\delta_C = \delta_{max} = \frac{ql^4}{120EI}$
	$\varphi_A = \varphi_B = \frac{q(l^3 - 2a^2l + a^3)}{24EI}$		$\delta_C = \delta_{max} = \frac{q(25l^4 - 40a^2l^2 + 16a^4)}{1920EI}$
	als $a \leq b$ $\varphi_A = \frac{M(l^2 - 3b^2)}{6EI}$	als $a \leq b$ $\varphi_B = \frac{M(3a^2 - l^2)}{6EI}$	als $a \leq b$ $\varphi_C = \frac{M(4a^2 - l^2)}{16EI}$
	$\varphi_A = \frac{qa^2(20l^2 - 15al + 3a^2)}{360EI}$ $\varphi_B = \frac{qa^2(10l^2 - 3a^2)}{360EI}$		$\delta_C = \delta_{max} = \frac{q}{aEI} \left( \frac{5(a-b)l^4}{768} + \frac{b^3(5l^2 - 2b^2)}{480} \right)$

Table 3-4 Statically determinate beams (Ir.E.O.E van Rotterdam: Sterkteleer 2 toegepaste mechanica)  
(Point C is in the middle of the beam)

### 3.2 Second moments of area and properties of plane figures

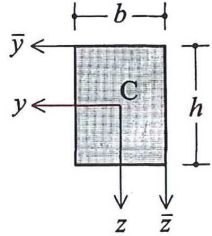
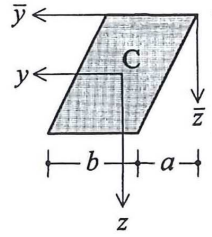
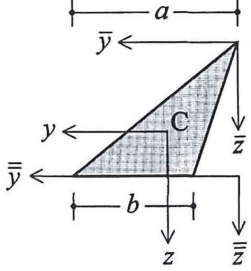
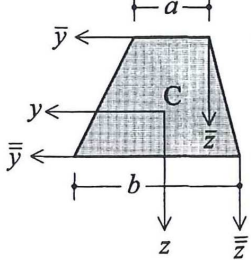
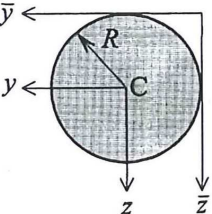
Figure	Area, coordinates centroid C	Second moments of area	
		centroidal	other
	Rectangle $A = bh$ $\bar{y}_C = \frac{1}{2}b$ $\bar{z}_C = \frac{1}{2}h$	$I_{yy} = \frac{1}{12}b^3h$ $I_{zz} = \frac{1}{12}bh^3$ $I_{yz} = 0$	$I_{\bar{y}\bar{y}} = \frac{1}{3}b^3h$ $I_{\bar{z}\bar{z}} = \frac{1}{3}bh^3$ $I_{\bar{y}\bar{z}} = \frac{1}{4}b^2h^2$
	Parallelogram $A = bh$ $\bar{y}_C = \frac{1}{2}(a+b)$ $\bar{z}_C = \frac{1}{2}h$	$I_{yy} = \frac{1}{12}(a^2 + b^2)bh$ $I_{zz} = \frac{1}{12}bh^3$ $I_{yz} = \frac{1}{12}abh^2$	$I_{\bar{z}\bar{z}} = \frac{1}{3}bh^3$
	Triangle $A = \frac{1}{2}bh$ $\bar{y}_C = \frac{1}{3}(2a-b)$ $\bar{z}_C = \frac{2}{3}h$	$I_{yy} = \frac{1}{36}(a^2 - ab + b^2)bh$ $I_{zz} = \frac{1}{36}bh^3$ $I_{yz} = \frac{1}{72}(2a-b)bh^2$	$I_{\bar{z}\bar{z}} = \frac{1}{4}bh^3$ $I_{\bar{y}\bar{z}} = \frac{1}{8}(2a-b)bh^2$ $I_{\bar{y}\bar{y}} = \frac{1}{12}bh^3$
	Trapezium $A = \frac{1}{2}(a+b)h$ $\bar{z}_C = \frac{1}{3} \frac{a+2b}{a+b} h$	$I_{zz} = \frac{1}{36} \frac{a^2 + 4ab + b^2}{a+b} h^3$	$I_{\bar{z}\bar{z}} = \frac{1}{12}(a+3b)h^3$ $I_{\bar{y}\bar{y}} = \frac{1}{12}(3a+b)h^3$
	Circle $A = \pi R^2$	$I_{yy} = I_{zz} = \frac{1}{4}\pi R^4$ $I_{yz} = 0$ $I_p = \frac{1}{2}\pi R^4$	$I_{\bar{y}\bar{y}} = I_{\bar{z}\bar{z}} = \frac{5}{4}\pi R^4$ $I_{\bar{y}\bar{z}} = \pi R^4$

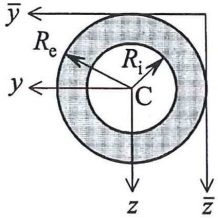
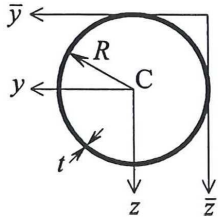
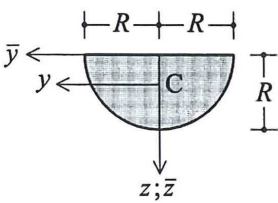
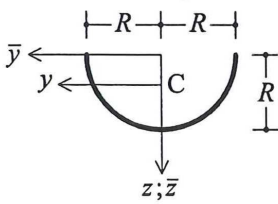
Figure	Area, coordinates centroid C	Second moments of area	
		centroidal	other
	<p>Thick-walled ring</p> $A = \pi(R_e^2 - R_i^2)$	$I_{yy} = I_{zz} = \frac{1}{4} \pi(R_e^4 - R_i^4)$ $I_{yz} = 0$ $I_p = \frac{1}{2} \pi(R_e^4 - R_i^4)$	
	<p>Thin-walled ring</p> $A = 2\pi R t$	$I_{yy} = I_{zz} = \pi R^3 t$ $I_{yz} = 0$ $I_p = 2\pi R^3 t$	$I_{\bar{y}\bar{y}} = I_{\bar{z}\bar{z}} = 3\pi R^3 t$
	<p>Semicircle</p> $A = \frac{1}{2} \pi R^2$ $\bar{y}_C = 0$ $\bar{z}_C = \frac{4}{3\pi} R = 0.424 R$	$I_{yy} = \frac{1}{8} \pi R^4 = 0.393 R^4$ $I_{zz} = (\frac{\pi}{8} - \frac{8}{9\pi}) R^4 = 0.110 R^4$ $I_{yz} = 0$	$I_{\bar{y}\bar{y}} = I_{\bar{z}\bar{z}} = \frac{1}{8} \pi R^4$ $I_{\bar{y}\bar{z}} = 0$
	<p>Semicircular ring</p> $A = \pi R t$ $\bar{y}_C = 0$ $\bar{z}_C = \frac{2}{\pi} R = 0.637 R$	$I_{yy} = \frac{1}{2} \pi R^3 t$ $I_{zz} = (\frac{\pi}{2} - \frac{4}{\pi}) R^3 t = 0.298 R^3 t$ $I_{yz} = 0$	$I_{\bar{y}\bar{y}} = I_{\bar{z}\bar{z}} = \frac{1}{2} \pi R^3 t$ $I_{\bar{y}\bar{z}} = 0$

Table 3-5 Second moments of area

properties of 2D shapes to be used for the moment-area theorems

(1)		<p>rectangle: <math>y = h</math></p> <p><math>A = bh</math></p> <p><math>x_C = \frac{1}{2}b</math></p>
(2)		<p>triangle: <math>y = h \left\{ 1 - \frac{x}{b} \right\}</math></p> <p><math>A = \frac{1}{2}bh</math></p> <p><math>x_C = \frac{1}{3}b</math></p>
(3)		<p>parabola: <math>y = h \left\{ 1 - \frac{x}{b} \right\}^2</math></p> <p><math>A = \frac{1}{3}bh</math></p> <p><math>x_C = \frac{1}{4}b</math></p>
(4)		<p>parabola: <math>y = h \left\{ 1 - \left( \frac{x}{b} \right)^2 \right\}</math></p> <p><math>A = \frac{2}{3}bh</math></p> <p><math>x_C = \frac{3}{8}b</math></p>
(5)		<p>parabola:</p> <p><math>A = \frac{2}{3}bh</math></p> <p><math>x_C = \frac{1}{2}b</math></p>
(6)		<p>trapezium: <math>y = h_1 + (h_2 - h_1) \frac{x}{b}</math></p> <p><math>A = \frac{1}{2}b(h_1 + h_2)</math></p> <p><math>x_C = \frac{1}{3}b \frac{h_1 + 2h_2}{h_1 + h_2}</math></p>

Table 3-6 Properties of plane shapes

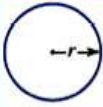
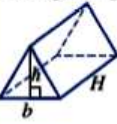
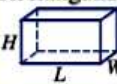
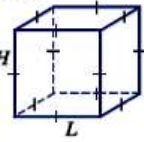
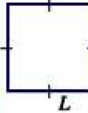
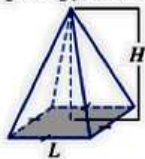
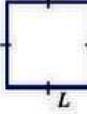
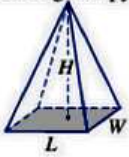
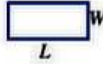
Shape	Cross-sectional shape	Volume
<p>Cylinder</p> 	 <p>Area = <math>\pi r^2</math></p>	<p><math>V = \text{area of a circle} \times \text{height}</math>  <math>= \pi r^2 \times H</math></p>
<p>Triangular prism</p> 	 <p>Area = <math>\frac{1}{2}bh</math></p>	<p><math>V = \text{area of a triangle} \times \text{height}</math>  <math>= \frac{1}{2}bh \times H</math>  <i>Note:</i> Lowercase <i>h</i> represents the height of the triangle.</p>
<p>Rectangular prism</p> 	 <p>Area = <math>L \times W</math></p>	<p><math>V = \text{area of a rectangle} \times \text{height}</math>  <math>= L \times W \times H</math></p>
<p>Cube</p> 	 <p>Area = <math>L^2</math></p>	<p><math>V = \text{area of a square} \times \text{height}</math>  <math>= L^2 \times H</math>  <math>= L^2 \times L</math>  <math>= L^3</math>                      (since in a square, <math>H = L</math>)</p>
<p>Cone</p> 		<p><math>V = \frac{1}{3} \times \text{area of a circle} \times \text{height}</math>  <math>V = \frac{1}{3} \pi r^2 \times H</math></p>
<p>Square pyramid</p> 		<p><math>V = \frac{1}{3} \times \text{area of a square} \times \text{height}</math>  <math>V = \frac{1}{3} L^2 \times H</math></p>
<p>Rectangular pyramid</p> 		<p><math>V = \frac{1}{3} \times \text{area of a rectangle} \times \text{height}</math>  <math>= \frac{1}{3} L \times W \times H</math></p>
<p>sphere.</p> 	 <p>Area = <math>\pi r^2</math></p>	<p><math>V = \frac{4}{3} \pi r^3</math>  <math>r</math> is the radius of the sphere.</p>

Table 3-7 Properties of 3D-objects (from: <http://cshsyear10maths.global2.vic.edu.au/>)

### 3.3 Natural oscillation frequencies

Natural frequencies of structures with a uniform and homogeneous section can be calculated according to  $f_n = \omega_n / 2\pi$  [Hz].

The angular velocity is  $\omega_n = C \sqrt{\frac{EI}{\mu L^4}}$  [rad/s],

where:

- $E$  [N/m<sup>2</sup>] = Youngs modulus (*elasticiteitsmodulus*)
- $L$  [m] = length of the beam/girder
- $I$  [m<sup>4</sup>] = moment of inertia (*traagheidsmoment*)
- $\mu$  [kg/m] = mass per running metre beam
- $C$  [m] = coefficient according to Table 3-8

		$n = 1$	$n = 2$	$n = 3$	$n = 4$	$n = 5$
clamped	free	 $C = 3.52$	 $C = 22.4$	 $C = 61.7$	 $C = 121.0$	 $C = 200.0$
simply supported	simply supported	 $C = 9.87$	 $C = 39.5$	 $C = 88.9$	 $C = 158.0$	 $C = 247.0$
clamped	clamped	 $C = 22.4$	 $C = 61.7$	 $C = 121.0$	 $C = 200.0$	 $C = 296.0$
free	free	 $C = 22.4$	 $C = 61.7$	 $C = 121.0$	 $C = 200.0$	 $C = 298.0$
clamped	simply supported	 $C = 15.4$	 $C = 50.0$	 $C = 104.0$	 $C = 178.0$	 $C = 272.0$
simply supported	free	 $C = 15.4$	 $C = 50.0$	 $C = 104.0$	 $C = 178.0$	 $C = 272.0$

Table 3-8 Natural frequency (eigen frequency)  $f_n$  and principal modes of vibration (patterns of motion).

The position of the nodes have been indicated by their distance to the support on the left

## 4. Some helpful computer programs

The table below refers to computer programmes available at the TU Delft. In this manual, however, the various programs are not or hardly dealt with. Instead, so-called “hand calculations” and design rules are given full attention.

Program	Description
AFDA	Program for level II probabilistic calculations
Cress	CRESS provides a collection of small routines important in coastal and river engineering (web based application <a href="http://www.cress.nl">www.cress.nl</a> )
D-Breakwat	Design program for rock-fill breakwaters
D-Geo Stability	Program for the calculation of stability of slopes using circular slide plains
D-Probed	Program calculating bed protections and pipe covers subjected to a combination of currents and (non-breaking) waves
D-Settlement	Program for settlement calculations
D-Sheetpiling	Program for stability calculations for sheet pile structures
DAMWAND	Simple program for stability calculations for sheet pile structures
DELFT3D*)	Advanced program for the calculation of morphological processes in the coastal zone
DUFLOW	Program for the calculation of flow in open waterways
GLOBPAP	Program for the probabilistic analysis of circular slide plains
HISWA*)	Program for wave height and wave period determination
MatrixFrame	Program for structural strength calculations for continuous beams, 2D and 3D frameworks, walls, etc.
MSEEP	Program for the calculation of groundwater flow
PLAXIS <sup>1)</sup>	Finite elements program for the stability of foundations and soil retaining structures. Also calculation of groundwater flow
Scia Engineer	All-in-one platform featuring strong 3D modelling. It uses a finite element engine, integrated multi-material code design and reporting tools enable to centralize the workflow. This programme can be downloaded from <a href="http://nemetschek-scia.com/">nemetschek-scia.com/</a> , where also a free student license can be obtained.
SWAN	Program for the determination of wave height and wave period calculations
UNIBEST*)	Program for calculation of morphological processes in the coastal zone
PC-Overslag	Program for the calculation of wave overtopping. This programme can be downloaded from <a href="http://www.helpdeskwater.nl/onderwerpen/applicaties-modellen/">www.helpdeskwater.nl/onderwerpen/applicaties-modellen/</a>

Table 4-1 Computer programmes available at TU Delft

<sup>1)</sup> These programs are not commonly available. Depending on the graduation project these may be made available in consultation with the graduation supervisor(s).

## 5. Units and conventions

### 5.1 Units

The world's most widely used system of physical units, both in everyday commerce and in science, is the International System of Units (abbreviated SI from the French "Système International d'unités"). A notable exception is the United States of America, which still uses many old units in addition to SI. The SI-standard is maintained by the Bureau International des Poids et Mesures in Sèvres, France. The seven SI base units are presented in Table 5-1.

quantity		unit	
name	symbol	name	symbol
length	$l$	metre	m
mass	$m$	kilogram	kg
time	$t$	second	s
electric current	$I$	ampere	A
thermodynamic temperature	$T$	kelvin	K
amount of substance	$n$	mole	mol
luminous intensity	$I_v$	candela	cd

Table 5-1 base units

Base units can be put together to derive units of measurement for other quantities. Some have been given names. Table 5-2 gives an overview of derived SI units relevant for hydraulic engineering.

quantity		unit		
name	symbol	name	non-SI units (generally used)	SI base units
acceleration	$a$	metre per second squared		$m s^{-2}$
angle	$\alpha, \beta, \dots$	radian	rad	1
angular velocity	$\omega$	radian per second	rad / s	$s^{-1}$
area	$A$	square metre		$m^2$
area moment of inertia	$I$	metre to the fourth power		$m^4$
axial rigidity	$EA$	newton per metre	$N m^{-1}$	$kg s^{-2}$
bending stiffness	$EI$	newton per square metre	$N m^2$	$kg m^{-1} s^{-2}$
density	$\rho$	kilogram per cubic metre		$kg m^{-3}$
dynamic viscosity	$\eta$	pascal second	$Pa s (N s / m^2)$	$kg m^{-1} s^{-1}$
energy, work, heat	$W$	joule	$J (N m)$	$kg m^2 s^{-2}$
first moment of area	$S$	cubic metre		$m^3$
force, weight	$F, G$	newton	N	$kg m s^{-2}$
frequency	$f$	hertz	Hz	$s^{-1}$
impulse, momentum	$p$	newton second	$N s$	$kg m s^{-1}$
kinematic viscosity	$\nu$	square metre per second		$m^2 \cdot s^{-1}$
moment of force, torque	$M$	newton metre	$N m$	$kg m^2 s^{-2}$
section modulus	$W$	cubic metre		$m^3$
power	$P$	watt	$W (J / s)$	$kg m^2 s^{-3}$
pressure, stress	$\sigma$	pascal	$Pa (N / m^2)$	$kg m^{-1} s^{-2}$
speed, velocity	$v$	metre per second		$m s^{-1}$
specific weight	$\gamma$	newton per cubic metre	$N / m^3$	$kg m^{-2} s^{-2}$
volume	$V$	cubic metre		$m^3$
wave number	$k$	reciprocal metre		$m^{-1}$
Young's modulus	$E$	newton per square metre	$N m^{-2}$	$kg m^{-1} s^{-2}$

Table 5-2 Selection of derived SI-units

The 'area moment of inertia', or 'second moment of area' in hydraulic engineering is mostly referred to as 'moment of inertia'. In some literature, the 'section modulus' is indicated as the 'moment of resistance'. The 'bending stiffness' is also known as 'flexural rigidity'. The 'Young's modulus' is also known as 'modulus of elasticity', 'elastic modulus' or 'tensile modulus'.

Depending on age and place, many non-SI units are in use. The most important non-SI units still in use are presented in Table 5-3. Extensive lists with conversion factors can be found on internet, see for example <http://www.unc.edu/~rowlett/units/>.

quantity		unit		
name	symbol	name	symbol	relation to SI-units
area	A	are	a	= 100 m <sup>2</sup>
energy	W	kilocalorie	Cal, kcal	= 4,1868 kJ
energy	W	kilowatt-hour	kWh	= 3,6 MJ
force	F	ton / tonnes (force)	tnf	= 1000 kgf ≈ 9,81 kN
force	F	pound	lb (lbf)	≈ 4,448 N
length	L	mile	mi	≈ 1609 m
length	L	nautical mile	nmi, NM	= 1852 m
length	L	yard	yd	= 0,9144 m
length	L	foot (international)	ft	= 0,3048 m
length	L	inch	in (")	= 0,0254 m
mass	m	slug	slug (lb-s <sup>2</sup> /ft)	= 14,59 kg
mass	m	ton / tonnes (mass)	t	= 1000 kg
power	P	horsepower (metric)	hp	≈ 735,499 W
pressure	σ	atmosphere	atm	= 101 325 Pa
pressure	σ	bar	bar	= 10 <sup>5</sup> Pa
speed, velocity	v	knot (international)	kn (kt)	= 0,514 m s <sup>-1</sup> (= 1 nmi/h)
temperature	T	degree Celsius	°C	= T <sub>K</sub> - 273.15
temperature	T	degree Fahrenheit	°F	= T <sub>K</sub> × 1.8 - 459.67
volume	V	litre	l or L	= 1 dm <sup>3</sup> = 0.001 m <sup>3</sup>
volume	V	gallon (imperial)	gal	≈ 4,546 × 10 <sup>-3</sup> m <sup>3</sup>
volume	V	gallon (USA)	gal	≈ 3,785 × 10 <sup>-3</sup> m <sup>3</sup>

Table 5-3 Non-SI units

Prefixes may be added to units to produce a multiple of the original unit. All multiples are integer powers of ten. See Table 5-4 for an overview of the most used prefixes.

name	symbol	factor
peta-	P	10 <sup>15</sup>
tera-	T	10 <sup>12</sup>
giga-	G	10 <sup>9</sup>
mega-	M	10 <sup>6</sup>
kilo-	k	10 <sup>3</sup>
hecto-	h	10 <sup>2</sup>
deca-	da	10 <sup>1</sup>
deci-	d	10 <sup>-1</sup>
cent-	c	10 <sup>-2</sup>
milli-	m	10 <sup>-3</sup>
micro-	μ	10 <sup>-6</sup>
nano-	n	10 <sup>-9</sup>
pico-	p	10 <sup>-12</sup>
femto-	f	10 <sup>-15</sup>

Table 5-4 SI-prefixes

For direct conversion of °C to °F and v.v., next formulae apply:

$$T_C = (T_F - 32)/1,8$$

$$T_F = 1,8 T_C + 32$$

Besides the related quantities of density and specific weight, in some anglo-saxon literature 'specific gravity' (sg) is used. This is defined as:  $sg = \frac{\gamma_{\text{specific material}}}{\gamma_{\text{water}, 4^\circ\text{C}}} = \frac{\rho_{\text{specific material}}}{\rho_{\text{water}, 4^\circ\text{C}}} [-]$ .

## 5.2 Conventions

In design practise, and also in this Manual, stresses and material properties are expressed in  $\text{N/mm}^2$ , only values for soundings are in MPa. Forces are generally expressed in kN.

The decimal mark and the thousands separator in numbers are written in the style that is used in most of Europe: a comma is used as decimal delimiter, and a blank space is used as digit grouping delimiter (for reading comfort). So, for example, one million newton with a precision of two decimals is written as 1 000 000,00 N.

Many authorities recommend that in scientific notation, when numbers are represented using powers of ten, the exponent of the 10 should be a multiple of 3. So, for example,  $1,234 \cdot 10^4$  should be written as  $12,34 \cdot 10^3$ .

## 6. Dutch translation of Hydraulic Structures keywords

### A

abutment	landhoofd
angle of internal friction	hoek van inwendige wrijving
apron	vlonder
aquifer	waterhoudende grondlaag
area moment of inertia	traagheidsmoment

### B

backwater curve	stuwkromme
barrier	kering
beam	ligger
bearing	ondersteuning(sconstructie)
bearing capacity	draagvermogen
bentonite	bentoniet
berth	ligplaats
berthing dolphin	meerstoel
blinding	werkvloer
bollard	bolder
bolt	bout
breakwater	golfbreker
buckle (to buckle)	knikken
building dock / construction dock	bouwdok
building pit / construction pit	bouwput
bulkhead	slingerschot / scheidingswand
buoyancy	opdrijving
buoyant force	opdrijvende kracht
buttress	schoor / steunbeer

### C

cable bridge / rope bridge	tuibrug
cantilever	kraagligger / console
capping beam	deksloof
cellular cofferdam	cellenwand
chamber lock	schutsluis
clearance	kielspeling / vrije ruimte
cofferdam	bouwkuip / kistdam
compression stress	drukspanning
confined aquifer	afsgeloten grondlaag met spanningswater
conceptual design	voorlopig ontwerp
construction pit / building pit	bouwput
creep	kruip
crest	kruin
culvert	duiker
cut and cover method	wanden-dakmethode
cut-off	coupure
cut-off screen	kwelscherm (ondoorlatend scherm)
cutting-edge	snijrand

### D

dam	stuwdam
deep foundation	paalfundering
density	dichtheid (soortelijke massa)
design value	rekenwaarde
dewatering gate	uitwateringsluis
diaphragm wall	diepwand
discharge sluice	uitwateringsluis
dissipation chamber	woelbak

dolphin	dukdalf
dragline	sleepgraver (dragline)
draught	diepgang
drop gate	zakdeur
dry dock	droogdok
<b>E</b>	
effective stress	korreldruk
embedded depth	inheidiepte
entry ramp	toerit (naar tunnel)
equilibrium state	evenwichtssituatie
excavator	graafmachine
expansion joint	dilatatievoeg
<b>F</b>	
falsework	steigerwerk / bekisting
fascine mattress	zinkstuk (van rijshout)
fender	stootblok
fetch	strijklengte
fillet weld	hoeklas
flange	flens
flexural rigidity	buigstijfheid
flood defence	waterkering
footing	fundament
formwork	bekisting
freeboard	waakhoogte
frontline waters	buitenwateren
<b>G</b>	
gantry crane	portaalkraan
girder	draagbalk / steunbalk
gravity floor	gewichtsvloer
ground level	maaiveld
guard lock	keersluis
guide beam	geleidebalk
guide work	geleidewerk
<b>H</b>	
hawser force	troskracht
heave	hydraulische grondbreuk
hinge	scharnier
hoist	takel
<b>I</b>	
immersed tunnel	afgezonken tunnel
inclined plane	hellend vlak
inflatable barrier	balgkering of schulpkering
influence coefficient	invloedscoëfficiënt
inland waters	binnenwateren
<b>J</b>	
jack	vijzel
jetty	steiger, golfbreker
<b>L</b>	
lay-by berth	wachtplaats
lean concrete	stampbeton
liquefaction	zettingsvloeiing
lock chamber	schutkolk
lock head	sluishoofd

**M**

masonry	metselwerk
mitre gate	puntdeur
modulus of subgrade reaction	beddingsconstante
mole	havenhoofd
moment diagram	momentenlijn
mooring facility	aanlegvoorziening
mooring force	aanlegkracht
mooring post	meerpaal
mould	mal

**N**

natural oscillation period	eigenperiode
navigation lock	schutsluis
navigation width	doorvaartbreedte
neap tide	doodtij
normal force diagram	normaalkrachtenlijn
nut	moer

**P**

pad footing	poer
pier	pijler
pile	paal
pillar	pilaar
piping	onderloopsheid
pivot	taats
plunger	zuiger
point of fixity	inklemmingspunt
prop	stempel
pulley	katrol
pumping station	gemaal

**Q**

quay	kade
quay wall	kademuur
quoin	wig

**R**

radial gate	segmentdeur
raking pile	schoorpaal
recess	uitsparing, inkassing
reinforcement	wapening
reinforcement bar yard	wapeningsvlechterij
reliability index	betrouwbaarheidsindex
roller gate	roldeur

**S**

scour	ontgroning, wegspoeling
screw	schroef
screw thread	schroefdraad
section modulus	weerstandsmoment
sector gate	sectordeur
seepage	onderloopsheid
self-weight	eigen gewicht
settlement	zetting
settling	klink
shallow foundation	fundering op staal
shear force	dwarskracht
shear force diagram	dwarskrachtenlijn
sheet pile wall	damwand
ship-lift	scheepslift
shop floor	werkvloer

shovel	laadschop
shutter	schuif / schot
shutter weir	klepkering / klepstuw
sill	dorpel, drempel
sill beam	dorpelbalk, drempelbalk
slackening structure	remmingwerk
slack water	kentering / doodtij
sliding gate	roldeur
sliding surface	glijvlak / schuifvlak
sluice caisson	doorlaatcaisson
slurry wall	diepwand
spalling force	spatkracht
span	overspanning
specific gravity	relatieve dichtheid
specific weight	soortelijk gewicht
stop lock	spuisluis
stop log	schotbalk
storm-surge barrier	stormvloedkering
strut	stempel / schoor(balk)
surcharge	bovenbelasting
suspension bridge	hangbrug / kettingbrug
sway	slingering
swell	deining
swivel	wartel / oogbout
<b>T</b>	
tender	aanbesteding
tensile stress	trekspanning
tie rod / tie bar	trekstang, ankerstaaf
timber	balk / hout
tow boat	sleepboot
trestle	aanloopsteiger
truss	spant, ligger
tug boat	sleepboot
turnbuckle	spanschroef
<b>U</b>	
unconfined aquifer	niet-afgesloten gondlaag met freatisch water
<b>V</b>	
valve	klep
vertical lift gate	hefdeur
visor dam	vizierstuw
void ratio	poriëngetal
<b>W</b>	
wale	verstevigingsbalk
waling	gording
walled building pit	bouwkuip
web	lijf (bijvoorbeeld van een H-balk)
weir	stuw
wedge	wig
wind set-up	opwaaing
winch	lier
<b>Y</b>	
yield stress	vloeigrens
Young's modulus	elasticiteitsmodulus

An extensive online technical dictionary (English-Dutch / Dutch-English) can be found at:  
<http://www.tecdic.com/>. A dictionary more specifically intended for hydraulic engineering is:  
<http://www.waterdictionary.info/>.



# Manual Hydraulic Structures

---

## **Part II: Loads**



## 7. Weight

### 7.1 General

In many cases, the most important load on a structure is gravity, because in most cases a structure's weight (a.k.a. 'dead weight') constitutes the largest load by far. Sometimes the weight works in favour of the structure:

- underwater concrete: to reduce the buoyancy (groundwater pressure)
- caisson: more weight means it can take more horizontal shear force
- immersed tunnel: weight is necessary to sink the tunnel to the bottom (of the river)

Sometimes the weight works to the disadvantage:

- bridges and gates: in every span, weight causes extra forces (and moments)
- shallow foundations: the larger the weight, the bigger and more expensive the footing

### 7.2 Design

The total weight of a structure can be found as follows:

$$G = \sum_i V_i \gamma_i$$

in which:  $G$  [kN] = weight of the structure  
 $V_i$  [m<sup>3</sup>] = volume of element  $i$   
 $\gamma_i$  [kN/m<sup>3</sup>] = specific weight of element  $i$

The specific weight of a material,  $\gamma$ , is the measure of the gravitational force acting on an object per unit of volume:

$$\gamma = \rho \cdot g$$

in which:  $\rho$  [kg/m<sup>3</sup>] = density (mass per unit of volume)  
 $g$  [m/s<sup>2</sup>] = acceleration due to gravity

$g \approx 9,81 \text{ m/s}^2$  in the Netherlands, at sea level.

The following table gives rough estimates of the specific weights of the most important construction materials:

material	specific weight
Steel	78 kN/m <sup>3</sup>
Concrete (reinforced or prestressed)	25 kN/m <sup>3</sup>
Concrete (not reinforced)	24 kN/m <sup>3</sup>
Bentonite slurry	11~13 kN/m <sup>3</sup>
Wood (soft)	6~7 kN/m <sup>3</sup>
Wood (hard)	8~10 kN/m <sup>3</sup>
Stone (excl. pores)	26 kN/m <sup>3</sup>
Gravel (dry)	16~17 kN/m <sup>3</sup>
Gravel (wet)	19~20 kN/m <sup>3</sup>
Sand (dry)	17~18 kN/m <sup>3</sup>
Sand (wet)	20~21 kN/m <sup>3</sup>
Clay	15~17 kN/m <sup>3</sup>
Peat	10~11 kN/m <sup>3</sup>

Table 7-1 Volumetric weights

For a more extensive overview of material and fluid densities, see for example <http://www.simetric.co.uk/>.

**Note.** Not only the structure's self-weight causes a load. Objects in the vicinity of the structure can also cause a (horizontal) load via the ground. This is why in calculations, one assumes a minimum evenly distributed vertical load (excluding the safety factor  $\gamma = 1,5$ ) of  $q_v = 20 \text{ kPa}$  next to a sheet pile or a retaining wall, unless it can be proved that no load (e.g. a concrete mixer truck) could ever reach the location.

## 8. Wind

revision: February 2008; Section 2 updated to Eurocode: February 2015

### 8.1 Theory

Wind is caused by uneven pressures in the atmosphere that exist in so-called high- and low-pressure areas. The wind climate is a stochastic process, which is described by a number of parameters, such as:

- wind direction
- wind velocity
- turbulence

The wind climate is determined by other factors besides the pressure differences, amongst which are the topography and the altitude. The parameters mentioned above are stochastic variables, which are estimated by statistically manipulating measured data concerning the wind climate. The data are gathered by meteorological institutes. Using a large number of meteorological stations, statistical data is collected for the description of the wind climate. The collection of data takes place at a set height: 10 m, above ground level and with a standardised terrain roughness (0,03 m).

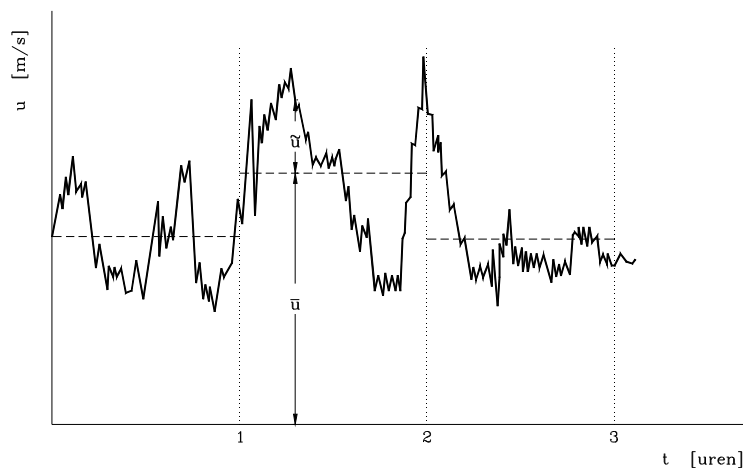


Figure 8-1 Wind velocity: one-hour average and fluctuation

The average wind velocity in an hour is described by the so-called long-term distribution (see Figure 2-1). The fluctuation of the wind velocity within the period of one hour is described by the short-term description, whereby an average value is distinguished from a value that fluctuates in the course of time:

$$\vec{u}(t) = \begin{bmatrix} u_x(t) \\ u_y(t) \\ u_z(t) \end{bmatrix} = \begin{bmatrix} \bar{u}_x \\ \bar{u}_y \\ \bar{u}_z \end{bmatrix} + \begin{bmatrix} \tilde{u}_x(t) \\ \tilde{u}_y(t) \\ \tilde{u}_z(t) \end{bmatrix}$$

in which:  $\vec{u}(t)$  [m/s] = vector of the wind velocity in all three directions given as a function of time within an hour

$\bar{u}_x$  [m/s] = average wind velocity in an hour in x-direction

$\tilde{u}_x(t)$  [m/s] = fluctuation of the wind velocity within an hour

The wind direction, wind velocity and turbulence in the lowest layers of the atmosphere play an important role in the design, realisation and use of hydraulic structures. The friction between the wind and the earth's surface is of large importance in this layer. Aspects such as the vegetation and buildings determine the friction.

In a neutrally stable atmosphere, the time-average wind velocity close to the surface follows a logarithmic profile (see also Figure 8-2):

$$\bar{u}(z) = \frac{u_*}{k} \ln\left(\frac{z}{z_0}\right)$$

where:  $\bar{u}(z)$  [m/s] = average wind velocity in an hour at a height  $z$

$u_*$  [m/s] = friction velocity, which describes the amount of turbulence

$$u_* = \sqrt{\frac{\tau_w}{\rho}}, \text{ where } \tau_w = \text{surface shear stress and } \rho = \text{fluid (air) density}$$

$k$  [-] = Von Kármán constant ( $\approx 0,41$ )

$z$  [m] = height above the surface (normally this is the earth or marine surface, but in urban areas the average height of buildings should be taken as surface level)

$z_0$  [m] = roughness height of the surface, dependent on the nature of the terrain  
The roughness height varies from 0,0002 m for water surfaces to 1,6 m for very large cities with tall buildings and skyscrapers.

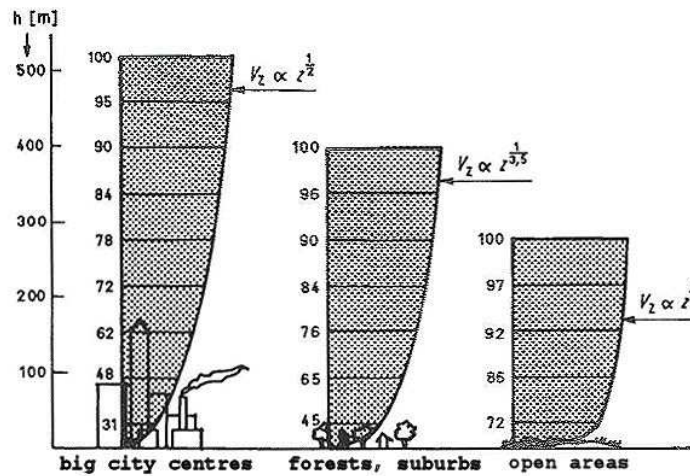


Figure 8-2 Logarithmic wind velocity profiles (from 'De Ingenieur', 31 July 1970)

The wind fluctuation occurring within an hour can be expressed as a standard deviation from the average:

$$\sigma_u = \sqrt{\int_0^{1 \text{ hour}} (u(t) - \bar{u})^2 dt}$$

The variation coefficient  $\sigma_u \cdot I \cdot \bar{u}$  is known as the turbulence intensity. The turbulence intensity  $I$  at a height  $z$  above the surface level can be approached by:

$$I(z) = \frac{k}{\ln\left(\frac{z}{z_0}\right)}$$

in which:  $k$  [-] = factor dependent on the surface. In rural area:  $k = 1,0$ ; in built-up area:  $k = 0,9$

From this, the standard deviation of the momentary wind velocity can be calculated with  $\sigma_u = \bar{u} \cdot I$

The wind velocity is subject to fluctuations with maximum and minimum velocities. The maximums are known as wind gusts. The maximum momentary wind velocity in a gust can be described with a Rayleigh

distribution: 
$$P(\hat{u} > \xi) = \exp\left(-\frac{(\xi - \bar{u})^2}{2\sigma_n^2}\right)$$

The probability distribution of the maximum wind velocity in a period with  $n$  gusts can be determined with:

$$P(\hat{u}_n < \xi) = P(\hat{u} < \xi)^n = \left( 1 - \exp\left(-\frac{(\xi - \bar{u})^2}{2\sigma_n^2}\right) \right)^n = \exp\left(-n \cdot \exp\left(-\frac{(\xi - \bar{u})^2}{2\sigma_n^2}\right)\right)$$

This probability distribution is a conditional probability distribution because  $\bar{u}$  must be known. For the determination of the unconditional probability distribution one is referred to the course CIE4130, "Probabilistic design".

The load of the wind on an object is determined by the flow around the object. This flow is an analogue of the flow around an object in a fluid flow (see Chapter 12).

The force on a structure in the wind direction (drag) and perpendicular to the wind direction (lift) is described by the following formulas:

$$F_D = \frac{1}{2} \rho u^2 C_D A \quad \text{and} \quad F_L = \frac{1}{2} \rho u^2 C_L A$$

The term  $\frac{1}{2} \rho u^2$  is known as the dynamic pressure.  $A$  is the surface area,  $C_D$  and  $C_L$  are coefficients that depend on, amongst other things, the shape of the structure.

The wind velocity is a random variable. Because the dynamic pressure is a function of the wind velocity, the dynamic pressure is also a random variable. The following is valid for the average dynamic pressure and the variation coefficient of the dynamic pressure:

$$\bar{p}_w = \frac{1}{2} \rho \bar{u}^2 \quad V_{p_w} = \frac{\partial p_w}{\partial u} \frac{I \cdot \bar{u}}{\bar{p}_w} = 2 \cdot I$$

The design dynamic pressure at a height  $z$  above ground level can generally be described as:

$$p_w(z) = (1 + \alpha \cdot 2 \cdot I(z)) \cdot \frac{1}{2} \cdot \rho \cdot (u(z))^2$$

The old Dutch Technical Basic Rules for Structures ("Technische Grondslagen voor Bouwconstructies, TGB") use the value  $\alpha = 3,5$ . This value depends on the desired safety level and can be determined by a risk analysis.

Just like the wind velocity, the force on an object will be part constant and part variable. The variable part is caused by variations of the wind velocity, but also by possible separation vortices. The latter is particularly relevant in cases of relatively slender elements (round towers, suspension cables and so forth). The variable part of the load can cause vibrations of the structure or object. The same way as for an object in a stationary flow in a fluid, the sensitivity to vibrations can be analysed using the Strouhal value (see Section 12.3).

## 8.2 (Preliminary) design of structures

According to Eurocode 1991, part 1-4 'General actions - Wind actions', wind loads on structures (lower than 200 m) and structural elements shall be determined taking account of both external and internal wind pressures. This section of the Manual endeavours to present the main design procedure for wind loads, but especially the determination of the structural factor and the force coefficient is quite complex. For details and additional information, one is referred to the original text of Eurocode 1-4. Furthermore, details can vary per country, so mind the National Annexes belonging to the general standard!

### Important preliminary note

The Eurocode distinguishes between wind pressure, which is relevant for the design of cladding (*gevelbekleding*), fixings and structural parts (Section 8.2.1), and wind force, which should be used for overall wind effects (Section 8.2.2).

### 8.2.1 Wind pressure on surfaces

The net pressure on a wall, roof or element is the difference between the pressures on the opposite surfaces taking due account of their signs. Pressure, directed towards the surface is taken as positive, and suction, directed away from the surface as negative. See Figure 8-3 for some examples.

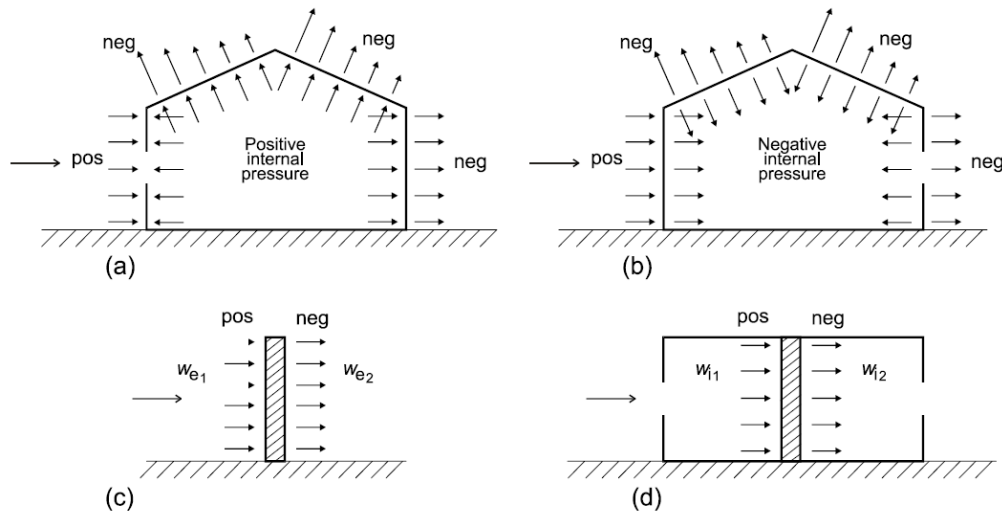


Figure 8-3 Pressure on surfaces (Eurocode 1)

The wind pressure acting on external surfaces  $w_e$  should be calculated according to:

$$w_e = q_p(z_e) \cdot c_{pe}$$

The wind pressure acting on the internal surfaces of a structure  $w_i$  should be obtained from:

$$w_i = q_p(z_i) \cdot c_{pi}$$

where:  $q_p(z_x)$  [kN/m<sup>2</sup>] = peak velocity pressure (*extreme stuwdruk*) at reference height  $z_x$   
 $z_x$  [m] = reference height for the external pressure  $z_e$  or internal pressure  $z_i$   
 $c_{px}$  [-] = pressure coefficient for the external pressure  $c_{pe}$  or internal pressure  $c_{pi}$

The value for the peak velocity pressure  $q_p$  can be calculated according to:

$$q_p(z) = [1 + 7 \cdot I_v(z)] \cdot \frac{1}{2} \cdot \rho \cdot v_m^2(z)$$

where:  $I_v(z)$  [-] = wind turbulence intensity at height  $z$   
 $\rho$  [kg/m<sup>3</sup>] = air density (recommended value is 1,25 kg/m<sup>3</sup>)  
 $v_m(z)$  [m/s] = mean wind velocity at height  $z$

The mean wind velocity  $v_m(z)$  depends on the terrain roughness, orography (= topographic relief of the terrain) and the basic wind velocity, but for the Netherlands a table is available where the value for the peak velocity pressure  $q_p$  can easily be found (Table 8-1). Three pressure zones are distinguished in the Netherlands (Figure 8-4).

$h$ m	peak velocity pressure					
	zone I		zone II		zone III	
	open	built-on	open	built-on	open	built-on
≤ 2	0.64	0.64	0.54	0.54	0.46	0.46
3	0.70	0.64	0.54	0.54	0.46	0.46
4	0.78	0.64	0.62	0.54	0.49	0.46
5	0.84	0.64	0.68	0.54	0.55	0.46
6	0.90	0.64	0.73	0.54	0.59	0.46
7	0.95	0.64	0.78	0.54	0.63	0.46
8	0.99	0.64	0.81	0.54	0.67	0.46
9	1.02	0.64	0.85	0.54	0.70	0.46
10	1.06	0.70	0.88	0.59	0.73	0.50
11	1.09	0.76	0.91	0.64	0.76	0.54
12	1.12	0.81	0.94	0.68	0.78	0.58
13	1.14	0.86	0.96	0.72	0.80	0.61
14	1.17	0.90	0.99	0.76	0.82	0.64
15	1.19	0.94	1.01	0.79	0.84	0.67
16	1.21	0.98	1.03	0.82	0.86	0.70
17	1.23	1.02	1.05	0.85	0.88	0.72
18	1.25	1.05	1.07	0.88	0.90	0.75
19	1.27	1.08	1.09	0.90	0.91	0.77
20	1.29	1.11	1.10	0.93	0.93	0.79
25	1.37	1.23	1.18	1.03	1.00	0.88
30	1.43	1.34	1.24	1.12	1.06	0.95
35	1.49	1.43	1.30	1.20	1.11	1.02
40	1.54	1.50	1.35	1.26	1.15	1.07
45	1.58	1.57	1.39	1.32	1.19	1.12
50	1.62	1.62	1.43	1.37	1.23	1.16

Table 8-1 Peak velocity pressure  $q_p$  [kN/m<sup>2</sup>] in the Netherlands as a function of the height above the surrounding level (*Eurocode 1*)Figure 8-4 Wind pressure zones in the Netherlands (*Eurocode 1, Dutch national annex*)

The external reference height  $z_e$  for windward walls of rectangular plan buildings depends on the aspect ratio  $h/b$  and is always the upper height of the different parts of the walls, see Figure 8-5. The recommended procedure is to take the height of the building as the reference height, but this can vary per national annex of the Eurocode.

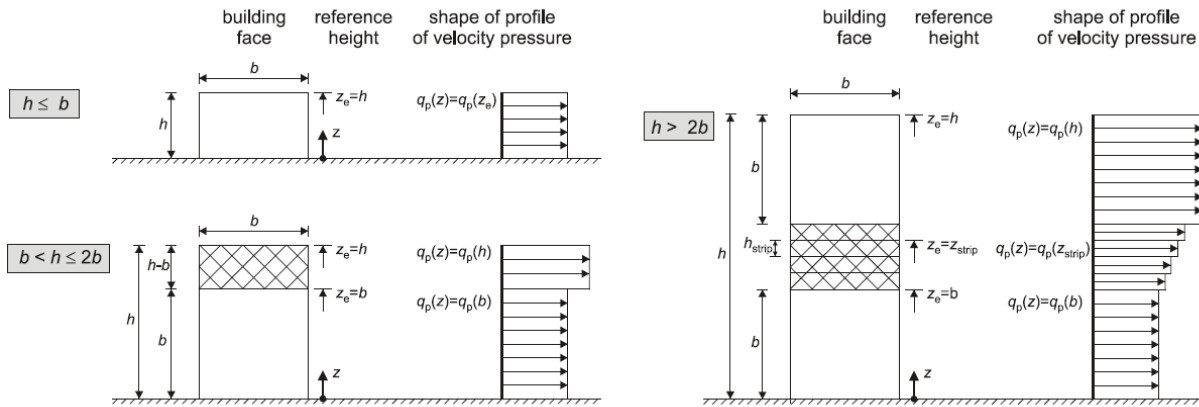


Figure 8-5 Reference height for wind loads (Eurocode 1)

The reference height  $z_i$  for the internal pressures should be equal to the reference height  $z_e$  for the external pressures on the faces which contribute by their openings to the creation of the internal pressure. If there are several openings, the largest value of  $z_e$  should be used to determine  $z_i$ .

External and internal pressures should be considered to act at the same time. For design conditions, the worst combination of external and internal pressures shall be considered. This has to be done for every combination of possible openings and other leakage paths.

The external pressure coefficient  $c_{pe}$  depends on the wind direction and on the size of the loaded area  $A$  that produces the wind action in the section to be calculated. The external pressure coefficients are given for loaded areas  $A$  of  $1 \text{ m}^2$  (indicated with  $C_{pe,1}$ ) and  $10 \text{ m}^2$  ( $C_{pe,10}$ ) in the tables. Values for  $C_{pe,1}$  are intended for the design of small elements and fixings with an area of  $1 \text{ m}^2$  or less, while values for  $C_{pe,10}$  may be used for the design of the overall load bearing structure of buildings.

The different configurations are presented in Figure 8-6 and the corresponding external pressure coefficients in Table 8-2.

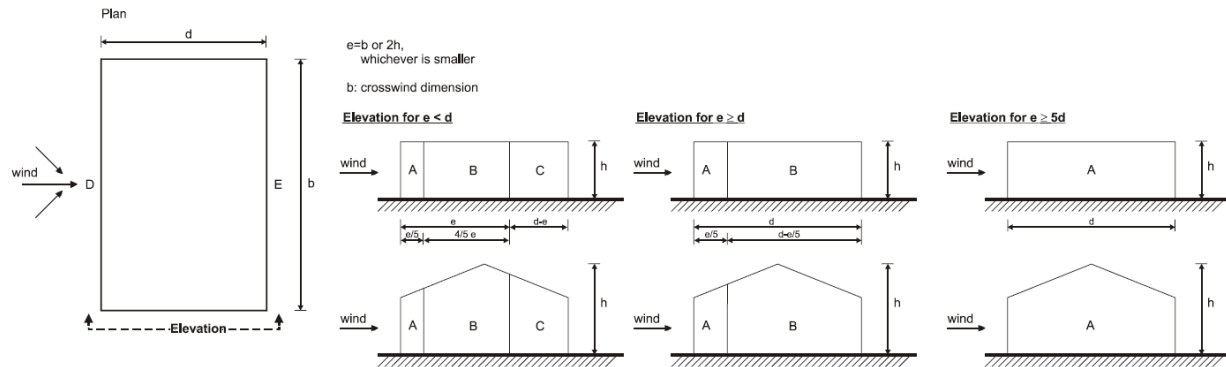


Figure 8-6 Key for vertical walls (Eurocode 1)

Zone	A		B		C		D		E	
	$C_{pe,10}$	$C_{pe,1}$								
5	-1,2	-1,4	-0,8	-1,1	-0,5		+0,8	+1,0	-0,7	
≤ 1	-1,2	-1,4	-0,8	-1,1	-0,5		+0,8	+1,0	-0,5	

Table 8-2 External pressure coefficients for the Netherlands (Eurocode 1 - Dutch national annex)

Reference is made to Eurocode 1 for the external pressure coefficients of all kinds of roofs and domes.

Internal pressure does not only depend on the shape of the structure, but also on the number of openings and their location relative to the wind direction. For structures with a 'dominant face' the internal pressure should be taken as a fraction of the external pressure at the openings of the dominant face. The following two equations can be used for internal pressure coefficient for faces with less than 30% openings:

- When the area of the openings at the dominant face is twice the area of the openings in the remaining faces,

$$c_{pi} = 0,75 \cdot c_{pe}$$

- When the area of the openings at the dominant face is at least 3 times the area of the openings in the remaining faces,

$$c_{pi} = 0,90 \cdot c_{pe}$$

The internal pressure coefficient of open silos and chimneys is  $c_{pi} = -0,60$  and of vented tanks with small openings it should be based on  $c_{pi} = -0,40$ . In these cases the reference height  $z_i$  is equal to the height of the structure.

For free-standing walls and parapets, the values of the *resulting* pressure coefficients  $c_{p,net}$  depend on the solidity ratio  $\phi$ . For solid walls,  $\phi = 1$ , and for walls which are 80% solid (i.e. have 20 % openings)  $\phi = 0,8$ . The pressure coefficients  $c_{p,net}$  mentioned in Table 8-3 should be used for the zones indicated in Figure 8-7. For porous walls and fences with a solidity ratio of less than 0,8 reference is made to Eurocode 1.

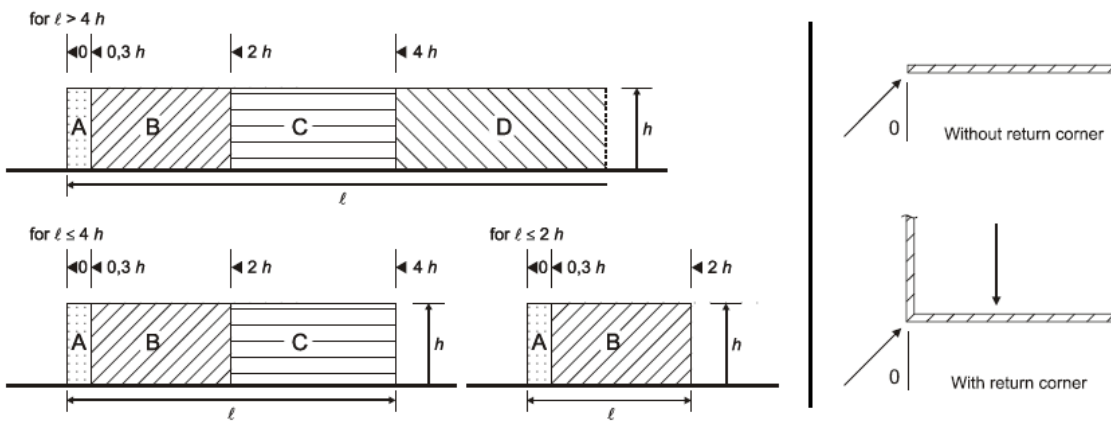


Figure 8-7 Key to zones of free-standing walls and parapets (Eurocode 1)

Solidity	Zone		A	B	C	D
$\phi = 1$	Without return corners	$l/h \leq 3$	2,3	1,4	1,2	1,2
		$l/h = 5$	2,9	1,8	1,4	1,2
		$l/h \geq 10$	3,4	2,1	1,7	1,2
	with return corners of length $\geq h^a$		2,1	1,8	1,4	1,2
$\phi = 0,8$			1,2	1,2	1,2	1,2

<sup>a</sup> Linear interpolation may be used for return corner lengths between 0,0 and  $h$

Table 8-3 Recommended pressure coefficients  $c_{p,net}$  for free-standing walls and parapets (Eurocode 1)

For details and specific regulations per country, reference is made to Eurocode 1, part 1-4 and the national annexes to this standard.

### 8.2.2 Wind forces on whole structures

For the determination of wind forces on whole structures or structural components, the peak velocity pressure should be multiplied with the area of the wall and several coefficients:

$$F_w = c_s c_d \cdot c_f \cdot q_p(z_e) \cdot A_{ref}$$

where:  $F_w$  [kN] = wind force on a structure or structural component  
 $c_s$  [-] = coefficient that takes into account the effect on wind actions from the non-simultaneous occurrence of peak wind pressures on the surface  
 $c_d$  [-] = coefficient for the effect of vibrations of the structure due to turbulence  
 $c_f$  [-] = force coefficient  
 $q_p(z_e)$  [kN/m<sup>2</sup>] = peak velocity pressure at reference height  $z_e$  (Table 8-1)  
 $A_{ref}$  [m<sup>2</sup>] = reference area of the surface

An alternative calculation method uses the wind pressures as calculated in the previous section:

- For external forces:

$$F_{w,e} = c_s c_d \cdot \sum_{surfaces} w_e \cdot A_{ref}$$

- For internal forces:

$$F_{w,i} = \sum_{surfaces} w_i \cdot A_{ref}$$

- For friction forces (on external surfaces  $A_{fr}$  parallel to the wind direction):

$$F_{fr} = c_{fr} \cdot q_p(z_e) \cdot A_{fr}$$

where  $c_{fr}$  [-] = friction coefficient according to Table 8-4.

Surface	Friction coefficient $c_{fr}$
Smooth (i.e. steel, smooth concrete)	0,01
Rough (i.e. rough concrete, tar-boards)	0,02
very rough (i.e. ripples, ribs, folds)	0,04

Table 8-4 Wind friction coefficients  $c_{fr}$

The force coefficient  $c_f$  of structural elements of rectangular section with the wind blowing normally to a face is determined by:

$$c_f = \psi_r \cdot \psi_\lambda \cdot c_{f,0}$$

where:  $\psi_r$  [-] = reduction factor for square sections with rounded corners.  $\psi_r$  depends on the Reynolds number and has a minimum value of 0,5.  
 For sharp edges  $\psi_r \approx 1,00$

$\psi_\lambda$  [-] = end-effect factor for elements with free-end flow.  
 $\psi_\lambda$  depends on the effective slenderness  $\lambda$  and the solidity ratio  $\phi$  of the structure.  
 The effective slenderness  $\lambda$  of polygonal, rectangular and sharp edged sections of structures is:

- for  $\ell \geq 50$  m,  $\lambda = 1,4 \cdot \ell/b$  or  $\lambda = 70$ , whichever is smaller
- for  $\ell < 15$  m,  $\lambda = 2,0 \cdot \ell/b$  or  $\lambda = 70$ , whichever is smaller
- for  $15 \text{ m} \leq \ell < 50$  m: linear interpolation should be used

The solidity ratio  $\varphi$  is the ratio between the net area (= the area excluding openings) and the overall envelope area  $A_c = l \cdot b$ . For closed structures,  $\varphi = 1,0$ . The end-effect factor can be determined when  $\lambda$  and  $\varphi$  are known with help of Figure 8-13.

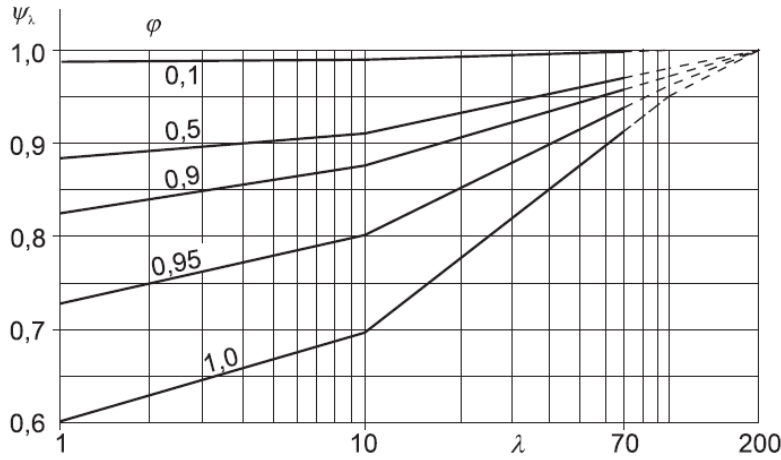


Figure 8-8 End-effect factor as a function of the effective slenderness (Eurocode 1)

$c_{f,0}$  [-] = force coefficient of rectangular sections with sharp corners and without free-end flow as given by Figure 8-9.

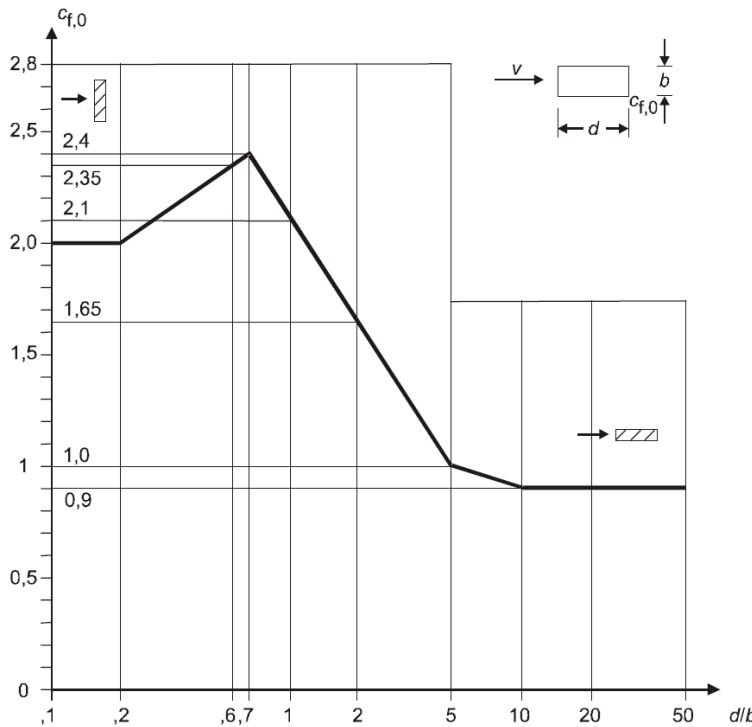


Figure 8-9 Force coefficient for rectangular sections with sharp corners and without free end flow

The coefficients  $c_s$  and  $c_d$  can be combined into one structural factor  $c_s c_d$ . For buildings with a height less than 15 m the value of  $c_s c_d$  may be taken as 1. For (rectangular) civil engineering works (other than bridges) the structural factor should be calculated according to:

$$c_s c_d = \frac{1 + 2 \cdot k_p \cdot I_v \cdot \sqrt{B^2 + R^2}}{1 + 7 \cdot I_v(z_s)}$$

where:  $k_p$  [-] = peak factor defined as the ratio of the maximum value of the fluctuating part of the response to its standard deviation:

$$k_p = \sqrt{2 \cdot \ln(\nu \cdot T)} + \frac{0,6}{\sqrt{2 \cdot \ln(\nu \cdot T)}} \text{ with a minimum of } k_p = 3,0$$

$T$  [s] = averaging time for the mean wind velocity ( $T = 600$  s)  
 $\nu$  [Hz] = up-crossing frequency as given in:

$$\nu = n_{1,x} \cdot \sqrt{\frac{R^2}{B^2 + R^2}} \text{ and } \nu \geq 0,8$$

$n_{1,x}$  [Hz] = natural frequency of the structure. The limit of  $\nu = 0,08$  Hz corresponds to a peak factor of 3,0.

$I_v$  [-] = turbulence intensity = the standard deviation of the turbulence  $\sigma_v$  divided by the mean wind velocity  $v_m(z)$ :

$$I_v(z) = \frac{\sigma_v}{v_m(z)} = \frac{k_f}{c_o(z) \cdot \ln(z/z_0)} \text{ for } z_{\min} \leq z \leq z_{\max}$$

$$I_v(z) = I_v(z_{\min}) \text{ for } z < z_{\min}$$

$k_f$  [-] = turbulence factor. The recommended value for  $k_f$  is 1,0.

$c_o$  [-] = orography factor. Where orography (e.g. hills, cliffs etc.) increases wind velocities by more than 5% the effects should be taken into account using the orography factor  $c_o$ . Otherwise  $c_o = 1,0$ .

$z_0$  [m] = roughness length as given in Table 8-5

$z_{\min}$  [m] = is the minimum height defined in Table 8-5.

$z_{\max}$  [m] = is to be taken as 200 m

Terrain category		$z_0$ m	$z_{\min}$ m
0	Sea or coastal area exposed to the open sea	0,003	1
I	Lakes or flat and horizontal area with negligible vegetation and without obstacles	0,01	1
II	Area with low vegetation such as grass and isolated obstacles (trees, buildings) with separations of at least 20 obstacle heights	0,05	2
III	Area with regular cover of vegetation or buildings or with isolated obstacles with separations of maximum 20 obstacle heights (such as villages, suburban terrain, permanent forest)	0,3	5
IV	Area in which at least 15 % of the surface is covered with buildings and their average height exceeds 15 m	1,0	10

Table 8-5 Roughness length  $z_0$  and minimum height  $z_{\min}$  (Eurocode 1)

$B^2$  [-] = background factor, allowing for the lack of full correlation of the pressure on the structure surface:

$$B^2 = \frac{1}{1 + 0,9 \cdot \left( \frac{b+h}{L(z_s)} \right)^{0,63}}$$

$L(z_s)$  [m] = turbulent length scale

It is on the safe side to use  $B^2 = 1,0$ .

$R^2$  [-] = resonance response factor, allowing for turbulence in resonance with the vibration mode:

$$R^2 = \frac{\pi^2}{2 \cdot \delta} \cdot S_L(z_s, n_{1,x}) \cdot R_h(\eta_h) \cdot R_b(\eta_b)$$

$\delta$  [-] = total logarithmic decrement of damping:

$$\delta = \delta_s + \delta_a + \delta_d$$

$\delta_s$  = logarithmic decrement of structural damping, for some structural types indicated in Figure 8-10, otherwise see Eurocode 1, Annex F.5

Structural type	structural damping, $\delta_s$
reinforced concrete buildings	0,10
steel buildings	0,05
mixed structures concrete + steel	0,08

Figure 8-10 logarithmic decrement of damping (Eurocode 1)

$\delta_a$  = logarithmic decrement of aerodynamic damping for the fundamental mode. If the modal deflections are constant over each height  $z$ , which is mostly the case,  $\delta_a$  may be determined with:

$$\delta_a = \frac{c_f \cdot \rho \cdot b \cdot v_m(z_s)}{2 \cdot n_1 \cdot m_e}$$

$n_1$  [Hz] = fundamental flexural frequency of the structure  
 $m_e$  [kg] = equivalent mass per unit length  
 $\rho$  [kg/m<sup>3</sup>] = air density ( $\approx 1,25$  kg/m<sup>3</sup>)

$\delta_d$  = logarithmic decrement of damping due to special devices (like tuned mass dampers and sloshing tanks etc.). If these special dissipative devices are added to the structure,  $\delta_d$  should be calculated by suitable theoretical or experimental techniques.

$S_L$  [m] = is the non-dimensional power spectral density function:

$$L(z) = L_t \cdot \left(\frac{z}{z_t}\right)^\alpha \quad \text{for } z \geq z_{min}$$

$$L(z) = L(z_{min}) \quad \text{for } z < z_{min}$$

$z_t$  [m] = reference height = 200m

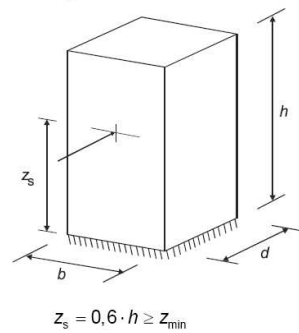
$z_{min}$  [m] = minimum height (Table 8-5)

$\alpha = 0,69 + 0,05 \cdot \ln(z_0)$ , where  $z_0$  = roughness length (Table 8-5)

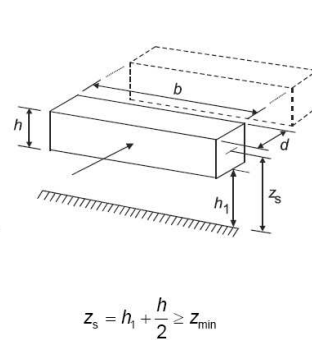
$L_t$  [m] = reference length scale = 300 m

$z_s$  [m] = reference height for determining the structural factor, see Figure 8-11

a) vertical structures such as buildings etc.



b) parallel oscillator, i.e. horizontal structures such as beams etc.



c) pointlike structures such as signboards etc.

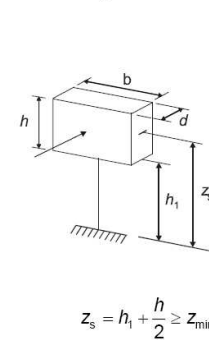


Figure 8-11 General shapes of structures and the reference height  $z_s$

For a preliminary design one could consider to use  $R^2 = 1$ , which could result in a over-estimation of the structural factor  $c_s c_d$  of up to 15% (the approved minimum value of  $c_s c_d$  is 0,85).

### 8.2.3 Abroad

If the wind situation (and particularly the wind velocity) is not comparable to the coast or inland areas of the Netherlands, the dynamic pressure can be determined with the following formula:

$$q = \frac{1}{2} \rho u^2 C_D$$

where:  $\rho$  [kg/m<sup>3</sup>] = air density:  $\rho = 1,25$  kg/m<sup>3</sup>  
 $C_D$  [-] = drag coefficient, dependent on Reynolds value:  $C_D \approx 0,7$

For a more accurate approximation of the drag coefficient  $C_D$ , see Chapter 12. This  $C_D$  value depends on a number of different factors, including the shape and size of the structure or object. The factors are dealt with in larger detail in NEN 6702.

The average velocity is dependent on the altitude, the location and the measurement time according to the formula:

$$u = \beta_{\Delta T} \left( \frac{h}{10 \text{ m}} \right)^\alpha u_{1 \text{ h}, 10 \text{ m}}$$

where:  $\beta_{\Delta T}$  [-] = correction factor for the duration of the gust  
 $h$  [m] = altitude of measurement  
 $\alpha$  [-] = parameter for roughness of terrain:  $\alpha = 0,13$  (coast),  $\alpha = 0,19$  (inland)  
 $u_{1 \text{ h}, 10 \text{ m}}$  [m/s] = average wind velocity at an altitude of 10 m, during one hour

The wind velocity is given as an average for one hour. A gust of 3 seconds can reach a higher average velocity. The difference is indicated by the parameter  $\beta_{\Delta T}$  (see following table).

The average wind velocity  $u_{1 \text{ h}, 10 \text{ m}}$  is dependent on both the location and the probability of exceedance  $T_{\text{year}}$ . According to the TGB (the old Dutch standard), the following values are applicable in the Netherlands.

	$\beta_{\Delta T}$	$T_{\text{year}} = 1 \times \text{per } 5$ years	$T_{\text{year}} = 1 \times \text{per } 75$ years
Land	1,75	$u_{1 \text{ h}, 10 \text{ m}} = 20,5$ m/s	$u_{1 \text{ h}, 10 \text{ m}} = 25,0$ m/s
Coast	1,40	$u_{1 \text{ h}, 10 \text{ m}} = 26,0$ m/s	$u_{1 \text{ h}, 10 \text{ m}} = 32,0$ m/s

Table 8-6 Wind velocities according to TGB

For other exceedance frequencies  $u_{1 \text{ h}, 10 \text{ m}}$  may be linearly interpolated and extrapolated over  $\log(T_{\text{year}})$ . The given wind velocities apply to the Netherlands. These values must be measured again for other areas.

#### Notes

- For slender structures it is necessary to consider the load in transverse direction ( $F_L = \frac{1}{2} \rho u^2 C_L$ ).
  - For slender structures it is necessary to test the structure for vibrations caused by gusts.
- (For this see the TGB 1972, or: Wind load, a commentary on the TGB ("Windbelasting, toelichting op de TGB" 1972).

### 8.3 Wind load on vessels

The Oil Companies International Marine Forum (OCIMF) issued a report with coefficients and procedures for computing wind and current loads on oil tankers. According to the second edition of this report, the resultant wind force on a moored tanker (a very large crude carrier, i.e.  $150\,000 < \text{DWT} < 500\,000$ ) can be calculated using the following equations.

$$F_{Xw} = \frac{1}{2} C_{Xw} \rho_w v_{w,10}^2 A_T \quad \text{and} \quad F_{Yw} = \frac{1}{2} C_{Yw} \rho_w v_{w,10}^2 A_L$$

in which:

$F_{Xw}$ [N]	=	longitudinal wind force (surge wind force)
$F_{Yw}$ [N]	=	lateral wind force (sway wind force)
$C_{Xw}$ [-]	=	longitudinal wind force coefficient, see Figure 8-12
$C_{Yw}$ [-]	=	lateral wind force coefficient, see Figure 8-13
$\rho_w$ $\text{kg/m}^3$	=	density of air ( $\approx 1,28 \text{ kg/m}^3$ )
$v_{w,10}$ [m/s]	=	wind velocity at 10 m elevation
$A_T$ $\text{m}^2$	=	transverse (head-on) wind area
$A_L$ $\text{m}^2$	=	longitudinal (broadside) wind area

(Longitudinal and transverse directions are with respect to the vessel length axis)

The wind force coefficients depend on the wind angle of attack, the extent of loading by cargo (fully loaded or only ballasted) and the bow configuration.

If the wind velocity is known at a different elevation than 10 metres above water surface, the following equation can be used for conversion:

$$v_{w,10} = u_w \left( \frac{10}{h} \right)^{1/7}$$

where  $u_w$  [m] = wind velocity at elevation  $h$  above ground/water surface.

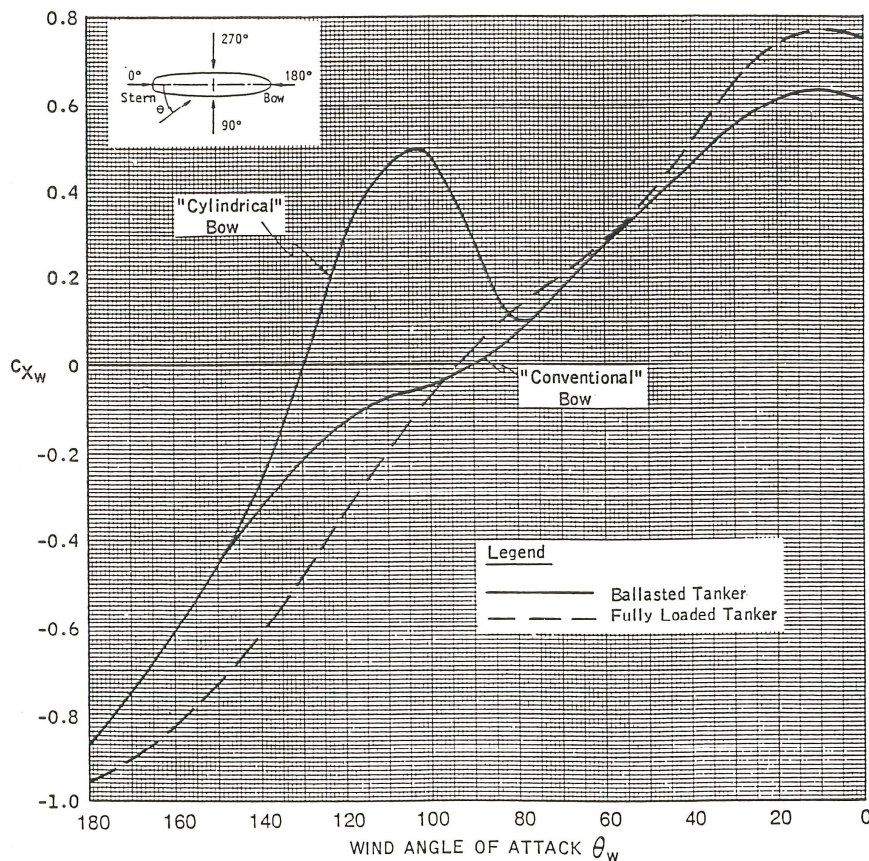


Figure 8-12 longitudinal wind force coefficient

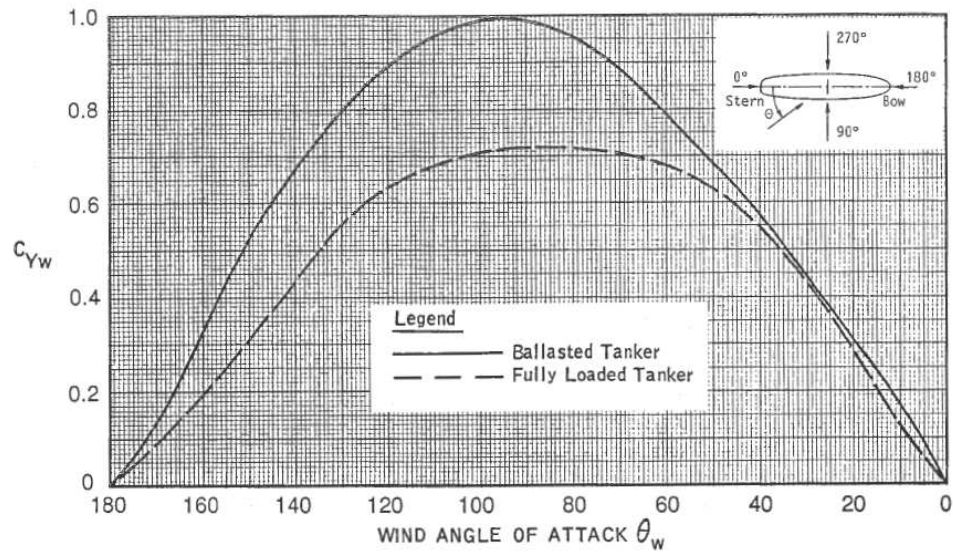


Figure 8-13 lateral wind force coefficient

## 8.4 Literature

- Nederlands Normalisatie-instituut: NEN 6702 "Technische grondslagen voor bouwconstructies", Belastingen en vervormingen, (TGB 1990), Delft 1990.
- Eurocode 1: Actions on structures - Part 1-4: General actions - Wind actions (NEN-EN 1991-1-4)
- Oil Companies International Marine Forum: Prediction of wind and current loads on VLCC's, second edition. Witherby & Co Ltd., London, 1994.

## 9. Hydrostatic pressure

### 9.1 Theory

Shear stresses only occur in fluids if there are velocity differences between the fluid particles. In a fluid at rest there is no shear stress and the pressures in one point are equal in all directions. This characteristic is known as Pascal's law. For flowing fluids, Pascal's law gives rather good approximations.

The hydrostatic (water) pressure in any given point under water is a function of the pressure head and the density of the water:

$$p = \rho_w g h$$

where:  $p$  [Pa] = water pressure  
 $h$  [m] = pressure head  
 $g$  [m/s<sup>2</sup>] = acceleration due to gravity  
 $\rho_w$  [kg/m<sup>3</sup>] = density of water ( $\rho_{w,salt} = 1025$ ;  $\rho_{w,fresh} = 1000$ )

In water at rest or in a uniform flow (no acceleration or deceleration) in an open waterway, the pressure head is equal to the water depth at the point considered. Largely varying flow velocities in open waterways correspond to largely curved flow lines. In such cases the pressure head is not equal to the water depth. In Chapters 11 and 14 this is treated in larger detail.

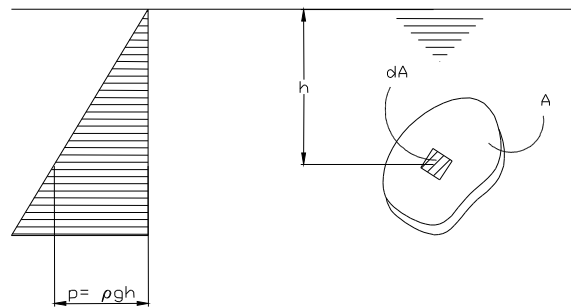


Figure 9-1 Water pressure

The force on a plain under water is calculated by integrating the pressure over the plain:

$$F = \int_A p \, dA$$

in which:  $F$  [N] = the force perpendicular to the plane  
 $dA$  [m<sup>2</sup>] = a small part of the area (see Figure 9-1)  
 $A$  [m<sup>2</sup>] = the total surface area

If the plane on which the force is working is straight, the force is equal to the product of the area of the plane and the water pressure in the mass centre of the plane. The components of the force in the x, y and z directions can be determined with:

$$F_x = \iint_A p \, dy \, dz \quad F_y = \iint_A p \, dx \, dz \quad F_z = \iint_A p \, dx \, dy$$

The co-ordinates of the line of action of the force in the x direction can be found with:

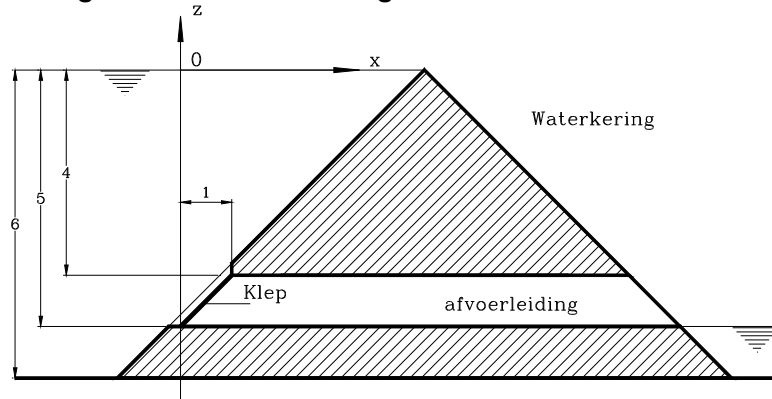
$$y_x = \frac{\iint_A p y \, dy \, dz}{F_x} \quad \text{and} \quad z_x = \frac{\iint_A p z \, dy \, dz}{F_x}$$

The lines of action of the forces  $F_y$  and  $F_z$  can be found in a similar manner.

The previous equations correspond exactly to the equations for the volumes and mass centres of the pressure diagrams. This makes it possible to determine the forces and their points of application for known shapes using relatively simple standard formulas.

## 9.2 Water pressure on gates

### Example: Force on a gate in a water-retaining structure



A 6 m high wall is part of a water-retaining structure (see figure). The wall has an angle of  $45^\circ$  with the vertical plane and retains up to 6 m water. The wall contains a rectangular gate with a width of 1 m. Calculate the horizontal and vertical forces acting on the gate and the coordinates of the point of action.

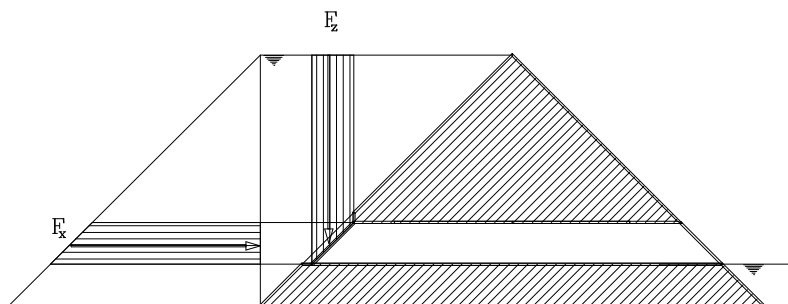
Solution:

The pressure is constant in  $y$ -direction (perpendicular to the paper). The water pressure as a function of  $x$  and  $z$  is:

$$p(x) = (5-x)\rho g \quad \text{and} \quad p(z) = -z\rho g$$

$$\text{The horizontal force on the gate is: } F_x = \int_{-5}^{-4} -z\rho g dz = \frac{9}{2}\rho g = 45 \cdot 10^3 \text{ N}$$

$$\text{The vertical force on the gate is: } F_z = \int_0^1 (5-x)\rho g dx = \frac{9}{2}\rho g = 45 \cdot 10^3 \text{ N}$$



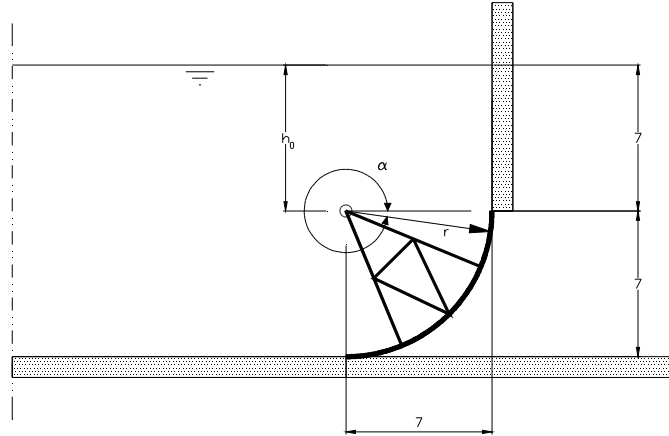
De coordinates of the point of action are:

$$x_F = \frac{\int_0^1 x(5-x)\rho g dx}{\int_0^1 (5-x)\rho g dx} = \frac{13}{27} = 0,48 \text{ m} \quad \text{and} \quad z_F = \frac{\int_{-5}^{-4} z^2 \rho g dx}{\int_{-5}^{-4} z \rho g dx} = \frac{-122}{27} = -4,52 \text{ m}$$

In case of a circular gate, the principle is the same. For practical reasons, however, it could be more convenient to use a polar system of coordinates. See the following example.

**Example: Force on a closed radial gate (horizontal axis)**

A weir with an underflow type outflow contains a radial gate that opens in upward direction. The gate has a radius of 7 metres and a width of 10 metres. The water height upstream of the weir is 14 metres.



Calculate the load on the radial gate in closed position. In this case there is no water behind the weir.

**Solution**

Because of the circular shape of the cross section of the radial gate, it is convenient to choose a polar system of coordinates in the x-z plane with centre in the axis of the circle. In that case,  $dA = dy r d\alpha$  is applicable.

The pressure on the gate can be expressed as a function of the angle with the positive x-axis. The function is:

$$p = (h_0 - r \sin(\alpha)) \rho g$$

where:  $h_0$  [m] = pressure height in the centre  
 $r$  [m] = the radius of the gate

The contribution of a strip over the width of the gate and a height  $r d\alpha$  to the exerted force on the gate is:

$$dF_x = (h_0 - r \sin(\alpha)) \rho g \cos(\alpha) b r d\alpha$$

$$dF_z = (h_0 - r \sin(\alpha)) \rho g \sin(\alpha) b r d\alpha$$

The load on the gate can be found by integrating these equations:

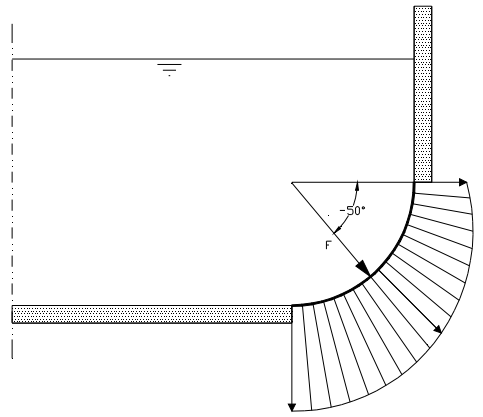
$$F_x = \int_{-\frac{\pi}{2}}^0 (h_0 - r \sin(\alpha)) \rho g \cos(\alpha) b r d\alpha = \rho g b r \left( h_0 + \frac{r}{2} \right) = 7,5 \cdot 10^6 \text{ N}$$

$$F_z = \int_{-\frac{\pi}{2}}^0 (h_0 - r \sin(\alpha)) \rho g \sin(\alpha) b r d\alpha = \rho g b r \left( -h_0 - \frac{\pi r}{4} \right) = -8,748 \cdot 10^6 \text{ N}$$

The direction of the force is:

$$\alpha_F = \arctan\left(\frac{F_z}{F_x}\right) = -50^\circ$$

The load and the resulting force are indicated in the following figure.



In most cases, however, it is easier to consider the vertical and horizontal component of the water pressure on an object separately. The resulting force in x-direction is equal to the summarized horizontal pressure on a projection of the gate to a vertical plane. The total force in z-direction is equal to the weight of the water volume above the gate. This is indicated in Figure 9-2.

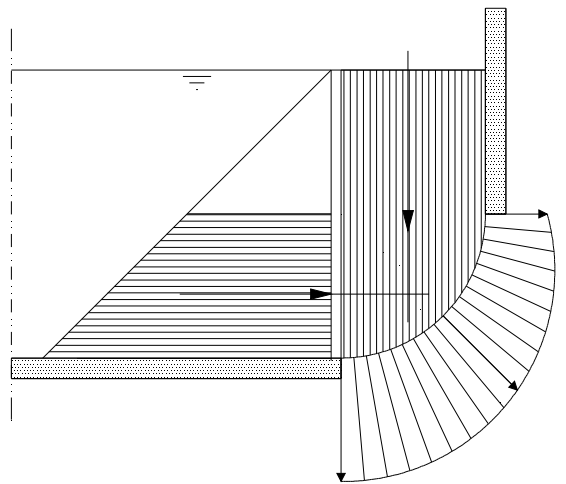


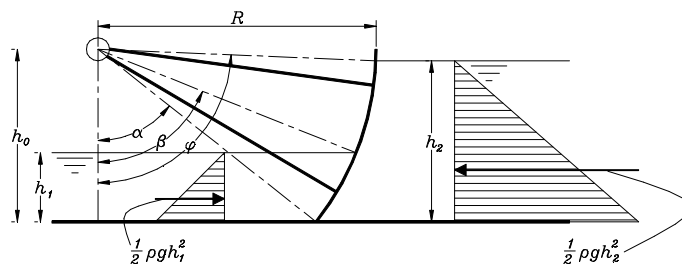
Figure 9-2 Simple determination of the forces

**Example: Calculation of load**

The resultant of the water pressure goes through the centre of the circle. With this one point on the line of action of the reaction force is known, after all "action = reaction". One can determine the direction and size of the reaction force in the hinge by calculating the resulting horizontal and vertical water pressures on the gate. The horizontal force in a hinge as a result of the water pressure can be determined simply using:

$$H = \frac{1}{2} \rho g (h_1^2 - h_2^2) \frac{L}{2}$$

$$= \frac{1}{4} \rho g L (h_1^2 - h_2^2)$$



Theoretically, the determination of the vertical load on the gate is not difficult, but due to the shape of the gate it is less simple. The total vertical load due to the water equals the lift force minus the weight of the water on the gate. The following figure shows an example of the weight of the water on the gate. The weight per metre of width equals  $\rho g A$ . The surface area  $A$  can be found with:  $A = A_1 - A_2 - A_3$

in which:

$$A_1 = \frac{\beta}{2} R^2 - \frac{1}{2} R \sin \beta R \cos \beta$$

$$= \frac{1}{2} (\beta - \sin \beta \cos \beta) R^2$$

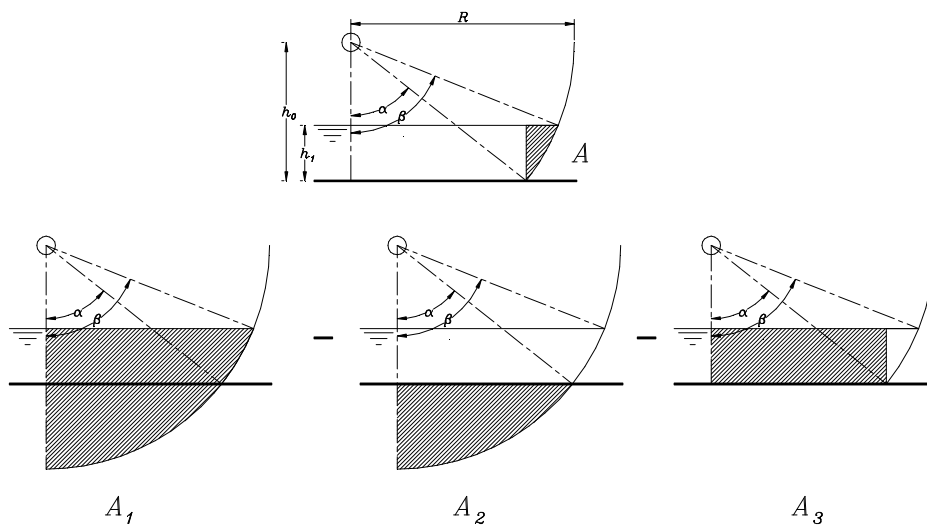
$$A_2 = \frac{\alpha}{2} R^2 - \frac{1}{2} R \sin \alpha R \cos \alpha$$

$$= \frac{1}{2} (\alpha - \sin \alpha \cos \alpha) R^2$$

$$A_3 = h_1 R \sin \alpha$$

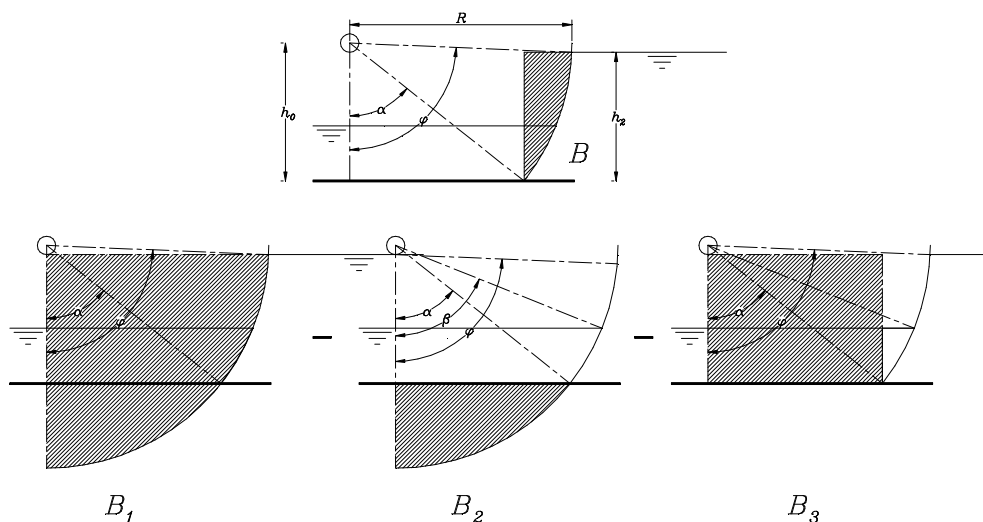
so:  $A = \frac{1}{2} (\beta - \alpha - \sin \beta \cos \beta + \sin \alpha \cos \alpha) R^2 - h_1 R \sin \alpha$

in which:  $\alpha = \arccos\left(\frac{h_0}{R}\right)$  and  $\beta = \arccos\left(\frac{h_0 - h_1}{R}\right)$



The upward force per metre of width can be found in exactly the same way using  $\rho g B$  (see the figure above), with:  
 $B = \frac{1}{2} (\varphi - \alpha - \sin \varphi \cos \varphi + \sin \alpha \cos \alpha) R^2 - h_1 R \sin \alpha$

in which:  $\alpha = \arccos\left(\frac{h_0}{R}\right)$  and  $\varphi = \arccos\left(\frac{h_0 - h_2}{R}\right)$

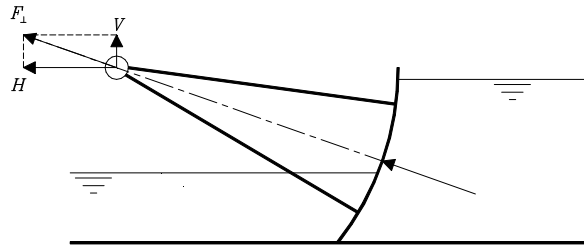


The vertical load on one hinge is:

$$V = \rho g(B - A) \frac{L}{2}$$

$$= \frac{1}{2} \rho g L \left( \frac{1}{2} (\varphi - \beta - \sin \varphi \cos \varphi + \sin \beta \cos \beta) R^2 - (h_2 - h_1) R \sin \alpha \right)$$

The resulting load perpendicular to the hinge is:  $F_{\perp} = \sqrt{H^2 + V^2}$



In the case of a radial gate with a vertical axis, the gate is curved in the horizontal plane to an arc with a centre that coincides with the position of the hinge. Thus the resultant of the water pressure load goes precisely through the hinge in the horizontal plane. The direction of the resultant depends on the lengthwise profile of the gate. In the vertical plane, the direction and the position of the resultant of the water pressure depends on the shape of the gate in the vertical cross section. Figure 9-3 shows a number of possible cross sections and the forces on the gate per metre. The position of the seal with the bottom is an important detail which determines the size of the upward force.

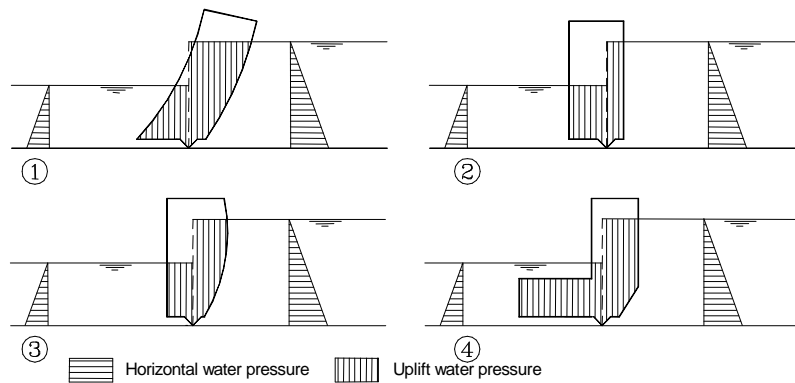


Figure 9-3 Loads dependent on the shape of the gate

For more information about the design of gates, see Chapter 49 of this manual (part IV).

## 10. Water, flow, water levels

### 10.1 River: discharge and water level

The discharge and water levels that are of importance for the design of a structure in or beside a river depend on the structure's function. For instance, for a water defence the maximum water level and thus the maximum discharge are important, whilst the sill of an inlet of an irrigation system will be designed for a minimal water level, thus a minimal river discharge.

The minimum and maximum discharges are random variables and have an extreme value distribution. For the statistical analysis of extreme maximum and minimum discharges, the series of observation data is usually too short to be able to decide which theoretical probability distribution to use. In practice the available observation material is sorted out and compared with a couple of theoretical probability distributions.

In the statistical analysis of the discharges, caution is required concerning the size of the series of observations. The quality of the statistical analysis does not always improve with the inclusion of more observations. In the course of time, changes of the river and the catchment area can render old observations useless. Furthermore, one must question the physical possibility of an extreme discharge. If a very high discharge causes flooding upstream of the point that the analysis is based on, the discharge will be more or less restricted.

In a stationary flow, the discharge can be described with an equilibrium equation, such as Chézy's and Manning's equations (see next section), in which the friction is in balance with the slope of the energy line. In the case of a discharge wave, such a simple equation does not suffice. Both inertia and retention are then of importance. The flow must be modelled as a so-called long wave. For equations for long waves, one is referred to the lecture notes "Open Channel Flow" (in Dutch: "Stroming in open waterlopen"), course code CTB3350 (Battjes and Labeur, 2014).

The propagation of a given discharge wave is usually calculated using a computer model. Such a computer model can be seen as a transformation of the discharge to the water level. By carrying out a large number of calculations with different discharges, for which the probability distribution is more or less known, the probability distribution of the water levels can be estimated. However, in practice, the water level is usually calculated for a chosen discharge with a certain frequency. This water level is then the design water level.

### 10.2 Flow in open water ways

Water flows if there is a difference of potential between two points. The flow velocity is dependent on the extent of the difference in potential and the resistance encountered by the water. Friction and sudden changes of the flow profile cause the resistance encountered by the flowing water.

#### Friction

Friction between water particles causes a logarithmical flow velocity change over the water height. The average velocity can be calculated using Chézy's or Manning's equation.

Chézy's equation is:

$$u_{gem} = C\sqrt{Ri} \quad \text{with } C = 5,75 \cdot \sqrt{g} \cdot \log \frac{12R}{k}$$

in which:	$u$	[m/s]	=	flow velocity
	$C$	[m <sup>1/2</sup> /s]	=	Chézy's coefficient
	$R$	[m]	=	hydraulic radius of the flow profile $\approx \frac{bh}{b+2h} \approx h$ (for: $b \gg h$ )
	$h$	[m]	=	depth of flow, i.e. water level
	$b$	[m]	=	flow width
	$i$	[-]	=	slope of the energy line in uniform flow this equals the slope of the river bed
	$k$	[m]	=	roughness of the edges of the flow profile

To find the relation between the discharge  $Q$  and the water depth  $h$  one generally uses:

$$h^{3/2} = \frac{Q}{C b i^{1/2}}$$

**Note.** For beds with sediment transport:  $k \approx 0,05 - 0,10$  m. On other cases  $k = 2 \cdot D_{90}$  can be used. ( $D_{90}$  is the diameter of the sieve through which 90 percent of the grains pass).

The disadvantage of the approximation of the flow velocity according to Chézy is that  $C$  isn't a constant. Therefore, internationally, Manning's equation is given preference.

**Manning's** equation is:

$$u_{gem} = \frac{1}{n} R^{2/3} \sqrt{i}$$

in which:  $n$  [-] = Manning's coefficient, dependent on the roughness of the riverbed [-].

This coefficient can easily be measured by determining the discharge  $Q$ , flow section  $A$ , slope  $i$  and water depth  $h$ . Henderson (1966) found the values given below:

Glass, smooth metal	$n = 0,010$
concrete made with wooden formwork (untreated)	$n = 0,014$
smooth earth, bare (no vegetation)	$n = 0,020$
river: clear and straight	$n = 0,025 - 0,030$
river: meandering and with shallows/ depths	$n = 0,033 - 0,040$
river: overgrown, meandering	$n = 0,075 - 0,150$

Table 10-1 Manning's coefficient (in  $m^{-1/3} s$ )

Chézy can be converted to Manning and vice versa, because:

$$C \sqrt{Ri} = \frac{1}{n} R^{2/3} \sqrt{i} \Rightarrow C = \frac{1}{n} R^{1/6}$$

Note that with increasing roughness of the bed,  $n$ , Chézy's coefficient decreases. Chézy's coefficient is therefore really a smoothness coefficient. By approximating, among other things, the  $\log$ -term in the Chézy equation, the riverbed roughness parameters  $k$  and  $n$  can be converted into each other:

$$n^{-1} \approx 8,3 \cdot \sqrt{g} \cdot k^{-1/6}$$

### **Change of flow profile**

The energy loss due to sudden changes of the flow profile can be estimated using the balance of impulse. In practice, however, local losses due to flow profile changes are taken in to account by changing Chézy's (or Manning's) coefficient.

## **10.3 Flow through and along structures**

Civil engineering works such as weirs, piers and sills, can influence the water level in a river. The extent of the influence is described by the discharge relationship of the structure.

Two possible situations for the discharge are distinguished for civil engineering works, namely:

- submerged flow: in this case the discharge depends on the difference in the total head in front of and behind the structure.
- free flow : in this case the discharge is purely dependent on the upstream total head (super-critical).

**Submerged flow**

Generally one can say the energy loss over a structure is:

$$\Delta H = \xi \frac{u^2}{2g}$$

in which:  $\xi$  [-] = loss coefficient  
 $u$  [m/s] = flow velocity at the structure

This can be also be written as:

$$u = \sqrt{\frac{2g\Delta H}{\xi}} \text{ [m/s]}$$

The relation between the discharge and the energy loss over the structure,  $Q$  [m<sup>3</sup>/s], is therefore:

$$Q = mA\sqrt{2g\Delta H}$$

in which:  $m$  [-] = discharge coefficient =  $\sqrt{\frac{1}{\xi}}$   
 $A$  [m<sup>2</sup>] = the smallest flow section at the work

The loss coefficient  $\xi$  can be determined experimentally. One can find tables on the standard method of doing this.

**Free flow**

In the case of free flow, the relationship between the discharge and water level is:

$$Q = mA\sqrt{2g(H_b - h_A)}$$

in which:  $H_b$  [m] = energy head upstream of the structure  
 $h_A$  [m] = pressure head in the smallest flow section

For flow and loads on walls, see Chapter 11 "Water, flow, wall".



$$F_u = \rho q(u_2 - u_1) \quad [\text{kN/m}]$$

The balance of forces is:  $F_1 - F_2 - F_s - F_u = 0$

From this the force on the flat sluice gate,  $F_s$ , can be determined.

To solve the given balance of impulse, the water levels and flow velocities must first be solved. This can be done using a combination of the rules for "Preservation of discharge (volume and mass)" and "Preservation of energy (Bernoulli)".

The following applies for the preservation of volume:  $Q = u \cdot A = \text{constant}$ .

For the preservation of energy:  $H = h + \frac{u^2}{2g} = \text{constant}$ .

In other words: the total head  $H$  equals the depth  $h$  plus the velocity head  $\frac{u^2}{2g}$ . The depth  $h$  can be divided further into a place dependent height  $z$  and a piezometric head  $\frac{p}{\rho g}$ .

Preservation of energy does not apply to places with turbulence or places with (large) wall friction losses (so  $H_1 = H_s \neq H_2$ ).

The situation is easiest to solve if the discharge  $q$  is known. In that case,  $u$  can be (iteratively) solved from:

$$u = \frac{q}{h} = \frac{q}{H - \frac{u^2}{2g}}$$

If there is a sharp-crested weir (*stuw*) somewhere in the canal (Figure 11-2), the discharge can be determined by applying Bernoulli's equation:

$$z_1 + \frac{u_1^2}{2g} + \frac{p_1}{\gamma} = z_2 + \frac{u_2^2}{2g} + \frac{p_2}{\gamma}$$

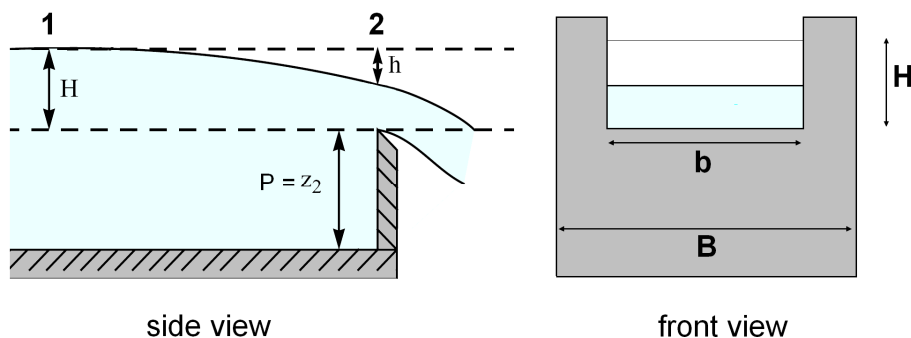


Figure 11-2 A sharp-crested weir in a canal

With help of Figure 11-2 it can be seen that Bernoulli's equation reduces to:

$$H + \frac{u_1^2}{2g} = (H - h) + \frac{u_2^2}{2g}, \text{ so } u_2 = \sqrt{2g \cdot \left( h + \frac{u_1^2}{2g} \right)}$$

where:  $u$  [m/s] = flow velocity  
 $g$  [m/s<sup>2</sup>] = gravitational acceleration  
 $h$  [m] = distance between the water surface above the weir and the still water surface  
 $H$  [m] = distance between the still water surface and of the weir crest (the 'head')

The theoretical discharge over the weir crest is:

$$Q_{theory} = \int_{z=0}^H (u_2 \cdot b) dz$$

where:  $b$  [m] = width of the notch  
 $z$  [m] = height above the weir crest

For a rectangular weir, the width is constant, so not a function of  $h$ . The theoretical discharge then is:

$$Q_{theory} = W \cdot \int_{z=0}^H \sqrt{2g \left( h + \frac{u_2^2}{2g} \right)} dz$$

By substituting for  $u_2$ , this can be formulated as:

$$Q_{theory} = \frac{2}{3} b \cdot \sqrt{2g} \cdot \left[ \left( H + \frac{u_1^2}{2g} \right)^{3/2} - \left( \frac{u_1^2}{2g} \right)^{3/2} \right]$$

If the upstream velocity head is negligible ( $H \gg (u_1/2g)$ ), this can be simplified to:

$$Q = \frac{2}{3} \cdot b \cdot \sqrt{2g} \cdot H^{3/2}$$

In a more general form, this equation is known as the Kindsvater-Carter rectangular weir equation (ISO, 1980):

$$Q = \frac{2}{3} \cdot (b + K_b) \cdot \sqrt{2g} \cdot (H + K_h)^{3/2} \cdot C_d$$

where:  $b + K_b$  [m] = effective width  
 $H + K_h$  [m] = effective head  
 $K_b$  [m] = coefficient to account for the viscosity (see Figure 11-3)  
 $K_h$  [m] = coefficient to account for the surface tension ( $K_h = 0,001$  m)  
 $C_d$  [-] = discharge coefficient (see Figure 11-4)

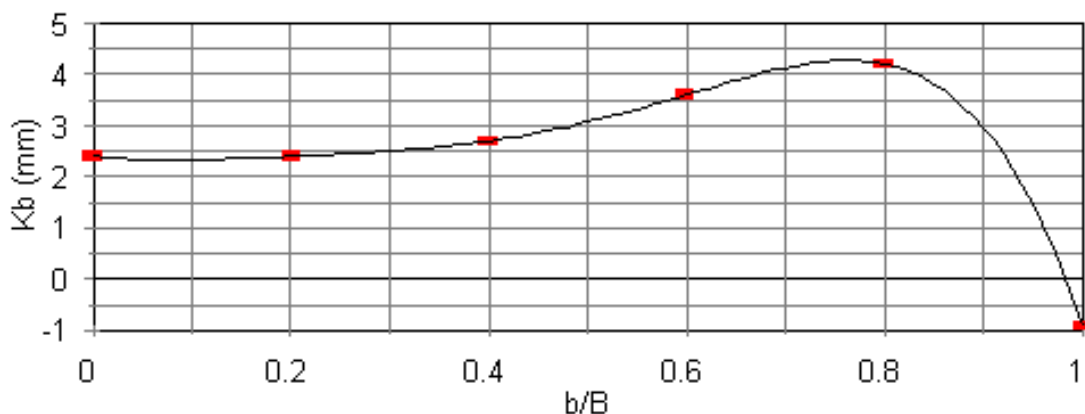


Figure 11-3  $K_b$  for a rectangular weir (LMNO Engineering)

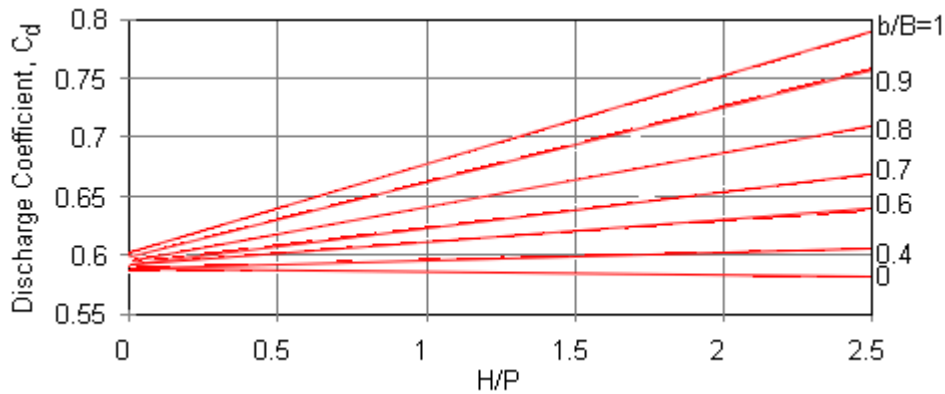


Figure 11-4 Rectangular weir discharge coefficient (ISO 1980)

For a triangular V-notch weir the width varies with the depth  $z$ , see Figure 11-5.

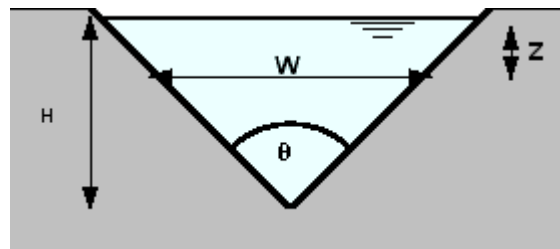


Figure 11-5 V-notch weir

The width can be described by:  $w = 2(H - z) \cdot \tan\left(\frac{\theta}{2}\right)$

The general equation for the theoretical discharge over the weir also applies to the V-notch weir:

$$Q = \int_{z=0}^H (u_2 \cdot w) dz$$

By substituting  $u_2$  and  $w$ , integrating and assuming that  $u_1 \ll H$ , the discharge over the V-notch can be described as:

$$Q = \frac{8}{15} \cdot \sqrt{2g} \cdot \tan\left(\frac{\theta}{2}\right) \cdot H^{5/2}$$

Also for V-notched weirs, losses occur due to the edges of the weir and contractions in the area of flow. These losses are accounted for by a discharge coefficient  $C_d$  [-]:

$$Q_{actual} = Q_{theory} \cdot C_d$$

The value of  $C_d$  for a specifically shaped weir can be found experimentally. From dimensional analysis and experiments, the *average* value for the discharge coefficient was found: for V-notch weirs:  $C_d = 0,60$  [-].

If the discharge is unknown, the entire flow pattern (also upstream and downstream) must be investigated to determine the discharge.

For a preliminary design, one can also use estimates for the eddy near a gate, such as:

$$\mu a \approx 0,7 \cdot a$$

$$h_s \approx 0,9 \cdot h_2$$

These values depend on the shape of the edge of the gate and cannot be calculated precisely. They should therefore be determined experimentally in a later stage of design.

It is good to realise that the largest static force usually originates at a closed gate. In that case the force is simply:

$$F_s = \frac{1}{2} \rho g (H_1^2 - H_2^2) = \frac{1}{2} \gamma_w (H_1^2 - H_2^2)$$

The flow under the gate will cause resonance of the gate (with tidal movements, two directions of flow are involved!). The determination of the size and frequencies of the resonance force is beyond the scope of this book.

### Example: The force on a flat open gate

#### Balance of impulse

A structure with a flat gate has been placed in a wide, open waterway with a rectangular flow section (see Figure 11-6). Supercritical flow occurs behind the gate. In the smallest flow section behind the gate, the depth of the water is  $\mu \cdot h = 0,62 \cdot 1,62 = 1,00$  m. The water in front of the weir rises to a total head of 5,05 m.

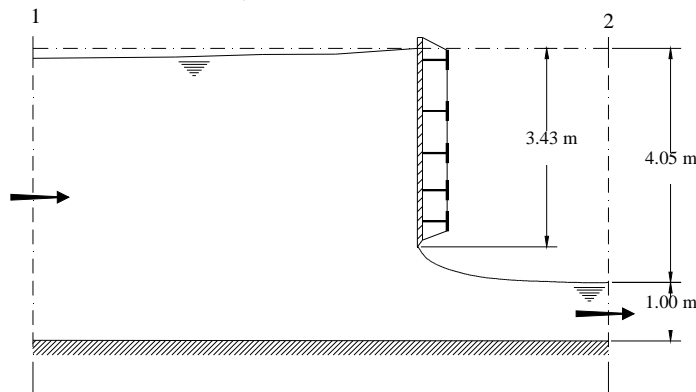


Figure 11-6 Gate in an open waterway

The task is to calculate the force on the flat gate, given that the flow lines in cross sections 1 and 2 are straight.

#### Solution

Because the flat gate is completely located in the acceleration zone, simple application of the balance of impulse is possible, once the flow velocities and water depth in cross section 1 have been determined using Bernoulli.

According to Bernoulli, the energy head = place dependent height + piezometric head + velocity head, or:

$$H = z + \frac{p}{\rho g} + \frac{u^2}{2g} \quad (\text{often: } z + \frac{p}{\rho g} = h)$$

Bernoulli in cross section 2:

$$H = h_2 + \frac{u_2^2}{2g} \Rightarrow u_2 = \sqrt{2g(H - h_2)} = \sqrt{2 \cdot 9,81 \cdot 4,05} = 8,91 \text{ m/s}$$

Continuity equation from 1 to 2:

$$u_1 h_1 = q = u_2 h_2 = 8,91 \text{ m}^2 / \text{s}$$

Bernoulli in cross section 1:

$$H = h_1 + \frac{u_1^2}{2g} \Rightarrow q + \frac{u_1^3}{2g} - H u_1 = 0 \Rightarrow u_1 = 1,83 \text{ m/s}$$

$$h_1 = \frac{q}{u_1} = 4,88 \text{ m}$$

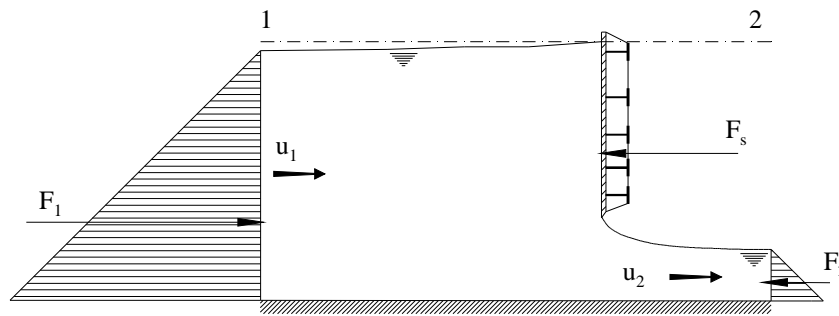


Figure 11-7 Balance of impulse

Because the flow lines in sections 1 and 2 are straight, there is a hydrostatic pressure distribution on the borders of balance area. The forces on the area are:

$$F_1 = \frac{1}{2} \rho g h_1^2 = 117 \text{ kN/m} \quad \text{and} \quad F_2 = \frac{1}{2} \rho g h_2^2 = 4,9 \text{ kN/m}$$

$F_s =$  to be determined using balance of impulse

$$\text{The balance equation: } F_1 - F_2 - F_s + \rho q (u_1 - u_2) = 0$$

From this one can derive the force on the flat gate:  $F_s = F_1 - F_2 + \rho q (u_1 - u_2) = 117 - 4,9 + 8,91 \cdot (1,83 - 8,91) = 49 \text{ kN/m}$

Note: One could simply use the hydrostatic pressure on the gates (underflow and overflow) for a first conservative estimation it is left to the reader to calculate the difference with the answer of the above example.

## 11.2 Potential flow and pressure distribution

The pressure distribution on a structure in the flow, and thus also on the point of application, cannot be determined using the balance of impulse. To do this, the potential flow theory may be used. However, one condition for the use of this theory is that the flow is free of rotations. This means the shear stresses are to be ignored. The potential flow theory will not be explained here, one is referred to the lecture notes "Open Channel Flow" (*Stroming in open waterlopen*), CTB3350 (Battjes & Labeur, 2014). An important property of a two-dimensional potential flow is that the flow lines and the equipotential lines are perpendicular to each other.

By drawing lines of equal potential at a distance  $\Delta\phi$  of each other and flow lines at a distance  $\Delta\psi$  of each other,  $\Delta\phi$  being equal to  $\Delta\psi$ , one creates a flow net consisting of squares. Such a net can be drawn iteratively by using the above-mentioned properties. The diagonals of the flow net in turn form another square flow net with the same properties. This characteristic can be used as a visual test of the constructed flow net. The following example serves as a clarification.

### Example: Force on an open gate (continuation)

#### Potential flow

Task: Calculate the pressure distribution on the gate given in the previous example.

#### Solution

Because the gate is located completely in a potential flow, the pressure distribution can be determined with a square flow net. The net is drawn in Figure 11-8.

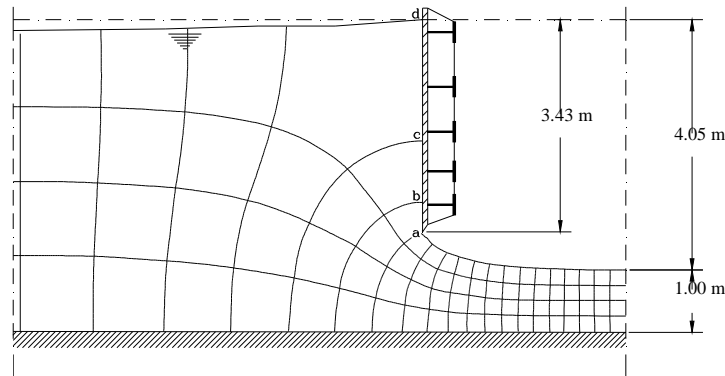


Figure 11-8 Square flow net

In points a and d in Figure 11-8 the pressure equals the atmospheric pressure because there is a free water surface in those points.

In points b and c, the pressures can be estimated using the flow net. The discharge per unit of width between two successive flow lines is:  $q_{square} = 8,91 \text{ m}^2/\text{s} / 4 \text{ squares} = 2,229 \text{ m}^2/\text{s}$ .

At point b the distance between the gate and the first flow line, measured along the equipotential line is approximately  $l = 0,65 \text{ m}$ . The flow velocity in point b is therefore  $u = q_{square} / l = 3,52 \text{ m/s}$ .

The potential in point b is  $H - z_b = 5,05 - 2,09 = 2,96 \text{ m}$

According to Bernoulli the pressure in point b is:

$$H = z + \frac{p}{\rho g} + \frac{u^2}{2g} \Rightarrow p = 1000 \cdot 9,81 \left( 2,96 - \frac{3,52^2}{2 \cdot 9,81} \right) = 23 \cdot 10^3 \text{ N/m}^2$$

At point c the potential is 1,96 m and the distance between the gate and the first flow line, measured along the equipotential line is about 1,31 m. The pressure in point c is calculated the same way as in point b and is  $18 \cdot 10^3 \text{ N/m}^2$ . The course of the piezometric head

$\frac{p}{\rho g}$  is indicated in Figure 11-9.

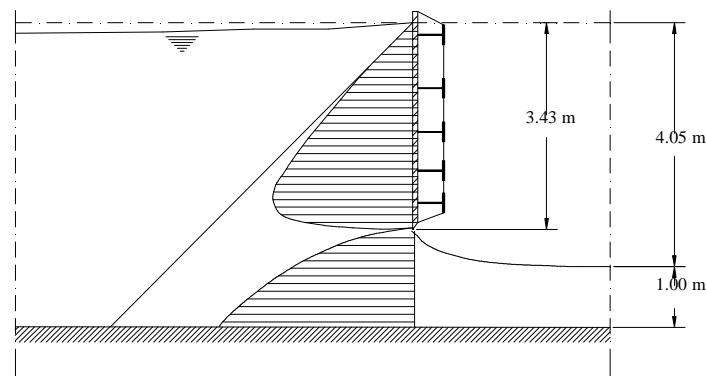


Figure 11-9 Course of piezometric head

### 11.3 Literature

ISO (1980). International Organization of Standards. ISO 1438/1-1980(E). Water flow measurement in open channels using weirs and venturi flumes - Part 1: Thin plate weirs. 1980. Available from Global Engineering Documents at <http://global.ihs.com>

Kindsvater, C. E. and R. W. Carter. 1959. Discharge characteristics of rectangular thin-plate weirs. Transactions, American Society of Civil Engineers. v. 24. Paper No. 3001.

## 12. Water, flow, slender structures

### 12.1 Drag and lift forces

An object, entirely in a uniform flow field, is subject to forces both in the direction of flow (drag force) and perpendicular to the flow (lift force). Drag and lift forces fluctuate in time. These forces cannot be determined theoretically with a linear flow theory such as Bernoulli's.

The reason the flow cannot be schematised as a potential flow is because of the occurrence of rotation, namely eddies behind the cylinder. A wake with a lower pressure is created directly behind the cylinder, which causes a resultant force in the direction of the wake. This turbulence also causes oscillations.

Experiments have shown that the resultant force on an object in the flow  $F$  [N] is reasonably proportional to the velocity head times the density of the fluid (compare this with Bernoulli's equation):

$$F \sim \rho g \frac{u^2}{2g} = \frac{1}{2} \rho u^2$$

in which:  $\rho$  [kg/m<sup>3</sup>] = density of water  
 $u$  [m/s] = de undisturbed flow velocity

The empirical formulas for drag and lift are:

$$F_D = \frac{1}{2} \rho u^2 (C_D + C'_D) A \quad \text{and} \quad F_L = \frac{1}{2} \rho u^2 (C_L + C'_L) A$$

in which:  $F_D$  [N] = drag force parallel to the flow direction  
 $F_L$  [N] = lift force perpendicular to the flow direction  
 $C_D$  [-] = drag coefficient (static)  
 $C_L$  [-] = lift coefficient (static)  
 $C'_D$  [-] = dynamic drag coefficient (time dependent)  
 $C'_L$  [-] = dynamic lift coefficient  
 $A$  [m<sup>2</sup>] = area facing flow, projected perpendicular to the flow direction

The fluctuation in time of the shapes of the wake and the eddies causes a fluctuation of the size and direction of the force, which, in turn, can cause oscillations. The drag force and lift force therefore consist of a static and a dynamic part. The corresponding coefficients are treated separately below.

#### Notes

- The drag force is parallel to the direction of flow (and not to the axis of the object!), the lift force is perpendicular to this.
- It is very important to notice that the turbulence of the water can wash out the soil behind a pile, thereby endangering the founding property of the pile. This erosion of the bed is called scour and is not discussed any further. When dimensioning a post, one must take this scour into account (less fixation and more effective pile length) or include bed protection measures. The scour behind a pile is 1.5 - 2 times the pile diameter in sandy soils.

### 12.2 Drag and lift forces, static part

The coefficients  $C_D$  and  $C_L$  are largely dependent on the shape of the structure and the flow around the structure, which are expressed in the Reynolds value,  $Re$  [-]:

$$Re = \frac{u d}{\nu}$$

in which:  $Re$  [-] = Reynolds value  
 $u$  [m/s] = flow velocity  
 $\nu$  [m<sup>2</sup>/s] = kinematic viscosity = 10<sup>-6</sup>  
 $d$  [m] = measure of length dependent on geometry

In the field of hydraulic engineering, the flow is usually turbulent ( $Re > 10^4$ ). The  $C_D$  coefficients for three different shapes (cylinder, plate and a streamlined wing) are given in

Figure 12-1. This figure shows that the  $C_D$  coefficient of a cylinder (pile) in the area  $10^5 < Re < 10^6$  is sensitive to fluctuations of  $Re$ . However, the  $C_D$  coefficients of angular objects, such as plates and beams, are barely dependent on  $Re$  in this turbulence area.

In the region  $10^5 < Re < 10^6$ , the wake behind a cylinder decreases for a larger Reynolds value, the separation points move further back. A smaller wake means a smaller resultant force. For objects with sharp edges, the separation points of the flow and thus the wake are more or less fixed. The resultant force on such objects is therefore less sensitive to fluctuations of  $Re$ .

Figure 12-1 shows that the shape of a pile is very important for the forces that result from flow against the pile.

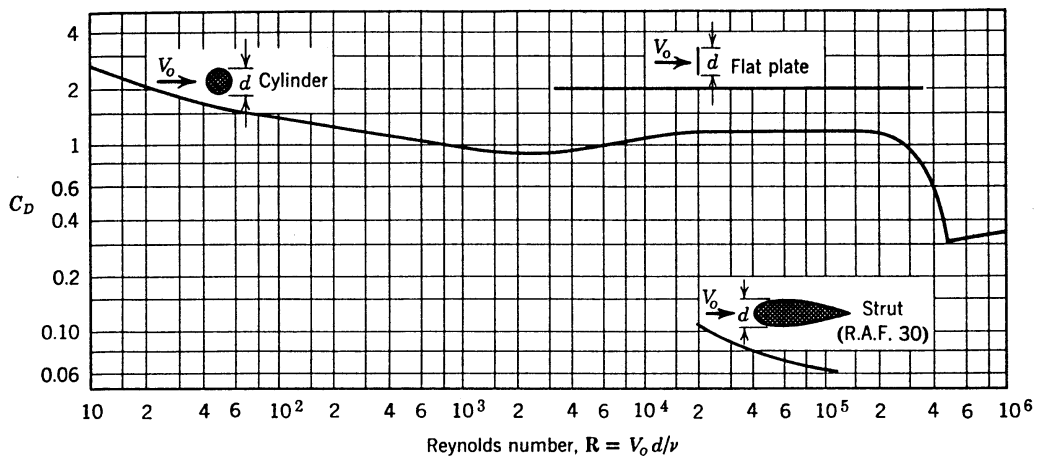


Figure 12-1  $C_D$  value of a cylinder, plate and streamlined wing

The static lift coefficient ( $C_L$ ) is zero for straight approaching flow.

The  $C_D$  and  $C_L$  coefficients of a bridge pile approached by flow at an angle are given in Figure 12-2. Three different shapes for the pile are indicated. The given coefficients are largest for the cylinder. However, this does not mean that the force on the cylinder is actually the largest, because the projected surface perpendicular to the flow is smaller for a cylinder than for the other given piles.

The more the shape of the pile deviates from a cylinder, the larger the force on the pile if the flow approaches at an angle.

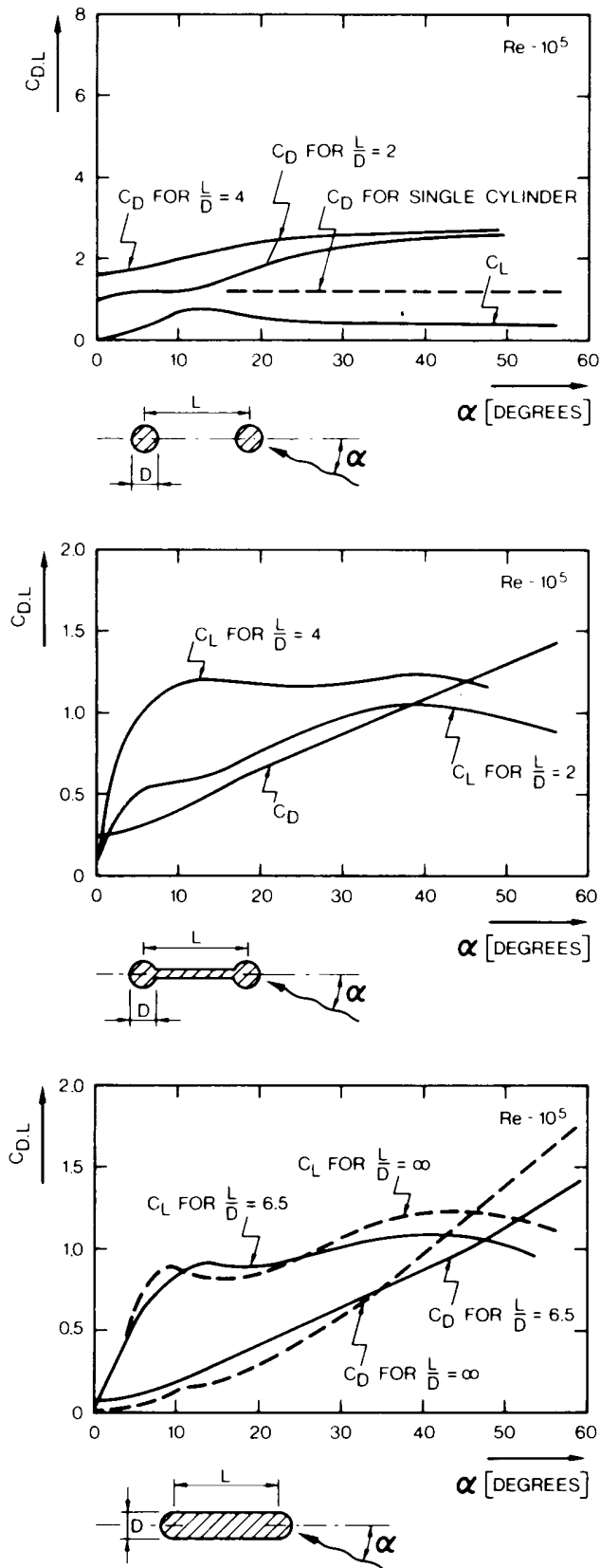


Figure 12-2  $C_D$  and  $C_L$  coefficients of various pile shapes in the case of flow at an angle (Apelt and Isaacs, 1986)

### 12.3 Drag and lift forces, dynamic part (vibrations)

A structure that has been placed in a stationary flow can start to vibrate. These lecture notes only include an introduction to the phenomenon of vibrations as a result of stationary flow, as the complexity of the subject doesn't allow for a full description here.

The most important vibrations in a structure in a stationary flow are caused by instability of the wake and the vortices behind and alongside the structure or by hydrodynamic instability. Due to fluctuations in time of the vortices and the wake, the size and direction of the resultant force on an object in a stationary flow also fluctuates in time. Figure 12-3 indicates the pressure distribution around a cylinder due to changing vortices. This figure clearly shows that there is a dynamic resultant load.

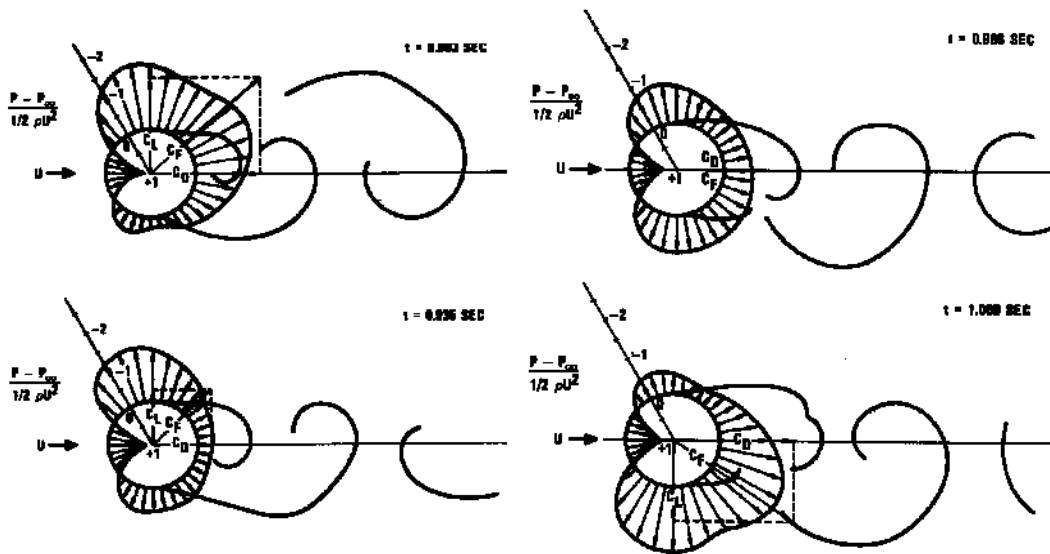


Figure 12-3 Fluctuation in time of the pressure and the wake with  $Re=1.12 \cdot 10^5$  (Drescher 1956)

The frequency  $f_s$  of vortex shedding behind an object standing in the flow is given by:

$$f_s = \frac{uS}{D}$$

- in which:  $u$  [m/s] = the flow velocity in an undisturbed flow  
 $S$  [-] = Strouhal number  
 $D$  [m] = the characteristic diameter perpendicular to the flow

The Strouhal number ( $S$ ), named after the Czech physicist Vincenc Strouhal, is a dimensionless number describing oscillating flow mechanisms. For cylinders, this number is given as a function of the Reynolds value ( $Re$ ) in Figure 12-4. For shapes with non-circular cross sections, reference is made to Figure 12-5.

Hydrodynamic instability occurs if a slight movement of an object is enforced by the flow, so that a small displacement can lead to vibrations with increasing amplitude. Depending on the stiffness of the structure hydrodynamic instability may occur. If  $f_s > f_n$ , no resonance will occur; here  $f_n$  is the natural oscillation frequency of the system (structure + water). This dynamic phenomenon is identical to a chimney swaying in the wind. Calculating the natural oscillation frequency is a study in its own right and is not covered in this course.

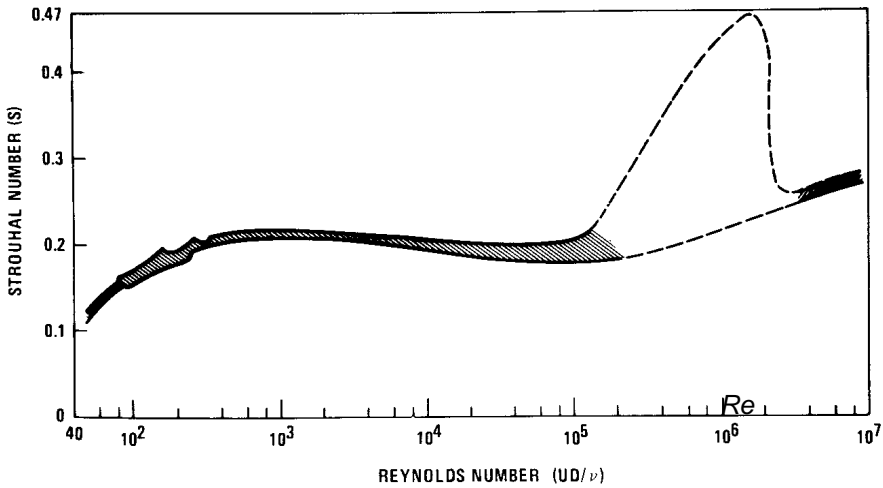


Figure 12-4 Strouhal number for cylinders

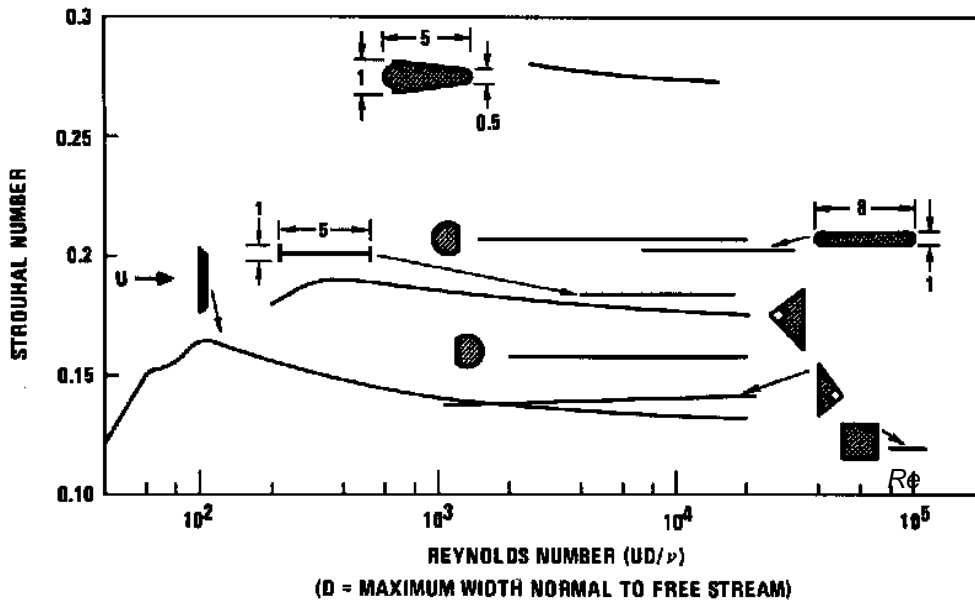


Figure 12-5 Strouhal number for non-circular cross sections

For the maximum dynamic drag coefficient (time dependent):

$$C_D' = 0,10 \text{ to } 0,5 \cdot C_D \quad \text{if: } f_s > f_n$$

$$C_D' = ? \text{ (danger of resonance)} \quad \text{if: } f_s < f_n$$

The static  $C_L$  coefficient is of course zero for a straight approaching flow ( $\alpha = 0$ ). The dynamic  $C_L'$  coefficient is not zero due to the time dependent turbulent oscillations. The value of  $C_L'$  is strongly dependent on the ratio  $\frac{f_s}{f_n}$  and increases largely near  $\frac{f_s}{f_n} = 1$ . Still no reasonably accurate expression is available for the value  $C_L'$ . For a preliminary design, one may therefore assume:

$$C_L' \approx C_D'$$

## 13. Water, tide and wind set-up

Extended and updated: February 2015

Water levels along the coast are mainly determined by the tide and by wind set-up. Furthermore, phenomena such as storm surges, shower oscillations, shower gusts and seiches are involved. These effects are explained below. Chapter 49 explains how they contribute to the determination of the height of flood defences.

### 13.1 Astronomical tide

#### Theory

One of the most characteristic properties of coastal waters is the tidal movement. Different tides can be distinguished according to the water motion direction, namely:

- vertical tides: raising and falling of the water level
- horizontal tides: tidal flows in tidal inlets/ outlets and creeks and along the coast.

The tidal movements on earth are caused mainly by the following 5 factors:

1. The gravitational pull of the moon on the seawater.
2. The monthly rotation of earth around the shared earth-moon axis (centrifugal force).
3. The daily rotation of earth around its own axis.
4. The inclination of the earth's rotation axis.
5. The gravitational pull of the sun on the seawater.

#### 1. The gravitational pull of the moon on seawater

The moon, and in lesser extent the sun, cause an uneven force distribution on the water due to the difference in distances between the points on earth and the moon, see figure below. The result is a semi-diurnal tide.

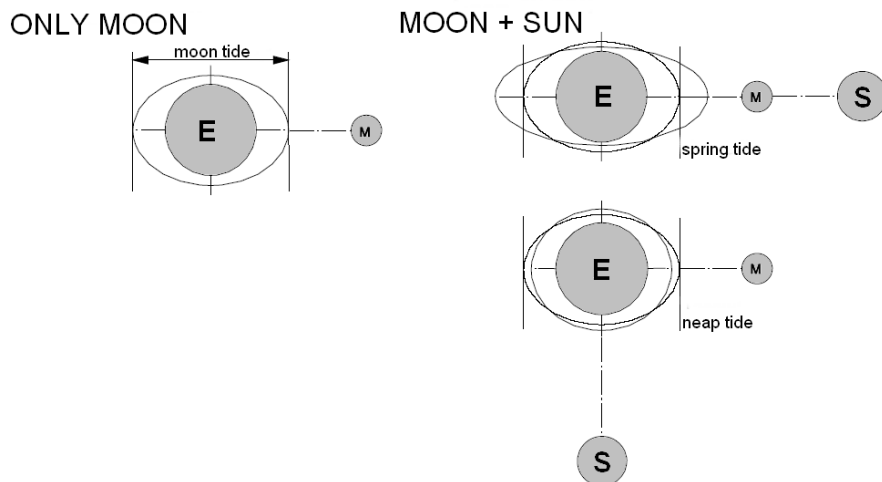


Figure 13-1 Pull of the moon and the sun

#### 2. Rotation around the shared earth-moon axis

The earth has a monthly rotation around the shared earth-moon axis. This axis is approximately  $0,6 r$  from the centre of earth. Because every point on earth covers the same distance for this rotation, the centrifugal force is the same everywhere on earth. (In this case one must not consider that the earth is rotating around its own axis, as this is taken into consideration in point 3.) Together these two forces form an elliptical force distribution around the earth. If the earth were covered entirely in water, the water mass would take the shape of an ellipsoid, as shown in Figure 13-2. This fictional situation is known as the equilibrium tide due to the moon.

#### 3. Rotation around own axis

The earth spins as it were under the water mass, thus causing two high tides and two low tides a day (semi diurnal tide) in an arbitrary location. There are, however, places on earth where the tidal flow is influenced by the presence of a continent to such an extent that there is only one high tide per day (diurnal tide) in these locations.

**4. Obliqueness rotation axis**

Due to the obliqueness of the rotational axis of the earth, the tidal movement during a semi diurnal tide is AB one time and A'B' another. This causes a daily inequality of the maximum tide (see Figure 13-3). In winter, the high tide at daytime (AB) is generally smaller than the high tide at night (A'B'). In the summer, the opposite applies.

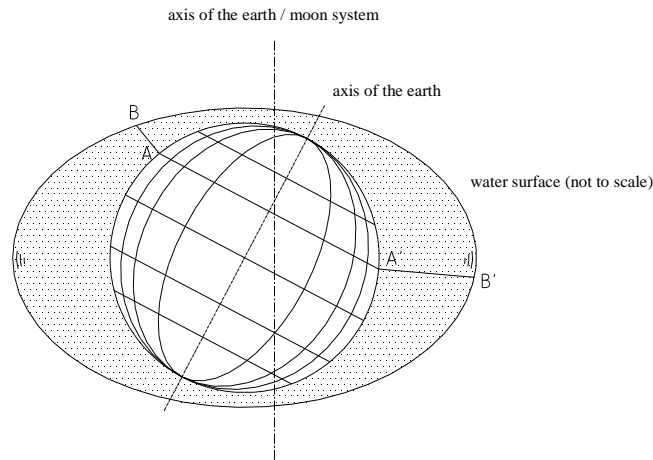


Figure 13-2 Two different high tides

**5. Gravitational pull of the sun on seawater**

The influence of the sun is confined to reinforcing or weakening the moon tide. If the sun and the moon are on the same side of the earth, they reinforce each other. The resulting tide is known as spring tide, if they counteract each other it is called neap tide. Spring tide occurs at full and new moons; neap tide occurs in the first and last quarters.

**(Preliminary) design**

In reality the astronomical tide bears little resemblance to the theoretical equilibrium tide. This is due to the presence of continents and the Coriolis effect, which causes the diversion of tidal flows. The true tidal water levels and the times of high and low tide can be predicted with a "harmonic analysis" or "Fourier analysis" of the data from measuring stations. These techniques are not discussed here.

Every year, the National Institute for Public Works and Water Management, Rijkswaterstaat, publishes predictions made using these methods in the booklet Tide tables for the Netherlands ("Getijtafels voor Nederland"). For a number of measuring stations, the booklet lists when high and low tides will occur at and what their corresponding water levels are.

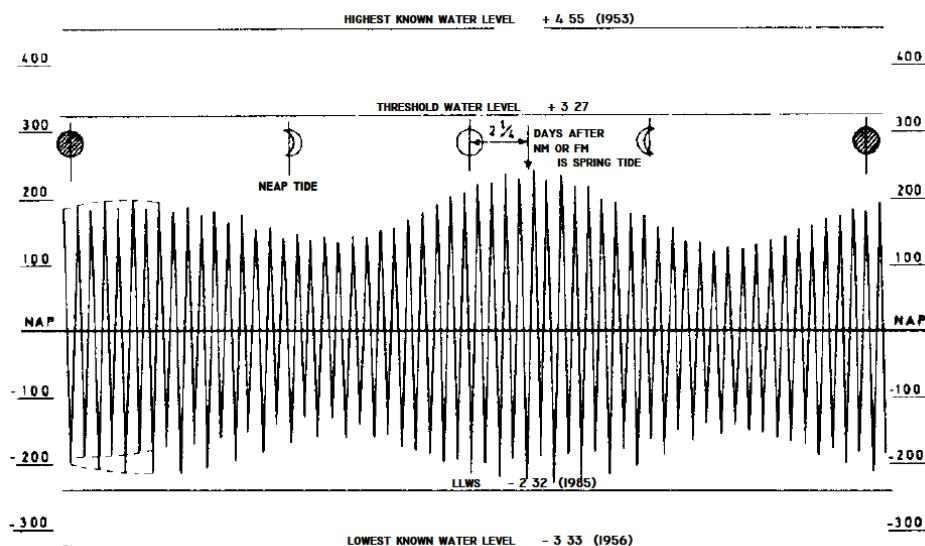


Figure 13-3 Water level in one month in Vlissingen

For some hydraulic engineering structures, the water level during an extreme storm surge is particularly important. See Section 13.3 "Storm surge" for tables with storm surge water levels.

Data on tides can be found at [www.rijkswaterstaat.nl/geotool/waterhoogte\\_tov\\_nap.aspx](http://www.rijkswaterstaat.nl/geotool/waterhoogte_tov_nap.aspx).

## 13.2 Wind set-up

In shallow seas, deltas, closed off creeks, and lakes, wind fields can influence the water level quite considerably by heading up the water (wind set-up). Figure 13-4 shows a model to approximate the wind set-up (*opwaaiing*).

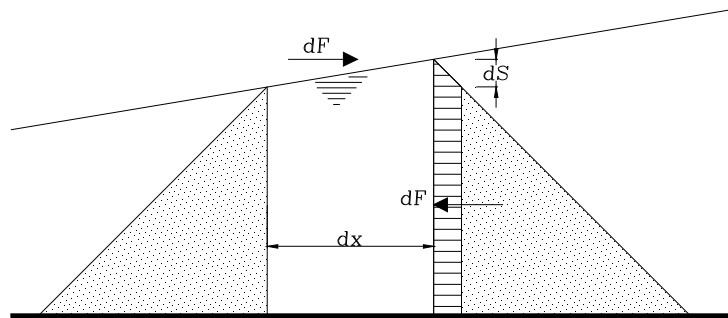


Figure 13-4 Balance of forces in case of wind set-up

The wind set-up in the equilibrium state is approximately:

$$\frac{dS}{dx} = C_2 \frac{u^2}{gd}$$

in which:  $S$  [m] = total wind set-up  
 $C_2$  [-] = constant  $\approx 3,5 \cdot 10^{-6}$  to  $4,0 \cdot 10^{-6}$   
 $d$  [m] = water depth  
 $u$  [m/s] = wind velocity

If the wind set-up is small compared with the water depth, in an area with a horizontal bed, the slope  $\frac{dS}{dx}$  is constant. The formula shows that the wind set-up increases with increasing wind velocity and fetch and decreasing water depth. The wind set-up is therefore of importance in river deltas, lakes and shallow seas. In coastal areas where the sea is deep, wind set-up hardly ever occurs. In the North Sea, the Wadden Sea and the IJsselmeer, the set-up can be as much as a couple of meters. In 1953 the rise in Vlissingen was 3,05 m.

If the water level at the edge of a basin is known, the course of the water level in the basin can be calculated with a simple numerical solution (Heun method):

$$d_x = d_{x-\Delta x} + \frac{dS}{dx} \Delta x - \Delta z_{x-\Delta x, x}$$

in which:  $d_x$  [m] = the water depth in point  $x$   
 $d_{x-\Delta x}$  [m] = the water depth in point  $x-\Delta x$   
 $\Delta z_{x-\Delta x, x}$  [m] = difference between the height of the bed in  $x$  and  $x-\Delta x$

In a closed basin or a lake, the total amount of water cannot change. This means that, provided the slope may be assumed constant, the surface of the water (by approximation) will tilt around the gravity line of the basin surface, perpendicular to the wind direction. The water in the area between the down-wind edge and the gravity centre is subjected to wind set-down (see Figure 13-5).

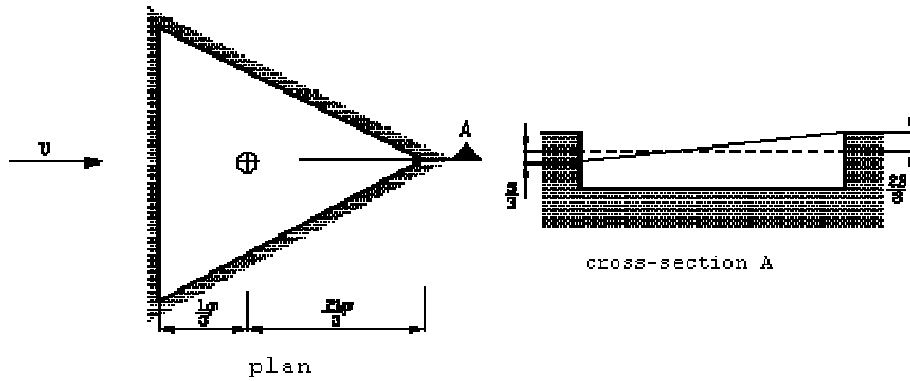


Figure 13-5 Wind set-up in a closed basin

The combination of tides and wind set-up is important, particularly for the design of most hydraulic engineering structures. If high tide coincides with strong winds (storm) a storm surge occurs. See the following section for tables with water levels in storm surges.

### 13.3 Storm surge

It is more or less possible to predict the timing and the water levels of a spring tide. The wind set-up in front of the coast can be calculated with a given wind velocity. By analysing wind data, it is possible to calculate the probability of occurrence of a spring tide and a certain wind set-up. Such a combination is known as a storm surge (*stormvloed*).

Because the calculation model for wind set-up contains a number of uncertainties, a different approach is used in practice. The Dutch Delta Committee based the determination of basic water levels upon as many observed storm surge levels as possible. In this way, it constructed a frequency distribution (an empirical relation). The design water level (storm surge level) for a chosen small normative exceedance frequency was then determined by extrapolation of measuring points, see the high water level measurements for Hoek van Holland in the following figure<sup>1</sup> (measured at a gauge (*peilschaal*) near the coast).

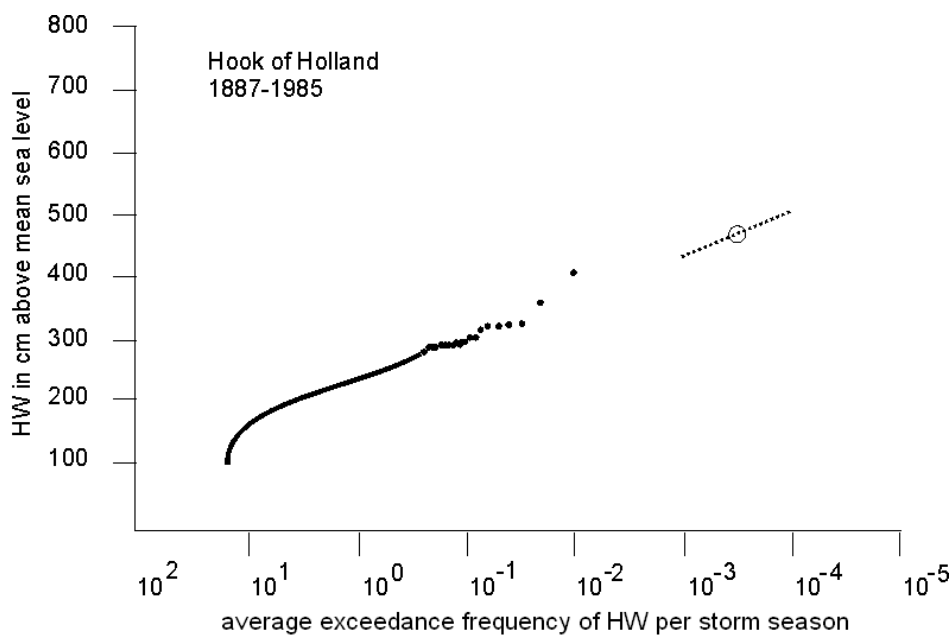


Figure 13-6 Water level exceedance frequencies at Hoek van Holland

<sup>1</sup> Notice that x- and y-axis are swapped in this figure, as usual with water levels, and the y-axis is plotted on a logarithmic scale. Also the direction of the y-axis deviates from the usual direction (y-values decrease towards the right of the graph).

HW (high water level) in this figure includes two phenomena: astronomical tide and wind set-up. In the Netherlands, the Delta Committee assigned normative water levels to areas surrounded by dikes or other flood defences (dike ring areas). The heights of the normative water levels were related to an economic optimum of investments in flood protection and consecutive risk reduction per dike ring area. For the economically most valuable parts of the Netherlands (the Randstad, dike ring number 14) the normative water level is related to an average exceedance frequency of 1/10 000 per year.

After profound analysis of the available data, it was found that the frequency of exceedance of a certain water level  $h_0$  can be described with an exponential function:

$$f(h > h_0) = e^{-\frac{h_0 - A}{B}}$$

where:

$$\begin{aligned} f \quad [\text{year}^{-1}] &= \text{exceedance frequency} \\ h \quad [\text{m}] &= \text{water level} \\ h_0 \quad [\text{m}] &= \text{reference level, for instance the height of structure} \\ A, B \quad [\text{m}] &= \text{constants} \end{aligned}$$

With help of this equation, the design water level can be found if the normative exceedance frequency is given. So, for Hoek van Holland the design water level is NAP + 5,00 m.

The table below gives water levels corresponding to certain probabilities of exceedance for a number of places (see Tidal Tables for the Netherlands, "Getijtafels voor Nederland", RIKZ).

HW/year	Delfzijl	Den Helder	Scheveningen	Vlissingen	Bath
$10^{-1}$	4,10 m	2,75 m	3,05 m	3,85 m	4,75 m
$10^{-2}$	4,95 m	3,40 m	3,70 m	4,40 m	5,45 m
$10^{-3}$	5,60 m	3,95 m	4,40 m	4,95 m	6,10 m
$10^{-4}$	6,20 m	4,45 m	5,15 m	5,50 m	6,75 m
1 Feb. 1953	-	3,25 m	3,97 m	4,55 m	5,60 m

Table 13-1 (Extreme) storm surge levels

The probability of exceedance is closely related to the frequency of exceedance. A difference is that a frequency can theoretically be more than 1,0, whereas a probability per definition cannot exceed this value. For small numbers, however, the difference is negligible. The relation is expressed as a complementary Gumbel distribution<sup>2</sup>:

$$P(h > h_0) = 1 - e^{-f(h > h_0) \cdot T}$$

For exceedance probabilities frequencies of less than 0,1, the exceedance frequency has about the same magnitude if the exceedance probability is considered over a period of one year ( $T = 1$ ), which we usually do<sup>3</sup>.

For foreign projects, however, there are often too few data to determine the design storm surge level on a statistical basis. In such cases the models for the tide and the wind set-up have to be used to estimate the storm surge level.

<sup>2</sup> The Gumbel distribution is a probability distribution of extreme values which can be applied to storm surge levels. Various types of extreme value distributions are treated in courses 'Bed, Bank and Shore Protection' (CIE4310) and 'Probabilistic Design in Hydraulic Engineering' (CIE5310)

<sup>3</sup> In practice, exceedance frequency and probability are therefore often confused. It should, however, be noticed that the units are different: a frequency is expressed as a number of occurrences per year, and a probability is dimensionless.

## 13.4 Other influences

Besides tides and wind set-up, other factors can influence the water level, such as:

1. Shower oscillations and shower gusts
2. Seiches
3. Relative sea level rise

These factors are discussed below.

### **Shower gusts and shower oscillations**

Shower gusts (*buiستوتن*) are single elevations of the sea water level caused by atmospheric depressions. Gusts are generated when a storm with low air pressure (e.g. 3 cm of water pressure less than the surrounding area) approaches the coast at wave velocity, thus building up an increasingly large wave. The duration of a gust can vary between a couple of minutes and more than one hour. The shower gust elevation at the Dutch coast can be up to 0,50 to 1,00 m during storm conditions.

If shower gusts appear in a more or less regular series, the phenomenon is called shower oscillations (*bui-oscillaties*). The period of a shower oscillation can vary from a couple of minutes to more than an hour; the amplitude in Dutch waters is usually about 0,20 to 0,30 m.

In Dutch waters, the gust effect dominates the effect of shower oscillations; this is why it is assumed that the effect of the latter is discounted in the contribution of the shower gust. The Dutch guide on the design of river dikes (*TAW Leidraad voor het ontwerpen van rivierdijken - deel 2: benedenrivierengebied, 1989*) recommended reducing the magnitude of the shower gust, depending on the extent of wave run-up. These values have been adopted by the Dutch guide on lake and sea dikes (*TAW Basisrapport bij de Leidraad voor meer- en zeedijken, 1999*).

During the passing of hurricane Hugo in Guadeloupe, a water level rise of 0,30 to 0,60 m was observed in deep water. In shallow water the rise was as much as 2,50 to 3,00 m.

### **Seiches**

A seiche is an oscillatory rise of the water level in a basin enclosed on three sides, caused by oscillation of the water level outside the basin. Particularly the shower oscillation within periods ranging from a couple of minutes to an hour can cause seiches, for instance a sheltered harbour. In general, when designing structures in closed areas or harbour basins seiches must be taken into account.

Because of the presence of the Hartelkering and the Maeslantkering, the importance of shower gusts, shower oscillations and seiches has become much less relevant behind these barriers. The Dutch committee on flood defence (TAW) therefore recommended to neglect these effects behind the barriers, until further research has been carried out (*TAW Technisch Rapport Ontwerpbelastingen voor het rivierengebied, 2007*).

### **Relative sea level rise**

Relative sea level rise is caused by a number of factors:

- Subsidence of the sea bottom due to geological processes and gas and oil extraction
- Increase of the average temperature, which causes melting of the polar caps and thermal expansion of the ocean water.

The relative sea level rise is still subject to research. An estimate of the relative level rise of the North Sea is 40 to 80 cm per century (Note on coastal defence 1990 – TR6 – Sea level rise, in Dutch: “Nota kustverdediging van 1990 - TR6 – Zeespiegelrijzing”). The Dutch Delta Committee 2008 made a prognosis of 130 cm in 100 year as a worst case scenario, based on forecast models. The observed trend, however, is 19 cm relative sea level rise per 100 year (inclusive land subsidence) and a deviation from this trend has not yet been observed.

The latest reports suggest that the increased average temperature is causing an increased precipitation in Antarctica, which compensates the accelerated melting of the southern polar cap. The melting of the northern polar cap does not affect the average sea level. The expanding volume of water due to decreasing density caused by higher temperatures is said to form the main contribution to sea water level rise.

## 14. Water, waves, theory

In hydraulic engineering different types of waves can be distinguished, such as:

- Translation waves (sloping front!), caused for instance by:
  - quickly emptying or filling a lock chamber on or from a canal section
  - opening or closing a hydropower station
- wind waves, caused by the wind skimming large water surfaces
- tides, caused by the position and rotation of celestial bodies
- discharge waves caused by precipitation or thaw
- ships' waves
- pressure waves, which can be created in closed pipes by sudden discharge changes.

With the exception of pressure waves, all the above are waves which occur on the water surface. These waves are divided into short and long waves. Short waves, such as wind waves and ships' waves, cannot be disregarded in the vertical component of the wave velocity in relation to the horizontal component, as is the case with long waves, such as tide and translation waves.

This chapter briefly describes translation waves and wind waves. Tides were covered in Section 13.1. Discharge waves were discussed in Section 10.1. Pressure waves in closed pipes will not be treated. When approaching shallows and obstacles, waves change their properties and can start to break. This is covered in Section 16 "Water, waves, shallows + breaking".

### 14.1 Translation waves

Translation waves can have different causes. One of the most common causes is emptying or filling a lock chamber. There are also natural processes that can cause a translation wave. Examples of these are dam breaches (of ice dams and natural soil dams) and tidal bores. Figure 14.1 gives a sketch of a translation wave. The propagation velocity of the wave is:

$$c = u \pm \sqrt{g \frac{(2d + \eta)(d + \eta)}{2d}}$$

in which:  $u$  [m/s] = the normal flow velocity  
 $d$  [m] = the water depth  
 $\eta$  [m] = the displacement of the water surface

For a relatively small  $\eta$ , the propagation velocity can be approached with:

$$c = u \pm \sqrt{gd}$$

The displacement of the water surface depends on the change of the discharge, the propagation velocity and the flow width:

$$\eta = \frac{\Delta Q}{Bc}$$

in which:  $\Delta Q$  [m<sup>3</sup>/s] = the change of discharge  
 $B$  [m] = the flow width

In the translation wave the pressure is hydrostatic. The pressure under a translation wave with elevation  $\eta$  is:

$$p = \rho g(d + \eta)$$

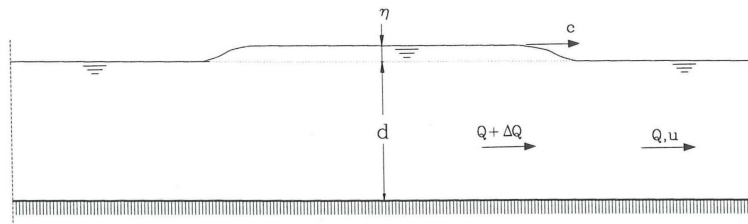


Figure 14-1 Translation wave

When the flow profile changes, a wave continues in the original direction and a wave reflects in the opposite direction. The same happens at the branching of a river.

When determining the displacement of the water surface with the continuing and reflected wave, the following applies, after the passing of the wave, at the point of profile adjustment:

- the water level to the left and the right of this point are equal
- the sum of the discharges equals zero.

## 14.2 Wind waves

### Linear wave theory (regular waves)

This chapter briefly gives a number of characteristics of wind waves. For a more extensive explanation and the derivation of the equations one is referred to the course Ocean Waves (CT4325). The terms involved in wave theory can best be defined using a picture of a single wave.

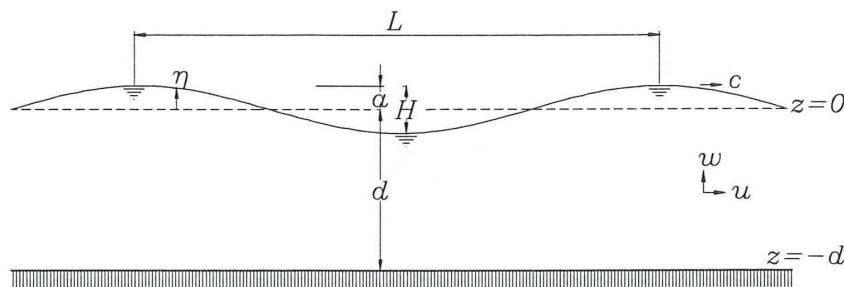


Figure 14-2 Sinusoidal wave shape

The most important terms are:

- $L$  The wavelength is the horizontal distance between two successive wave crests (or troughs).
- $T$  The period is the time, which passes at a certain fixed point between the passing of two consecutive wave crests
- $f$  The frequency is defined as the number of waves per unit of time, which equals the inverse of the period ( $= 1/T$ )
- $c$  The wave velocity (also known as the propagation velocity or phase velocity) with which the wave crest travels
- $\eta$  The displacement of the water surface
- $a$  The amplitude of the wave
- $H$  The wave height is the difference in height between the highest and the lowest point of the wave profile ( $H=2a$ )
- $H/L$  The steepness is the ratio wave height to wavelength
- $u$  and  $w$  The velocity components of the orbital movement of the water particles
- $p$  The water pressure
- $d$  The water depth

Figure 14-2 shows a schematised, sinusoidal, vertical cross section of the water surface, which is perpendicular to the direction of the wave crests.

This schematisation is used in linear wave theory. The true shape of short waves is highly dependent on the steepness ( $H/L$ ).

If  $H/L \leq 1/40$ , the shape of the wave is comparable to a sinusoid. For larger values of  $H/L$ , the shape will bear more resemblance to a trochoid.

The following applies in case of the sinusoidal approximation of the displacement of the water surface:

$$\eta(r, t) = a \sin\left(\frac{2\pi t}{T} - \frac{2\pi r}{L} + \alpha\right) \quad \text{or} \quad \eta(r, t) = a \sin(\omega t - kr + \alpha)$$

in which:  $\omega = \frac{2\pi}{T}$  [rad/s] = angular frequency

$k = \frac{2\pi}{L}$  [rad/m] = wave number

$t$  [s] = point in time

$r$  [m] = place measured in the wave direction

$\alpha$  [rad] = phase

**Note.**

In American literature the following equation is used for the displacement of the surface:

$$\eta(r, t) = a \cos(kr - \omega t + \alpha). \text{ This means a phase shift of } \pi/2.$$

The wave velocity  $c$ , the wavelength  $L$  and the period  $T$  are related to each other according to the following equation:

$$c = \frac{L}{T} = \frac{\omega}{k}$$

From theoretical derivations, relations follow between the wave velocity, the wavelength and the water depth, such as:

$$c = \sqrt{\frac{g}{k} \tanh(kd)} \quad \text{or} \quad c = c_o \tanh(kd)$$

$$L = \frac{gT^2}{2\pi} \tanh(kd) \quad \text{or} \quad L = L_o \tanh(kd)$$

$$\text{in which: } c_o = \frac{gT}{2\pi}$$

$$L_o = \frac{gT^2}{2\pi}$$

In shallow water ( $d \leq \frac{1}{25}L$ ),  $\tanh(x) \approx x$ . Therefore, the wave velocity in shallow water can be written as:

$$c = \sqrt{\frac{g}{k} \tanh(kd)} \approx \sqrt{gd}$$

When observing waves it is noticeable that a wave group does not move at the same velocity as individual waves. A wave group propagates with a smaller velocity than the individual waves, whereby the waves overtake each other. The wave front moves at the so-called group velocity:

$$c_g = nc \quad \text{with} \quad n = \frac{1}{2} + \frac{kd}{\sinh(2kd)} \quad \text{for deep water: } n = \frac{1}{2}$$

All water particles in a wave move in a more or less elliptic course. The movement of the particles decreases the deeper they are below the water surface. The elliptical movement of the water parts is known as orbital movement.

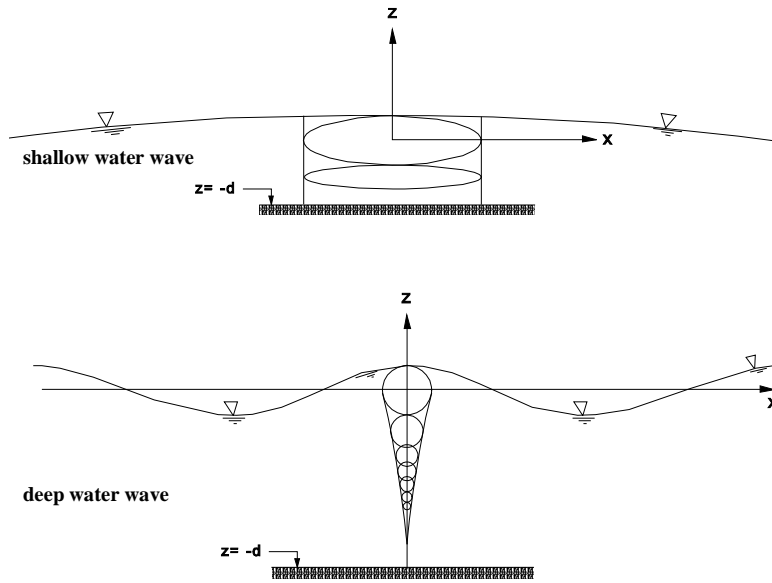


Figure 14-3 Orbital movement

The maximal horizontal and vertical components of the orbital velocity of a water particle are given by:

$$\hat{u} = \omega a \frac{\cosh(k(d+z))}{\sinh(kd)} \quad \text{and} \quad \hat{w} = \omega a \frac{\sinh(k(d+z))}{\sinh(kd)}$$

in which:  $\hat{u}$  [m/s] = maximal horizontal velocity

$\hat{w}$  [m/s] = maximal vertical velocity

$z$  [m] = co-ordinate of the considered depth relative to the average water surface

As is evident from the formula, the water velocity is largest at  $z = 0$  and smallest at  $z = -d$ .

The pressure in a given point at a depth  $z$  below the average water line is:

$$p = -\rho g z + \rho g a \frac{\cosh(k(d+z))}{\cosh(kd)} \sin(\omega t - kr) \quad \text{for } z < 0$$

The pressure in a point above the average water line can be approximated by linear interpolation:

$$p = \rho g (\eta - z) \quad \text{for } z > 0$$

In the preceding, a possible flow velocity of the water was not taken into account. The given equations only apply for a co-ordinate system fixed to the undisturbed water surface. In a flow the equations are for a co-ordinate system that moves along with the flow. Relative to a fixed point, the propagation velocity and phase velocity are to be adjusted as follows:

$$c' = c + \vec{U} \vec{e}_r \quad \text{and} \quad \omega' = \omega + \vec{k} \cdot \vec{U} = \sqrt{gk \tanh(kd)} + \vec{k} \cdot \vec{U}$$

A wave has kinetic and potential energy. The potential energy is related to the displacement of the water surface and the kinetic energy is related to the orbital movement.

The total mechanical energy of one wave is:

$$E = \frac{1}{8} \rho g H^2 L \quad (\text{per } m' \text{ wave crest})$$

The average energy per unit of surface area is thus:

$$E = \frac{1}{8} \rho g H^2$$

This energy plays an important part in the description of waves in a wave field.

A summary of linear wave theory is given in Table 8-1.

Relative depth Characteristics	Shallow Water $\frac{h}{L} < \frac{1}{20}$	Transitional water depth $\frac{1}{20} < \frac{h}{L} < \frac{1}{2}$	Deep Water $\frac{h}{L} > \frac{1}{2}$
Wave Celerity	$c = \frac{L}{T} = \sqrt{gh}$	$c = \frac{L}{T} = \frac{gT}{2\pi} \tanh kh$	$c = c_0 = \frac{L}{T} = \frac{gT}{2\pi}$
Wave Length	$L = T\sqrt{gh}$	$L = \frac{gT^2}{2\pi} \tanh kh$	$L = L_0 = \frac{gT^2}{2\pi}$
Group Velocity	$c_g = c = \sqrt{gh}$	$c_g = nc = \frac{1}{2} \left[ 1 + \frac{2kh}{\sinh 2kh} \right] \cdot c$	$c_g = \frac{1}{2} c_0 = \frac{gT}{4\pi}$
Energy Flux (per m width)	$F = Ec_g = \frac{1}{2} \rho g a^2 \sqrt{gh}$	$F = Ec_g = \frac{1}{2} \rho g a^2 nc$	$F = \frac{T}{8\pi} \rho g^2 a^2$
Particle velocity			
Horizontal	$u = a \sqrt{\frac{g}{h}} \sin \theta$	$u = \omega a \frac{\cosh k(h+z)}{\sinh kh} \sin \theta$	$u = \omega a e^{kz} \sin \theta$
Vertical	$w = \omega a \left( 1 + \frac{z}{h} \right) \cos \theta$	$w = \omega a \frac{\sinh k(h+z)}{\sinh kh} \cos \theta$	$w = \omega a e^{kz} \sin \theta$
Particle displacement			
Horizontal	$\xi = -\frac{a}{\omega} \sqrt{\frac{g}{h}} \cos \theta$	$\xi = -a \frac{\cosh k(h+z)}{\sinh kh} \cos \theta$	$\xi = -a e^{kz} \cos \theta$
Vertical		$\zeta = a \frac{\sinh k(h+z)}{\sinh kh} \sin \theta$	$\zeta = a e^{kz} \sin \theta$
Subsurface pressure	$p = -\rho g z + \rho g a \sin \theta$	$p = -\rho g z + \rho g a \frac{\cosh k(h+z)}{\cosh kh} \sin \theta$	$p = -\rho g z + \rho g a e^{kz} \sin \theta$
$a = \frac{H}{2} \quad \omega = \frac{2\pi}{T} \quad k = \frac{2\pi}{L} \quad \theta = \omega t - kx$			

Table 14-1 Summary of linear (Airy) wave theory - wave characteristics

**Wave fields (irregular waves)**

The previous section described the so-called regular wave. In a wave field generated by wind, there are many waves, with different periods, phases, wave heights and wave directions.

The water surface in a wave field is erratic and single waves cannot be distinguished. With a Fourier analysis, however, it is possible to describe this erratic surface as the sum of a large number of sinusoidal waves with different wave heights  $a$ , angular frequencies  $\omega$  and phases  $\alpha$ .

The movement of the water surface can be described as:

$$\eta(\vec{r}, t) = \sum_i \sum_j a_i \sin(\omega_i t - \vec{k}_{i,j} \cdot \vec{r} + \alpha_{i,j})$$

$$\text{in which: } \vec{k}_{i,j} = \begin{bmatrix} k_i \cos(\theta_j) \\ k_i \sin(\theta_j) \end{bmatrix}$$

$\theta_j =$  angle between the wave direction and the positive x-axis

If the consideration is limited to one point, the model becomes a one dimensional random-phase model:

$$\eta(t) = \sum_i a_i \sin(\omega_i t + \alpha_i)$$

The properties of a wave field are set in an energy spectrum. For the theoretical background and the formal definition of the energy spectrum, one is referred to the book used for the course on wind waves (*Waves in oceanic and coastal waters*, Holthuijsen, 2005).

Continuing with the one dimensional random-phase model, the energy spectrum is:

$$E_{\eta\eta}(f) \Delta f = \sum_{f_i=f}^{f+\Delta f} \frac{1}{2} a_i^2$$

A two-dimensional spectrum of frequency and direction is:

$$E_{\eta\eta}(f, \theta) \Delta f \Delta \theta = \sum_{f_i=f}^{f+\Delta f} \sum_{\theta_j=\theta}^{\theta+\Delta\theta} \frac{1}{2} a_{i,j}^2$$

A number of important characteristics of a wave field can be expressed in the moments of the spectrum. These moments are defined as:

$$m_n = \int_0^{\infty} f^n E_{\eta\eta}(f) df$$

One of the characteristics is the significant wave height. The significant wave height  $H_s$  is the average of the highest 1/3 of the waves. The relation between this wave height and the spectrum is:

$$H_s = 3.8 \sqrt{m_0}$$

The momentary wave height has a Rayleigh probability distribution. The exceedance probability of a given wave height within a given wave field is:

$$P(H > x) = \exp\left(-2\left(\frac{x}{H_s}\right)^2\right)$$

For the continuation of wave heights and exceedance probabilities, see the next chapter.

## 15. Water, waves, wave heights

updated: February 2015

### 15.1 Estimate of wave height and period if no measurements are available

The most important waves are waves generated by the wind. If a structure is to be dimensioned for a certain wave height, this wave height has to be known (measurements). If no measurements are available, the significant wave height and wave period can be estimated by using equations as proposed by Charles L. Bretschneider. These equations were later on improved by Young and Verhagen (1996):

$$\tilde{H} = \tilde{H}_\infty \left\{ \tanh(0.343 \tilde{d}^{1.14}) \cdot \tanh \left( \frac{4.41 \cdot 10^{-4} \tilde{F}^{0.79}}{\tanh(0.343 \tilde{d}^{1.14})} \right) \right\}^{0.572}$$

$$\tilde{T} = \tilde{T}_\infty \left\{ \tanh(0.10 \tilde{d}^{2.01}) \cdot \tanh \left( \frac{2.77 \cdot 10^{-7} \tilde{F}^{1.45}}{\tanh(0.10 \tilde{d}^{2.01})} \right) \right\}^{0.187}$$

in which:

$\tilde{H}$	[-]	$= \frac{gH_{m0}}{U_{10}^2}$	$\tilde{T}$	[-]	$= \frac{gT_p}{U_{10}}$
$\tilde{F}$	[-]	$= \frac{gF}{U_{10}^2}$	$\tilde{d}$	[-]	$= \frac{gd}{U_{10}^2}$
$F$	[m]	= fetch [m]			
$d$	[m/s]	= water depth [m]			
$U_{10}$	[m/s]	= wind velocity at an altitude of 10 m [m/s]			
$T_p$	[s]	= peak wave period (= most common period)			
$\tilde{H}_\infty$	[-]	= dimensionless wave height at deep water = 0,24			
$\tilde{T}_\infty$	[-]	= dimensionless wave period at deep water = 7,69			

Besides the improved Bretschneider formula given above, the Groen and Dorrestein nomograms are also very well known. These nomograms are shown in Figure 15-2 and Figure 15-3. Figure 15-2 should be used for deep and transitional water ( $d/L > 0,1$ ) and Figure 15-3 for shallow water ( $d/L < 0,1$ ). One should use these nomograms cautiously: neither is dimensionless. Because Groen and Dorrestein used different data sets than Bretschneider, their findings are not identical.

For the water depth  $d$  it is recommended by the TAW to use one value, like the average depth of a lake or river, if suitable, or the water height above a river foreland (*uiterwaard*). The influence of local deep trenches is usually neglected.

For the estimation of wave heights just in front of flood defences, it is recommended to use an effective fetch, which takes the shape of the water body into account. The effective stretch in a random situation is the weighted average of the projections  $\ell(\alpha)$  on the wind direction of all fetches in all directions  $\alpha$  (see Figure 15-1), according to:

$$F_e = \frac{\int_{-\alpha_m}^{\alpha_m} w(\alpha) \cdot \ell(\alpha) \cdot d\alpha}{\int_{-\alpha_m}^{\alpha_m} w(\alpha) \cdot d\alpha}$$

where:

$w(\alpha)$	[-]	= weight function. Recommended function is: $w(\alpha) = \cos(\alpha)$
$\ell(\alpha)$	[m]	= fetch in wind direction
$\alpha$	[°]	= deviation from wind direction in point of interest
$\alpha_m$	[°]	= boundary angle for wind directions that influence the effective fetch

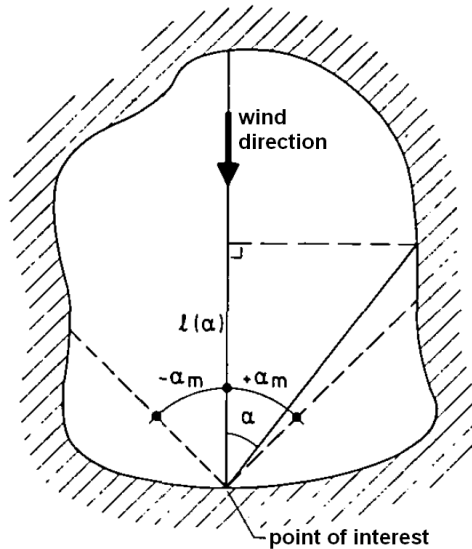


Figure 15-1 Definition sketch for determining the effective fetch (Holthuijsen, 1980)

## 15.2 The design wave height

The significant wave height  $H_s$  is the average of the highest 1/3 of the waves. This wave occurs regularly and is therefore a much lower than the design wave height  $H_d$ . If the effects of shallow water can be disregarded with a small wave height, a Rayleigh distribution can be assumed. The probability of exceedance of a given wave height within a given wave field is:

$$\Pr(H > x) = e^{-2\left(\frac{x}{H_s}\right)^2}$$

Therefore, the probability that the design wave height  $H_d$  is exceeded during a storm with  $N$  waves is:

$$\Pr(H > H_d) = 1 - e^{-N \cdot e^{-2(H_d/H_s)^2}}$$

For a storm along the coast one can assume  $T_{storm} = 2$  h. For rivers and the IJsselmeer,  $T_{storm} = 4$  h can be supposed. Presuming  $T_{wave} = 3$  s, the number of waves  $N$  along the coast is:

$$N = \frac{T_{storm}}{T_{wave}} \approx 2400$$

If one allows an exceedance probability  $\Pr(H > H_d) = 0,10$ , the design wave height  $H_d$  is:

$$H_d = 2,25 H_s$$

To ascertain the design wave length one may assume that the shape of the energy spectrum essentially does not change for light and heavy storms, so:

$$L_d \approx L_s$$

This wave can change shape because it reaches shallow water (refraction, shoaling and breaking) or obstacles (diffraction and reflection). This is treated in the next chapter.

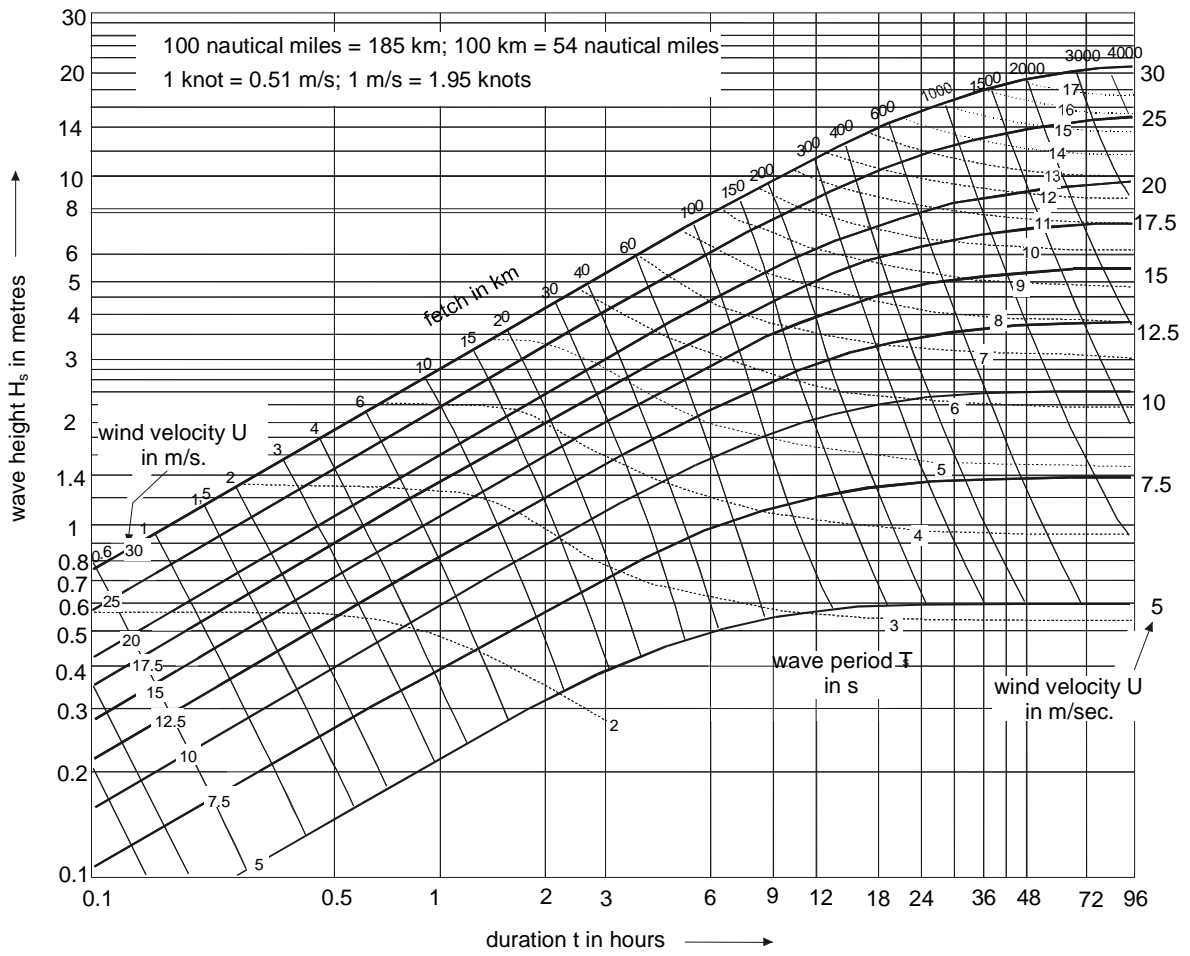


Figure 15-2 Nomogram, valid for deep and transitional water ( $d/L > 0,1$ ) (Groen and Dorrestein, 1976)

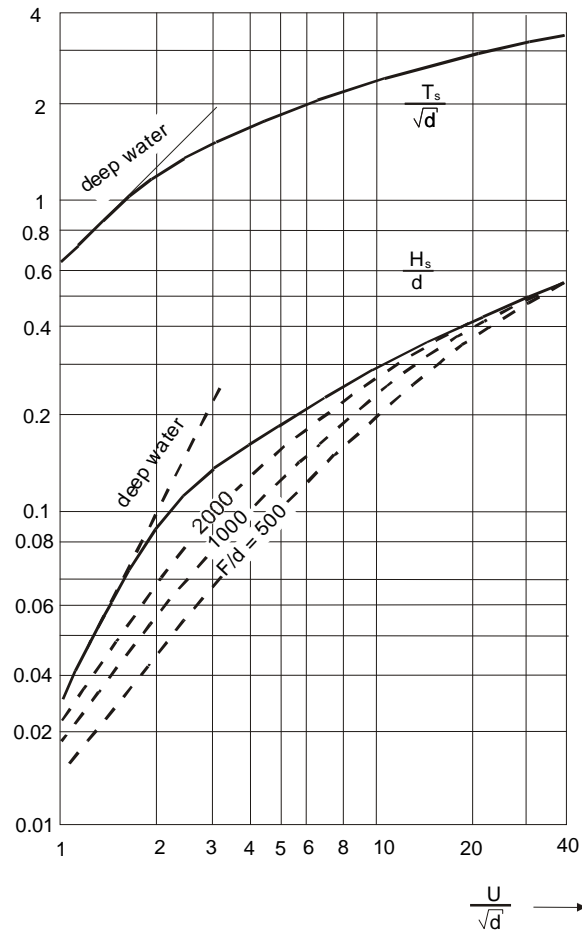


Figure 15-3 Nomogram, valid for shallow water ( $d/L < 0,1$ ) (Groen and Dorrestein, 1976)

### 15.3 Literature

Bretschneider, C.I. (1958) *Revisions in wave forecasting: deep and shallow water*. Proceedings of the 6th Conference on Coastal Engineering, pp. 30-67

Groen, P. and R. Dorrestein (1976) *Zeegolven*. Opstellen op oceanografisch en maritiem meteorologisch gebied nr. 11. Derde herziene druk. KNMI. Staatsdrukkerij- en uitgeverijbedrijf 's-Gravenhage

Holthuijsen, L.H. (1980) *Methoden voor golfvoorspelling*. TAW.

Holthuijsen, L.H. (2008) *Waves in oceanic and coastal waters*. Cambridge University Press, ISBN 978-0-521-86028-4

Young, I.R. and L.A. Verhagen (1996) *The growth of fetch-limited waves in water of finite depth. Part 1: Total energy and peak frequency*. Coastal Engineering 29, pp. 47-78

## 16. Water, waves, shallows + breaking

When waves approach the coast, a number of changes occur, caused by the change of water depth. Due to the smaller depth, the wave velocity decreases and the wave front turns so it runs increasingly parallel to the depth contours (refraction). As a result, the wave crests become narrower, the wave becomes more concentrated and the wave height increases. At the same time, the wave velocity decreases, thereby reducing the wavelength, causing a further increase of the wave height (shoaling). So, the wave height increases and the wave length reduces. At a certain point, the waves are so steep that they break. This section considers these three phenomena:

1. Refraction
2. Shoaling
3. Breaking of waves

Besides that, the effect of an obstacle is also discussed. The two most well-known consequences are:

1. Diffraction
2. Reflection

Unless stated otherwise, regular waves are assumed in this chapter.

### 16.1 Shallows: refraction

If a wave approaches a sloping coastline at an angle, the propagation velocity will vary along the wave crest due to the difference in water depth along the wave crest. After all:

$$c = \sqrt{\frac{g}{k} \tanh(kd)} = c_0 \cdot \tanh(kd)$$

In shallow water the propagation velocity is smaller. Therefore, with decreasing depth, the wavelength shortens. The wave front decelerates in the first part to reach shallow water. The wave front will thus turn. This causes a bend of the propagation velocity towards the coast. This phenomenon is known as refraction.

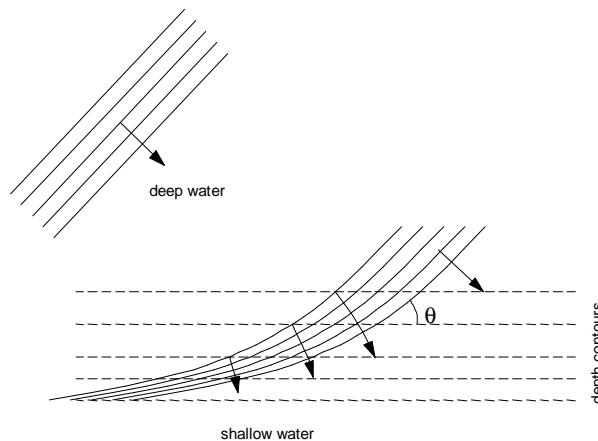


Figure 16-1 Refraction

In the case of a coast with straight parallel depth contours, the angle between the wave crest and a contour line can be derived directly from the local depth and the angle between the wave crests and a parallel contour line in deep water (Figure 16-1). This relation is called Snell's law and reads as follows:

$$\frac{\sin(\theta_1)}{\sin(\theta_0)} = \tanh(k_1 d_1) \quad \text{for:} \quad \frac{\sin(\theta_1)}{\sin(\theta_0)} = \frac{c_1}{c_0} = \frac{c_0 \tanh(k_1 d_1)}{c_0} = \tanh(k_1 d_1) = \frac{L_1}{L_0}$$

in which:  $\theta_0$  = the angle between the wave crest and the contour line in deep sea

$\theta_1$  = the angle between the wave crest and the contour line in shallow water

**From shallow to deep**

If one knows the angle of the wave ray, the wave height and wavelength in shallow water, one can calculate the wave ray angle in deep water using the above equation or the dotted line in Figure 16-2.

**From deep to shallow**

If the angle of the wave ray, the wave height and the wavelength in deep water are known, the angle of the wave ray in shallow water cannot be calculated using the equation above. The equation requires the wavelength in shallow water, for which the following applies:

$$L_1 = L_0 \tanh(k_1 d_1) \quad \text{met:} \quad k_1 = \frac{2\pi}{L_1}$$

So  $\frac{\sin(\theta_1)}{\sin(\theta_0)}$  as a function of  $d/L_0$  is an implicit function, which has to be solved iteratively. The inverse solution is given as a solid line in the graph below, plotted against the relative water depth  $d/L_0$  (water depth  $d$  in shallow water, divided by the wavelength  $L_0$  in deep water).

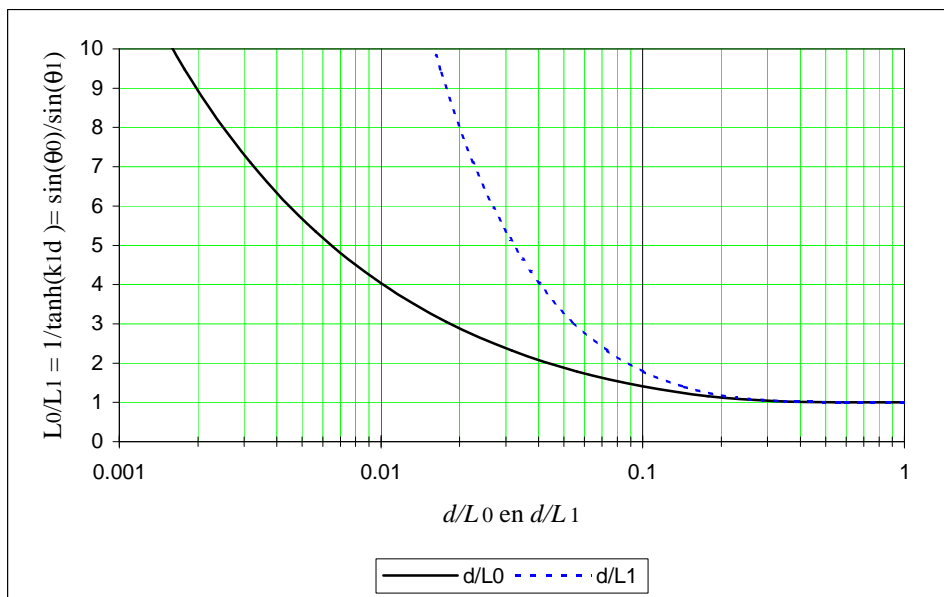


Figure 16-2 Relation between depth and wavelength ( $d$  = depth,  $L_1$  = wavelength at considered depth,  $L_0$  = wavelength in deep water)

Depending on the concentration or spread of wave rays, the wave height will increase or decrease. Generally, for the wave height in shallow water:

$$H = K_s K_r H_0$$

in which:  $K_r$  [-] = the refraction coefficient  
 $K_s$  [-] = the shoaling coefficient (see next section)

In the case of straight parallel depth contours, the wave height decreases with a factor:

$$K_r = \sqrt{\frac{b_0}{b_1}} = \sqrt{\frac{\cos(\theta_0)}{\cos(\theta_1)}}$$

with:  $b$  = the wave crest width

This is because the wave crest width  $b$  continues to increase while the wave crest turns, which causes a reduction of the energy density and thus also of the wave height. The change of wavelength in shallow water also leads to a change of the energy density and the wave height, but that phenomenon is called shoaling and is covered in the next section.

Refraction also occurs when a wave enters an area with a current (along the coast). In this case, the wave will turn more or less in the direction of the current.

## 16.2 Shallows: shoaling

When the water depth decreases, the propagation velocity and the wavelength are reduced with a constant period. This influences the wave height.

### Theory

Chapter 14 showed that the wave energy per unit of surface area equals:

$$E = \frac{1}{8} \rho g H^2$$

The group velocity is:

$$c_g = n c \quad \text{with} \quad n = \frac{1}{2} + \frac{k d}{\sinh(2 k d)} \quad \text{and} \quad c = \sqrt{\frac{g}{k} \tanh(k d)} = c_0 \cdot \tanh(k d)$$

The energy flux is the amount of energy that passes a certain point per unit of width. This energy flux equals:

$$F = E \cdot c_g = \text{constant}$$

and is constant for non-breaking waves (no loss of energy) and straight approaching waves (no change of width).

The wave height is therefore:

$$H^2 = \frac{\text{constant}}{n \cdot c}$$

The wave height in a shallow area,  $H_1$ , is therefore dependent on the wave height in deep water,  $H_0$ , according to:

$$\frac{H_1}{H_0} = K_s = \sqrt{\frac{c_{g,0}}{c_{g,1}}} = \sqrt{\frac{c_0 n_0}{c_1 n_1}} = \sqrt{\frac{1}{\tanh(k d) n_1}} = \sqrt{\frac{1}{\tanh(k d) \left(1 + \frac{2 k d}{\sinh(2 k d)}\right)}}$$

The shoaling coefficient is therefore a function of the wave number  $k$  and the water depth  $d$ :

$$K_s = \frac{1}{\sqrt{\tanh(k d) \left(1 + \frac{2 k d}{\sinh(2 k d)}\right)}} \quad \text{with:} \quad k d = 2\pi \frac{d}{L}$$

This solution is represented by the dotted line in the figure below. If the wave height and wavelength are known in a certain shallow area, these can be used to calculate the wave height in deep water. The inverse, using this solution and a known wave height and a known wave length in deep water to calculate the wave height in shallow water is not possible. The problem is that  $L$  and thus also  $k$  are dependent on the depth  $d$  and on themselves, for:

$$L = L_0 \tanh(k d) = L_0 \tanh\left(\frac{2\pi d}{L}\right)$$

This is an implicit function. The shoaling coefficient, a function of the water depth  $d$  and wavelength in deep water  $L_0$ , can therefore only be solved iteratively. This solution is represented by the solid line in Figure 16-3.

Besides shoaling, refraction also influences the wave height, for this see the previous section.

### (Preliminary) design

The wave height  $H_1$  of regular (non-breaking) waves in shallow water depends on the wave height in deep water  $H_0$ , the refraction coefficient  $K_r$ , and on the shoaling coefficient  $K_s$ , according to:

$$H_1 = K_r K_s H_0$$

In Figure 16-4 the shoaling coefficient is given as a function of the relative water depth (water depth  $d$  in shallow water, divided by the wavelength  $L_0$  in deep water).

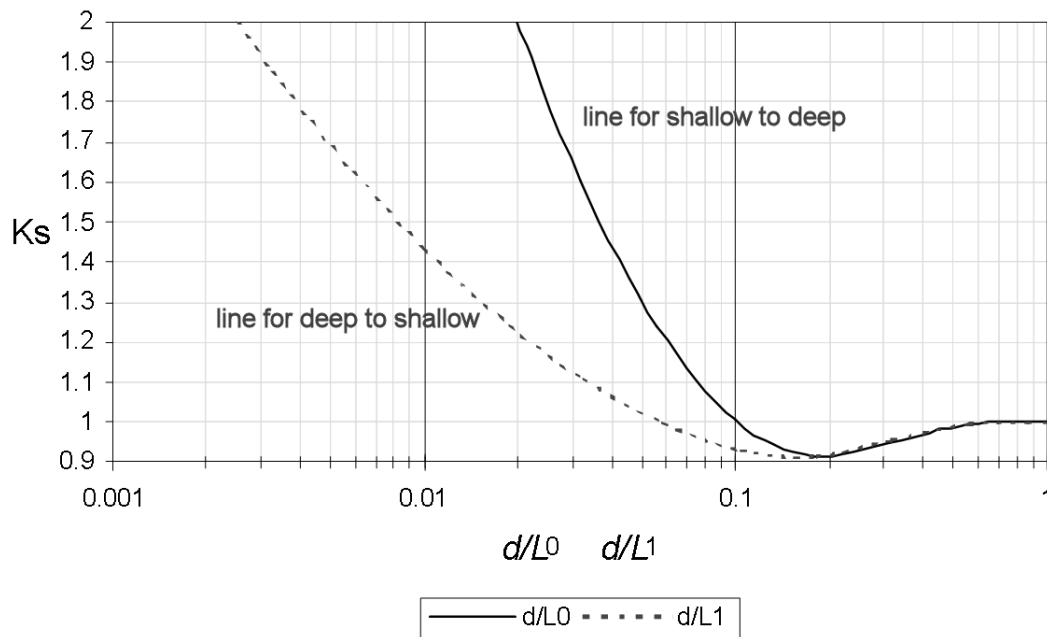


Figure 16-3 Relation between  $K_s$  and  $d/L$  ( $L$  = wavelength at considered depth,  $L_o$  = wavelength at deep sea)

For the refraction parameter, the following equation has been found:

$$K_r = \sqrt{\frac{\cos(\theta_o)}{\cos(\theta_1)}}$$

To calculate the refraction ( $\theta_o \Rightarrow \theta_1$ ), see previous section.

The theory given above only applies for regular waves that don't break (or haven't yet broken).

### 16.3 Shallows: breaking waves

Distinction should be made between individual waves (for the calculation of loads on structures) and significant waves (for the calculation of run-up, overtopping, stability of stones).

#### Individual waves

Due to the decreasing wavelength and the increasing wave height in shallow areas, the steepness of the wave increases. Waves will theoretically break if they become too steep, or if the water depth becomes too little with respect to the wave height:

- $\frac{H}{L} \geq \frac{1}{7}$

or:

- $\frac{H}{d} \geq 0,78$

There are also more complex formulas for the shallowness criterion, e.g. by Miche. In spite of the theoretically deduced criterion, individual non-breaking waves with a ratio of  $H/d = 1,2$  have been observed under very specific circumstances.

#### Significant waves

When calculating breaking for a wave spectrum, the significant wave height  $H_s$  should be used. This is the average height of the 1/3 highest waves. It is often assumed that breaking occurs if

- $\frac{H_s}{d} \geq 0,4$  to  $0,5$

The way in which a wave breaks on a smooth slope with a constant slope angle depends on the steepness of the wave and the slope of the bed. This is characterised with the breaker parameter (Iribarren):

$$\xi = \frac{\tan \alpha}{\sqrt{H_s/L_o}}$$

in which:  $\alpha$  [°] = angle of the slope  
 $H_s$  [m] = significant wave height  
 $L_o$  [m] = wavelength in deep water

Depending on the value of the breaker parameter, different types of breaking occur, as is shown in Figure 16-4.

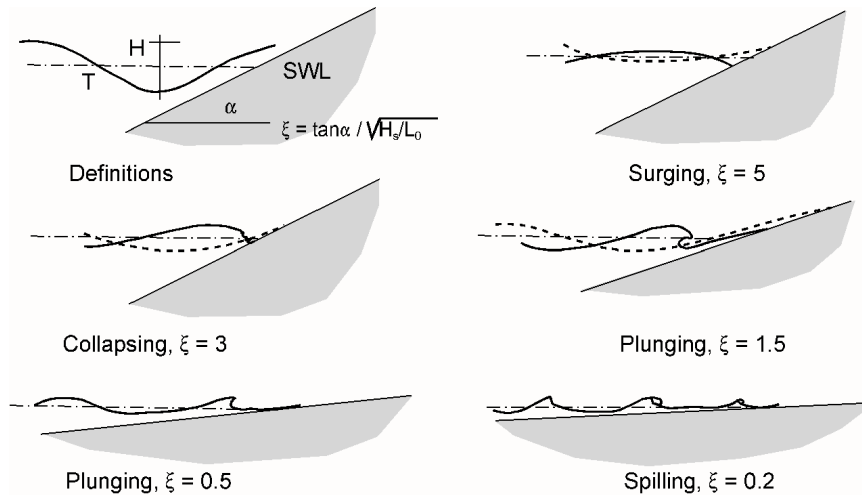


Figure 16-4 Types of breaking

**Notes**

- The depth profile need not be constant in time. Shallows can appear or disappear. It is therefore important to find out if the bed consists of rock or sand.
- The depth can depend on the tide and on the wind set-up (storm surge).
- Changes of depth also mean changes of refraction, shoaling and breaking.

The validity of wave theories is depicted in Figure 16-5.

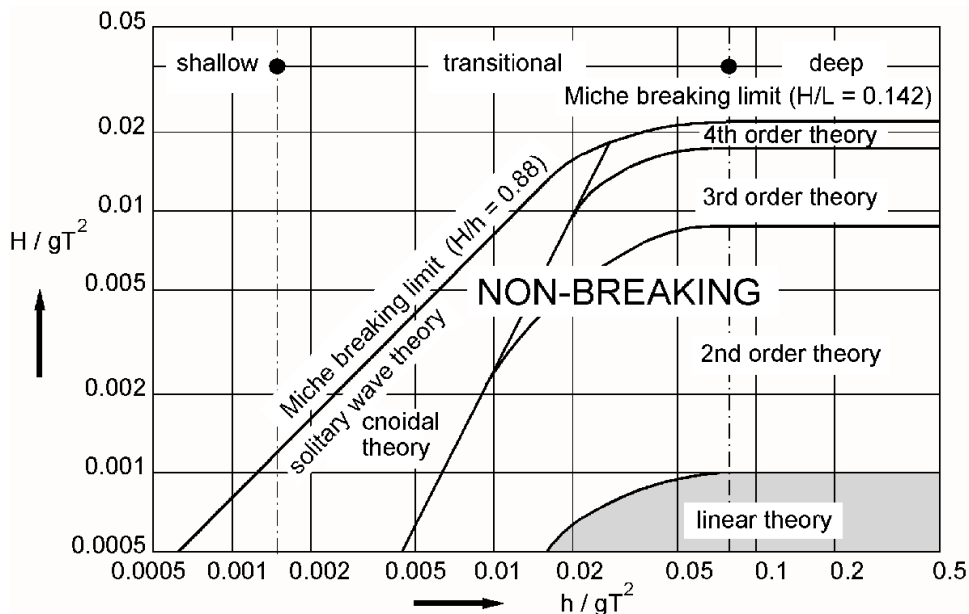


Figure 16-5 Validity of wave theory (Le Méhauté, 1976 / Introduction to bed, bank and shore line protection, CIE4310)

## 16.4 Obstacle: reflection

If waves run into a structure they can break or reflect. The reflection can be partial or complete. Characteristics of completely reflected waves are:

- the energy of the reflected wave equals the energy of the incoming wave
- the period of the reflected wave equals the period of the incoming wave
- the reflected wave is in phase with the incoming wave.

The consequence of the above is that a standing wave with (in case of complete reflection) a wave height twice the size of an incoming wave is created in front of the structure. If the reflection is partial, the wave height of the standing wave will be less. In general the following applies:

$$H = (1 + \chi) \cdot H_i$$

in which:  $H$  [m] = the wave height of the standing wave  
 $H_i$  [m] = the wave height of the incoming wave  
 $\chi$  [-] = the reflection coefficient  $\leq 1$

The value of  $\chi$  depends on the permeability, roughness and slope of the structure and on the steepness of the incoming waves and the water depth in front of the structure.

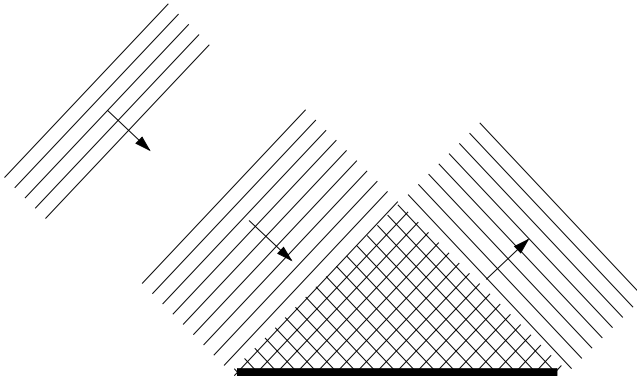


Figure 16-6 Reflection

The load on the wall can be calculated according to Chapter 18 "Water, waves, wall, non-breaking".

## 16.5 Obstacle: diffraction

If there's an obstacle in the course of a wave (e.g. a breakwater or an island), wave motion still occurs in the shadow zone behind the obstacle. The transfer of energy apparently not only takes place in the wave direction. The wave crests bend round the object shaped like circular arcs. This phenomenon is called diffraction.

The wave height changes due to diffraction, whereby the wave height on the lee side of the object is smaller than that of the incoming wave, whilst the wave height next to the object is often larger than that of the incoming wave.

Generally:

$$H = K_d H_o$$

where:  $K_d$  [-] = the diffraction coefficient

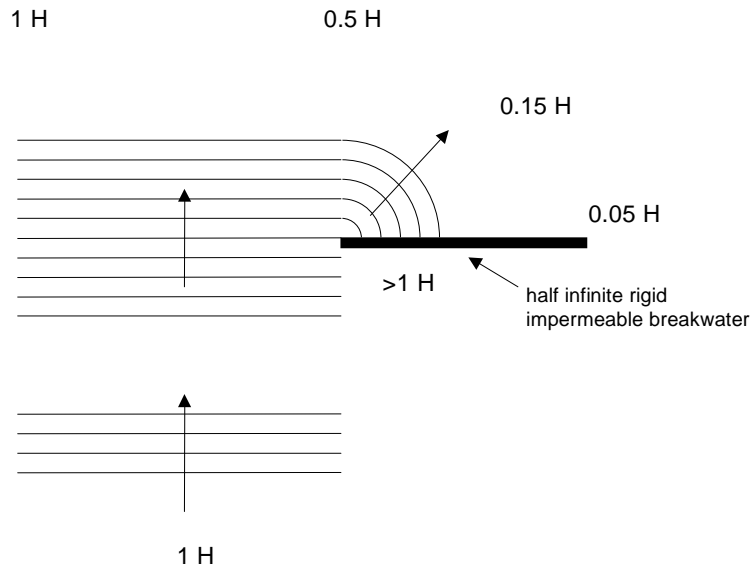


Figure 16-7 Diffraction

The "Shore Protection Manual" (CERC 1984) gives a large number of diagrams for the estimation of  $K_d$  with different wave directions. The Shore Protection Manual can be found on the internet on [www.google.com](http://www.google.com) with search request 'coastal engineering manual'. Figure 16-8 is taken from the book 'Oceanographical Engineering' by Robert Wiegel (1964). It shows the diagram for waves moving straight towards a breakwater. The distances in x- and y-direction are divided by the wavelength  $L$ .

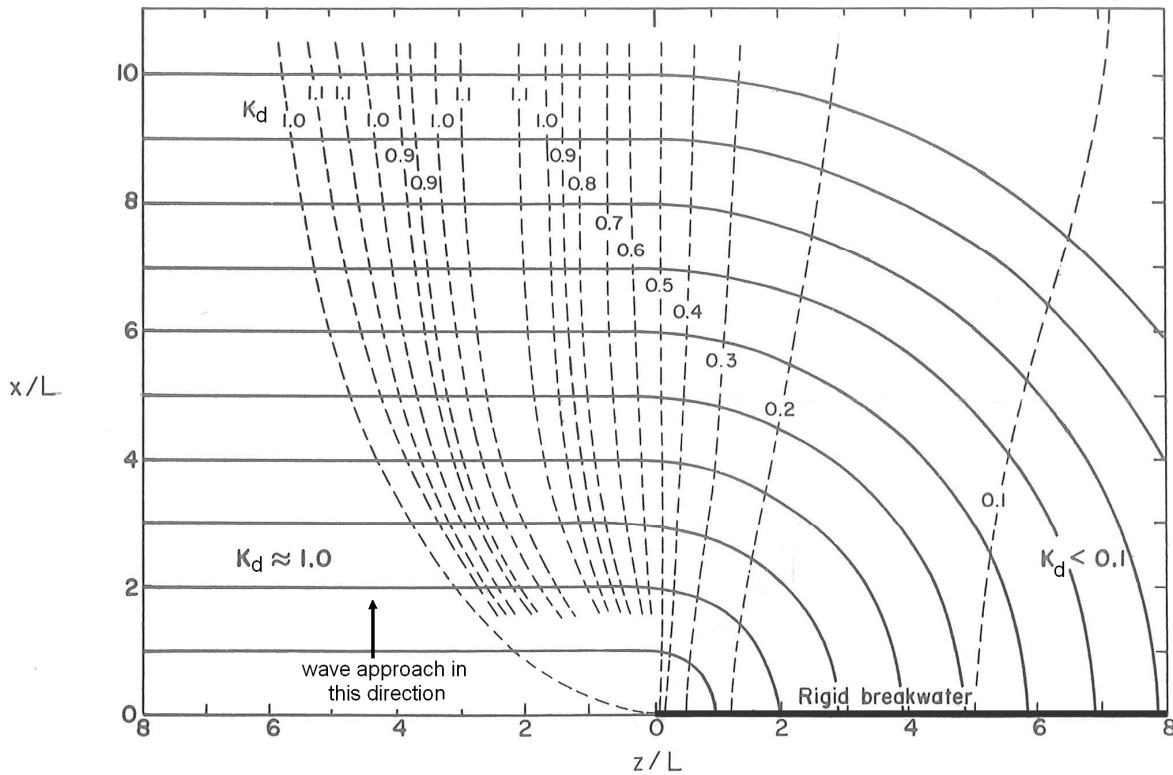


Figure 16-8 Diffraction coefficients for straight incoming waves (Wiegel, 1964)

For waves approaching from other directions relative to the breakwater, reference is made to literature, like *Diffraction of periodic sea waves along a vertical breakwater* by Penny and Price (1952).

## 17. Water, waves, run-up + overtopping

SLS overtopping requirements added: February 2016

For the design of slanting structures (a slope or a wall) it is important to know how far a wave can run up the slope, or how much water can go over the structure. In the first place, this depends on the average water level (= tide + wind set-up) and in the second place on the height of the waves attacking the structure.

This chapter covers the following two phenomena:

1. Wave run-up (*golfooploop*)
2. Wave overtopping (*golfoverslag*)

These phenomena play a role in determining the crest height of flood defences and the top of structure level of other hydraulic structures.

### 17.1 Wave run-up

#### General

The wave run-up  $R$  is the vertical distance between the average water level and the highest point on a slope that is reached by water running up the slope. This applies for both breaking and non-breaking waves (see Figure 17-1).

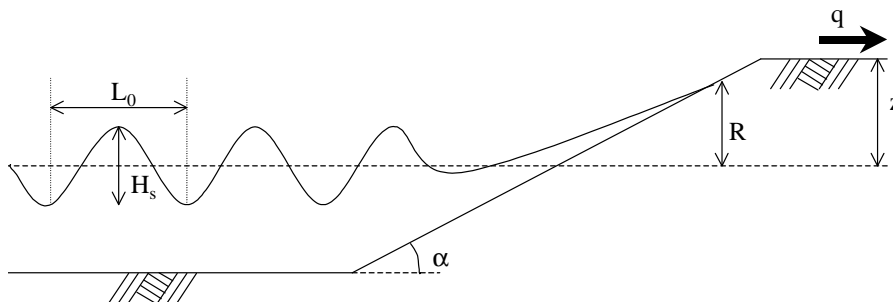


Figure 17-1 Wave run-up

The wave run-up depends on:

- The wave field
- The geometry of the flood defence
- The roughness of the surface

The Dutch Delta Committee assumed that a dike would fail if 40 to 60 waves would have overtopped the dike (caused by failure of the inner slope). This is about 2% of the number of waves in an average storm along the Dutch coast. As a rule of thumb, the following 'old Delft formula' could be used to calculate the crest freeboard related to an acceptable amount of run-up on dikes:

$$R_{2\%} = 8 \cdot H_s \cdot \tan(\alpha)$$

where:

- |           |     |   |
|-----------|-----|---|
| $R_{2\%}$ | [m] | = the value of run-up exceeded by 2% of the waves |
| $H_s$     | [m] | = the significant wave height                     |
| $\alpha$  | [°] | = the angle of the slope with the horizontal      |

This old Delft formula is valid for the Dutch coast under storm conditions and:

- relatively gentle slopes (1:3)
- "normal" wave steepness (between 4 and 5%)

With help of some extra parameters the old Delft formula can be made a bit more sophisticated:

$$R_{2\%} = 8 \cdot H_s \cdot \tan(\alpha) \cdot \gamma_f \cdot \gamma_b \cdot \gamma_\beta$$

where:

- $\gamma_f$  [-] = factor taking the slope roughness into account
- $\gamma_b$  [-] = berm influence factor
- $\gamma_\beta$  [-] = influence factor for oblique wave attack

(See below for an explanation of these factors)

I.A. Hunt found out that the factor of '8' in the old Delft formula actually is related to the wave steepness, which can be represented by the breaker parameter (Iribarren parameter)  $\xi$  (see section 16.3):

$$R_u = f(\xi) \cdot H_s,$$

or to be more precise:

$$R_{u2\%} = 1,5 \cdot \gamma_f \cdot \gamma_b \cdot \gamma_\beta \cdot H_s \cdot \xi_p$$

where the maximum of  $R_{u2\% \max} = 3 \cdot H_s$

J.W. van der Meer fine-tuned Hunt's equation. For deterministic calculations it reads:

$$R_{2\%} = 1,75 \cdot \gamma_b \cdot \gamma_f \cdot \gamma_\beta \cdot \xi_{m-1,0} \cdot H_{m0} \quad \text{with a maximum of:} \quad R_{2\%, \max} = 1,00 \cdot \gamma_f \cdot \gamma_\beta \cdot \left( 4,3 - \frac{1,6}{\sqrt{\xi_{m-1,0}}} \right) \cdot H_{m0}$$

where the breaker parameter (Iribarren parameter) is defined by:

$$\xi_{m-1,0} = \frac{\tan \alpha}{\sqrt{H_{m0} / L_0}} = \frac{\tan \alpha}{\sqrt{H_s / (1,56 \cdot T_{m-1,0}^2)}}$$

$H_{m0}$  = estimate of the significant wave height from spectral analysis =  $4\sqrt{m_0}$ .  $H_{m0} \approx H_s$   
 $T_{m-1,0}$  is a calculated wave period that follows from the wave spectrum. In about 80% of the cases,  
 $T_{m-1,0} \approx 0,9 \cdot T_p$

The Van der Meer equation has been adopted by the CUR-TAW-guidelines and the European Overtopping Manual (see Section 17.2 for more background on this Manual). A definition sketch is presented in Figure 17-1.

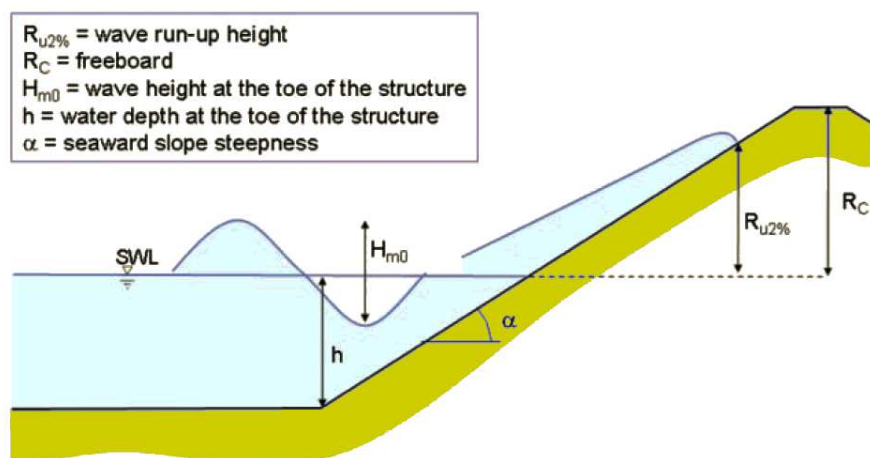


Figure 17-1 Definition of some parameters for the calculation of overtopping [European Overtopping Manual 2007]

**Roughness (factor  $\gamma_f$ )**

The reduction factor  $\gamma_f$  that takes the roughness and the permeability of the surface into account is:

- 1,00 for asphalt, concrete with a smooth surface
- 0,95 for concrete blocks, block mats
- 0,70 for gravel, gabions
- 0,60 for quarry stone (rip-rap)
- 0,50 for cubes (random positioning)
- < 0,50 for X-blocs, tetrapods, dollosses (see European Overtopping Manual for more data)

**Berm influence (factor  $\gamma_b$ )**

A berm reduces the wave run-up and its influence can be taken into account by using a berm influence factor  $\gamma_b$  (also known as the *shoulder reduction factor*). The magnitude of the berm influence factor depends on the length of the berm  $B_b$  and the water depth above the berm  $h_B$ .

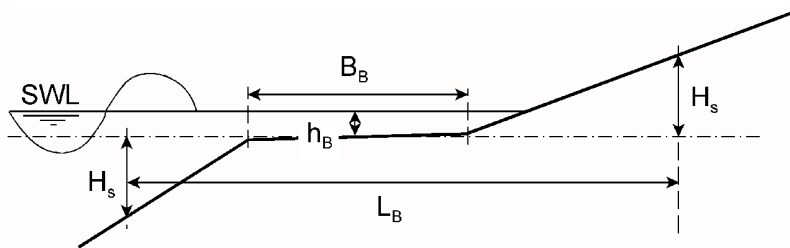


Figure 17-2 Definitions berm reduction

At both sides of the berm, the slope is intersected at a vertical distance  $H_S$  from the horizontal centre plane of the berm, giving a length  $L_B$ .  $h_B$  is the distance between SWL and the berm level (can be negative or positive).  $\gamma_b$  finally becomes:

$$\gamma_b = 1 - \frac{B_B}{L_B} \left[ 0,5 + 0,5 \cos \left( \pi \frac{h_B}{x} \right) \right]$$

$$x = z_{2\%} \quad \text{for } z_{2\%} > -h_B > 0 \quad (\text{berm above SWL})$$

$$x = 2H_S \quad \text{for } 2H_S > h_B \geq 0 \quad (\text{berm below SWL})$$

With limits:  $0,6 \cdot \gamma_b < 1$ . The equation above shows that a berm on SWL is most efficient. For more information, see TAW (2002).

If there is no berm, no berm influence factor should be used in overtopping or run-up calculations.

**Angle of incidence (factor  $\gamma_\beta$ )**

For oblique waves the angle of wave attack is defined as the angle between the direction of propagation of waves and the axis perpendicular to the structure (for perpendicular wave attack:  $\beta = 0^\circ$ ). For short-crested waves:

$$\gamma_\beta = 1 - 0,0022 \beta \quad \text{for } : 0^\circ \leq \beta \leq 80^\circ$$

$$\gamma_\beta = 0,824 \quad \text{for } \beta > 80^\circ$$

So, at an angle of  $80^\circ$  (fetch waves) the reduction is only 18%, compared to perpendicular wave attack.

**Foreshore reduction**

On very shallow foreshores waves will break; the wave spectrum transforms and is flattened. Also the waves are no longer Rayleigh-distributed. According to TAW (2002) one should use for the calculation of  $\xi$  not the  $T_{m0}$ , but the  $T_{m-1,0}$ , which is  $m_1/m_0$  (the first negative moment of the spectrum divided by the zero order moment of the spectrum). In case no detailed spectrum information is available, one may use  $T_{m-1,0} \approx 0,9 T_p$ . For the wave height on the shallow foreshore one should use the  $H_{m0}$  on the foreshore.

**Example wave run-up**

Given a sea dike with a slope on gabions, steepness 1:4 and no berm. The waves are perpendicular to the dike and  $H_s = 2,5$  m,  $T_p = 8$  s.

How much is the run-up ( $R_{2\%}$ )?

Using the old Delft Formula:  $R = 8 \cdot 2,5 / 4 = 5,0$  m

Using the CUR-TAW equation:

$T_{m-1,0} = 0,9 \cdot T_p = 7,2$  s (in this example)

$$\xi = \frac{\tan \alpha}{\sqrt{H/L}} = \frac{0,25}{\sqrt{2,5 / (1,56 \cdot 7,2^2)}} = 1,42$$

$\gamma_f = 0,70$  (gabions)

$R_{2\%} = 1,75 \cdot 2,5 \cdot 1,42 \cdot 0,70 = 4,35$  m ( $< 0,70 \cdot (4,3 - 1,6/\sqrt{1,42}) = 5,18$  m)

**17.2 Wave overtopping**

Overtopping waves can jeopardise a civil engineering work if they cause erosion or softening of the foundations. Wave overtopping can also cause a nuisance for the surroundings. To prevent severe wave overtopping, the design of the structure should therefore include a sufficient freeboard above the design water level.

For wave overtopping considerations, the wave run-up  $R_n$  simply exceeds the crest height  $z$ . The wave overtopping is usually characterised by an overtopping discharge  $q$  per metre of the water defence, averaged over time. This discharge depends on the wave height, the wave steepness, the slope and the existing freeboard. This concerns overtopping discharges averaged over time. In reality, a far larger discharge can occur for a short time, depending on the percentage of overtopping waves. With the results of several investigations, a global relationship between all of these factors can be derived.

In the Netherlands, the old 2%-run-up requirement has been replaced by critical overtopping discharges (TAW, Leidraad Zee- en Meerdijken, 1999).

**Overtopping of structures with a slope**

In August 2007, the EurOtop team released the "Wave Overtopping of Sea Defences and Related Structures: Assessment Manual", in short: "European Overtopping Manual" (EurOtop team 2007). That manual gives "guidance on analysis and/or prediction of wave overtopping for flood defences attacked by wave action." It replaces the older Dutch "Technical Report Wave Run-up and Wave Overtopping at Dikes" of TAW, Technical Advisory Committee on Flood Defences, author: J.W. van der Meer, and two other (foreign) reports.

The Overtopping Manual gives maximum overtopping discharges, to be used for the design of hydraulic structures where waves could overtop. Distinction should be made between serviceability limit state (SLS) and ultimate limit state (ULS) requirements. ULS requirements concern the structural integrity (structural safety) of the hydraulic structure itself. SLS requirements are related to the direct impact on pedestrians, vehicles and property behind the defence. Maximum overtopping discharges and volumes are given in Table 17-1 for ULS and Table 17-2 for SLS.

Next to these ULS and SLS requirements, the storage capacity of the water system behind the defence could restrict the allowable overtopping volume. This could become more critical if sea water overtops into a fresh water basin or lake (regarding salt intrusion).

Hazard type and reason	mean discharge $q$ (l/s/m)
<b>Embankment seawalls / sea dikes</b>	
No damage if crest and rear slope are well protected	50-200
No damage to crest and rear face of grass covered embankment of clay	1-10
No damage to crest and rear face of embankment if not protected	0,1
<b>Promenade or revetment seawalls</b>	
Damage to paved or armoured promenade behind seawall	200
Damage to grassed or lightly protected promenade or reclamation cover	50

Table 17-1 ULS requirements for overtopping [*European Overtopping Manual 2007*]

Hazard type and reason	mean discharge $q$ (l/s/m)	max. volume $V_{max}$ (l/m)
<b>For pedestrians</b>		
Trained staff, well shod and protected, expecting to get wet; overtopping flows at lower levels only, no falling jet, low danger of fall from walkway	1 - 10	500 at low level
Aware pedestrian, clear view of the sea, not easily upset or frightened, able to tolerate getting wet, wider walkway	0,1	20 - 50 at high level or velocity
<b>For vehicles</b>		
Driving at low speed, overtopping by pulsating flows at low flow depths, no falling jets, vehicle not immersed	10 - 50	100 - 1000
Driving at moderate or high speed, impulsive overtopping giving falling or high velocity jets	0,01 - 0,05	5 - 50 at high level or velocity
<b>For property behind the defence</b>		
significant damage or sinking of larger yachts	50	5000 - 50 000
sinking small boats set 5 - 10 m from wall; damage to larger yachts	10	1000 - 10 000
Building structure elements	1	-
Damage to equipment set back 5 - 10 m	0,4	-

Table 17-2 SLS requirements for overtopping [*European Overtopping Manual 2007*]

The principal equation used for wave overtopping is:

$$\frac{q}{\sqrt{g \cdot H_{m0}^3}} = a \cdot e^{\left(\frac{-b R_c}{H_{m0}}\right)}$$

where:

$$\frac{q}{\sqrt{g \cdot H_{m0}^3}} \quad [-] \quad = \quad \text{dimensionless overtopping discharge}$$

$$q \quad [\text{m}^3/\text{s}/\text{m}] \quad = \quad \text{overtopping discharge}$$

$$\frac{R_c}{H_{m0}} \quad [-] \quad = \quad \text{the relative crest freeboard}$$

$$R_c \quad [\text{m}] \quad = \quad \text{crest height}$$

$$H_{m0} \quad [\text{m}] \quad = \quad \text{estimate of significant wave height from spectral analysis} = 4\sqrt{m_0} \approx H_s$$

(See Figure 17-1 for a definition sketch)

Further needed parameters according to the Overtopping Manual:

$$a \quad [-] = \frac{0,067}{\sqrt{\tan \alpha}} \gamma_b \cdot \xi_{m-1,0}$$

$$b \quad [-] = \frac{4.3}{\xi_{m-1,0} \cdot \gamma_b \cdot \gamma_f \cdot \gamma_\beta \cdot \gamma_v}$$

$\xi_{m-1,0}$  [-] = breaker parameter (see previous section)

$\gamma_b$  [-] = influence factor of a berm (see previous section)

$\gamma_f$  [-] = influence factor for the permeability and roughness of the slope, sometimes written as  $\gamma_R$  (see previous section)

$\gamma_\beta$  [-] = factor for oblique wave attack

$$\gamma_\beta = 1 - 0,0033|\beta| \quad \text{for } 0^\circ \leq \beta \leq 80^\circ$$

$$\gamma_\beta = 0,736 \quad \text{for } \beta > 80^\circ$$

Note:  $\gamma_\beta$  has different values for run-up and overtopping calculations!

$\gamma_v$  [-] = influence factor for a vertical wall on top of the crest (see below)

The breaker parameter also referred to as surf similarity or Iribarren number is defined as:

$$\xi_{m-1,0} = \frac{\tan \alpha}{\sqrt{H_{m0} / L_{m-1,0}}}$$

where  $\tan \alpha$  is the slope of the front face of the structure and  $L_{m-1,0}$  being the deep water wave length:

$$L_{m-1,0} = \frac{g \cdot T_{m-1,0}^2}{2 \cdot \pi} \quad [\text{m}]$$

In another shape, the overtopping equation reads:

$$q = a \cdot e^{\left(\frac{-b R_c}{H_{m0}}\right)} \cdot \sqrt{g \cdot H_{m0}^3},$$

which is valid for  $\xi_{m-1,0} < 5,0$ . In case of shallow foreshores, other formulas are recommended.

The European Overtopping Manual gives a maximum of  $q_{\max} = 0,2 \cdot e^{\left(\frac{-2,3 \cdot R_c}{H_{m0} \cdot \gamma_f \cdot \gamma_\beta}\right)} \cdot \sqrt{g \cdot H_{m0}^3}$ .

The wave steepness  $s_0$  ( $= H_{m0} / L_{m-1,0}$ ) can vary from 0,04 (steep storm waves) and 0,01 (long waves due to swell or wave breaking).

### Influence of vertical walls on top of a slope (factor $\gamma_v$ )

The reduction due to relatively small vertical walls on top of the slope can amount up to 35%. This topic has to be studied further, but based on experience up to now the next equation could be applied:

$$\gamma_v = 1,35 - 0,0078 \cdot \alpha_{\text{wall}}$$

where  $\alpha_{\text{wall}}$  is the slope of the wall (for vertical walls,  $\alpha_{\text{wall}} = 90^\circ$ ).

The European Overtopping Manual restricts the equation above to the next conditions:

- the average slope of  $1,5 H_{m0}$  below the still water line to the foot of the wall (excluding a berm) must lie between 1 : 2,5 to 1 : 3,5.
- the width of all berms together must be no more than  $3 H_{m0}$ .
- the foot of the wall must lie between about  $1,2 H_{m0}$  under and above the still water line;
- the minimum height of the wall (for a high foot) is about  $0,5 H_{m0}$ . The maximum height (for a low foot) is about  $3 H_{m0}$ .

If there is no vertical wall on top of a slope, of course no correction factor  $\gamma_v$  should be used in the overtopping calculation.

**Example: Overtopping**

Consider a sea dike like in Figure 17-1 with a smooth slope and a crest height  $R_c = 1,5$  m. The slope is 1:3, which corresponds with an angle  $\alpha$  of  $18^\circ$ . There is no vertical wall on top of the slope.

Wave parameters:

$$H_{m0} = 2 \text{ m}$$

$$L_{m-1,0} = 50 \text{ m}$$

the approach angle  $\beta$  is  $20^\circ$

Calculate the overtopping discharge during a storm.

**Solution:**

$$\gamma_b = 1,0$$

$$\gamma_f = 1,0$$

$$\gamma_\beta = 1 - 0,0033 \cdot 20 = 0,934$$

$$\gamma_v = 1,0$$

$$\xi_{m-1,0} = \frac{\tan \alpha}{\sqrt{H_{m0}/L_{m-1,0}}} = \frac{\tan(18^\circ)}{\sqrt{0,04}} = 1,62$$

( $H_{m0}/L_{m-1,0} = 0,04$  for storm waves)

$$a = \frac{0,067}{\sqrt{\tan \alpha}} \cdot \gamma_b \cdot \xi_{m-1,0} = \frac{0,067}{\sqrt{\tan 18^\circ}} \cdot 1 \cdot 1,62 = 0,19$$

$$b = \frac{4,3}{\xi_{m-1,0} \cdot \gamma_b \cdot \gamma_f \cdot \gamma_\beta \cdot \gamma_v} = \frac{4,3}{1,62 \cdot 1,0 \cdot 1,0 \cdot 0,934 \cdot 1,0} = 2,84$$

$$q = a \cdot e^{\left(\frac{-b \cdot R_c}{H_{m0}}\right)} \cdot \sqrt{g \cdot H_{m0}^3} = 0,19 \cdot e^{\left(\frac{-2,84 \cdot 1,5}{2}\right)} \cdot \sqrt{9,81 \cdot 2,0^3} = 0,200 \text{ m}^3/\text{s/m} = 200 \text{ l/s/m}$$

What would happen if the dike would be 2 meter higher?

$$q = a \cdot e^{\left(\frac{-b \cdot R_c}{H_{m0}}\right)} \cdot \sqrt{g \cdot H_{m0}^3} = 0,19 \cdot e^{\left(\frac{-2,84 \cdot 3,5}{2}\right)} \cdot \sqrt{9,81 \cdot 2,0^3} = 0,012 \text{ m}^3/\text{s/m} = 12 \text{ l/s/m}$$

**Overtopping of vertical walls**

This section deals with wave overtopping over entire vertical walls, so not with (relatively small) vertical walls on top of a slope. To calculate the amount of wave overtopping over vertical walls or vertical structures like caisson breakwaters and navigation locks (including the gates), Franco and colleagues proposed the following equation (Franco et. al., 1994):

$$\frac{q}{\sqrt{g \cdot H_s^3}} = a \cdot e^{-b \frac{R_c}{\gamma \cdot H_s}}$$

where:

$R_c$	[m]	= crest freeboard
$q$	[m <sup>3</sup> /m/s]	= specific discharge
$a, b$	[-]	= empirical coefficients
$\gamma$	[-]	= geometrical parameter
$H_s$	[m]	= significant wave height
$g$	[m/s <sup>2</sup> ]	= gravity acceleration

For rectangular shapes:  $a = 0,192$ ,  $b = 4,3$ ,  $\gamma = 1$ .

In the European Overtopping Manual two types of wave conditions in front of the vertical wall are distinguished: If the waves are relatively small compared to the local water depth, or in case of gentle wave steepnesses, they will not critically influenced by the toe or approach slope of the structure. The resulting loads on the structure are rather smooth-varying. These conditions are called 'non-impulsive'. The other type of conditions, the 'impulsive' conditions, occurs if the waves are larger in relation to the local water depth. Some waves will break violently against the wall with forces up to 40 times more than under non-impulsive conditions. This also leads to higher overtopping volumes.

Whether or not the wave conditions are impulsive, can be determined with help of the impulsiveness parameter  $h^*$ . Conditions are considered to be impulsive if  $h^* < 0,2$  and non-impulsive if  $h^* > 0,3$ . For the intermediate range overtopping volumes should be calculated for both conditions and the largest value should be used for the design.

The impulsiveness parameter can be calculated according to:

$$h^* = 1,35 \frac{h_s}{H_{m0}} \cdot \frac{2\pi h_s}{g T_{m-1,0}^2}$$

where:

$h_s$ [m]	=	water depth at the front of the structure
$H_{m0}$ [m]	=	estimate of significant wave height from spectral analysis $\approx H_s$
$g$ [m/s <sup>2</sup> ]	=	gravity acceleration
$T_{m-0,0}$ [s]	=	average wave period (defined by $m_{-1}/m_0$ )

The overtopping volumes for deterministic design can then be calculated according to:

$$\frac{q}{h^2 \sqrt{g h_s^3}} = 2,8 \cdot 10^{-4} \left( h^* \frac{R_c}{H_{m0}} \right)^{-3,1}, \quad \text{valid for } 0,03 < h^* \frac{R_c}{H_{m0}} < 1,0 \text{ for impulsive conditions } (h^* < 0,2)$$

and

$$\frac{q}{\sqrt{g H_{m0}^3}} = 0,04 \cdot e^{-1,8 \frac{R_c}{H_{m0}}}, \quad \text{valid for } 0,1 < \frac{R_c}{H_{m0}} < 3,5 \text{ for non-impulsive conditions } (h^* > 0,3):$$

For equations for probabilistic design, battered walls and vertical walls with parapets, composite walls and other shapes, the reader is referred to the European Overtopping Manual.

### Note

*If non-breaking waves are reflected by a vertical structure, interference of incoming and reflecting waves will occur. This will result in a standing wave with a height twice as much as the incoming wave. In the overtopping volume equation, however, the wave height of the incoming wave, not the standing wave, should be used, because the parameters in the equations already include this effect.*

## 17.3 Literature

Franco, L., M. de Gerloni, Meer, J.W. van der (1994). *Wave overtopping on vertical and composite breakwaters*. Proceeding of the 24th International Conference on Coastal Engineering. Kobe, pp 1030-1044

Eurotop team (2007). *Wave overtopping of sea defences and related structures: Assessment manual "European Overtopping Manual"*. To be downloaded from: [www.overtopping-manual.com](http://www.overtopping-manual.com) (mind the errata!)

## 18. Water, waves, wall, non-breaking

Updated: February 2015

Civil engineering works located on the sea side of a breaker zone, can be subjected to loads by non-breaking waves. Non-breaking waves also occur in waterways and lakes in which the wave height is limited. Unlike around slender structures, the wave pattern is influenced by a wall. The wave height in front of the wall is determined by refraction and diffraction (see Sections 16.4 and 16.5).

There are five methods to calculate the load on a wall due to non-breaking waves. They are given in the table below with a description of when they are applied.

No	Method	Design phase	Notes
1	Rule of thumb	preliminary estimate	conservative
2	Linear theory	preliminary (and final) design	-
3	Sainflou	preliminary design	simple!
4	Rundgren	final design	not in this handbook
5	Goda	final design	also for sills!

Table 18-1 Summary of methods

### 18.1 Rule of thumb

According to linear wave theory for non-breaking waves against a vertical wall, the wave height  $H$  in front of the wall is double the incoming wave height  $H_i$ , in the case of total reflection. In short:

$$H = 2H_i \quad \text{and with} \quad H = 2a: \quad a = H_i \quad \text{is valid.}$$

This causes a temporary water level rise. If this is considered as a stationary load, the following rule of thumb can be applied to calculate the maximum wave force  $F_{max}$  [N] against a wall:

$$F_{max} = \frac{1}{2}\rho g H_i^2 + d\rho g H_i$$

in which:  $\rho$  [kg/m<sup>3</sup>] = density of water  
 $g$  [m/s<sup>2</sup>] = gravity acceleration  
 $H_i$  [m] = the wave height of an incoming wave (= 2  $a$ )  
 $a$  [m] = amplitude of the wave (half the wave height)  
 $d$  [m] = depth of the breakwater

This can be used for a quick estimate of the upper boundary value of the wave load.

### 18.2 Linear theory

For non-breaking waves against a vertical wall, the force on a wall can be determined using the pressure distribution in a vertical, taken from wave theory. As mentioned before, according to linear wave theory, the wave height  $H$  in front of the wall:

$$H = 2H_i \quad \text{and with} \quad H = 2a: \quad a = H_i \quad \text{is valid.}$$

The maximum pressure against a wall in case of reflection is then:

$$\rho = \rho g H_i \frac{\cosh(k(d+z))}{\cosh(kd)} \quad \text{for} \quad -d < z < 0$$

$$\rho = \left(1 - \frac{z}{H_i}\right) \rho g H_i \quad \text{for} \quad 0 < z < H_i$$

in which:  $H_i$  [m] = wave height of an incoming wave

$k$  [ $\text{m}^{-1}$ ] = the wave number of the incoming wave ( $= 2\pi/L$ )

The force per linear metre follows from integration over the water depth:

$$F = \int_{-d}^0 \rho g H_i \frac{\cosh(k(d+z))}{\cosh(kd)} dz + \int_0^{H_i} \left(1 - \frac{z}{H_i}\right) \rho g H_i dz$$

$$= \rho g H_i \left( \frac{(\exp(kd) - \exp(-kd))}{2k \cosh(kd)} + \frac{H_i}{2} \right)$$

In the case of a large wavelength, the wave pressure approaches the hydrostatic pressure (= rule of thumb). Figure 18-1 gives an example of this. The figure illustrates the wave pressures for different wavelengths, which are to be added to the hydrostatic pressure corresponding to the still water level.

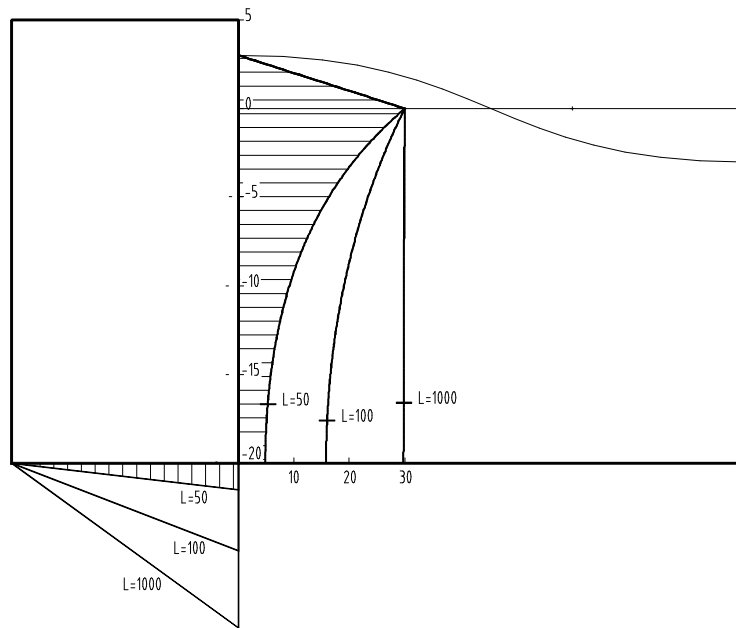


Figure 18-1 Linear wave theory: wave pressure

### 18.3 Sainflou

In practice another simple approximation is often used for the calculation of the total force on a wall. This method is known as Sainflou's method. This approach is shown schematically in Figure 18-2 and only applies to non-breaking waves. The approach is based on Stokes' second order wave theory. The incoming waves have the shape of a trochoid and complete reflection ( $\chi = 1$ ) is assumed. Due to interference of reflected waves with incoming waves, peaks in front of the wall will reach an amplitude with the magnitude of the incoming wave height.

The still water level in front of the vertical wall will increase with  $h_0$  [m]:

$$h_0 = \frac{1}{2} \cdot k \cdot H_{in}^2 \cdot \coth(k \cdot d)$$

where:

- $h_0$  [m] = increase of the mean water level in front of the structure
- $H_{in}$  [m] = height of the incoming wave; not influenced by the presence of the wall
- $d$  [m] = water depth in front of the sill, 2 or 3 wave lengths away from the wall
- $k$  [ $\text{m}^{-1}$ ] = wave number of the incoming wave:
 
$$k = \frac{2\pi}{L_0} \quad \text{or} \quad k = \frac{2\pi}{L}$$
- $L$  [m] = wave length

For 100% reflection:  $H_{refl} = 2 \cdot H_{in}$ , where  $H_{refl}$  is the height of the wave that originates from the interference of the incoming and the reflected wave.

Sainflou and Stokes's second order wave theory lead to the same maximum pressures at mean water level and near the bed as the linear theory; viz.:

$$p_1 = \rho \cdot g \cdot (H_{in} + h_0)$$

$$p_0 = \frac{\rho \cdot g \cdot H_{in}}{\cosh(k \cdot d')}$$

where:

$d'$  [m] = water depth above foundation level of the structure.

The pressure between  $p_0$  and  $p_1$  is assumed to be linear. Therefore Sainflou leads to an overestimation of the load for steep waves.

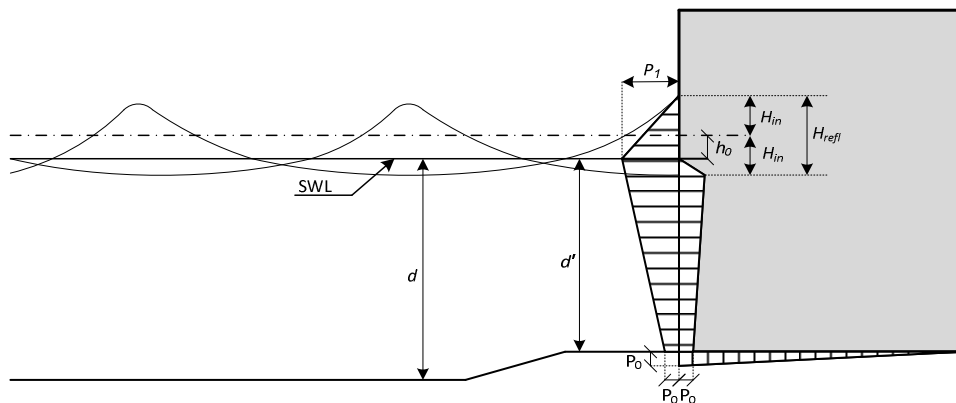


Figure 18-2 Sainflou: wave pressure

## 18.4 Rundgren

Based on adapted higher order wave theory, Rundgren adapted Sainflou's formulas. The adapted formulas were used to make the graphs in the Shore Protection Manual (CERC, 1984). In these graphs, overtopping and oblique approach are taken into account, which reduces the load. Rundgren's wave theory is not covered in this manual.

## 18.5 Goda

Goda (1985, 1992) made a general expression for the wave pressure on a caisson on a rockfill sill. This expression can also be used for broken and breaking waves. Worldwide Goda's equations are used often for the design of vertical breakwaters, see Figure 18-3. Goda's equations don't have an analytical base but rather an empirically foundation.

For the determination of the design wave height  $H_D$  and the design wavelength  $L_D$ , see the method in this book in Chapters 15 and 16. Goda proposed his own formula for  $H_D$  and  $L_D$  however, these are not dealt with in this manual.

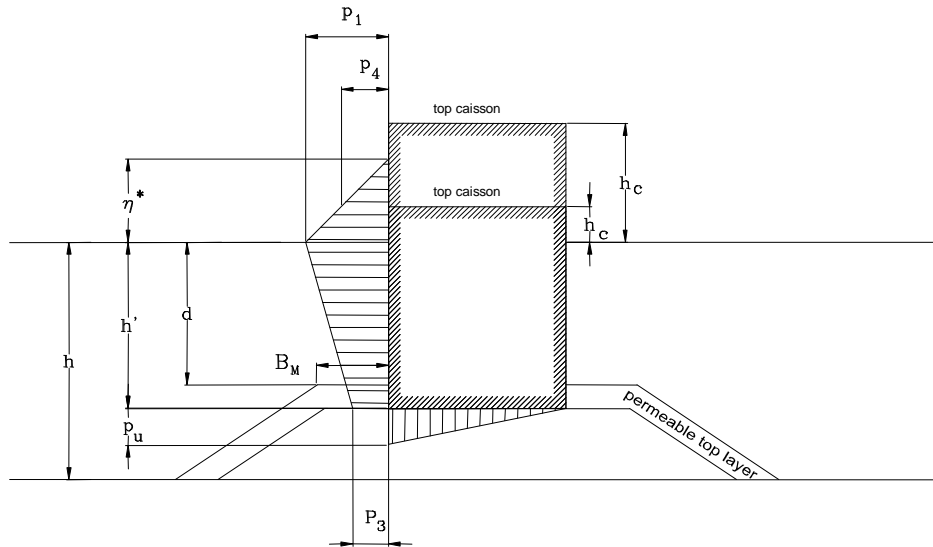


Figure 18-3 Goda (modified by Tanimoto): wave pressure

The sill height is  $h - d$ .

The sill width is  $B_m$ .

The maximum wave pressures are:

$$p_1 = 0,5 (1 + \cos(\beta)) (\lambda_1 \alpha_1 + \lambda_2 \alpha_2 \cos^2(\beta)) \rho g H_D$$

$$p_3 = \alpha_3 p_1$$

$$p_4 = \alpha_4 p_1$$

$$p_u = 0,5 (1 + \cos(\beta)) \lambda_3 \alpha_1 \alpha_3 \rho g H_D$$

in which:  $\beta$  = the angle of the incoming wave

$$\eta^* = 0,75 (1 + \cos(\beta)) \lambda_1 H_D$$

$$\alpha_1 = 0,6 + 0,5 \left( \frac{4\pi h / L_D}{\sinh(4\pi h / L_D)} \right)^2$$

$$\alpha_2 = \min \left( \frac{(1 - d/h_b)(H_D/d)^2}{3}, \frac{2d}{H_D} \right)$$

$$\alpha_3 = 1 - (h'/h) \left( 1 - \frac{1}{\cosh(2\pi h / L_D)} \right)$$

$$\approx \frac{1}{\cosh(kd)} \quad (\text{without sill})$$

$$\alpha_4 = 1 - \frac{h_c^*}{\eta^*}$$

$$h_c^* = \min(\eta^*, h_c)$$

$\lambda_1, \lambda_2, \lambda_3$  = factors dependent on the shape of the structure and on wave conditions;  
(vertical wall and non-breaking waves:  $\lambda_1 = \lambda_2 = \lambda_3 = 1$ )

$h_b$  = water depth at a distance  $5H_D$  from the wall

$H_D$  = design wave height (see Chapters 15 and 16)

$L_D$  = design wavelength (see Chapters 15 and 16)

$d$  = water depth above the top of the sill

$h'$  = water depth above the wall foundations plane

$h$  = water depth in front of the sill.

## 19. Water, waves, wall, breaking

### 19.1 Introduction

For the description of conditions in which a wave breaks, see Section 16.3 "Shallows: breaking".

For unbroken waves, the pressure distribution in the wave is a measure for the force on the wall. In the case of breaking waves this is not so. For those waves it is mainly the velocity with which the water particles hit the wall that is of importance. The shape of the breaking wave and possible air that is caught between the structure and the breaking wave largely influence the maximum wave shock and the course of the pressure distribution in time. The load due to breaking waves is still a point of research. The dynamic character of the load is an essential facet of breaking waves. Due to the collision between the wave and the structure a transfer of impulse takes place. At the moment of impact a relatively high pressure occurs, which only lasts a very short time (in the order of 0,01 s). Because of the short time span, this pressure is not representative for the stability of a structure (due to the inertia of mass). This pressure can be of importance for the strength of the structure (partial collapse).

If possible, it is better to prevent waves to break before they hit the structure, so that the shock will be less. In most cases it is therefore more economical not to place too high a sill in front of a straight wall, so that the waves won't break and the load of the non-breaking waves is governing (*maatgevend*).

The sections below describe three models for breaking and broken waves. These models are:

- Minikin
- CERC 1984, broken waves
- Goda-Takahashi

These models are no more than rough estimates.

### 19.2 Minikin

Minikin's model is based on both laboratory tests and on prototype measurements. Figure 19-1 gives a diagram of the model. It is based on a maximum dynamic pressure at the still water level and on a parabolic decline to zero over the distance  $H_b/2$  above and below the still water level plus an increase of the hydrostatic pressure as a result of the displacement of the water surface.

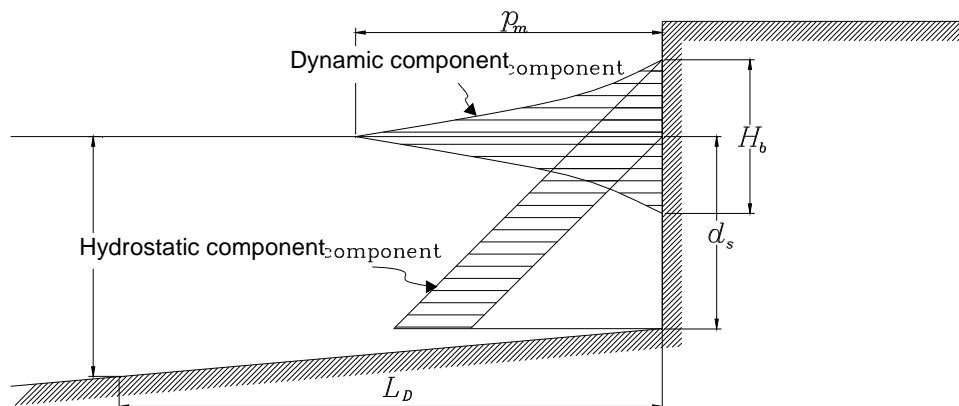


Figure 19-1 Minikin: broken wave pressure

The maximum pressure is:

$$p_m = \frac{1}{2} C_{mk} \pi \rho g \frac{H_b}{L_D} \frac{d_s}{D} (D + d_s)$$

where:  $C_{mk}$  [-] = coefficient of the impact  $\approx 2$   
 $H_b$  [m] = breaker height  
 $d_s$  [m] = depth in front of the wall  
 $D$  [m] = depth at one wavelength in front of the wall  
 $L_D$  [m] = wavelength at depth  $D$

Minikin found  $C_{mk} \approx 2$ .

The resultant force according to Minikin is:

$$F = \frac{P_m H_b}{3} + \frac{\rho g H_b}{2} \left( \frac{H_b}{4} + d_s \right)$$

### Note

Minikin's method is unfortunately described incorrectly in CERC (1984). In the original publication by Minikin (1963), the pressure on the wall was expressed in tonnes per square foot. This is not correct. It should be ton force per square foot. This mistake was overseen in conversion to SI units for the CERC 1984 and has led to a formula for  $p_m$  which gives values that are far too large. This is why many publications warn against Minikin's method, mentioning that the equation gives values that are 10 to 15 times too large, whilst the original method actually gave far lower values. One is advised not to use equations derived from Minikin (except for the corrected equations given above).

## 19.3 CERC 1984

According to CERC 1984, the model for broken waves merely gives an indication of the load. If accurate estimates are needed of the maximum load on a structure due to breaking waves, more thorough research must be carried out for the specific situation. Like Minikin's model, the model assumes a dynamic and a hydrostatic component of the water pressure on the structure.

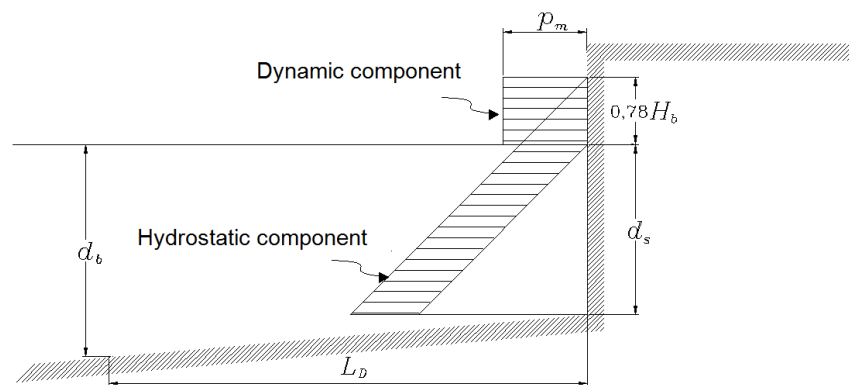


Figure 19-2 CERC 1984: broken wave pressure

The dynamic component is derived from the wave propagation velocity  $c$  at the moment the waves started to break. The broken wave is considered a translation wave with the propagation velocity:

$$c = \sqrt{gd_b}.$$

The dynamic pressure is:

$$p_m = \rho g \frac{c^2}{2g} = \frac{\rho g d_b}{2}$$

where:  $d_b$  [m] = the water depth where the wave broke

As in Minikin's model, the hydrostatic component of the load is caused by the displacement of the water surface. The total load as a result of the broken wave is therefore:

$$F = \rho g h_c \left( \frac{d_b}{2} + \frac{h_c}{2} + d_s \right)$$

in which:  $h_c$  [m] = the height of the broken wave (translation wave) =  $0,78 H_b$

## 19.4 Goda-Takahashi

Goda's model was already given in the previous chapter. According to Takahashi and others (1994), a couple of factors need to be adjusted for waves that break on the berm of the sill on top of which a caisson has been placed:

$$\lambda_1 = \lambda_3 = 1$$

$$\lambda_2 = \max\left(1, \frac{\alpha_1}{\alpha_2}\right)$$

where:  $\alpha_i$  = impulse coefficient

The impulse coefficient is determined with the following equations:

$$\alpha_i = \alpha_n \alpha_m$$

$$\alpha_m = \min\left(\frac{H_D}{d}, 2\right)$$

$$\alpha_n = \frac{\cos(\delta_2)}{\cosh(\delta_1)} \quad \text{if } \delta_2 \leq 0$$

$$\alpha_n = \frac{1}{\cos(\delta_1) \sqrt{\cosh(\delta_2)}} \quad \text{if } \delta_2 > 0$$

$$\delta_1 = 20 \delta_{11} \quad \text{if } \delta_{11} \leq 0$$

$$\delta_1 = 15 \delta_{11} \quad \text{if } \delta_{11} > 0$$

$$\delta_2 = 4,9 \delta_{22} \quad \text{if } \delta_{22} \leq 0$$

$$\delta_2 = 3,0 \delta_{22} \quad \text{if } \delta_{22} > 0$$

$$\delta_{11} = 0,93 \left( \frac{B_M}{L_D} - 0,12 \right) + 0,36 \left( \frac{h-d}{h} - 0,6 \right)$$

$$\delta_{22} = -0,36 \left( \frac{B_M}{L_D} - 0,12 \right) + 0,93 \left( \frac{h-d}{h} - 0,6 \right)$$

where:  $B_M$  [m] = width of the berm in front of the wall (see Figure 18-3)

The dimensions of the berm have an important influence on the extent of the load. Figure 19-3 shows this influence for an example.

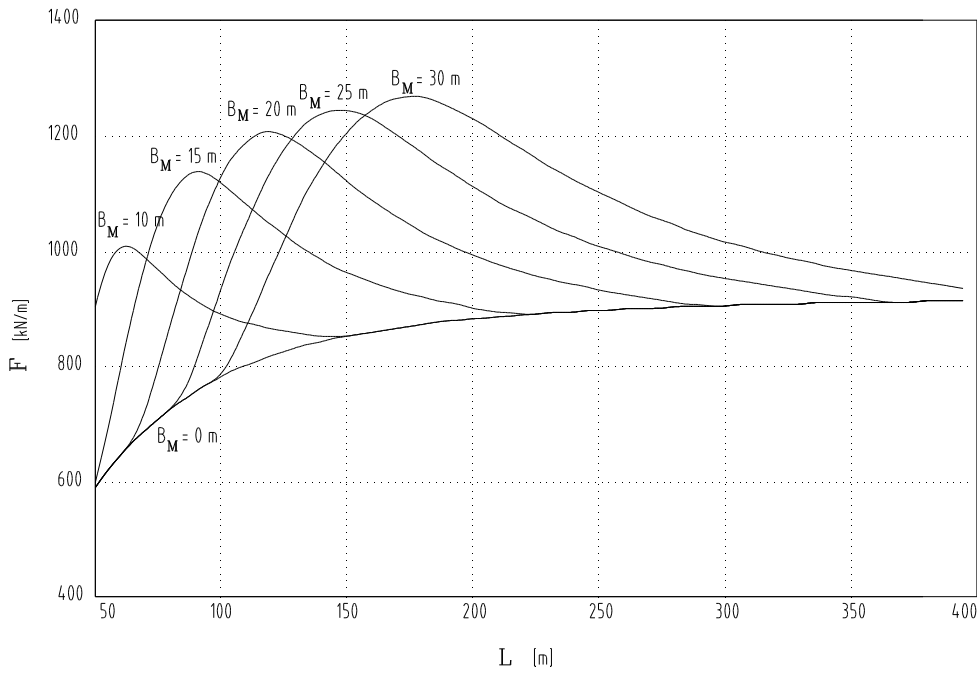


Figure 19-3 Influence of a berm on the wave load ( $H_D = 6\text{ m}$ ,  $h = 9\text{ m}$ ,  $h' = 7\text{ m}$ ,  $d = 5\text{ m}$ ,  $h_c = \infty$ )

### 19.5 Comparison

Figure 19-4 shows a comparison of the different models. The wave load was calculated for various different wave periods, for a given configuration (a caisson on a quarry stone sill).

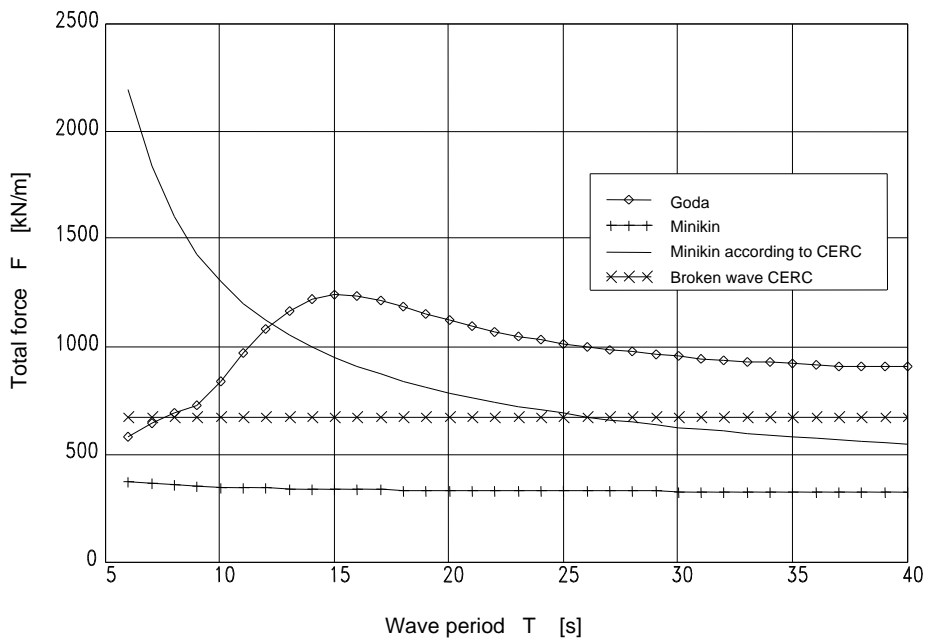


Figure 19-4 Comparison of Minikin, Goda and broken waves according to CERC 1984 ( $H_D = 6\text{ m}$ ,  $h = 9\text{ m}$ ,  $h' = 7\text{ m}$ ,  $d = 5\text{ m}$ ,  $h_c = \infty$ )

The comparison of the different calculation models revealed that there are considerable differences between the results of the models, particularly when waves with periods between 6 and 15 seconds are considered. When applying the models, one could consider upper and lower boundaries, where Minikin's model is clearly a lower boundary for the above-mentioned periods.

One reason for the deviation between the models could be the different researchers' ways of measuring the wave load. The wave force of a breaking wave varies in time. The moment the wave breaks against the structure, the impact is the largest, during a very short time span the pressure against the wall is extremely high. Directly after the impact the pressure decreases very quickly and stays constant a while at a certain level of pressure. This is shown schematically in Figure 19-5. This schematisation is known as the "church roof" load. The response of the structure under a "church roof" load depends on the stiffness and on the inertia of the structure. These determine the speed of reaction of the structure. A structure with little inertia (mass) and a large stiffness will be more sensitive to short impulse loads than a structure with a larger inertia.

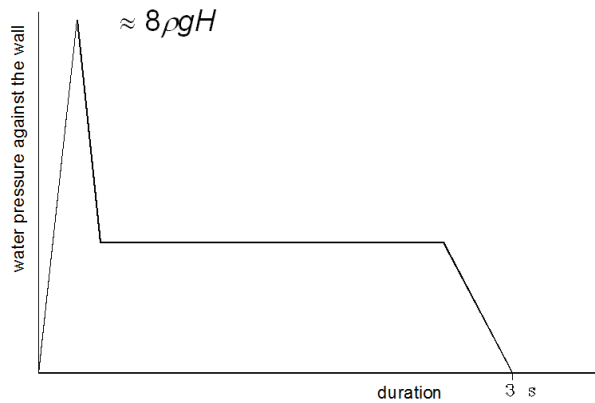


Figure 19-5 Course of the load in time

The wave load and the response of the structure are still subject to research.

Figure 19-6 shows the force  $F$  on a smooth wall for different wave steepnesses ( $s = H / L$ ), according to the four given methods. Here, the sill height in the Goda formulas is kept equal to zero, even though, the Goda formulas were derived for a caisson on a sill.

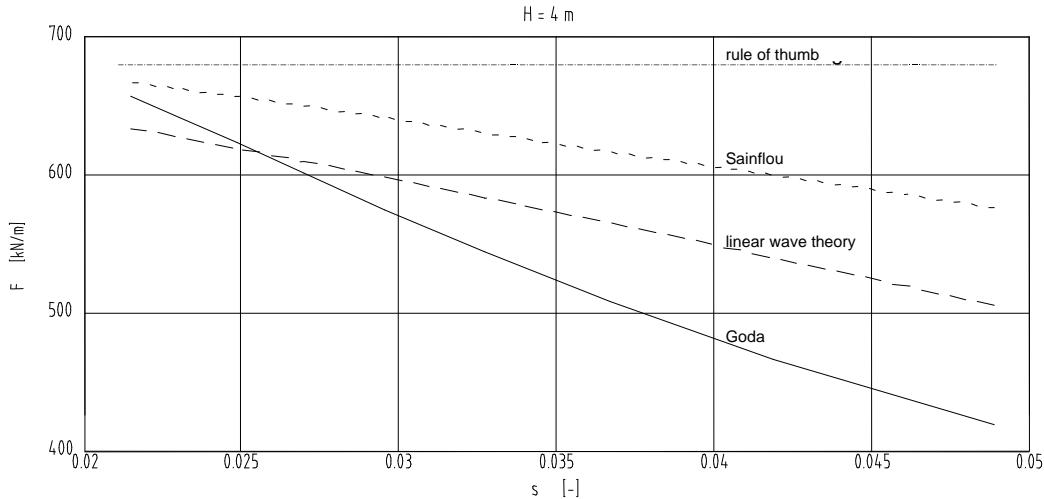


Figure 19-6 Wave load  $F$  of non-breaking waves ( $H = 4\text{ m}$ ) as a function of the steepness  $s$  ( $h = h' = d = h_b = 15\text{ m}$ )

The wave load of a four-metre high wave on the same wall is plotted as a function of the wave period in Figure 19-7.

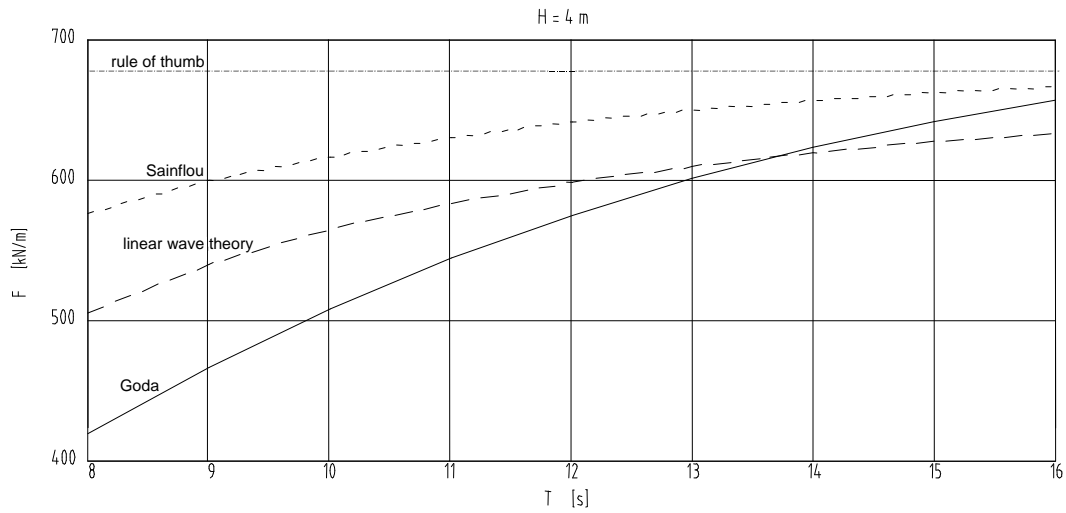


Figure 19-7 Wave load  $F$  of non-breaking waves ( $H = 4$  m) as a function of the period  $T$  ( $h = h' = d = h_b = 15$ m)

The graphs do not begin at “zero”, so the graphs give a distorted view. The differences between the linear wave theory and Sainflou or Goda are no more than 10% or 20%. Particularly for long waves (hence not very steep), the rule of thumb has a small error.

## 20. Water, waves, slender structure, non-breaking

Analogous to the formulation of the force on an object in a stationary flow, Morison (1950) found a relation between the force on a vertical pile as a function of the velocity and the acceleration of water particles in a wave. The part of the force that is caused by the flow velocity is the drag force and the part that is caused by the acceleration of the water particles is the inertia force.

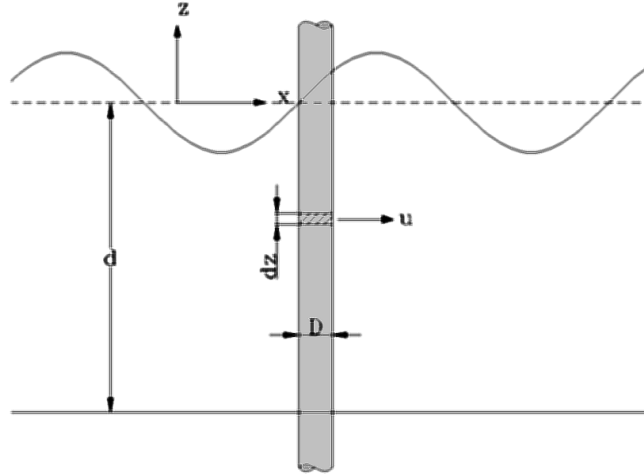


Figure 20-1 Wave load on a slender structure

### 20.1 Theory

Morison's formula for a fixed body in an oscillatory flow includes an inertia part and a drag part:

$$\frac{dF}{dz} = p(t, z) = p_i + p_D = C_i \rho \frac{\pi D^2}{4} \frac{du}{dt} + C_D \frac{1}{2} \rho D u |u|$$

where: $p(t, z)$	[N/m]	=	pile force per unit of length of the pile at time $t$ and in position $z$ [N/m]
$p_i$	[N/m]	=	inertia force (per unit of length of the pile)
$p_D$	[N/m]	=	drag force (per unit of length of the pile)
$C_i$	[-]	=	inertia coefficient $\approx 2,0$
$C_D$	[-]	=	drag coefficient (for low flow velocities $C_D \approx 1,2$ , see Section 20.3)
$\rho$	[kg/m <sup>3</sup> ]	=	density of the water
$D$	[m]	=	diameter of the pile
$u$	[m/s]	=	horizontal velocity of the water particles: $u = \omega a \frac{\cosh(k(d+z))}{\sinh(kd)} \sin(\omega t)$
$\frac{du}{dt}$	[m/s <sup>2</sup> ]	=	horizontal acceleration of the water: $\frac{du}{dt} = \omega^2 a \frac{\cosh(k(d+z))}{\sinh(kd)} \cos(\omega t)$
$\omega$	[rad/s]	=	angular frequency ( $2\pi/T$ )
$k$	[rad/m]	=	wave number ( $2\pi/L$ )
$d$	[m]	=	depth

Because the velocity and the acceleration of the water particles are not in phase, the maximum total force is smaller than the sum of the maximum drag force and the maximum inertia force.

The force on the pile over time is found by integration:

$$F(t) = \int_{-d}^{\eta} p(t, z) dz = \int_{-d}^{\eta} p_i dz + \int_{-d}^{\eta} p_D dz = C_i \rho \frac{\pi D^2}{4} \int_{-d}^{\eta} \frac{du}{dt} dz + C_D \frac{1}{2} \rho D \int_{-d}^{\eta} u |u| dz$$

The moment on the pile relative to the bed is found by integrating the wave pressure multiplied by the height on the pile:

$$M(t) = \int_{-d}^{\eta} p(t, z)(z + d) dz = \int_{-d}^{\eta} p_i(z + d) dz + \int_{-d}^{\eta} p_D(z + d) dz$$

## 20.2 (Preliminary) design

The maximum force and the maximum moment in the above integrals are generally solved as follows:

$$F_{\max} = F_I + F_D = C_I K_I H \rho g \frac{\pi D^2}{4} + C_D K_D H^2 \frac{1}{2} \rho g D$$

$$M_{\max} = F_I d S_I + F_D d S_D$$

where:  $C_I$  [-] = inertia coefficient  $\approx 2,0$   
 $C_D$  [-] = drag coefficient (for small flow velocities  $C_D \approx 1,2$ , see Section 20.3)  
 $K_I$  [-] = correction for extent of inertia force  
 $K_D$  [-] = correction for extent of drag force  
 $S_I$  [-] = correction for position of resultant inertia force  
 $S_D$  [-] = correction for position of resultant drag force  
 $H$  [m] = wave height  
 $D$  [m] = diameter pile  
 $d$  [m] = depth

The "Shore Protection Manual" (CERC 1984) gives graphs with the maximum values of the coefficients  $C_D$ ,  $K_I$ ,  $K_D$ ,  $S_I$ ,  $S_D$ . These graphs are also included in the following sections. The values of the coefficients depend on the wave period, the phase, the water depth and the applicable wave theory for the determination of the velocity of the water particles.

The graphs show various different curves. These depend on the ratio:

$$\frac{H}{H_b}$$

in which:  $H_b$  [m] = wave height when breaking (see Section 16.3)

Just like a body in a constant flow, a pile in a wave is subjected to a lifting force perpendicular to the direction of the wave and the axis of the pole. This force is caused by fluctuations of the vortexes next to and behind the pile. Due to resonance of the pile, these forces have been known to be 4,5 times larger than the drag force. In most cases the lift force is of the same order of magnitude as the drag force.

For a preliminary design, the maximum lift force can be approximated by:

$$F_{L,\max} = C_L \frac{1}{2} \rho g D H^2 K_{D,\max}$$

in which:  $C_L$  [-] = lift coefficient  
 $K_{D,\max}$  [-] = maximum value of  $K_D$

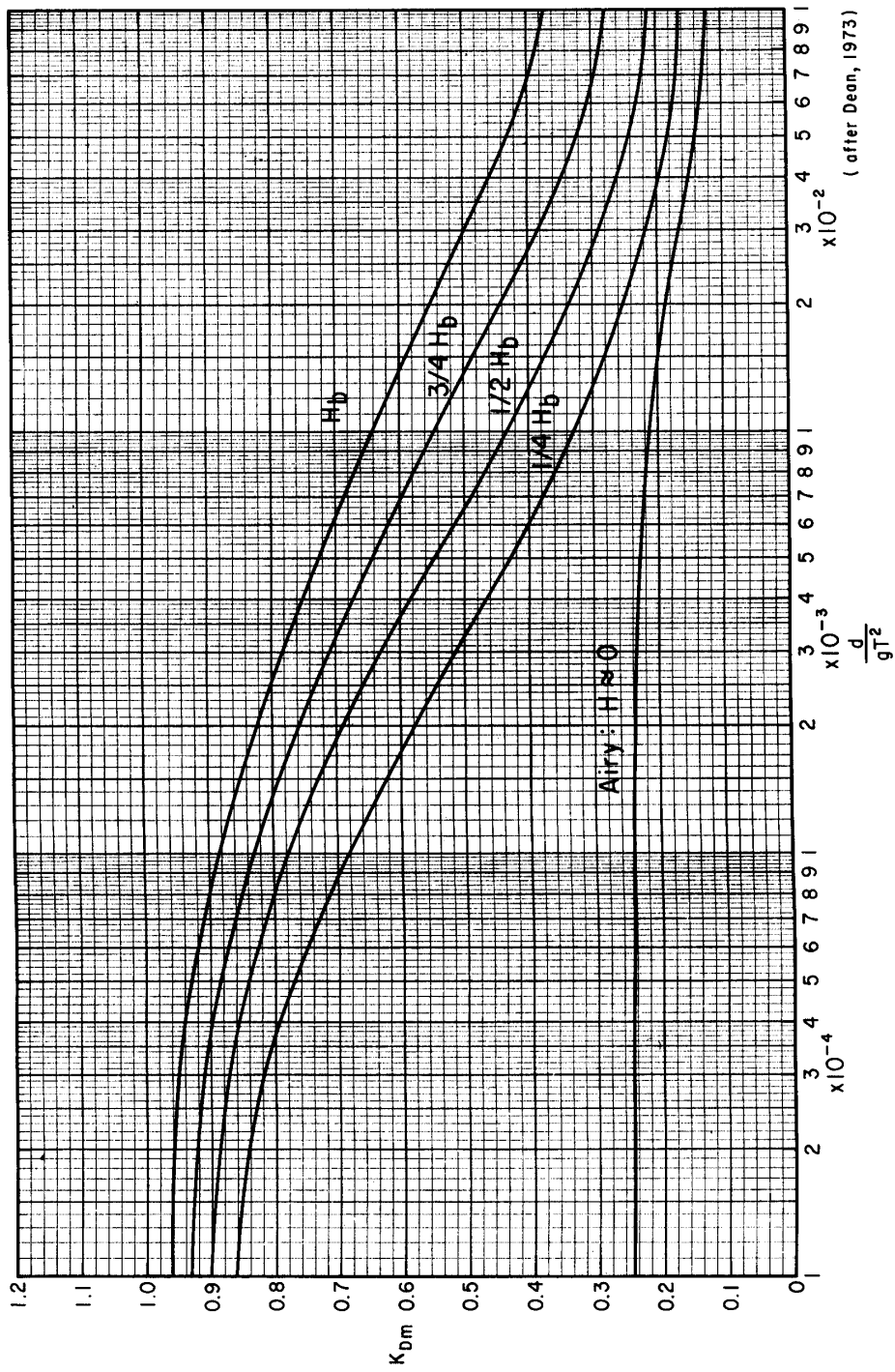
The lift coefficient  $C_L$  is unknown, but in most cases:

$$0 < C_L < C_D$$

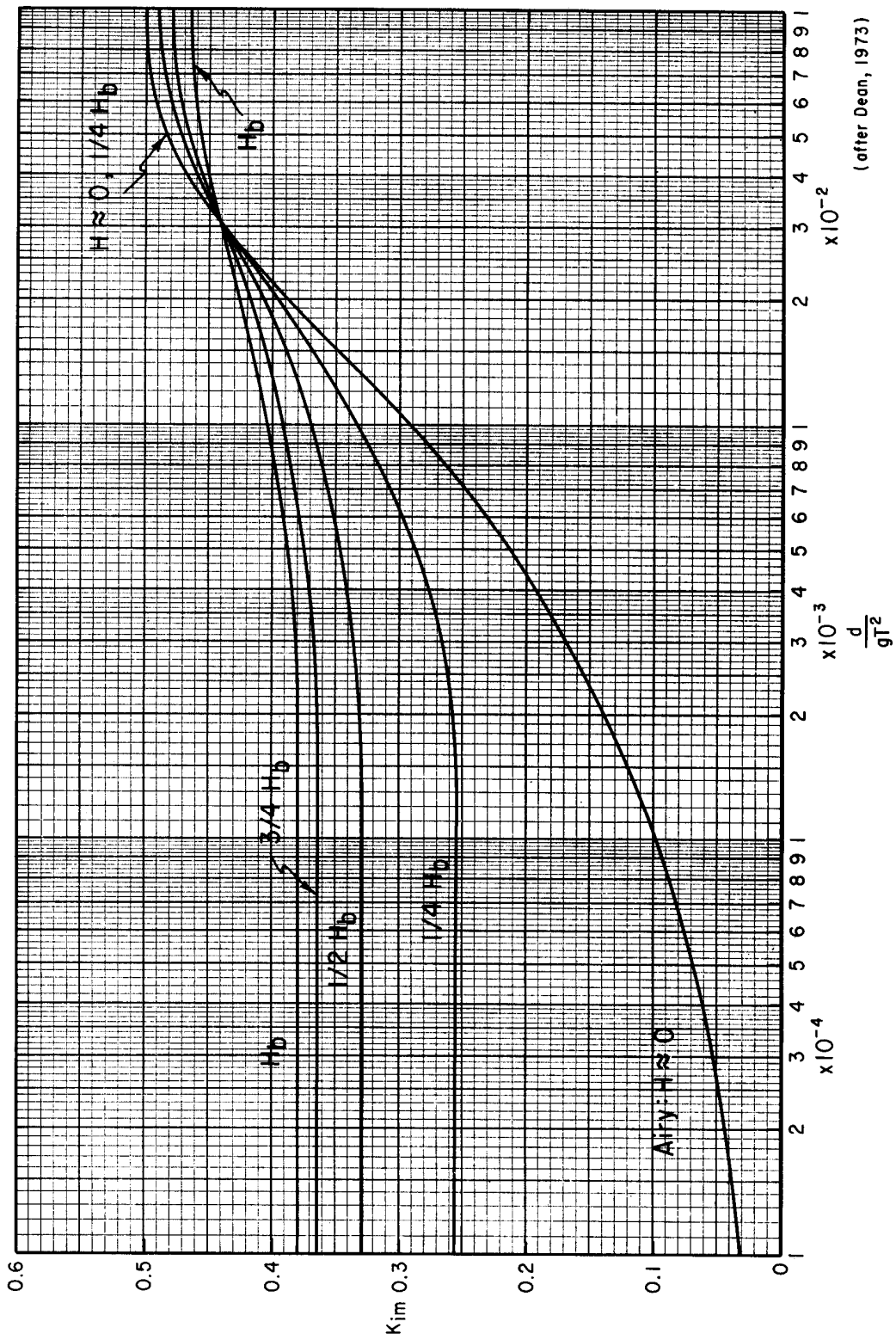
is valid. This can be used to determine a safe upper bound.



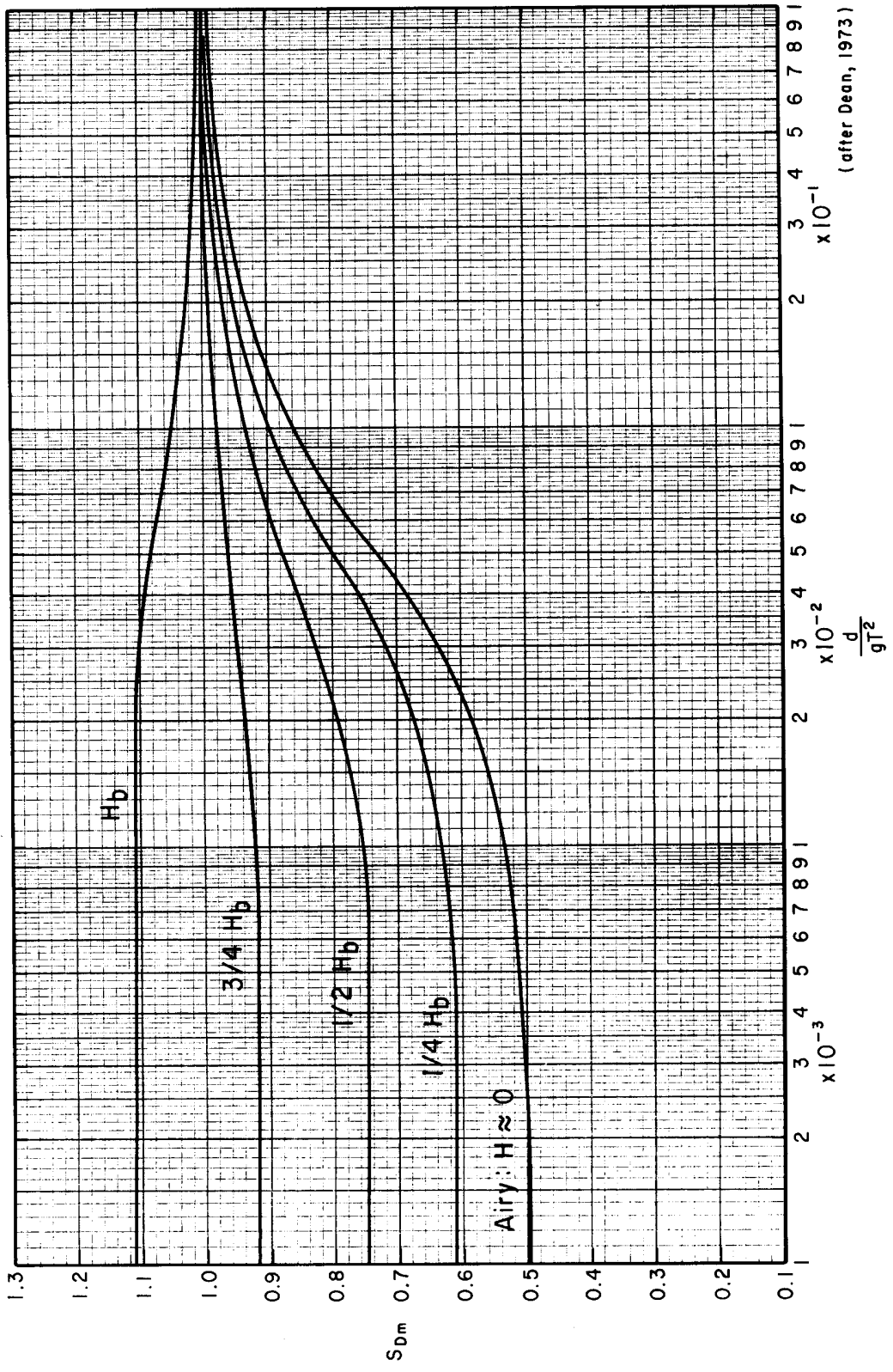
### 20.4 $K_p$ coefficient



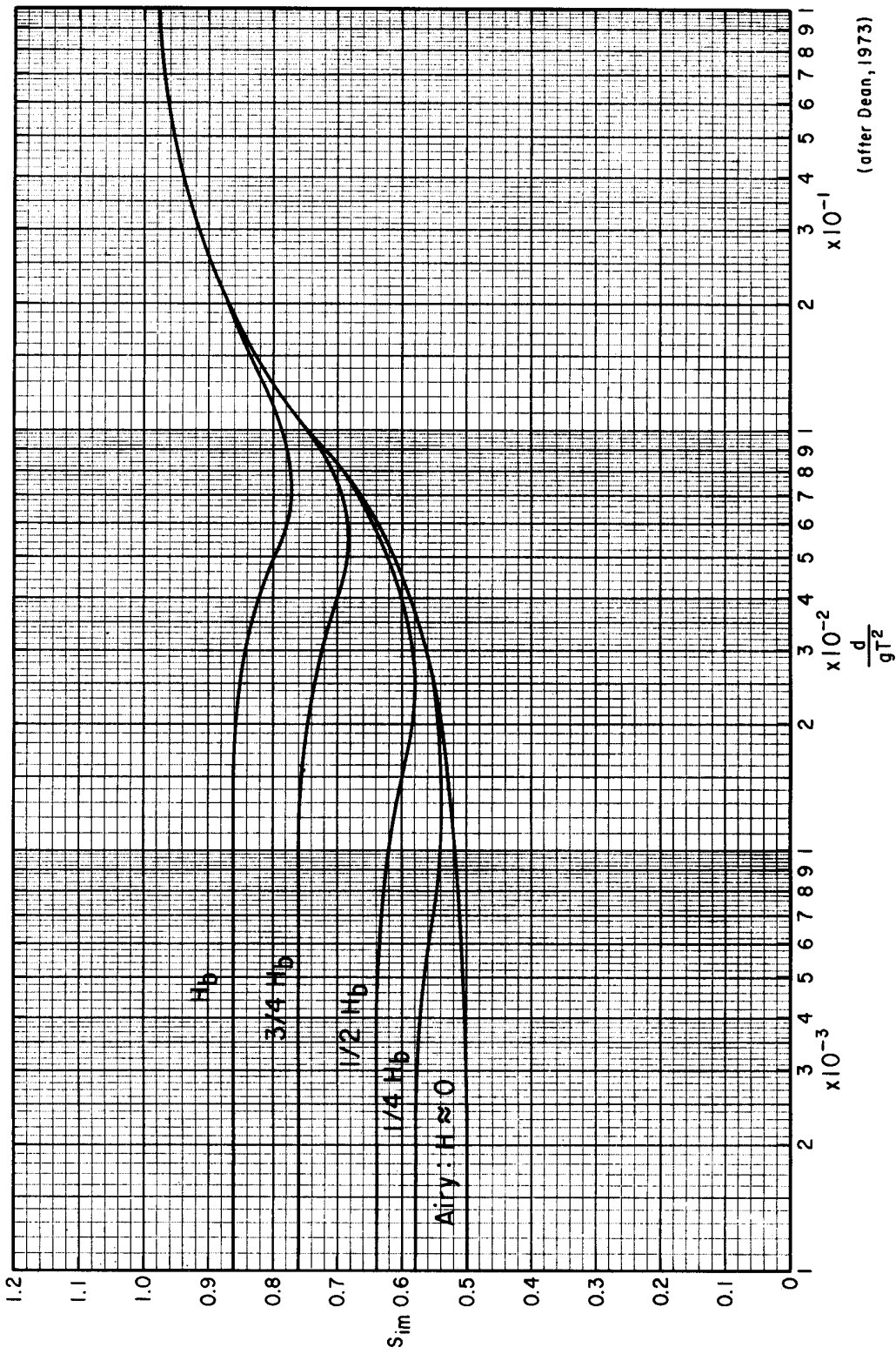
### 20.5 $K_f$ coefficient



20.6  $S_p$  coefficient



20.7  $S_1$  coefficient



## 21. Water, waves, slender structure, breaking

In a breaking wave the water particles have large horizontal velocities. In this case the accelerations are subordinate to the velocity of the water. Consequently, the inertia force on a slender structure is negligible relative to the drag force. The maximum force on a pile can therefore be approximated using the reduced formula:

$$F_{\max} = F_D = C_D^* K_D H^2 \frac{1}{2} \rho g D$$

In this case, the maximum moment on the pile is:

$$M_{\max} = F_D d S_D$$

Observations revealed that the value of  $C_D^*$  in breaking waves is 2,5 times larger than in non-breaking waves:

$$C_D^* \approx 2,5 \cdot C_D$$

Thus, the known values of  $C_D$  for non-breaking waves can be used (see Section 20 "Water, waves, slender structures").

Breaking waves in shallow water involve super-critical flow ( $C_D = 0,7$ ). In these conditions, one can assume the following for the preliminary design of cylindrical piles:

$$C_D^* \approx 2,5 \cdot 0,7 \approx 1,75$$

$$K_D \approx 1,0$$

$$S_D \approx 1,11$$

$$H = H_b \quad [-] = \text{height of the breaking wave}$$

$$d = d_b \quad [-] = \text{depth at which the wave breaks}$$

Section 16.3 "Shallows: breaking" mentions the following about breaking:

Theoretically the wave breaks at a steepness of  $H/L = 1/7$ . The depth also limits the wave height. It has been theoretically deduced that an individual wave will break when  $\frac{H}{d} \geq 0,78$  (there are also more complex formulas e.g. by Miche). However, individual waves with a ratio of  $\frac{H}{d} = 1,2$  have been observed.

When calculating breaking for a wave spectrum:

$$\frac{H_s}{d} = 0,4 \sim 0,5$$

## 22. Ice

extended with design rules: February 2015

One distinguishes four ways in which ice can exert a load on a hydraulic engineering work. These are:

- Thermal expansion.
- Ice accumulation.
- Collision.
- Ice attachment.

### 22.1 Thermal expansion

During the freezing process of a layer of ice on water, the thickness of the ice increases without an increase of the ice area. There is hardly any expansion perpendicular to the direction of growth of the ice. Therefore, the freezing process itself does not generate any loads.

After the freezing process, changes of the ice temperature can cause loads. This thermal expansion of the ice can sometimes cause static horizontal loads. This only applies if the ice is restricted in its expansion. Examples of this are the forces on structures on the banks of frozen lakes and the forces on the piles of berths as a result of the expansion of the ice between the piles.

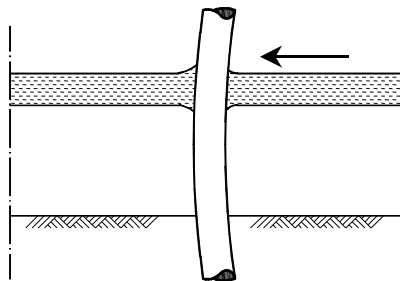


Figure 22-1 Thermal expansion.

The thermal expansion of ice is comparable to the temperature load as described in Chapter 23 "Temperature". On average, the coefficient of thermal expansion is about  $\alpha = 5,5 \cdot 10^{-5} \text{ } ^\circ\text{C}^{-1}$ .

The expansion causes stresses both in the structure loaded by the ice and in the ice itself. These stresses create equilibrium in the interface between the structure and the ice. The upper limit of these stresses is the yield stress of the structure or of the ice.

The yield stress of the ice largely depends on the density and the composition of the ice. The salinity (salt concentration), the extent of water pollution and the temperature are hence important factors involved. It is therefore not possible to give a general yield stress of ice. It is very much linked to the location where the ice was formed and also the temperature history of the ice.

Research into the yield stress of ice has been carried out in several different locations. The yield stress varies between 20 and 300 kN/m<sup>2</sup>. The large spread of the values of the strength show that knowledge of the local ice strength is of large importance.

An important phenomenon associated with thermal expansion is the buckling of the ice surface in places where the ice shows irregularities. Thus a completely new situation is created with respect to thermal expansion.

### 22.2 Ice accumulation

As a result of a slight current, ice can accumulate against a structure. A current beneath the ice causes a shear force along the ice, which is in equilibrium with forces on the structure. Due to the accumulation of ice against the structure in slowly flowing water, a static horizontal load is created.

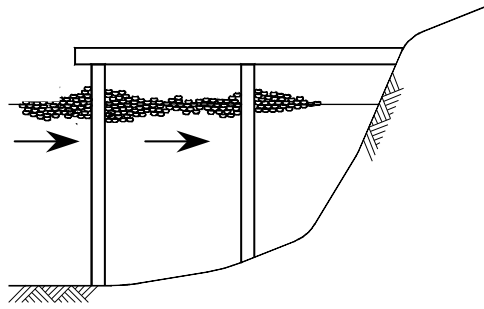


Figure 22-2 Accumulation of ice

### 22.3 Collision

The dynamic horizontal load on a structure is caused by colliding blocks of ice, which were carried along by the wind and the current. This is particularly of importance for structures in rivers and along coasts with a considerable current.

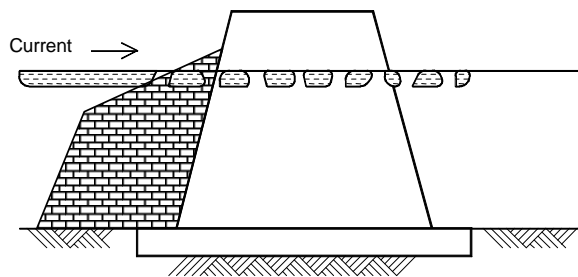


Figure 22-3 Collision of ice floes and breaking on an ice breaker

The impact of large ice sheets that collide against a structure can be compared with the impact of ships that run into a structure. The fact that the mass and particularly the velocity of the colliding ice sheet determine the load on a structure follows from the equations in Chapter 29 "Shipping, berthing". Here, too, the stresses are in equilibrium in the interface between the structure and the ice. If the maximum yield stress of the ice is exceeded, it will collapse. It is known that the stresses are maximal in the outer fibres, as a result of bending. Therefore, collapse of the ice takes place sooner in a case of bending than in case of a uniformly distributed normal force.

This knowledge can be used to reduce or prevent forces on structures. An angled slope or an oblique edge in front of a structure can make the ice buckle and thus prevents the ice sheet from sliding into the structure.

### 22.4 Ice attachment

The static vertical load on a structure as a result of the attachment of ice onto a structure is of particular importance when water levels vary. Ice attachment can occur anywhere between the high and the low water levels. Under water this mass causes an upward force and above water it results in a downward load on the structure.

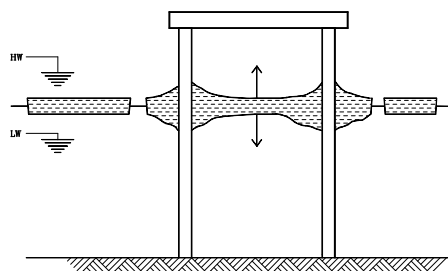


Figure 22-4 Ice attachment

## 22.5 Design rules

It should be judged per situation whether ice loading is relevant for the design of hydraulic structures. For example, there can be ice loading from frozen surface water acting on a quay wall, but at the same time the ground water on the other side of the wall can be frozen too, mainly or partly eliminating the outer ice load.

The Dutch Guidelines Design Hydraulic Structures (*Richtlijnen Ontwerp Kunstwerken, ROK, 2013*) of Rijkswaterstaat prescribe an ice load of  $400 \text{ kN/m}^1$  on the walls of lock chambers, at the expected water level during ice conditions. ROK also specifies the directions and locations of ice loads on gates:

- For thermal expansion: in length direction of the lock chamber, 0,20 m below the upstream water level;
- For accumulating ice: perpendicular to the gate, at upstream water level;
- For attached ice: in vertical direction, equally distributed over the cross rails (*regels*) that are located under water.

The Dutch Manual Sheetpile Walls (*Handboek Damwandconstructies, CUR-publication 166*) states that in most cases, ice loads will appear not to be critical for the design of sheet pile walls. For retaining walls adjacent to open water, the combination of ice load, ship impact and wave load should not be considered. Either ice load or the combination of ship impact and wave load are governing. For the estimation of horizontal ice loads on sheetpile walls, it can generally be assumed that the ice layer has a thickness of 0,50 m and a compressive strength of 1,5 MPa for sea water and 2,5 MPa for fresh water. Because this load will vary over the contact surface from 0 to the compressive strength of ice, a levelling coefficient of 0,33 may be applied. This leads to the following design values for corresponding line loads, acting at the most unfavourable water level: 250 kN/m for sea water and 400 kN/m for fresh water (corresponding with the value mentioned in the ROK).

For the strength calculation of structural members a concentrated load of 1500 kN should be used, if ice could act on these members<sup>4</sup>. In intertidal areas, where ice floes (*schotsen*) can origin, a horizontal line load of 100 kN/m can be used and possibly also vertical loads (not quantified in CUR 166). All these values only apply to long walls; for short sheetpile walls (like those used for the construction of bridge piers), reference is made to the German manual on quay walls, the EAU (see below).

CUR 166 also mentions line loads coming from thermal expansion of enclosed ice. The magnitude of these loads depends on the initial temperature of the ice, the temperature gradient and the thickness of the ice [m], see Figure 22-5.

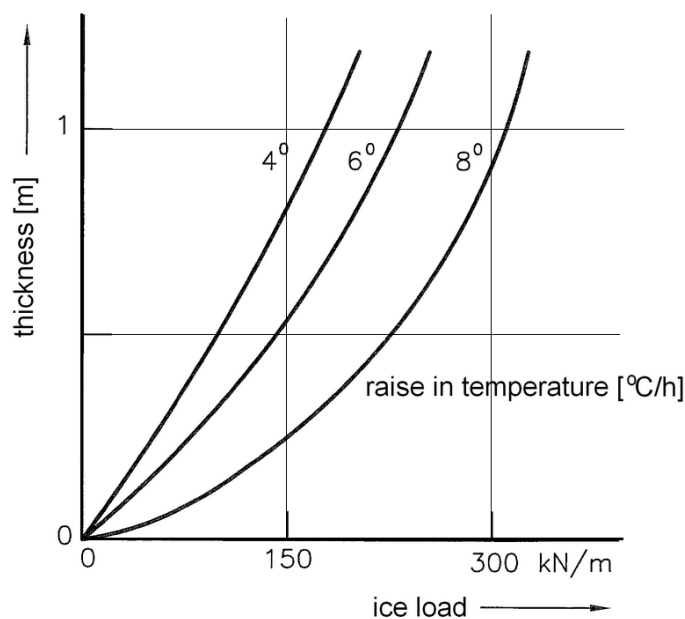


Figure 22-5 Loads caused by thermal expansion of ice (CUR 166)

<sup>4</sup> This seems a very high value, so for the dimensioning of specific structural members one should judge whether situations can occur that can indeed inflict such a force.

The German manual on quay walls, the *Empfehlungen des Arbeitsausschusses "Uferneifassungen"* (EAU, 2012) gives rules to calculate the compressive strength of ice and measured maximum thickness of ice layers (in Germany, varying from 0,35 to 0,80 m).

According to the EAU, concentrated ice loads on vertical piles can be calculated with:

$$P_p = k \cdot \sigma_0 \cdot \sqrt{d} \cdot h^{1,1}$$

where:  $P_p$  [N] = concentrated ice load (force)  
 $\sigma_0$  [N/m<sup>2</sup>] = uniaxial compressive strength of ice related to a specific expansion rate  $\varepsilon = 0.001 \text{ s}^{-1}$   
 $d$  [m] = width of the pile  
 $h$  [m] = thickness of the ice  
 $k$  [m<sup>0,4</sup>] = empirical coefficient; for floating ice:  $k = 0,564$ ;  
 for ice frozen onto the pile:  $k = 0,793$

The horizontal uniaxial compressive strength of ice,  $\sigma_0$ , can be calculated according to:

$$\sigma_0 = 2,700 \cdot \varepsilon^{0,33} \cdot \varphi_B$$

and

$$\varphi_B = 19,37 + 36,18 \cdot S_B^{0,19} \cdot |\vartheta_m|^{-0,69}$$

where  $\varepsilon$  [s<sup>-1</sup>] = specific expansion rate =  $0.001 \text{ s}^{-1}$   
 $\varphi_B$  [m‰] = porosity of the ice layer  
 $S_B$  [m‰] = salinity of the ice  
 (usual values are: < 1 ‰ for fresh water, and 35 ‰ for sea water)  
 $\vartheta_m$  [°C] = temperature in the middle of the ice layer

The Ice Handbook for Engineers gives the following equation for static ice load:

$$F_{static} = k_c \cdot \sigma_c \cdot D \cdot h$$

where  $F_{static}$  [N] = static ice load  
 $k_c$  [-] = degree of confinement (*opsluiting*) of the ice in front of the structure, varying from 1 to 3  
 $\sigma_c$  [N/m<sup>2</sup>] = average uniaxial compressive strength of the total ice thickness  
 $D$  [m] = width of the structure  
 $h$  [m] = ice thickness

Vertical loads on single piles due to attached ice on rising or falling water levels can be calculated according to the Russian national standard SNiP 2.06.04.82 (1995):

$$A_V = \left( 0,6 + \frac{0,15 \cdot D}{h} \right) \cdot 0,4 \cdot \sigma_0 \cdot h^2$$

where:  $A_V$  [kN] = vertical ice load on a pile  
 $h$  [m] = thickness of the ice layer  
 $D$  [m] = diagonal of the pile  
 $\sigma_0$  [kN/m<sup>2</sup>] = compressive strength of the ice layer

For piles being part of a pile group, or piles next to fixed structures, a geometrical reduction factor  $f_g$  may be applied to  $A_V$  (see the EAU or SNiP for details).

## 22.6 Literature

- CUR 166: Handboek Damwandconstructies, CUR, 2012
- EAU, Empfehlungen des Arbeitsausschusses "Ufereinfassungen", Springer Verlag, 2012
- Ice handbook for engineers, version 1.2. Luleå Tekniska Universitet - Institutionen för samhällsbyggnad. Luleå, 2009
- ROK, Richtlijnen voor het Ontwerp van Kunstwerken. Rijkswaterstaat 2013
- SNiP 2.06.04.82 Нагрузки и воздействия на гидротехнические сооружения (волновые, ледовые и от судов). Russian standard 'Loads and actions on hydraulic engineering structures (wave and ice generated and from ships). Moscow, 1995.

## 23. Temperature

### 23.1 General

Temperature changes of structures and parts of structures usually lead to deformations and stresses. The cause of the temperature change can be both internal and external. Examples of external causes are:

- accumulation of warmth due to solar rays (daytime)
- loss of heat due to warmth emission (night time)
- adaptation to a changing air temperature
- cooling due to wind
- cooling due to precipitation
- cooling due to the evaporation of water in or on the structure
- warming or cooling due to activities in the structure (heating, air conditioning)

An internal cause of temperature change is the development of heat during the setting and hardening of concrete (hydration heat).

The temperature spread in a cross section of a structure element depends on the heat flow through the element. Some examples of possible temperature profiles are shown in Figure 23-1.

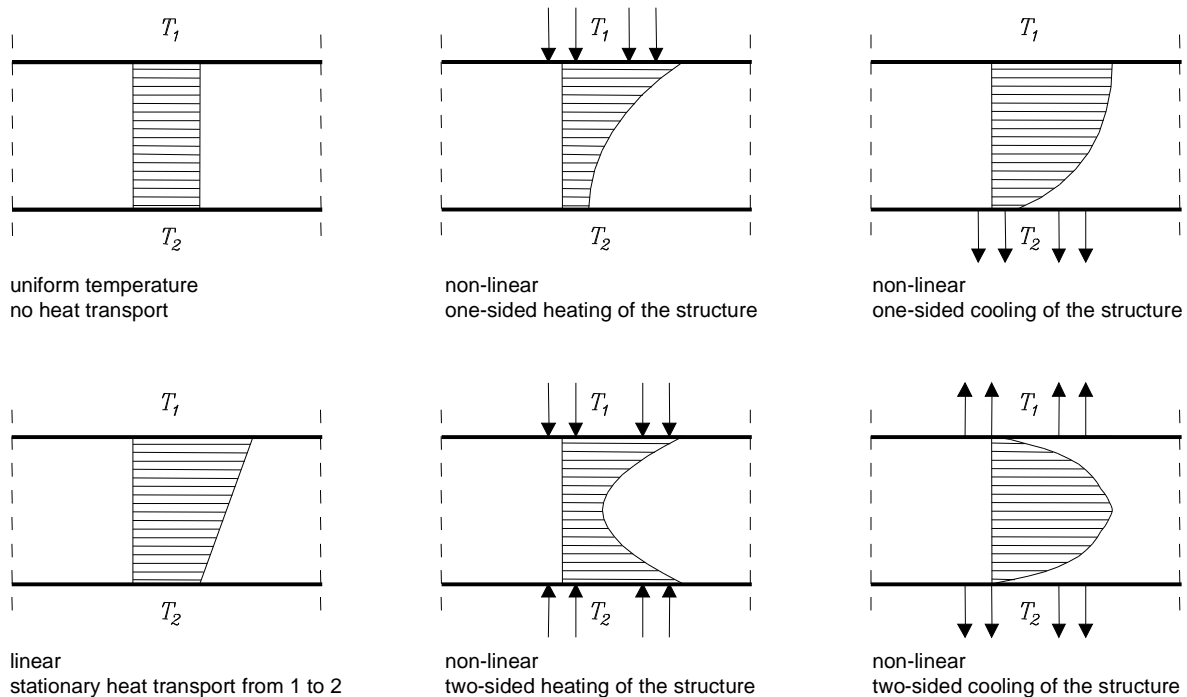


Figure 23-1 Temperature profiles

### 23.2 Unobstructed thermal deformation

#### Temperature change

When the temperature of an unobstructed object changes its length increases or decreases linearly according to:

$$\epsilon = \frac{\Delta \ell}{\ell} = \alpha \Delta T$$

- in which:  $\epsilon$  [-] = the strain (*rek*)  
 $\Delta \ell$  [m] = the change in length  
 $\ell$  [m] = the length at the reference temperature  
 $\alpha$  [°C<sup>-1</sup>] = the linear expansion coefficient  
 $\Delta T$  [°C] = the change in temperature

The linear expansion coefficients of a number of materials are given below:

Concrete	$1,0 \cdot 10^{-5} \text{ } ^\circ\text{C}^{-1}$
Steel	$1,2 \cdot 10^{-5} \text{ } ^\circ\text{C}^{-1}$
Ice	$5,5 \cdot 10^{-5} \text{ } ^\circ\text{C}^{-1}$

Table 23-1 Linear coefficients of expansion

It is noticeable that the linear expansion coefficients of concrete and steel are almost equal. This is useful because otherwise temperature fluctuations in reinforced concrete would create more problems. Figure 23-2 shows an example of the elongation of a simple beam due to a temperature increase. The shape of the beam is not relevant for the linear expansion.

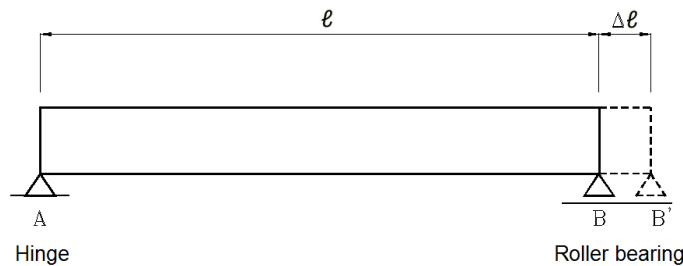


Figure 23-2 Increase in the length of a beam due to a total rise in temperature

After a temperature change, one can determine the position of all points on an arbitrary object relative to a fixed point because the shape of an object is not of importance. An example is given in Figure 23-3.

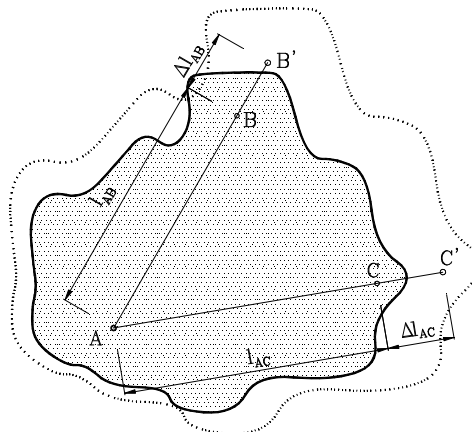


Figure 23-3 Change of the area of a sheet due to a total rise in temperature

### Temperature gradient

The preceding applies for a total temperature change (of the entire body). However, it is also possible that a temperature gradient occurs in the body. Figure 23-4 shows an example of this. There is a temperature rise on the underside and a temperature decrease on top. The consequence is a shortening on the upper side and a lengthening at the bottom of the beam, causing a curvature of the beam.

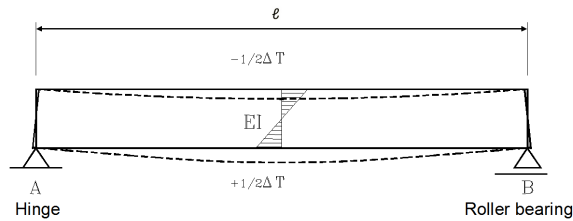


Figure 23-4 Temperature gradient in a beam

The curvature of the beam is equal in all places along the beam and amounts to:

$$\kappa = \frac{\varepsilon_b - \varepsilon_o}{h} = -\frac{\alpha \Delta T}{h}$$

The angle of rotation of the beam is found by integrating the curvature over the length:

$$\varphi_B = \varphi_A + \int_0^x \kappa dx = \varphi_A + \kappa x$$

The deflection is found by integrating the angle of rotation:

$$f_x = \int_0^x \left( \varphi_A + \int_0^x \kappa dx \right) dx = \varphi_A x + \frac{1}{2} \kappa x^2$$

Using the boundary conditions at the two supports one finds:

$$\varphi_A = -\frac{1}{2} \kappa \ell = \frac{\alpha \Delta T \ell}{2h}$$

The deflection in the middle is therefore:

$$f_m = -\frac{1}{4} \kappa \ell^2 + \frac{1}{8} \kappa \ell^2 = -\frac{1}{8} \kappa \ell^2 = \frac{\alpha \Delta T \ell^2}{8h}$$

In the case of a plate instead of a beam, the deflection must be considered in two directions. If the plate can deform unrestrainedly, it will rest on the corners if it bulges out.

For a temperature change of the beam, in which the temperature change is in the same direction both on top and in the bottom, one can distinguish an average temperature change and a temperature gradient. The change in length and the deflection can be calculated using the equations derived for the deformations.

The preceding, assumed a linear course of the temperature over the height of the structure. In reality, the course of the temperature is often not linear but curved. In such a case, the temperature course is divided into an average temperature, a linear temperature gradient and a so-called characteristic temperature. The linear temperature gradient is chosen such that the remaining characteristic temperature does not cause any deformations. An example is given in Figure 23-5. As regards the characteristic temperature, the following applies:

$$\int_0^h (T_e - T_0) dz = 0 \quad \text{and} \quad \int_0^h (T_e - T_0) z dz = 0$$

in which:  $h$  [m] = height of the structure  
 $T_e$  [°C] = characteristic temperature  
 $T_0$  [°C] = reference temperature

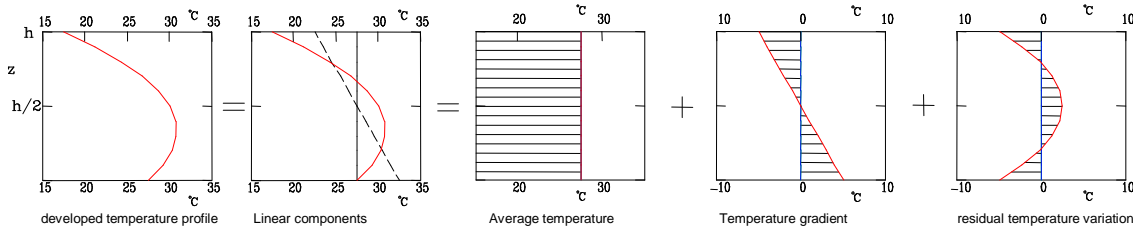


Figure 23-5 Arbitrary temperature distribution

The characteristic temperature does not cause any resulting deformations, but it does cause stresses. For a construction material such as concrete, one must take these stresses into account. This is of particular importance for the two-sided cooling of a thick structure during and after the setting of the concrete (hydration heat), causing tensile stress in the concrete.

### 23.3 Restrained thermal deformation

#### Temperature change

If the deformations of a structure due to temperature changes can take place without restraints, no stresses occur in the material. Generally, however, the deformation is restrained. This is usually the result of the boundary conditions of the supports, which in turn are determined by possible adjoining structure elements and the surroundings. As an example consider a structure buried in the ground. In the case of restrained deformation, the total deformation equals the unrestrained temperature deformation minus the deformation resulting from the stress increase.

The restriction of the linear expansion of a beam can be schematised as a beam with a spring in the roller bearing (see Figure 23-6).

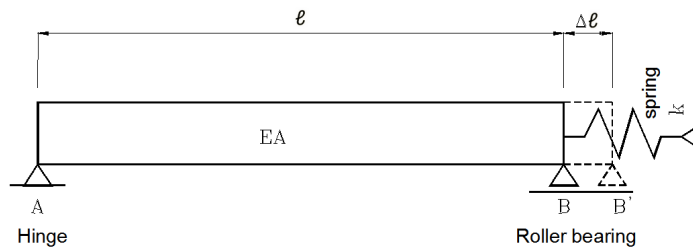


Figure 23-6 Restrained deformation due to temperature change

The elongation of the beam results in a force in the spring equal to:

$$F = k \Delta l$$

where:  $k$  [kN/m] = the stiffness of the spring

The occurring deformation is equal to the unrestrained temperature deformation minus the linear elastic deformation:

$$\Delta l = \alpha \Delta T \ell - \frac{F \ell}{EA}$$

This leads to the force  $F$ :

$$\frac{F}{k} = \alpha \Delta T \ell - \frac{F \ell}{EA} \Rightarrow F = \frac{\alpha \Delta T \ell}{\frac{1}{k} + \frac{\ell}{EA}}$$

If  $k = EA$ , 50% of the unrestrained deformation occurs. If  $k > 100 \cdot EA$  a fully restrained deformation is involved.

**Temperature gradient**

The restraint of the rotation of a beam due to the supports can also be schematised by a rotation spring (see Figure 23-7). The moment in the bearing then equals:

$$M = c \cdot \varphi$$

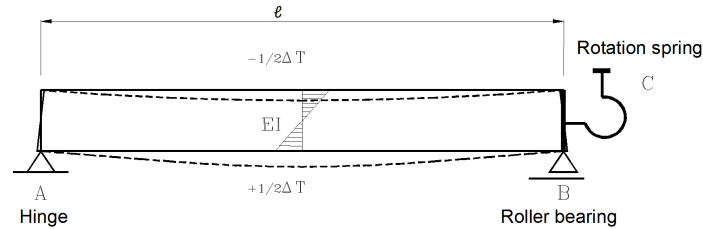


Figure 23-7 Restrained rotation

The rotation in the bearing equals the unrestrained temperature deformation minus the linear elastic deformation:

$$\varphi = \frac{\alpha \Delta T \ell}{2h} - \frac{M \ell}{3EI}$$

where:  $\alpha$  [ $^{\circ}\text{C}^{-1}$ ] = linear expansion coefficient  
 $h$  [m] = height of the beam

The moment is therefore:

$$\frac{M}{c} = \frac{\alpha \Delta T \ell}{2h} - \frac{M \ell}{3EI} \Rightarrow M = \frac{\alpha \Delta T \ell}{2h \left( \frac{1}{c} + \frac{\ell}{3EI} \right)}$$

**Longitudinal direction**

If the deformations of a plate are restrained, one must take the deformation in all directions into account. Close to the supports of the plate, where the deformation is restrained, shrinkage can cause a considerable tensile stress. This tensile stress is parallel to the supports. This is why concrete slabs should contain sufficient reinforcement in the direction perpendicular to the span (longitudinal reinforcement). The tensile stress will propagate further into the field as the slab is wider (see

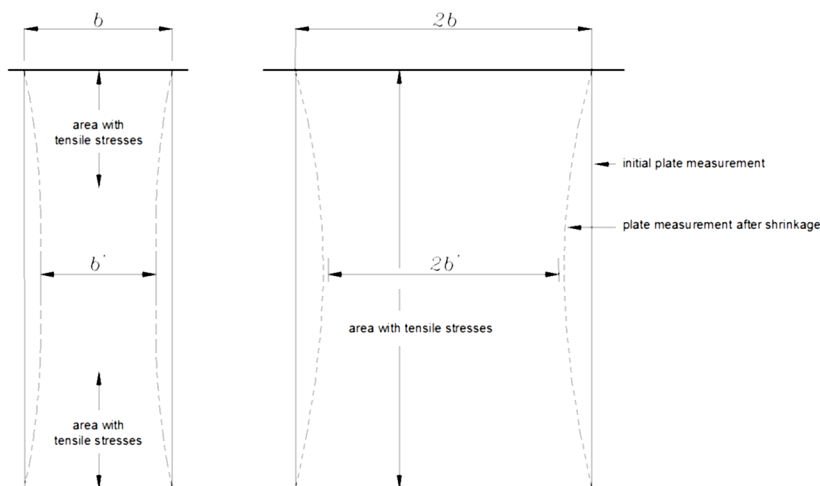


Figure 23-8).

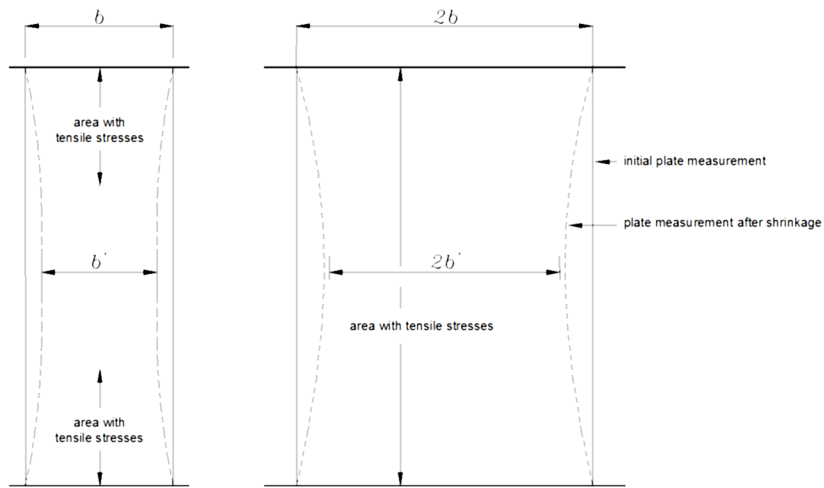


Figure 23-8 Effect of the width of a slab

**Note**

For compound structures one has to take in account that different temperatures create different expansions. For example an oil pipe with warm oil on a (cold) jetty needs an expansion loop.

## 24. Soil - loading and stresses

The effective soil stress is often the most important load on a structure, next to water pressure. After all, the effective soil stress is the only load on the entire structure that adjusts itself (up to a certain point) to the other loads: It resists the forces acting on the soil, creating equilibrium. Unless the ground collapses (actively or passively), the ground pushes back, both in normal direction and in shear direction, as much as the structure pushes the ground.

The load caused by the effective stress on the structure is never calculated by considering the load as such, but by calculating all other loads and considering the effective stress as the *balancing item*. One should not forget to check whether this load will ever exceed the maximum compression stress and the maximum shear stress of the soil during any construction or operational phases. For the maximum soliciting stresses, see Chapter 38 and for the bearing capacity of the soil see Chapter 32.

One must also remember to check that this load never causes the maximum displacement (and particularly the displacement difference) to be exceeded during any construction or operational phases.

If the maximum forces or displacements are likely to be exceeded, the design of the structure should be adjusted. The calculations of the loads then start anew and the design is therefore an iterative process.

This chapter describes the distribution of loads in soil in vertical and horizontal direction. The resistance, or strength, of soil against loads is described in part III of this manual (Chapter 32).

### 24.1 Vertical soil stress

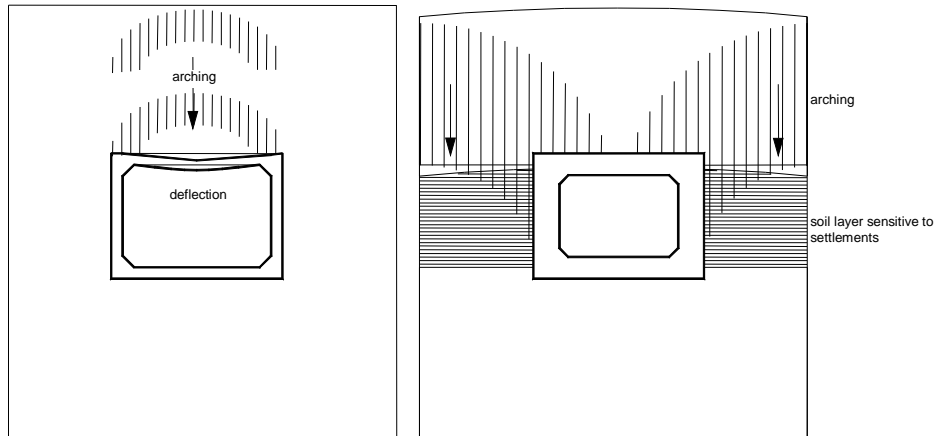
The exception to the rule given above, which states that the effective pressure can only be calculated as a balancing item of the other loads, is the vertical effective pressure on top of a structure. The vertical loads occur on horizontal and diagonal planes of structures in the ground, e.g. cellars and tunnels. The total load corresponds to the weight of the ground. One has to divide total stresses into inter-granular stresses and water pressures (see Chapter 27 "Soil, groundwater").

The vertical effective pressure (load) for a soil system with  $n$  dry layers and  $m$  wet layers can be determined according to:

$$\sigma_v' = \sigma_v - \rho \quad \text{i.e.:} \quad \sigma_v' = \sum_{i=1}^n \gamma_{d,i} d_i + \sum_{j=1}^m \gamma_{n,j} d_j - \rho$$

in which:	$\sigma_v'$	[kN/m <sup>2</sup> ]	= vertical inter-granular stress (= effective pressure)
	$\sigma_v$	[kN/m <sup>2</sup> ]	= total vertical stress
	$\gamma_{d,i}$	[kN/m <sup>3</sup> ]	= dry volumetric weight of soil layer $i$ : $\gamma_{d,i} = \rho_{d,i} g$
	$\gamma_{n,j}$	[kN/m <sup>3</sup> ]	= wet volumetric weight of soil layer $j$ : $\gamma_{n,j} = \rho_{n,j} g$
	$\sigma$	[kg/m <sup>3</sup> ]	= volumetric mass of a soil layer
	$d_i$	[m]	= thickness of soil layer $i$ above the considered plane
	$n$	[-]	= number of dry layers above the considered plane
	$m$	[-]	= number of wet layers above the considered plane
	$\rho$	[kN/m <sup>2</sup> ]	= water pressure in the considered plane

The interaction between the structure and the ground is different from the interaction between the structure and the groundwater. The groundwater does not have any shear stiffness and the groundwater pressures do not depend on possible deformations of the structure. This is different for the soil. In soil it is possible that deformations of a structure or the surrounding ground cause a redistribution of the total stresses. For instance, in a tunnel of limited dimensions arching can occur in transverse direction, thereby more or less relieving the roof of the tunnel of stresses. A stiff structure can also be subjected to a larger load if there are settlements of the surrounding ground, because the surrounding ground is "suspended" from the structure.

Figure 24-1 Arching (Left  $K_a < 1$ , right  $K_p > 1$ )

### **Pressure under a structure / surcharge**

Loads on ground level result in a change of the stresses in the subsoil. The horizontal and vertical earth pressures on a structure will consequently increase. There are various models to calculate the increase of the earth pressure as a result of a load on ground level. The best known are models by Boussinesq, Flamant and Newmark. For these methods the reader is referred to the lecture notes Soil Mechanics (A. Verruijt / S. van Baars).

The ratio between the stiffness of the structure and the stiffness of the soil has an important influence on the soil pressure distribution under the structure. There are several models or schematisations in use for soil stiffness. Depending on the model, the influence on soil pressure distribution, especially the spreading of pressure, is either less or more significant, see below in this Section under 'stress distribution'. Generally the Winkler model is used for soil stiffness, which models the soil as a system of mutually independent vertical springs with stiffness  $k$ .

Considering the stiffness ratio soil-structure, an extreme case is to assume an infinitely stiff structure. This assumption implies that the foundation surface remains level. In combination with the Winkler soil stiffness model the calculation of the soil pressure distribution is analogous to the calculation of a cross-section of a beam with normal and shear forces, and bending moments (For a foundation  $\Sigma V$  and  $\Sigma H$  are the equivalent of normal and shear force respectively; the resulting overturning moment  $\Sigma M$  is the equivalent of the bending moment). Therefore the stress in point  $(x,y)$  under an infinitely stiff structure, the whole contact surface remains under pressure, is:

$$\sigma_{x,y} = \frac{V}{A} + \frac{M_y}{I_y} x + \frac{M_x}{I_x} y$$

in which:

- $I_y$  = the moment of inertia of the foundation around the  $y$ -axis
- $I_x$  = the moment of inertia of the foundation around the  $x$ -axis
- $A$  = the area of the foundation =  $b \cdot h$
- $V$  = the vertical load
- $M_y$  = moment in  $y$  direction relative to the centre of mass of the foundation  
 $M_y = V e_x$
- $M_x$  = moment in  $x$  direction relative to the centre of mass of the foundation  
 $M_x = V e_y$

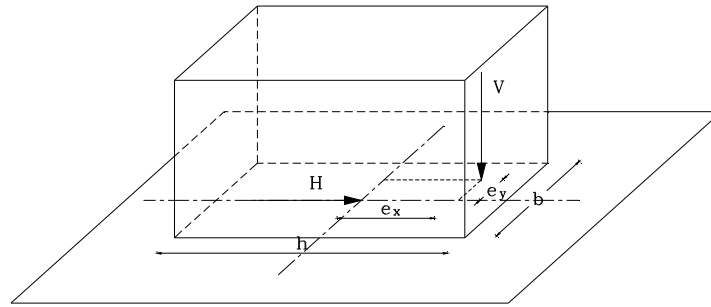


Figure 24-2 Stiff structure on a shallow foundation

Since the entire foundation surface remains under pressure, the working line of the resulting force lies within the core of the foundation surface. The dimensions of the core of the surface can easily be determined using:

$$e_b = \frac{W_b}{A} ; e_o = \frac{W_o}{A} ; e_l = \frac{W_l}{A} ; e_r = \frac{W_r}{A}$$

in which:  $e_b, e_o, e_l, e_r$ : dimensions of the core according to Figure 24-3

$$W_b = \text{section modulus } \frac{I_x}{y_b}$$

$$W_l = \text{section modulus } \frac{I_y}{x_l}$$

$$W_o = \text{section modulus } \frac{I_x}{y_o}$$

$$W_r = \text{section modulus } \frac{I_y}{x_r}$$

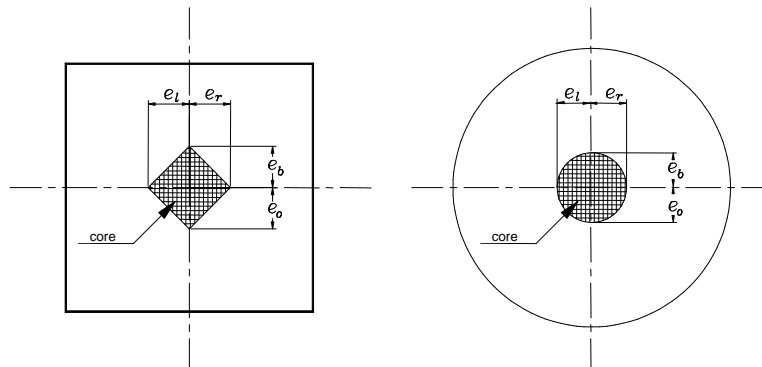
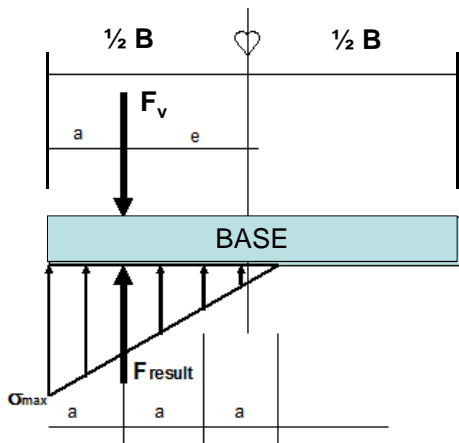


Figure 24-3 The cores of a square and a circular cross-section

If the resultant of the loads lies outside the core of the foundation surface, the previous equations for the stresses in the foundation plane do not apply.

Large eccentricities, the resulting force has a working line outside the core of the foundation surface, considerably complicate the calculation of soil pressure distributions under the foundation.

A well-known solution for a rectangular foundation assumes a triangular soil pressure distribution for the part of the base that remains in contact with the soil. For equilibrium of forces ( $\Sigma V = \Sigma H = \Sigma M = 0$ ) the working line of the resultant of the soil pressure should be the same line as the one for the resultant of the loads. Using the position of the centre of gravity for a triangle, one-third of the base, the maximum (required) soil pressure can be determined easily (see Figure 24-4).



$$F_v = F_{result} = \frac{1}{2} \cdot \sigma'_{max,soil} \cdot 3a \Rightarrow$$

$$\sigma'_{max,soil} = \frac{2 \cdot F_v}{3a}$$

Figure 24-4 Pressures in the case of a very eccentric load

If the structure is not infinitely stiff relative to the soil, use of the Winkler model for the soil stiffness only yields approximate results. For finite stiffness of the structure, relative to the soil stiffness, the way to determine the soil pressure distribution more accurate is to use the theories on elastic or elasto-plastic half spaces. Reference is made to the work of Hetenyi – “Beams on elastic foundation” [1946].

Vertical stress distribution under a structure or top load

A stress at ground level will spread in depth due to the shear stresses in the soil. The course of the stresses was solved by Flamant. The spread of the stress somewhat resembles a Gaussian curve. Because this is difficult in calculations, for a preliminary design one can spread the stress below an angle of 45°, as shown in the figure below.

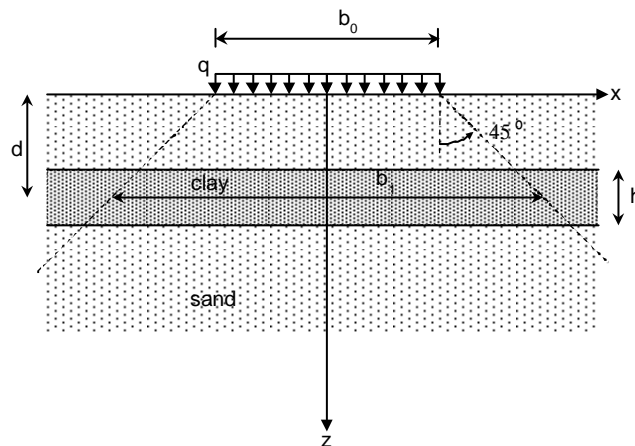


Figure 24-5 Simplified stress spread in depth

The contributing width  $b_1$  and length  $l_1$  are then:

$$b_1 = b_0 + 2d \quad \text{and:} \quad l_1 = l_0 + 2d$$

The average increase in stress in the clay layer due to the load is then:

$$\Delta \bar{\sigma}' = \frac{b_0 l_0}{b_1 l_1} q$$

The strain in the clay layer is subsequently calculated with:  $\Delta \sigma' = E_{oed} \Delta \epsilon$  (Hooke) or, even better, with Koppejan (see following section).

The total settlement  $u$  then follows from:

$$u = h\Delta\varepsilon$$

### Notes

- Computer programmes are faster at calculations than man and therefore do not use this simplified stress spreading method, but methods such as Flamant.

Flamant's solution is based on one of Boussinesq's solutions (point force on an infinite half space); which is why computer programmes often state the stress spreading method is based on Boussinesq. Flamant (1892) found a solution for the stresses in an infinite half-space<sup>5</sup> subjected to a line load. On the basis of superposition, this solution can be transformed to a solution for a strip-shaped load.

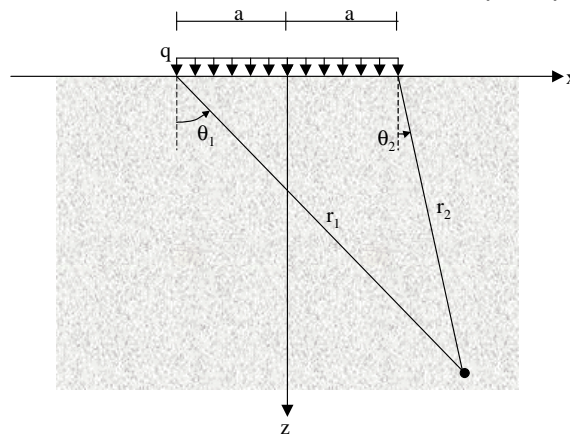


Figure 24-6 Strip load (Flamant)

The stresses in an arbitrary point in this homogenous half-space are:

$$\sigma'_{zz} = \frac{q_v}{\pi} [(\theta_1 - \theta_2) + \sin \theta_1 \cos \theta_1 - \sin \theta_2 \cos \theta_2]$$

$$\sigma'_{xx} = \frac{q_v}{\pi} [(\theta_1 - \theta_2) - \sin \theta_1 \cos \theta_1 + \sin \theta_2 \cos \theta_2]$$

$$\sigma'_{xz} = \frac{q_v}{\pi} [\cos^2 \theta_2 - \cos^2 \theta_1]$$

## 24.2 Horizontal soil stress

When determining the total horizontal soil stress acting on a structure, the water pressure ( $p$ ) and the effective vertical soil pressure ( $\sigma'$ ) should be considered separately:

$$\sigma_{soil,h} = \sigma_h' + p$$

The reason for this is that the magnitude of water pressure at a certain depth is the same in all directions (law of Pascal), but soil pressure is not.

The horizontal groundwater pressure  $p$  at a certain depth is equal (in magnitude, not in direction) to the vertical groundwater pressure at that depth and is determined according to Chapter 27 "Soil, groundwater".

The relation between the horizontal and the vertical effective pressure is regularly assumed to be constant (first assumption):

$$\sigma_h' = K \cdot \sigma_v'$$

There are three types of soil behaviour under stress. The first type occurs when soil is at rest, so when it does not deform due to deflection or sliding aside of a structure. This state of stress is called 'neutral

<sup>5</sup> A half-space is either of the two parts into which a plane divides the three-dimensional (Euclidean) space

stress'. The second type of soil behaviour under stress occurs when the soil becomes less compacted than at rest, due to, e.g., deflection of a sheetpile wall, or the sliding aside of a gravity structure away from the soil body. This is called active soil stress. The third type of soil stress, the passive stress, occurs when the soil is compressed due to movement of a wall in the direction of the soil. These three types of soil behaviour are explained in the following sections.

### **Neutral soil stress (Jaky's theory)**

Hungarian J. Jaky studied the relation between vertical and horizontal soil at rest and published his results in 1944 in Hungarian. He assumed a constant relation between the horizontal and the vertical effective pressure:

$$\sigma'_h = K \cdot \sigma'_v$$

where:

$\sigma'_h$	[Pa]	=	horizontal soil pressure
$\sigma'_v$	[Pa]	=	vertical soil pressure
$K_0$	[-]	=	neutral soil pressure coefficient
$\phi$	[°]	=	angle of internal friction

The relation between the horizontal and vertical effective pressures without deformation is the neutral soil pressure coefficient. This coefficient is unknown and difficult to measure. To simplify matters one often uses J.Jaky's formula:

$$\sigma'_h = K_0 \cdot \sigma'_v \quad \text{with: } K_0 = 1 - \sin(\phi)$$

This formula was first published in 1944 and still seems to be relatively accurate for the limit values. It works well for water ( $\phi = 0$  so:  $K_0 = 1 - \sin(\phi) = 1$ ) and seems to work fairly well for sand ( $\phi \approx 30^\circ$  so:  $K_0 = 1 - \sin(\phi) \approx 0,5$ ). This formula is very popular, for want of anything better, but not very scientific. Overloaded soil generally shows a far higher value.

The accuracy of Jaky's neutral soil pressure coefficient is often disputed, but at least it gives values between 0 and 1, and leads to conservative results, so it is still being used. A study in 2005 even led to the conclusion that it is surprising that the equation is a good representation of the true stress ratio in soils at rest (Michalowski, 2005 Journal of Geotechnical and Geo-environmental engineering ASCE).

Large shallow foundations expand due to temperature changes, so in these cases one must take a larger pressure on the vertical walls into account than predicted by Jaky. In this case:

$$\sigma'_{h,n} = K_0 \cdot \sigma'_v \quad \text{with: } K_0 \approx 1$$

Eurocode 7 also takes the over-consolidation ratio (OCR) into account for the horizontal soil pressure. The over-consolidation ratio is the relation between the original effective vertical soil pressure and the actual effective vertical soil pressure at the same depth. The neutral soil pressure coefficient should then be calculated according to:

$$K_0 = (1 - \sin \phi) \cdot \sqrt{OCR}$$

This equation should not be used for 'very high values of OCR'.

If the ground level behind the wall deviates from the horizontal plain with an angle  $\beta$ , the horizontal effective soil may be calculated using:

$$K_{0,\beta} = K_0 \cdot (1 + \sin \beta)$$

**Notes**

- If a structure is sensitive to seasonal temperature changes (resulting in stress increment in the structure), a soil pressure coefficient of  $K = 1,0$  should be used under the following two conditions:
  - The horizontal effective pressure on the wall of a tunnel or open excavation acts unfavourably;
  - The bottom of the structure is wider than 15 m.
- For the variable load at ground level next to an open excavation or an excavated building site, an evenly distributed surface load of at least 20 kN/m<sup>2</sup> or VOSB class 45 should be used.

**Active and passive soil stress (Rankine's theory)**

Figure 24-1 shows the various types of soil deformation due to movement of walls or structures.

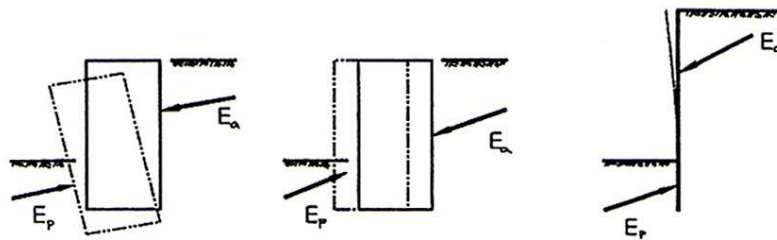


Figure 24-1 Soil deformation due to rotation, displacement or deflection of a wall or structure

Soil under active stress develops less horizontal soil pressure than soil under passive stress. In principle, the horizontal soil pressure is undetermined; only a lower and an upper limit can be given, corresponding to two types of ground collapse: maximum active, or maximum passive. According to Rankine (based on Mohr-Coulomb and smooth horizontal walls), and including cohesion, these lower and upper limits are as follows:

$$\sigma'_{h,min} = K_a \sigma'_v - 2c\sqrt{K_a} \quad \text{with} \quad K_a = \frac{1 - \sin \phi'}{1 + \sin \phi'} \quad \text{coefficient of active soil pressure}$$

$$\sigma'_{h,max} = K_p \sigma'_v + 2c\sqrt{K_p} \quad K_p = \frac{1 + \sin \phi'}{1 - \sin \phi'} \quad \text{coefficient of passive soil pressure}$$

The maximum and minimum horizontal effective pressures correspond to a state of ground collapse. The maximum effective pressure depends on the passive soil pressure coefficient  $K_p$  and the minimum effective pressure depend on the active soil pressure coefficient  $K_a$ .

The value of the real horizontal effective soil pressure lies somewhere between the maximum and minimum pressure and depends mainly on the horizontal displacement of the wall. The horizontal soil pressure develops gradually between the two limit states, see Figure 24-2.

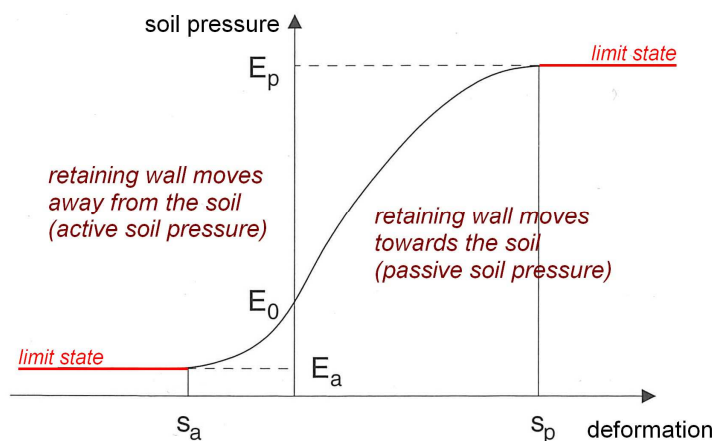


Figure 24-2 Horizontal soil pressure versus deformation of the soil

The horizontal soil pressure can be influenced by cold flow, temperature changes and the loading history.

### Horizontal soil pressure on a vertical wall

Using Mohr's circle, William Rankine, a Scottish civil engineer, found a definition for the maximum and minimum horizontal effective stresses with a given vertical pressure. The reasoning behind it is that a sliding surface occurs due to the combinations of vertical and horizontal stresses. This means that the Mohr circles have a tangent line  $\tau = c' + \sigma' \tan(\varphi')$ .

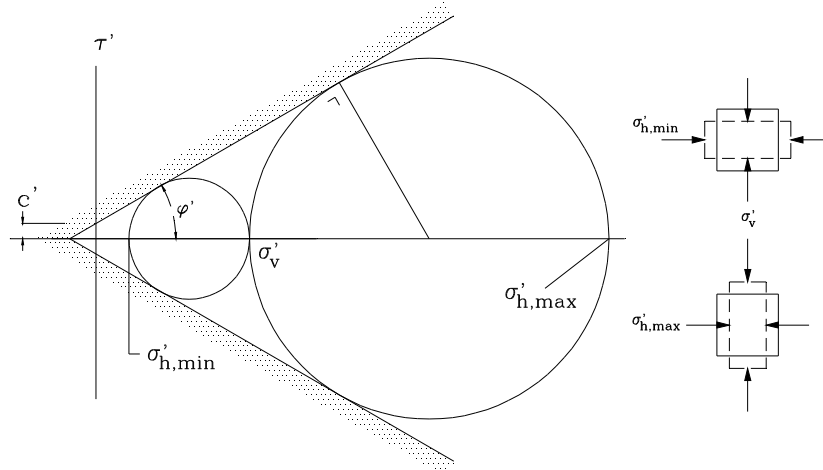


Figure 24-3 Rankine

When a straight wall without shear stress collapses, straight sliding surfaces are created. Using some trigonometry one can derive the maximum and minimum horizontal effective stresses for a straight wall without shear stresses:

$$\sigma'_{h,\min} = K_a \sigma'_v - 2c \sqrt{K_a} \quad \text{with: } K_a = \frac{1 - \sin \varphi'}{1 + \sin \varphi'}$$

$$\sigma'_{h,\max} = K_p \sigma'_v + 2c \sqrt{K_p} \quad \text{with: } K_p = \frac{1 + \sin \varphi'}{1 - \sin \varphi'}$$

If the soil is non-cohesive (like sand),  $c = 0$  which simplifies the equation.

Please bear in mind that in reality,  $K_p$  is limited to a maximum value of about 7,5. If the soil retaining structure cannot deform or displace, or if displacements are not tolerable,  $K_0$  should be used instead of  $K_a$  and  $K_p$ .

### Horizontal pressure on an oblique wall (*hellende wand*)

The load on a soil retaining structure can differ from these maximum and minimum effective stresses. This is due to:

1. the friction of the soil along the wall
2. a possibly increasing ground level
3. the possible obliqueness of the soil retaining structure.

The general formulation of the horizontal pressure then is:

$$\sigma'_{h,\min} = K_{a,h,\sigma} \sigma'_v + K_{a,h,c} c$$

$$\sigma'_{h,\max} = K_{p,h,\sigma} \sigma'_v + K_{p,h,c} c$$

in which:  $K_{a,h,\sigma}$  = active coefficient for the effective stress  
 $K_{a,h,c}$  = active coefficient for the cohesion  
 $K_{p,h,\sigma}$  = passive coefficient for the effective stress  
 $K_{p,h,c}$  = passive coefficient for the cohesion

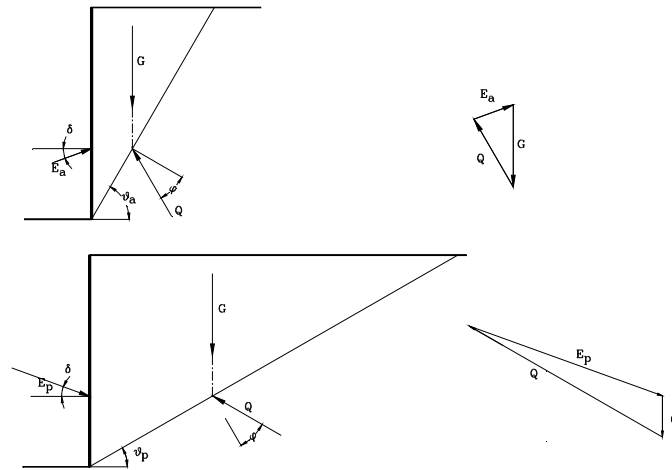


Figure 24-4 Balance of forces in the case of straight sliding surfaces

The balance of forces based on equilibrium considerations of a wedge of soil sliding along a straight sliding surface, corresponding to Rankine's state of stress, is schematised in Figure 24-4. The resultant force  $E_a$  or  $E_p$  on the soil retaining structure forms an angle  $\delta$  with the normal to the retaining wall. The horizontal component of the ground pressure is found by resolving the total ground pressure into its horizontal and vertical components.

Formulas for the coefficients of horizontal ground pressure have been derived for homogenous (non-layered) soil (by Müller/Breslau):

$$K_{a,h,\sigma} = \frac{\cos^2(\phi + \alpha)}{\cos^2(\alpha) \left( 1 + \sqrt{\frac{\sin(\phi + \delta) \sin(\phi - \beta)}{\cos(\alpha - \delta) \cos(\alpha + \beta)}} \right)^2}$$

$$K_{p,h,\sigma} = \frac{\cos^2(\phi - \alpha)}{\cos^2(\alpha) \left( 1 - \sqrt{\frac{\sin(\phi - \delta) \sin(\phi + \beta)}{\cos(\alpha - \delta) \cos(\alpha + \beta)}} \right)^2}$$

$$K_{a,h,c} = -\frac{2 \cos(\phi) \cos(\beta) (1 - \tan(\alpha) \tan(\beta)) \cos(\alpha - \delta)}{1 + \sin(\phi + \delta - \alpha - \beta)}$$

$$K_{p,h,c} = \frac{2 \cos(\phi) \cos(\beta) (1 - \tan(\alpha) \tan(\beta)) \cos(\alpha - \delta)}{1 - \sin(\phi - \delta + \alpha + \beta)}$$

in which:  $\alpha$  = the obliqueness of the structure (see Figure 24-5)

$\beta$  = the angle of the ground level (see Figure 24-5)

$\phi$  = angle of internal friction

$\delta$  = the angle between the resultant force exerted on the soil retaining wall and the normal to this wall (see Figure 24-5) (assumption  $\delta \approx 0,8$  to  $0,9 \cdot \phi$ , see Section 32.3)

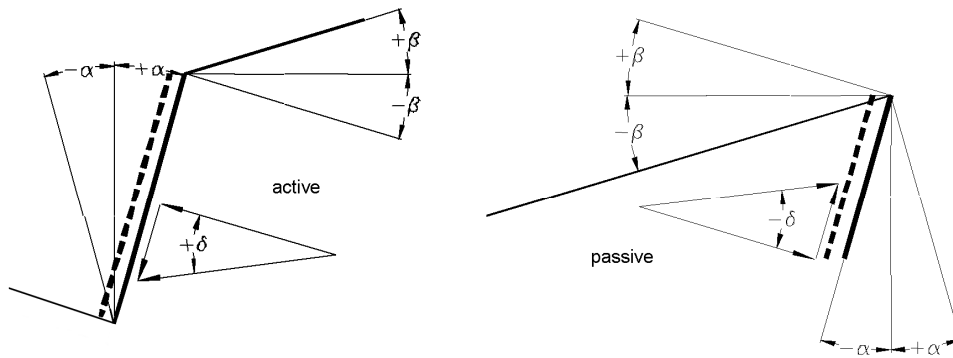


Figure 24-5 Definition of angles

The aforementioned formulas assume straight sliding surfaces. For angles of internal friction ( $\phi$ ) higher than  $30^\circ$ , curved sliding planes are more realistic (the theory of curved sliding surfaces is not discussed in this manual). If nevertheless the Müller / Breslau equations are used for these higher values of  $\phi$ , the resulting values for  $K_{p,h,c}$  are unrealistically high. In reality,  $K_{p,h,c}$  is limited to a maximum value of about 7. This also applies to the simplified equations.

**Infinite surface load next to a wall**

In the case of a surface load  $q$  that reaches infinitely far in two directions, the additional horizontal load on an oblique wall is:

$$\Delta\sigma'_{h,min} = K_{a,h,\sigma} q \frac{\cos(\alpha)\cos(\beta)}{\cos(\alpha + \beta)} \quad \Delta\sigma'_{h,max} = K_{p,h,\sigma} q \frac{\cos(\alpha)\cos(\beta)}{\cos(\alpha + \beta)}$$

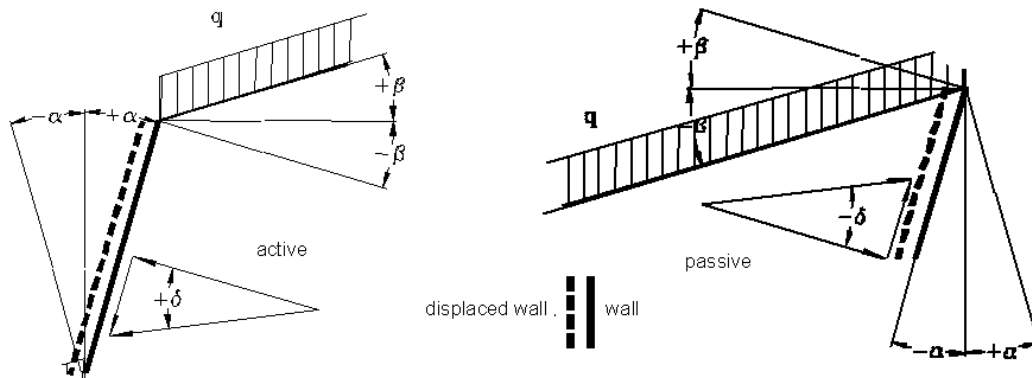


Figure 24-6 Infinitely extended surface load

For vertical walls, where  $\alpha = \beta = 0^\circ$ , these equations reduce to:

$$\Delta\sigma'_{h,min} = K_{a,h,\sigma} q \quad \Delta\sigma'_{h,max} = K_{p,h,\sigma} q$$

**Finite surface load next to a wall**

If the load is merely exerted on a strip along the side of the soil retaining structure, the horizontal load on the structure is smaller at the bottom of the wall. An approximation of the horizontal load on the soil-retaining structure is given in Figure 24-7. In this case one assumes that the surface loads spreads to a depth  $b$  that is determined by the active sliding surface that could occur behind the surface load. It is also assumed that the load reduces to zero over a height of  $\frac{1}{2}b$ .

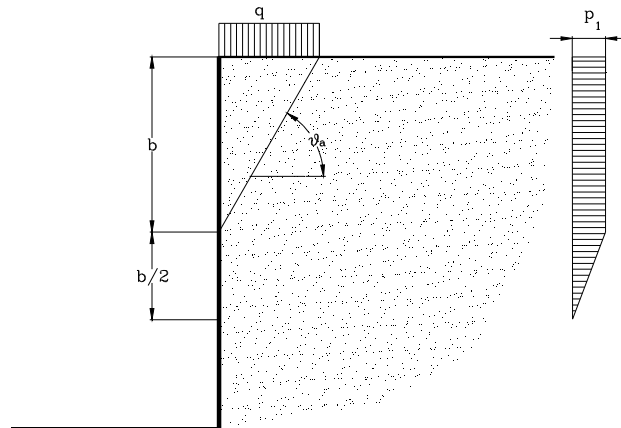


Figure 24-7 Load on a strip next to the soil retaining structure

The influence at a depth  $b$  is calculated using angle  $\vartheta_a$  for active soil and  $\vartheta_b$  for passive soil:

$$\tan \vartheta_a = \tan \varphi + \sqrt{\frac{(1 + \tan^2 \varphi) \cdot \tan \varphi}{\tan \varphi + \tan \delta}} \quad \text{and} \quad \tan \vartheta_p = -\tan \varphi + \sqrt{\frac{(1 + \tan^2 \varphi) \cdot (-\tan \varphi)}{-\tan \varphi + \tan \delta}}$$

By approximation the additional horizontal load  $\Delta\sigma'_h$  is:

$$\Delta\sigma'_h = p_1 = qK_{a,h,\sigma}$$

(For a more accurate solution see Section 24.1).

**Infinite surface load at a distance of a wall**

In the case of a very extensive load at some distance from the soil retaining structure, the top of the structure will have a smaller load. An approximation of the horizontal load on the structure is given in Figure 24-8.

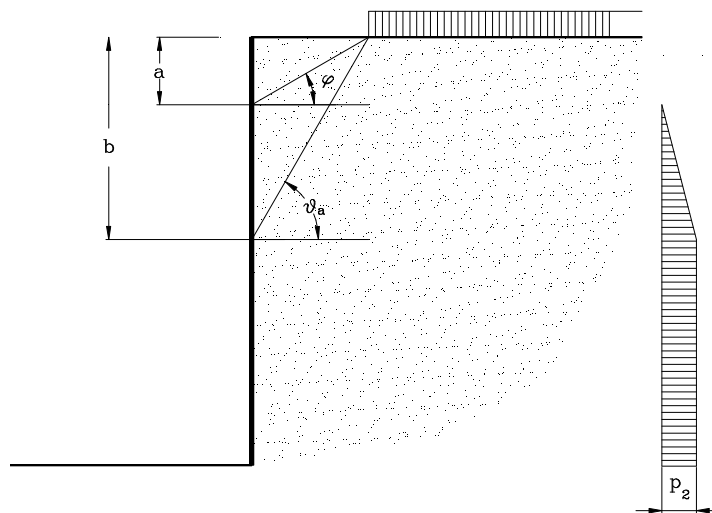


Figure 24-8 Extensive load at a distance from the structure

In this case, too, the maximum horizontal soil pressure is:  $p_2 = qK_{a,h,\sigma}$

### Finite surface load at a distance of a wall

One can approximate the horizontal load due to a strip load at some distance from the soil retaining structure according to Figure 24-9.

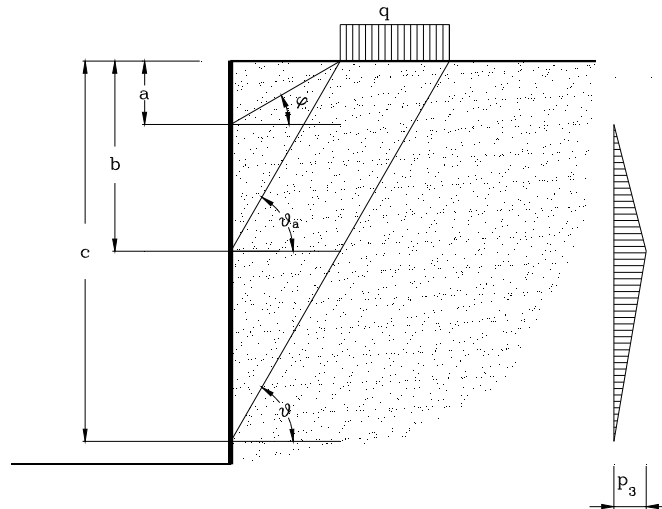


Figure 24-9 Strip load at some distance from the structure

In this case the maximum horizontal earth pressure due to the surface load is:

$$p_3 = \frac{2qs\theta}{c-a}$$

in which:

$$\theta = \frac{\sin(\vartheta_a - \varphi) \cos(\delta)}{\cos(\vartheta_a - \varphi - \delta)}$$

$s$  = the width of strip where the load is exerted  
 $a, c$  = see Figure 24-9

(For a more accurate solution see Section 24.1).

### Horizontal stress distribution next to a finite surface load

The stress on a retaining wall next to a surface load at a certain distance of that wall may be assumed to vary over angles of  $\pm 45^\circ$ , like depicted in Figure 24-10. It gradually decreases further aside, until the retaining wall does not experience any influence of the surface load any more.

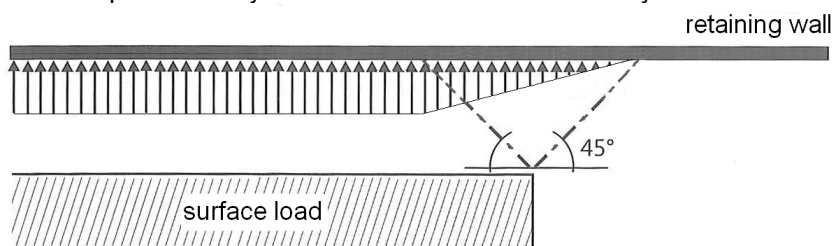


Figure 24-10 Top view of a situation with horizontal stress distribution next to a finite surface load (adapted from EAU 2012)

### Horizontal pressure on piles

For a three-dimensional situation, as for piles, one can increase  $K_p$  and the cohesion due to shell behaviour. The Danish structural engineer Jørgen Brinch Hansen, who was specialised in soil mechanics, gives one method for this in his book "The ultimate resistance of rigid piles against transversal forces". The 3-D values for the coefficient of passive earth pressure and the cohesion as a result of shell behaviour is built into the programme code in the computer program D-sheetpiling. The calculation is too complicated to discuss in this Manual.

## 25. Soil, settlement

Settlements (*zettingen*) occur as a result of raising the effective stresses in the subsoil. For instance, this could be by placing a foundation or by lowering the groundwater level. Settlements as such are usually not a problem for a structure, as long as the settlements are even. Only for flood defences the lowering of the crest due to settlements should be taken into account (regarding critical overtopping discharges), also when the settlement is even.

Uneven settlements can create large stresses in a structure. There are several causes for this:

- Uneven foundation pressure
- Different sized foundation elements (even if the pressure is equal!). Wide elements will settle more than narrow elements with an equal foundation pressure because the stress in the heart of the structure is spread out less and thus works to a larger depth.
- Local deviations from the soil properties. Locally the soil may be stiffer or less stiff, which causes uneven settlements for even loads.
- Changes of the horizontal stresses due to a nearby structure excavation or a (bored) tunnel.

According to NEN 6740, article 5.2.2.2, no span (foundation beams!) may undergo a rotation due to settlement differences larger than:

$$\frac{\Delta z}{\ell} = \theta = 1/300$$

For shallow foundations, the settlement can be calculated according to Chapter 33 (Part III). For pile foundations, the above requirement is usually met. To check the design of pile foundations, see Chapter 43 (compression piles) and the lecture notes on deep foundations (part of the course material for "Hydraulic Structures 1").

For excavations (building site) the consequences of the swelling of weaker soil layers located at a larger depth must also be taken into account. For excavations (building site), a pipe located nearby could undergo a rotation (see figure below). This can also be tested using the rotation condition given above.

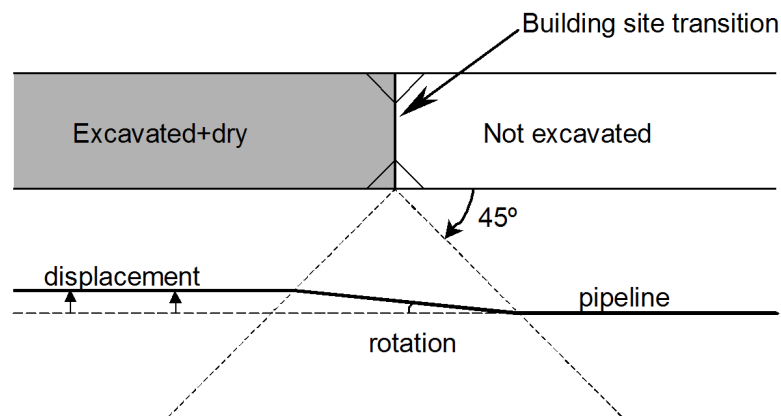


Figure 25-1 Rotation of a pipe near a building site excavation

If one expects problems due to excessive settlement differences, one can take the following measures:

- Using equal foundation pressures.
- Using equal-sized foundation elements.
- Applying soil improvement measures.
- Demanding stricter requirements for the structure excavation or (bore) tunnel.
- Applying pile foundations.
- Introducing movement joints.
- Reducing the distance between joints.
- Changing the statically indeterminate structure into a statically determinate structure.

Figure 25-2 indicates the difference between a statically determinate beam (two supports) and a statically indeterminate beam (three supports). In the first case the forces and moments are not influenced by the settlement of a support. In the second case the moment above the settled middle support decreases and the moment in the field thus increases.

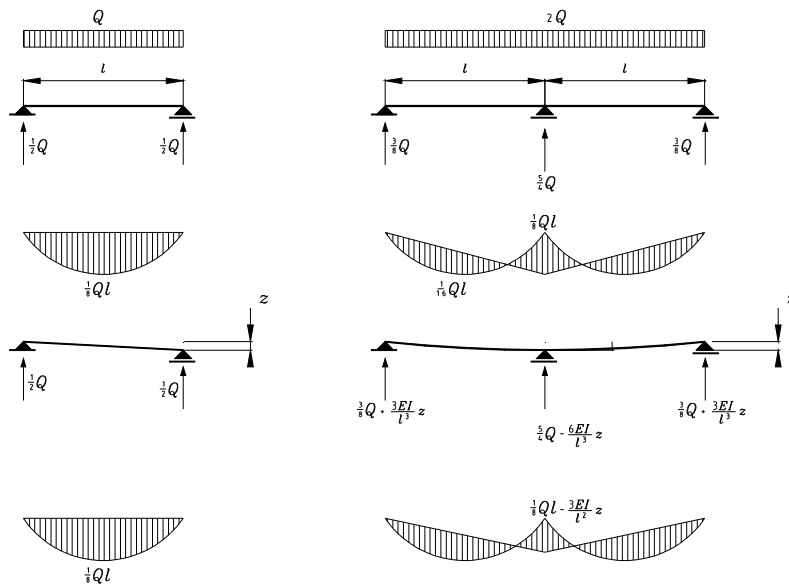


Figure 25-2 Forces and moments as a result of the settlement of a support

Settlements can be taken into account in the structural calculations in two ways, namely:

- Taking an imposed deformation into account
- Schematising the ground as a spring

The schematisation of the ground as a spring is not an accurate method because the ground does not behave like a spring. It is preferable to take the settlements into account as imposed deformations, whereby the settlements are determined using the distribution of forces in the structure initially neglecting the settlements. This way the settlements are overestimated and the calculated load is conservative. It is possible to carry out the calculations a number of times, thus iterating, to estimate the loads more accurately.

For both methods of calculation, see Chapters 32 and 33 (Part III).

## 26. Soil, earthquake

### 26.1 General

For the design of a hydraulic engineering work it is important to know whether earthquakes occur in the area where construction is to take place. The horizontal accelerations induced by earthquakes largely affect:

1. The ground  
Particularly due to the ratio between the horizontal and the vertical ground stresses. This can lead to plastic deformation of the ground.
2. Structures (above and below ground level);  
These structures are also subjected to the same accelerations in both horizontal and vertical directions.

The theory of the generation of earthquakes assumes that the earth's crust consists of plates that move very slowly relative to each other. At the interface between the plates (the fault line), elastic deformation takes place until a maximum shear stress is exceeded. At that moment the earth's crust deforms plastically and the potential energy of the elastic deformation is released. This occurs as a jerky deformation (waves and vibrations).

Earthquakes can also be caused by deformations in the earth's crust. Examples are earthquakes due to gas and oil extraction.

### 26.2 Richter scale

The Richter scale is mostly used to register and classify earthquakes. The Richter scale is derived from the maximum registered amplitude of the quake and the distance from the point of registration to the epicentre of the earthquake. The epicentre is the projection of the point of origin of the quake on the Earth's crust. The Richter scale value is called the magnitude of the earthquake. This magnitude is independent of the location of the measurement of the amplitude. Though every earthquake has a unique magnitude that is the same in all locations on earth, the effect of the earthquake is not the same everywhere. Therefore, the magnitude of an earthquake cannot be used for a good estimation of the amount of damage to or load on a structure. The table below, however, can be used to give a global indication of the effects.

Earthquake Severity	
Richter Magnitudes	Earthquake effects
Less than 3,5	Generally not felt, but recorded
3,5 - 5,4	Often felt, but rarely causes damage.
Under 6,0	At most slight damage to well-designed buildings. Can cause major damage to poorly constructed buildings over small regions.
6,1 - 6,9	Can be destructive in areas up to about 100 kilometres across where people live.
7,0 - 7,9	Major earthquake. Can cause serious damage over larger areas.
8,0 or larger	Large earthquake. Can cause serious damage in areas several hundred kilometres across.

Table 26-1 Effects related to the Richter scale

Another indication is that the energy related to magnitude 1 corresponds to a car (1000 kg) falling to the ground from a height of 100 metres. For every single increase of magnitude, the number of cars can be multiplied by thirty. Hence, for magnitude 8, one would have to drop 22 billion cars from the Dom tower in Utrecht.

To determine the Richter scale a nomogram can be used, which requires the distance to the epicentre and the maximum amplitude as input. An example of such a nomogram is given in Figure 26-1.

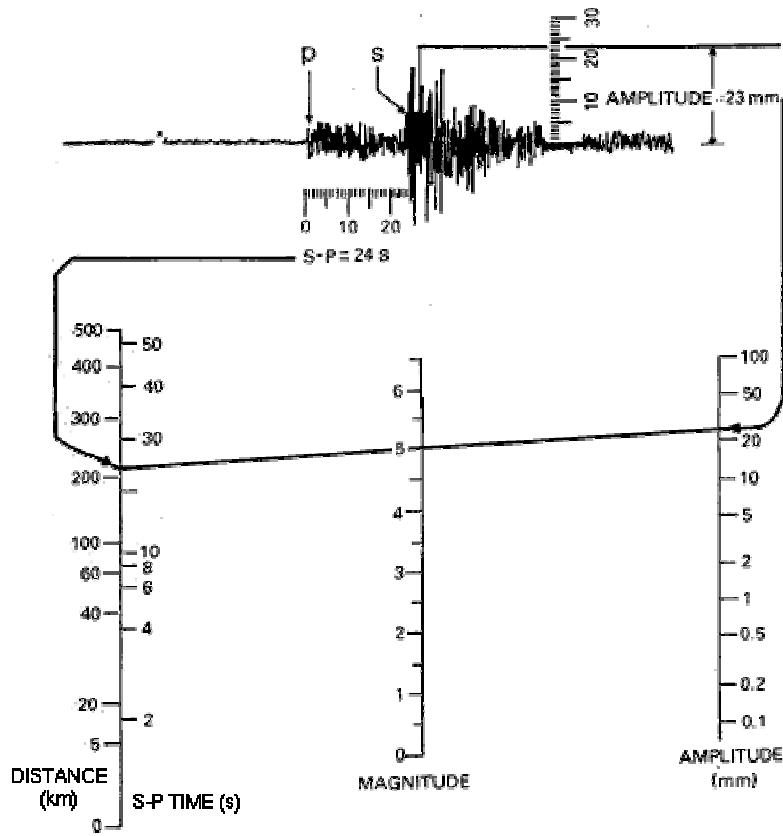


Figure 26-1 Determination of the magnitude of an earthquake on the Richter scale

Figure 26-2 shows the areas where earthquakes of magnitude IV or larger were registered in 1996.

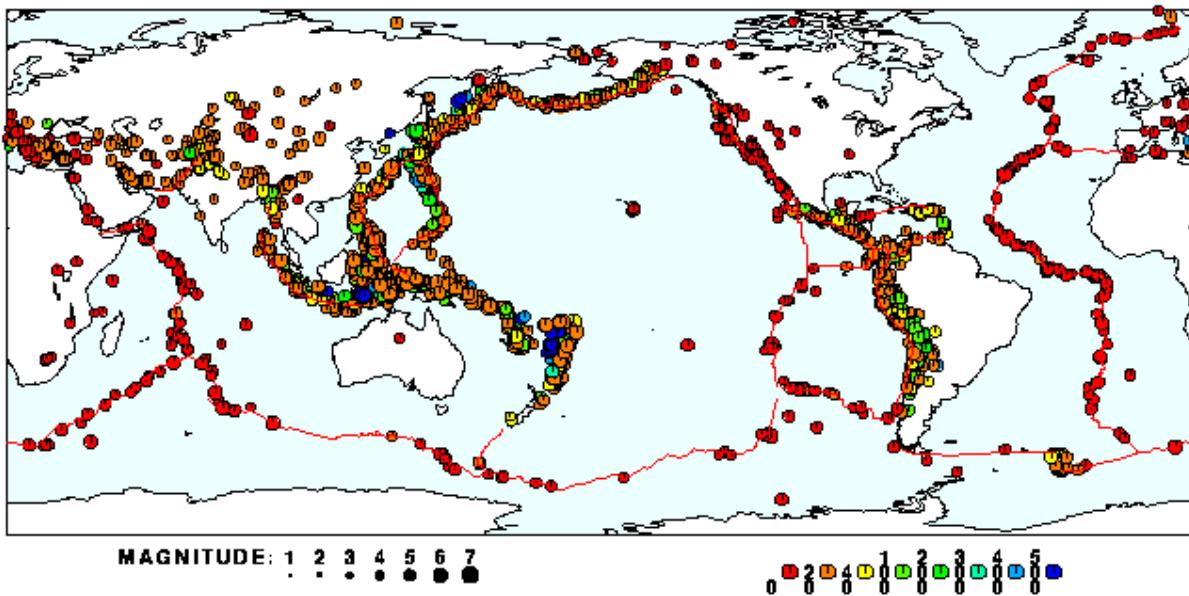


Figure 26-2 Observed earthquakes of 1996 ( $M \geq 4$ )

## 26.3 Design

In the Netherlands, designs rarely take earthquakes into account, unless large consequences (and thus large risks) are involved, for instance, such as for nuclear power plants. Even the storm surge barriers in the Delta Works were not dimensioned for earthquakes. The probability that (serious) damage is caused by an earthquake is very small and the probability that it happens during a storm surge is negligible.

In cases where earthquakes are used for the dimensioning, civil engineers need a measure with which the load on a structure can be determined. In fact, a constructor is only interested in the maximum acceleration of the ground. This is why the intensity according to the Mercalli scale is a better measure than the Magnitude according to Richter. Amongst other factors, the intensity depends on the distance to the epicentre and the structure of the earth's crust.

The propagation and damping of waves and vibrations in the earth's crust depend on a large number of factors, such as, for instance, the soil types and the layered composition and the density variation of the earth's crust. Due to damping, the intensity of the earthquake decreases as the distance relative to the epicentre increases. Local registrations and experiences are of large importance for the estimation of the nature and extent of earthquake loads.

Figure 26-3 can be used for the estimation of earthquake intensities in the Netherlands.

For the estimation of the horizontal acceleration  $a$  at a certain intensity, one can use the classification given in Table 26-2.

Intensity	Description	Acceleration [m/s <sup>2</sup> ]
I	Only registered by seismographs	0,01
II	Very weak; only felt in favourable circumstances	0,02
III	Weak; felt by a few people; vibrations similar to those of passing traffic	0,05
IV	Moderate; felt by many; tremors as vibrations cause by heavy traffic; doors and windows rattle	0,1
V	Fairly strong; generally felt by everybody; hanging objects sway; clocks stop running	0,2
VI	Strong; shock reactions; objects in houses fall over; trees move; insufficiently solid houses are damaged	0,5
VII	Very strong; many buildings are damaged; chimneys break; waves in ponds; church bells ring	1,0
VIII	Destructive; panic; general damage to buildings; weak buildings are partially destroyed	2,0

Table 26-2 Intensities according to the Modified Mercalli Scale (1931)

### **Buildings**

For buildings, the accelerations in all directions of the earth's surface are of particular importance. These accelerations cause dynamic loads. The dynamic character of the loads does not always stand out equally well in different structure regulations and norms. In the various regulations the earthquake load is often calculated as a static load, a function of the mass of the elements of the structure, in all directions. The stiffness of the elements of the structure is not always taken into account.

The equivalent static method (ESM) approaches the dynamic behaviour of the structure by also relating the size of the load to the structure's lowest natural frequency. This and other methods to determine the earthquake load are described in specialised literature on seismic design of reinforced concrete structures. The essence of most of these methods is that the structure is schematised as a mass-spring system with freedom of movement in all directions.

For a description of earthquakes as a statistic process, one is referred to the lecture notes *Statistic vibrations* (in Dutch: "Stochastische trillingen") (Vrouwenvelder, 1997).

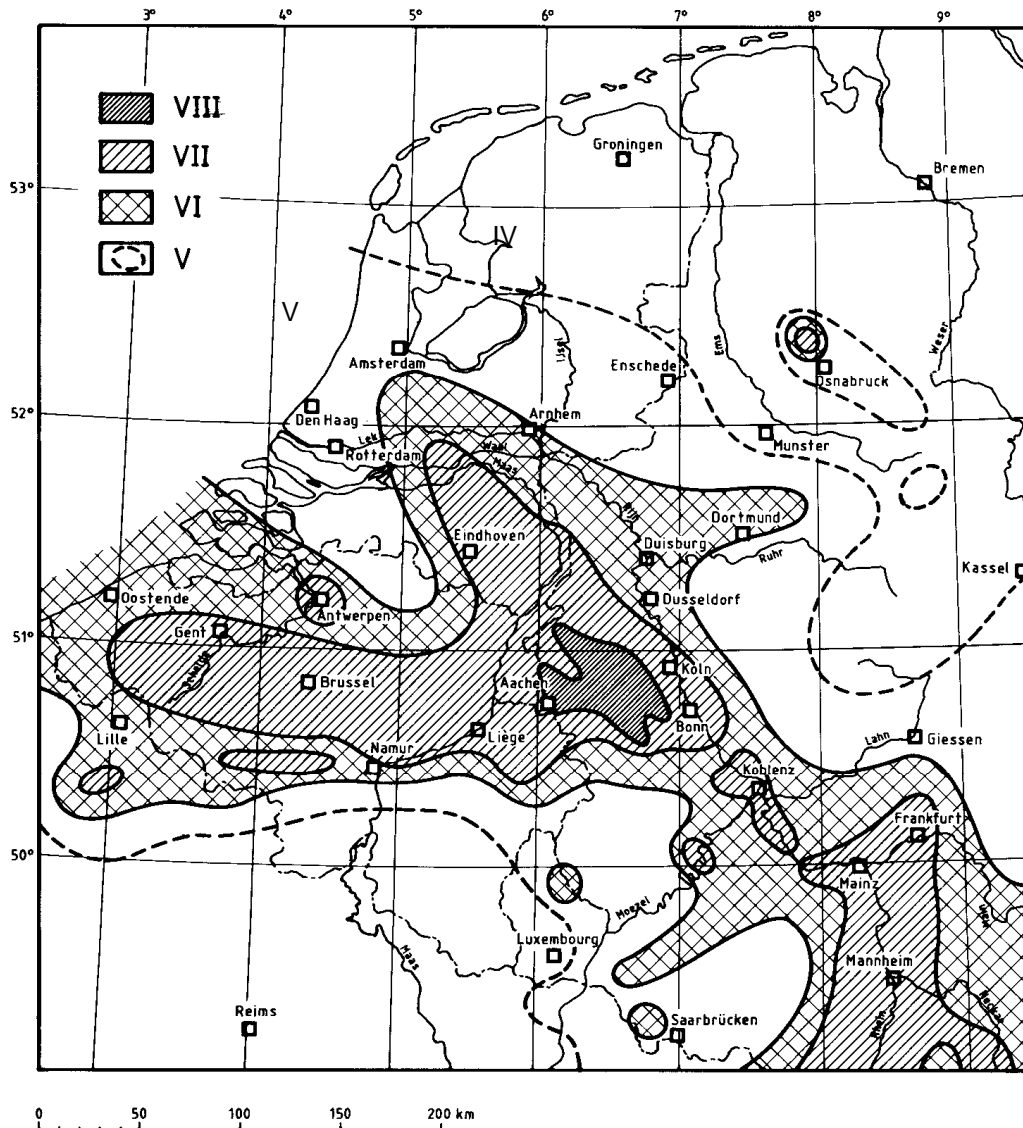


Figure 26-3 Earthquake intensities in and around the Netherlands (Modified Mercalli Scale)

### Soil

For soil retaining structures it is unusual to schematise the structure as a mass-spring system. The difficulty with such a schematisation is estimating the mass of the soil to be retained in earthquake conditions.

The German manual on quay walls, the EAU (*Empfehlungen des Arbeitsausschusses Ufereinfassungen*, Wilhelm Ernst & Sohn, München), gives an approximation method that is simple in application. This approach considers the maximum horizontal acceleration constant and assumes that the maximum horizontal and vertical accelerations do not occur simultaneously (the fact that this assumption is not always correct was shown in Kobé, Japan).

With these assumptions, the resultant acceleration can be found by vectorial addition of gravity and the horizontal acceleration caused by the earthquake. The calculation is based on a fictitious rotation of the system, such that the resultant acceleration coincides with the gravitational acceleration. This means that both the sheet piling and the ground level in front of and behind the retention structure are given a rotation according to Figure 26-4.

The rotation amounts to  $\tan\left(\frac{a}{g}\right)$ .

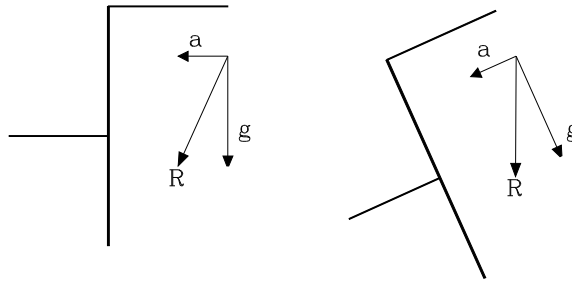


Figure 26-4 Fictitious rotation of the soil retaining structure and the ground level as a result of horizontal accelerations

Using the general horizontal ground pressure coefficients  $K_a$  and  $K_p$ , as given in Chapter 35 (Part III), the horizontal ground pressure can also be determined for a rotated schematisation. The true horizontal load is found by resolving the force into its true horizontal and vertical components.

For the soil below the groundwater level, the mass of the water must also be taken into account. This is done by correcting the rotation, for this one is referred to the German guidelines on quay wall design, the EAU 2012.

## 27. Soil, groundwater

An important aspect of the soil is the presence of groundwater. Groundwater largely influences both the strength and the stiffness behaviour of the ground. Furthermore, groundwater is also responsible for a large load on the structure.

Sometimes the load of the groundwater is only temporarily undesirable. If that is the case, one can opt for drainage. That is why this chapter also considers groundwater flow and drainage. Groundwater flow can cause erosion, this is known as pipng.

These six facets of groundwater are discussed below in the following order:

- Load
- Groundwater flow
- Piping
- Drainage
- Influencing strength
- Influencing stiffness

### 27.1 Groundwater pressure

In the Netherlands, many structures placed in the ground are also found to be in the groundwater, due to the high groundwater level. The structure therefore undergoes an upward load. If there is no groundwater flow (e.g. seepage or consolidation), this load is identical to that of a floating object (see Chapter 3):

$$p = \rho \cdot g \cdot h$$

where:  $p$  [Pa] = (ground)water pressure  
 $\rho$  [kg/m<sup>3</sup>] = the density of the water (salt = 1025 kg/m<sup>3</sup>; fresh = 1000 kg/m<sup>3</sup>)  
 $g$  [m/s<sup>2</sup>] = the gravitational acceleration  
 $h$  [m] = the piezometric head or piezometric height

For excavations, one must always check if this load on the bottom of a clay layer, building site floor or cellar floor won't allow the structure to burst open. There should be a sufficient safety margin between the upward groundwater load and the downward load of the weight of the clay layer or structure ( $\gamma_{m,g} = 1,1$ ) or the tensile force of the tension piles ( $\gamma_{m,b4} = 1,4$ ).

By loading a layer of little permeable soil (clay or peat), the piezometric head temporarily increases. Consolidation gradually reduces the piezometric head back to its initial value (see Part III, section 32.4). Due to groundwater flow some layers (particularly the deeper Pleistocene sand layers) have a different piezometric head, which causes seepage. In the vicinity of rivers the piezometric head in sand layers is closely related to the river water level (see note).

The water level in a soil layer is easy to measure using a piezometer. That is why the groundwater stress in deeper layers is always measured using a piezometer. For soil layers close to ground level the water levels in ditches are conveniently assumed. Due to run-off ground level is often considered a maximum piezometric head in polders.

Naturally, groundwater flow occurs around a water retaining structure and thus the groundwater pressure is not constant. This is described in the next section.

#### Note

*Before the fall of the Berlin Wall, the German government built a new 100 million Euro parliament building (Reichstag) in Bonn, beside a river. Once the car park in the basement had been completed, high water levels were encountered in the river. The levels above ground had not yet been constructed and thus did not provide compensatory weight. The company that had to place sheet piling around the excavated building site had experienced delays, leaving the groundwater and river water free reign to destroy the structure, Which consequently happened. Nobody dared to implement the only alternative (flooding the car park to provide additional weight) to save the Reichstag for fear of water damage to the basement.*

## 27.2 Groundwater flow

### Theory

In many cases of groundwater flow one can assume that the specific discharge is linearly proportional to the hydraulic gradient:

$$q = -k \cdot i$$

in which:  $q$  [m/s] = specific discharge (=  $Q / A$ )  
 $k$  [m/s] = permeability coefficient  
 $i$  [-] = hydraulic gradient:  $i = \frac{dh}{ds}$   
 $h$  [m] = potential, piezometric head  
 $s$  [m] = distance along a fictitious flow line

This is called Darcy's law. This law only applies if the potential flow is laminar. Thereto the following applies:

$$Re = \frac{ud}{\nu} < 1$$

in which:  $Re$  [-] = the Reynolds value  
 $u$  [m/s] = the fluid's filtration velocity  
 $d$  [m] = diameter of the soil particles  
 $\nu$  [m<sup>2</sup>/s] = kinematic viscosity

$Re > 1$  occurs for soil particles with large diameters (stone) and for large flow velocities, which don't usually occur in groundwater flow.

A rough indication of the permeability of various types of soil is given below:

Soil type	$k$ [m/s]
Gravel	$10^{-2}$
Coarse sand	$10^{-3}$
Moderately coarse to moderately fine sand	$10^{-3}$ to $10^{-4}$
Fine sand	$10^{-4}$ to $10^{-5}$
Clay	$10^{-9}$ to $10^{-11}$

Table 27-1 Permeability versus soil type

Groundwater flow can thus be described using the theory of potential flow. This means that a two-dimensional groundwater flow can be analysed using a flow net (see Example).

The following applies between the flow lines:

$$q da = -k \frac{dh}{ds} da = \text{constant}$$

in which  $da$  [m] = distance between two successive flow lines

Because the successive flow lines and equipotential lines create a square, the following applies:

$\frac{da}{ds} = \text{constant}$ . Because  $k$  is a constant, the potential difference between two successive equipotential lines is constant.

With a given potential in two locations, the course of the potential and the specific discharge along a flow line are fixed in a flow net.

Erosion below structures due to groundwater flow is treated in section 38.4 (part IV of this manual).

### Example groundwater flow

The water level in a canal is lowered using a water retaining structure. The structure has a length of 20 m and is 1.5 m thick. Beneath the structure, sheet piling with a length of 5.5 meters can be found. The ground below the structure consists of 17 m of sand and below that an impermeable layer. The water depth to the left of the structure is 6 m and to the right it is 3 m.

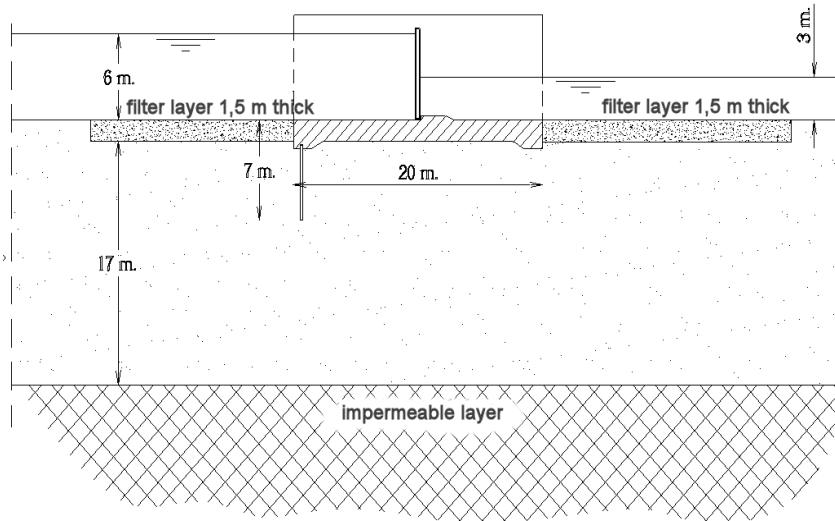


Figure 27-1 Water retaining structure

Determine the water pressure against the bottom of this structure using equipotential lines and to compare it with a water pressure that declines linearly along the structure. The potential loss over the filter layer may be ignored.

### Solution

Using the property that equipotential lines are perpendicular to flow lines, a net can iteratively be drawn in which the flow lines and equipotential lines form squares as best as possible. The outermost equipotential lines are formed by the bed contours to the left and to the right of the structure. The outermost flow lines are formed by the structure and the impermeable layer.

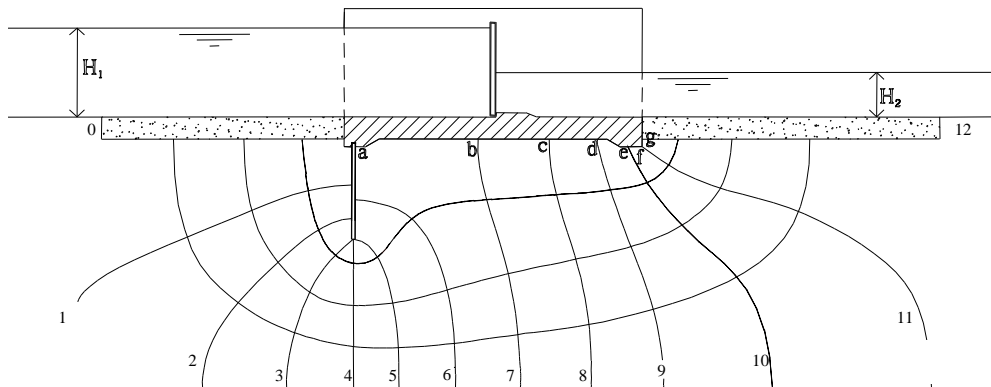


Figure 27-2 Equipotential lines under the structure

per equipotential line the potential is reduced by :  $\Delta H = \frac{H_1 - H_2}{12} = \frac{3}{12} = 0,25 \text{ m}$

Point a is between potential 6 and 7:

potential in point a:  $H_1 + d_{filter} - (6,3 \times 0,25) = 6 + 1,5 - 6,3 \times 0,25 = 5,9 \text{ m}$

potential in point b:  $6 + 1,5 - (7 \times 0,25) = 5,8 \text{ m}$

potential in point c: 5,5 m

potential in point d: 5,3 m

potential in point e: 5,0 m

potential in point f: 4,8 m

potential in point g: 4,5 m

Figure 27-3 shows the result of the net of potential and flow lines.

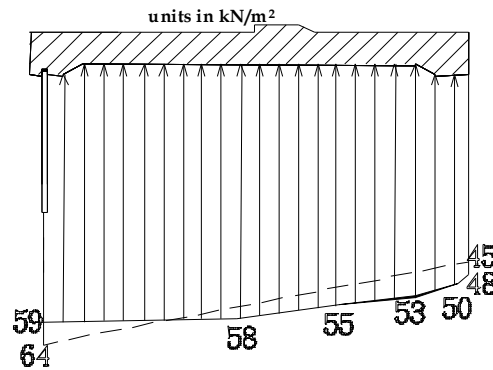


Figure 27-3 Solution groundwater pressure

The dotted line is based on a linearly declining water pressure. In this case the pressure behind the sheet piling is 64  $\text{KN/m}^2$  ( $= 45 + 30 \cdot \frac{20}{2 \cdot (7 - 1,5) + 20}$ ). This linearly declines to 45  $\text{KN/m}^2$  downstream (equivalent of 4.5 m of water). This

reveals that the linear pressure distribution is a slight underestimation of the real pressure, but is applicable for a preliminary design. The moment on the structure is overestimated using the linear pressure distribution.

### 27.3 Drainage

When an area is being drained the groundwater flow is usually 3-dimensional, so the given 2-dimensional flow net method cannot be used. For calculations involving drainage, the water levels and the groundwater pressures, see Chapter 48 (in part IV of this manual).

### 27.4 Influences on strength

The soil's shear strength depends on the cohesion, the angle of internal friction and the so-called inter-granular stress (also known as effective stress). The inter-granular stress, also known as effective soil stress ( $\sigma'$ ) depends on the total stress and the water pressure:

$$\sigma' = \sigma - p$$

in which:  $\sigma$  [Pa] = total stress  
 $p$  [Pa] = water pressure (also denoted as  $\sigma_w$ )

This shows that the presence of groundwater reduces the effective stress and thus the shear stress of the soil, as:

$$\tau = c' + \sigma'_n \cdot \tan(\varphi)$$

As regards the shear stress  $\tau$ , it is therefore important to keep the water pressure under the structure as low as possible. That is why the sheet pile in Figure 27-2 is on the upstream side. A separate chapter is dedicated to loads caused by inter-granular stress  $\sigma'$  (Chapter 24).

## 27.5 Influence on stiffness

Another soil property which is largely influenced by the presence of groundwater is the course of the compaction of the soil as a result of an increase of the ground pressure. In the case of impermeable soil (clay, peat), an increase of the total stress often causes a proportional increase of the water pressure. This is because water cannot flow out of the pores quickly enough when the soil is compressed. The water can be considered incompressible and accounts for the entire increase of pressure. The result is a high total stress and water pressure and a relatively low effective stress. As a consequence of the increase of the water pressure, groundwater will flow to a place with a lower potential. This way, the water pressure and the effective stress adjust to the load.

In this case, the compression process depends on the speed with which the groundwater can flow out of the pores. This process of reducing the water pressure and increasing the effective stress is called the consolidation process. The presence of groundwater therefore causes a temporary increase of stiffness in compressible, impermeable soil.

For this see also in part III, Chapters 33 ('Settlement') and 34 ('Stiffness').

## 28. Shipping, hydraulic aspects

Water movements created by sailing and manoeuvring ships can be of importance for structures in ports and shipping lanes. These water movements are:

- Return current
- Water level depression
- Ships wakes
- Propeller wash

Generally, these hydraulic loads on a structure are inferior to the other loads. However, the hydraulic loads are of large importance to the stability of flexible structures adjoining the hydraulic engineering work. For the design of such structures one is referred to the book for course CIE4310: "Introduction to Bed, bank and Shore protection" (Schiereck, 2001).

## 29. Shipping, berthing

### 29.1 Introduction

Berthing a ship (*aanleggen van een schip*) to a structure and collision of a ship against a structure are, theoretically, the same process. The only differences are the velocity and the extent of control of the process. In the following sections only berthing is discussed. The calculation for the load during collisions is the same as that for the berthing load, however, the velocity taken into account is larger during a collision.

A number of aspects are of importance in relation to the load of a berthing ship on a structure. These aspects are:

- dimensions of the ship
- mass of the ship
- velocity of the ship
- stiffness of the ship's hull
- mass of the water moving along with the ship, known as the hydrodynamic or added mass
- approach angle
- stiffness of the mooring structure
- geometry of the mooring structure
- place where the ship hits the structure
- current
- wind

### 29.2 Theory

A schematic representation of a berthing vessel including the main parameters relevant to calculating the berthing impact is depicted in Figure 29-1.

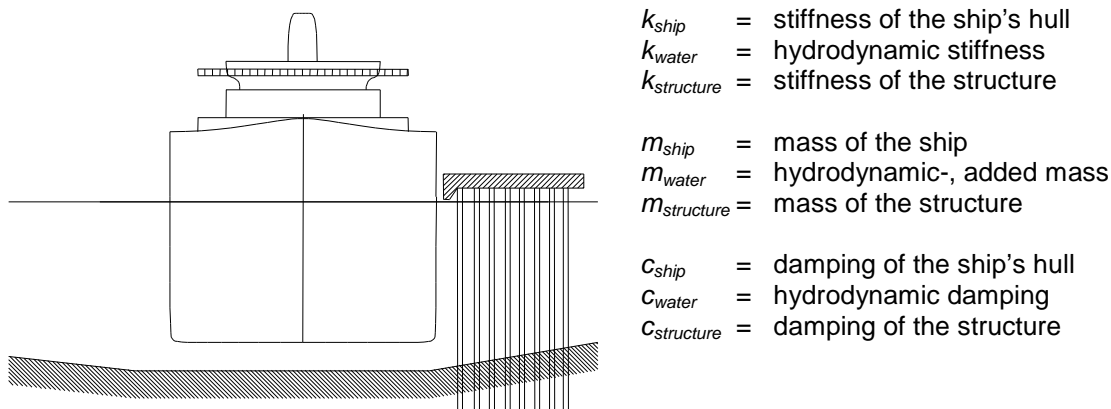


Figure 29-1 A berthing vessel and main parameters related to berthing impact

Together with the water that moves along, the ship to be moored has the following amount of kinetic energy:

$$E_{kin} = \frac{1}{2}(m_s + m_w)v_s^2$$

in which:  $E_{kin}$  [Nm] = kinetic energy  
 $m_s$  [kg] = mass of the ship  
 $m_w$  [kg] = mass of the water moving with the ship; additional mass  
 $v_s$  [m/s] = velocity of the ship and water ( $\perp$  structure)

The kinetic energy has to be absorbed by the berthing structure and it is a measure of the load on a structure. The maximum force that develops between the ship and the berthing structure largely depends on the stiffness of the whole ship-water-structure system. This system can be schematised as a mass-spring-dashpot system (*massa-veer-dempersysteem*).

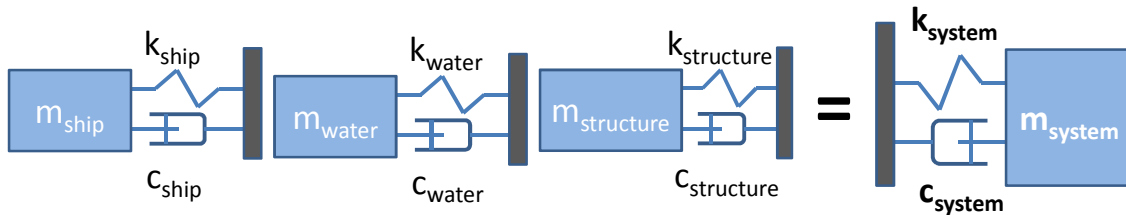


Figure 29-2 Schematisation of a berthing vessel as a mass-spring-dashpot system

In a preliminary design damping will be neglected, which results in a conservative calculation of the berthing load on the structure. Without damping, which dissipates energy, all of the kinetic energy is transformed into potential energy. The potential energy in a spring is:

$$E_{pot} = \int_0^{\Delta x} k(x) x dx \quad \text{for a linear spring system:} \quad E_{pot} = \int_0^{\Delta x} k x dx = \frac{1}{2} k \Delta x^2$$

Where  $\Delta x$  is the displacement of the spring, and  $k$  is the spring stiffness of the total system, i.e.: structure + ship; the water stiffness has been neglected. (The stiffness of the structure:  $\frac{1}{k_{structure}} = \frac{1}{k_{concrete}} + \frac{1}{k_{fender}}$ .

Usually  $k_{fender} \ll k_{concrete}$ ).

Compared to the mass of the ship plus added water mass, the mass of the structure (the part that would move) is negligible. Hence, the maximum potential energy in the spring equals the maximum kinetic energy of the ship and the water. For a linear elastic structure, equating potential and kinetic energy

gives:  $E_{pot,max} = E_{kin,max} \Leftrightarrow \frac{1}{2} k \Delta x^2 = E_{kin,max} \Leftrightarrow \Delta x = \sqrt{\frac{2 E_{kin,max}}{k}}$

### 29.3 Design

The force on a linear elastic structure is:

$$F = k \Delta x = \sqrt{2 k E_{kin,max}}$$

This formula clearly shows the influence of the stiffness of the structure on the resultant force of the ship on the structure and therefore also of the structure on the ship. Because the stiffness of the structure is not known until after the design phase, the load of a ship on a structure is not given as a force, but as an amount of kinetic energy that needs to be absorbed.

The total amount of kinetic energy to be absorbed by the structure is equal to:

$$E_{kin} = \frac{1}{2} m_s v_s^2 C_H C_E C_S C_C \quad \text{or:} \quad E_{kin} = \frac{1}{2} (m_s + m_w) v_s^2 C_E C_S C_C$$

- in which:
- $C_H$  [-] = hydrodynamic coefficient =  $\frac{m_s + m_w}{m_s}$
  - $C_E$  [-] = eccentricity coefficient
  - $C_S$  [-] = softness coefficient
  - $C_C$  [-] = configuration coefficient
  - $m_s$  [kg] = mass of the ship
  - $v_s$  [m/s] = velocity of the ship (component  $\perp$  structure)

These parameters are discussed below.

Besides the amount of kinetic energy to be absorbed during mooring, other forces on the ship must also be taken into account, such as wind and current. These forces are transferred to the structure via the ship.

### Structure stiffness $k$

The stiffness of the structure depends both on the structure (including the foundation) and on the used fenders. In very stiff structures the fenders are normative. Assuming a cell-fender with the spring characteristics given below and a diameter of 0,80 m, one finds a fender stiffness of:

$$k_{\text{fender}} \approx \frac{1100 \text{ kN}}{10\% \cdot 0,80 \text{ m}} \approx 14 \text{ MN}$$

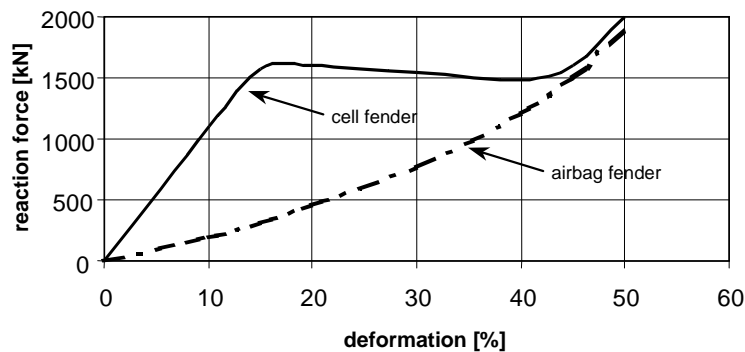


Figure 29-3 Force versus deformation of a cell-fender and an airbag fender.

Of course, this stiffness of the cell-fender only applies up to a deformation of 15%. After that, the behaviour is no longer linear and the reaction force remains fairly constant at 1,5 MN. The advantage of the cell-fender is that it absorbs a lot of energy by means of a relative large deformation, without increasing force (rectangular shaped area under the curve). The disadvantage is that the mooring force is very large for possible small boats; during the first initial deformation the force rapidly increases to a first maximum (triangular shaped area under the curve). Airbag fenders deform more than cell-fenders, but also cause smaller mooring forces for small boats.

### Velocity of the ship $v_s$

The velocity with which a ship berths is an important factor, after all, the kinetic energy is proportional to the square of the velocity. A large number of measurements revealed that the berthing speed depends on the ship's dimensions, the type of load (cargo) and the berthing conditions.

In good berthing conditions, one could use Table 29-1 for mooring speeds.

ship [ton]	Observed velocity [m/s]	Design velocity [m/s]
<10 000	0,10 ~ 0,30	0,20
10 000 ~ 50 000	0,10 ~ 0,20	0,15
>50 000	0,10 ~ 0,15	0,15

Table 29-1 Berthing speeds in good conditions (velocity component  $v_s \perp$  structure)

As the observed velocities exceed the design velocities one can conclude that the design velocities are too low. One is therefore advised to assume the maximum observed velocities instead.

The design velocity as given in Figure 29-4 is as a function of both the ship's dimensions and the berthing conditions. As the velocities in this figure are sometimes lower than the observed velocities, one is advised not to assume velocities lower than the maximum observed velocities given in the table above.

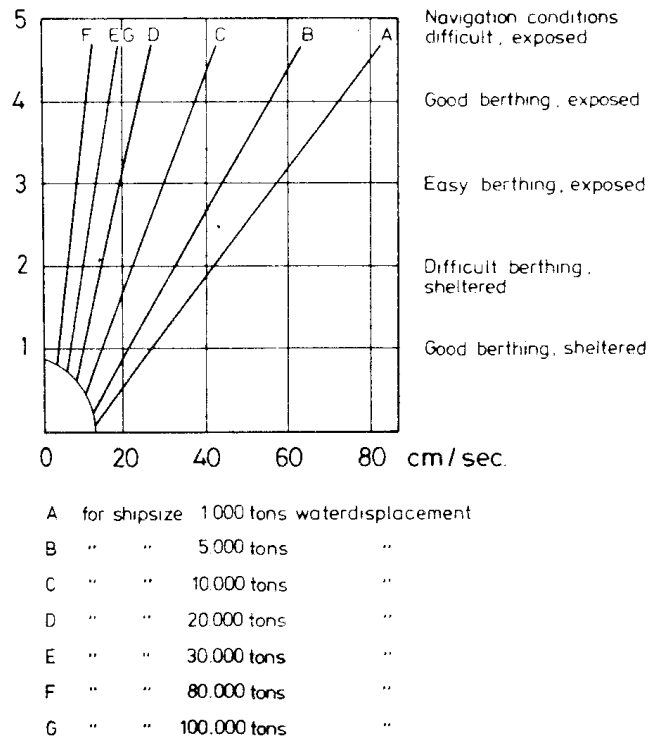


Figure 29-4 Design velocity

**Hydrodynamic coefficient  $C_H$**

The hydrodynamic coefficient is in fact simply the ratio between the mass of the ship plus the water moving with the ship and the mass of the ship:

$$C_H = \frac{m_s + m_w}{m_s}$$

The mass of the ship that should be used to calculate the hydrodynamic coefficient is the total water displacement of the loaded ship (FLD = full load displacement). The additional mass of the water depends on, amongst other factors, the movement of the ship in three-dimensional space. Several models have been developed to determine the hydrodynamic additional mass, they are based on the potential theory or on the theory regarding the preservation of impulse.

However, here a simple approximation that can be used for a preliminary design suffices. This approximation is based on the potential theory and is known as Stelson Mavils' equation:

$$m_w = \rho L \frac{1}{4} \pi D^2$$

in which:  $\rho$  [kg/m<sup>3</sup>] = density of (sea)water  
 $L$  [m] = length of the ship  
 $D$  [m] = draught of the ship

(Compare the formula with Morison's formula, see Chapter 20 "Water, waves, slender structure")

The equation for the hydrodynamic coefficient can be simplified further with an assumption for the block coefficient  $C_b$ :

$$C_b \approx \frac{\pi}{4}$$

$$m_s = \rho L B D C_b$$

$$C_H = \frac{m_s + m_w}{m_s} \approx 1 + \frac{D}{B}$$

**Note:** Vasto-Costa formula reads as follows  $C_H = 1 + \frac{2D}{B}$  use of this well-known formula is wide spread. Engineering judgement is required!

### Coefficient of eccentricity $C_E$

The coefficient of eccentricity takes into account the energy dissipation caused by the yawing (*bijdraaien*) of the ship when it moors eccentrically against the structure. This yawing is shown in Figure 29-5.

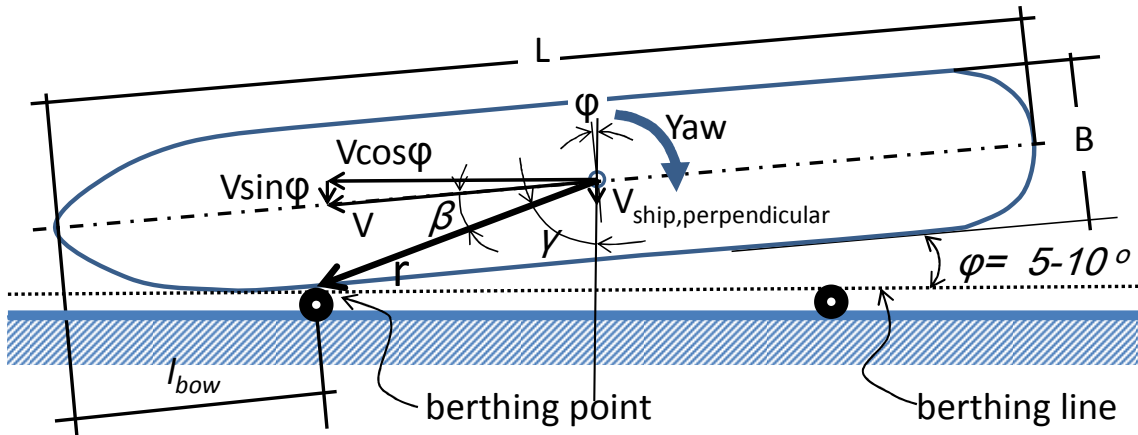


Figure 29-5 Eccentric berthing

If the movement of the ship at time of impact with the structure can be described solely as a translation of the centre of gravity, then the coefficient of eccentricity is:

$$C_E = \frac{k^2 + r^2 \cos^2(\gamma)}{k^2 + r^2} \quad \gamma = 90^\circ - \beta - \varphi \quad r = \sqrt{\left(\frac{1}{2}L - \ell_{bow}\right)^2 + \frac{1}{4}B^2}$$

in which:

- $k$  [m] = radius of gyration (*traagheidsstraal*) of the ship
- $r$  [m] = the radius between the gravity centre of the ship and the berthing point
- $\beta$  [°] = the angle between radius  $r$  and the ship's velocity along the axis of the ship
- $\gamma$  [°] = the angle between radius  $r$  and the ship's velocity perpendicular to the berthing line
- $\varphi$  [°] = the berthing angle; the angle between the ship's axis and the berthing line
- $\ell_{bow}$  [m] = distance between the bow tip and the point where the straight part of the hull starts to curve to the bow

The radius of gyration of the ship can be approximated by:

$$k = (0,19C_b + 0,11)L$$

in which:  $C_b$  [-] = block coefficient =  $C_b = \frac{V}{LBD}$

- $L$  [m] = length of the ship
- $B$  [m] = width of the ship
- $D$  [m] = draught of the ship
- $V$  [m<sup>3</sup>] = (volumetric) water displacement of the ship

The smaller the value of  $C_b$ , the larger the load  $F$ . Therefore a small  $C_b$  is governing. The following approximation applies:  $0,6$  (slender ships)  $\leq C_b \leq 0,95$  (container ships)

**Softness coefficient  $C_S$** 

The softness coefficient takes into account the elasticity of the ship's side. This coefficient depends on the stiffness of the structure and that of the ship's shell and takes into account the part that is taken on by the structure. In the case of weak structures, such as, for instance, a wooden pier with fenders, nearly all of the energy is absorbed by the structure because the deflection of the ship's shell is negligible. In this case  $C_S = 1$ .

For a relatively stiff structure, such as a quay with wooden support beams and car tyres, the deflection of the ship's shell will not be entirely negligible compared with the deflection of the structure. In this case  $C_S = 0,9$  can be used for design purposes.

**Configuration coefficient  $C_C$** 

The berth configuration coefficient or cushion factor takes into account the dissipation of energy due to the fact that water has to be squeezed away from the space between the ship and quay structure. If the structure is closed, e.g. a straight vertical sheetpile wall, a cushion of water between the structure and ship will slow the ship down. For a closed quay and parallel mooring ( $\theta = 0^\circ$ ) this can lead to a 20% reduction of the amount of energy to be absorbed. If there is a small angle between the ship and the quay ( $\theta = 5^\circ$ ) this reduction can disappear almost entirely because the water can simply flow away. If the structure is open, e.g. a jetty, no hydrodynamic damping will occur.

Therefore the limit values of the configuration coefficient are:  $0,8 \leq C_C \leq 1,0$ .

For safety reasons, one can assume  $C_C = 1,0$  for a preliminary design.

For a numerical example of the berthing of a ship to a jetty, see part IV, Chapter 46 ('Pile groups').

## 30. Shipping - mooring forces

### 30.1 Theory

Forces in mooring ropes (also called 'hawsers' (*trossen*)) are caused by:

- Loads on the ship such as wind, current and water level differences (filling a lock!)
- Movements of the ship, the mass of the ship and the stiffness of the mooring cables are of importance in this respect.
- Pre-stressing forces in the mooring cables

Pre-stressing forces in the cables are generated during the hauling in and after mooring. The fracturing force of the cables and the number of cables limit the mooring force. Increasingly, modern quays and mooring structures are equipped with "quick release hooks". These release the mooring cables automatically if a maximum force is exceeded. So-called yielding bolts are used to connect the structure with conventional bollards and mooring bits, which are still used often in heavy quay structures and sluices. The yielding bolts yield when the maximum acceptable force is exceeded.

### 30.2 Preliminary design

For a preliminary design one can assume the mooring forces for seagoing vessels, self-propelled barges (for inland waterways) (*binnenvaartschepen*) and yachts (*plezierjachten*) as specified in the tables below.

Seagoing vessels	
water displacement of ship [ton] <sup>6)</sup>	mooring force
	[kN]
< 2 000	0 - 100
2 000 ~ 10 000	100 - 300
10 000 ~ 20 000	300 - 600
20 000 ~ 50 000	600 - 800
50 000 ~ 100 000	800 - 1000
100 000 ~ 200 000	1000 - 1500
> 200 000	1500 - 2000

Table 30-1 Mooring forces of sea going ships per bolder

Inland barges	
class of ship <sup>7)</sup>	mooring force [kN]
CEMT Class I + II	140
CEMT Class III + IV	210
CEMT Class V + VI	280

Table 30-2 Mooring forces of inland barges per bolder

Yachts	
class of ship	mooring force [kN]
Yachts	55

Table 30-3 Mooring forces of yachts per bolder

<sup>6</sup> Example: Water displacement of a seagoing ship = 70 000 tonnes: Mooring force =  $800 + 200 \cdot (70-50) / (100-50) = 880$  kN.

<sup>7</sup> The CEMT barge class definitions can be found in the 'Richtlijnen Vaarwegen 2011' of *Rijkswaterstaat* (downloadable from internet).

# Manual Hydraulic Structures

---

## **Part III: Materials**



## 31. Soil - properties

Section 31.5 extended: February 2015

### 31.1 Stiffness and strength

Before collecting or calculating parameters one must be aware of whether the type of problem that has to be dealt with is:

- a strength problem (e.g. the stability of a dike),
- a stiffness problem (e.g. the settlement of a road) or
- a mixed problem (e.g. the foundation of a structure).

Specific tests exist to determine the strength parameters (e.g. the direct shear test) and the stiffness parameters (e.g. the oedometer test). Tests to determine both types of parameters also exist (e.g. triaxial compression test).

Most calculations also distinguish between problems of strength and stiffness. Koppejan's settlement calculation, for example, is a stiffness calculation. Prandtl and Brinch Hansen's bearing capacity calculation is a strength calculation and the spring model used to calculate sheet piling (like D-Sheet Piling) is a mixed model; the model produces estimates of both strength and displacement(s). The problem, the parameters and the calculation must correspond.

### 31.2 Soil investigation

Loads on hydraulic engineering works are transferred to the subsoil. The properties of the soil are therefore of great importance for the design and the dimensioning of a structure. The nature of the loads on the structure and the properties of the subsoil determine the choice of the type of foundation.

A number of techniques are available to investigate the subsoil. This includes:

- soundings
- borings
- water pressure measurements
- vane shear tests (determination of  $c_u$ )
- pump tests
- (seismic research)
- (nuclear research)

These research methods are suitable to investigate the layered composition of the soil and to estimate some soil parameters. The subsoil is usually composed of different types of soil layers. First, an attempt is made at establishing the structure of the soil layers. For this, see Section 31.3 "Determination soil type". After that, the necessary soil parameters are determined for every soil layer. Fieldwork provides all the required information, but to determine the soil parameters more accurately laboratory tests are needed. It is best to obtain soil samples by boring; these samples can then subsequently be tested in a laboratory.

The most important laboratory tests for alluvial soil types (sand and clay) are:

- consolidation test (= oedometer test) (determination of stiffness and permeability)
- triaxial compression test (determination of stiffness and strength)
- (permeability test)
- (direct shear test)
- (Cassagrande's test)

For rock and stone-like materials other parameters are determined, such as the compression strength, the splitting strength, the density and the permeability.

Tests mentioned above can be used to calculate the representative parameters of a given soil layer. For this see Section 31.4 "Determination of soil parameters from laboratory tests".

If no laboratory tests are available, a few soil parameters one can be estimated empirically, using the  $q_c$  values of the soundings. For this refer to Section 31.5 "Determination of soil parameters from cone penetration tests values".

One can also use Dutch experience values. Table 31-4 of Section 31.6 gives the representative low values of some important soil parameters for a number of soil types. Besides the aforementioned parameters the following parameters are given:

$\gamma$  = volumetric weight

$q_c$  = sounding value

$C_{sw}$  = swelling coefficient (to be used instead of  $C_c$  in case of pressure reduction)

$E$  = Young's modulus [N/mm<sup>2</sup>]

$f_{undr}$  = undrained shear strength =  $c_u$

### 31.3 Determination soil type

The best way to determine what soil type a soil layer consists of is to carry out borings in different locations and to analyse the samples in a laboratory. Usually one opts for a cheaper alternative. In this case only a few borings and a (much) larger number of cone penetration tests (CPT) are carried out (e.g. every 25 metres). The cheaper CPT's (*sonderingen*) are then linked to the more expensive boring samples, to determine the soil profile and the soil characteristics of every layer that has been distinguished.

There are two types of CPT's, which depends on the cone being used. One measures both the cone resistance and the local friction and one measures the cone resistance and the (pore) water pressure.

The CPT including water pressure measurements clearly shows:

- where the impermeable layers (clay and peat) are.
- how well the layer seals off water.
- what the water pressure is at a greater depth, in the permeable layers (sand and gravel).

The CPT including local friction measurement clearly shows which soil layers are present and is therefore used most often. There is a strong correlation between the soil type and the friction ratio, see table below. The friction ratio is the sleeve friction divided by the cone resistance and is therefore dimensionless. Nowadays the cylindrical electronic penetrometer with friction sleeve is often used for soundings.

Soil type	Friction ratio > than: (cylindrical <b>electronic</b> cone)	Friction ratio > than: ( <b>mechanical</b> friction sleeve cone)
moderate to coarse sand	0,4 %	1,0 %
moderately fine sand	0,6 %	1,3 %
fine sand	0,8 %	1,6 %
silty sand	1,1 %	1,9 %
clayey sand	1,4 %	2,6 %
sandy clay <b>or</b> loam	1,8 %	2,8 %
silt	2,2 %	3,1 %
silty clay	2,5 %	3,6 %
clay	3,3 %	4,3 %
humus clay	5,0 %	6,3 %
peat	8,1 %	8,0 %

Table 31-1 Friction ratio versus soil type

**Notes**

- It is advisable to always carry out a couple of borings; firstly because the percentages in the table above are not always correct, secondly because a boring provides a lot of visual information and thirdly because a boring is necessary to obtain soil samples for laboratory tests.
- It is important that one first compares the table above with the values found by borings. One should therefore always carry out a sounding near a boring.
- If weak soil layers are present (especially for an excavation (building site)), it is sensible to have a couple of CPTs that include water pressure measurements carried out, because these measurements distinguish well between permeable and non-permeable soil layers.

**31.4 Determination of soil parameters from laboratory tests**

For the weak soil layers compression test are usually carried out in case of settlement questions, for strength questions triaxial test are usual. For stronger soil layers (sand and gravel), usually only triaxial tests are performed. From these tests one can determine the strength and stiffness parameters for a certain soil layer.

In calculations the 5% upper or lower limit values are to be used. For soil both the real average value  $x_{avg}$  and the real average spread  $\sigma$  are unknown. That is why an average value  $x_{avg}$  and the standard deviation  $\sigma$  are first determined with tests. Subsequently, the student- $t$  method can be used to calculate the representative upper or lower limits of the average  $x_{rep}$ :

$$x_{rep} = x_{avg,5\%char} = x_{avg} \pm t_{5\%} \cdot \sigma \cdot \frac{1}{\sqrt{n}}$$

in which  $n$  is the number of tests.

The value of  $t_{5\%}$  depends on the number of samples  $n$ :

$n$	2	3	4	5	6	7	8	9	10	11	21	$\infty$
$t_{5\%}$	6,31	2,92	2,35	2,13	2,01	1,94	1,89	1,86	1,83	1,81	1,72	1,64

Table 31-2 Student- $t$  distribution

**31.5 Determination of soil parameters from cone penetration tests**

If no laboratory tests have been carried out, one can estimate the stiffness and strength parameters of the soil layers for a preliminary design with rules of thumb using the sounding values ( $q_c$ ), or else by using Table 31-4 of Section 31.6.

Electric Cone penetration tests (CPTs) provide a fast, repeatable and economical way to determine soil stratigraphy and soil types. There are various ways to determine soil types from these tests, using the measured cone resistance  $q_c$ , the sleeve friction  $f_s$  and, if available, the pore pressure  $u$ . Instead of the sleeve friction, the friction ratio  $R_f$  is often used:

$$R_f = \frac{f_s}{q_c} \cdot 100$$

where  $R_f$  [%] = friction ratio  
 $f_s$  [MPa] = CPT sleeve friction  
 $q_c$  [MPa] = CPT cone resistance

Peter Robertson developed a classification chart that is used in practice for the determination of soil (behaviour) types. The simplest version of this chart, which was published by Robertson in 1986 and updated in 2010, uses the CPT-values of the cone resistance and the friction ratio, see Figure 31-1. The cone resistance is made dimensionless by dividing it with the atmospheric pressure  $p_a$  (0,1 MPa).

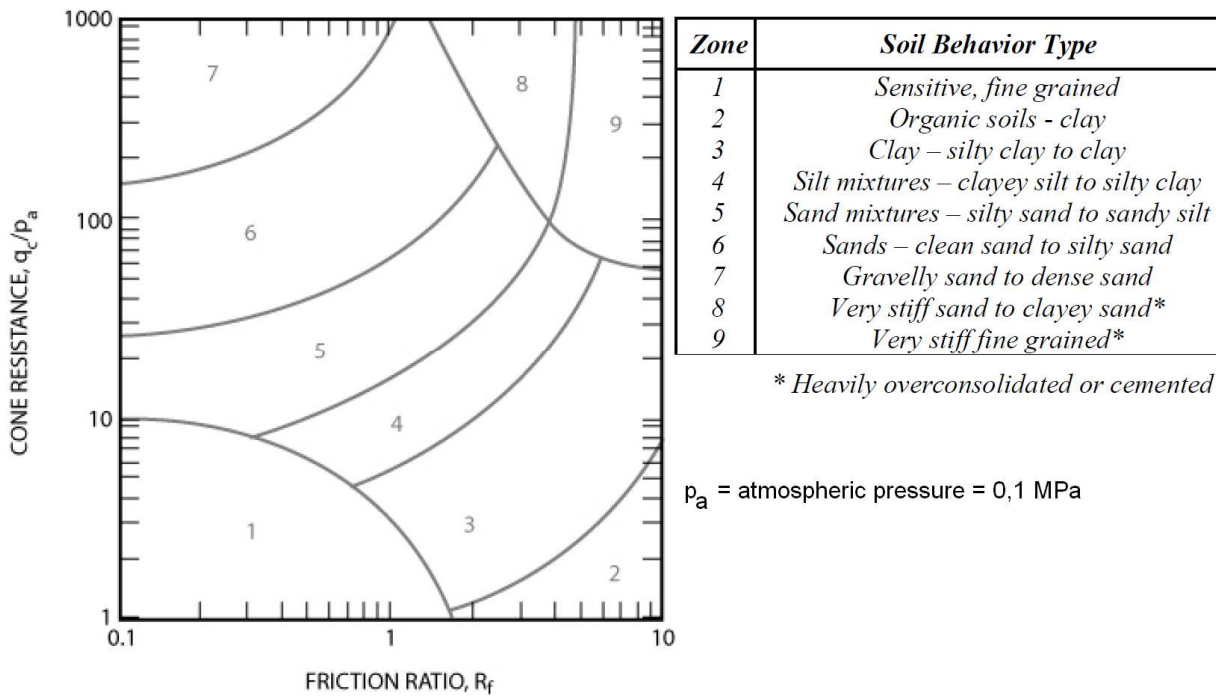


Figure 31-1 Soil classification chart based on CPT cone resistance and friction ratio (Robertson 1986, 2010)

The chart is global in nature and can provide reasonable predictions of soil behaviour type for CPT soundings up to about 20 m in depth. Overlap in some zones should be expected and the zones should be adjusted somewhat based on local experience.

Robertson improved this chart by using a normalized cone resistance  $Q_t$  and a normalized friction ratio  $F_R$ :

$$Q_t = \frac{q_t - \sigma_{vo}}{\sigma'_{vo}}$$

$$F_R = \frac{f_s}{q_t - \sigma_{vo}} \cdot 100$$

where:  $Q_t$  [-] = normalized cone resistance  
 $F_R$  [%] = normalized friction ratio  
 $q_t$  [MPa] = measured CPT cone resistance, corrected for pore pressure:  
 $q_t = q_c + (1 - \alpha) \cdot u_2$  if the pore pressure filter is directly behind the cone tip  
 $q_t = q_c + (1 - \alpha) \cdot \{\beta(u_1 - u_0) + u_0\}$  if the filter is situated in the cone tip  
 $q_t = q_c$  in sandy soils, or if pore pressures were not measured  
 $u_0$  = hydrostatic water pressure  
 $u_1$  = water pressure if the pore pressure filter is situated in the cone tip  
 $u_2$  = water pressure if the pore pressure filter is situated behind the cone tip  
 $\alpha$  = net area ratio of the cone because of the slit behind the cone tip  
 $\alpha$  is usually determined from laboratory calibration, with typical values between 0,70 and 0,85  
 $\beta$  = factor for the differing soil types for the conversion of  $u_1$  to  $u_2$   
 mostly  $\beta = 0,8$  is used  
 $\sigma_{vo}$  [MPa] = total vertical soil stress determined using the specific weight per soil layer  
 $\sigma'_{vo}$  [MPa] = effective vertical soil stress determined using the specific weight per soil layer  
 $f_s$  [MPa] = measured CPT cone resistance (not corrected)

The normalized chart is shown in Figure 31-2.

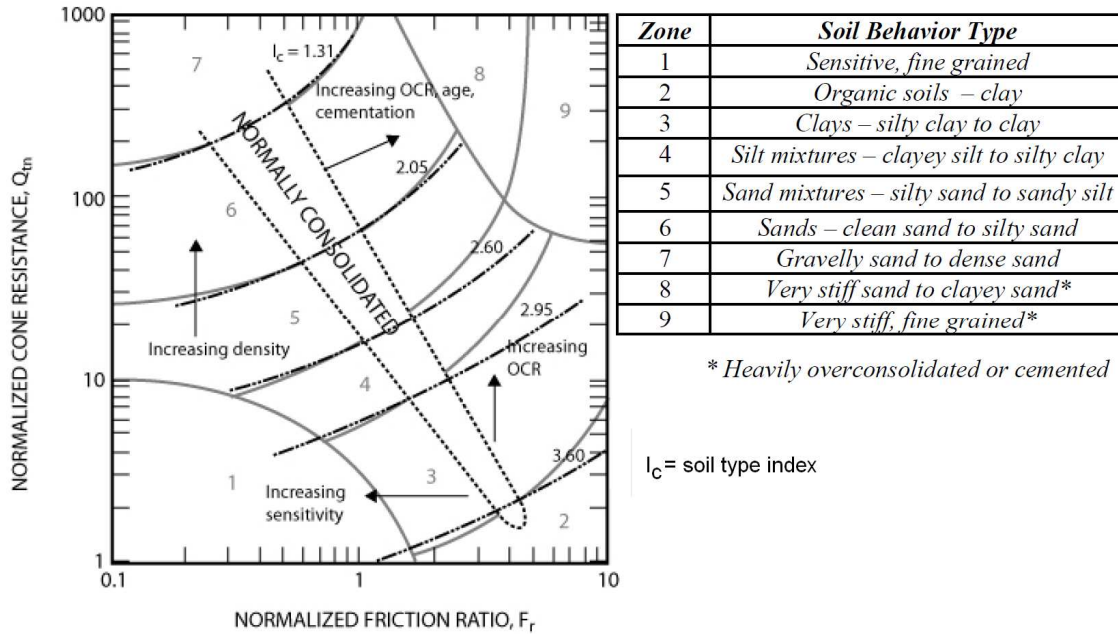


Figure 31-2 Normalized chart for the classification of soil types on basis of SPT (Robertson 1990, 2010)

This normalized chart corrects for unequal cone end area effects and some other effects related to specific characteristics of the CPT. The normalized chart in general provides more reliable identification of soil types than the non-normalized chart, although when the in-situ vertical effective stress is between 50 and 150 kPa, there is often little difference between the two charts. The advantage of the non-normalized chart is that it can be used in real-time to evaluate the soil type during and immediately after the CPT. The normalized chart can only be used after the CPT during post-processing, because it requires information on soil specific weights and groundwater conditions that are not available during the CPT.

In this double-logarithmic chart, the boundaries between the soil types can be approximated by concentric circles. A soil type index, describing these circles, can be defined by:

$$I_c = \sqrt{\left(3,47 - \log\left(\frac{q_c}{\rho_a}\right)\right)^2 + \left(\log R_f + 1,22\right)^2}$$

(use the basic CPT-values for the non-normalized chart)

Instead of the charts, the following table can be used now to identify soil types (which is very suitable for automated identification of soil types).

Zone	Soil Behavior Type	I <sub>c</sub>
1	Sensitive, fine grained	N/A
2	Organic soils – clay	> 3.6
3	Clays – silty clay to clay	2.95 – 3.6
4	Silt mixtures – clayey silt to silty clay	2.60 – 2.95
5	Sand mixtures – silty sand to sandy silt	2.05 – 2.6
6	Sands – clean sand to silty sand	1.31 – 2.05
7	Gravelly sand to dense sand	< 1.31
8	Very stiff sand to clayey sand*	N/A
9	Very stiff, fine grained*	N/A

Table 31-3 Soil types related to soil type index I<sub>c</sub>

**Sand (rules of thumb)**

The Young's modulus  $E$  results from:

$$E_{oed} = \frac{(1-\nu)}{(1+\nu)(1-2\nu)} E$$

with:

$E_{oed}$  = constrained modulus (*modulus bij zijdelingse opsluiting*):

$$\begin{aligned} E_{oed} &= 4 q_c && 0 < q_c < 10 \text{ MPa} \\ &= 2 q_c + 20 \text{ MPa} && \text{for: } 10 < q_c < 50 \text{ MPa} \\ &= 120 \text{ MPa} && 50 \text{ MPa} < q_c \end{aligned}$$

$\nu$  [-] = Poisson's ratio (*dwarscontractiecoëfficiënt*):  $\nu = 0,3$

Other parameters for sand:  $c' = 0$  and  $\phi' = 29^\circ + \frac{q_c}{4 \text{ MPa/}^\circ}$

For sand calculations assume the drained values (so the parameters with an  $\times'$ , instead of  $\times_u$ ).

If there are no known values of  $q_c$  or if these values vary too much, one can use the following as a rough estimate for clean sand:

$$\begin{aligned} E &= 250 \cdot \sigma_v' \\ \phi &= 32^\circ \end{aligned}$$

For unloading and reloading, the following applies (for sand, clay and peat):

$$E_{\text{unload/reload}} \approx (3 \sim 5) \cdot E'$$

**Clay, peat and loam (rules of thumb)**

$$\begin{aligned} c_u &= f_{\text{undr}} = \frac{q_c}{20} && \text{(clay/loam)} \\ c_u &= f_{\text{undr}} = \frac{q_c}{30} && \text{(peat, humous clay)} \\ E_u &\approx E = 100 \cdot f_{\text{undr}} && \text{(clay/peat)} \\ E_u &\approx E = 40 \cdot f_{\text{undr}} && \text{(loam)} \\ \nu &= 0,4 \\ \nu_u &= 0,5 \end{aligned}$$

For clay, peat and loam one must distinguish between a short term load (undrained, so parameters with an  $\times_u$ ) and a long term load (drained, so parameters with an  $\times'$ ). For the drained stiffness  $E'$  the assumption  $E_u \approx E'$  does not take creep into account. For calculations concerning the stiffness of drained soil, it is preferable to use the primary and secondary settlement constants  $C_p$  and  $C_s$ .

The following applies for unloading and reloading (for sand, clay and peat):

$$E_{\text{unload/reload}} \approx (3 \sim 5) \cdot E$$

**31.6 Determination of soil parameters with the Eurocode table**

The table on the next page is table 1 from Eurocode 7. It shows the representative values  $X_{rep}$  for different soil types. The table is based on values found in practice in the Netherlands. These values can be used in the Netherlands as an estimate if no laboratory research is available.

Soil type Main type	Representative value <sup>a)</sup> of the soil property										$c_u$ (= $f_{ult}$ ) kPa			
	$\gamma$ kN/m <sup>3</sup>	$\gamma_{sat}$ kN/m <sup>3</sup>	$q_c$ <sup>d)</sup> Mpa	$C_p$ -	$C'_s$ -	$C_c / (1+e_0)$ <sup>e)</sup>	$C_\phi$	$C_{sw} / (1+e_0)$ <sup>f)</sup>	$E_{100}$ <sup>g)</sup> Mpa	$\phi$ <sup>h)</sup> °		$c'$ kPa		
gravel	17	19	15	500	∞	0,0046	0	0,0015	45	32,5	0	-		
	18	20	25	1000	∞	0,0023	0	0,0008	75	35	0			
	19	20	30	1200 1400	∞	0,0019 0,0016	0	0,0006 0,0005	90	37,5 40	0			
slightly silty	18	20	10	400	∞	0,0058	0	0,0019	30	30	0	-		
	19	21	15	600	∞	0,0038	0	0,0013	45	32,5	0			
	20	21	25	1000 1500	∞	0,0023 0,0015	0	0,0008 0,0005	75 110	35 40	0			
clean	17	19	5	200	∞	0,0115	0	0,0038	15	30	0	-		
	18	20	15	600	∞	0,0038	0	0,0013	45	32,5	0			
	19	20	25	1000 1500	∞	0,0023 0,0015	0	0,0008 0,0005	75 110	35 40	0			
slightly silty clayey	18	19	20	21	12	450 650	∞	0,0051 0,0035	0	0,0017 0,0012	35 50	27 32,5	0	-
	18	19	20	21	8	200 400	∞	0,0115 0,0058	0	0,0038 0,0019	15 30	25 30	0	
	19	19	1	25	650	0,0920	0,0037	0,0307	2	27,5 30	0	50		
loam <sup>a)</sup>	20	20	2	45	1300	0,0511	0,0020	0,0170	3	27,5 32,5	1	100	-	
	21	22	3	70 100	1900 2500	0,0329 0,0230	0,0013 0,0009	0,0110 0,0077	5 7	27,5 35	2,5 3,8	200 300		
	19	20	2	45 70	1300 2000	0,0511 0,0329	0,0020 0,0013	0,0170 0,0110	3 5	27,5 35	0 1	50 100		
clay	14	14	0,5	7	80	0,3286	0,0131	0,1095	1	17,5	0	25	-	
	17	17	1	15	160	0,1533	0,0061	0,0511	2	17,5	5	50		
	19	20	2	25 30	320 500	0,0920 0,0767	0,0037 0,0031	0,0307 0,0256	4 10	17,5 25	13 15	100 200		
slightly sandy	15	15	0,7	10	110	0,2300	0,0092	0,0767	1,5	22,5	0	40	-	
	18	18	1,5	20	240	0,1150	0,0046	0,0383	3	22,5	5	80		
	20	21	2,5	30 50	400 600	0,0767 0,0460	0,0031 0,0018	0,0256 0,0153	5 10	22,5 27,5	13 15	120 170		
greatly sandy	18	20	1	25 50	320 1680	0,0920 0,0164	0,0037 0,0007	0,0307 0,0055	2 5	27,5 32,5	0 1	0 10	-	
	13	13	0,2	7,5	30	0,3067	0,0153	0,1022	0,5	15	0 1	10		
	15	16	0,5	10 15	40 60	0,2300 0,1533	0,0115 0,0077	0,0767 0,0511	1 2	15	0 1	25 30		
peat	10	12	0,1	5 7,5	20 30	0,4600 0,3067	0,0230 0,0153	0,1533 0,1022	0,2 0,5	15	1 2,5	10 20	-	
	12	13	0,2	7,5 10	30 40	0,3067 0,2300	0,0153 0,0115	0,1022 0,0767	0,5 1,0	15	2,5 5	20 30		
	0,05	-	-	-	-	0,25	-	-	-	0,10	-	0,20		

<sup>a)</sup> The table gives the low and the high characteristic value of the average of the soil type concerned. If an increase of the characteristic value of a soil property would lead to a situation that is more unfavourable than the given low value for that property, the value on the right should be used. If there is no value mentioned on the right side of a cell, then the value just below it should be used. This is, for example, the case for negative friction on a pile where a higher value for  $\phi'$ ,  $c'$  and  $C_u$  also results in a high value of the negative friction. The table gives the high characteristic average values for  $C_c / (1+e_0)$ ,  $C_\phi$  and  $C_{sw} / (1+e_0)$ .

<sup>b)</sup> Loose:  $0 < R_n < 0,33$ ; moderate:  $0,33 < R_n < 0,67$ ; solid:  $0,67 < R_n < 1,00$ .

<sup>c)</sup> The  $\gamma$ -values are applicable to a natural moisture content

<sup>d)</sup> The values for  $q_c$  (cone resistance) given in this table should be considered as entry values for use of the table and should not be used in calculations.

<sup>e)</sup> The values concern saturated loam

<sup>f)</sup> The  $C_\phi$ -values are valid for a trajectory of stress increase of at least 100%.

<sup>g)</sup> For gravel, sand and to a lesser extent also for loam and sandy clay,  $q_c$ ,  $E_{100}$ ,  $\phi'$  and the compressibility coefficients  $C_p$ ,  $C_c / (1+e_0)$  and  $C_{sw} / (1+e_0)$  are normalised for an effective soil stress  $\sigma'_v$  of 100 kPa. In that sense the equation  $q_{c,base} = q_{c,measured} \cdot C_\phi$  should be used, where  $C_\phi = (100 / \sigma'_v)^{0,67}$ . For an angle of internal friction  $\phi'$  and cohesion  $c'$  it applies that these are dependent on the consistency of the soil. This implies that this conversion is also needed for  $\phi'$  and  $c'$ . If  $q_{c,base}$  would become larger than the value given in the table, the value given in the lowest row of the concerning soil type should be used.

<sup>h)</sup> The Youngs' modulus in case of recurrent stress can be considered to be three times the given value.

Example: in clean sand at a depth of 5 m below water it is measured that:  $q_{c,base} = 9$  MPa and  $\sigma'_v = 50$  kPa.  $C_\phi$  then is  $2^{0,67} \approx 1,6$  and  $q_{c,base} = 9 \cdot 1,6 = 14,4$  MPa. This means that  $E = 45$  MPa,  $\phi' = 32,5^\circ$ ,  $C_p = 600$ ,  $C_c / (1+e_0) = 0,0038$  and  $C_{sw} / (1+e_0) = 0,0013$ .

Table 31-4 Indicative soil properties according to Eurocode 7 NEN-EN9997 (to be verified by on-site soil investigation!)

### 31.7 Soil parameters and models

In all engineering sciences an effort is made to link analytical, numerical and physical models. Below the analytical Mohr-Coulomb model and some numerical models are linked, by means of the soil properties, to soil investigation results (= 'real' physical model).

#### **Mohr-Coulomb (general)**

##### **Strength:**

In the Mohr-Coulomb model the following expressions are derived for drained and undrained shear strengths respectively:

$$\begin{aligned} \text{Drained:} \quad \tau_{\max} &= c' \cdot \cos(\phi) + \frac{1}{2}(\sigma_h' + \sigma_v') \cdot \sin(\phi) \\ \text{Undrained:} \quad f_{\text{undr}} = c_u = \tau_{\max} &= c' \cdot \cos(\phi) + \frac{1}{2}(\sigma_h' + \sigma_v') \cdot \sin(\phi) \end{aligned}$$

The stresses  $\sigma_v'$  and  $\sigma_h'$  can be assumed equal to the stresses before loading because during the quick loading the normal effective stresses and thus also the strength of the undrained soil does not change.

The difference between the above mentioned Mohr-Coulomb strength and the Coulomb strength is quite significant:

$$\tau_{\max} = c' + \sigma_n' \cdot \tan(\phi) \quad (\text{Coulomb})$$

##### **Stiffness:**

$$E_{\text{oed}} = \frac{(1-\nu)}{(1+\nu)(1-2\nu)} E$$

$$K = \frac{E}{3(1-2\nu)}$$

$$G = \frac{E}{2(1+\nu)} \quad (\tau = G\gamma)$$

$$\sigma_h' = K_0 \cdot \sigma_v' \quad \text{with:} \quad K_0 = \frac{\nu}{1-\nu} \quad (\text{which differs from Jaky's formula: } K_0 = 1 - \sin\phi)$$

According to Mohr-Coulomb, the difference between the stiffness to be taken into account for drained or undrained loading of clay is merely a factor:

$$\frac{E_u}{E'} = \frac{1+\nu_u}{1+\nu'} \quad \text{with:} \quad \nu_u = 0,5 \quad \text{and} \quad \nu' = 0,3 \quad \Rightarrow \quad \frac{E_u}{E'} = 1.15$$

In reality the difference is bigger because Mohr-Coulomb does not take creep into account. For clay and peat it is better to assume:

$$\frac{E_u}{E'} \approx 2 \text{ to } 3$$

It is even better to use Koppejan's settlement formulas (Section 34.2) and the primary and secondary settlement constants  $C_p$  and  $C_s$  in calculations.

In the case of unloading and reloading one can assume that a little creep occurs, thus one can presume:

$$E_{\text{relief / reapplication}} \approx (3 \sim 5) \cdot E'$$

**Winkler**

Soil is often modelled as a set of uncoupled linear springs, known as the Winkler model. See Chapter 33 for a further description.

**D-sheet Piling (spring model)**

D-Sheet Piling (named Msheet in earlier days) is a computer programme for the calculation of (mostly) sheet pile walls and laterally loaded piles. It is based on Winkler's spring model. When using the programme, a choice has to be made between the use of either straight or curved slip planes in the soil. The physical reality is such that the friction between the sheet piling or pile and the soil results in curved slip planes instead of straight planes. For hand calculations curved slip planes are far too difficult to calculate. For convenience, one uses straight slip planes instead. However, the straight slip planes model calculates a strength that is too optimistic, hence less safe. To arrive at a more conservative, safe, strength the wall friction angle  $\delta$  should be reduced more in straight than in the curved slip planes model. Using D-Sheet Piling, or similar computer programmes, it is anyway better to choose for curved slip planes, because it is more accurate (the computer does the extra/more difficult computation).

For the calculation of slip planes with wall friction angle  $\delta$  Eurocode 7, NEN 9997-1+C1:2012 applies:

Qualitative description wall surface	More specific definition Roughness wall surface	Wall friction angle $\delta$	
		Straight slip surface	Curved slip surface
Toothed	$> 10 d_{50}$	$2/3 \varphi'_k$	$\leq \varphi'_k$
Rough	$0.5 d_{50} - 10 d_{50}$	$2/3 \varphi'_k$	$\leq \varphi'_k - 2.5^\circ$ with a maximum of $27.5^\circ$
Half rough	$0.1 d_{50} - 0.5 d_{50}$	$2/3 \varphi'_k$	$2/3 \varphi'_k$
Smooth	$0.1 < d_{50}$	$0^\circ$	$0^\circ$

\* For clay, loam, sand and pebbles

\*\* For diaphragm walls the wall friction angle has to be reduced more than for steel walls

The stiffness (modulus of sub grade reactions for the springs) is discussed in Section 33.2 "Modulus of subgrade reaction". The strength of the soil is covered in Chapter 32.

**Plaxis (finite elements model)**

Plaxis can calculate using several soil models. All models require a reduction of the friction at the soil-structure interfaces.

For vertical interfaces one can assume:  $R_{\text{interface}} \approx 0,8$  so:  $\tan(\delta) \approx 0,8 \cdot \tan(\phi)$

For horizontal interfaces one can assume:  $R_{\text{interface}} \approx 0,67$  so:  $\tan(\delta) \approx \frac{2}{3} \cdot \tan(\phi)$

For this see Section 32.3 "Soil - strength, Horizontal bearing capacity (resistance against sliding)".

If the Soft-Soil (Creep) Model is used in Plaxis, the following applies for clay and peat:

$$\lambda^* = \frac{1}{C'_p}$$

$$\kappa^* \approx \frac{1 - \nu_{\text{unloading}}}{1 + \nu_{\text{unloading}}} \cdot \frac{1 + 2K_0}{C_p} \quad \text{with: } \nu_{\text{unloading}} \approx 0,15 \quad \text{and: } K_0 \approx 0,60$$

$$\mu^* \approx \frac{1}{\ln(10)} \cdot \frac{1}{C'_s}$$

### 31.8 Literature

Paul W. Mayne, Matthew R. Coop, Sarah M. Springman, An-Bin Huang and Jorge G. Zornberg. *Geomaterial behavior and testing*. Proceedings of the 17th International Conference on Soil Mechanics and Geotechnical Engineering, 2009.

Peter K. Robertson. *Soil classification using the cone penetration test*. Canadian Geotechnical Journal, NRC Research Press, 1990

Peter K. Robertson. *Soil behaviour type from the CPT: an update*. 2nd International symposium on Cone Penetration Testing. 2010

Peter K. Robertson and K.L. Cabal (Robertson). *Guide to Cone Penetration Testing for Geotechnical Engineering*. Gregg Drilling & Testing, Inc. 5th Edition, November 2012

A. Verruijt. *Soil mechanics*. Delft University of Technology, 2001, 2012

## 32. Soil - strength

This chapter covers some of the classic methods concerning the strength of soil, namely:

- Mohr-Coulomb (general)
- Prandtl and Brinch Hansen (vertical bearing capacity)
- Horizontal bearing capacity
- Fellenius and Bishop (stability of a slope, including reinforced earth)

In general, the soil strength should be sufficient to resist all acting loads.

### 32.1 Soil strength schematization (Mohr-Coulomb)

Various models are available to schematise the strength of soil. The most important models are the Mohr-Coulomb model and the Cam Clay model. This manual only discusses the Mohr-Coulomb model. Mohr's circle of stress shows all stress combinations possible in the soil. Coulomb's line of collapse shows which combination leads to collapse and when. These two parts together form the Mohr-Coulomb model.

#### **Mohr**

Mohr's circle of stress shows all stress combinations in a two-dimensional space, given that there are two planes with zero shear stress, in which only a normal stress acts. The directions of the normal stresses in these two planes are called the principal directions. If the stresses in two planes are known, all states of stress are defined by Mohr's circle (Figure 32-1).

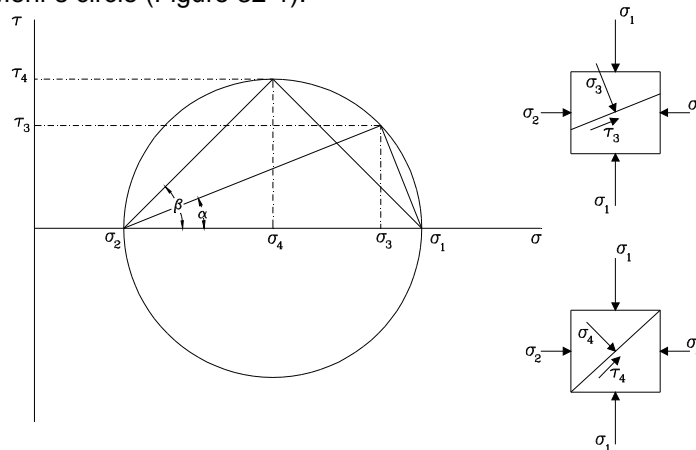


Figure 32-1 Mohr's circle

#### **Coulomb**

Coulomb assumes a strength that is expressed by the shear resistance. If this resistance to shear is exceeded a plane of slip is created. The maximum shear resistance is:

$$\tau_{\max} = c' + \sigma'_n \tan(\delta)$$

in which:  $\tau_{\max}$  [kPa] = max shear stress on a given plane  
 $c'$  [kPa] = cohesion  
 $\delta$  [°] = angle of internal friction  
 $\sigma'_n$  [kPa] = the effective normal stress in a given plane

As long as the shear stress  $|\tau| \leq c' + \sigma'_n \tan(\delta)$  no sliding will occur.

### Mohr-Coulomb

Contrary to Coulomb's collapse, the Mohr-Coulomb model assumes that not one ( $\sigma_n'$ ) but two stresses ( $\sigma_v'$  and  $\sigma_h'$ ) determine the maximum failure value of the shear stress (or shear resistance)  $\tau$ . After all, Mohr's circle considers whether collapse is possible in all directions. Figure 32-2 shows the maximum absorbable shear stress in the  $\sigma, \tau$  plane.

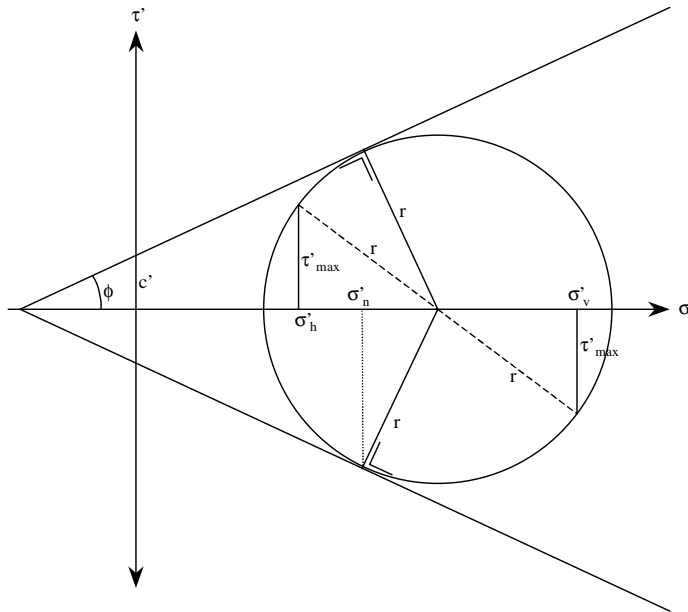


Figure 32-2 Maximum absorbable shear stress according to Mohr-Coulomb

According to Mohr-Coulomb the following applies:

$$\tau_{\max} = c' \cdot \cos(\phi) + \frac{1}{2}(\sigma_h' + \sigma_v') \cdot \sin(\phi)$$

Therefore for undrained materials (clay and peat):

$$c_u = \tau_{\max} = c' \cdot \cos(\phi) + \frac{1}{2}(\sigma_h' + \sigma_v') \cdot \sin(\phi)$$

For this the stresses  $\sigma_v'$  and  $\sigma_h'$  before the application of the load can be assumed because the water pressure absorbs all normal stresses during the application of the load. Consequently, the shear stress remains constant.

### 32.2 Vertical bearing capacity (Prandtl & Brinch Hansen)

The Brinch Hansen method is often used for determining the maximum bearing resistance  $F$  of a foundation. This method is based on Prandtl's theoretical slip surfaces (Figure 32-3). One distinguishes between drained and undrained situations. Undrained situations occur in cohesive impermeable soils, in which pore water pressures increase directly after the load is applied. In undrained soil an undrained shear strength  $c_u$  is used instead of  $c'$ , which is used for drained soil layers. For undrained soil, also  $\phi = 0$  is used for clay and low values of  $\phi$  for sand.

Long-term loads on clay and peat are, of course, calculated as on drained soils!

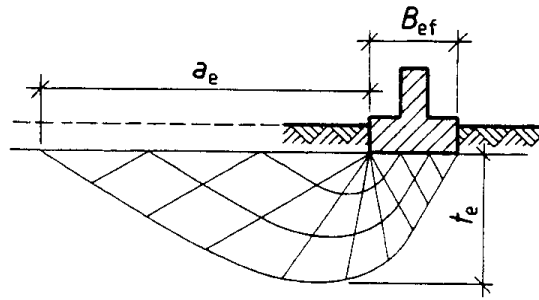


Figure 32-3 Prandtl's slip surfaces

Brinch Hansen extended Prandtl's formulas to include reduction factors for the influence of a possible shear force  $H$  and the relation between the foundation's width  $B$  and length  $L$ . Buisman found equations for the maximum depth ( $D_{max}$ ) and width ( $B_{max}$ ) of the slip body (Figure 32-4):

$$D_{max} = \frac{B \cdot \cos \varphi}{2 \cdot \cos \alpha_f} e^{\alpha_f \cdot \tan \varphi} \quad \text{and} \quad B_{max} = \tan \alpha_f \cdot e^{\frac{\pi}{2} \cdot B \cdot \tan \varphi} = \sqrt{N_q} \cdot B$$

where

$\varphi$  = angle of internal friction,

$\alpha_f$  = angle as depicted in Figure 32-4:  $\alpha_f = \frac{\pi}{4} + \frac{\varphi}{2}$

$N_q$  = bearing capacity factor (see next page)

These equations apply to homogeneous soil, but they could give an indication of the maximum dimensions of the slip body in layered soil. The depth  $D_{max}$  of the slip body is restricted to  $3 B$  and the horizontal dimension  $B_{max}$  to  $1 B$ . For undrained soil the angle of internal friction  $\varphi$  is zero, in which case  $D_{max} = B/\sqrt{2}$  en  $B_{max} = B$ .

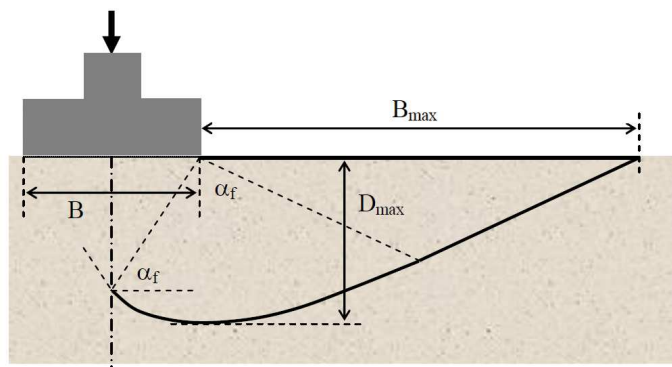


Figure 32-4 Maximum depth and width of a slip body according to Buisman (De Smedt, 2013)

The following discusses a method which is somewhat simplified, compared to the TGB 1990 (old Dutch standard) and the Eurocode 9997-1+C1, and applies for well-permeable soil.

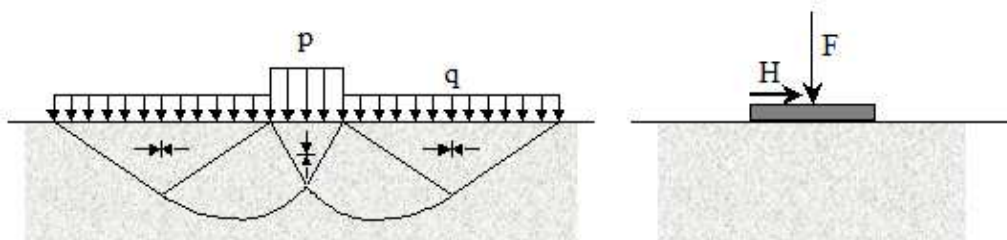


Figure 32-5 Collapse of soil under a structure according to Prandtl and Brinch Hansen

The maximum bearing capacity can be approximated by:

$$F_{\max} = p'_{\max} \cdot A$$

where:

$$p'_{\max} = c' N_c s_c i_c + q' N_q s_q i_q + 0,5 \gamma' B \cdot N_\gamma s_\gamma i_\gamma,$$

consisting of contributions from cohesion (index  $c$ ), surcharge including soil coverage ( $q$ ) and capacity of the soil below the foundation ( $\gamma$ ).

The bearing capacity factors are:

$$N_c = (N_q - 1) \cot \phi' \quad N_q = \frac{1 + \sin \phi'}{1 - \sin \phi'} e^{\pi \tan \phi'} \quad N_\gamma = 2(N_q - 1) \tan \phi'$$

The shape factors ( $B \leq L \leq \infty$ ) are:

$$s_c = 1 + 0,2 \frac{B}{L} \quad s_q = 1 + \frac{B}{L} \sin \phi' \quad s_\gamma = 1 - 0,3 \frac{B}{L}$$

In case of an inclined load, which causes a horizontal component, the bearing capacity is considerably reduced. The inclination factors to deal with an inclined direction of the resulting force ( $B \leq L \leq \infty$ ) are:

For *drained* soil:

For  $H$  parallel to  $L$  and  $L/B \geq 2$  :

$$i_c = \frac{i_q N_q - 1}{N_q - 1} \quad i_q = i_\gamma = 1 - \frac{H}{F + Ac' \cot \phi'}$$

For  $H$  parallel to  $B$  :

$$i_c = \frac{i_q N_q - 1}{N_q - 1} \quad i_q = \left( 1 - \frac{0,70 H}{F + Ac' \cot \phi'} \right)^3 \quad i_\gamma = \left( 1 - \frac{H}{F + Ac' \cot \phi'} \right)^3$$

For *undrained* soil:

$$i_c = 0,5 \left( 1 + \sqrt{1 - \frac{H}{Af_{undr}}} \right) \text{ for the rest, see above.}$$

Only the part of the foundation slab which has effective stresses underneath is included in the effective width  $B$ . The factors for the bearing force are also given in the figure below.

$\phi'_{e,d}$	$N_c$	$N_q$	$N_\gamma$
0°	5	1	0
5°	6.5	1.5	0
10°	8.5	2.5	1
15°	11	4	2
20°	15	6.5	4
22.5°	17.5	8	6
25°	20.5	10.5	9
27.5°	25	14	14
30°	30	18	20
32.5°	37	25	30
35°	46	33	46
37.5°	58	46	68
40°	75	64	106
42.5°	99	92	166

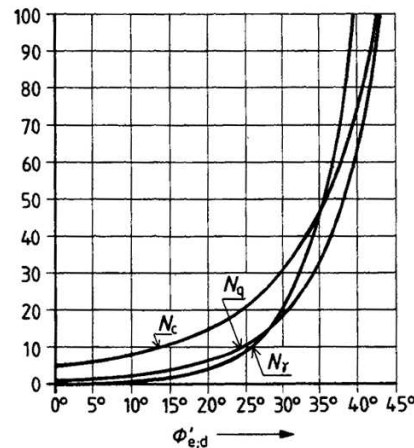
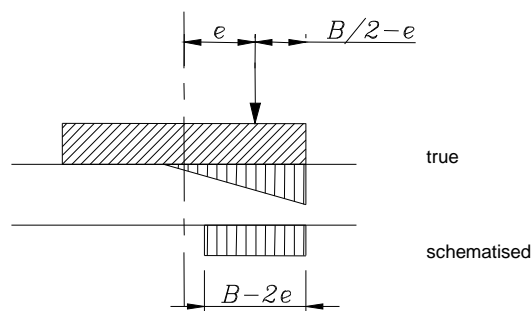


Figure 32-6 Bearing force factors as functions of the angle of internal friction

Clarification of the symbols:

$p'_{max}$	[kPa]	= maximal average effective stress on the effective foundation area
$A$	[m <sup>2</sup> ]	= effective foundation area
$c'$	[kPa]	= (weighted) cohesion (design value)
$q'$	[kPa]	= effective stress at the depth of, but next to foundation surface (design value) = $\sigma'_{v,z;0} = \gamma_{f,g} \cdot \sum_{i=1}^{i=n} (d_i \cdot \gamma_{car}) - u$
$u$	[kN/m <sup>2</sup> ]	= water pressure
$n$	[-]	= number of horizontal soil layers between the construction depth and the soil cover level
$\gamma$	[kN/m <sup>3</sup> ]	= (weighted) effective volumetric weight of the soil below construction depth (design value)
$d_i$	[m]	= thickness of layer $i$
$\gamma_{car}$	[kN/m <sup>3</sup> ]	= characteristic volumetric weight of the soil, for which: - for a soil layer above groundwater level: $\gamma_{car} = \gamma_{rep}$ ; - for a soil layer under groundwater level: $\gamma_{car} = \gamma_{sat;rep}$ ;
$\gamma_{rep}$	[kN/m <sup>3</sup> ]	= representative value of the volumetric weight with natural humidity
$\gamma_{sat;rep}$	[kN/m <sup>3</sup> ]	= saturated volumetric weight
$\gamma_{f,g}$	[-]	= load factor for a favourable load
$\chi_c$	[-]	= factor for the influence of cohesion
$\chi_q$	[-]	= factor for the influence of the soil cover
$\chi_\gamma$	[-]	= factor for the influence of the effective volumetric weight of the soil
$\phi'_{e;d}$	[°]	= (weighted) effective angle of internal friction (design value)
$H$	[kN]	= shear force, i.e.: component of the force in the plane of the foundation surface (design value)
$F$	[kN]	= component of the exerted force perpendicular to the foundation surface (design value)
$f_{undr}$	[kPa]	= design value of the undrained shear strength = $c_u$
$L$	[m]	= length of the effective foundation area, for circular slabs: $L = B$
$B$	[m]	= width of the effective foundation area, for circular slabs: $L = B$ For an eccentrically loaded foundation $B$ is approximated by $B-2e$ See the following figure:



### Note

- The factors for the bearing force are too conservative. This is because it is assumed that the factors do not influence each other, which is incorrect.
- The factors for the shape of the foundation and particularly for the horizontal load are not substantiated scientifically but they are based on empirical relations, experiments, calculations, etc.
- For a horizontal load  $H$  one not only has to apply a reduction in the calculation of the vertical bearing force  $F$ , but one also has to check if sliding can occur (e.g. using Coulomb).
- The reduction of the vertical bearing force  $F$  as a result of the horizontal load  $H$  is considerable. Assuming  $H/F = 0,30$  results in  $i_q = 0,50$ !

Layered soil

If the foundation's subsoil is layered, one can fill in the average soil properties in the previous equations according to:

$$\phi' = \frac{\sum_{i=1}^{i=n} h_i \phi_i X_i}{\sum_{i=1}^{i=n} h_i X_i} \quad c' = \frac{\sum_{i=1}^{i=n} h_i c_i X_i}{\sum_{i=1}^{i=n} h_i X_i} \quad \gamma' = \frac{\sum_{i=1}^{i=n} h_i \gamma_i X_i}{\sum_{i=1}^{i=n} h_i X_i}$$

in which:

- $h_i$  [m] = thickness of layer  $i$ ,
- $\phi_i$  [°] = the design value of the effective angle of internal friction for layer  $i$
- $n$  [-] = the number of horizontal layers between the influence depth  $t_e$  and the depth of the bottom of the foundation element;
- $X_i$  [m] = distance between the centre of layer  $i$  to the influence depth  $D_{max}$  (see Figure 32-4),
- $h_j$  [m] = the thickness of layer  $j$ ,
- $t_e$  [m] = the influence depth;  $t_e = 1,5 B$
- $c_i$  [kPa] = the design value for the effective cohesion of layer  $i$
- $\gamma_i$  [kN/m<sup>3</sup>] = the design value for the effective volumetric weight of layer  $i$

Using the previous equations one can determine the dimensions of a foundation iteratively. As a first estimate one often uses a rule of thumb which assumes that the soil under and next to the foundation does not collapse if the work-line of resultant force intersects the core of the foundation surface (see Section 37.2).

**32.3 Horizontal bearing capacity (resistance against sliding)****Theory**

Horizontally loaded foundations transfer their load to the subsoil by means of friction in the foundation plane and possibly passive earth pressure behind the foundation. To calculate the maximum friction against the foundation surface one normally uses Coulomb's formula:

$$\tau_{max} = f \sigma_n'$$

- in which:  $\tau_{max}$  [kPa] = maximum shear stress in the foundation surface
- $f$  [-] = coefficient of friction =  $\tan(\delta)$
- $\delta$  [°] = angle of friction between foundation slab and soil
- $\sigma_n'$  [kPa] = the effective normal stress under the foundation

One might wonder whether the cohesion of a soil layer should also be included in the formula above, but on grounds of sensitivity to settlements, foundations are never situated directly on cohesive materials but always on sand or gravel, making this question irrelevant.

The coefficient of friction between concrete and sand is usually in the order of 40% to 50%. For the coefficient of friction between steel and sand roughly the same values are found.

The angle of friction parameter  $\delta$  is a parameter that belongs to Coulomb's model of friction. The angle of internal friction  $\phi$  is a parameter that corresponds to Mohr-Coulomb's model of friction. These are different models. Coulomb's model of friction is based on one stress: the normal stress  $\sigma_n'$ , whilst Mohr-Coulomb's model of friction is based on two stresses:  $\sigma_v'$  and  $\sigma_n'$ .

Assuming the normal stress  $\sigma_n'$  and the stress perpendicular to this  $\sigma_{\perp}'$  it is possible to work  $\phi$  into  $\delta$ :

$$\tan(\delta) = \frac{1}{2} \sqrt{(1+K)^2 \cdot \sin^2(\phi) - (1-K)^2} \quad \text{with: } K = \frac{\sigma_{\perp}'}{\sigma_n'}$$

If  $K = 1$  then:  $\tan(\delta) = \sin(\phi)$

### **Design**

Usually  $\sigma_h' < \sigma_v'$  is valid for soil layers, because  $K_0 < 1$ .

For horizontal surfaces the normal stress (vertical) is therefore greater than the stress perpendicular to this (horizontal):

$$\sigma_n' > \sigma_{\perp}'$$

By approximation one can assume:

$$\tau_{\max} = \tan(\delta) \sigma_n' \quad \text{with: } \delta \approx \frac{2}{3} \phi$$

For vertical surfaces the normal stress (horizontal) is therefore smaller than the vertical stress perpendicular to this:

$$\sigma_n' < \sigma_{\perp}'$$

By approximation one can assume:

$$\tau_{\max} = \tan(\delta) \sigma_n' \quad \text{with: } \delta \approx 0,8 \text{ to } 0,9 \cdot \phi$$

The values given above can be derived theoretically. Furthermore, these values are also found experimentally.

## **32.4 Stability of slopes (Fellenius and Bishop)**

Many methods for checking the stability of slopes are based on circular slip surfaces. The earth mass above the failure arc is divided into slices, of which one, with a width  $b$  and (average) height  $h$ , has been drawn. If one considers the moments relative to the centre of the circle, the following applies for the driving moment:

$$M_a = \sum \gamma b h R \sin(\alpha)$$

which considers the sum of the contributions of all slices and where  $\gamma$  is the volumetric weight of soil. If the ground mass is composed of several layers, one may have to deal with different volumetric weights over the height  $h$ . If the water table is found above the sliding surface one must take into account the volumetric weight of wet soil below the water table and the weight of dry soil above it (unless there is also capillary rise, as tends to be the case particularly for clay and peat). Possible water above ground level should also be taken into account.

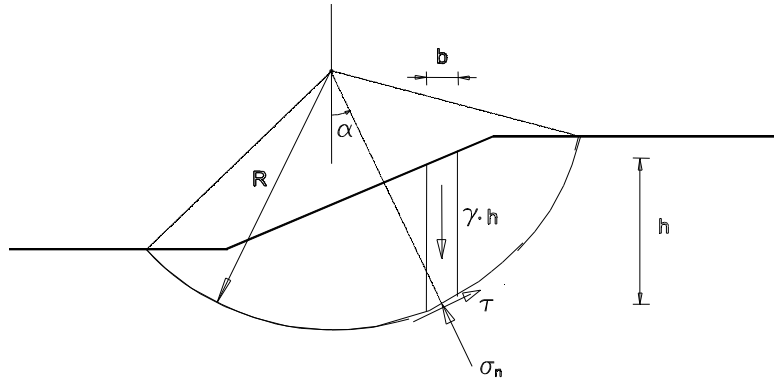


Figure 32-7 The principle of a slip surface calculation

The resisting moment is:

$$M_w = \sum \tau b \frac{1}{\cos(\alpha)} R$$

in which  $b/\cos(\alpha)$  approximates the length of the circumference over the slice width  $b$ .

Fellenius assumes that the shear stress  $\tau$  along the whole circumference is a factor  $F$  smaller than the maximum shear stress that can be developed. This factor is also called the stability factor and it can be considered a type of safety coefficient.

Therefore the shear stress can be denoted as:

$$\tau = \frac{1}{F} (c' + \sigma_n' \cdot \tan(\phi'))$$

in which:

$c'$	[kPa]	=	cohesion
$\sigma_n'$	[kPa]	=	normal effective stress, with $\sigma_n' = \sigma_n - p$
$\phi'$	[-]	=	angle of internal friction
$p$	[kPa]	=	water pressure

### **Fellenius**

Fellenius assumes that the slices do not exert any force on each other. The balance of forces along the radial leads to:

$$\sigma_n' \cdot b \frac{1}{\cos \alpha} = \gamma b h \cos(\alpha) \Leftrightarrow \sigma_n' = \gamma h \cos^2(\alpha)$$

Inserting the normal stress produces:

$$\tau = \frac{1}{F} (c' + (\gamma h \cos^2(\alpha) - p) \tan(\phi'))$$

A balance of moments around the centre of the circle means that the driving moment  $M_a$  equals the resisting moment  $M_r$ . Together this results in the following formula by Fellenius for safety:

$$F = \frac{\sum \{ [c' + (\gamma h \cos^2 \alpha - p) \tan \phi'] / \cos \alpha \}}{\sum \gamma h \sin \alpha}$$

**Bishop**

Due to the shear force that is created under a slice, the vertical balance should really be corrected, so that:

$$\gamma h = \sigma_n' + p + \tau \cdot \frac{\sin \alpha}{\cos \alpha}$$

Inserting this in the driving moment  $M_d$  leads to Bishop's iterative formula:

$$F = \frac{\sum \frac{c' + (\gamma h - p) \tan \phi'}{\cos \alpha (1 + \tan \alpha \cdot \tan \phi' / F)}}{\sum \gamma h \sin \alpha}$$

The stability check consists of dividing the soil, for instance into 10 slices of equal width, measuring  $\alpha$  and  $h$  for each slice and then determining the safety factor  $F$ . The verification is carried out for several sliding surfaces (different centre points and radii). The smallest value of  $F$  (corresponding to the most critical sliding surface) has to be greater than  $\underline{F} = 1,2$  for temporary building works (e.g. excavated building sites) or  $\underline{F} = 1,3$  for permanent works.

The aforementioned method of calculation entails a lot of work. Particularly if one considers that several slope angles have to be investigated in order to find the steepest possible slope. This is why the calculations are always carried out by a computer programme (e.g. Mstab).

For an infinite slope of dry, non-cohesive material, one finds:

$$F = \frac{\tan \phi'}{\tan \alpha}$$

**Note:**

*One should not value the calculated safety factor too much, because the entire method is questionable.*

*Some of the flaws are:*

- *the circular sliding surface is not entirely correct because the soil can deform.*
- *the calculations only include the balance of moment and not the complete balance of force.*
- *the transfer of forces between the slices is not taken into account.*

*The groundwater pressures are not always well known, but they are very important. A high groundwater pressure reduces the safety factor. In little permeable soil types, the water pressure certainly needs (a lot of) time to adjust to the drainage and to the dewatering of an excavated building site. Using values for the water pressure that are too optimistic in calculations has led to the collapse of slopes (sliding) in many cases. Measures against this include:*

- *designing with more realistic values (and thus shallower slopes).*
- *dewatering the area earlier.*
- *draining the excavated building site slowly.*
- *applying sand drains or geo-drains for faster drainage of little permeable soil layers in places where sliding surfaces can be expected.*

**Reinforced earth (Terre Armée)**

A reinforced earth wall is a wall consisting of prefab slabs piled on top of each other. Two strips of geotextile (or zinc-coated steel), which disappear horizontally in the soil behind the wall, are attached to each slab. Due to the weight of the soil, the strips can absorb a tensile force and hold the individual elements in place. The collapse mechanism of the entire wall can be solved with Fellenius and Bishop but that requires calculating the extra tensile force of the strips correctly. The part of the strip outside of the sliding circle (see Figure 32-8) can absorb an additional force in the order of:

$$F_{strip} = 2bl_{eff}\sigma'_v \tan \delta$$

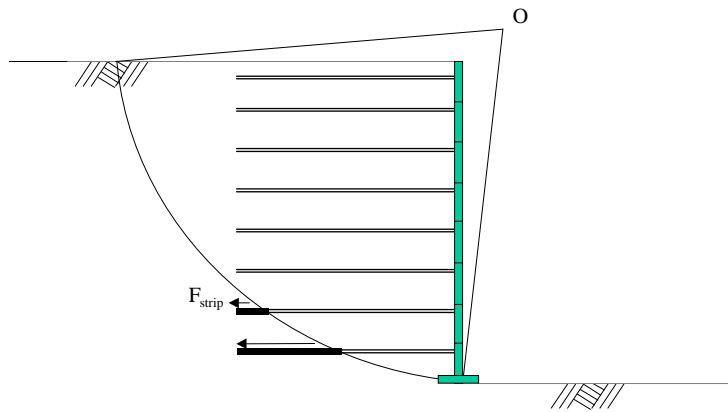


Figure 32-8 Extra stability due to reinforced earth

**Note**

Next to no computer programmes can calculate reinforced earth. The programmes that do calculations with geo-textiles (nearly) never include the correct effective length in calculations (including Mstab). Plaxis, however, does calculate this length properly.

### 33. Soil - stiffness

Schematizations of soil stiffness are used for determining the flow of forces through the structure and for estimates of the displacement of the structure. The two most frequently used models:

1. Winkler model, based on the schematization of the soil into a set of uncoupled linear springs.
2. Elastic solid foundation model. This model is based on the relation between stress, strain and the Young's modulus.

For conceptual design the use of the Winkler model is often more convenient, therefore the Elastic solid foundation model will not be elaborated here.

#### 33.1 Spring schematisation

For design calculations involving the stiffness properties of soil, the soil is often modelled as a set of uncoupled linear springs, known as the Winkler model. This is a popular schematization because it is a simple model, easy to use.

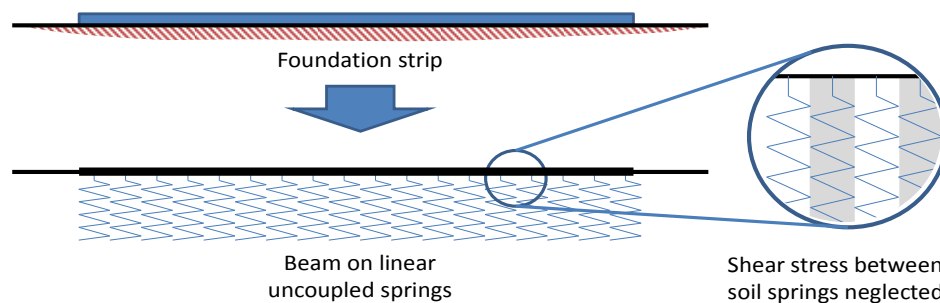


Figure 33-1 Winkler foundation model

Since a linear relationship between the action on the foundation, suppose pressure  $p$ , and the deflection  $w$  is assumed:

$$p = k_o \cdot w$$

where  $k_o$  [N/m<sup>2</sup>/m] = foundation modulus

For beams with width  $b$ , we use  $p = k \cdot w = k_o \cdot b \cdot w$  (unit of  $k$ : N/m/m).

If the foundation is infinitely stiff the foundation modulus  $k_o$  is in fact fully determined by the soil characteristics. For the infinite stiff foundation,  $k_o$  is better known as the modulus of subgrade reaction  $k$  (*beddingsconstante*).

Note: the modulus of subgrade reaction is in fact not a soil parameter; i.e. not only soil parameters influence its value but the geometry of the structure as well.

As downside of the simple Winkler model the following can be mentioned:

- The springs are not linked or coupled to each other (see Figure 33-1), while in reality the soil elements are linked by means of shear stresses.
- The spread of stress in the subsoil is not really included in the schematisation because of the independent, uncoupled behaviour of every spring.
- The soil is not a spring and definitely does not behave as a linear one.
- Springs have a spring constant  $k$  (generally  $k=EA/l$ ). The schematisation as spring therefore requires a "contributing depth", to account for  $l$ , which is unknown.

Figure 33-2 shows the real and the calculated pressure distributions under a very stiff foundation, using the linear spring model for soil. The biggest difference is the soil pressure near the edges of the foundation.

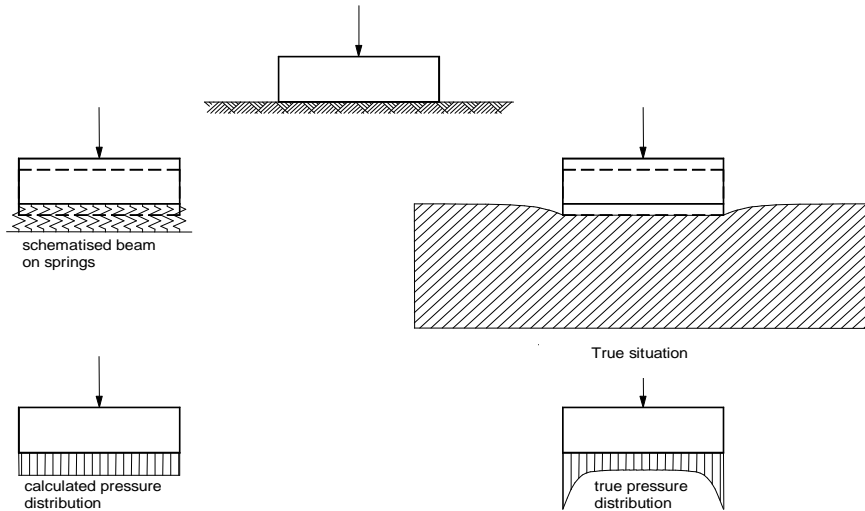


Figure 33-2 Calculated versus true pressures

In the case of an infinitely stiff plate, the foundation pressure is, neither in reality nor according the continuum theory, constant. The pressure along the edge is, after all, higher than in the middle. According to the “spring” method, the pressure is the same everywhere.

For foundations of limited dimensions, settlements not only depend on the stiffness of the soil and the stresses in the foundation plane, but also on the dimensions of the structure. Figure 33-3 shows the settlements for a foundation slab of  $\phi$  75 cm and for a slab of  $\phi$  150 cm. In both cases, the settlement of the largest foundation slab is bigger than the settlement of the smaller plate, for the same soil stiffness and equal pressures on the foundation surface.

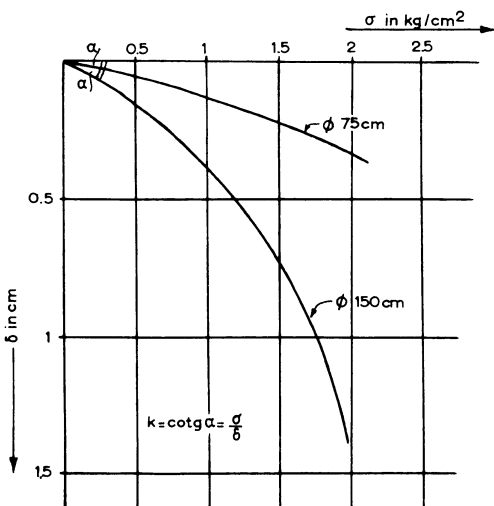


Figure 33-3 measured settlements for two foundation slabs

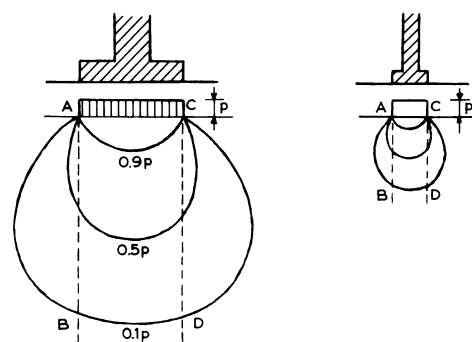


Figure 33-4 Influence depth of a foundation strip

This can be explained by the spread of the load in subsoil. Figure 33-4 shows the influence of the size of the foundation slab on the spread of the load in the subsoil. By approximation the depth of influence of the foundation is directly proportional to the dimensions of the foundation area. The area of the foundation should therefore be taken into account in the calculation of the modulus of sub grade reaction.

### 33.2 Modulus of subgrade reaction

Estimating the stiffness of a structure is usually relatively easy. The bending stiffness (or flexural rigidity) of a beam is characterised by its  $EI$  value. Estimating the stiffness of soil, however, is a lot more difficult. The modulus of subgrade reaction (*beddingsconstante*) is defined as:

$$k = \frac{\sigma}{\delta}$$

in which:  $k$  [Pa/m] = modulus of subgrade reaction  
 $\sigma$  [Pa] = the (effective) stress at the bottom of, under the foundation surface  
 $\delta$  [m] = the displacement of the foundation surface

This section discusses three different types of modulus of sub grade reactions:

- Vertical modulus of subgrade reactions
- Horizontal modulus of subgrade reactions for (sheet pile) walls
- Horizontal modulus of subgrade reactions for piles

### 33.3 Vertical modulus of subgrade reaction (using Flamant)

The solution for surface loads was already treated in Section 24.1. The stresses in an arbitrary point in a homogenous half space are:

$$\sigma'_{zz} = \frac{q_v}{\pi} [(\theta_1 - \theta_2) + \sin \theta_1 \cos \theta_1 - \sin \theta_2 \cos \theta_2] \quad \sigma'_{xz} = \frac{q_v}{\pi} [\cos^2 \theta_2 - \cos^2 \theta_1]$$

$$\sigma'_{xx} = \frac{q_v}{\pi} [(\theta_1 - \theta_2) - \sin \theta_1 \cos \theta_1 + \sin \theta_2 \cos \theta_2]$$

Because all stresses have been solved, all strains and therefore also all displacements can be solved. The following is valid for the  $z$ -axis:

$$\varepsilon_{zz(x=0)} = \frac{2q_v}{\pi E} [\theta_1(1-2\nu) + \sin \theta_1 \cos \theta_1(1+\nu)] \Rightarrow$$

$$u_{z(x=0)} = \int_{z=0}^{z=\infty} \varepsilon_{zz(x=0)} \delta z \approx \frac{2aq_v}{E}(1+\nu)[1,762 \cdot (1-2\nu) + 1,443]$$

The modulus of subgrade reaction for the  $z$ -axis is then:

$$k_{(x=0)} = \frac{q_v}{u_{z(x=0)}} \approx \frac{E}{2a} \cdot \frac{1}{(1+\nu)[1,762 \cdot (1-2\nu) + 1,443]}$$

A reasonable estimate for the modulus of subgrade reaction of drained soil is:

$$k \approx 0,31 \cdot \frac{E}{2a} \quad (\nu = 0,3)$$

A reasonable estimate for the modulus of subgrade reaction of undrained soil is:

$$k \approx 0,53 \cdot \frac{E}{2a} \quad (\nu_u = 0,5 \text{ and } E_u = \frac{1+\nu_u}{1+\nu} E)$$

The geometry (width of the load:  $2a$ ) is clearly present in the modulus of sub grade reaction, which proves that the value of  $k$  depends on the geometry of the structure.

For line loads one does not use the modulus of subgrade reaction per area unit, but per length unit of the line load. This modulus of subgrade reaction  $k'$  has a different dimension ( $[\text{kN}/\text{m}^2]$  instead of  $[\text{kN}/\text{m}^3]$ ) and is independent of the width of the line load, because:

$$k' = \frac{k}{2a} \approx 0,31 \cdot E \quad (\nu = 0,3)$$

### 33.4 Horizontal modulus of subgrade reaction for (sheet piling) walls

This section explains what modulus of subgrade reactions should be used according to CUR 166 to calculate a sheet pile wall with a spring model. The figure below is used to calculate the horizontal stress-displacement relationship.

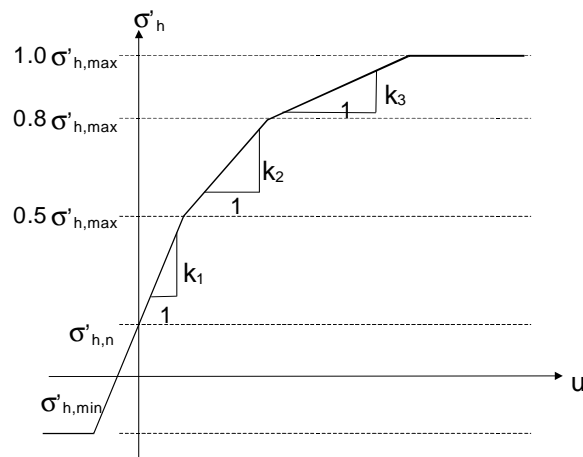


Figure 33-5 Horizontal stress-displacement relationship

In the figure the following applies:

$$\begin{aligned}\sigma'_{h,\min} &= K_a \sigma'_v - 2c\sqrt{K_a} \\ \sigma'_{h,\max} &= K_p \sigma'_v + 2c\sqrt{K_p} \\ \sigma'_{h,n} &= K_0 \sigma'_v\end{aligned}$$

where:

$$\text{coefficient of active horizontal soil stress} \quad K_a = \frac{1 - \sin \phi'}{1 + \sin \phi'}$$

$$\text{coefficient of passive horizontal soil stress} \quad K_p = \frac{1 + \sin \phi'}{1 - \sin \phi'}$$

$$\text{coefficient of neutral horizontal soil stress} \quad K_0 = 1 - \sin \phi'$$

The aforementioned formulas assume straight sliding surfaces. For angles of internal friction ( $\phi$ ) higher than  $30^\circ$ , curved sliding planes are more realistic. If nevertheless the above mentioned equations are used for these higher values of  $\phi$ , the resulting values for  $K$  are unrealistically high. In reality,  $K$  is limited to a maximum value of about 7.

		$k_1$ [kN/m <sup>3</sup> ]		$k_2$ [kN/m <sup>3</sup> ]		$k_3$ [kN/m <sup>3</sup> ]	
		$k_{low}$	$k_{high}$	$k_{low}$	$k_{high}$	$k_{low}$	$k_{high}$
<b>sand</b>	$q_c$ [MPa]						
loose	5	12000	27000	3270	7360	1000	2250
moderate	15	20000	45000	5460	12270	1670	3750
firm	25	40000	90000	10900	24550	3330	7500
<b>clay</b>	$f_{undr}$ [kPa]						
weak	25	2000	4500	400	900	200	450
moderate	50	4000	9000	1090	2460	240	530
firm	200	6000	13500	2570	5790	670	1500
<b>peat</b>	$f_{undr}$ [kPa]						
weak	10	1000	2250	275	615	85	185
moderate	30	2000	4500	400	900	200	450

Table 33-1 Horizontal modulus of sub grade reactions (CUR 166)

The stress-displacement relationship is split into three branches. The modulus of subgrade reactions for these three branches are given in Table 33-1. They depend on the type of soil. The modulus of subgrade reactions are determined according to CUR 166.

#### Note

- To calculate the displacement normative  $k$ -values are used, i.e.:  $k_{low}$ .
- To calculate the forces and moments, two calculations are carried out. One with  $k_{low}/1.3$  and a second with  $k_{high}$ . It is impossible to tell which of the two is normative in advance, although in most cases the calculation with the low modulus of sub grade reactions is normative.

### 33.5 Horizontal modulus of subgrade reactions for piles

For horizontally loaded piles horizontal modulus of subgrade reactions are used. The pressure distribution around a pile is completely different to the distribution around a wall. This also means different modulus of subgrade reactions are to be used. According to Menard these constants can best be based on the radial elasticity modulus  $E_{menard}$ . According to Menard, the following relationship between the modulus of subgrade reaction and the radial elasticity modulus is valid for piles:

$$\frac{1}{K_h} = \frac{1}{3 \cdot E_{menard}} \left( 4,0 \cdot \left( 2,65 \cdot \frac{D}{0,60\text{m}} \right)^\alpha + \alpha \cdot \frac{D}{2} \right) \quad (D \geq 0,60 \text{ m})$$

$$\frac{1}{K_h} = \frac{D}{E_{menard}} \cdot \frac{4,0 \cdot (2,65)^\alpha + 3\alpha}{18} \quad (D < 0,60 \text{ m})$$

One can measure  $E_{menard}$  by blowing up a balloon in a boring hole and by measuring which radial deformation occurs at a given pressure. In most cases, however,  $E_{menard}$  is not measured. Usually the  $q_c$  has been found from soundings. In that case the following empirical relationship between Menard's elasticity modulus and the cone resistance can be used:

$$E_{menard} = q_c \cdot f$$

Type of soil	$f$	$\alpha$
gravel	-	1.4
sand	0,8 to 1,0	1/3
silt	2,0 to 3,0	1/2
clay	3,0	2/3
peat	3,0 to 4,0	1.0

Table 33-2 Empirical relationships

One can calculate using the dynamic stiffness for short-term loads, such as a collision against a bridge piling. The dynamic stiffness is greater than the static stiffness, for instance:

$$E_{dynamic} = 3 \cdot E_{static}$$

This linear stiffness behaviour is limited by the strength behaviour of piles. The derivation of the three-dimensional  $K_p$  values (with shell behaviour) is complex and goes beyond the scope of this manual. See "The ultimate resistance of rigid piles against transversal forces" by Brinch Hansen. This is a standard part of the single pile module of the computer programme D-Sheet Piling.

## 34. Soil - settlement

slightly revised: February 2011; revised: February 2015

Settlement is the process of soil compression. It is an important phenomenon for hydraulic engineering because it results in a decrease of the ground level including all structures resting on shallow foundations. Especially for flood defences this is relevant because settlement will reduce their water retaining height, which immediately affects their primary function if the design does not sufficiently take this effect into account. Furthermore, uneven settlements should be avoided or compensated for, in order to prevent structural failure due to too high stresses in the structure.

Settlement can take place in the subsoil (*zetting*) or in an embankment (*klink*). Land subsidence, by the way, also causes a drop in ground level, but this takes place at another geological scale and should also be taken into account when designing flood defences.

Settlement can mainly be caused by two different natural phenomena. It can be caused by expulsion of water out of the pores between the soil particles due to an increase in vertical loading, which is called 'consolidation'. It can also be the result of an ongoing, slower, densification process during which the soil properties gradually change, which is called 'creep' (*kruip*), 'secondary settlement' or 'secular effect'.

These phenomena and the opposite effect of compression (relaxation of soil) are described in the following sections, starting with consolidation.

### 34.1 Consolidation

#### Theory

Consolidation is the process that involves decrease in water content of a saturated soil due to loading, without replacement of water by air. Especially long term static loads cause expulsion of water which results in a reduction in volume without a change of its shape. The degree of consolidation,  $U$ , indicates how much water (pressure) has already dissipated. The following applies for one-dimensional consolidation:

$$U = 1 - \frac{8}{\pi^2} \sum_{j=1}^{\infty} \frac{1}{(2j-1)^2} \cdot e^{\left( -\frac{(2j-1)^2 \cdot \pi^2 \cdot c_v \cdot t}{4 \cdot h^2} \right)}$$

Or by approximation:

$$U \approx \frac{2}{\sqrt{\pi}} \sqrt{\frac{c_v \cdot t}{h^2}} \quad \text{if } (U \leq 0,5) \quad \text{and} \quad U \approx 1 - \frac{8}{\pi^2} \cdot e^{\left( -\frac{\pi^2 \cdot c_v \cdot t}{4 \cdot h^2} \right)} \quad \text{if } (U > 0,5)$$

in which:  $c_v$  [m<sup>2</sup>/s] = coefficient of (vertical) consolidation (oedometer test)

$h$  [m] = drainage height. If a soil layer is drained on the top and from below, the drainage height  $h$  is half the height of the double drained soil layer.

$t$  [s] = time

The above degree of consolidation is not valid for vertical drainage. For that, see the next section.

The following is valid for the vertical consolidation "constant"  $c_v$ :

$$c_v = \frac{k_v}{\gamma_w m_v}$$

No sensible estimates can be made of  $c_v$ . This is because both the vertical permeability  $k_v$  and the vertical soil stiffness  $m_v$  vary too much per soil layer. Furthermore,  $k_v$  and  $m_v$  decrease during consolidation due to their dependence on the stresses! The only reasonable solution is to do oedometer tests for the correct stress path.

The duration of one-dimensional consolidation:

$$t_{99\%} \approx \frac{1,78 \cdot h^2}{c_v}$$

At time  $t_{99\%}$ , the pressure has adjusted 99%. From then on it can be assumed that  $U = 1$ .

Depending on how the excess pore-water is dissipated, two or three-dimensional consolidation is involved. In literature one can find equations for the adjustment of the water pressure in time for both two and three-dimensional consolidation (Lambe and Whitman, 1969).

Theoretically, in the case of one-dimensional loading (oedometer test, horizontal strain is zero), 100% of the load goes to the water pressure and 0% to the effective stress (so:  $U_0 = 0$ ). In the case of plain stress loading (triaxial test, horizontal stress is constant), 33% goes to the water pressure and 67% to the vertical effective stress ( $U_0 = 0,67!!!$ ). In a combination, plain-strain loading (biaxial test) 50% goes to the water pressure and 50% to the effective stress ( $U_0 = 0,50$ ). In reality, most loads are in principle something in between a one-dimensional load and a plain-strain load. That is why it would be better to use:

$$U_0 \approx 0,25$$

The total consolidation process goes therefore much faster than the equation of the degree of consolidation suggests. More information on this topic can be found in other literature (A.Verruijt, 1987).

### **Vertical drainage**

The best-known vertical drainage systems are sand drains and synthetic geo-drains. Vertical drainage is applied to accelerate the consolidation process. The most important reason for accelerating the consolidation process is the problem that one starts construction too late. An additional matter is that the drainage costs can sometimes be earned back by interest savings by being able to purchase the land later. Drawbacks of vertical drainage are:

- the extra costs,
- the environmental drawbacks (plastic in the soil),
- the degradation of the seal against vertical water transport ("piercing the polder").

One must realise that the vertical drainage does not accelerate the secondary settlement (creep). If one doesn't satisfy a certain residual settlement requirement, vertical drainage is not a solution in all cases. Preferably one should consider working with a longer settlement period or with temporary embankments.

In the case of vertical drainage, there is a constant horizontal drainage distance for all soil layers. This makes calculating the degree of consolidation per layer easier. The following is valid:

$$U_h = 1 - e^{-\frac{8T_h}{\mu}}$$

where:

$U_h$  [-] = horizontal degree of consolidation (for vertical drainage)

$T_h$  [-] = time factor for horizontal flow:

$$T_h = \frac{c_h \cdot t}{D^2}, \text{ where:}$$

$c_h$  [m<sup>2</sup>/s] = horizontal consolidation coefficient (oedometer test)

$D$  [m] = equivalent drain distance:

$$D = 1,05 \cdot \ell \text{ (for triangular pattern of drainage)}$$

$$= 113 \cdot \ell \text{ (for square pattern of drainage)}$$

$\ell$  [m] = distance between two vertical drains

$$c_h = \frac{k_h}{m_v \cdot \gamma_w}$$

$\mu$  [-] = a function mainly related to drain spacing and size and the extent of soil disturbance due to drain installation (smear effect). The basic form of  $\mu$  for ideal drain with no smear effect can be expressed as follows:

$$\mu = \frac{n^2}{n^2 - 1} \left[ \ln(n) - \frac{3}{4} + \frac{1}{n^2} \left( 1 - \frac{1}{4n^2} \right) \right], \text{ where:}$$

$$n [-] = \frac{D}{d}$$

$$d \text{ [m]} = \text{equivalent drain thickness: } d = \frac{2(b+t)}{\pi}$$

### Notes

- In some literature 'consolidation' has the meaning of the primary settlement. In this Manual 'consolidation' is considered the cause of primary settlement.
- Densification of an embankment ('klink' in Dutch) can consist of three effects: primary settlement, secondary (creep) settlement and lateral deformation. Lateral, or horizontal, deformation (expansion) does not influence the total volume, so it results in a decreased embankment height.
- The horizontal permeability of a soil layer can be greater (or smaller) than the vertical permeability.
- The distance  $\ell$  between two drains is generally between 1 and 3 m.
- A triangular pattern is always more economical than a square pattern.

The cross-section of narrow synthetic drains is  $b \times t = 100 \times 4 \text{ mm}^2$ . The cross-section of wide synthetic drains is  $b \times t = 300 \times 4 \text{ mm}^2$ .

## 34.2 Primary settlement and creep

In practice, the compressibility of soil is an important property regarding settlement problems. Compression is the decrease in volume without the change of shape.

Soil is not a linearly elastic material. Generally the stiffness increases with an increase of the average compressive stress ( $\sigma'_0$ ) caused by higher loading. Due to this increase in loading the soil particles will come closer together (the porosity decreases), increasing the number of contact points and enlarging the areas of contact. As a result, water residing in the pores will be expelled. This phenomenon is called 'primary settlement'.

A related phenomenon is secondary settlement, also called 'creep' or 'secular effect'. Creep is the ongoing compression under a constant load, where the soil properties gradually change. Also here water is expelled out of the pores. This compaction goes on practically forever, also if the pore pressures have been long reduced to zero.

Internationally, the Anglo-Saxon method is often used to determine soil settlement. This method comprises primary and secondary settlement and is expressed by the symbol  $\varepsilon$  that represents the relative settlement, so the reduction of the height of a soil layer ( $\Delta H$ ) divided by the initial layer height ( $H$ ):

$$\varepsilon = \varepsilon_p + \varepsilon_s ,$$

and  $\Delta H = \varepsilon \cdot H$ . The total settlement of  $n$  soil layers thus is  $\Delta H_{total} = \sum_{i=1}^n \Delta H_i$ .

The equation for the primary compression comes from Karl von Terzaghi:

$$\varepsilon_p = \frac{C_c}{1 + e_0} \log \left( \frac{\sigma'_{v,i} + \Delta\sigma'_v}{\sigma'_{v,i}} \right)$$

in which:  $\varepsilon_p$  [-] = relative primary settlement =  $\Delta H_p / H_p$   
 $C_c$  [-] = primary compression coefficient  
 $e_0$  [-] = initial void ratio (*poriëngetal*) (see Section 34.3)  
 $\sigma'_{v,i}$  [kPa] = initial vertical effective stress  
 $\sigma'_v$  [kPa] = (new) vertical effective stress =  $\sigma'_{v,i} + \Delta\sigma'_v$

The equation for creep has been developed by prof. Keverling Buisman:

$$\varepsilon_s = C_\alpha \log(t)$$

in which:  $\varepsilon_s$  [-] = relative secondary settlement (= creep) =  $\Delta H_s / H_s$   
 $C_\alpha$  [-] = secondary compression coefficient  
 $t$  [day] = time

This formula has no advantages, but it does have three disadvantages:

- The initial pore value  $e_0$  is unknown and difficult to estimate.
- The formula for secondary compression is not intended for weak soil.
- The formula for secondary compression is nonsense. The value of the pressure difference  $\Delta\sigma'$  is not even included in the formula!

The equation according to linear elasticity is also used:

$$\varepsilon = m_v \Delta\sigma$$

in which:  $m_v$  = (vertical) compression constant =  $1 / E_{oed}$

Because in principle soil is not a linear elastic material, this formula has limited applicability. The constant  $m_v$  depends on the state of stress and can only be assumed constant in a limited stress course.

The most used method for determination of the compressibility in the Netherlands is proposed by Koppejan. The relative compression of a soil layer with a certain degree of consolidation can be calculated with the following equation, based on Koppejan's original formula from 1948:

$$\varepsilon = \left( \frac{U}{C'_p} + \frac{1}{C'_s} \log(t) \right) \cdot \ln \left( \frac{\sigma'_{v,i} + \Delta\sigma'_v}{\sigma'_{v,i}} \right)$$

in which:  $\varepsilon$  [-] = relative compression =  $\Delta H / H$   
 $H$  [m] = layer thickness  
 $U$  [-] = degree of consolidation (see Section 34.1)  
 $C'_p$  [-] = primary compression coefficient ( $\sigma'_v > \sigma'_{limit}$ )  
 $C'_s$  [-] = secondary compression coefficient ( $\sigma'_v > \sigma'_{limit}$ )  
 $C_p$  [-] = primary compression coefficient ( $\sigma'_v < \sigma'_{limit}$ )  
 $C_s$  [-] = secondary compression coefficient ( $\sigma'_v < \sigma'_{limit}$ )  
 $t$  [day] = time  
 $\Delta\sigma'_v$  [kPa] = increase of the vertical effective stress in the weak layer  
 $\sigma'_{v,i}$  [kPa] = initial vertical effective stress  
 $\sigma'_v$  [kPa] = (new) vertical effective stress =  $\sigma'_{v,i} + \Delta\sigma'_v$

This equation comprises both primary settlement and creep, taking the degree of consolidation into account.

**Notes**

- Be aware that the formula is confusing. It contains both an e-log and a 10-log.
- Usually  $t_{\infty} = 10\,000$  days (= 30 years) is considered the maximum settlement time.
- On completion of a structure, the usual requirement is that the total surplus settlement  $< 0,30$  m, i.e.:  $H(\varepsilon_{t_{\infty}} - \varepsilon_{t_{opl}}) \leq 0,30$  m.
- If both sand layers and clay or peat layers are present, the compression of the sand layers is usually negligible.
- Take spreading of the load in the soil into account. A spread of the stress under an angle of 45 degrees is customary (for slabs both in lengthways and widthways directions: For a square slab with length = D,  $\Delta\sigma'$  is reduced to  $1/9^{\text{th}}$  at a depth D (see Section 24.1).
- The parameters  $C'_p$  and  $C'_s$  follow from oedometer tests on samples obtained by (tube sample) borings. For a preliminary design the values in the table in section 31.6 "Determination of soil parameters with the Eurocode table" suffice.

One should really also take the limit stress  $\sigma'_{limit}$  into account. That is the maximum inter-granular stress ever reached in a soil layer. If the initial granular stress is less than the limit stress ( $\sigma'_i < \sigma'_{limit}$ ), the soil will react a lot stiffer (approximately a factor 3 to 5). It is better to divide the settlement calculation into a stiff part before the stress reaches its limit and a weak part thereafter:

$$\varepsilon = \left( \frac{U}{C'_p} + \frac{1}{C'_s} \log(t) \right) \ln \left( \frac{\sigma'_{limit}}{\sigma'_{v,i}} \right) + \left( \frac{U}{C'_p} + \frac{1}{C'_s} \log(t) \right) \ln \left( \frac{\sigma'_v}{\sigma'_{limit}} \right)$$

**34.3 Soil relaxation**

Excavations (e.g. for a construction site) relieve the soil situated at a greater depth. This causes relaxation (= swell) of the soil. In turn this causes the bed to rise in time.

To determine the total relaxation  $\Delta h_{total}$  the following formula is used:

$$\frac{\Delta h_{total}}{h} = \frac{C_{sw}}{(1 + e_0)} \cdot \log \left( \frac{\sigma'_i + \Delta\sigma}{\sigma'_i} \right)$$

in which:

- $h$  [m] = initial thickness of the relaxing layer  
 $C_{sw}$  [-] = swell or relaxation coefficient (*zwellcoëfficiënt*, or *zwellingsmodulus*)  
 (see Table 31-4)  
 $e_0$  [-] = initial void ratio (*poriëngetal*)  
 $\sigma'_i$  [N/m<sup>2</sup>] = initial effective stress  
 $\Delta\sigma$  [N/m<sup>2</sup>] = reduction of the effective stress due to the excavation

The void ratio is defined with:

$$e = \frac{V_{pores}}{V_{grains}}$$

in which:

- $V_{pores}$  [m<sup>3</sup>] = volume of the pores, which is the volume of water if the soil is completely saturated  
 $V_{grains}$  [m<sup>3</sup>] = volume of the solid material (sediment grains)

If the relaxation is (partially) restricted, for instance by the presence of a submerged concrete floor with tensile piles, this leads to an increase of the effective stress below the floor. For relaxation a secondary effect (creep) is not taken into account in calculations, so the extent of the effective stress against the floor depends on the consolidation of the swelling layer and on the extent of the change of the effective stress due to the excavation.

If the stiffness of the soil is linear when it is relieved of its load, one can pose:

$$\sigma'_{relaxation} = (1-U) \cdot \Delta\sigma'_{excavate}$$

The calculation of the degree of consolidation  $U$ , the moment the floor is constructed is carried out according to Section 34.1 "Consolidation". For this one can assume that:

$$c_{v,relaxation} \approx 4 \cdot c_v,$$

because the stiffness ( $1/m_v$ ) is far greater when being relieved of pressure, which has consequences for  $c_v$  according to:

$$c_v = \frac{k_v}{\gamma_w m_v}$$

### 34.4 Literature

Barron, R.A.: *Consolidation of fine grained soils by drain wells*. Transactions of American Society for Civil Engineers, Vol. 113, No. 2346, pp. 718-724. 1948

Smedt, F. De: *Grondmechanica*. Vrije Universiteit Brussel. 2013.

Verruijt, A. and S. van Baars: *Grondmechanica*. VSSD, Delft, 2005.

## 35. Concrete

major revision: February 2011

Concrete is a commonly used and very suitable construction material, particularly for non-moving parts of hydraulic structures. The design of concrete structures is a profession in itself. It should be realised that the theory of concrete for hydraulic engineering purposes has other emphases than the theory for the more common utility construction branch, because of the following reasons:

1. In utility construction one can often schematize structural element as bending beams. In structural hydraulic engineering the concrete structures are often not slender and often have complex 3-D shapes.
2. In hydraulic structures the concrete parts below the water surface are under pressure. A pre-tensile stress is present on all sides. This does not exist in utility construction.
3. The reinforcement steel in hydraulic structures in sea water must be well protected from corrosion. This is why often pre-stressed reinforcement is used to reduce the crack width to zero.

### 35.1 Properties of concrete

For design calculations European standards should be used: for concrete NEN-EN 1992-1-1:2005 (Eurocode 2: Design of concrete structures). For the theory about this subject, the course of CT2051 and CT3051 is recommended. The prescribed characteristics for concrete classes currently available in the Netherlands are presented in Table 35-1 (EN 206-1 table 7 and EN 1992-1-1 table 3.1).

Concrete class (old)	Concrete class	$f_{ck,cil}$ (MPa)	$f_{ck}$ (MPa)	$f_{cm}$ (MPa)	$f_{ctm}$ (MPa)	$f_{ctk, 0.05}$ (MPa)	$f_{ctk, 0.95}$ (MPa)	$E_{cm}$ (GPa)
B15	C12/15	12	15	20	1.6	1.1	2.0	27
B25	C20/25	20	25	28	2.2	1.5	2.9	30
B35	C30/37	30	35	38	2.9	2.0	3.8	33
B45	C35/45	35	45	43	3.2	2.2	4.2	34
B55	C45/55	45	55	53	3.8	2.7	4.9	36
B65	C55/67	55	67	63	4.2	3.0	5.5	38

Table 35-1 Characteristics of concrete classes

$f_{ck,cil}$	[MPa]	= characteristic compressive cylinder strength of concrete at 28 days
$f_{ck}$	[MPa]	= characteristic compressive cube strength
$f_{cm}$	[MPa]	= mean value of concrete cylinder compressive strength after 28 days ( $f_{cm} = f_{ck} + 8$ )
$f_{ctm}$	[MPa]	= mean value of axial tensile strength of concrete: $f_{ctm} = 0,30 \cdot f_{ck}^{(2/3)}$ for qualities $\leq$ C50/60; $f_{ctm} = 2,12 \cdot \ln(1 + (f_{ck}/10))$ for qualities $>$ C50/60
$f_{ctk, 0.05}$	[MPa]	= characteristic axial tensile strength of concrete ( $f_{ctk, 0.05} = 0,7 f_{ctm}$ 5% fractile)
$f_{ctk, 0.95}$	[MPa]	= characteristic axial tensile strength of concrete ( $f_{ctk, 0.95} = 1,3 f_{ctm}$ 95% fractile)
$E_{cm}$	[GPa]	= secant modulus of elasticity of concrete ( $E_{cm} = 22 [(f_{cm})/10]^{0,3}$ ) ( $f_{cm}$ in MPa)

The design value for concrete compressive strength can be computed as follows:

$$f_{cd} = \frac{\alpha_{cc} \cdot f_{ck}}{\gamma_C}$$

The design value for concrete tensile strength can be computed as follows:

$$f_{ctd} = \frac{\alpha_{ct} \cdot f_{ctk,0.05}}{\gamma_c}$$

Where:

$f_{cd}$	[MPa]	= design value of concrete compressive strength
$f_{ctd}$	[MPa]	= design value of concrete tensile strength
$\alpha_{cc}$	[-]	= coefficient taking account of long term effects on the compressive strength and of unfavourable effects resulting from the way the load is applied ( $\alpha_{cc} = 1,0$ )
$\alpha_{tc}$	[-]	= coefficient taking account of long term effects on the compressive strength and of unfavourable effects resulting from the way the load is applied ( $\alpha_{tc} = 1,0$ )
$f_{ck}$	[MPa]	= characteristic compressive cylinder strength of concrete at 28 days
$f_{ctk,0.05}$	[MPa]	= characteristic axial tensile strength of concrete (5% fractile)
$\gamma_c$	[-]	= partial safety factor for concrete

An overview of the partial safety factors for materials for ultimate limit states for concrete ( $\gamma_c$ ) and steel ( $\gamma_s$ ) is given in Table 35-2.

Design situations	$\gamma_c$ for concrete	$\gamma_s$ for reinforcement steel	$\gamma_s$ for prestressing steel
Persistent & Transient loads	1,5	1,15	1,1
Accidental loads	1,2	1,0	1,0

Table 35-2 Partial safety factors for material

## 35.2 Properties of reinforcement steel

For reinforcement steel TGB 1990 gives material properties for some steel classes:

Steel type		$f_{yk}$ [N/mm <sup>2</sup> ]	$f_{yd}$ [N/mm <sup>2</sup> ]	$\epsilon_{uk}$ [N/mm <sup>2</sup> ]
Bars	FeB 220 HWL	220	190	5,00
	FeB 400 HWL, HK	400	350	4,00
	FeB 500 HWL, HK	500	435	3,25
	FeB 500 HKN	500	435	2,75
Wire fabrics (wapeningsnetten)	FeB 500 HKN, HWN	500	435	2,75

Table 35-3 Characteristics of reinforcement steel classes according to the old TGB 1990 standard

Where:

$f_{yk}$	[N/mm <sup>2</sup> ]	= characteristic yield strength of reinforcement
$f_{yd}$	[N/mm <sup>2</sup> ]	= design yield strength of reinforcement
$\epsilon_{uk}$	[-]	= characteristic strain ( <i>rek</i> ) of reinforcement or prestressing steel at maximum load

The TGB 1990 standard has been replaced by a NEN standard that shows some differences regarding the characteristic values of reinforcement steel classes. The NEN standard (NEN 6008) applies only in a limited part of Europe. The most frequently used reinforcement steel class is B500B.

Reinforcement steel classes	$\varnothing$ [mm]	$R_e$ [MPa]	$R_m/R_e$ [-]	$A_{gt}$ [%]
B500A	4-16	500	1,05 (1,03 for $\varnothing \leq 5.5\text{mm}$ )	3,0 (2,0 for $\varnothing \leq 5.5\text{mm}$ )
B500B	6-50	500	1,08	5,0
B500C	6-50	500	1,15 (1,13 for $\varnothing \leq 12\text{mm}$ )	7,5 (7,0 for $\varnothing \leq 12\text{mm}$ )

Table 35-4 Characteristics of reinforcement steel classes according to the NEN 6008 standard

Where:

$\varnothing$	[mm]	=	nominal diameter
$R_e$	[MPa]	=	characteristic yield strength of reinforcement ( $f_{yk}$ )
$R_m$	[MPa]	=	characteristic tensile strength of reinforcement ( $f_{tk}$ )
$R_m/R_e$	[-]	=	minimum ratio tensile strength/yield strength ( $f_{tk}/f_{yk}$ )
$A_{gt}$	[-]	=	minimum percentage total elongation at maximum force
A	[-]	=	indicates a smooth, dented or ribbed profile
B	[-]	=	indicates a dented or ribbed profile
C	[-]	=	indicates a ribbed profile

Commonly used reinforcement bar diameters in Hydraulic Engineering are  $\varnothing$  12,16,20,25 and 32.

The Young's modulus of reinforcement steel ( $E_s$ ) is  $2,0 \cdot 10^5 \text{ N/mm}^2$

### 35.3 Properties of prestressed steel

In principle the function of prestressing is to prevent the occurrence of cracks in the concrete structure by creating compressive stresses in a structural member where one normally would expect tensile stresses. The elimination of tensile stresses does not only result in the prevention of cracks in the concrete, but also in a more economical use of materials (slender structures). In Figure 35-1 the principle of prestressing is visualized for a simply supported beam (*vrijopgelegde balk*) on two supports. The load on the beam results in compressive stresses above the centroid (*neutrale lijn*) and tensile stresses below the centroid as indicated in the left stress diagram. As the result of prestressing a normal force is exerted, resulting in an evenly distributed compressive stress over the whole cross-section of the beam (middle stress diagram). This compressive stress eliminates the tensile stress at the underside of the beam and reinforces the compressive stress at the topside, resulting in compressive stresses over the whole cross-section (right stress diagram).

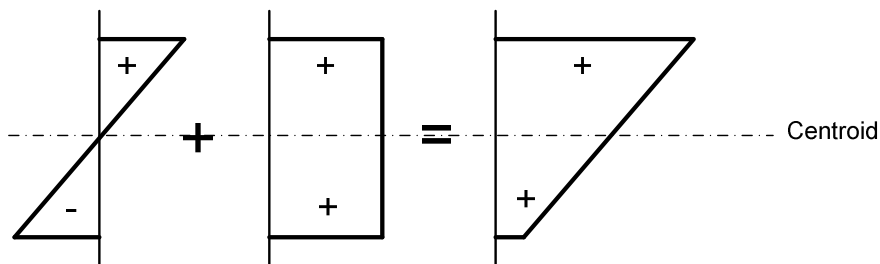


Figure 35-1 the principle of prestressing.

The following methods for prestressing concrete are used:

1) Pre-tensioning (*voorspanning met aanhechting, VMA*):

This principle is mainly used in the prefabrication of concrete members. In the factory the tendons (*voorspanwapening*) are pre-stretched before the concrete is poured. After the concrete has hardened enough the tendons are released. The force present in the tendons is absorbed via adhesion (friction) between the steel and the concrete.

2) Post-tensioning (*voorspanning zonder aanhechting, VZA*):

Here the tendons are situated in a protective tube. After pouring the concrete they are slightly tensioned in order to prevent attachment with the cement water. After a certain period, when the

concrete has reached a strength determined by the structural engineer, the tendons are pre-stressed to approximately 20% of their capacity. This is called pre-stressing the dead weight (*eigen gewicht aanspannen*). When the concrete has reached its ultimate strength the tendons are pre-stressed to 100% of their capacity.

There are three types of prestressing steels, namely: wire (*voerspandraad*), strands (*voorspanstreng*) and bars (*voorspanstaven*). The properties of these three types are described in the following standards, NEN-EN 10138-2 (draft) "wire", NEN-EN 10138-3 (draft) "strand" and NEN-EN 10138-4 (draft) "bars". Furthermore the NEN- EN 10138-1 (draft) "general requirements" and NEN-EN 1992-1 are applicable. In Table 35-5 the characteristic values for certain diameters of all three types of prestressing steel are presented, for information regarding other available diameters the reader is referred to the standards mentioned above.

Steel type	$d$ [mm]	$S_n$ [mm <sup>2</sup> ]	$f_{pk}$ [N/mm <sup>2</sup> ]	$f_{p0.1k}$ [N/mm <sup>2</sup> ]	$\epsilon_{uk}$ [-]
<b>Wire</b>					
Y1860C	4,0	12,57	1860	1599	0,035
Y1770C	6,0	28,27	1770	1521	0,035
Y1670C	8,0	38,48	1670	1437	0,035
Y1570C	10,0	78,54	1570	1299	0,035
<b>Strand</b>					
Y1860S3 class A	6,5	23,40	1860	1598	0,035
Y1770S7 class A	16,0	150,00	1770	1587	0,035
Y1960S3 class B	6,5	21,10	1960	1687	0,035
Y1960S7 class B	9,0	50,00	1960	1680	0,035
<b>Bar</b>					
Y1030H	26,0	531	1030	834	0,035
Y1030H	40,0	1257	1030	835	0,035
Y1230H	26,0	531	1230	1079	0,035
Y1230H	40,0	1257	1230	1080	0,035

Table 35-5 Characteristic values for prestressing steels.

Where:

- $d$  : nominal diameter
- $S_n$  : nominal cross-sectional area
- $f_{pk}$  : characteristic value for the tensile strength of prestressing steel
- $f_{p0.1pk}$  : characteristic 0.1% yield boundary for prestressing steel
- $\epsilon_{uk}$  : characteristic strain (*rek*) of reinforcement or prestressing steel at maximum load

The design value for the tensile strength is equal to:  $f_{pd} = \frac{f_{p0.1k}}{\gamma_s}$

The design value for the characteristic yield boundary can be computed as follows:  $\epsilon_{ud} = 0,9 \cdot \epsilon_{uk}$ .

The Young's modulus for prestressing steel ( $E_p$ ) is  $2,05 \cdot 10^5$  N/mm<sup>2</sup> for wire and bars and  $1,95 \cdot 10^5$  N/mm<sup>2</sup> for strands.

## 35.4 Concrete cover

The concrete cover on the outer reinforcement bar of a structure serves to protect the reinforcement against external influences such as rain water, soil, corrosive liquids or fumes or the like, which can lead to corrosion of the reinforcement. When the concrete cover is too thin or insufficiently dense there is a risk that the reinforcement starts to oxidize (*roesten*). This will lead to reduction of the bar diameter and hence the force that the reinforcement can absorb decreases. Since rust has a larger volume than the original steel there is a probability that the concrete cover is pushed off the reinforcement. This will lead to further corrosion and a further decrease of the absorbable force. It is obvious that the reinforcement in an

aggressive environment requires a thicker concrete cover than in a dry environment. Hence the thickness of the concrete cover depends on the environment in which the concrete structure is located. The environment characteristics are expressed via an exposure classification, see Figure 35-6. The minimum required concrete cover on the outer reinforcement bar for each exposure class is presented in Figure 35-7.

Exposure classification			
Class	Corrosion induced by	Class	measure of humidity
X0	no risk		very dry
XC	carbonation	XC1	dry or persistently wet
		XC2	wet, seldom dry
		XC3	moderate humidity
		XC4	alternating wet and dry
XD	chlorides (excl. seawater)	XD1	moderate humidity
		XD2	wet, seldom dry
		XD3	alternating wet and dry
XS	seawater	XS1	exposed to salt in the air, no direct contact with seawater
		XS2	persistently submerged
		XS3	tidal-, splash- and spray-zone
XF	freeze/thaw attack	XF1	not fully saturated with water, without de-icing salt
		XF2	not fully saturated with water, with de-icing salt
		XF3	fully saturated with water, without de-icing salt
		XF4	fully saturated with water, with de-icing salt
XA	chemical attack	XA1	weakly aggressive chemical environment
		XA2	moderately aggressive chemical environment
		XA3	highly aggressive chemical environment

Notation: XC1 X stands for exposure; the letter indicates process that causes the corrosion and the number indicates the humidity

Table 35-6 Exposure classification of the environment in which the structure is situated.

Exposure classification	Concrete cover (c) [mm]		
	slab, wall	beam, pad footing ( <i>poer</i> ), truss ( <i>spant</i> )	column
X0	-	-	-
XC1	15	25	30
XC2 to XC4 XF1 and XF3	25	30	35
XD1 to XD3 XS1 to XS4 XF2 and XF4 XA1 to XA3	30	35	40

A surcharge of 5 mm to the minimum concrete cover should be applied in case of:

- a finished (*nabewerkt*) surface;
- an uncontrollable surface;
- concrete with a characteristic cube compressive strength (*kubusdruksterkte*)  $f_{ck} < 25 \text{ N/mm}^2$

Note that when the situations above occur simultaneously, the surcharges should be superimposed.

Table 35-7 Minimum concrete cover on the outer reinforcement bar

## 35.5 Reinforced and prestressed concrete

To design reinforced or prestressed concrete structures the following limit states have to be considered:

- 1) Ultimate limit states, leading to failure of the structure;
- 2) Serviceability limit states; leading to restriction of use of the structure.

### ultimate limit state:

- fracture due to bending and / or normal force
- fracture due to shear force
- fracture due to punching
- fracture due to torsion

### serviceability limit state:

- unacceptable deformation
- unacceptable cracking (*scheuren*)

For a more elaborate consideration of the limit states, reference is made to the TGB 1990 (NEN 6720, chapter 8). Bending and shear force are discussed briefly here because they are of importance in a preliminary design.

### Bending and/or normal force

The limit state involving bending and normal force is:

$$M_{Ed} = M_{Rd} \quad \text{en} \quad N_{Ed} = N_{Rd}$$

in which:  $M_{Ed}$  [Nm] = design value of the maximum occurring bending moment  
 $M_{Rd}$  [Nm] = maximum allowable bending moment  
 $N_{Ed}$  [Nm] = design value of the normal force  
 $N_{Rd}$  [Nm] = maximum allowable normal force

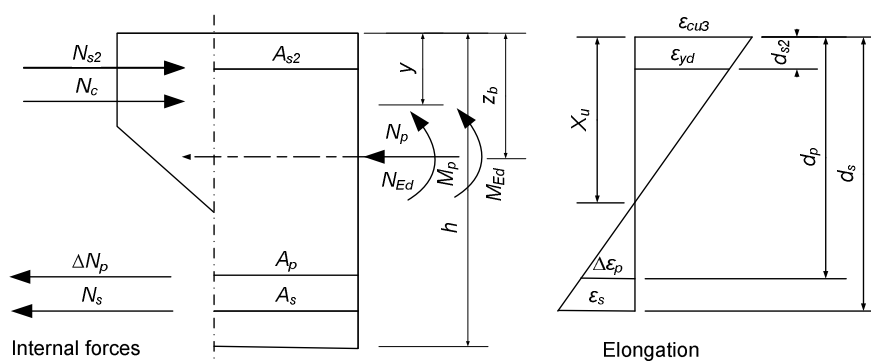


Figure 35-2 Forces and strains in concrete

The maximum allowable moment and normal force are:

$$M_{Rd} = (N_p + N_{Ed})(z_b - y) + \sum N_s(d_s - y) + \sum \Delta N_p(d_p - y)$$

$$N_{Rd} = N_c + N_{s2} - N_p - \Delta N_p - N_s$$

Where:  $N_p$  [N] = design value for the effective normal compression force as a result of the pre-stressing force  
 $M_p$  [Nm] = design value for the effective moment force as a result of the pre-stressing force  
 $N_{Ed}$  [N] = design value of the normal force (excluding pre-stressing force); if the normal force is a tensile force replace  $+N_{Ed}$  with  $-N_{Ed}$   
 $N_c$  [N] = design value of the compression resultant =  $0,75 \cdot x_u \cdot f_{cd}$

$f_{cd}$	[N/m <sup>2</sup> ]	= design value of concrete compressive strength
$N_s$	[N]	= tensile force in the reinforcement steel
$N_{s,2}$	[N]	= compressive force in the reinforcement steel
$\Delta N_p$	[N]	= increase of the force in the pre-stressing reinforcement relative to the initial pre-stressing force ( $\Delta N_p = A_p \cdot \Delta \sigma_{pu}$ )
$A_p$	[m <sup>2</sup> ]	= cross-sectional area of the pre-stressed element
$\Delta \sigma_{pu}$	[N/m <sup>2</sup> ]	= increase of the stress in the pre-stressing reinforcement relative to the initial pre-stressing stress
$y$	[m]	= distance between the compression stress resultant and the edge with the highest compression = $7/18 x_u$ (for $\leq C50/60$ )
$x_u$	[m]	= height of the concrete compression zone
$d_s$	[m]	= the distance between the tensile reinforcement and the edge with highest compression
$d_{s2}$	[m]	= the distance between the reinforcement in the compression zone and the edge with most compression
$d_p$	[m]	= the distance between the pre-stressing steel and the edge with most compression
$z_b$	[m]	= the distance between the elastic line of gravity and the edge with most compression
$h$	[m]	= total height of the structure
$\epsilon_{cu3}$	[m]	= ultimate compressive strain in the concrete

When determining  $x_u$  one must take into account that:  $\epsilon_{cu3} = 0,0035$ .

Furthermore, there are requirements for the maximum value of  $x_u$  if the normal force is small ( $N_{Ed} < 0,1 \cdot f_{cd} \cdot A_c$ ) due to the rotation capacity, for this the reader is referred to TGB 1990 (NEN 6720 art 8.1.3).

To calculate the required reinforcement, the requirement should be satisfied that the reinforcement steel must yield before the concrete will fail and the minimum of the reinforcement percentage must be large enough to be sure there will be no brittle failure when cracking of the concrete occurs (*brosse breuk*). If the structure is mainly loaded by a moment force, the required reinforcement steel can easily be calculated with help of Table 35-8. Note that Table 35-8, Table 35-9, Table 35-10 and the flowchart below only apply to reinforced concrete and not for pre-stressed concrete. The flowchart is used to compute the reinforcement percentage needed in a structural member when the bending moment for the ultimate limit state is known.

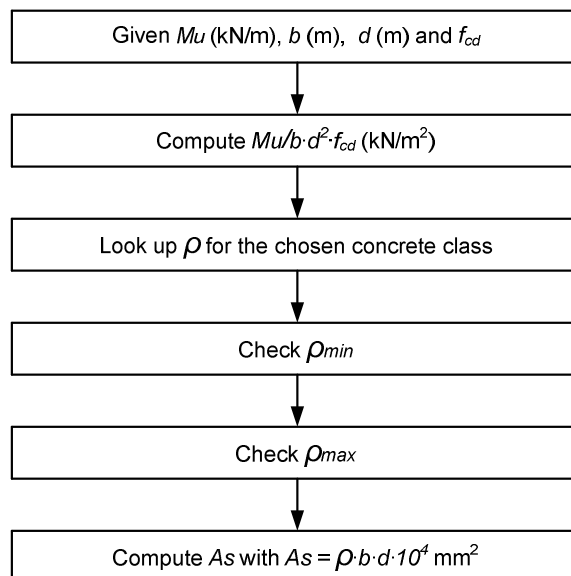


Figure 35-3 Flowchart for the preliminary design of reinforcement using the GTB-tables.

$\frac{M_d}{bd^2 f_{cd}}$	$\psi$	$k_x$	$k_z$	$\rho$ [%]				
				C20/25	C28/35	C35/45	C45/55	C53/65
10	0,010	0,013	0,99	0,03	0,05	0,06	0,08	0,09
20	0,020	0,027	0,99	0,07	0,10	0,13	0,15	0,18
30	0,030	0,240	0,98	0,10	0,15	0,19	0,23	0,27
40	0,041	0,055	0,98	0,14	0,20	0,25	0,31	0,37
50	0,051	0,068	0,97	0,18	0,25	0,32	0,39	0,46
60	0,062	0,083	0,97	0,21	0,30	0,39	0,47	0,56
70	0,073	0,097	0,96	0,25	0,35	0,45	0,55	0,66
80	0,084	0,112	0,96	0,29	0,41	0,52	0,64	0,75
90	0,095	0,127	0,95	0,33	0,46	0,59	0,72	0,85
100	0,106	0,141	0,94	0,37	0,51	0,66	0,81	0,95
110	0,117	0,156	0,94	0,40	0,56	0,73	0,89	1,05
120	0,129	0,172	0,93	0,44	0,62	0,80	0,98	1,16
130	0,140	0,187	0,93	0,48	0,68	0,87	1,06	1,26
140	0,152	0,203	0,92	0,52	0,73	0,94	1,15	1,36
150	0,164	0,219	0,91	0,57	0,79	1,02	1,24	1,47
160	0,176	0,235	0,91	0,61	0,85	1,09	1,34	1,58
170	0,188	0,251	0,90	0,65	0,91	1,17	1,43	1,69
180	0,201	0,268	0,90	0,69	0,97	1,25	1,53	1,80
190	0,214	0,285	0,89	0,74	1,03	1,33	1,62	1,92
200	0,227	0,303	0,88	0,78	1,10	1,41	1,72	2,04
210	0,240	0,320	0,88	0,83	1,16	1,49	1,82	2,16
220	0,253	0,337	0,87	0,87	1,22	1,57	1,92	2,27
230	0,267	0,356	0,86	0,92	1,29	1,66	2,03	2,39
240	0,281	0,375	0,85	0,97	1,35	1,75	2,13	2,52
250	0,295	0,393	0,85	1,02	1,43	1,83	2,24	2,64
260	0,310	0,413	0,84	1,07	1,50	1,93	2,35	2,78
270	0,325	0,433	0,83	1,12	1,57	2,02	2,47	2,91
280	0,340	0,453	0,82	1,17	1,64	2,11	2,58	3,05
290	0,356	0,475	0,81	1,23	1,72	2,21	2,70	3,19
300	0,372	0,496	0,81	1,28	1,80	2,31	2,82	3,34
310	0,388	0,517	0,80	1,34	1,87	2,41	2,94	3,48
320	0,405	0,540	0,79	1,40	1,96	2,51	3,07	3,63

Table 35-8 Reinforcement percentages for rectangular cross-sections, reinforced with B500B, loaded by bending without normal force, With  $M_u$  in kNm;  $b$  and  $d$  in m<sup>1</sup> and  $f_{cb}$  in N/mm<sup>2</sup>

Where:

$M_u$  [kNm] = ultimate absorbable bending moment (*breukmoment*)

$k$  [-] = ratio between the strength of concrete and steel  $\left( k = \frac{f_{yd}}{f_{cd}} \right)$

$f_{yd}$  [N/mm<sup>2</sup>] = design yield strength of reinforcement  $\left( f_{yd} = \frac{f_{yk}}{\gamma_s} \right)$

$f_{cd}$  [N/mm<sup>2</sup>] = design value of concrete compressive strength  $\left( f_{cd} = \frac{f_{ck}}{\gamma_c} \right)$

$\rho$  [%] = reinforcement percentage

$b$  [mm] = cross-sectional width

$\psi$  [%] = mechanical reinforcement percentage:  $\psi = k \cdot \rho$

$$k_x = \frac{x_u}{d} \quad k_z = \frac{z_u}{d}$$

$x_u$  = height of the of the compressive zone (*hoogte drukzone*):  $x_u = d \cdot \frac{\rho \cdot k}{0,75}$

$z_u$  = arm of internal leverage (*inwendige hefboomsarm*):

$$z_u = d \cdot (1 - 0,52 \cdot \rho \cdot k) = d - \beta \cdot x_u, \text{ where } \beta = 0,75 \cdot 0,52 = 0,39$$

$d$  [mm] = effective height of the cross-section (*nuttige hoogte*):

$$d = h - (c + \frac{1}{2} \varnothing)$$

$h$  [mm] = height of the cross-section

$c$  [mm] = concrete cover

$\varnothing$  [mm] = bar diameter (*kenmiddellijn*)

$A_s$  [mm<sup>2</sup>] = total cross-sectional area of the reinforcement

	C20/25	C28/35	C35/45	C45/55
$\rho_{min}$	0,15	0,18	0,21	0,24

Table 35-9 Minimum reinforcement percentage ( $\rho_{min}$ ) for B500B.

	C20/25	C28/35	C35/45	C45/55
$\rho_{max}$	1,38	1,94	2,49	3,05

Table 35-10 Maximum reinforcement percentage ( $\rho_{max}$ ) for B500B.

To check an already existing concrete structural member, the maximum allowable bending moment can be computed using the following equation (see the book *Constructie leer Gewapend Beton of course CTB2220*):

$$M_u = A_s \cdot f_{yd} \cdot d \cdot (1 - 0,52 \cdot \rho \cdot k) \quad \text{and} \quad M_{ed} \leq M_u$$

Where:

$M_{ed}$  [Nm] = design value for the bending moment in the ultimate limit state

$M_u$  [Nm] = ultimate absorbable bending moment

$A_s$  [m<sup>2</sup>] = total cross-sectional area of reinforcement

$k$  [-] = ratio between the strength of concrete and steel  $\left( k = \frac{f_{yd}}{f_{cd}} \right)$

$f_{yd}$  [N/m<sup>2</sup>] = design yield strength of reinforcement

$f_{cd}$  [N/m<sup>2</sup>] = design value of concrete compressive strength

$\rho$  [-] = reinforcement ratio  $\left( = \frac{A_s}{b \cdot d} \right)$

$b$  [m] = width of the concrete structure

Automatically the equation can also be used to calculate the necessary reinforcement, when the load is known.

### Example calculation maximum bending moment

**Given:**

A concrete beam with size of  $b \times h = 300 \times 600$  mm<sup>2</sup>, is reinforced by stirrups of  $\varnothing 8$  mm and longitudinal reinforcement of  $4 \varnothing 16$  ( $4 \cdot 201 = 804$  mm<sup>2</sup>). The concrete class is C20/25 and the reinforcement steel class is B500B. The beam is situated in a marine environment and has a finished, uncontrollable surface.

**Question:** Calculate the maximum allowable bending moment.

**Answer:**

$$b = 300 \text{ mm}, h = 600 \text{ mm}, c = 35 + 5 + 5 = 45 \text{ mm}$$

$$d = h - (c + \varnothing_{\text{stirrups}} + 1/2 \varnothing_{\text{longitudinal reinforcement}}) = 600 - 45 - 8 - 8 = 539 \text{ mm}$$

$$\text{The design value of the concrete compressive strength of C20/25 is: } f_{cd} = \frac{f_{ck}}{\gamma_c} = \frac{25}{1.5} = 16\frac{2}{3} \text{ N/mm}^2$$

$$\text{The design yield strength of the reinforcement B500B is: } f_{yd} = \frac{f_{yk}}{\gamma_s} = \frac{500}{1.15} = 435 \text{ N/mm}^2$$

From Figure 35-2 it can be deduced that  $N_s = N_c$

$$N_s = A_s \cdot f_{yd} = 4 \cdot 201 \cdot 435 = 349\,740 \text{ N}$$

$$N_c = \frac{3}{4} \cdot x_u \cdot f_{cd} \cdot b = \frac{3}{4} \cdot x_u \cdot 16,67 \cdot 300 = 3751 \cdot x_u$$

$$349\,740 = 3751 \cdot x_u$$

$$x_u = 93 \text{ mm}$$

The centre of mass of the concrete compression zone lays a distance  $\beta \cdot x_u$  from the upper side of the concrete beam.

$$z = d - \beta \cdot x_u = 539 - 0,39 \cdot 93 = 502,7 \text{ mm}$$

$$M_{Rd} = A_s \cdot f_{yd} \cdot z = 804 \cdot 435 \cdot 502,7 = 175,8 \cdot 10^6 \text{ Nmm} = 175,8 \text{ kNm}$$

### Example determination of the required amount of reinforcement steel in the cross-sectional area of a beam.

**Given:** a reinforced concrete beam with size of  $b \times h = 300 \times 600 \text{ mm}^2$ . The concrete quality is C20/25, the steel quality is B500B.  $M_{Ed} = 320 \text{ kNm}$ . The beam is situated in a marine environment and has a finished, uncontrollable surface.

**Question:** Calculate the amount of reinforcement needed in the concrete beam.

**Answer:**

Concrete strength class C20/25, so  $f_{cd} = 16,67 \text{ N/mm}^2$ ; steel quality B500B, so Table 35-8 is applicable.

Since  $M_{Ed}$  must be smaller than or equal too  $M_u$ , the most economical way of reinforcing is found by taking  $M_{Ed} = M_u$ .

$$c = 35 + 5 + 5 = 45 \text{ mm}$$

$$d = h - (c + \varnothing_{\text{stirrups}} + 1/2 \varnothing_{\text{longitudinal reinforcement}}) = 600 - 45 - 8 - 8 = 539 \text{ mm}$$

$$\frac{M_u}{b \cdot d^2 \cdot f_{cd}} = \frac{320}{0,30 \cdot 0,539^2 \cdot 16,67} = 220 \Rightarrow \text{read in Table 35-8 that for C20/25 } \rho = 0,78\%$$

Table 35-9: minimum reinforcement percentage is 0,15%  $\Rightarrow$  OK

Table 35-10: maximum reinforcement percentage is 1,38%  $\Rightarrow$  OK

$$A_s = \rho \cdot b \cdot d \cdot 10^4 = 0,78 \cdot 0,30 \cdot 0,539 \cdot 10^4 = 1262 \text{ mm}^2$$

**Question:** Calculate height of the of the compressive zone  $x_u$ .

Using Table 35-8:

$$\text{Read value in column } k_x = \frac{x_u}{d} \text{ for } \rho = 0,78\% \Rightarrow 0,303, \text{ so } x_u = k_x \cdot d = 0,303 \cdot 539 = 163 \text{ mm}$$

$$\text{Using } x_u = d \cdot \frac{\rho \cdot k}{0,75} : \text{Read value in column } \psi (= k \cdot \rho) \text{ for } \rho = 0,78\% \Rightarrow k \cdot \rho = 22,7\%$$

$$x_u = d \cdot \frac{\rho \cdot k}{0,75} = 539 \cdot \frac{0,227}{0,75} = 163 \text{ mm}$$

**Question:** Calculate the arm of internal leverage  $z_u$ .

Using Table 35-8:

Read value in column  $k_z = \frac{z_u}{d}$  for  $\rho = 0,78\% \Rightarrow 0,88$ , so  $z_u = k_z \cdot d = 0,88 \cdot 539 = 474 \text{ mm}$

Using  $z_u = d \cdot (1 - 0,52 \cdot \rho \cdot k)$ :

Read value in column  $\psi$  for  $\rho = 0,78\% \Rightarrow \psi = 22,7\%$

$$z_u = d \cdot (1 - 0,52 \cdot \rho \cdot k) = 539 \cdot (1 - 0,52 \cdot 0,227) = 475 \text{ mm}$$

### Example check of a reinforced concrete beam with help of Table 35-8

Given: a reinforced concrete beam,  $b \times h = 300 \times 600 \text{ mm}^2$ ,  $d = 539 \text{ mm}$ .  $M_{Ed}$  is increased from 250 to 255 kNm. The concrete quality is C20/25 and the steel quality of the reinforcement is B500B. The reinforcement percentage is 0,75%

Question: Calculate if the existing beam is able to bear the increased load.

Answer:

Using Table 35-8:

The design value of the concrete compressive strength of C20/25 is:  $f_{cd} = \frac{f_{ck}}{\gamma_c} = \frac{25}{1,5} = 16\frac{2}{3} \text{ N/mm}^2$

The design yield strength of the reinforcement B500B is:  $f_{yd} = \frac{f_{yk}}{\gamma_s} = \frac{500}{1,15} = 435 \text{ N/mm}^2$

$$k = \frac{f_{yd}}{f_{cd}} = \frac{435}{16,67} = 26, \text{ so } \psi = 0,75 \cdot 26 = 19,58\%$$

read in Table 35-8 that for  $\psi = 19,58\%$ ,  $\frac{M_u}{b \cdot d^2 \cdot f_{cd}} \approx 180$

$$M_u = 175 \cdot b \cdot d^2 \cdot f_{cd} = 180 \cdot 0,30 \cdot 0,539^2 \cdot 16,67 = 261,5 \text{ kNm}$$

$$M_{ed} \leq M_u \Rightarrow 255 \leq 261,5, \text{ so OK}$$

Using  $M_u = A_s \cdot f_{yd} \cdot d \cdot (1 - 0,52 \cdot \rho \cdot k)$ :

$$\rho = \frac{A_s}{b \cdot d} \Rightarrow A_s = \frac{\rho \cdot b \cdot d}{100} = \frac{0,75 \cdot 300 \cdot 539}{100} = 1213 \text{ mm}^2$$

$$M_u = A_s \cdot f_{yd} \cdot d \cdot (1 - 0,52 \cdot \rho \cdot k) = 1213 \cdot 435 \cdot 539 \cdot (1 - 0,52 \cdot 0,195) = 255,6 \cdot 10^6 \text{ Nmm} = 255,6 \text{ kNm}$$

$$M_{ed} \leq M_u \Rightarrow 255 \text{ kNm} \leq 255,6 \text{ kNm}, \text{ so OK}$$

As expected both methods lead to the same result.

## Shear force

The design value for the shear resistance  $V_{Rd,c}$  **without** shear reinforcement is given by

$$V_{Rd,c} = \left[ C_{RD,c} \cdot k \cdot (100 \cdot \rho_1 \cdot f_{ck})^{1/3} + k_1 \cdot \sigma_{cp} \right] \cdot b_w \cdot d \quad [\text{N}]$$

With a minimum of

$$V_{Rd,c} = (v_{\min} + k_1 \cdot \sigma_{cp}) \cdot b_w \cdot d \quad [\text{N}],$$

where  $f_{ck}$  [N/mm<sup>2</sup>] = characteristic compressive cylinder strength of concrete at 28 days in MPa

$$k \quad [-] = 1 + \sqrt{\frac{200}{d}} \leq 2,0 \text{ with } d \text{ in mm}$$

$$\rho_1 \quad [-] = \text{reinforcement ratio for longitudinal reinforcement} = \frac{A_{sl}}{b_w \cdot d} \leq 0,02;$$

$A_{sl}$  [mm<sup>2</sup>] = the area of the tensile reinforcement, which extends more than  $(l_{bd} + d)$  beyond the section considered

$b_w$  [mm<sup>2</sup>] = the smallest width of the cross-section in the tensile area

$\sigma_{cp}$  [N/mm<sup>2</sup>] = compressive stress in the concrete from axial load or prestressing:

$$\sigma_{cp} = N_{Ed} / A_C < 0,2 \cdot f_{cd}$$

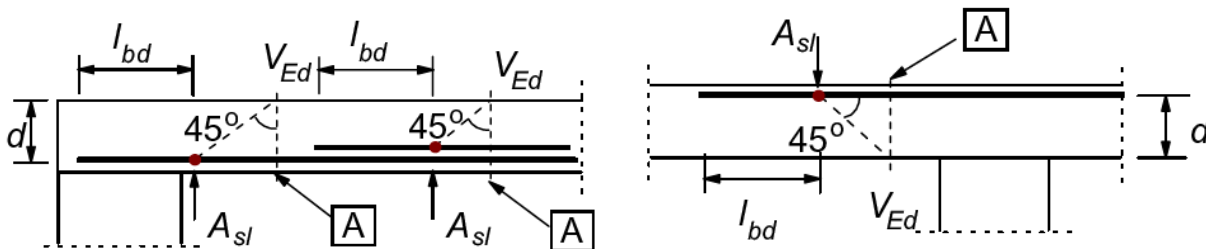
$N_{Ed}$  [N] = the axial force in the cross-section due to loading or prestressing ( $N_{Ed} > 0$  for compression)

$A_C$  [mm<sup>2</sup>] = the area of the concrete cross-section [mm<sup>2</sup>]

$k_1$  [-] = a coefficient, in the Netherlands: 0,15

$C_{RD,c}$  [-] = a coefficient, in the Netherlands:  $0,18 / \gamma_c = 0,18 / 1,5 = 0,12$

$$v_{\min} \quad [] = 0,035 \cdot k^{3/2} \cdot f_{ck}^{1/2}$$



**A** - section considered

Figure 35-4 Reinforced concrete structural member without shear reinforcement.

The design of members **with** shear reinforcement is based on a truss model (*vakwerkmodel*).

In Figure 35-5 the following notations are shown:

$\alpha$ : angle between shear reinforcement and the beam axis perpendicular to the shear force (measured positive as shown in the figure)

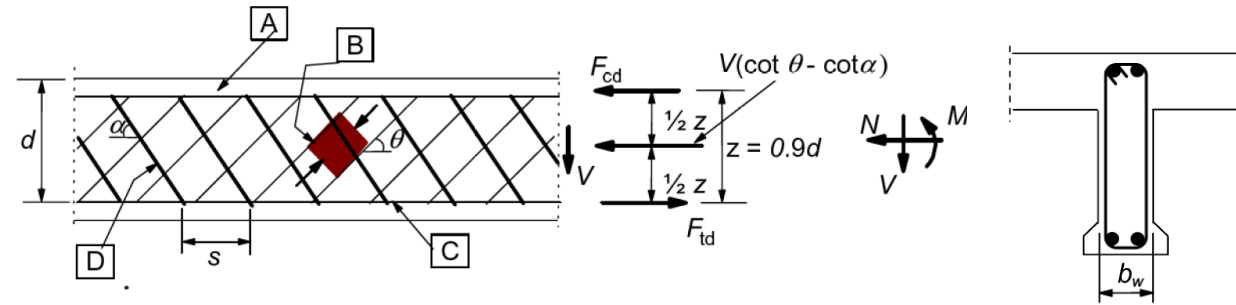
$\theta$ : angle between the concrete compression strut and the beam axis perpendicular to the shear force

$F_{td}$ : design value of the tensile force in the longitudinal reinforcement

$F_{cd}$ : design value of the concrete compression force in the direction of the longitudinal member axis.

$b_w$ : the smallest width of the cross-section in the tensile area

$z$ : arm of internal leverage, for a member with constant depth, corresponding to the bending moment in the element under consideration. In the shear analysis of reinforced concrete without axial force, the approximate value  $z = 0,9 \cdot d$  may normally be used.



[A] - compression chord, [B] - struts, [C] - tensile chord, [D] - shear reinforcement

Figure 35-5 Inclined shear reinforcement

The angle  $\theta$  should be limited. The recommended upper and lower limits are:  $21,8^\circ \leq \theta \leq 45^\circ$ .

### **Vertical shear reinforcement**

For members with vertical shear reinforcement, the shear resistance,  $V_{Rd}$  is the smaller value of :

$$V_{Rd,s} = \frac{A_{sw}}{s} \cdot z \cdot f_{ywd} \cdot \cot \theta \quad (\text{stirrups governing})$$

Where:

$A_{sw}$  = the cross-sectional area of the shear reinforcement (two times because the reinforcement crossed two times the cross-sectional area of the concrete).

$s$  = the spacing of the stirrups

$f_{ywd}$  = the design yield strength of the shear reinforcement

And

$$V_{Rd,max} = \frac{\alpha_{cw} b_w z \cdot v_1 \cdot f_{cd}}{\cot \theta + \tan \theta} \quad (\text{concrete compressive struts governing})$$

Where:

$v_1$  = strength reduction factor for concrete cracked in shear. Recommended is that  $v_1 = v$

$$\text{and } v = 0,6 \left( 1 - \frac{f_{ck}}{250} \right)$$

$\alpha_{cw}$  = coefficient taking account of the state of the stress in the compression chord. The recommended value of  $\alpha_{cw}$  is as follows:

- 1 for non pre-stressed structures
- $(1 + \sigma_{cp} / f_{cd})$  for  $0 < \sigma_{cp} \leq 0,25 \cdot f_{cd}$
- 1,25 for  $0,25 \cdot f_{cd} < \sigma_{cp} \leq 0,5 \cdot f_{cd}$
- $2,5 \cdot (1 - \sigma_{cp} / f_{cd})$  for  $0,5 \cdot f_{cd} < \sigma_{cp} \leq 1,0 \cdot f_{cd}$

$\sigma_{cp}$  = the mean compressive stress, measured positive, in the concrete due to the design axial force. This should be obtained by averaging it over the concrete section taking account of the reinforcement. The value of  $\sigma_{cp}$  need not be calculated at a distance less than  $0,5 \cdot d \cdot \cot \theta$  from the edge of the support.

The maximum effective cross-sectional area of the shear reinforcement,  $A_{sw,max}$  for  $\cot \theta = 1$  is given by:

$$\frac{A_{sw,max} \cdot f_{ywd}}{b_w \cdot s} \leq \frac{1}{2} \cdot \alpha_{cw} \cdot v_1 \cdot f_{cd}$$

**Inclined shear reinforcement**

For members with inclined shear reinforcement (*schuine dwarskrachtwapening*), the shear resistance is the smaller value of:

$$V_{Rd,s} = \frac{A_{sw}}{s} \cdot z \cdot f_{ywd} \cdot (\cot \theta + \cot \alpha) \cdot \sin \alpha \quad (\text{stirrups governing})$$

and

$$V_{Rd,max} = \frac{\alpha_{cw} \cdot b_w \cdot z \cdot v_1 \cdot f_{cd} \cdot (\cot \theta + \cot \alpha)}{1 + \cot^2 \theta} \quad (\text{concrete compressive struts governing})$$

The maximum effective shear reinforcement,  $A_{sw,max}$  for  $\cot \theta = 1$  follows from:

$$\frac{A_{sw,max} \cdot f_{ywd}}{b_w \cdot s} \leq \frac{\frac{1}{2} \cdot \alpha_{cw} \cdot v_1 \cdot f_{cd}}{\sin \alpha}$$

**Example calculation of required shear reinforcement**

**Given:** A pier with a deck of concrete slabs, supported by crossbeams,  $b \times h = 450 \times 800 \text{ mm}^2$ , which in turn are supported by two longitudinal beams,  $b \times h = 450 \times 800 \text{ mm}^2$ . The longitudinal beams are reinforced with a main reinforcement consisting of bars  $\varnothing 32 \text{ mm}$  and stirrups of  $\varnothing 12 \text{ mm}$ . The concrete class is C28/C35. The steel is B500B. The concrete cover is 40 mm.

The design value of the concentrate loads ( $F_d$ ) is 800 kN. The dead weight of the longitudinal beams is neglected in this example. The reinforcement ratio for longitudinal reinforcement ( $\rho_1$ ) is 0,01. Inclined stirrups are used in the longitudinal beam.

**Question:** Calculate the required shear reinforcement of the longitudinal beam.

**Answer:**

Determine the force distribution (see Figure 35-6).

$$R_{Ad} = R_{Bd} = 1200 \text{ kN}$$

$$V_{Ad} = V_{Bd} = V_{Ed} = 800 \text{ kN}$$

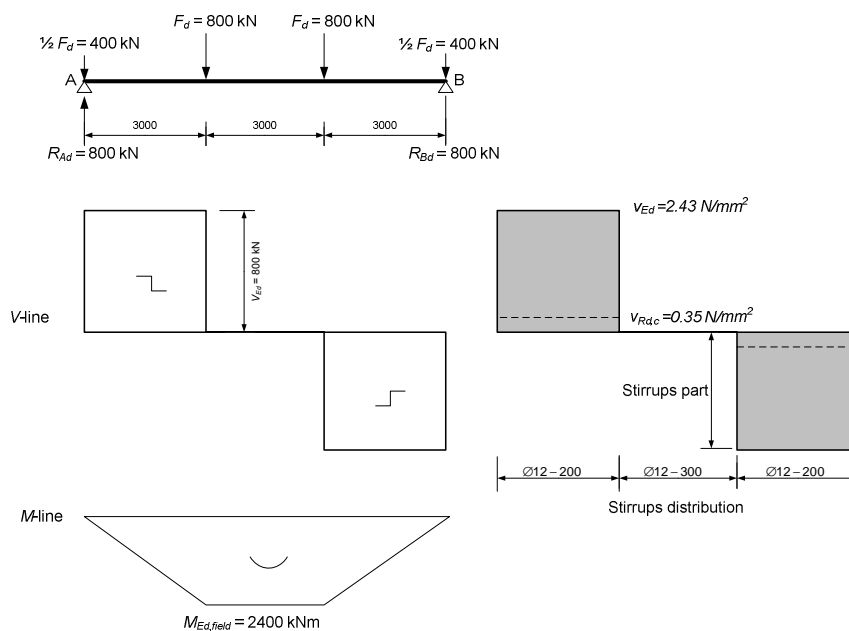


Figure 35-6 V-line and M-line longitudinal beam.

Determine the shear stress  $V_{Rd,c}$

$$d = h - c - \varnothing_{st} - \frac{1}{2}\varnothing_r = 800 - 40 - 12 - \frac{1}{2} \cdot 32 = 732 \text{ mm}$$

$$V_{Rd,c} = \left[ C_{Rd,c} \cdot k \cdot (100 \cdot \rho_1 \cdot f_{ck})^{1/3} \right] \cdot b_w \cdot d = \left[ 0,12 \cdot \left( 1 + \sqrt{\frac{200}{732}} \right) \cdot (100 \cdot 0,1 \cdot 20)^{1/3} \right] \cdot 450 \cdot 732 = 352 \cdot 10^3 \text{ [N]}$$

(which should be more than the minimum of

$$V_{Rd,c} = v_{\min} \cdot b_w \cdot d = 0,035 \cdot k^{3/2} \cdot f_{ck}^{1/2} \cdot d \cdot b = 0,035 \cdot 1,523^{3/2} \cdot 20^{1/2} \cdot 732 \cdot 450 = 96\,879 \text{ N})$$

( $V_{Rd,c} = 352 \cdot 10^3$ ) < ( $V_{Ad} = 800 \cdot 10^3$ ), so shear reinforcement is needed!

The distance between the stirrups then is:

$$V_{Rd,s} = \frac{A_{sw}}{s} \cdot z \cdot f_{ywd} (\cot \theta + \cot \alpha) \sin \alpha$$

$$\theta = 21,8 \quad \alpha = 90^\circ \quad z = 0,9d = 659 \text{ mm}$$

$$A_{sw} = 2 \cdot \frac{1}{4} \cdot \pi \cdot 12^2 = 226,20$$

$$\frac{A_{sw}}{s} = \frac{V_{Rd,s}}{z \cdot f_{ywd} (\cot \theta + \cot \alpha) \sin \alpha} = \frac{800\,000}{659 \cdot 435(2,5 + 0)1} = 1,12 \text{ mm}^2/\text{mm}$$

$$s = \frac{A_{sw}}{1,12} = 202 \text{ mm}$$

So the maximum distance between the stirrups is 200 mm over the first 3 m from the supports and 300 mm in the middle 3m of the longitudinal beam

### Note

*In the walls of many hydraulic structures, there are large areas in which the shear force has reached its maximum while the bending moment is zero. In this case pure tension is found in the concrete wall, which needs special attention.*

## 35.6 Stiffness of the concrete structure

For statically indeterminate structures, the stiffness (EI) of the elements used in the calculations has considerable influence, not only on the resulting deformation and displacements, but on the flow of forces through the structure (global force effect) and the resulting internal forces in each individual member (local force effect) as well. Figure 35-7 illustrates this effect for a U-shaped cross section on a pile foundation. The correct stiffness has to be used in hand or computer calculations to find the governing (internal) load distributions M, N and V.

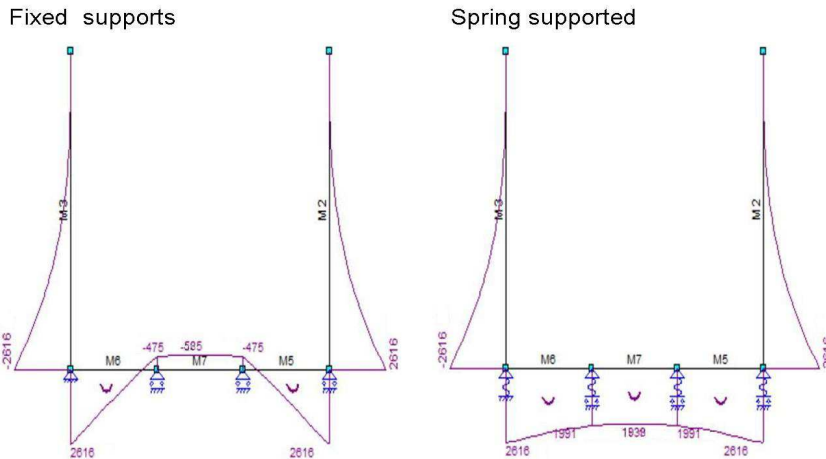


Figure 35-7 Influence of foundation stiffness on force distribution in the structure

Unfortunately the stiffness of a reinforced concrete section or element changes depending on crack development. There is a significant difference in bending stiffness between the non-cracked and the cracked concrete cross-section. After occurrence of the first cracks, further loading will go hand in hand with a decreasing stiffness of the concrete. This is easily demonstrated by a *M-k* diagram, here *k* is curvature (*kromming*), see Figure 35-8.

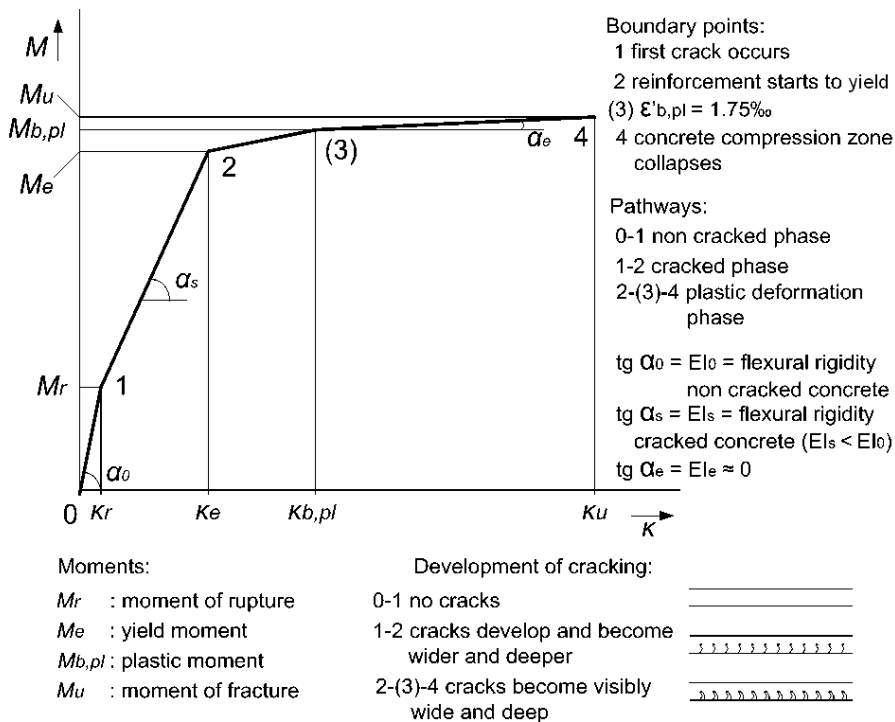


Figure 35-8 *M-k*-diagram

The bending stiffness of a concrete section, having to resist a certain *M*, is equal to the tangent of the line in the *M-k*-diagram:

$$EI_x = \tan \alpha_x = \frac{M_x}{\kappa_x} \quad \text{and} \quad \kappa_x = \frac{M_x}{EI_x}$$

So, for a certain bending moment the intersection with the line in the *M-k*-diagram has to be determined first to find the value of the curvature on the *x*-axis. Finally the tangent of the line connecting the origin with the intersection point can be found, using the equation above and hence the bending stiffness corresponding to that moment.

To construct a  $M$ - $\kappa$ -diagram, all the  $M$ - $\kappa$  combinations have to be computed. The curvature  $\kappa$  can be determined as follows:

$$\kappa = \frac{\varepsilon'_b + \varepsilon_s}{d}$$

To find the correct stiffness of the whole structure the  $M$ - $\kappa$ -diagram has to be constructed for every different concrete section, for each type of concrete and reinforcement percentage ( $\rho$ ). This is a lot of work, often too much work for the level of precision required. In the following subsections first an approximation of concrete stiffness will be presented, then development of the  $M$ - $\kappa$ -diagram will be further explained for detailed calculations.

### **First design calculations with concrete EI gestimate**

For uncracked cross-sections the bending stiffness of concrete  $EI_0$  can be gestimated/computed as follows:

$$EI_0 = E'_b \cdot I$$

Where:

$$E'_b = 22250 + 250 \cdot f_{ck} \quad \text{for } 15 \leq f_{ck} \leq 65 \text{ (NEN6720)}$$

$$E'_b = 35900 + 40 \cdot f_{ck} \quad \text{for } 65 \leq f_{ck} \leq 105 \text{ (CUR 97)}$$

$$I = \frac{1}{12} \cdot b \cdot h^3 \quad \text{for rectangular cross-sections}$$

For cracked cross-sections the bending stiffness  $EI_g$  can be computed as follows:

$$EI_g = 0,5 \cdot E_s \cdot A_s \cdot h^2$$

Where:

$E_s$  [N/m<sup>2</sup>] = Youngs' modulus of steel

$A_s$  [m<sup>2</sup>] = area of the reinforcement steel present in the cross-sectional area of the beam

$f_{ck}$  [N/m<sup>2</sup>] = characteristic compressive strength

$b$  [m] = width of the cross-section

$h$  [m] = height of the cross-section

(source: 'construeren in gewapend beton' - part 2, Kamerling 1978)

### **More detailed calculation of concrete stiffness with M-K diagram**

In this subsection the critical points of pure bending, i.e. bending moment  $M$  without normal force  $N$ , will be explained using stress-strain diagrams (*spanning-rek diagrammen*) in the end leading to the  $M$ - $\kappa$ -diagram, see Figure 35-8.

#### Non-cracked beam (ongescheurde balk)

At the instant that the concrete tensile strength  $f_{ctd}$  is reached, the deformation diagram and stress diagram look like depicted in Figure 35-9. The bending moment equals the moment of rupture  $M_r$  (*scheurmoment*) and the concrete is just not cracked. In this stage the concrete's compressive strength is still very small because the mean value of the axial tensile strength of concrete  $f_{ctm}$  is much smaller than the design value of the concrete compressive strength  $f_{cb}$ , so that  $\varepsilon'_b \ll 1,75\text{‰}$ .

#### Cracked beam

When the load only increases a little the tensile zone in the concrete will crack and the tensile forces will be concentrated in the existing reinforcement. The centroid (*neutrale lijn*) displaces in upward direction. The load can be increased further until the reinforcement reaches its yield stress  $f_{yd}$ . The corresponding deformation and stress diagrams are depicted in Figure 35-10. The concrete is cracked so it does not have a tensile strength any longer. The deformation of the concrete at the compression side of the beam ( $\varepsilon'_b$ ) is still smaller than 1,75‰. The corresponding bending moment is the yield moment (*vloeimoment*). At this point the deformation of the steel changes from elastic to plastic.

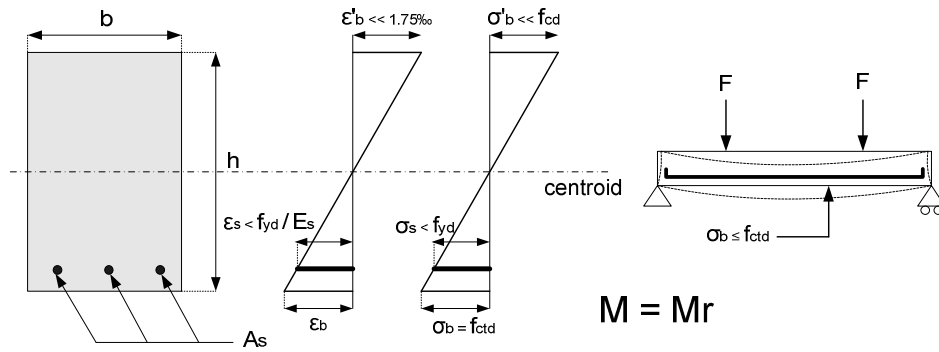


Figure 35-9 Deformation and stress diagram for a non-cracked beam

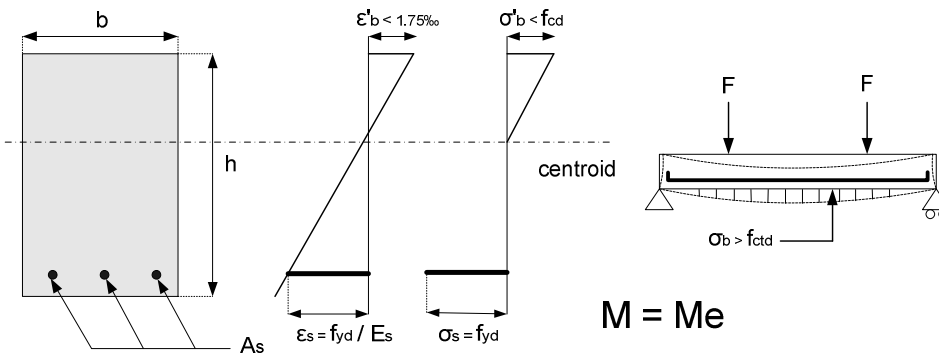


Figure 35-10 Deformation and stress diagram for a cracked beam

**Compression strain in concrete (*betonstuik*)**

When the load on the beam is increased further, at a certain moment the deformation of the concrete at the compression side of the beam will reach the value of 1,75‰ in the extreme pressure fibre (*uiterste drukvezel*). At the moment the compression strain of 1,75‰ is reached and the corresponding bending moment is equal to the plastic moment  $M_{b,pl}$ . The corresponding deformation and stress diagrams are depicted in Figure 35-11.

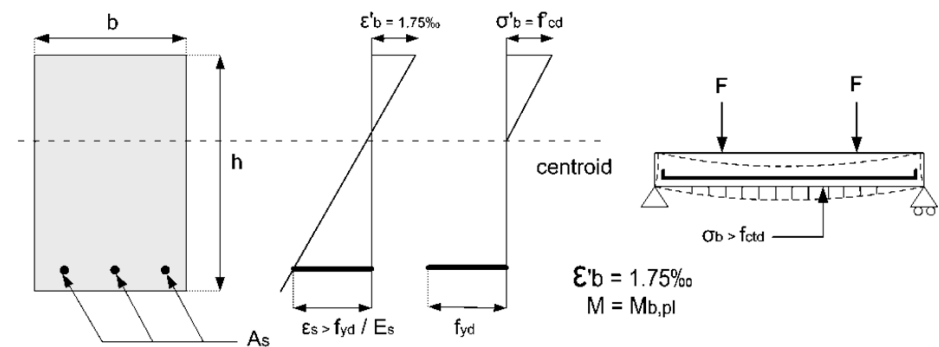


Figure 35-11 Deformation and stress diagram when the compression strain in the concrete has reached a value of 1.75‰.

When the load on the beam increases even further, the compression strain in the concrete will reach eventually a value of 3,50‰ in the extreme pressure fibre. If the beam reaches its point of collapse, the corresponding bending moment is the moment of fracture  $M_u$  (*breukmoment*). The corresponding deformation and stress diagrams are shown in Figure 35-12.

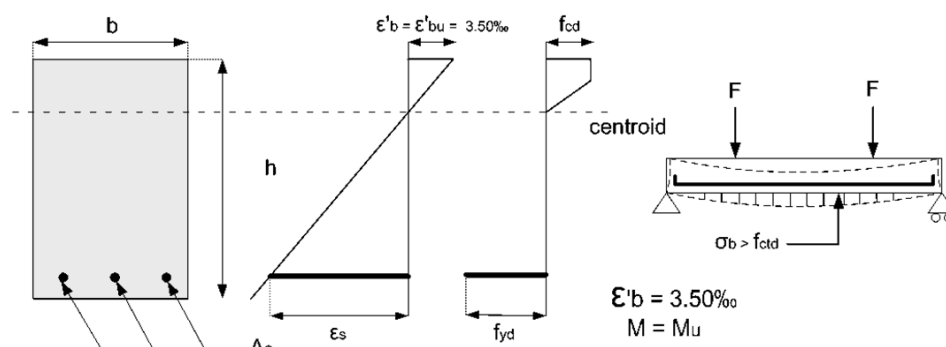


Figure 35-12 Deformation and stress diagram when the compression strain in the concrete has reached a value of 3.50‰.

### 35.7 Literature

Nederlands Normalisatie instituut, Eurocode 2: "Design of concrete structures – Part 1: Specification, performance, production and conformity" (NEN-EN 206-1), november 2005, Nederlands Normalisatie instituut.

Nederlands Normalisatie instituut, Dutch supplement to NEN-EN 206-1: "Concrete - Part 1: Specification, performance, production and conformity" (NEN 8005), februari 2008, Nederlands Normalisatie instituut.

Nederlands Normalisatie instituut, Eurocode 2: "Design of concrete structures – Part 1-1: "General rules and rules for buildings" (NEN-EN 1992-1-1), april 2005, Nederlands Normalisatie instituut.

Nederlands Normalisatie instituut, National Annex to NEN-EN 1992-1-1 Eurocode 2: "Design of concrete structures – Part 1-1: "General rules and rules for buildings" (NEN-EN 1992-1-1/NB), november 2007, Nederlands Normalisatie instituut.

Nederlands Normalisatie instituut, NEN 6008: "Steel for the reinforcement of concrete", juli 2008, Nederlands Normalisatie instituut.

Nederlands Normalisatie instituut, NEN-EN 10080: "Steel for the reinforcement of concrete – Weldable Reinforcing steel - General", juni 2005, Nederlands Normalisatie instituut

Nederlands Normalisatie instituut, NEN-EN 10138-1 Draft: "Prestressing steels – Part 1: General requirements", september 2000, Nederlands Normalisatie instituut.

Nederlands Normalisatie instituut, NEN-EN 10138-2 (Draft): "Prestressing steels – Part 2: Wire", september 2000, Nederlands Normalisatie instituut.

Nederlands Normalisatie instituut, NEN-EN 10138-3 (Draft): "Prestressing steels – Part 3: Strand", september 2000, Nederlands Normalisatie instituut.

Nederlands Normalisatie instituut, NEN-EN 10138-4 (Draft): "Prestressing steels – Part 4: Bars", september 2000, Nederlands Normalisatie instituut.

Ing. R. Sagel and ing. A.J. van Dongen, Constructie leer: Gewapend beton, december 2004, ENCI media, 's Hertogenbosch.

## 36. Steel

major revision: February 2011

Steel is a frequently used material for particularly moveable parts of hydraulic structures and for temporary structures. A well-known example of a temporary structure is the building pit, where the sheet pile wall, the struts and the wales consist of steel elements. Steel structural elements for building pits are dealt with in Chapters 39 to 41 in part IV of this manual. The present chapter deals with the characteristics of steel and the most important calculation checks for beams, according to European standard EN 1993-1-1. More detailed information can be found in the books "(over)spannend staal", and the lecture notes of CTB2220 ("Beton- en staalconstructies"). Reinforcement steel to be used in concrete structures is dealt with in Chapter 35 of this Manual. For an example calculation of struts and wales in a cofferdam, see part IV, Chapter 40.

### 36.1 General

#### **Characteristics of steel**

The most common types of construction steel are S235 and S355. For the most important properties, see Table 36-1.

material property ↓ / steel quality →	S235	S275	S355
yield stress $f_y$ at 20 °C [N/mm <sup>2</sup> ]	235	275	355
tensile strength $f_u$ [N/mm <sup>2</sup> ]	360	430	510
Young's modulus	$E = 210\,000 \text{ N/mm}^2$		
Shear modulus ( <i>glijdingsmodulus</i> )	$G = \frac{E}{2(1+\nu)} \approx 81\,000 \text{ N/mm}^2$		
Poisson's ratio in elastic stage	$\nu = 0,3$		
Coefficient of linear thermal expansion	$\alpha = 12 \cdot 10^{-6} \text{ per } ^\circ\text{C} \text{ (for } T \leq 100 \text{ } ^\circ\text{C)}$		

Table 36-1 Steel characteristics for S235, S275 and S355

In this chapter, the partial material factors  $\gamma_M$  should be applied to the various characteristic values of resistance as follows:

- Resistance of cross-sections for all classes:  $\gamma_{M0} = 1,0$
- Resistance of members to instability assessed by member checks:  $\gamma_{M1} = 1,0$
- Resistance of cross-sections in tension to fracture:  $\gamma_{M2} = 1,25$
- Resistance of various joints, see EN 1993-1-8

#### **Ultimate limit state (ULS)**

The following aspects should be checked in the ultimate limit state (ULS):

- Exceedance of the yield stress caused by tension, compression, bending, shear and torsion
- Global buckling (of bars, beams or columns) (*knik*)
- Lateral buckling (of beams, columns) (*kip*)
- Local (plate) buckling (*plooï*)
- Fatigue

#### **Serviceability limit state (SLS)**

For the serviceability limit state the following should explicitly be checked:

- Deformation / deflection (also plays a significant role for second order effects in ULS)

**First or second order analysis?**

The internal forces and moments may generally be determined using either:

- First-order analysis, using the initial geometry of the structure or
- Second-order analysis, which also takes into account the influences of the deformation of the structure.

First order analysis may be used for the structure if the increase of the relevant internal forces or moments or any other change of the structural behaviour caused by deformations can be neglected. This condition may be assumed to be fulfilled, if the following criterion is satisfied:

$$\alpha_{cr} = \frac{F_{cr}}{F_{Ed}} \geq 10 \quad \text{for elastic analysis}$$

$$\alpha_{cr} = \frac{F_{cr}}{F_{Ed}} \geq 15 \quad \text{for plastic analysis}$$

Where:

$\alpha_{cr}$  [-] = amplification factor to further increase the design load that will result in elastic instability in a global mode

$F_{Ed}$  [kN] = design force acting on the structure

$F_{cr}$  [kN] = elastic buckling force for global instability mode based on initial elastic stiffnesses

For single storey frames on the basis of elastic global analysis, second order sway effects due to vertical loads may be calculated by increasing the horizontal loads  $H_{Ed}$  (e.g. wind) and equivalent loads  $V_{Ed}$  due to imperfections and other possible sway effects according to first order theory by a factor:

$$\frac{1}{1 - \frac{1}{\alpha_{cr}}}$$

**Classification of cross-sections**

Calculation methods for structural elements need to be appropriate with respect to the deformation characteristics of the profile (mostly dependent on the width/thickness-ratio). The plastic theory, for instance, should only be used if the profile is able to sufficiently deform in a plastic way. For the sake of convenience, standards (like the old NEN 6770 - *TGB staaI*) make use of classifications to indicate what calculation methods have to be used. This classification is useful to determine the extent to which the resistance and rotation capacity of cross-sections is limited by its local buckling resistance.

Four classes of cross-sections are defined, as follows (see also Table 36-2):

- Class 1: plastic cross-sections which can form a plastic hinge with the rotation capacity of plastic analysis without reduction of the resistance. Plastic theory may be used for the calculation of cross-sections and determination of the load distribution.
- Class 2: compact cross-sections (*gedrongen doorsneden*) which can develop their plastic moment resistance, but have limited rotation capacity because of local buckling. Plastic theory may only be used for the calculation of cross-sections.
- Class 3: semi-compact cross-sections in which the stress in the extreme compression fibre of the steel member assuming an elastic distribution of stresses can reach the yield strength, but local buckling is liable to prevent development of the plastic moment resistance. Elastic theory should be used for both cross-section calculations and load distribution determination. No buckling calculation is required.
- Class 4: slender cross-sections where local buckling will occur before yield stress occurs in one or more parts of the cross-section. Elastic theory should be used for both cross-section calculations and load distribution determination. Buckling calculation is required.

type of plate	type of load	class 1 (plastic)	class 2 (semi-plastic)	class 3 (elastic)
flange rolled I-profile 	pressure	$b/t_f \leq 10$ all HE-profiles	$b/t_f \leq 11$	$b/t_f \leq 15$
web rolled I-profile 	bending pressure	$h_w/t_w \leq 72$ $h_w/t_w \leq 33$	$h_w/t_w \leq 83$ $h_w/t_w \leq 38$	$h_w/t_w \leq 124$ $h_w/t_w \leq 42$
walls rolled square tube 	pressure	$b/t \leq 33$	$b/t \leq 38$	$b/t \leq 42$
wall cylindrical tube 	pressure or bending	$d/t \leq 50$	$d/t \leq 70$	$d/t \leq 90$

Table 36-2 Cross-section classes for steel profiles (S235) (from: (over)spannend staal Construeren A).

## 36.2 Strength

Possible internal forces in a cross-section are:

- tension
- compression
- bending moment
- shear
- torsion
- combination of bending moment and shear
- combination of bending moment and axial force

### Tension

The design value of the tension force  $N_{Ed}$  at each cross-section shall be smaller than the design tension

resistance (*maximaal toelaatbare trekkracht*)  $N_{t,Rd}$ :  $\frac{N_{Ed}}{N_{t,Rd}} \leq 1,0$

For sections with holes the design tension resistance  $N_{t,Rd}$  shall be the smallest value of:

a) the design plastic resistance of the gross cross-section  $N_{pl,Rd} = \frac{A \cdot f_y}{\gamma_{M0}}$

b) the design ultimate resistance of the net cross-section at holes for fasteners  $N_{u,Rd} = \frac{0,9 \cdot A_{net} \cdot f_u}{\gamma_{M2}}$

### Compression

The design value of the compression force  $N_{Ed}$  at each cross-section shall satisfy:  $\frac{N_{Ed}}{N_{c,Rd}} \leq 1,0$

The design compression resistance (*maximaal toelaatbare drukkracht*) of the cross-section for uniform compression  $N_{c,Rd}$  shall be determined as follows:

$$N_{c,Rd} = \frac{A \cdot f_y}{\gamma_{M0}} \quad \text{for class 1, 2 or 3 cross-sections}$$

$$N_{c,Rd} = \frac{A_{eff} \cdot f_y}{\gamma_{M0}} \quad \text{for class 4 cross-sections}$$

### **Bending moment**

The design value of the bending moment  $M_{Ed}$  at each cross-section should satisfy:  $\frac{M_{Ed}}{M_{c,Rd}} \leq 1,0$

The design resistance for bending around one principal axis of a cross-section is determined as follows:

$$M_{c,Rd} = M_{pl,Rd} = \frac{W_{pl} \cdot f_y}{\gamma_{M0}} \quad \text{for class 1 or 2 cross sections}$$

$$M_{c,Rd} = M_{el,Rd} = \frac{W_{el,min} \cdot f_y}{\gamma_{M0}} \quad \text{for class 3 cross sections}$$

$$M_{c,Rd} = \frac{W_{eff,min} \cdot f_y}{\gamma_{M0}} \quad \text{for class 4 cross sections}$$

Where  $W_{el,min}$  and  $W_{eff,min}$  correspond to the fibre with the maximum elastic stress.

### **Shear**

The design value of the shear force  $V_{Ed}$  at each cross-section should satisfy  $\frac{V_{Ed}}{V_{c,Rd}} \leq 1,0$

Where  $V_{c,Rd}$  is the design shear resistance (*maximaal opneembare dwarskracht*).

For plastic design  $V_{c,Rd}$  is the design plastic shear resistance  $V_{pl,Rd}$ . In absence of torsion the design plastic shear resistance is given by:

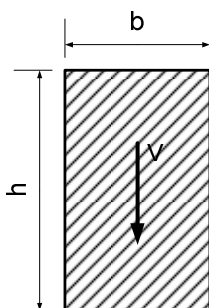
$$V_{pl,Rd} = \frac{A_v (f_y / \sqrt{3})}{\gamma_{M0}} \quad \text{Where } A_v \text{ is the shear area [mm}^2\text{].}$$

For verification of the design elastic shear resistance  $V_{c,Rd}$  the following criterion for a critical point of the cross-section may be used unless the buckling verification in section 5 of EN 1993-1-5 is applicable:

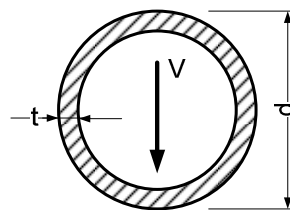
$$\frac{\tau_{Ed}}{f_y / (\sqrt{3} \gamma_{M0})} \leq 1,0 \quad \text{Where } \tau_{Ed} \text{ may be obtained from: } \tau_{Ed} = \frac{V_{Ed} \cdot S}{I \cdot t}$$

Where:

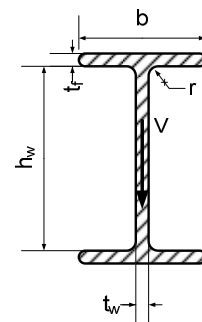
- $V_{Ed}$  [N] = design value of the shear force  
 $S$  [mm<sup>3</sup>] = first moment of area (*statisch moment*) with respect to the centroidal axis of the portion of the cross-section between the point where shear has to be considered and the boundary of the cross-section.  
 $I$  [mm<sup>4</sup>] = second moment of area (*traagheidsmoment*) of the entire cross-section.  
 $t$  [mm] = thickness at the considered point



$$\tau_{Ed} = \frac{V_{Ed}}{b \cdot h}$$



$$\tau_{Ed} = \frac{V_{Ed}}{\frac{1}{2} \cdot \pi \cdot d \cdot t - \frac{1}{4} \cdot \pi \cdot t^2}$$



$$\tau_{Ed} = \frac{V_{Ed}}{t_w \cdot h_w}$$

### **Torsion**

For members subject to torsion for which distortional deformations may be disregarded, the design value of the torsional moment  $T_{Ed}$  at each cross-section should satisfy:  $\frac{T_{Ed}}{T_{Rd}} \leq 1,0$

Where  $T_{Rd}$  is the design torsional resistance (*torsiemomentweerstand*) of the cross-section.

The total torsional moment  $T_{Ed}$  at any cross-section should be considered as the sum of two internal effects:  $T_{Ed} = T_{t,Ed} + T_{w,Ed}$

Where  $T_{t,Ed}$  is the internal St. Venant torsion (*inwendige St. Venantse wringing*)

$T_{w,Ed}$  is the internal warping torsion (*inwendige wringing met verhinderde welving*)

The following stresses due to torsion should be taken into account:

- the shear stresses  $\tau_{t,Ed}$  due to St. Venant torsion  $T_{t,Ed}$
- the direct stresses  $\sigma_{w,Ed}$  due to the bi-moment  $B_{Ed}$  and shear stresses  $\tau_{w,Ed}$  due to warping torsion  $T_{w,Ed}$ .

The above method is prescribed in standard EN-1993, which is meant for use in mechanical engineering. For this course CT3330, it will go too far for detailing this. For checks on torsion, the calculation method mentioned in TGB1990 (Technische Grondslagen voor Bouwconstructies 1990) may be used in the Netherlands (the way of calculation differs per country).

### **Combination of bending and shear**

Where shear force is present, its effect on the moment resistance (*maximaal opneembare moment*) should be taken into account, except if the shear force is less than half the plastic shear resistance (in which case it may be neglected). Otherwise the reduced moment resistance calculated using a reduced yield strength should be taken as the design resistance of the cross-section:  $(1 - \rho) \cdot f_y$  for the shear area, where:

$$\rho = \left( \frac{2 \cdot V_{Ed}}{V_{pl,Rd}} - 1 \right)^2 \quad \text{and} \quad V_{pl,Rd} = \frac{A_v \cdot (f_y / \sqrt{3})}{\gamma_{M0}}$$

in which  $A_v$  = shear area (slide plane) and  $\gamma_{M0}$  = partial factor for cross-sections for the resistance to instability (in most cases  $\gamma_{M0} = 1,0$ ).

If also torsion is present,  $\rho$  should be obtained from  $\rho = \left( \frac{2 \cdot V_{Ed}}{V_{pl,T,Rd}} - 1 \right)^2$ , but should be taken 0 if

$V_{Ed} \leq 0,5 \cdot V_{pl,T,Rd}$ , where  $V_{pl,T,Rd}$  depends on the profile shape (see NEN-EN 1993-1-1, article 6.2.7).

### **Combination of bending and axial force**

**For class 1 and 2 cross-sections**, the following criterion should be satisfied:  $M_{Ed} \leq M_{N,Rd}$

Where  $M_{N,Rd}$  is the design plastic moment resistance reduced due to the axial force  $N_{Ed}$ .

For a rectangular solid section without fastener holes  $M_{N,Rd}$  should be taken as:

$$M_{N,Rd} = M_{pl,Rd} \left[ 1 - \left( N_{Ed} / N_{pl,Rd} \right)^2 \right]$$

For double symmetrical I- and H-sections or other flanges sections, the effect of the axial force on the plastic moment resistance around the y-y axis does not have to be taken into account if both the following criteria are satisfied:

$$N_{Ed} \leq 0,25 \cdot N_{pl,Rd} \quad \text{and} \quad N_{Ed} \leq \frac{0,5 \cdot h_w \cdot t_w \cdot f_y}{\gamma_{M0}}$$

The effect of the axial force on the plastic moment resistance around the z-z axis may be neglected if

$$N_{Ed} \leq \frac{h_w \cdot t_w \cdot f_y}{\gamma_{M0}}$$

For bi-axial bending the following criterion may be used:

$$\left[ \frac{M_{y,Ed}}{M_{N,y,Rd}} \right]^\alpha + \left[ \frac{M_{z,Ed}}{M_{N,z,Rd}} \right]^\beta \leq 1,0$$

in which  $\alpha$  and  $\beta$  are constants, which may conservatively be assumed to be 1, otherwise as follows:

- I- and H-sections:  $\alpha = 2$  and  $\beta = 5 \cdot n$  but  $\beta \geq 1$
- Circular hollow sections:  $\alpha = 2$  and  $\beta = 2$
- Rectangular hollow sections:  $\alpha = \beta = \frac{1,66}{1 - 1,13 \cdot n^2}$  but  $\alpha$  and  $\beta \leq 6$

Where  $n = N_{Ed} / N_{pl,Rd}$

In absence of shear force, **for Class 3 cross-sections** the maximum longitudinal stress  $\sigma_{x,Ed}$  should satisfy the criterion:  $\sigma_{x,Ed} \leq \frac{f_y}{\gamma_{M0}}$ , where  $\sigma_{x,Ed}$  is the design value of the local longitudinal stress due to moment and axial force taking account of relevant fastener holes (*boutgaten*).

In absence of shear force, **for Class 4 cross-sections** the maximum longitudinal stress  $\sigma_{x,Ed}$  calculated using the effective cross-sections should satisfy the criterion:  $\sigma_{x,Ed} \leq \frac{f_y}{\gamma_{M0}}$ , where  $\sigma_{x,Ed}$  is the design value of the local longitudinal stress due to moment and axial force taking account of fastener holes, which are relevant here. The following criterion should be met:

$$\frac{N_{Ed}}{A_{eff} \cdot f_y / \gamma_{M0}} + \frac{M_{y,Ed} + N_{Ed} \cdot e_{Ny}}{W_{eff,y,min} \cdot f_y / \gamma_{M0}} + \frac{M_{z,Ed} + N_{Ed} \cdot e_{Nz}}{W_{eff,z,min} \cdot f_y / \gamma_{M0}} \leq 1,0$$

Where:

- $A_{eff}$  [mm<sup>2</sup>] = effective area of the cross-section when subjected to uniform compression
- $W_{eff,min}$  [mm<sup>3</sup>] = effective section modulus (corresponding to the fibre with the maximum elastic stress) of the cross-section when subjected only to moment about the relevant axis
- $e_N$  [mm] = shift of the relevant centroidal axis when the cross-section is subjected to compression only

### **Combination of bending, shear and axial force**

Provided that the design value of the shear force  $V_{Ed}$  does not exceed 50% of the design plastic shear resistance  $V_{pl,Rd}$ , no reduction of the resistance defined for bending and axial force need be made, except where shear buckling reduces the section resistance, see EN 1993-1-5.

Where  $V_{Ed}$  exceeds 50% of  $V_{pl,Rd}$  the design resistance of the cross-section to combinations of moment and axial force should be calculated using a reduced yield strength:

$$(1 - \rho) \cdot f_y \text{ for the shear area where } \rho = \left( \frac{2 \cdot V_{Ed}}{V_{pl,Rd}} - 1 \right)^2.$$

### 36.3 Stability

Buckling (*knik*) is a failure mechanism that occurs due to a normal force acting on a beam (or other structural element). Lateral buckling (*kip*) occurs if there is a shear force acting in the element. Both are displacements in the direction perpendicular to the load direction. Dependent on the forces, this failure mechanism must be checked.

#### **Buckling resistance**

A structural part under compression should be verified against buckling as follows:  $\frac{N_{Ed}}{N_{b,Rd}} \leq 1,0$

Where:

$$\begin{aligned} N_{Ed} \quad [\text{kN}] &= \text{the design value of the compression force} \\ N_{b,Rd} \quad [\text{kN}] &= \text{the design buckling resistance of the compression member} \end{aligned}$$

For structural members with non-symmetric Class 4 sections the additional moment  $\Delta M_{Ed}$  due to the eccentricity of the centroidal axis of the effective section should be taken into account.

The design buckling resistance of a compression member should be taken as:

$$N_{b,Rd} = \frac{\chi \cdot A \cdot f_y}{\gamma_{M1}} \quad \text{for Class 1, 2 and 3 cross-sections}$$

$$N_{b,Rd} = \frac{\chi \cdot A_{\text{eff}} \cdot f_y}{\gamma_{M1}} \quad \text{for Class 4 cross-sections}$$

Where  $\chi$  is the reduction factor for the relevant buckling mode, to be taken from Figure 36-1.

#### **Buckling curves**

For axial compression in members the value of  $\chi$  for the appropriate non-dimensional slenderness  $\bar{\lambda}$  should be determined using the relevant buckling curve.

$$\bar{\lambda} = \sqrt{\frac{A \cdot f_y}{N_{cr}}} \quad \text{for Class 1, 2 and 3 cross-sections}$$

$$\bar{\lambda} = \sqrt{\frac{A_{\text{eff}} \cdot f_y}{N_{cr}}} \quad \text{for Class 4 cross-sections}$$

$N_{cr}$  is the elastic critical force for the relevant buckling mode based on the gross cross-sectional properties.

The appropriate buckling curve should be obtained from Table 36-3. Values of the reduction factor  $\chi$  for the appropriate non-dimensional slenderness  $\bar{\lambda}$  may be obtained from Figure 36-1.

For slenderness  $\bar{\lambda} \leq 0,2$  or for  $\frac{N_{Ed}}{N_{cr}} \leq 0,04$  the buckling effects may be ignored and only cross-sectional checks apply.

Table 6.2: Selection of buckling curve for a cross-section

Cross section	Limits	Buckling about axis	Buckling curve	
			S 235 S 275 S 355 S 420	S 460
Rolled sections 	$h/b > 1,2$	y-y z-z	$t_f \leq 40$ mm	a a <sub>0</sub>
			$40 < t_f \leq 100$	b a
	$h/b \leq 1,2$	y-y z-z	$t_f \leq 100$ mm	b a
			$t_f > 100$ mm	d c
Welded I-sections 	$t_f \leq 40$ mm	y-y z-z	b c	b c
	$t_f > 40$ mm	y-y z-z	c d	c d
Hollow sections 	hot finished	any	a	a <sub>0</sub>
	cold formed	any	c	c
Welded box sections 	generally (except as below)	any	b	b
	thick welds: $a > 0,5t_f$ $b/t_f < 30$ $h/t_w < 30$	any	c	c
U-, T- and solid sections 		any	c	c
L-sections 		any	b	b

Table 36-3 Buckling curves for various cross-sections.

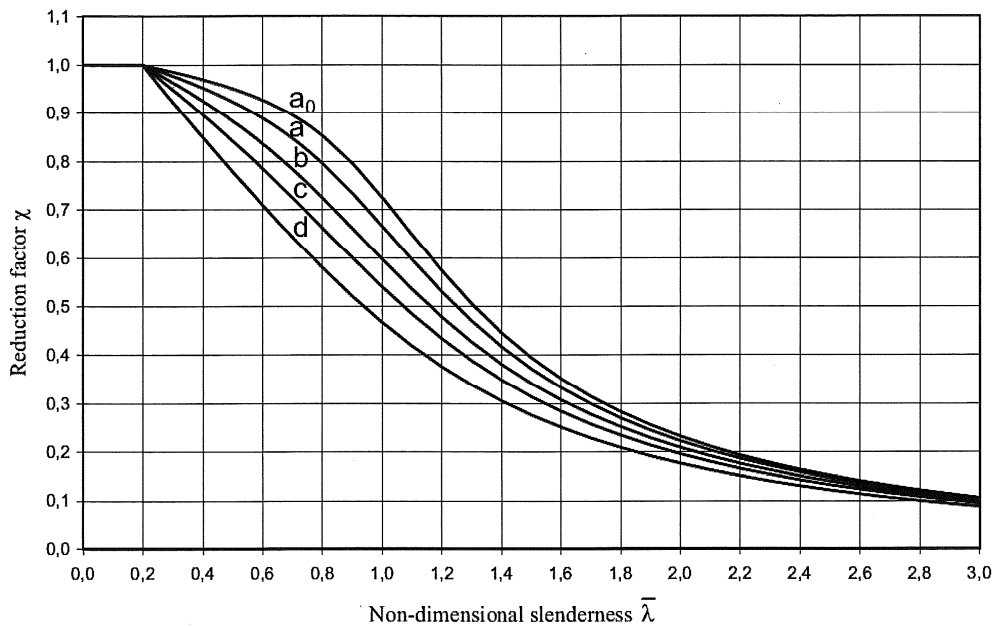


Figure 36-1 Relation between the reduction factor  $\chi$  and the non-dimensional slenderness (from: NEN-EN 1993-1-1)

Note: in the older standard NEN 6770,  $\chi$  is indicated with  $\omega_{buc}$  (buckling factor) and  $\bar{\lambda}$  with  $\lambda_{rel}$  (relative slenderness).

**Slenderness for flexural buckling (buigingsknik)**

The non-dimensional slenderness  $\bar{\lambda}$  is given by

$$\bar{\lambda} = \sqrt{\frac{A \cdot f_y}{N_{cr}}} = \frac{L_{cr}}{i} \frac{1}{\lambda_1} \quad \text{for Class 1, 2 and 3 cross-sections}$$

$$\bar{\lambda} = \sqrt{\frac{A_{eff} \cdot f_y}{N_{cr}}} = \frac{L_{cr}}{i} \sqrt{\frac{A_{eff}}{A}} \quad \text{for Class 4 cross-sections,}$$

Where:  $L_{cr}$  [m] = buckling length in the buckling plane considered (=  $l_{ef}$  in Figure 36-2)

$i$  [m] = radius of gyration around the relevant axis, determined using the properties of the cross-section

$\lambda_1$  [] =

$$\lambda_1 = \pi \cdot \sqrt{\frac{E}{f_y}} = 93,9 \cdot \varepsilon$$

$\varepsilon$  [] =

$$\varepsilon = \sqrt{\frac{235}{f_y}}$$

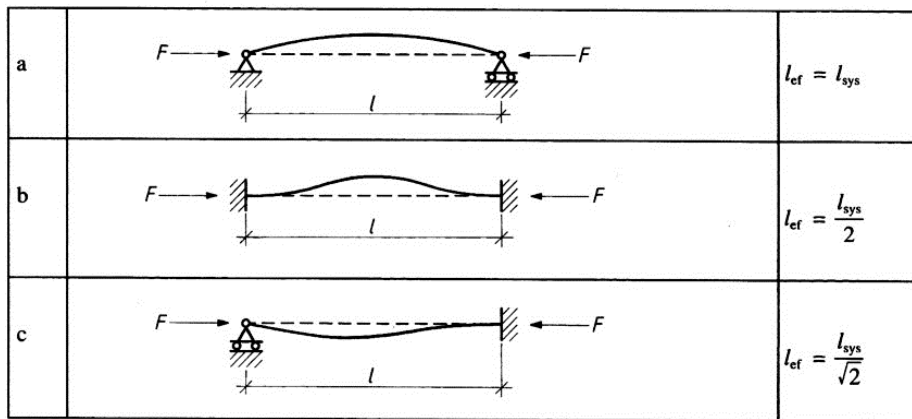


Figure 36-2 Effective buckling length.

**Uniform members in bending****Buckling resistance (kipweerstand)**

A laterally unrestrained member subject to major axis bending should be verified against lateral torsional buckling as follows:

$$\frac{M_{Ed}}{M_{b,Rd}} \leq 1,0$$

Where  $M_{Ed}$  [Nm] = design value of the moment

$M_{b,Rd}$  [Nm] = design buckling resistance moment

The design buckling resistance moment of a laterally unrestrained beam should be taken as:

$$M_{b,Rd} = \chi_{LT} \cdot W_y \cdot \frac{f_y}{\gamma_{M1}}$$

Where:

$W_y$  [m<sup>3</sup>] = the appropriate section modulus as follows:

$W_y = W_{pl,y}$  for Class 1 or 2 cross-sections

$W_y = W_{el,y}$  for Class 3 cross-sections

$W_y = W_{eff,y}$  for Class 4 cross-sections

$\chi_{LT}$  [-] = the reduction factor for lateral-torsional buckling

### Lateral torsional buckling curves (*kipkrommen*)

For determining the value of the reduction factor  $\chi_{LT}$  the curve of Figure 36-1 can be used, and

$$\bar{\lambda}_{LT} = \sqrt{\frac{W_y \cdot f_y}{M_{cr}}}$$

in which  $M_{cr}$  is the elastic critical moment for lateral-torsional buckling and is based on gross cross-sectional properties and takes into account the loading conditions, the real moment distribution and the lateral restraints. Recommended values for lateral buckling curves for cross-sections, see Table 36-4.

cross-section	Limits	Buckling curve
rolled I-sections	$h/b \leq 2$	a
	$h/b > 2$	b
welt I-sections	$h/b \leq 2$	c
	$h/b > 2$	d
other cross-sections	-	d

Table 36-4 buckling curves per cross-section.

## 36.4 Welded connections

The most often used type of weld in steel structures and especially temporary steel structures, is the fillet weld (*hoeklas*). This is the only type of weld discussed here, based on the general weld calculations.

Three types of connections in the building pit example have to be designed:

1. Pipe strut – long waling (Figure 36-3)
2. Short waling – long waling (4 corners of the building pit) (Figure 36-4)
3. H-beam strut – waling (struts shoring the wales in the corners with an angle of 45°).

These connections can be chosen to be designed as rigid connections or hinges. Especially for a temporary structure such as a building pit, rigid connections are an appropriate choice for all 3 types of connections, but most of the time hinges are preferred. The welds will have to transfer normal forces, shear and bending moments, but the span moments will mostly be smaller. The connection can be strengthened with extra steel plates or stiffeners (*schotjes, kopplaat*).



Figure 36-3 Welded connection of pipe strut and waling. The picture on the left (cofferdam near Sebastiaansbrug in Delft, 2007) shows a wale consisting of single H-profile, whereas the drawing on the right depicts the more common case of a double profile.

The theory that is stated in this section applies only to weldable structural steel with a material thickness larger or equal to 4 mm. For welds on thinner material the reader is referred to EN 1993-1-3. Also the mechanical properties, such as the yield strength ( $f_y$ ); ultimate tensile strength ( $f_u$ ); etc., of the weld material should be equivalent or better than the parent material, this ensures that the weld is at least as strong as the materials welded together.

Fillet welds may be used for connecting parts where the fusion faces form an angle between  $60^\circ$  and  $120^\circ$ . Fillet welds finishing at the ends or sides of parts that are connected should continue, full-size, around the corner for a distance of at least twice the leg length of the weld; unless access or the configuration of the joint renders this impracticable. Since a fillet weld is roughly rectangular in cross-section the leg length is defined as the length along the base material, or in other words the length of the sides of the triangle that make an angle of  $90^\circ$  (see Figure 36-4). Note that the leg length can also be unequal, however this is not common practise.

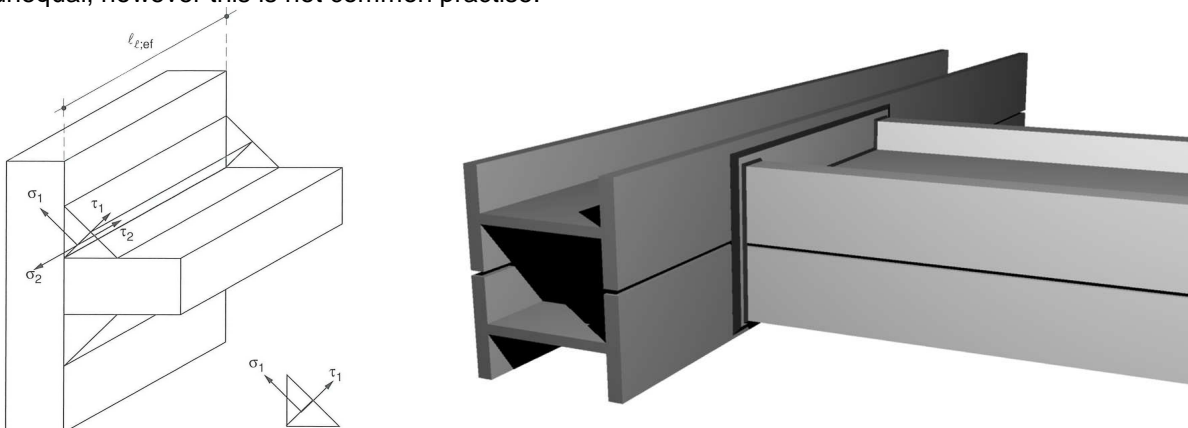


Figure 36-4 Connection between two walings, with front plate ( $\sigma_1 = \sigma_\perp$  and  $\sigma_2 = \sigma_\parallel$ )

Normal forces in the structural members will either act parallel or rectangular to the weld. They cause a stress in the direction parallel or rectangular to the weld,  $\sigma_\parallel$  or  $\sigma_\perp$  respectively. The bending moments on a rigid welded connection also cause stresses in these directions.

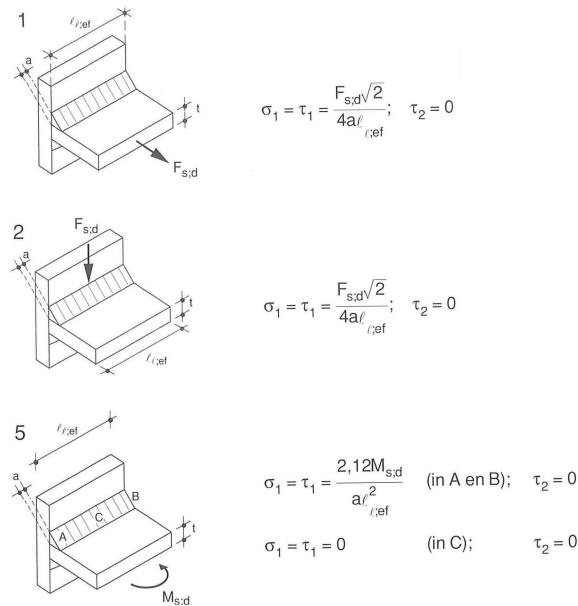


Figure 36-5: Standard cases 1, 2 and 5 of a normal force and shear force in a connected member. (Overspannend staal– Construeren A)

Figure 36-5 shows three basic standard cases of fillet welds connecting rectangular members with one weld per side;  $\ell_{eff}$  is the effective length of the member,  $a$  is the throat thickness.

#### 1. Normal force in connected member

$$\sigma_{\perp} = \tau_{\perp} = \frac{F_d \cdot \sqrt{2}}{4 \cdot a \cdot \ell_{eff}} ; \tau_{\parallel} = 0$$

#### 2. Shear force or load in connected member, perpendicular to the weld length

$$\sigma_{\perp} = \tau_{\perp} = \frac{\sqrt{2} \cdot F_d}{4 \cdot a \cdot \ell_{eff}} ; \tau_{\parallel} = 0$$

#### 5. A bending moment on the connected member

A concentrated load on the member is modelled as a concentrated load plus a bending moment on the connection. The stresses resulting from the bending moment alone are:

In points A and B:  $\sigma_{\perp} = \tau_{\perp} = \frac{3 \cdot M_{s;d}}{\sqrt{2} \cdot a \cdot \ell_{eff}^2} ; \tau_{\parallel} = 0$

In point C:  $\sigma_{\perp} = \tau_{\perp} = 0 ; \tau_{\parallel} = 0$

According to European standard EN 1993-1-8 the design resistance of a fillet weld can be determined using either the directional method or the simplified method, which will be discussed in the remainder of this section. Important notions are the effective length ( $\ell_{eff}$ ) and the effective throat thickness ( $a$ ) of the weld.

The effective length of a fillet weld should be taken as the length over which the fillet is full-size. This may be taken as the overall length of the weld reduced by twice the effective throat thickness. Provided that the weld is full-size throughout its length including starts and terminations, no reduction in effective length need be made for either the start or the termination of the weld. Note: a fillet weld with an effective length less than 30 mm or less than 6 times its throat thickness, whichever is larger, should not be designed to carry load.

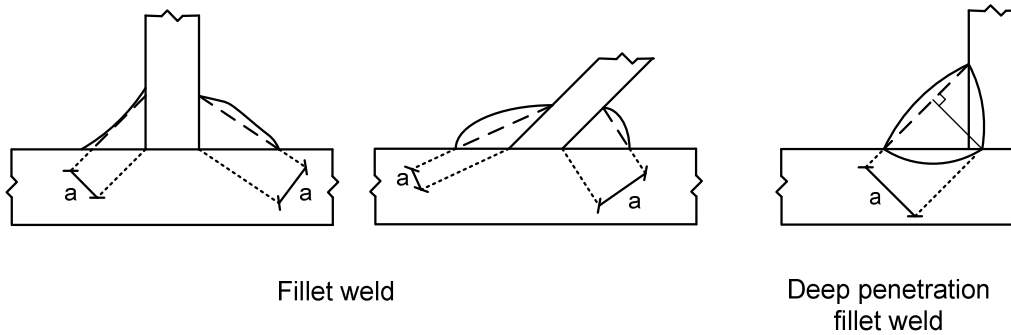


Figure 36-6 Throat thickness of a (deep penetration) fillet weld.

The effective throat thickness of a weld should be taken as the height of the largest triangle (with equal or unequal legs) that can be inscribed within the fusion faces and the weld surface, measured perpendicular to the outer side of this triangle, see Figure 36-6. The effective throat thickness of a fillet weld should not be less than 3 mm for practical reasons. In determining the design resistance of a deep penetration fillet weld, one may take the its additional throat thickness into account (see Figure 36-6), provided that preliminary tests show that the required penetration can be achieved consistently.

### Directional method

In this method the forces transmitted by a unit length of weld are resolved into components parallel and transverse to the longitudinal axis of the weld and normal and transverse to the plane of its throat ( $a$ ). The design throat area ( $A_w$ ) should be taken as  $A_w = \sum a \cdot l_{eff}$  and should be assumed concentrated in the root of the weld.

An uniform distribution of stress is assumed on the throat section of the weld, leading to normal and shear stresses as shown in Figure 36-7.

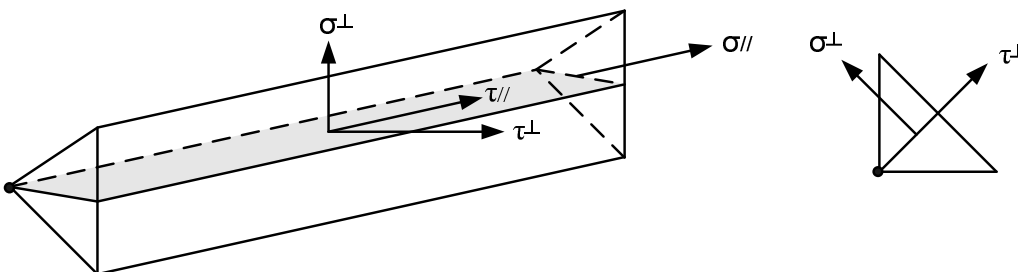


Figure 36-7 stresses on the throat section of a fillet weld.

Where:

- $\sigma_{\perp}$  [N/mm<sup>2</sup>] = normal stress perpendicular to the throat
- $\sigma_{//}$  [N/mm<sup>2</sup>] = normal stress parallel to the axis of the weld
- $\tau_{\perp}$  [N/mm<sup>2</sup>] = shear stress (in the plane of the throat) perpendicular to the axis of the weld
- $\tau_{//}$  [N/mm<sup>2</sup>] = shear stress (in the plane of the throat) parallel to the axis of the weld

The design resistance of the filled weld is sufficient if the following equations are both satisfied:

$$\sigma_d = \sqrt{\sigma_{\perp}^2 + 3(\tau_{\perp}^2 + \tau_{//}^2)} \leq \frac{f_u}{\beta_w \cdot \gamma_{M2}} \quad \text{and} \quad \sigma_{\perp} \leq \frac{0,9 \cdot f_u}{\gamma_{M2}}$$

Where:

- $f_u$  [N/mm<sup>2</sup>] = nominal tension strength of the weaker part joined
- $\beta_w$  [-] = appropriate correlation factor taken from Table 36-5
- $\gamma_{M2}$  [-] = partial factor for the tensile strength ( $\gamma_{M2} = 1,25$ )

Using these criteria the throat thickness of the weld can be determined, as stated before the practical minimum amounts to 3 mm. Note that the stress parallel to the axis,  $\sigma_{//}$ , is not considered when verifying the design resistance of the weld.

When welds connect parts with two different material strengths, the weld should be designed using the properties of the material with the lower strength grade.

Steel grade	Tensile stress	Correlation factor
S235	360 N/mm <sup>2</sup>	0,80
S275	275 N/mm <sup>2</sup>	0,85
S355	360 N/mm <sup>2</sup>	0,90
S420	360 N/mm <sup>2</sup>	1,00
S460	360 N/mm <sup>2</sup>	1,00

Table 36-5 correlation factor for fillet welds

### **Simplified method**

Alternatively the design resistance of a fillet weld may be assumed to be adequate if, at every point along its length, the resultant of all the forces per unit length transmitted by the weld satisfy the following criterion:

$$F_{w,Ed} \leq F_{w,Rd}$$

Where:

$$F_{w,Ed} \text{ [N/mm]} = \text{design value of the weld force per unit length}$$

$$F_{w,Rd} \text{ [N/mm]} = \text{design weld resistance per unit length}$$

Independent of the orientation of the weld throat plane to the applied force, the design resistance per unit length should be determined from:

$$F_{w,Rd} = f_{vw,d} \cdot a \quad \text{where} \quad f_{vw,d} = \frac{f_u}{\sqrt{3} \cdot \beta_w \cdot \gamma_{M2}}$$

Where:

$$f_{vw,d} \text{ [N/mm}^2\text{]} = \text{design shear strength of the weld}$$

**Example fillet weld**Given:

The pipe strut has a circle shaped cross-section, which will be welded upon the flanges of the double HEB-profile waling.

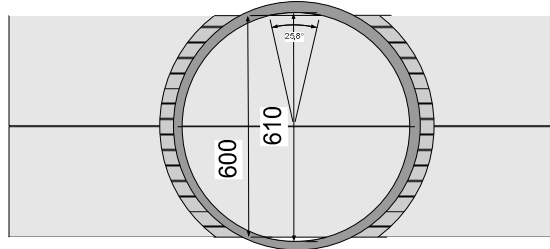


Figure 36-6: circular cross-section of pipe strut welded on flanges of double I-beam (weld only on the outer circumference)

Particulars of the connection are:

CHS 610-20 and 2 HEB 800 ( $h = 800$  mm,  $b = 300$  mm); both S235.

$D_{inner}$  pipe strut = 570 mm

Thickness pipe strut ( $t$ ) = 20 mm

Thickness flanges ( $t_f$ ) = 33 mm

Forces and moments:

$N = 2000$  kN  $\rightarrow$

$V = 41,4$  kN  $\uparrow$

$M = 289,8$  kNm

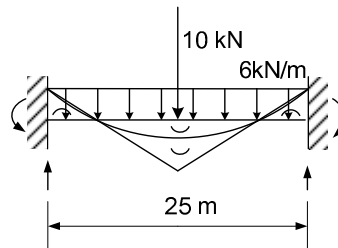


Figure 36-7: clamped/wedged beam

Asked:

Estimate the weld thickness and check the occurring stresses in the weld.

Elaboration:

Width flanges  $2 \cdot b = 2 \cdot 300 = 600$  mm

Circumference<sub>outer</sub>  $2\pi r = 1916$  mm

As  $D_{outer} > 600$ , part of the circumference is outside the flanges.

The part of the pipe on the flange will be welded upon the flange:

$\Delta \text{angle} = 360 - (600/610) \cdot 360 = 6^\circ$

$\Delta \text{circumference} = 6 / 360 \cdot 2\pi r = 0,02 \cdot 1916 = 38,32$  mm

$l_{eff \text{ total}} = 1916 - 39 = 1877$  mm.

The welded connections at both ends of the pipe strut will be rigid in reality. Therefore the bending moments in the connection will be assumed as follows:

$M_A = 1/2 q l^2 + 1/8 FL = 940,6$  kNm

Assumption  $a = 6$  mm

$$\sigma_{\perp} = \tau_{\perp} = \frac{\sqrt{2} \cdot F_d}{4 \cdot a \cdot l_{eff}} = \frac{\sqrt{2} \cdot 2000 \cdot 10^3}{4 \cdot 6 \cdot 1877} = 63 \text{ N/mm}^2 \quad (\text{compression})$$

$$\sigma_{\perp} = \tau_{\perp} = \frac{\sqrt{2} \cdot F_d}{4 \cdot a \cdot l_{eff}} = \frac{\sqrt{2} \cdot 41,4 \cdot 10^3}{4 \cdot 6 \cdot 1877} = 1,30 \text{ N/mm}^2 \quad (\text{shear})$$

$$\sigma_{\perp} = \tau_{\perp} = \frac{3 \cdot M_d}{\sqrt{2} \cdot a \cdot \ell_{\text{eff}}^2} = \frac{2,12 \cdot 940,6 \cdot 10^6}{6 \cdot 1877^2} = 94 \text{ N/mm}^2$$

Use the effective welding length per side of the pipe:  $\ell_{\text{eff}}$  of  $\frac{1}{2} \cdot$  circumference.

Using the directional method, both equations must be satisfied:

$$\sqrt{\sigma_{\perp}^2 + 3(\tau_{\perp}^2 + \tau_{\parallel}^2)} \leq \frac{f_u}{\beta_w \cdot \gamma_{M2}} \quad \text{and} \quad \sigma_{\perp} \leq \frac{0,9 \cdot f_u}{\gamma_{M2}}$$

$$\sqrt{158^2 + 3 \cdot (158^2 + 0^2)} \leq \frac{360}{0,8 \cdot 1,25} \quad \text{and} \quad 158 \leq \frac{0,9 \cdot 360}{1,25}$$

$$316 \leq 360 \Rightarrow \text{OK}$$

$$158 \leq 259 \Rightarrow \text{OK}$$

Or, using the simplified method for determining the design resistance of the fillet weld:

$$F_{w,Rd} = \frac{f_u}{\sqrt{3} \cdot \beta_w \cdot \gamma_{M2}} \cdot a = \frac{360}{\sqrt{3} \cdot 0,8 \cdot 1,25} \cdot 6 = 1247 \text{ N/mm}^1$$

$$F_{w,Ed} \leq F_{w,Rd}$$

$$a \cdot (\sum \sigma_{\perp} + \sum \tau_{\perp}) \leq 1247 \text{ N/mm}^1$$

$$6 \cdot (158 + 158) \leq 1247 \text{ N/mm}^1$$

$$1896 \text{ N/mm}^1 \leq 1247 \text{ N/mm}^1 \Rightarrow \text{not OK}$$

Assume a throat thickness of 10 mm:

$$F_{w,Rd} = \frac{f_u}{\sqrt{3} \cdot \beta_w \cdot \gamma_{M2}} \cdot a = \frac{360}{\sqrt{3} \cdot 0,8 \cdot 1,25} \cdot 10 = 2078 \text{ N/mm}^1$$

$$F_{w,Ed} \leq F_{w,Rd}$$

$$a \cdot (\sum \sigma_{\perp} + \sum \tau_{\perp}) \leq 2078 \text{ N/mm}^1$$

$$10 \cdot (95 + 95) \leq 2078 \text{ N/mm}^1$$

$$1900 \text{ N/mm}^1 \leq 2078 \text{ N/mm}^1 \Rightarrow \text{ok}$$

Note that the simplified method results in a thicker weld, this is a result of the trade off between the accuracy and the difficulty of the calculation.

The high connection forces are a result of the stiffness of the welded connection.

NB. The deformations of a temporary structure such as struts are not often checked. They could be estimated using forget-me-nots from structural mechanics and then checked against the requirements.

### 36.5 Bolt connections

The partial safety factor  $\gamma_M$  for the tensile strength of bolts (*bouten*) is  $\gamma_{M2} = 1,25$ . The partial safety factor for the preload of high strength bolts is  $\gamma_{M7} = 1,1$ . Detailed information about connections made by bolts can be found in EN 1993-1-8. The rules in this standard are valid for the bolt classes given in Table 36-6.

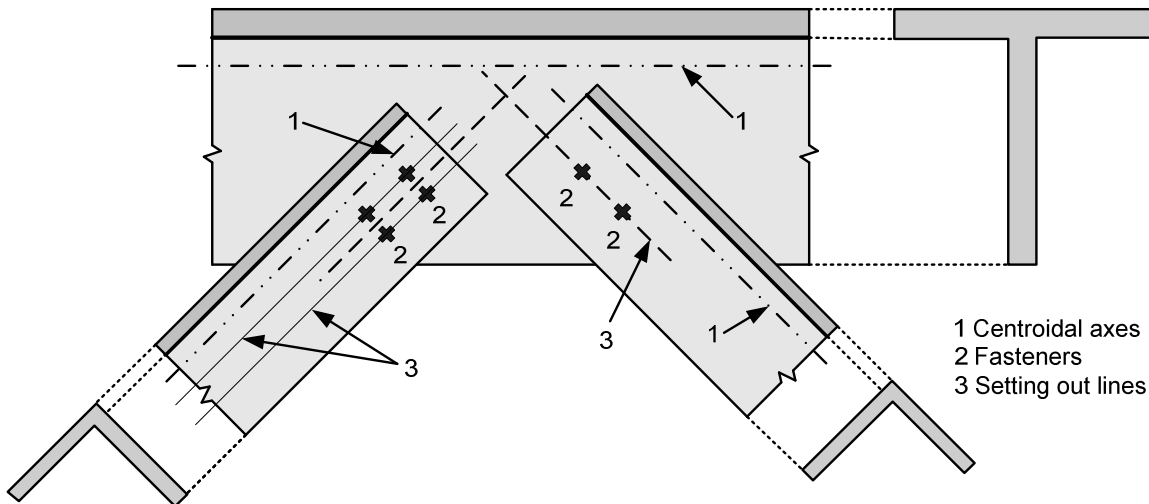


Figure 36-8 Two angular sections (*hoekprofiel*) are bolted to a T-profile

The yield strength  $f_{yb}$  and the ultimate tensile strength  $f_{ub}$  for bolt classes 4.6, 4.8, 5.6, 5.8, 6.8, 8.8 and 10.9 are given in Table 36-6. These values should be adopted as characteristic values in design calculations.

Bolt class	4.6	4.8	5.6	5.8	6.8	8.8	10.9
$f_{yb}$ (N/mm <sup>2</sup> )	240	320	300	400	480	640	900
$f_{ub}$ (N/mm <sup>2</sup> )	400	400	500	500	600	800	1000

Table 36-6 Bolt classes (Nominal values of the yield strength and the ultimate tensile strength for bolts.)



Figure 36-9 Cofferdam for the construction of the metro line in Thessaloniki, with bolt connections struts-wales (August 2009)

**Categories of bolted connections***Shear connections*

Bolted connections loaded in shear should be designed as one of the following categories:

- Category A : Bearing type  
In this category bolts from class 4.6 up to and including class 10.9 should be used. No preloading and special provisions for contact surfaces are required. The design ultimate shear load should not exceed the design shear resistance, nor the design bearing resistance.
- Category B : Slip-resistant at serviceability limit state  
In this category preloaded bolts from classes 8.8 and 10.9 should be used. Slip should not occur at the serviceability limit state. The design serviceability shear load should not exceed the design slip resistance. The ultimate shear load should not exceed the design shear resistance, nor the design bearing resistance.
- Category C : Slip-resistant at ultimate limit state  
In this category preloaded bolts from classes 8.8 and 10.9 should be used. Slip should not occur at the ultimate limit state. The design ultimate shear load should not exceed the design slip resistance, nor the design bearing resistance. In addition for a connection in tension, the design plastic resistance of the net cross-section at bolt holes should be checked at the ultimate limit state.

*Tension connections*

Bolted connections loaded in tension should be designed as one of the following categories:

- Category D : Non-preloaded  
In this category bolts from class 4.6 up to and including class 10.9 should be used. No preloading is required. This category should not be used where the connections are frequently subjected to variations of tensile loading. However, they may be used in connections designed to resist normal wind loads.
- Category E : Preloaded  
In this category preloaded bolts from classes 8.8 and 10.9 with controlled tightening in conformity with 1.2.7 Reference Standards: Group 7 should be used.

**Positioning of holes for bolts (and rivets)**

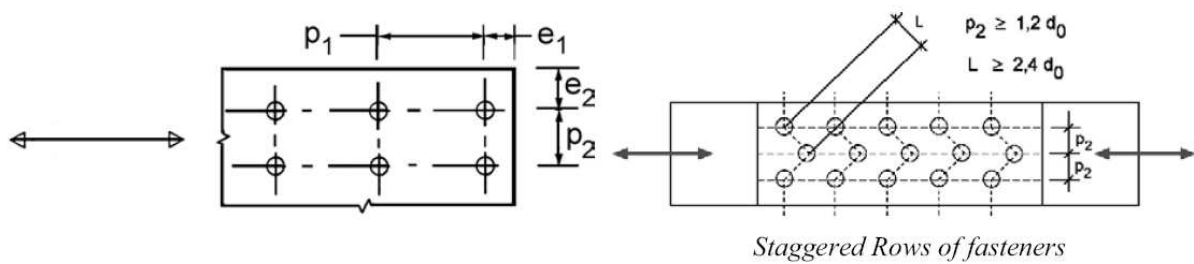
Minimum and maximum spacing and end and edge distances for bolts (*bouten*) and rivets (*klinknagels*) are given in Table 36-7.

Distances and spacings, see figure 26-10	Minimum	Maximum <sup>1) 2) 3)</sup>		
		Structures made from steels conforming to EN 10025 except steels conforming to EN 10025-5		Structures made from steels conforming to EN 10025-5
		Steel exposed to the weather or other corrosive influences	Steel not exposed to the weather or other corrosive influences	Steel used unprotected
End distance $e_1$	$1,2 d_0$	$4t + 40$ mm		The larger of $8t$ or 125 mm
Edge distance $e_2$	$1,2 d_0$	$4t + 40$ mm		The larger of $8t$ or 125 mm
Distance $e_3$ in slotted holes	$1,5 d_0$ <sup>4)</sup>			
Distance $e_4$ in slotted holes	$1,5 d_0$ <sup>4)</sup>			
Spacing $p_1$	$2,2 d_0$	The smaller of $14t$ or 200 mm	The smaller of $14t$ or 200 mm	The smaller of $14t_{min}$ or 175 mm
Spacing $p_{1,0}$		The smaller of $14t$ or 200 mm		
Spacing $p_{1,i}$		The smaller of $28t$ or 400 mm		
Spacing $p_2$ <sup>5)</sup>	$2,4 d_0$	The smaller of $14t$ or 200 mm	The smaller of $14t$ or 200 mm	The smaller of $14t_{min}$ or 175 mm
<p><sup>1)</sup> Maximum values for spacing, edge and end distances are unlimited, except for the following cases:  - for compression members in order to avoid local buckling and to prevent corrosion in exposed members and;  - for exposed tension members to prevent erosion.</p> <p><sup>2)</sup> The local buckling resistance of the plate in compression between the fasteners should be calculated according to EN 1993-1-1 using <math>0,6 p_1</math> as buckling length. Local buckling between the fasteners need not to be checked if <math>p_1 / t</math> is smaller than <math>9 \epsilon</math>. The edge distance should not exceed the local buckling requirements for an outstand element in the compression members, see EN 1993-1-1. The end distance is not affected by this requirement.</p> <p><sup>3)</sup> <math>t</math> is the thickness of the thinner outer connected part.</p> <p><sup>4)</sup> The dimensional limits for slotted holes are given in 1.2.7 Reference Standards: Group 7.</p> <p><sup>5)</sup> For staggered rows of fasteners a minimum line spacing of <math>p_2 = 1,2 d_0</math> may be used, provided that the minimum distance, <math>L</math>, between any two fasteners is greater or equal than <math>2.4 d_0</math>, see figure 26-10 b).</p>				

Table 36-7 Minimum and maximum spacing, end and edge distances of bolts

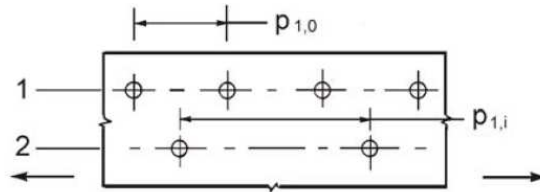
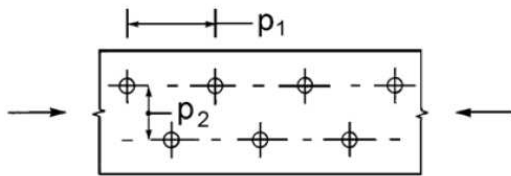
Where:

- $e_1$  [mm] = the end distance from the centre of a fastener hole to the adjacent end of any part, measured in the direction of load transfer
- $e_2$  [mm] = the edge distance from the centre of a fastener hole to the adjacent edge of any part, measured at right angles to the direction of load transfer
- $e_3$  [mm] = the distance from the axis of a slotted hole to the adjacent end or edge of any part
- $e_4$  [mm] = the distance from the centre of the end radius of a slotted hole to the adjacent end or edge of any part
- $p_1$  [mm] = the spacing between centres of fasteners in a line in the direction of load transfer
- $p_{1,0}$  [mm] = the spacing between centres of fasteners in an outer line in the direction of load transfer
- $p_{1,i}$  [mm] = the spacing between centres of fasteners in an inner line in the direction of load transfer
- $p_2$  [mm] = the spacing measured perpendicular to the load transfer direction between adjacent lines of fasteners
- $d_0$  [mm] = the hole diameter for a bolt, a rivet or a pin



a) Symbols for spacing of fasteners

b) Symbols for staggered spacing



$p_1 \leq 14 t$  and  $\leq 200$  mm

$p_2 \leq 14 t$  and  $\leq 200$  mm

$p_{1,0} \leq 14 t$  and  $\leq 200$  mm

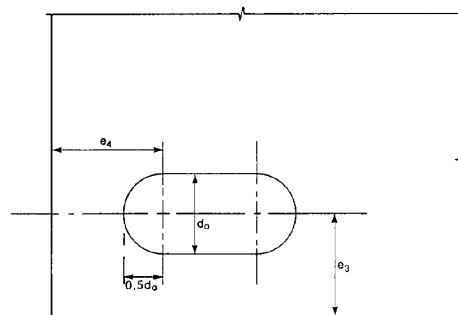
$p_{1,i} \leq 28 t$  and  $\leq 400$  mm

1 outer row

2 inner row

c) Staggered spacing in compression members

d) Staggered spacing in tension members



e) End and edge distances for slotted holes

Figure 36-10 Symbols for end and edge distances and spacing of fasteners.

### Design resistance of individual fasteners

The design resistance for an individual fastener subjected to shear and/or tension is given in Table 36-8. For preloaded bolts the design preload,  $F_{p,Cd}$ , to be used in design calculations is:

$$F_{p,Cd} = 0,7 \cdot f_{ub} \cdot A_s / \gamma_{M7}$$

where:

$F_{p,Cd}$ [N]	=	design preload
$f_{ub}$ [N/mm <sup>2</sup> ]	=	ultimate tensile strength
$A_s$ [mm <sup>2</sup> ]	=	tensile stress area of the bolt
$\gamma_{M7}$ [-]	=	partial factor for preload of high strength bolts ( $\gamma_{M7} = 1,1$ )

In single lap joints with only one bolt row, the bolts should be provided with washers (*ringen*) under both the head and the nut (*moer*). The design bearing resistance (*stuwweerstand*) for each bolt should be limited to:

$$F_{b,Rd} \leq 0,7 \cdot f_u \cdot d \cdot t / \gamma_{M2}$$

where:

$F_{b,Rd}$ [N]	=	design bearing resistance
$f_u$ [N/mm <sup>2</sup> ]	=	tensile stress
$d$ [mm]	=	nominal bolt diameter
$t$ [mm]	=	thickness of the thinner outer connected part
$\gamma_{M2}$ [-]	=	partial factor for the tensile strength ( $\gamma_{M2} = 1,25$ )

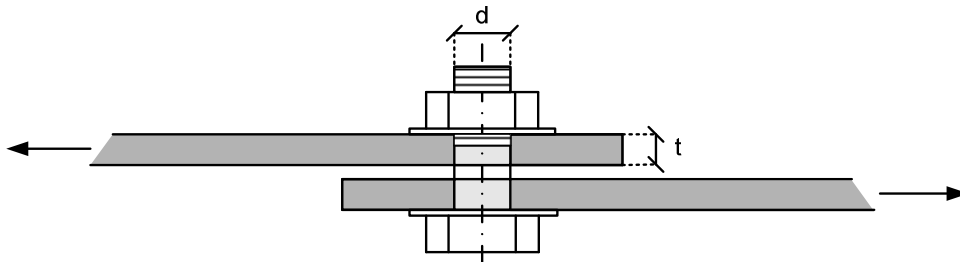


Figure 36-11 Single lap joint with one row of bolts

Failure mode	Bolts	Rivets
Shear resistance per shear plane	$F_{v,Rd} = \frac{\alpha_v \cdot f_{ub} \cdot A}{\gamma_{M2}}$ <ul style="list-style-type: none"> <li>- where the shear plane passes through the threaded portion of the bolt (<math>A</math> is the tensile stress area of the bolt <math>A_s</math>) <ul style="list-style-type: none"> <li>- for classes 4.6, 5.6, 8.8: <math>\alpha_v = 0.6</math></li> <li>- for classes 4.8, 5.8, 6.8 and 10.9: <math>\alpha_v = 0.5</math></li> </ul> </li> <li>- where the shear plane passes through the unthreaded portion of the bolt (<math>A</math> is the gross cross-section of the bolt): <math>\alpha_v = 0.6</math></li> </ul>	$F_{v,Rd} = \frac{0.6 \cdot f_{ur} \cdot A_0}{\gamma_{M2}}$
Bearing resistance <sup>1) 2) 3)</sup>	$F_{b,Rd} = \frac{k_1 \cdot \alpha_b \cdot f_u \cdot d \cdot t}{\gamma_{M2}}$ <ul style="list-style-type: none"> <li>- where <math>\alpha_b</math> is the smallest of <math>\alpha_d</math>; <math>\frac{f_{ub}}{f_u}</math> or 1,0</li> <li>- in the direction of load transfer: <ul style="list-style-type: none"> <li>- for end bolts: <math>\alpha_d = \frac{e_1}{3 \cdot d_0}</math>; for inner bolts: <math>\alpha_d = \frac{p_1}{3 \cdot d_0} - \frac{1}{4}</math></li> </ul> </li> <li>- perpendicular to the direction of load transfer: <ul style="list-style-type: none"> <li>- for edge bolts: <math>k_1</math> is the smallest of <math>2.8 \cdot \frac{e_2}{d_0} - 1.7</math> or 2,5</li> <li>- for inner bolts: <math>k_1</math> is the smallest of <math>1.4 \cdot \frac{p_2}{d_0} - 1.7</math> or 2,5</li> </ul> </li> </ul>	
Tension resistance <sup>2)</sup>	$F_{t,Rd} = \frac{k_2 \cdot f_{ub} \cdot A_s}{\gamma_{M2}}$ <p>where <math>k_2 = 0.63</math> for countersunk bolt, otherwise <math>k_2 = 0.9</math></p>	$F_{t,Rd} = \frac{0.6 \cdot f_{ur} \cdot A_0}{\gamma_{M2}}$
Punching shear resistance	$B_{p,Rd} = \frac{0.6 \cdot \pi \cdot d_m \cdot t_p \cdot f_u}{\gamma_{M2}}$	No check needed
Combined shear and tension	$\frac{F_{v,Ed}}{F_{v,Rd}} + \frac{F_{t,Ed}}{1.4 \cdot F_{t,Rd}} \leq 1.0$	
<sup>1)</sup> The bearing resistance $F_{b,Rd}$ for bolts <ul style="list-style-type: none"> <li>- in oversized holes is 0,8 times the bearing resistance for bolts in normal holes.</li> <li>- in slotted holes, where the longitudinal axis of the slotted hole is perpendicular to the direction of the force transfer, is 0,6 times the bearing resistance for bolts in round, normal holes.</li> </ul> <sup>2)</sup> For countersunk bolt: <ul style="list-style-type: none"> <li>- the bearing resistance <math>F_{b,Rd}</math> should be based on the plate thickness <math>t</math> equal to the thickness of the connected plate minus half the depth of the countersinking.</li> <li>- for the determination of the tension resistance <math>F_{t,Rd}</math> the angle and depth of countersinking should conform with 1.2.4 Reference Standards: Group 4, otherwise the tension resistance <math>F_{t,Rd}</math> should be adjusted accordingly.</li> </ul> <sup>3)</sup> When the load on a bolt is not parallel to the edge, the bearing resistance may be verified separately for the bolt load components parallel and normal to the end.		

Table 36-8 Design resistance for individual fasteners subjected to shear and/or tension

where:

$F_v, R_d$	[N]	= the design shear resistance per bolt
$F_b, R_d$	[N]	= the design bearing resistance per bolt
$F_t, R_d$	[N]	= the design tension resistance per bolt
$F_v, E_d$	[N]	= the design shear force per bolt for the ultimate limit state
$F_t, E_d$	[N]	= the design tensile force per bolt for the ultimate limit state
$B_p, R_d$	[N]	= the design punching shear resistance of the bolt head and the nut
$f_u$	[N/mm <sup>2</sup> ]	= tensile stress
$f_{ub}$	[N/mm <sup>2</sup> ]	= ultimate tensile strength
$f_{ur}$	[N/mm <sup>2</sup> ]	= the specified ultimate tensile strength of the rivet
$\alpha_v$	[-]	= factor defined in the table
$\alpha_d$	[-]	= factor defined in the table
$\alpha_b$	[-]	= factor defined in the table
$A$	[mm <sup>2</sup> ]	= the gross cross-section area of bolt
$A_s$	[mm <sup>2</sup> ]	= the tensile stress area of the bolt
$A_0$	[mm <sup>2</sup> ]	= the area of the rivet hole
$\gamma_{M2}$	[-]	= partial factor for the tensile strength ( $\gamma_{M2} = 1,25$ )
$t_p$	[mm]	= the thickness of a plate
$k_1$	[-]	= factor defined in the table
$k_2$	[-]	= factor defined in the table
$e_1$	[mm]	= the end distance from the centre of a fastener hole to the adjacent end of any part, measured in the direction of load transfer
$e_2$	[mm]	= the edge distance from the centre of a fastener hole to the adjacent edge of any part, measured at right angles to the direction of load transfer
$p_1$	[mm]	= the spacing between centres of fasteners in a line in the direction of load transfer
$p_2$	[mm]	= the spacing measured perpendicular to the load transfer direction between adjacent lines of fasteners
$d_m$	[mm]	= the mean of the across points and across flats dimensions of the bolt head or the nut, whichever is smaller
$d_0$	[mm]	= the hole diameter for a bolt, a rivet or a pin

### **Group of fasteners**

The design resistance of a group of fasteners may be taken as the sum of the design bearing resistances  $F_{b,Rd}$  of the individual fasteners, provided that the design shear resistance  $F_{v,Rd}$  of each individual fastener is greater than or equal to the design bearing resistance  $F_{b,Rd}$ . Otherwise the design resistance of a group of fasteners should be taken as the number of fasteners multiplied by the smallest design resistance of any of the individual fasteners.

## 36.6 Fatigue

This section presents an introduction to the phenomenon of fatigue and it refers to the lecture notes of CIE5126 on fatigue by M.H. Kolstein. In this section only the basic principles are treated, for more detailed information on this subject the reader is referred to the NEN-EN 1993-1-9 "Fatigue".

Fatigue is the progressive and localized structural damage that occurs when a material is subjected to cyclic loading. Final failure occurs in regions of tensile stress, if the reduced governing cross-section of the structural member becomes insufficient to bear the repetitive peak load without rupture. Fatigue is a major threat for structures under dynamic loads, such as bridges, cranes and offshore structures, where the live load presents a high portion of the total load. This is mostly the case in steel structures, where the dead weight is relatively low compared to the total load. Fatigue mainly leads to static failure by rupture (cracking) or buckling.

For a simple check, follow these design steps:

1. Locate the stress areas in the structure
2. Locate geometrical stress concentrations in the structure
3. Determine the fatigue strength
4. Determine the dynamic loads resulting in fatigue
5. Define the number of cycles  $n$ , using a cycle counting method
6. Check if damage will occur ( $D_d = \sum (n_i / N_i) \leq 1$ ) (Miner's summation)

Ad 1/2. Design simple structural details. Start checking fatigue in critical sections, such as welds, connections, changes in structural member and high live load/dead load ratio etc.

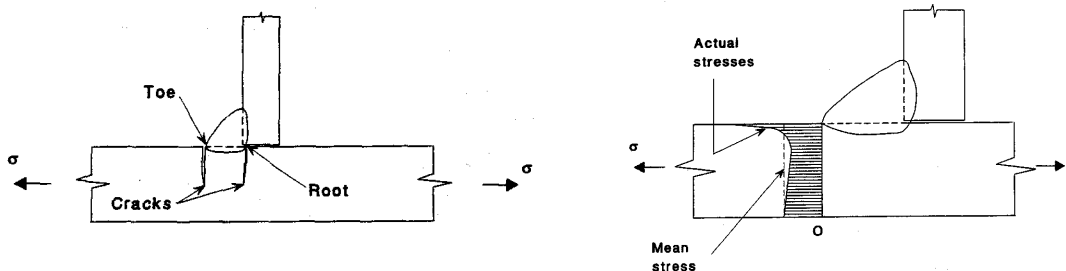


Figure 36-12: Discontinuities, stress peaks and cracks at the toe of a fillet weld

Ad3. Fatigue strength

The fatigue strength of a weld component is defined as the stress range ( $\Delta\sigma_R$ ) between the minimum and maximum stress in the cycle which would cause failure of the structural member when fluctuating with a constant amplitude for a specified number of cycles ( $N_R$ ). The number of cycles to failure  $N_R$  is known as the endurance or fatigue life.

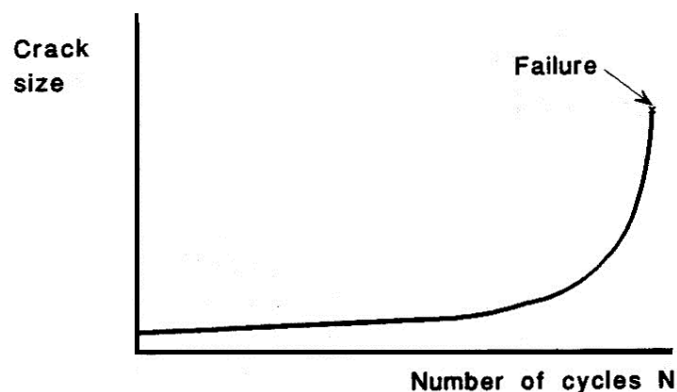


Figure 36-13: Typical crack growth curve

$$N_R = \frac{d}{\Delta\sigma_R^m} \quad \text{or} \quad \log N_R = \log d - m \cdot \log \Delta\sigma_R$$

Where:

- $m$  = slope of the fatigue strength curve (3 for most welded details)
- $d$  = design weld strength parameter, or the fatigue detail category coefficient, dependent on the stress range, see Table 36-9.

Detail Category $\Delta\sigma_c$ [N/mm <sup>2</sup> ]	$d$		$m$ [-]
160	7,962	$10^{12}$	3
140	5,636	$10^{12}$	3
125	3,990	$10^{12}$	3
112	2,825	$10^{12}$	3
100	2,000	$10^{12}$	3
90	1,416	$10^{12}$	3
80	1,002	$10^{12}$	3
71	0,710	$10^{12}$	3
63	0,502	$10^{12}$	3
56	0,356	$10^{12}$	3
50	0,252	$10^{12}$	3
45	0,178	$10^{12}$	3
40	0,126	$10^{12}$	3
36	0,089	$10^{12}$	3

Table 36-9 Classification table

$\Delta\sigma_c$  is the characteristic value for the weld-class applied, and represents the value for the stress range that is exceeded  $10^7$  times during the lifetime of the structure (see Figure 36-12).

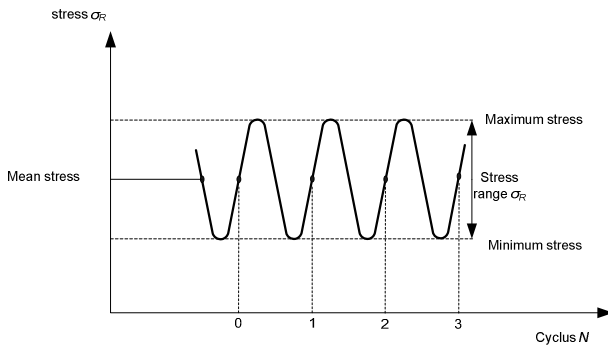


Figure 36-12: Constant amplitude stress history

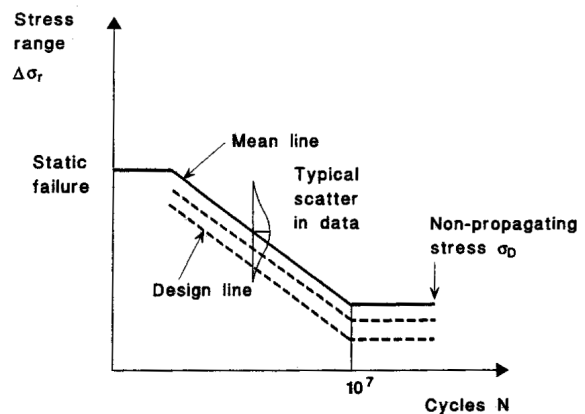


Figure 36-13: Typical S-N curve for constant amplitude tests

Beyond 5-10 million cycles, the stress range is generally too small to allow crack propagation under constant amplitude loading. Beneath this limit stress range cracks will not grow. The force fluctuation shall be calculated using the elasticity theory. No plastic redistribution is permitted because that would decrease the safety margin of the design.

Ad. 6 Calculation of damage.

The load spectrum is often simplified into a limited number of bands, see Figure 36-14. The damage per band is defined as  $n / N$ , where  $n$  is the number of cycles in the band and  $N$  is the endurance belonging to that stress range.

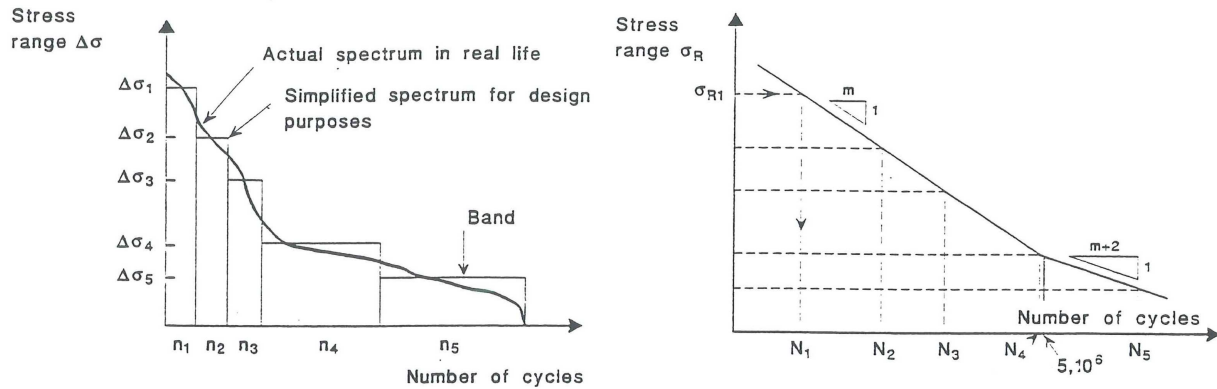


Figure 36-14 Simplification of stress spectrum and determination of endurance for each band (from lecture notes CT5126)

The damage during the design life ( $D_d$ ) as a result of all stress bands should not exceed unity:

$$D_d = \sum \frac{n_i}{N_i} \leq 1$$

In the design, the following aspects should be taken into account:

- Fatigue depends on the whole service loading sequence, not just one extreme load event.
- Fatigue is very sensitive to the geometry of details. Details should be simple and smoothness of the stress path should be ensured.
- In wett steel structures, fatigue cracks will almost certainly start to grow from welds, because
  - most welding processes leave minute metallurgical discontinuities from which cracks may grow (peak stresses at discontinuity).
  - At the toes of butt welds, sharp changes of direction often occur. Discontinuities at these points cause local stress concentrations, therefore cracks will grow faster.
- Fatigue requires more accurate prediction of elastic stress.
- A structure designed on fatigue makes more demands on workmanship and inspection.
- The static design safety margins are not sufficient for fatigue, therefore during the conceptual design should be checked whether fatigue is likely to be critical.
- Check areas of high live load/dead load ratios first on fatigue.

#### Example fatigue (simplified)

An offshore structure is dynamically loaded by wave impact. The load exerted on the structure as a result of the impact is 25 000 kN/m<sup>2</sup>, it is assumed that the impact is either present or absent. The waves have an average period of 30 seconds. Determine the fatigue strength of the structure and check if damage will occur within the required lifetime of 50 years. The characteristic value of the weld-class applied ( $\Delta\sigma_c$ ) is 80 N/mm<sup>2</sup>.

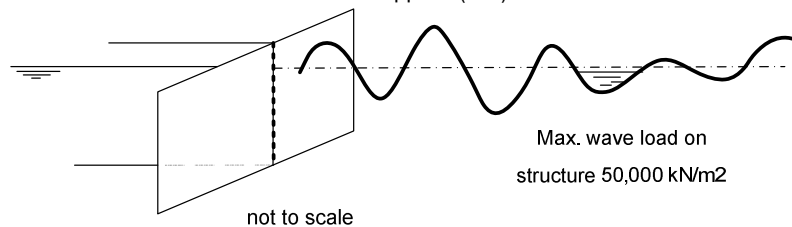


Figure 36-15 Fatigue load on offshore structure

- Step 3) Determine the fatigue strength:
- maximum load: 25 000 kN/m<sup>2</sup>
  - minimum load: 0 kN/m<sup>2</sup>
  - Stress range (interval)  $\Delta\sigma_R = 25\,000\text{ kN/m}^2 = 25\text{ N/mm}^2$

Step 4) Determine the dynamic loads resulting in fatigue:

Using Table 36-9 for  $\Delta\sigma_c = 80 \text{ N/mm}^2$ , one finds that the value for  $d$  is  $1,002 \cdot 10^{12}$ .

The design life expressed as the number of cycles related to a constant stress range (endurance) is:

$$N_R = \frac{d}{\Delta\sigma_R^m} = \frac{1,002 \cdot 10^{12}}{25^3} \approx 64,128 \cdot 10^6 \text{ cycles}$$

Step 5) Define the number of cycles  $n$ :

The design life time is 50 years and the average period of the load is 30 seconds, so the average number of cycles occurring during the life time amounts to:

$$n = \frac{50 \cdot 365 \cdot 24 \cdot 60 \cdot 60}{30} = 52,56 \cdot 10^6 \text{ cycles}$$

Step 6) Check if damage will occur during the design life:

$$D_d = \sum \frac{n}{N_R} = \sum \frac{52,560 \cdot 10^6}{64,128 \cdot 10^6} = 0,82 \leq 1 \Rightarrow \text{no damage will occur.}$$

## 36.7 Literature

Nederlands Normalisatie instituut, *Eurocode 3: "Design of steel structures – Part 1-1: General rules for buildings"* (NEN-EN 1993-1-1), januari 2006, Nederlands Normalisatie instituut.

Nederlands Normalisatie instituut, *Eurocode 3: "Design of steel structures – Part 1-8: Design of joints"* (NEN-EN 1993-1-8), januari 2006, Nederlands Normalisatie instituut.

Nederlands Normalisatie instituut, *Eurocode 3: "Design of steel structures – Part 1-9: Fatigue"* (NEN-EN 1993-1-9), januari 2006, Nederlands Normalisatie instituut.

# Manual Hydraulic Structures

---

## **Part IV: (temporary) structures**



## 37. Stability of structures on shallow foundations

New chapter: February 2011; updated February 2015; 'Piping' section slightly improved February 2016

Hydraulic structures have to be stable and not get into motion due to loads. This implies that there has to be a horizontal, vertical and rotational stability. This can be expressed with the following well-known equations:

$$\begin{aligned}\Sigma H_{total} &= 0 \\ \Sigma V_{total} &= 0 \\ \Sigma M_{total} &= 0,\end{aligned}$$

where

$$\begin{aligned}\Sigma H_{total} \text{ [kN]} &= \text{total of the horizontal components of the solliciting and resisting forces} \\ \Sigma V_{total} \text{ [kN]} &= \text{total of the vertical components of the solliciting and resisting forces} \\ \Sigma M_{total} \text{ [kNm]} &= \text{total of the moment caused by the solliciting and resisting forces}\end{aligned}$$

Another threat to the stability is groundwater flow under the structure, which can lead to internal erosion or undermining of the structure if sediment particles are moved away with the flow. External erosion, i.e., erosion in front of a structure, can also lead to collapse. These five criteria are elaborated in the remainder of this chapter.

### 37.1 Horizontal stability

The total of the horizontal forces acting on a hydraulic structure based on a shallow foundation will be transferred to the subsoil (Figure 37-1). The friction force of the subsoil should resist the resulting total acting horizontal force, otherwise it will slide aside. This friction force is determined by the total of the forces solliciting (acting) on the structure in vertical direction (or the total of the vertical components of the forces,  $\Sigma V$ ), multiplied by a dimensionless friction coefficient  $f$ . The friction force should not be less than the total of acting horizontal forces ( $\Sigma H$ ), to prevent the structure from sliding aside. In equation form:

$$\Sigma H < f \cdot \Sigma V$$

The dead weight of the structure and buoyant forces should be included in  $\Sigma V$ .

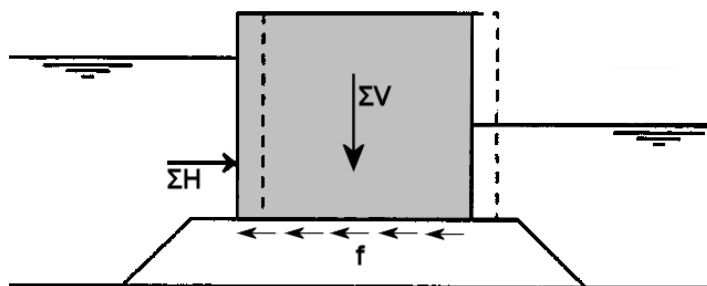


Figure 37-1 Slip-off principle sketch

Depending on the failure mechanism, more specifically the position and alignment of the slip surface, a certain type of friction develops. Some critical slip planes:

1. friction between structure and subsoil:  $f = \tan(\delta)$ , with  $\delta$  = friction angle between structure and subsoil. If  $\delta$  is unknown, it can be approximated:  $\delta \approx \frac{2}{3} \varphi$  ( $\varphi$  is angle of internal friction of the subsoil). The friction coefficient for concrete-rubble is about 0,5; in case of a rubble bed: 0,6 (Dutch Deltaworks). Values for cast concrete on soil are given in Table 37-1.
2. Internal friction of the subsoil:  $f = \tan(\varphi)$ , with  $\varphi$  is the angle of internal friction of the subsoil.
3. A deeper soil layer with a low sliding resistance.

Interface Materials	Friction Coefficient, f
Mass concrete on the following foundation materials:	
Clean sound rock	0.70
Clean gravel, gravel--sand mixtures, coarse sand	0.55 to 0.60
Clean fine to medium sand, silty medium to coarse sand, silty or clayey gravel	0.45 to 0.55
Clean fine sand, silty or clayey fine to medium sand	0.35 to 0.45
Fine sandy silt, nonplastic silt	0.30 to 0.35
Very stiff and hard residual or preconsolidated clay	0.40 to 0.50
Medium stiff and stiff clay and silty clay	0.30 to 0.35

Table 37-1 Friction coefficient for cast concrete on soil [USACE Technical Letters]

### 37.2 Rotational stability

Between soil and the structure only compression stresses can develop. For the stability of shallow foundation structures, tensile stresses should not be taken into account for force equilibrium. Especially the adhesive and cohesive properties of sand are very poor, so in general, tensile stress cannot be provided by the subsoil. Therefore, it is usually stipulated that the soil stresses necessary for rotational stability may only be compressive (so, no tensile stresses allowed). This is the case if the resulting action force intersects the core of the structure. The core is defined as the area extending to 1/6 of the structure width on both sides of the middle of the structure (point K). In equation form:

$$e_R = \frac{\sum M}{\sum V} \leq \frac{1}{6}b \tag{37.1}$$

where:  $e_R$  [m] = distance from the moment centre (K) to the intersection point of the resulting force and the bottom line of the structure

$\sum V$  [N] = total of the acting vertical forces (or vertical components)

$\sum M$  [N] = total of the acting moments, preferably around point K, halfway the width

$b$  [m] = width of the structure

See Figure 37-2 for an illustration.

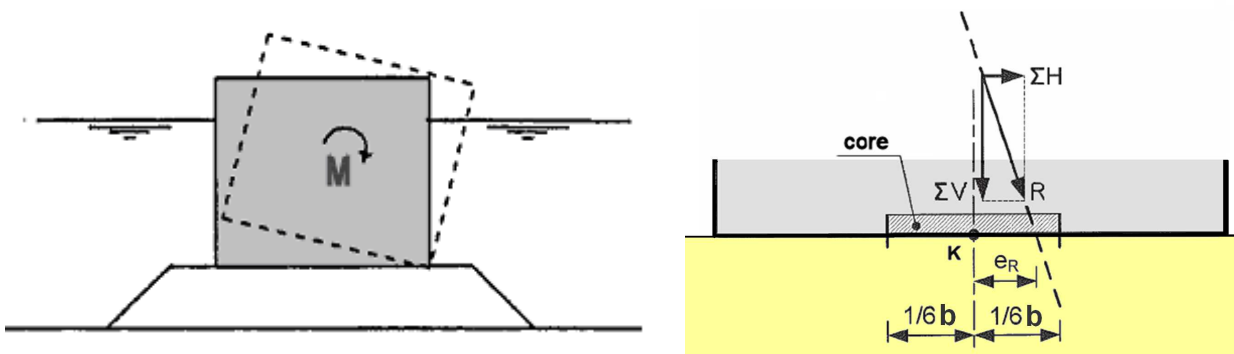


Figure 37-2 The action line of the resulting force should intersect the core of the structure  
The rotation depicted on the left side is very unusual. In reality, if there is a maximum load acting in just one point (the corner), the soil under the corner will immediately collapse. The adjoining soil then will start bearing the load.

If, however, the action line of the resulting force is situated outside the core of the structure, only part of the soil below the structure will contribute to the bearing, see Figure 37-3. In that case, the no-tensile criterion is not met. It actually can occur that even in this case the maximum occurring soil stress is not exceeded and the situation is not really problematic.

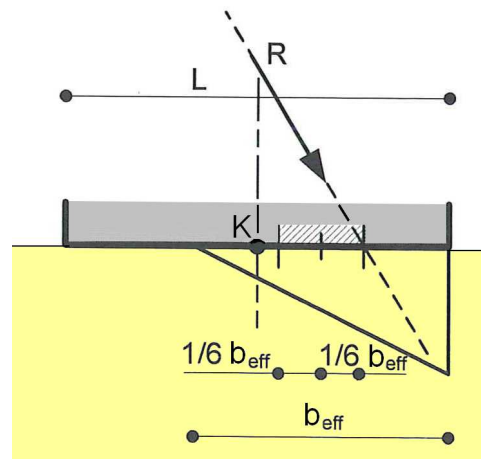


Figure 37-3 Action line of resultant force does not intersect the core of the structure

### 37.3 Vertical stability

The vertical effective soil stress, required to resist the acting loads ( $\sigma_{k,max}$ ), should not exceed the maximum bearing capacity of the soil ( $p'_{max}$ ), otherwise the soil will collapse:

$$\sigma_{k,max} < p'_{max} \quad (37.2)$$

The maximum acting load on the soil can be calculated with:

$$\sigma_{k,max} = \frac{F}{A} + \frac{M}{W} = \frac{\sum V}{b \cdot \ell} + \frac{\sum M}{\frac{1}{6} \ell b^2} \quad (37.3)$$

where:  $\sum V$  [N] = total of the acting vertical forces (or vertical components)  
 $A$  [m<sup>2</sup>] = area of the bottom plate  
 $W$  [m<sup>3</sup>] = section modulus of the contact area of the bottom plate  
 $b$  [m] = width of the structural element  
 $\ell$  [m] = length of the structural element  
 $\sum M$  [kNm] = total of the acting moments, preferably around point K, halfway the width

The bearing capacity  $p'_{max}$  can be calculated according to TGB 1990 (NEN 6744), which gives the Brinch Hansen method for determining the maximum bearing capacity of a foundation. This method takes into account the influence of cohesion, surcharge including soil coverage and capacity of the soil below the foundation, see Section 32.2 of this Manual (Part III).

As a rule of thumb (instead of the Brinch Hansen calculation), the bearing capacity of densely packed sand is often assumed to be 500 kN/m<sup>2</sup> (= 0,5 N/mm<sup>2</sup>).

The minimum acting load on the soil can be calculated with:

$$\sigma_{k,min} = \frac{F}{A} - \frac{M}{W} = \frac{\sum V}{b \cdot \ell} - \frac{\sum M}{\frac{1}{6} \ell b^2} \quad (37.4)$$

Because soil cannot or barely cope with tensile forces,

$$\sigma_{k,min} > 0 \quad (37.5)$$

### 37.4 Piping (internal backward erosion)

Groundwater flow under or besides a water or soil retaining structure is caused by a potential difference across the structure. Piping (*onderloopsheid*, or *achterloopsheid*) can occur at the plane separating the impermeable structure and a loose grain layer (Figure 37-4). Piping is the flow of water through a pipe-like channel that has been created by internal erosion. This phenomenon can occur along the foundation plane of a structure but also along a retention wall. Piping is also possible in dikes. Little "sand volcanoes" appear where the water flows out at ground level.

It is important to realise that two basic conditions have to be met before piping can occur:

1. The duration of the water level difference has to be sufficiently long to start this mechanism. This is the reason why piping under normal Dutch sea dikes has not yet been observed: water levels along the coast highly depend on tidal fluctuations.
2. Sand particles must have a possibility to extrude. So, if the ground level at the lower water table side is relatively high, piping becomes unlikely, just like in case of a closed and sufficiently strong surface. Before erosion can start, rupture of the top layer should occur. In case of low-permeable cohesive soil layer this phenomenon is called *uplift*; for sand (aquifer material) the term *heave* is used.

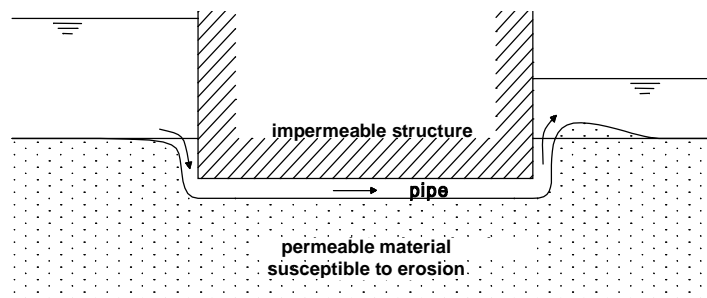


Figure 37-4 Piping

Empirical formulas based on research describe the critical situations in which piping can occur. The most famous are the Bligh and Lane formulas. According to these formulas there is a limit state with a critical ratio between the differential head and the seepage distance. More recent research has confirmed this. For the results of this research and the design rules that have been derived from it, one is referred to (Sellmeijer, 1988). It should be realised that the Bligh and Lane formulas are quite inaccurate and that they should only be used to get a first impression about possible piping problems.

W.G. Bligh was among the first to compose a formula for a safe seepage distance. He studied different structures like weirs, dams and barrages, mainly in the USA, India and France. Based on his observations, he developed a 'critical average gradient model' which determines the critical ratio between head difference and seepage length.

E.W. Lane extended Bligh's theory based on an investigation of over 200 masonry dams. Lane concluded that vertical structural parts are less likely to lead to a "pipe" (or 'line' or 'path') than horizontally placed parts. This is because the walls of a vertical line are more likely to collapse due to gravity, thereby blocking the line, than horizontal lines. In Lane's formula slopes with an angle of  $45^\circ$  or larger are treated as vertical, slopes at less than  $45^\circ$  are considered horizontal.

A sketch with horizontal and vertical seepage paths under a structure is presented in Figure 37-5.

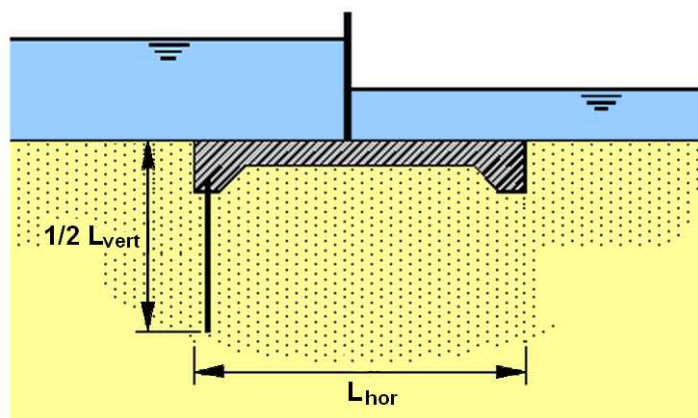


Figure 37-5 Horizontal and vertical seepage paths

Bligh assumes  $L = \sum L_{vert} + \sum L_{hor}$  and Lane assumes  $L = \sum L_{vert} + \sum \frac{1}{3} L_{hor}$ . On grounds of Lane's assumption, the soil constants also undergo changes compared to Bligh's constants (see Table 37-2). It should be noticed that for pile-founded structures  $L_{hor}$  should not be included in the total seepage length  $L$ , unless it is certain that the soil volume below the structure cannot decrease over time (which would lead to inter-space between soil and structure)

Piping method:	Bligh		Lane	
criterion	$L \geq \gamma \cdot C_B \cdot \Delta H$		$L \geq \gamma \cdot C_L \cdot \Delta H$	
used seepage length	$L = \sum L_{vert} + \sum L_{hor}$		$L = \sum L_{vert} + \sum \frac{1}{3} L_{hor}$	
	$C_B$	$i_{max}$	$C_L$	$i_{max}$
<b>Soil type:</b>				
Very fine sand / silt /sludge	18	5,6 %	8,5	11,8 %
Fine sand	15	6,7 %	7,0	14,3 %
Middle fine sand	-	-	6,0	16,7 %
Coarse sand	12	8,3 %	5,0	20,0 %
(fine) gravel (+sand)	5-9	11,1 – 20,0 %	4,0	25,0 %

Table 37-2 Safe seepage distance for piping

where:  $L$  [m] = total seepage distance, which is the distance through the soil where the water flow is impeded by the soil structure<sup>1</sup>  
 $C_B$  [-] = Bligh's constant, depends on soil type  
 $C_L$  [-] = Lane's constant, depends on soil type  
 $\Delta H$  [m] = differential head across structure  
 $\gamma$  [-] = safety factor (1,5)  
 $i_{max}$  [-] = maximum (allowed) hydraulic gradient =  $\Delta H / L$

In the Dutch design practice, both methods are being applied. Bligh's method is most suitable for the design of dikes, whereas Lanes' method is used to estimate whether piping will occur under water retaining structures because of the possibility of vertical piping lines.

J.B. Sellmeijer more recently (1988) developed a mathematical model to describe piping. The design rules resulting from this model lead to more favourable dimensions for the required horizontal piping line, compared to Bligh's method. Sellmeijers original model, however, is not applicable for vertical piping lines and is only suitable for the dimensioning of dikes. That is why he formulated additional design rules for the dimensioning of heave (*hydraulische grondbreuk*) behind seepage screens. These new design rules can be used if the piping criterion of Lane doesn't suffice.

According to Sellmeijer a piping channel becomes critical if its length exceeds half of the seepage length. If this occurs, the piping channel will progressively increase until failure. The observation of sand boils therefore does not immediately imply failure, but it is not very well possible to determine how safe the structure then still is.

<sup>1</sup> Notice that the horizontal distance under *pile-founded* structures should not be included in the horizontal seepage distance  $L_{hor}$ , because the subsoil can easily settle a bit while the pile-founded structure remains at its place (because of its foundation in a deep, stable ground layer). This results in an open space under the structure, where the water can flow without significant hindrance.

The critical water level difference can be computed with an empirical equation:

$$\Delta H = \alpha \cdot c \cdot L \cdot \left( \frac{\gamma_p}{\gamma_w} - 1 \right) \cdot (0,68 - 0,1 \cdot \ln c) \cdot \tan \theta_R > 0 \quad (37.6)$$

$$\alpha = \left( \frac{D}{L} \right)^{\frac{0,28}{\left( \frac{D}{L} \right)^{2,8} - 1}} ; c = \eta \cdot d_{70} \cdot \left( \frac{1}{\kappa L} \right)^{1/3} ; \kappa = \frac{\nu}{g} \cdot k$$

where:

$\alpha$	[-]	=	coefficient to include the limited thickness of the sand layer
$c$	[-]	=	erosion resistance coefficient for the soil layer
$L$	[m]	=	(horizontal) seepage length
$\gamma_p$	[kN/m <sup>3</sup> ]	=	specific weight of wet soil
$\gamma_w$	[kN/m <sup>3</sup> ]	=	specific weight of water
$\theta_R$	[°]	=	rolling friction angle
$D$	[m]	=	thickness of the sand layer
$\eta$	[-]	=	White's constant
$d_{70}$	[m]	=	0,70 grain size fractile of the sand
$\kappa$	[-]	=	intrinsic permeability
$\nu$	[m <sup>2</sup> /s]	=	kinematic viscosity
$k$	[m/s]	=	permeability
$g$	[m <sup>2</sup> /s]	=	gravitational acceleration

This method can only be used if sufficient specific soil parameters are known.

If a structure does not meet requirements for piping, the following solutions could be considered:

1. using (longer) sheet piling upstream as a screen against seepage
2. grout columns (making the soil impermeable and cohesive) (upstream)
3. inserting a diagonal protective textile in the ground (in front of the structure)
4. inserting a filter structure (downstream)

#### Notes

1. *The full and one third part of respectively the vertical and horizontal planes may only be taken into account if the following conditions are satisfied:*
  - *The building material must be in direct contact with undisturbed soil*
  - *The walls must be closed and must have a water-tight connection with the rest of the structure*
2. *The first condition means that if a structure has a pile foundation, which may allow settlements that create a split between the structure and the soil, the seepage path along the bottom slab may not be counted, unless extra measures are taken to seal the split.*
3. *One must not consider under-seepage only, but must also take backward seepage into account. Cut-off walls to prevent this are obviously placed in the same plane as the normal cut-off walls to prevent under-seepage. Furthermore, these walls are extended sideways beyond the loose ground of the building site.*
4. *It is very important to compact the soil around the structure so it erodes less easily.*

### 37.5 Scour protection

Bottom scour may affect the waves in front of the structure, which can lead to gradual dislocation of the sill and can decrease the geotechnical stability of the breakwater (Figure 37-6). Under the worst conditions, the scour depth in front of vertical breakwaters may reach values up to 0,7 times the original water depth.

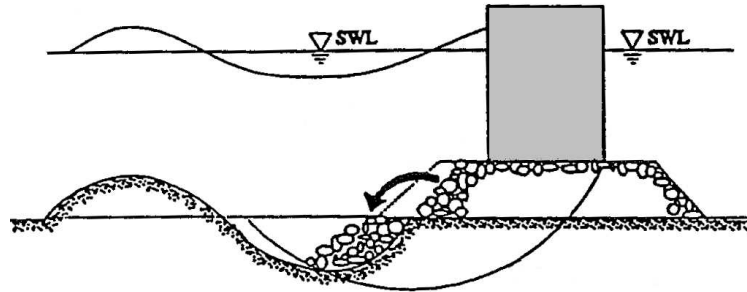


Figure 37-6 Effect of bottom scour on breakwater stability

Scour can be prevented by applying geometrically tight granular filters and more or less impermeable layers like concrete, asphalt and geotextile, see lecture notes of course CIE4310 'Bed, bank and shore protection' (Schiereck 2001).

#### Horizontal dimensions

In order to prevent scour at both sides of a closure dam, quite some research on the required length of a bed protection has been carried out during the execution of the Deltaworks in the Netherlands. This is reported by Pilarczyk in Section 2.4.9 of 'Closure of tidal basins' (In 't Veld, 1987). Details can also be found in the lecture notes on 'Bed, bank and shore protection' (Schiereck, 2001).

Because of turbulence and because there is only little transport over the protection, at the end of the scour protection an erosion hole is formed. The maximum depth of the hole at a given moment ( $h_{max}$ ) (Figure 37-7) can be calculated with the Breusers formula. When this scour hole becomes too deep, a critical slope 1:n can be exceeded in which case sliding is probable to occur. For normal packed sand this will result in normal sliding, but for loosely packed sand this may lead to liquefaction (*zettingsvloeiing*).

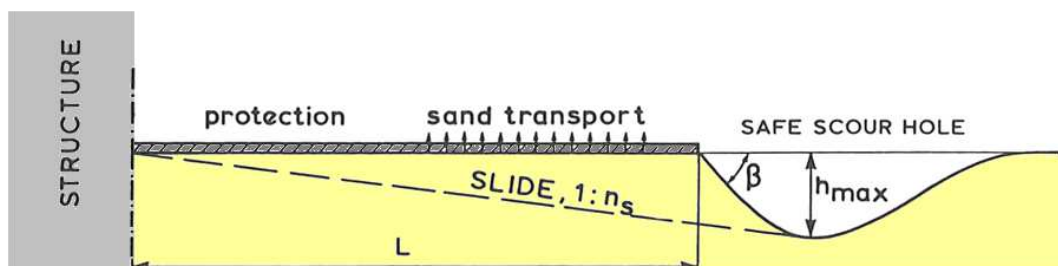


Figure 37-7 Length of bottom protection

For a first estimate, the required length of the bottom protection can be calculated with:

$$L \geq \gamma \cdot n_s \cdot h_{max} , \quad (37.7)$$

where:

$\gamma$	[-]	= safety factor ( $\geq 1,0$ )
$1:n_s$	[-]	= average slope of the slide
$h_{max}$	[m]	= maximum scouring depth

$n_s \approx 6$  for densely packed, or cohesive material,  $n_s \approx 15$  for loosely packed material

The upper scour slope,  $\beta$ , is usually much less steep than the natural slope of sediment under water. Usual values for  $\beta$  vary between  $18^\circ$  and  $26^\circ$ .

The time dependent scour formula of Breusers requires quite some information, which is difficult to obtain. A simplification can be achieved by calculating the equilibrium depth of the scour hole and assuming that there is no sand coming from upstream (clear water scour). In that case the maximum (= equilibrium) scour depth is given by:

$$\frac{h_{\max}}{h_0} = \frac{(0,5 \cdot \alpha \cdot u) - u_c}{u_c} \quad \text{for } (0,5 \cdot \alpha \cdot u) - u_c > 0 \quad (37.8)$$

where:

$h_0$	[m]	= initial water height
$h_{\max}$	[m]	= maximum depth of the scour hole (= equilibrium depth)
$u$	[m/s]	= depth-averaged flow velocity at the end of the bed protection
$u_c$	[m/s]	= critical velocity regarding begin of motion of sand particles
$\alpha$	[-]	= a coefficient to include turbulence effects. The value of $\alpha$ is in the order of 3.

The critical velocity  $u_c$  can be calculated with the Shields equation:

$$u_c = C \sqrt{\psi_c \cdot \Delta \cdot D_{n50}} \quad (37.9)$$

where:

$D_{n50}$	[m]	= median nominal diameter of sand particles
$C$	[ $\sqrt{\text{m/s}}$ ]	= Chézy coefficient: $C = 18 \cdot \log\left(12 \frac{R}{k_r}\right)$ and $k_r$ [m] = equivalent sand roughness $\approx 2 \cdot D_{n50}$
$\Delta$	[-]	= relative density: $\Delta = \frac{\rho_s - \rho_w}{\rho_w}$
$\psi_c$	[-]	= Shields (stability) parameter

The Shields parameter depends on the dimensionless grain diameter  $d_*$ :

$$d_* = D_{50} \cdot 3 \sqrt{\frac{\Delta \cdot g}{\nu^2}}$$

where  $\nu$  [ $\text{m}^2/\text{s}$ ] = kinematic viscosity

Figure 37-8 shows the relation between the shields parameter  $\psi_c$  and the dimensionless grain diameter  $d_*$  (lower horizontal axis). For normal circumstances (temperature, density), the value of  $\psi_c$  can be directly related to  $D_{50}$  (upper horizontal axis). Line 1 in this graph should be used for determining the scour depth. It indicates the threshold of motion of all grains. Line 2 should be used for stability calculations of the bed protection, because it indicates the threshold where no grains at all are moving.

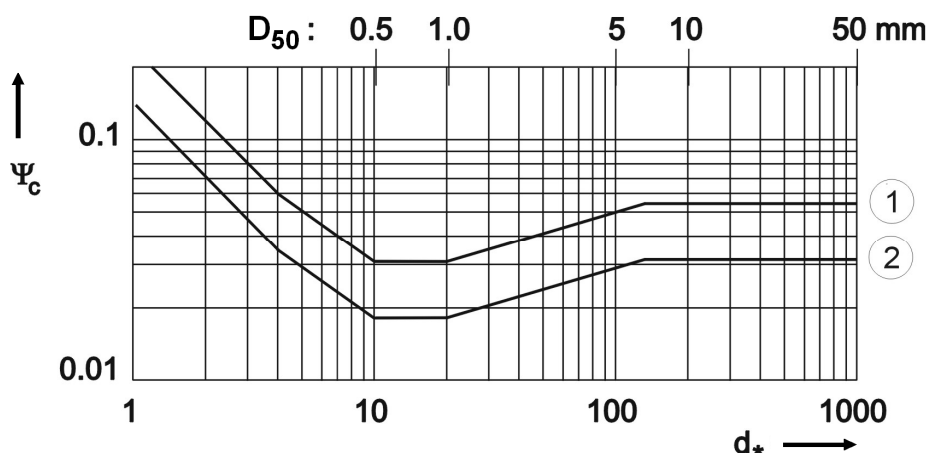


Figure 37-8 Relation between the Shields parameter and  $d_*$  or  $D_{50}$  for usual conditions (Schiereck 2001)

### **Maximum scouring depth**

If no information is available, the maximum scouring depth may be assumed to be of the same magnitude as the (initial) water depth  $h_0$ . This assumption, however, is rather rough and only to be used as a first indication.

### **Top and filter layers**

(Partly translated from lecture notes Hydraulic Engineering CTB1120)

In general, there are three types of scour protection, viz.:

- granular filter
- asphalt concrete
- geotextile

The granular filter type is the most commonly used and will be dealt with in the following paragraphs.

A granular filter should be designed in such a way, that grains in the basic layer cannot pass the holes of the filter. The holes in the granular filter exist of the pores in the grain packet that are interconnected by small pore channels. If the diameter of the pore channels  $D_c$  is smaller than the diameter of the governing grains of the basic layer  $D_b$ , no transport can take place, irrespective of the value of the water level slope, the direction and type (stationary or not) of the flow.

It has been empirically found that the diameter of a characteristic pore channel  $D_c$  in a granular layer meets with:  $D_c \approx 0,2 D_{f15}$  ( $D_{f15}$  is the size of the holes in a sieve, through which passes 15 percent by weight of the material, see Dutch standard NEN 2560).

The governing grain size of the basic layer is about  $D_{85}$ . If grains with the governing diameter cannot be transported, also smaller grains cannot be transported.

A layer is geometrically tight, if

$$\frac{D_{f15}}{D_{b85}} < 5. \quad (37.10)$$

This only applies if the sieve curve of the basic material does not differ too much from the curve of the filter material. If a layer is widely graded, internal instability can occur. In that case, the small grains can be transported through the channels of the big ones. Internal stability can be expected if:

$$\frac{D_{60}}{D_{10}} < 10, \quad (37.11)$$

which should also be the case for a filter layer.

To avoid overpressure perpendicular to the separating layer, the filter layer should be more permeable for water than the basic layer. In general, smaller grain diameters imply smaller permeability. In graded layers principally small grains of about  $D_{15}$  determine the permeability. During the lifetime of the structure, the diameters of the pore channels can decrease because of siltation with material from the basic layer, or because of deterioration (*verwering*). It is difficult to check up on this effect and eventual repairs are practically nearly impossible. Therefore, an extra requirement for permeability should be met:

$$\frac{D_{f15}}{D_{b15}} > 5 \quad (37.12)$$

For geotextile filters, similar rules apply. A geotextile is considered to be tight if the larger fraction of the grains of the basic layer cannot pass the characteristic pores of the geotextile:

$$O_{90} < D_{b90}, \text{ which is very strict, and usually: } O_{90} < 2D_{b90}$$

where  $O_{90}$  = the diameter of the fraction of which 90 weight-percentage remains on the geotextile after 10 minutes of sieving (so it is not an indication for the pore size distribution!)

If the basic material has a wide gradation ( $D_{60}/D_{10} > 10$ ),  $D_{60}$  in the equation can be replaced with  $D_{50}$ .

To avoid overpressure in vertical direction, the filter should be more permeable than the basic material. In this case the permeability coefficient of the geotextile should be more than the permeability coefficient of the basic layer:

$$k_{ng} > \gamma k_b \quad (37.13)$$

where:

$$\begin{aligned} k_{ng} \quad [\text{m/s}] &= \text{permeability coefficient of the geotextile} \\ \gamma \quad [-] &= \text{safety coefficient, dependent on the composition of the basic material:} \\ &\quad \gamma = 2,5 \text{ for a uniform grain distribution,} \\ &\quad \gamma = 10 \text{ for a highly graded material } (D_{60}/D_{10} > 10) \\ k_b \quad [\text{m/s}] &= \text{permeability coefficient of the basic layer} \end{aligned}$$

The permeability can be determined with help of a straightforward test, using a glass tube filled with soil, connected with two reservoirs of water - see the book on 'Soil Mechanics' by Verruijt/Van Baars, Section 8.1.

### 37.6 References

Bligh, W.G. (1915) Submerged weirs founded on sand. In: Dams and weirs, 1915.

Huis in 't Veld, J.C. (1987) Closure of tidal basins, Delft University press, ISBN 90-6275-287-X.

Kanning, W. (2013) The weakest link. Spatial variability in the piping failure mechanism of dikes. PhD-thesis Delft University of Technology.

Lane, E.W. (1935) Security from under-seepage. Masonry dams on earth foundations. Transactions American Society of Civil Engineers, no. 100.

Schiereck, G.J. (2001) Introduction to Bed, Bank and Shore Protection, VSSD, ISBN ISBN 978-90-407-1683-6.

Schweckendiek, T. (2014) On reducing piping uncertainties. A Bayesian decision approach. PhD-thesis Delft University of Technology.

Sellmeijer, J.B. (1988) On the mechanism of piping under impervious structures. PhD-thesis Delft University of Technology.

## 38. Stability of floating elements

Minor revision: February 2011, additional clarifications: February 2015

To ensure that floating elements do not undesirably move or rotate, they should be statically and dynamically stable. The stability of a floating element depends on forces and moments, and the shape of the element.

### 38.1 Static stability

#### **Equilibrium of vertical forces**

Vertical forces establish an equilibrium if the buoyant force (*opwaartse kracht*) equals the weight of the floating body (including all ballast). For a floating body, this buoyant force has the same magnitude as the weight of the displaced volume of fluid (Archimedes' principle: a floating body displaces its own weight of fluid).

A vertical equilibrium is usually reached if the element is floating, or if it is resting on the bottom of the water body. If there is no equilibrium, a completely immersed element will move upward or downward until an equilibrium state is reached. An element will move upward if the buoyancy is more than the total weight of the element. Then, at a certain moment, the part of the element rising out of the water will result in a decrease of the buoyant force in such an amount that this buoyant force equals the weight of the element. It then stops moving upward. An element, conversely, will sink if the weight of the element exceeds the buoyant force, until it reaches the bottom. The bottom will resist the downward directed force and will stop the element moving down.

#### **Equilibrium of moments**

For the design of large-scale prefabricated elements, vessels and dredging equipment, not just the weight is of importance. There must also be an assurance that the elements do not tilt in an unacceptable degree during the floating transport or the immersing procedure. Tilting can be initiated by the mooring forces, wave motions, and inlet of water during immersion, etc. Elements must therefore be designed or equipped in such a way that a rotation, caused by external factors, is corrected by a righting moment that will return the element to its original position.

If the sum of moments around the point of rotation (= point of gravity) equals zero, the element will not incline to tilt. This principle is illustrated in Figure 38-1, where equilibrium is not reached yet. It will tilt in such a way that an equilibrium will be reached.

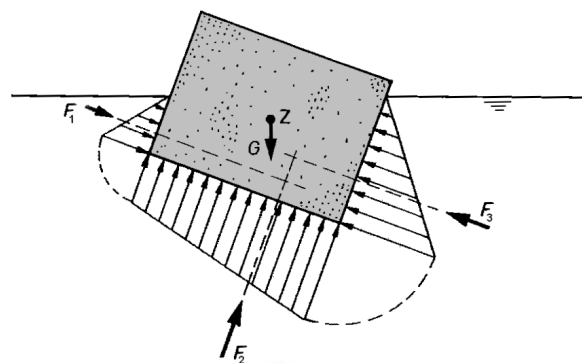


Figure 38-1 Forces acting on a floating element (Nortier, 1991)

### Static stability - metacentric height

A check of the equilibrium of moments (previous paragraph) is sufficient if an element is floating in still water. In reality, however, this is rarely the case. This is why also the 'sensitivity to tilting' has to be taken into account. A measure for the resistance to tilting is given by the 'metacentric height'. The principle is illustrated in Figure 38-2. The left side depicts the cross-section of a floating element (like a caisson). On the right side the same element is showed in tilted position. The rotation angle is  $\varphi$ .

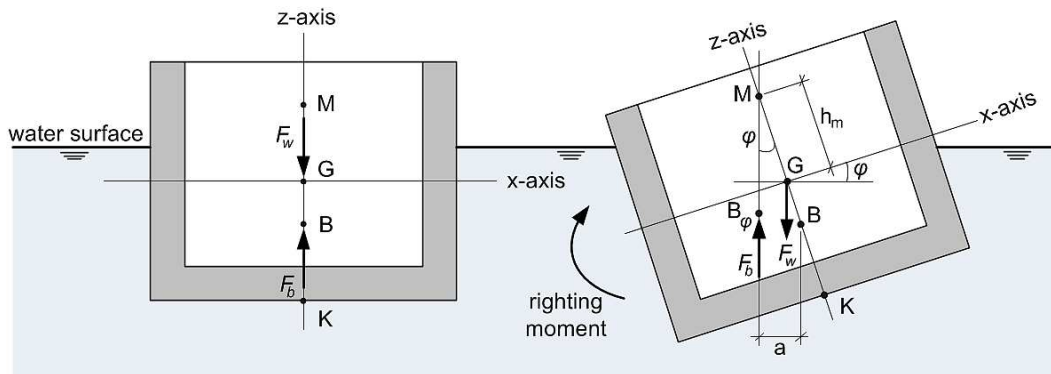


Figure 38-2 Floating element

Indicated are three points, which are of importance in the evaluation of the stability:

- B is the centre of buoyancy (*drukingspunt*), the point of application of the buoyant force  $F_b$  in state of equilibrium (the state in which the axis of symmetry of the element is vertical). B is therefore the centre of gravity of the displaced water. In a rectangular container (caisson), B is found halfway between the water surface and the bottom of the element. In tilted position the centre of buoyancy shifts to a new position because the geometry of the displaced volume has changed. The shifted centre of buoyancy is indicated with  $B_\varphi$  and the horizontal shift is  $a$  [m].
- G is the centre of gravity (*zwaartepunt*) of the element. If the element is filled with a layer of gravel or water for the benefit of the immersing procedure (not shown in Figure 38-2), this weight should also be taken into account when calculating G. Not only will this ballast lower the centre of gravity, it will also increase the draught and will therefore raise B relative to the bottom. If the element heels over, the centre of gravity generally remains fixed with respect to the element because it just depends upon the position of the element's weight and ballast. The centre of gravity at the same time is the rotation point.
- M is the metacentre; the point of intersection of the axis of symmetry, the z-axis, and the action line of the buoyant force in tilted position. For small rotations ( $\varphi < 10^\circ$ ) the metacentre is a fixed point (see lecture notes OE4652, 'Floating Structures' for a proof). The determination of point M is explained below.

For static stability, rotation of the element should be compensated by a righting moment caused by the buoyant force and the weight of the element. This is the case if M is located over G: the line segment  $\overline{GM}$ , also known as the metacentric height  $h_m$ , must be positive.

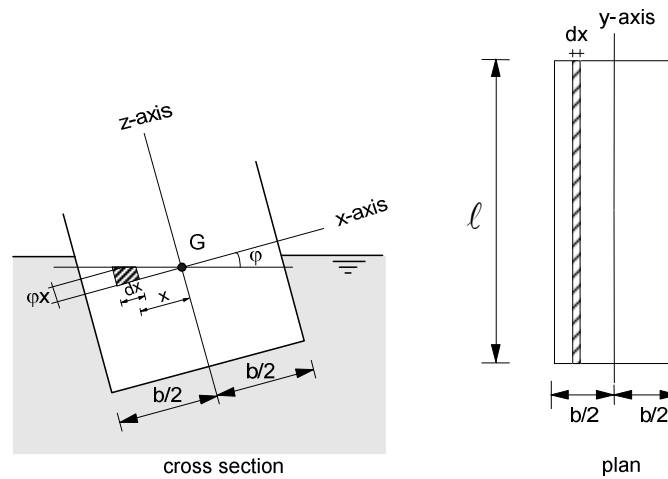


Figure 38-3 Tilted element

Figure 38-3 shows an element with a rotation  $\phi$ . The part  $dx$ , which has been forced under water by the rotation, experiences a buoyant force:

$$dF_b = \phi x dx \ell \rho_w g \tag{38.1}$$

in which  $\rho_w$  is the volumetric mass of water. This equation is only valid for rotations smaller than  $10^\circ$  in which case  $\tan \phi \approx \phi$  [rad]!

Relative to G this gives a moment  $dM = x dF_b = \phi x^2 dx \ell \rho g$ .

Over the entire width this means a righting (corrective) moment of:  $M = \int_{x=-b/2}^{+b/2} \phi x^2 dx \ell \rho g$ , which could

$$\text{be rewritten as } M = \phi \rho g \int_{x=-b/2}^{+b/2} x^2 \ell dx \tag{38.2}$$

Because  $\int_{x=-b/2}^{+b/2} x^2 \ell dx$  represents the area moment of inertia (a.k.a. 'second moment of area') relative to the y-axis,  $I_{yy}$ , the expression for the moment can be formulated as:

$$M = \phi \rho g I_{yy}, \text{ in which } I_{yy} = \frac{1}{12} \ell b^3. \tag{38.3}$$

The point of application of the buoyant force ( $F_b$ ) in a state of rest, is the centre of buoyancy B. A rotation  $\phi$  leads to a translation of the line of action of  $F_b$  over a distance  $a$  (see Figure 38-2).  $M = F_b \cdot a$ , so:

$$a = \frac{M}{F_b} = \frac{\phi \rho g I_{yy}}{\rho g V} = \frac{\phi I_{yy}}{V_{dw}} \tag{38.4}$$

In this equation,  $V_{dw}$  is the volume of the immersed part of the element (= the volume of the displaced water).

$$\text{Because } \sin \phi = \frac{a}{\overline{BM}}, \overline{BM} = \frac{a}{\sin \phi} \approx \frac{a}{\phi} \tag{38.5}$$

$$\text{So, } \overline{BM} \approx \frac{I_{yy}}{V_{dw}} \tag{38.6}$$

For small rotations ( $\phi < 10^\circ$ ) the metacentre is a fixed point, but  $\overline{BM}$  increases because the position of B will go down. In case of considerable rotations, the metacentre displaces upward and sideways in the opposite direction in which the ship has rolled and is no longer situated directly above the centre of gravity.

If M is positioned above G, a righting moment  $F_b h_m \varphi = \rho g V_{dw} h_m \varphi$  is created, which tries to return the element to its stable position.

For small seagoing vessels a metacentric height  $h_m$  of at least 0,46 m is required. A ship with a small metacentric height will be "tender" - have a long roll period. A low metacentric height increases the risk of a ship capsizing in rough weather and more likely to develop "synchronized rolling". It also puts the vessel at risk of potential for large angles of heel if the cargo or ballast shifts. If a ship with low  $h_m$  is damaged and partially flooded, the metacentric height will be reduced further and will make it even less stable.

For large ships  $h_m$  should be at least 1,1 m, but not too large because in that case the vessel will be too 'stiff': it will snap back upright too quickly after a wave or wind gust has passed, which will cause heavy stresses in the structural parts of the vessel, maybe shifting of the cargo and not unlikely sea sickness of the persons on board.

The requirements for caissons and tunnel elements are less tight: 0,5 m suffices for  $h_m$ . If M is positioned below G, the element is unstable and will tilt.

### **Check design static stability**

The check of the static stability (in this case also known as the outset stability, because only small rotations of the element are investigated) is made up of the following steps:

- Calculate the weight  $F_w$  and the position of the gravity centre G of the floating element with reference to K ( $\overline{KG}$ ). K is the intersection of the z-axis with the bottom line of the element. In general,

$$\overline{KG} = \frac{\sum V_i \cdot e_i \cdot \gamma_i}{\sum V_i \cdot \gamma_i}, \quad (38.7)$$

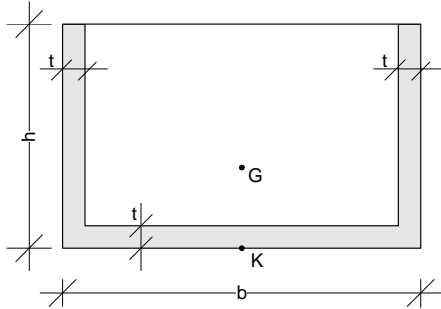
where  $V_i$  [m<sup>3</sup>] = volume of element  $i$   
 $\gamma_i$  [kN/m<sup>3</sup>] = specific weight of element  $i$   
 $e_i$  [m] = distance between gravity centre of element  $i$  and reference level  
 (which is a horizontal plane through point K)

- Calculate the draught  $d$  of the element.
- Locate the centre of buoyancy B and calculate its position above the bottom of the element. This distance is  $\overline{KB}$ . In case of rectangular elements,  $\overline{KB} = \frac{1}{2}d$
- Determine the shape of the area at the fluid surface and compute the smallest area moment of inertia  $I$  for that shape (this is the most unstable). For rectangular elements:  $I_{yy} = \frac{1}{12} \cdot \ell \cdot b^3$ .
- Compute the volume of the displaced water  $V_{dw}$ .
- Compute  $\overline{BM} = \frac{I_{yy}}{V_{dw}}$
- Calculate  $h_m = \overline{GM} = \overline{KB} + \overline{BM} - \overline{KG}$
- Theoretically, if  $h_m > 0$ , the body is stable. In practice,  $h_m > 0,50$  m is recommended. If  $h_m < 0,50$ , additional measures are required.

Besides the static stability, the dynamic stability (the oscillation) must also be checked. This will be explained later in this chapter.

### Example metacentre

Check the static stability of a reinforced concrete element, floating in a salty lake. See the following figure.



$l = 25,00$  m (outside dimension)  
 $b = 8,00$  m  
 $h = 4,50$  m  
 $t = 0,50$  m (also for head walls)  
 $\gamma_{\text{concrete}} = 25,00$  kN/m<sup>3</sup>  
 $\gamma_{\text{water}} = 10,06$  kN/m<sup>3</sup>

The total weight of the element is:

$$F_w = \{(25,00 \times 8,00 \times 4,50) - (24,00 \times 7,00 \times 4,00)\} \times 25,00 = 5700 \text{ kN (don't forget the head walls!).}$$

Because of the asymmetry, the position of the centre of gravity G will be lower than halfway the element height:

$$\begin{aligned} \overline{KG} &= \frac{b \times h \times l \times \frac{h}{2} - (b-2t)(h-t)(l-2t)\left(t + \frac{(h-t)}{2}\right)}{b \times h \times l - (b-2t)(h-t)(l-2t)} = \\ &= \frac{900,00 \times 2,25 - 672,00 \times 2,50}{900,00 - 672,00} = 1,513 \text{ m} \end{aligned}$$

The draught is:

$$d = \frac{F_w}{b \times l \times \gamma_w} = \frac{5700}{8,00 \times 25,00 \times 10,06} = 2,833 \text{ m, so distance } \overline{KB} = d / 2 = 1,417 \text{ m.}$$

$$I_{yy} = \frac{1}{12} l \times b^3 = \frac{1}{12} \times 25,00 \times 8,00^3 = 1067 \text{ m}^4;$$

$$V_{dw} = l \times b \times d = 25,00 \times 8,00 \times 2,833 = 566,7 \text{ m}^3.$$

$$\overline{BM} = \frac{I_{yy}}{V_{dw}} = \frac{1067}{567} = 1,882 \text{ m}$$

$$h_m = \overline{KB} + \overline{BM} - \overline{KG} = 1,417 + 1,882 - 1,513 = 1,786 \text{ m}$$

$h_m > 0,50$  m, so the element is statically stable.

### Measures for unstable elements

If the element is unstable, the design should be altered or additional measures have to be taken.

Examples of design alterations are:

- widening of the element, thereby increasing the area moment of inertia  $I$  (usually the floor thickness will increase too, because of strength requirements).
- making the floor of the element heavier. This lowers G and increases the draught (if the transport route allows for this), which raises B relative to the bottom of the element. Unfortunately  $V$  also increases, which decreases  $\overline{BM}$ , but the other effects dominate, so the stability is increased.

Examples of additional measures are:

- adding ballast to the element (below the point of gravity) during transport.
- the use of stabilising pontoons or vessels (see
- Figure 38-4a), which increases  $I_{yy}$ .
- linking two elements during the floating transport (see

- Figure 38-4b), which increases  $I$ . Before the elements are disconnected at their destination, extra ballast must be applied to ensure the stability of the individual elements.

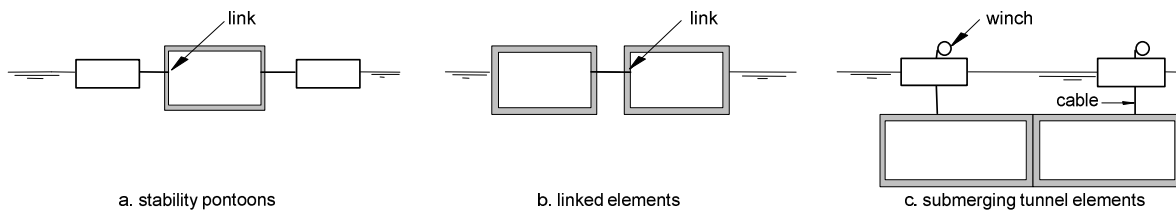


Figure 38-4 Stabilizing measures

If the required stability is achieved, one can opt to alter the design or use additional measures. Of course combinations of both are also possible.

Stability during immersion

Floating tunnel elements generally owe their stability to their large area moment of inertia. Once the elements have been given extra ballast, they immerse under water and no longer have a plane intersected by the waterline. The area moment of inertia is then zero. Stability is then only achieved if B is positioned above G. However, the elements are lowered on four cables using winches placed on four pontoons (see Figure 38-4c). This way, the elements are lowered accurately and in a controlled fashion. The element and the four pontoons together act as one system, which, around the pontoons, does have a plane that is intersected by the waterline and thus has an area moment of inertia. By positioning the pontoons as closely to the corners of the element as possible, large moments of inertia arise, both in the transverse direction and alongside the element.

Water ballast in the immersing process (free surface effect)

The use of water as ballast to immerse elements is attractive because it is a fast method and filling up with water can be simply accomplished by opening the valves (mostly placed in or just above the floor).

If a closed element (i.e., with a roof) is completely filled with water, it acts in effect as a solid mass. This means that its weight can be regarded as being concentrated at its centre of gravity. If the element is only partly filled, or completely but not having a roof, the water surface is free to move and therefore possesses inertia. This causes a destabilising effect for the element, which can also be observed from Figure 38-5a. Due to the rotation, the depth of the ballast water increases on the left and reduces on the right. This results in a moment which amplifies the rotation. If the inner space of the element is partitioned, as is shown in Figure 38-5b, the moment driven by the ballast water decreases.

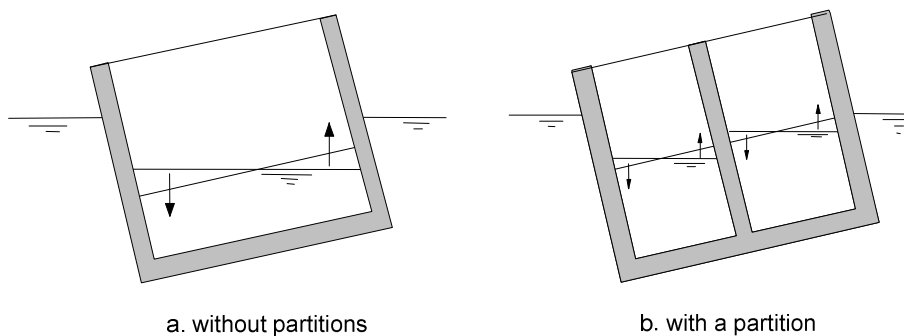


Figure 38-5 Water ballast

The unfavourable influence of the ballast water on the stability can be discounted by defining  $I$  as:

$$I_{yy} = I_{caisson} - \sum I_{comp,i} \tag{38.8}$$

in which:

- $I_{caisson}$  [ $m^4$ ] = area moment of inertia of the plane intersected by the waterline if there would be no water in the caisson
- $I_{comp}$  [ $m^4$ ] = area moment of inertia of the ballast water area relative to the gravity centre line of the compartment concerned

It should be noticed that Steiners theorem (*verschuivingsregel van Steiner*) is not applicable here. This can be explained with help of a somewhat different approach to the free surface effect (just another explanation of the same phenomenon):

The centre of gravity of a compartment filled with a fluid will shift if the caisson (including the compartment) is tilted. It shifts towards the lowest side of the compartment (moving away from the bottom of the caisson). The shift of the gravity centre of the compartment in horizontal direction, similar to equation (38.4) that expresses the shift of the centre of buoyancy, is:

$$\overline{gg'} = \frac{I_{comp}}{V_{comp}} \cdot \varphi \quad (38.9)$$

where:

$$\begin{aligned} I_{comp} \quad [m^4] &= \text{area moment of inertia of a compartment relative to its own axis through} \\ &\quad \text{the water surface in the compartment} \\ V_{comp} \quad [m^3] &= \text{volume of water in the compartment} \\ \varphi \quad [\text{radians}] &= \text{rotation angle} \end{aligned}$$

If the density of the liquid in the compartment differs from the water outside the caisson, this should be taken into account according to:

$$\overline{gg'} = \frac{\rho_{comp}}{\rho_{outside\ water}} \cdot \frac{I_{comp}}{V_{dw}} \cdot \varphi \quad (38.10)$$

The shift of the gravity centre of the compartment results in a shift in the gravity centre of the entire caisson. This shift of the gravity centre of the entire caisson in horizontal direction is:

$$\overline{GG'} = \frac{\overline{gg'} \cdot V_{comp}}{V_{dw}} = \frac{\left( \frac{I_{comp}}{V_{comp}} \cdot \varphi \right) \cdot V_{comp}}{V_{dw}} = \frac{I_{comp}}{V_{dw}} \cdot \varphi \quad (38.11)$$

where:

$$\begin{aligned} \overline{gg'} \quad [m] &= \text{horizontal shift of the gravity centre of the compartment} \\ V_{comp} \quad [m^3] &= \text{volume of the water in the compartment} \\ V_{dw} \quad [m^3] &= \text{total volume of 'outside water' displaced by the caisson} \\ \varphi \quad [\text{radians}] &= \text{rotation angle} \end{aligned}$$

This corresponds to a rise of the gravity centre of the caisson of  $\overline{GG''}$  (in z-direction):

$$\overline{GG''} = \frac{\overline{GG'}}{\varphi} = \frac{I_{comp}}{V_{dw}} \cdot \frac{\varphi}{\varphi} = \frac{I_{comp}}{V_{dw}}, \quad (38.12)$$

which is also called the 'free surface correction'.

For multiple compartments, the free surface corrections for the separate compartment have to be added up to find the total free surface correction.

The rise of the gravity centre could be expressed as a decrease of the value of  $\overline{BM}$ :

$$\overline{BM'} = \overline{BM} - \overline{GG''} = \frac{I_{caisson}}{V_{dw}} - \sum \frac{I_{comp,i}}{V_{dw}} = \frac{I_{caisson} - \sum I_{comp,i}}{V_{dw}}, \quad (38.13)$$

so actually the shift of the caisson gravity centre can be expressed as a decrease of the area moment of inertia:

$$I_{yy} = I_{caisson} - \sum I_{comp,i}, \text{ indeed without applying Steiners theorem. Q.E.D.}$$

---

### Example ballast water and compartmentation

Suppose that in Figure 38-5a the external width of the element is 10 m and the internal width is 9 m. Let us consider 1 m length of the element (perpendicular to the plane of drawing).

Without ballast water:  $I = \frac{1}{12} \times 1 \times 10^3 = 83,3 \text{ m}^4 / \text{m}$

With ballast water:  $I = 83,3 - \frac{1}{12} \times 1 \times 9^3 = 22,5 \text{ m}^4 / \text{m}$

The use of a partition, as shown in Figure 38-5b, has a positive effect on the stability. Suppose that the dimensions are equal to those in the previous calculation example and that the partition wall (bulk head) is 0.4 m thick, in that case:

With partition walls (and the compartments filled with water):  $I = 83,3 - 2 \times \frac{1}{12} \times 1 \times 4,3^3 = 70,0 \text{ m}^4 / \text{m}$

A larger number of partitions increases  $I$ , and therefore increases the stability.

Notice that the area moment of inertia for an empty compartmented caisson is the same as for an empty caisson without compartments. The area intersecting the water plane, after all, is the same in both circumstances.

---

Not only in transverse direction, as treated above, but particularly lengthways is the creation of compartments beneficial for the stability!

The partitions, which incidentally won't always be used and not for every type of prefab element, also have the following advantages:

- Smaller spans (and so smaller moments and shear forces) of outer walls, floor and if present, roof.
- Realization of a better flow of forces. Concentrated loads (*puntlasten*) like shipping and crane wheel loads can be resisted more easily.
- Correcting the tilt (trimming) during the immersing process, by letting more (or less) water into one compartment than into the other.

### Notes

- *Water is let into ballast tanks during the immersion of tunnel elements. These tanks are of limited sizes, in order to keep  $I_{comp}$  as small as possible.*
- *Working without tanks: letting water straight into the elements, immediately leads to tilting, especially lengthways.*
- *Rainwater tanks used by farmers are often used as ballast tanks. These tanks are easy to fix and remove and are also relatively inexpensive.*
- *The mentioned stability problems do not occur if sand or gravel is used as ballast material, provided that the material is spread evenly (so there is no unnecessary tilt) and that a coincidental unwanted tilt does not lead to the sliding of the ballast material.*

### 38.2 Dynamic stability

Not only the static stability but also the dynamic stability should be checked. If an element is transported over water, it will be affected by waves or swell (*deining*). This can cause the element to swing (*slingeren*), which can cause problems with respect to navigability and clearance (*kielspeling*).

#### Swing

If the dimensions (length or width) of a floating element are too small compared to the length of the waves or swell, the element will start swinging on the waves (*rolling* or *pitching*). In practice, the following rule of thumb is being used in engineering practice:

$$L_w < 0,7 \cdot \ell_e \quad \text{or} \quad Lw < 0,7 \cdot b_e$$

(dependent on the direction of the waves relative to the caisson)

where:

$$\begin{aligned} L_w \quad [\text{m}] &= \text{wave length} \\ \ell_e \quad [\text{m}] &= \text{length of the floating element} \\ b_e \quad [\text{m}] &= \text{width of the element} \end{aligned}$$

If this condition does not apply, problems due to swinging of the element can be expected.

#### Natural oscillation

Worse than just swaying on the waves or on the swell is the movement of an element if the period of the water movements comes close to the natural oscillation period (*eigenperiode*) of the element. In order to prevent this, one must ensure that the natural oscillation period of the element differs significantly larger from that of the waves or swell. For example, long swell was a problem for the transport of caissons in the bay of South Africa. If the natural oscillation period could be a problem and adjustments of the design or additional measures do not offer a solution, or are too expensive, the transportation and positioning at the final location should be postponed until favourable wave conditions come back. This can, however, lead to serious delays and thus larger costs. Therefore one should conduct a cost optimisation: on the one hand the costs of additional measures and/or design alterations, on the other hand the costs of possible delays.

Ignoring the hydrodynamic mass (the additional water mass) and damping, the natural oscillation period  $T_0$  can be calculated by considering the angular acceleration and the righting moment of the floating body. For small rotational angles, the body can be assumed to oscillate around its metacentre. The angular acceleration by definition is:

$$\alpha(t) = -\frac{d\omega}{dt} = -\frac{d^2\varphi}{dt^2} \quad [\text{rad/s}^2] \quad (38.14)$$

where:

$$\begin{aligned} \omega \quad [\text{m/s}] &= \text{angular velocity} \\ \varphi \quad [\text{rad}] &= \text{rotation after time } t \\ t \quad [\text{s}] &= \text{time} \end{aligned}$$

The direction of the angular acceleration  $\alpha(t)$  is towards the equilibrium position, hence the minus sign. The mass moment of inertia (so not the second moment of area, also called the area moment of inertia!) of the floating body about the centre of gravity is:

$$I_G = \frac{G}{g} j^2 \quad [\text{kg m}^2] \quad (38.15)$$

where:

$$\begin{aligned} G \quad [\text{N}] &= \text{weight of the floating body} \\ g \quad [\text{m/s}^2] &= \text{gravity acceleration} \\ j \quad [\text{s}] &= \text{radius of gyration about the horizontal axis through the gravity centre} \end{aligned}$$

The radius of gyration (*polaire traagheidsstraal*)  $j$  can be found according to:

$$j = \sqrt{\frac{I_{polar}}{A}}, \quad (38.16)$$

where  $A$  is the area of concrete in a vertical cross-section.

The polar moment of inertia  $I_{polar}$  is a measure for accelerated rotation and should in this case be considered around the  $y$ -axis:

$$I_{polar} = \int_A r^2 dA = I_{xx} + I_{zz}, \quad (38.17)$$

where  $I_{xx}$  = rectangular moment of inertia respective to the  $z$ -axis, and  $I_{zz}$  = rectangular moment of inertia respective to the  $x$ -axis, both in relation to the centre of gravity  $G$ .

The mass moment of inertia of the body about the metacentre is:

$$I_M = \frac{G}{g} (j^2 + h_m^2) \quad (38.18)$$

where:

$$h_m \text{ [m]} = \text{metacentric height}$$

If the metacentric height is small compared to the radius of gyration,  $I_G \approx I_M$ . For small angles of rotation, the righting moment equals the mass moment of inertia multiplied with the angular acceleration:

$$M = I \cdot \varphi = G h_m \varphi = I_G \frac{-d^2 \varphi}{dt^2} \quad (38.19)$$

After substituting the equation for  $I_G$ , it is obtained that:

$$G h_m \varphi = -\frac{G}{g} j^2 \frac{d^2 \varphi}{dt^2} \quad (38.20)$$

It can then be deduced that:

$$\frac{d^2 \varphi}{dt^2} + \frac{g \cdot h_m \cdot \varphi}{j^2} = 0 \quad (38.21)$$

The solution of an equation in the shape  $\frac{d^2 y}{dx^2} + a^2 y = 0$  is given by  $y = A \cdot \sin(ax) + B \cdot \cos(ax)$ , so in our case the solution is:

$$\varphi = A \cdot \sin \sqrt{\frac{g \cdot h_m}{j^2}} \cdot t + B \cdot \cos \sqrt{\frac{g \cdot h_m}{j^2}} \cdot t \quad (38.22)$$

If  $t = 0$ , also  $\varphi = 0$  and therefore  $B = 0$ , it follows from equation (38.22) that :

$$A \cdot \sin \left( \frac{g \cdot h_m}{j^2} \right) \cdot t = 0 \quad (38.23)$$

If still  $\varphi = 0$ , and  $t = \frac{1}{2} T_0$  (where  $T_0$  is the period of a complete oscillation), this can be rewritten as:

$$A \cdot \sin \left( \frac{g \cdot h_m}{j^2} \right) \cdot \frac{T_0}{2} = 0 \quad (38.24)$$

Since  $A \neq 0$ , this is only true if:

$$\sin\left(\frac{g \cdot h_m}{j^2}\right) \cdot \frac{T_0}{2} = 0 \quad (38.25)$$

The simplest solution of this equation is:

$$\sqrt{\frac{g \cdot h_m}{j^2}} \cdot \frac{T_0}{2} = \pi \quad (38.26)$$

from which the expression for the natural oscillation period can be found:

$$T_0 = \frac{2 \pi j}{\sqrt{g \cdot h_m}} \quad (38.27)$$

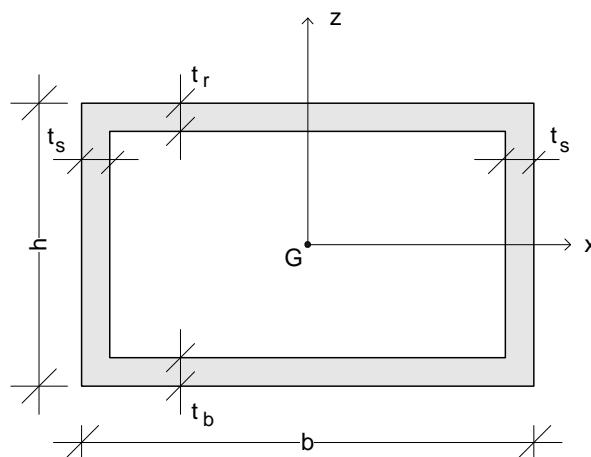
If the natural oscillation frequency is much larger than the wave or swell frequency, the element is dynamically stable for oscillations (rotation). Wave period statistics for the Dutch North Sea can be found on internet: <http://www.golflimaat.nl>.

A large natural oscillation period is gained by a large polar inertia radius. A large metacentric height, however advantageous for the static stability, decreases the natural oscillation period.

The same type of calculation has to be carried out for dynamic stability for pitching (vertical translation instead of rotation), but this calculation method is not discussed here. A good example of pitching is the rolled up mat that was used for the Oosterschelde storm surge barrier. This floating roll weighed 9000 tonnes and moved 0,60 m up and down in calm seas ( $H = 0,20$  m en  $T = 9$  s). Pitching can also be a problem for dredging vessels, because the cutter can hit the seabed.

### Example dynamic stability

Given: A caisson with a rectangular cross-section and a roof will be transported and immersed somewhere in a Dutch inland waterway. All walls (including the head walls), the bottom and the roof have a thickness of  $t$  metres. The caisson has a length of  $\ell$  metres.



$$\begin{aligned} \ell &= 20,00 \text{ m} \\ b &= 8,00 \text{ m} \\ h &= 5,00 \text{ m} \\ t_r &= t_b = t_s = 0,50 \text{ m} \end{aligned}$$

**Question:** Calculate the polar inertia radius of this caisson.

### Elaboration:

For a start, assume the caisson to have no head walls. In that case,  $I_{xx}$  and  $I_{zz}$  are constant over the entire length of the caisson.

$$I_{xx} = \frac{1}{12} b h^3 - \frac{1}{12} (b - 2t_s) (h - t_r - t_b)^3 \rightarrow I_{xx} = \frac{1}{12} \times 8,0 \times 5,0^3 - \frac{1}{12} (8,0 - 2 \times 0,5) (5,0 - 2 \times 0,5)^3 = 46,0 \text{ m}^4$$

$$I_{zz} = \frac{1}{12} h b^3 - \frac{1}{12} (h - t_r - t_b) (b - 2t_s)^3 \rightarrow I_{zz} = \frac{1}{12} \times 5,00 \times 8,00^3 - \frac{1}{12} (5,00 - 2 \times 0,50) (8,00 - 2 \times 0,50)^3 = 99,0 \text{ m}^4$$

$$I_{polar} = I_{xx} + I_{zz} = 46,0 + 99,0 = 145,0 \text{ m}^4$$

$A$  = area of concrete in the cross-section =  $(5,00 \cdot 8,00) - (4,00 \cdot 7,00) = 12,00 \text{ m}$ .

$$j = \sqrt{\frac{I_{polar}}{A}} = \sqrt{\frac{145,0}{12,0}} = 3,476 \text{ m}$$

For a more precise calculation, the presence of head walls should be taken into account for the calculation of the polar inertia radius. For intermediate cross-sections, the moments of inertia are calculated above ( $I_{xx}$  and  $I_{zz}$ ). For the head walls applies:

$$I_{xx,h} = \frac{1}{12} b h^3 = \frac{1}{12} \times 8,00 \times 5,00^3 = 83,3 \text{ m}^4$$

and

$$I_{zz,h} = \frac{1}{12} h b^3 = \frac{1}{12} \times 5,00 \times 8,00^3 = 213,3 \text{ m}^4,$$

so the polar moment of inertia for the head walls is:  $I_{polar,h} = I_{xx,h} + I_{zz,h} = 83,3 + 213,3 = 296,6 \text{ m}^4$

and the radius of gyration of the head walls is:  $j_h = \sqrt{\frac{I_{polar,h}}{A_h}} = \sqrt{\frac{296,6}{5,0 \times 8,0}} = 2,723 \text{ m}$

To obtain the radius of gyration of the entire caisson, the radius of the intermediate section and the head walls have to be 'averaged':

$$j_{resulting} = \frac{j(\ell - 2t) + j_h(2t)}{\ell} = \frac{3,476(25,00 - 2 \times 0,50) + 2,723(2 \times 0,50)}{25,00} = 3,446 \text{ m}$$

With  $j_{resulting}$  and  $h_m$ , the natural oscillation period of the element can be calculated.

In this case,  $h_m = 0,88 \text{ m}$ , so  $T_0 = \frac{2\pi j_{resulting}}{\sqrt{h_m g}} = \frac{2 \times \pi \times 3,446}{\sqrt{0,88 \times 9,81}} = 7,369 \text{ s}$ . This normally spoken is far more than the wave

periods to be expected in inland waterways, so dynamic instability is not to be expected.

Note. If the floating element is asymmetrical, the calculation of  $I_{xx}$  and  $I_{zz}$  is more complicated because the parallel axis theorem (a.k.a. Steiner's theorem) should be used. For example, if it has no roof,

$$I_{xx} = \frac{1}{12} b t_b^3 + b t_b \left( \overline{KG} - \frac{1}{2} t_b \right)^2 + 2 \left\{ \frac{1}{12} t_s (h - t_b)^3 + t_s (h - t_b) \left( t_b + \frac{1}{2} (h - t_b) - \overline{KG} \right)^2 \right\}$$

and

$$I_{zz} = \frac{1}{12} t_b b^3 + 2 \left\{ \frac{1}{12} (h - t_b) \cdot t_s^3 + (h - t_b) \cdot t_s \cdot \left( \frac{1}{2} b - \frac{1}{2} t_s \right)^2 \right\}$$

See Figure 38-6 for clarification of the application of Steiner's theorem in the calculation of  $I_{xx}$  and  $I_{zz}$ .

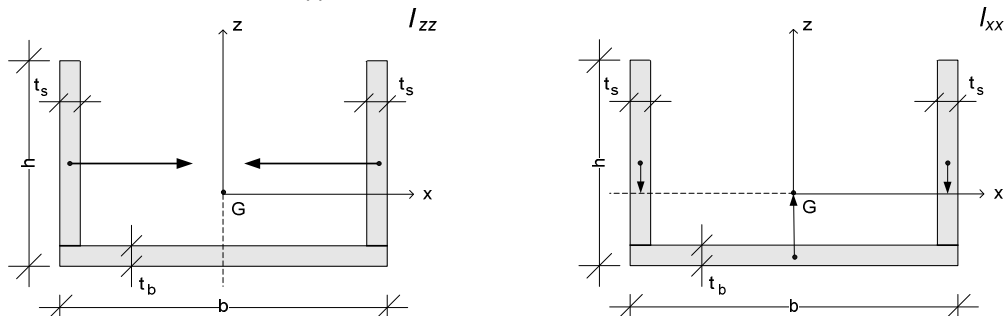


Figure 38-6 Translation direction for application of Steiner's theorem to calculate  $I_{xx}$  and  $I_{zz}$ .

### 38.3 References

- Barltop, N..D.P. et al: *Floating Structures: a guide for design and analysis*. Centre for Marine and Petroleum Technology (CMPT), 1998.
- Eugene A. Avallone and Theodore Baumeister, eds.: *Mark's Standard Handbook for Mechanical Engineers*. McGraw-Hill, New York, 1996.
- J.J.M. Journée and W.W. Massie: *Offshore Hydromechanics*. Lecture notes OE4620. Delft University of Technology. August 2001. Chapter 2.
- Robert L. Mott: *Applied Fluid Mechanics*. Pearson, Prentice Hall, 2006. Chapter 5
- I.W. Nortier and P. de Koning: *Toegepaste Vloeistofmechanica. Hydraulica voor Waterbouwkundigen*. 7th edition. Stam Techniek, Houten, 1991. Section 2.5
- H.J. Pursey. *Merchant Ship Stability*. 4th edition. Brown, Son & Ferguson, Glasgow, 1969.
- <http://www.golfklimaat.nl>, Rijkswaterstaat, accessed: July 2007.
- [http://www.codecogs.com/library/engineering/fluid\\_mechanics/floating\\_bodies](http://www.codecogs.com/library/engineering/fluid_mechanics/floating_bodies), accessed: August 213.

## 39. Soil retaining structures

(major revision: February 2011, improved and extended: January 2014)

A soil retaining wall is a structure intended to resist lateral (= horizontal) soil pressure. Retaining walls are needed if the required slope of the surface exceeds the angle of repose (*hoek van natuurlijk talud*) of the soil. If this maximum angle to the horizontal is exceeded, the soil will start sliding if not hindered by a wall. Retaining walls are also applied if water has to be retained.

There are mainly three types of soil retaining structures (Figure 39-1):

1. Gravity walls (*gewichtconstructies*)
  - including L- walls and reinforced earth (*terre armée*), often masonry (*metselwerk*) or concrete
2. Sheet pile walls (*damwanden*)
  - cantilever (*onverankerd*) or anchored (*verankerd*), including combi-walls (*combiwanden*), mostly steel profiles, sometimes prestressed concrete sheetpiles (*spanwanden*)
3. Diaphragm walls (also called slurry walls; *diepwanden*), in reinforced concrete

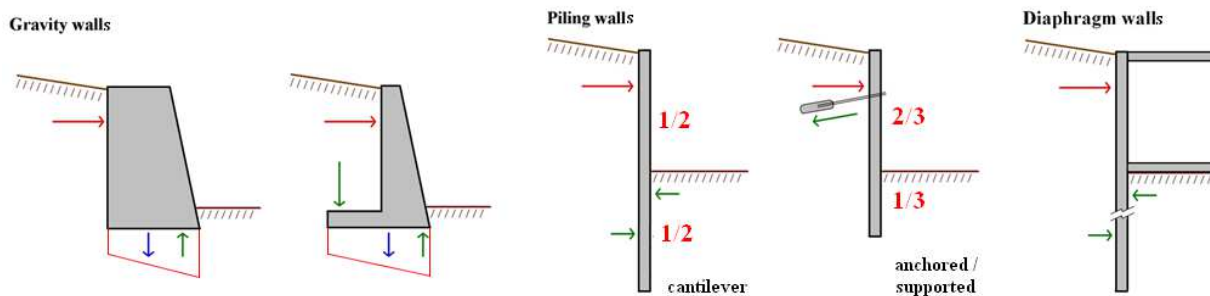


Figure 39-1 Five types of soil retaining walls (from: Wikimedia Commons, modified)

The following sections elaborate on the most interesting of these types. The designs of all these types have in common that:

- The structure and the soil body as a whole should be stable
- The retaining wall is sufficiently embedded in the soil
- The wall elements are able to resist the load (especially the largest occurring bending moments)

Gravity walls derive their stability from a combination of their shape and mass. They typically have a shallow foundation and their stability can be calculated according to Chapter 37. Horizontal displacements of gravity walls are normally spoken not allowed. Therefore the design of these soil retaining structures should be based on the situation of neutral soil stress on both sides of the structure (as active and passive soil stresses only develop after the structure exhibits some displacement)<sup>2</sup>. The neutral soil pressure coefficient can be estimated using the formula proposed by Jaky:  $K_0 \approx 1 - \sin \phi$ , where  $\phi$  is the angle of internal friction of the soil. If the friction angle is very small, e.g. soft clays, the neutral soil pressure coefficient is close to 1. The neutral soil pressure coefficient of sand is close to approximately 0,5-0,7.

<sup>2</sup> In some foreign literature active and passive soil stress is prescribed for the design of these structures, apparently allowing some displacement. It is advised to think very critically before accepting the allowance of displacement and the use of active and passive soil stresses.

### 39.1 Sheet piling

The least expensive soil retaining wall is usually made of steel sheet piling, particularly if it is only needed temporarily (excavated building site) and can be reclaimed. Sheet pile walls are generally used in soft soils and tight spaces. They are usually made of steel and can be installed one by one, or more usual in pairs. The sheets are connected by special joints or interlocks, see Figure 39-3. When installed in pairs, two sheets are connected before installation by tack welds (*hechtlassen*) or by continuous filled welds (*hoeklassen*) along the joints (or interlocks, *sloten*). Another method to join two sheets to make pairs is to pinch (*vastknijpen*) the joints.

Sheet piles can also be made of prestressed concrete (*spanwanden*), wood or synthetic materials. Installation into the soil can be done by driving (*heien*), vibrating (*trillen*) or pressing-in (*drukken*) (Figure 39-2).



Figure 39-2 Driving a sheet pile  
(<http://www.hjfoundation.com/Services/Sheet-Piling/>)

<b>LARSEN section</b> Interlock design conforming to DIN EN 10248-2 and E 67 of EAU 2004	
<b>LARSEN 43, 430</b> Interlock design conforming to DIN EN 10248-2 and E 67 of EAU 2004	
<b>HOESCH section</b> (finger-and-socket interlock) Interlock design conforming to DIN EN 10248-2 and E 67 of EAU 2004	
<b>PEINE interlock steel/ PEINE sheet piling</b> Interlock design conforming to DIN EN 10248-2 and E 67 of EAU 2004	
<b>UNION straight-web section</b> Interlock design conforming to DIN EN 10248-2 and E 67 of EAU 2004	
<b>KL lightweight section</b> Interlock design conforming to DIN EN 10249-2	

Figure 39-3 Various joint types  
(ThyssenKrupp sheet piling handbook)

There are two main profile types of sheet piles: U-profiles (like the 'Larssen' profiles) and Z-profiles (like the 'Hoesch' profiles). Two U-profiles together are not symmetrical which leads to oblique deflection when subjected to load. This reduces the strength and stiffness of these profiles by tenths. Z-profiles don't have this problem. If the heaviest sheet pile profile is insufficient regarding strength or stiffness, one should choose a combi-wall. It is least expensive to use steel quality S235. If this meets the demands for stiffness but not for strength, it is advisable to opt for steel with a higher yield stress rather than for heavier profiles. The AZ-type profiles from ArcelorMittal are relatively stiff.

Table 39-1, Table 39-2 and Table 39-3 give details for the most common sheet pile profiles in the Netherlands.

#### Notes

- See <http://www.tk-steelcom.com.au/documents/sheetpile-handbook-full.pdf> for details of many Hoesch and Larssen profiles, connections and combinations. ArcelorMittal profiles can be found on: <http://sheetpiling.arcelormittal.com/>
- Sheet pile walls do not only need a strength and stiffness design, but also a vibrating or driving design.

**HOESCH sections** (Finger-and-socket interlock)

	Section modulus		Weight		Second moment of inertia $I_y$ cm <sup>4</sup> /m	Section width b mm	Wall height h mm	Back thickness t mm	Web thickness s mm
	$W_y$ cm <sup>3</sup> /m	cm <sup>3</sup> / Single pile	kg/m <sup>2</sup> Wall	kg/m Single pile					
HOESCH 1105	<b>1100</b>	633	<b>101.0</b>	58.1	<b>14300</b>	575	260	8.8	8.8
HOESCH 1205	<b>1140</b>	655	<b>107.0</b>	61.5	<b>14820</b>	575	260	9.5	9.5
HOESCH 1205 K	<b>1200</b>	690	<b>112.5</b>	64.7	<b>15600</b>	575	260	10.2	10.2
HOESCH 1255	<b>1250</b>	719	<b>118.0</b>	67.9	<b>16250</b>	575	260	10.8	10.8
HOESCH 1605	<b>1600</b>	920	<b>107.0</b>	61.5	<b>28000</b>	575	350	9.2	8.1
HOESCH 1705	<b>1720</b>	989	<b>116.0</b>	66.7	<b>30100</b>	575	350	10.0	9.0
HOESCH 1705 K	<b>1700</b>	978	<b>117.0</b>	67.3	<b>29750</b>	575	350	9.5	9.5
HOESCH 1805	<b>1800</b>	1035	<b>125.0</b>	71.9	<b>31500</b>	575	350	10.8	9.9
HOESCH 2305	<b>2320</b>	1334	<b>142.3</b>	81.8	<b>40600</b>	575	350	11.5	8.4
HOESCH 2405	<b>2400</b>	1380	<b>148.0</b>	85.1	<b>42000</b>	575	350	12.1	9.0
HOESCH 2505	<b>2480</b>	1426	<b>152.0</b>	87.4	<b>43400</b>	575	350	12.5	9.5
HOESCH 2555 K	<b>2540</b>	1460	<b>155.0</b>	89.1	<b>44450</b>	575	350	12.8	10.0
HOESCH 2555	<b>2550</b>	1466	<b>158.0</b>	90.9	<b>44625</b>	575	350	13.0	10.0
HOESCH 2605	<b>2600</b>	1495	<b>162.3</b>	93.3	<b>45500</b>	575	350	13.3	10.3
HOESCH 2506 <sup>1)</sup>	<b>2500</b>	1688	<b>143.0</b>	96.5	<b>55000</b>	675	440	12.6	11.2
HOESCH 2606 <sup>1)</sup>	<b>2600</b>	1754	<b>150.0</b>	101.3	<b>57200</b>	675	440	13.2	12.0
HOESCH 2706 <sup>1)</sup>	<b>2700</b>	1823	<b>157.5</b>	106.3	<b>59400</b>	675	440	13.9	12.9
HOESCH 3406	<b>3420</b>	2308	<b>166.1</b>	112.1	<b>82940</b>	675	485	13.5	10.8
HOESCH 3506	<b>3500</b>	2363	<b>171.7</b>	115.9	<b>84880</b>	675	485	14.0	11.4
HOESCH 3606	<b>3600</b>	2370	<b>177.0</b>	119.5	<b>87300</b>	675	485	14.5	12.0
HOESCH 3706	<b>3700</b>	2497	<b>183.9</b>	124.1	<b>89730</b>	675	485	15.1	12.7
HOESCH 3806	<b>3780</b>	2498	<b>188.5</b>	127.2	<b>91665</b>	675	485	15.5	13.2

<sup>1)</sup> Rolling/delivery on request only.

Lengths from 30 m to 36 m on request.

The basis for billing is the weight of the single pile (kg/m).

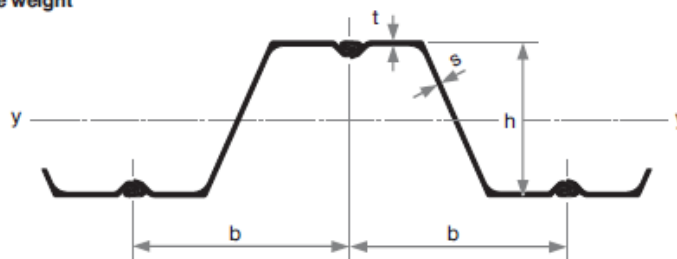
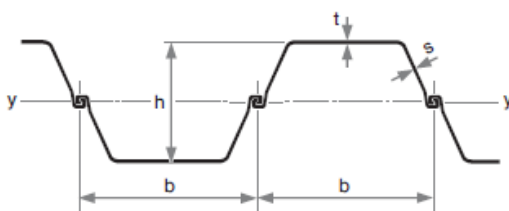


Table 39-1 Sheetpile profiles, Hoesch type (from: Sheet piling handbook)

**LARSSEN sections**

	Section modulus		Weight		Second moment of inertia	Section width	Wall height	Back thickness	Web thickness
	$W_y^{1)}$ cm <sup>3</sup> /m	cm <sup>3</sup> / Single pile	kg/m <sup>2</sup> Wall	kg/m Single pile	$I_y$ cm <sup>4</sup> /m	b	h	t	s
	Wall	Single pile	Wall	Single pile	Wall	mm	mm	mm	mm
LARSSEN 755	2000	580	127.5	95.6	45000	750	450	11.7	10.0
LARSSEN 703	1210	414	96.4	67.5	24200	700	400	9.5	8.0
LARSSEN 703 K	1300	426	103.0	72.1	25950	700	400	10.0	9.0
LARSSEN 703 10/10 <sup>3)</sup>	1340	437	108.0	75.6	26800	700	400	10.0	10.0
LARSSEN 704	1600	529	115.0	80.5	35200	700	440	10.2	9.5
LARSSEN 600	510	109	94.0	56.4	3840	600	150	9.5	9.5
LARSSEN 600 K	540	123	99.0	59.4	4050	600	150	10.0	10.0
LARSSEN 601	745	251	77.2	46.3	11520	600	310	7.5	6.4
LARSSEN 602	830	265	89.0	53.4	12870	600	310	8.2	8.0
LARSSEN 603	1200	330	108.0	64.8	18600	600	310	9.7	8.2
LARSSEN 603 K	1240	340	113.5	68.1	19220	600	310	10.0	9.0
LARSSEN 603 10/10 <sup>3)</sup>	1260	350	116.0	69.6	19530	600	310	10.0	10.0
LARSSEN 604	1620	425	124.2	74.5	30710	600	380	10.5	9.0
LARSSEN 605	2020	520	139.2	83.5	42370	600	420	12.5	9.0
LARSSEN 605 K	2030	549	144.5	86.7	42550	600	420	12.2	10.0
LARSSEN 606 n	2500	605	157.0	94.2	54375	600	435	14.4	9.2
LARSSEN 607 n	3200	649	190.0	114.0	72320	600	452	19.0	10.6
LARSSEN 22 10/10 <sup>3)</sup>	1300	369	130.0	65.0	22100	500	340	10.0	10.0
LARSSEN 23	2000	527	155.0	77.5	42000	500	420	11.5	10.0
LARSSEN 24	2500	547	175.0	87.5	52500	500	420	15.6	10.0
LARSSEN 24/12	2550	560	185.4	92.7	53610	500	420	15.6	12.0
LARSSEN 25	3040	562	206.0	103.0	63840	500	420	20.0	11.5
LARSSEN 43	1660	483	166.0	83.0	34900	500	420	12.0	12.0
LARSSEN 430	6450	—	234.5 <sup>2)</sup>	83.0	241800	708 <sup>4)</sup>	750	12.0	12.0



1) The section modulus values may only be used in static computations if at least every second interlock in the wall is cramped to adsorb shear forces.

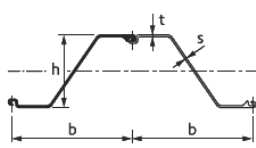
2) Wall assembly fabricated from LARSSEN 43 sections. Where quad pile assemblies are supplied, allowance must be made for the weight of the weld seams and reinforcements.

3) Rolling/delivery on request only.

4) With the use of quadruple piles  
W = 1416 mm

Lengths from 30 m to 36 m on request. The basis for billing is the weight of the single pile (kg/m).

Table 39-2 Sheetpile profiles, Larssen type (from Sheet piling handbook)



	Width	Height	Thickness		Mass		Moment of inertia	Elastic section modulus
	b	h	t	s	single pile	wall		
	mm	mm	mm	mm	kg/m	kg/m <sup>2</sup>	cm <sup>4</sup> /m	cm <sup>3</sup> /m
<b>AZ<sup>®</sup>-700 &amp; AZ<sup>®</sup>-770</b>								
AZ 12-770	770	344	8.5	8.5	72.6	<b>94.3</b>	21 430	<b>1 245</b>
AZ 13-770	770	344	9.0	9.0	76.1	<b>98.8</b>	22 360	<b>1 300</b>
AZ 14-770	770	345	9.5	9.5	79.5	<b>103.2</b>	23 300	<b>1 355</b>
AZ 14-770-10/10	770	345	10.0	10.0	82.9	<b>107.7</b>	24 240	<b>1 405</b>
AZ 12-700	700	314	8.5	8.5	67.7	<b>96.7</b>	18 880	<b>1 205</b>
AZ 13-700	700	315	9.5	9.5	74.0	<b>105.7</b>	20 540	<b>1 305</b>
AZ 13-700-10/10	700	316	10.0	10.0	77.2	<b>110.2</b>	21 370	<b>1 355</b>
AZ 14-700	700	316	10.5	10.5	80.3	<b>114.7</b>	22 190	<b>1 405</b>
AZ 17-700	700	420	8.5	8.5	73.1	<b>104.4</b>	36 230	<b>1 730</b>
AZ 18-700	700	420	9.0	9.0	76.5	<b>109.3</b>	37 800	<b>1 800</b>
AZ 19-700	700	421	9.5	9.5	80.0	<b>114.3</b>	39 380	<b>1 870</b>
AZ 20-700	700	421	10.0	10.0	83.5	<b>119.3</b>	40 960	<b>1 945</b>
AZ 24-700	700	459	11.2	11.2	95.7	<b>136.7</b>	55 820	<b>2 430</b>
AZ 26-700	700	460	12.2	12.2	102.9	<b>146.9</b>	59 720	<b>2 600</b>
AZ 28-700	700	461	13.2	13.2	110.0	<b>157.2</b>	63 620	<b>2 760</b>
AZ 24-700N	700	459	12.5	9.0	89.7	<b>128.2</b>	55 890	<b>2 435</b>
AZ 26-700N	700	460	13.5	10.0	96.9	<b>138.5</b>	59 790	<b>2 600</b>
AZ 28-700N	700	461	14.5	11.0	104.1	<b>148.7</b>	63 700	<b>2 765</b>
AZ 36-700N	700	499	15.0	11.2	118.6	<b>169.5</b>	89 610	<b>3 590</b>
AZ 38-700N	700	500	16.0	12.2	126.4	<b>180.6</b>	94 840	<b>3 795</b>
AZ 40-700N	700	501	17.0	13.2	134.2	<b>191.7</b>	100 080	<b>3 995</b>
AZ 42-700N	700	499	18.0	14.0	142.1	<b>203.1</b>	104 930	<b>4 205</b>
AZ 44-700N	700	500	19.0	15.0	149.9	<b>214.2</b>	110 150	<b>4 405</b>
AZ 46-700N	700	501	20.0	16.0	157.7	<b>225.3</b>	115 370	<b>4 605</b>
<b>AZ<sup>®</sup></b>								
AZ 18	630	380	9.5	9.5	74.4	<b>118.1</b>	34 200	<b>1 800</b>
AZ 18-10/10	630	381	10.0	10.0	77.8	<b>123.4</b>	35 540	<b>1 870</b>
AZ 26	630	427	13.0	12.2	97.8	<b>155.2</b>	55 510	<b>2 600</b>
AZ 46	580	481	18.0	14.0	132.6	<b>228.6</b>	110 450	<b>4 595</b>
AZ 48	580	482	19.0	15.0	139.6	<b>240.6</b>	115 670	<b>4 800</b>
AZ 50	580	483	20.0	16.0	146.7	<b>252.9</b>	121 060	<b>5 015</b>

Table 39-3 Sheetpile profiles, ArcelorMittal AZ type (from: ArcelorMittal brochure Z-profiles 2013-2)

### Calculation of sheet pile walls: general principles

Sheetpile walls tend to rotate and deform because of differences in horizontal soil pressure before and behind the wall. The wall as a whole rotates around a deep point. Deformations occur because sheetpile walls have relatively low stiffnesses. The local displacements are the result of the rotation of the whole wall and the local deformation of the wall.

Hermann Blum assumed that the local displacement of sheet pile walls would result in immediate yielding of the soil at both the active and passive side, instead of gradual development of shear stresses in the soil. This means that large soil deformations are assumed, resulting in the occurrence of maximum shear stresses in the soil. At the active side minimum soil stresses will occur and at the passive side maximum soil stresses are present (Figure 39-4). As a result it is assumed that no elastic deformation occurs. This is of course a simplification of the real situation, just as the assumption that the active and passive wedge have straight slip planes.

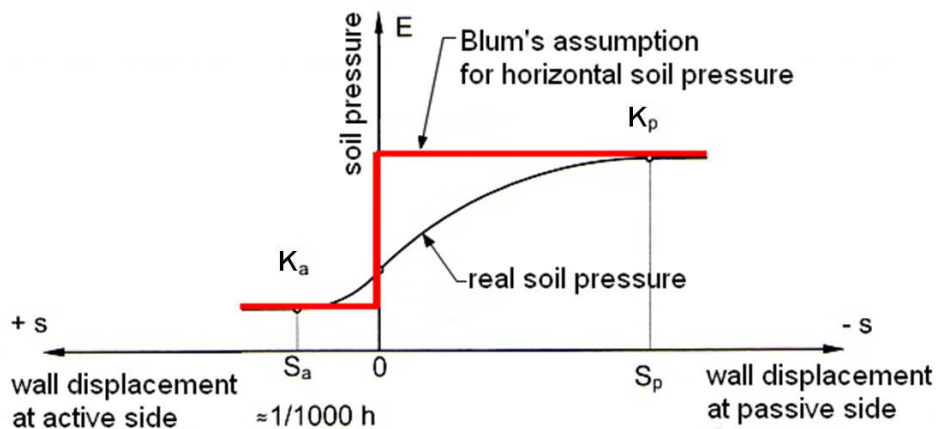


Figure 39-4 Blum's assumption regards horizontal soil pressure

The embedded depth, hence the length, of the wall should be long enough to provide a balance in horizontal pressures and forces, as well as an moment equilibrium to prevent turning over of the wall. If vertical stresses or forces act on the wall, e.g., the vertical component of an inclined anchor rod, or a vertical line load coming from a top structure, the friction stress along the wall should be high enough to prevent subsidence of the wall.

Deep slip planes should also be checked, because sheet pile walls could also mobilise larger soil bodies with slip planes below the active and passive wedges (Figure 39-5). These slip planes can be checked with help of the methods of Krantz, who assumed a straight slip plane, and Bishop, who assumed a circular slip plane (see also Section 41.4).

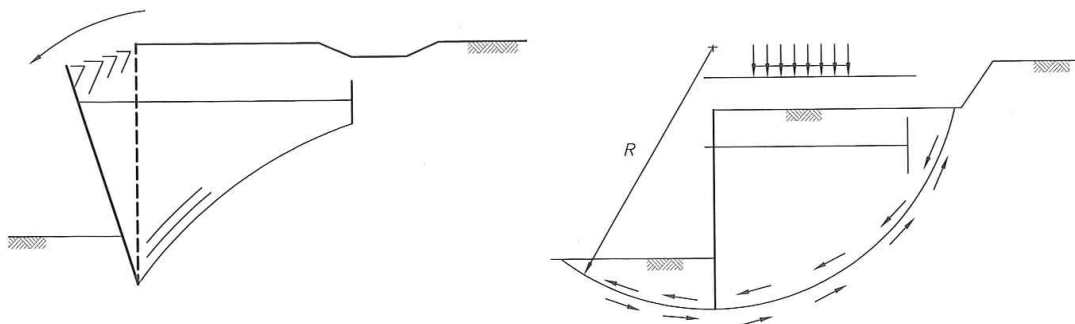


Figure 39-5 Deep slip planes: a straight plane (left) and a circular plane (right)

Other points of attention regards stability of sheet pile walls are piping and scour, which could lead to failure of the wall (see sections 37.4 and 37.5 for the calculation methods).

For the calculation of the required length and profile of sheet pile walls, it is important to make a good schematisation of the soil pressures and of the structure. The schematisation described in this Manual is based on the theory of Hermann Blum (1931, 1950, 1951).

The following sections explain some 'classical' methods to calculate the length and profile of sheet pile walls. These simple methods can be used for analytical (hand)calculations as a first rough estimate. Elastoplastic and finite element methods can be used for more detailed dimensioning of sheet pile walls.

### Calculation of cantilever sheet pile walls

An unsupported sheetpile wall mechanically acts as a cantilever (*uitkragende ligger*). The pressure of the soil at the active side leads to a tendency of the wall towards the passive side. This tendency does not only exist of a translation effect (because of an imbalance of horizontal forces) but also of a rotational effect (because of an imbalance of moments). Because of the flexibility of the wall, also a deformation of the sheet piles is to be expected. Figure 39-6 shows the deflections and deformations of a cantilever sheet pile wall in a rather extreme extent (failure state).

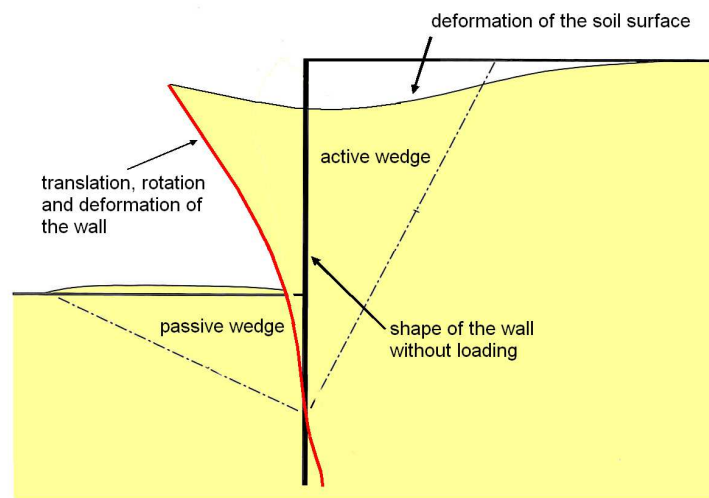


Figure 39-6 Deflection and deformation of a cantilever sheet pile wall due to loading (very much exaggerated)

An increase of the sheet pile length, and accordingly an increase in acting loads (until a certain depth), results in rapidly increasing deformations and an increasing claim on the bending capacity of the structure. Cantilever sheetpile walls are therefore usually not used as (part of) permanent structures. For temporary structures, like most cofferdams, they can only be used in case of relative low retaining heights.

### Schematisation of cantilever sheetpile walls according to Blum

As a result of the forces exerted on the sheet pile wall and the assumption that the sheet piles are infinitely rigid, the sheet pile wall inclines to turn around point D, see Figure 39-7A. Accordingly a clamping load (*inklembelasting*) will develop under point D, which resists the turning of the wall (Figure 39-7B). If the length of a sheet pile wall is somewhat longer than strictly necessary to ensure equilibrium, the passive soil pressure does not need to develop over the entire length of the embedded part of the wall. Because of this extra length the toe will act as a clamped edge (*inklemming*), in which the lowest part has the tendency to move to the right resulting in a pressure to the left. In combination with the passive soil pressure that is directed to the right this will constitute a clamping moment.

In order to calculate the needed embedded depth, the real pressure diagram is replaced by a schematised diagram, see Figure 39-7C. Blum proposed to replace the clamping load under point D by a concentrated load (*Ersatzkraft*, or substitute force  $Q$ ) acting through point D. The theoretical embedded depth can then be calculated considering an equilibrium of forces around point D. Since the passive pressure at the front side of the wall is underestimated in this schematisation, the deviation is corrected by increasing the computed theoretical embedded depth ( $t$ ) by a factor  $\alpha$  (usually 20%). This is done in such a way that the needed shear force,  $Q$ , in point D can be delivered ( $Q = F_{p,h} - F_{a,h}$ ). Note that the magnitude of the field moment is not influenced by this schematisation.

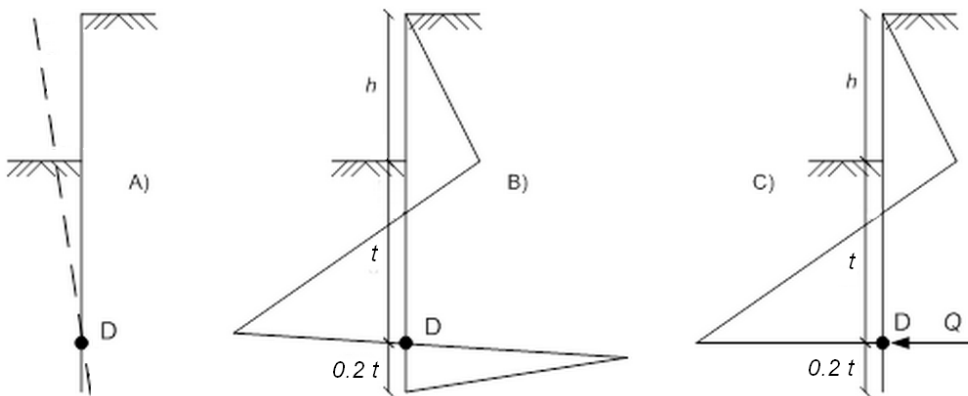


Figure 39-7 sheetpile with rotation point (A), 'real' ground pressure diagram (B) and schematized pressure diagram (C).

The factor  $\alpha$  that is used to increase the theoretical embedded depth  $t_0$ , varies between 1,05 and 1,60, depending on the water level difference, anchorage and toe schematisation. Table 39-4 gives an overview of the various values for this factor  $\alpha$ .

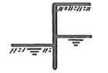
wall type	 small water head	 big water head	 very big water head or only water pressure
cantilever	1,20	1,30	1,40 - 1,60
anchored and fixed toe	1,10	1,15	1,20 - 1,30
anchored and toe free supported	1,05	1,10	1,15 - 1,20

Table 39-4 Increment factor  $\alpha$  for the embedded depth (from: Hoesch Spundwand-Handbuch 1980)

Calculation method of the length (depth) and profile of a cantilever sheet pile wall:

- Step 1. Calculate the resulting horizontal soil stresses at the active and passive side as a function of  $t$ .
- Step 2. Calculate the embedded depth  $t$  considering an equilibrium of moments around point D.
- Step 3. Calculate the maximum moment in the sheetpile wall to determine the required section modulus.
- Step 4. Choose a suitable sheetpile profile from the product specifications of the manufacturer.

### Example calculation cantilever sheet pile wall (length and profile)

The embedded depth will be calculated for a sheet pile wall in homogeneous sand as shown in Figure 39-8.

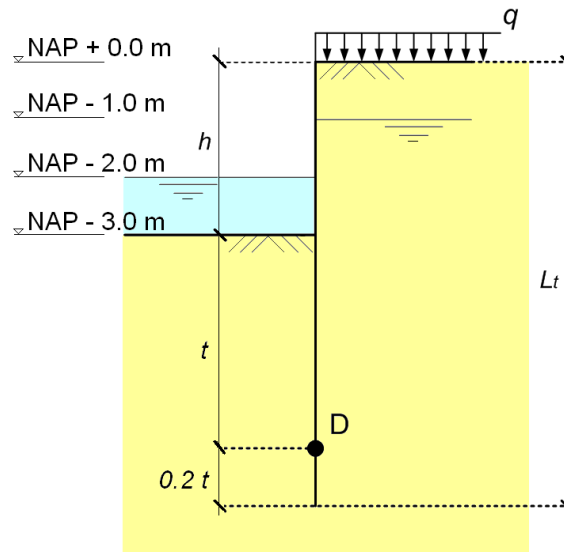


Figure 39-8 situation and soil profile.

#### Given

surcharge at the surface	22	[kN/m <sup>2</sup> ]
specific weight of dry sand ( $\gamma_d$ )	18	[kN/m <sup>3</sup> ]
specific weight of saturated sand ( $\gamma_s$ )	20	[kN/m <sup>3</sup> ]
specific weight of water ( $\gamma_w$ )	10	[kN/m <sup>3</sup> ]
angle of internal friction of the sand ( $\varphi$ ):	30	[°]
cohesion of the sand ( $c$ ):	0	[kN/m <sup>2</sup> ]
wall friction for a smooth wall ( $\delta$ ):	0	[°]

ground and water levels are indicated in the figure.

#### Question

Compute the required length and profile of the sheet piles. Do not use safety factors for this example.

#### Elaboration

##### Step 1. Calculate the resulting horizontal soil stresses at the active and passive side.

First the vertical stresses should be calculated. This is done for the water and the soil separately. Then the horizontal stresses acting on the wall are calculated. The horizontal water stresses are equal to the vertical water stresses (Law of Pascal) and the horizontal effective stress is found by multiplying the vertical effective stress with the active and passive soil coefficients. This is shown in Figure 39-9. For  $\varphi = 30^\circ$ ,  $K_a = 0,33$  and  $K_p = 3,0$  (see section 24.2 for the equations).

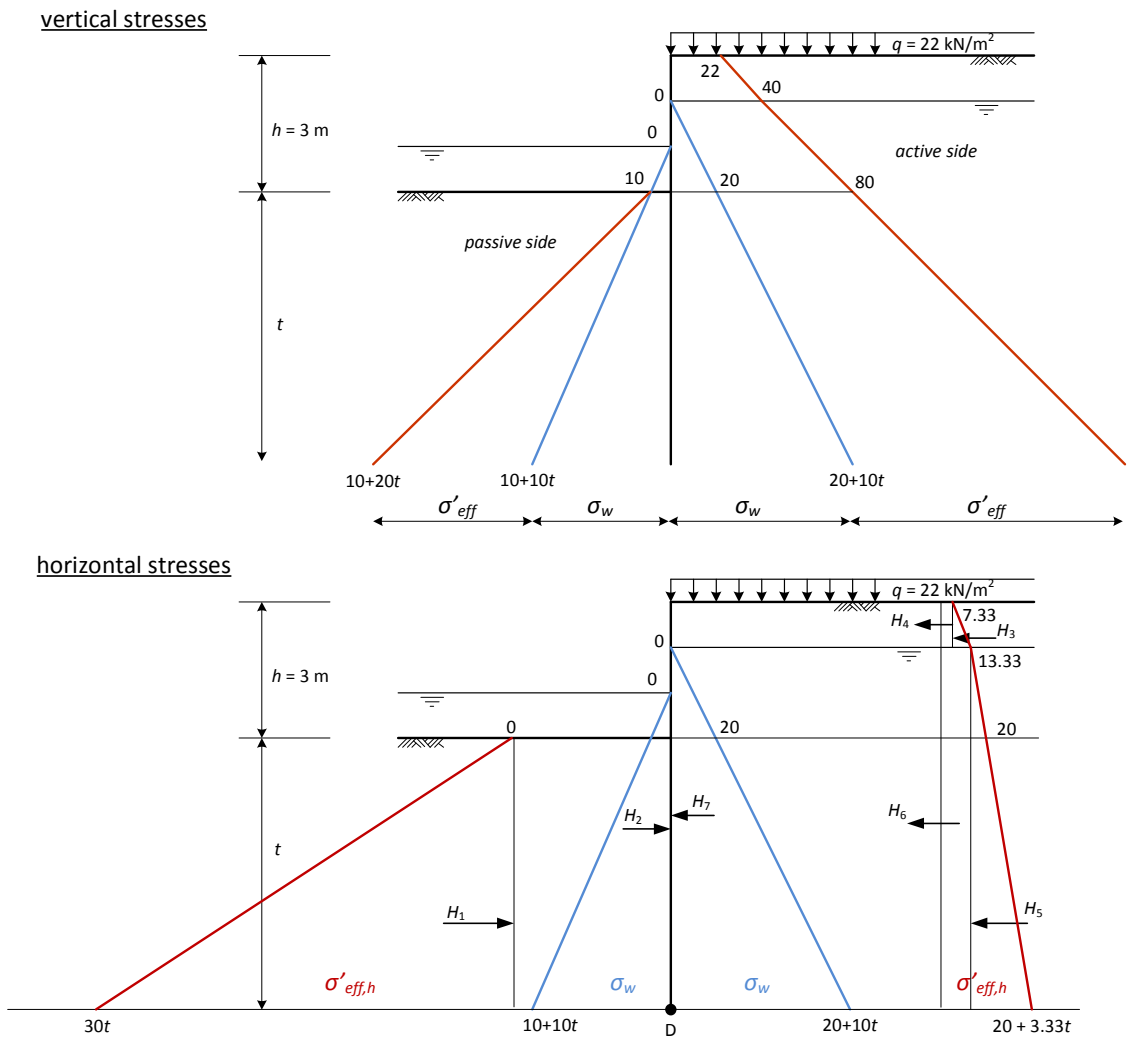


Figure 39-9 Vertical and horizontal stresses

Step 2. Calculate the embedded depth  $t$  considering an equilibrium of moments around point D.

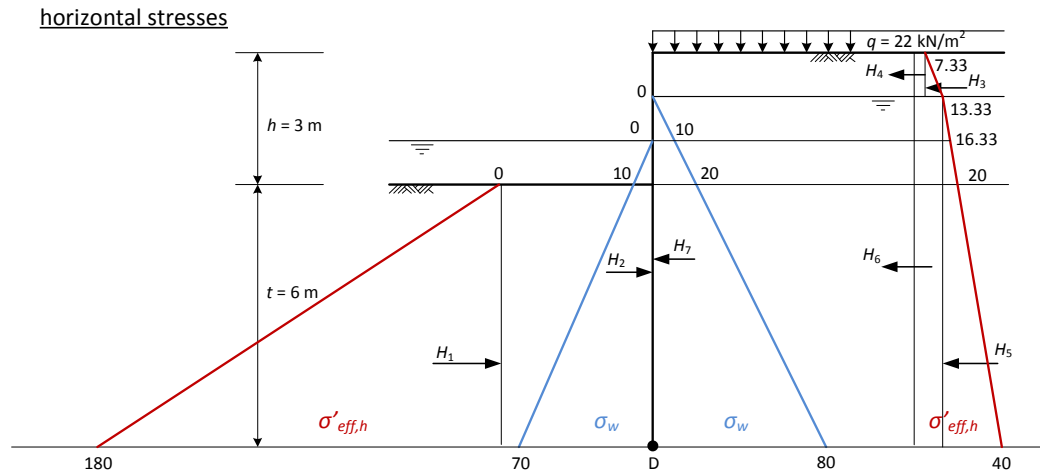
This is done in the following table. First the resulting horizontal forces are calculated, then the arm from point D to the work lines of these forces is determined. The resulting moment about point D is a third degree equation with one variable.

force [kN/m]		arm [m]	moment [kNm/m]
$H_1 = \frac{1}{2} \cdot 30t \cdot t =$		$\frac{1}{3} t$	$- 5 t^3$
$H_2 = \frac{1}{2} \cdot (10 + 10t) (1 + t) =$	- 5    - 10 t	$\frac{1}{3}(t + 1)$	$- 12/3 \quad - 5 t \quad - 5 t^2 \quad - 12/3 t^3$
$H_3 = \frac{1}{2} \cdot (13^{1/3} - 7^{1/3}) \cdot 1 =$	3	$t + 2^{1/3}$	7    + 3 t
$H_4 = 7^{1/3} \cdot 1 =$	$7^{1/3}$	$t + 2^{1/2}$	$18^{1/3} \quad + 7^{1/3} t$
$H_5 = \frac{1}{2} \cdot (20 + 3^{1/3} t - 13^{1/3}) \cdot (t+2) =$	$6^{2/3} \quad + 6^{2/3} t \quad + 1^{2/3} t^2$	$\frac{1}{3} (t + 2)$	$4^{4/9} \quad + 6^{2/3} t \quad + 3^{1/3} t^2 \quad + 5^{5/9} t^3$
$H_6 = 13^{1/3} \cdot (t + 2) =$	$26^{2/3} \quad + 13^{1/3} t$	$\frac{1}{2} (t + 2)$	$26^{2/3} \quad + 26^{2/3} t \quad + 6^{2/3} t^2$
$H_7 = \frac{1}{2} \cdot (20 + 10t) \cdot (t + 2) =$	20    + 20 t    + 5 t <sup>2</sup>	$\frac{1}{3} (t + 2)$	$13^{1/3} \quad + 20 t \quad + 10 t^2 \quad + 1^{2/3} t^3$
$\Sigma H - Q =$	$58^{2/3} \quad + 30 t \quad - 13^{1/3} t^2$	$\Sigma M_D =$	$68^{1/9} \quad + 58^{2/3} t \quad + 15 t^2 \quad - 4^{4/9} t^3$

$$\Sigma M_D = 0 \rightarrow 68^{1/9} + 58^{2/3} t + 15 t^2 - 4^{4/9} t^3 = 0 \rightarrow t = 6,00 \text{ m}$$

The substitute force Q then is  $58^{2/3} + 30 \cdot 6 - 13^{1/3} \cdot 6^2 = 241,33 \text{ kN/m}$ .

Mistakes are easily made, so it would be wise to check the calculation until now. This is done by redrawing the horizontal stress figure, but now with 6.00 substituted for  $t$  (directly in the graph). All partial horizontal forces and arms can now be directly calculated, without making use of the variable  $t$ . The sum of moments about D should still be zero.

Figure 39-10 Horizontal stresses for  $t = 6.00$  m

$$\begin{aligned}
 M_1 &= -0.5 \cdot 180 \cdot 6 \cdot 6/3 = & -1080,00 \\
 M_2 &= -0.5 \cdot 70 \cdot 7 \cdot 7/3 = & -571,67 \\
 M_3 &= 0.5 \cdot (13,33-7,33) \cdot 1 \cdot 8,33 = & +25,00 \\
 M_4 &= 7,33 \cdot 1 \cdot 8,5 = & +62,33 \\
 M_5 &= 0.5 \cdot (40-13,33) \cdot 8 \cdot 8/3 = & +284,44 \\
 M_6 &= 13,33 \cdot 8 \cdot 8/2 = & +426,67 \\
 M_7 &= 0.5 \cdot 80 \cdot 8 \cdot 8/3 = & +853,33 \\
 \Sigma M &= & 0,10 \approx 0 \\
 &\rightarrow \text{Check OK!}
 \end{aligned}$$

Step 3. Calculate the maximum moment in the sheetpile wall to determine the required section modulus.

The resulting stress diagram is drawn first, which is used to draw the shear force diagram (*dwardskrachtenlijn*) in order to find the moment diagram (*momentenlijn*). The maximum moment in the sheetpile wall can be found with help of this moment diagram.

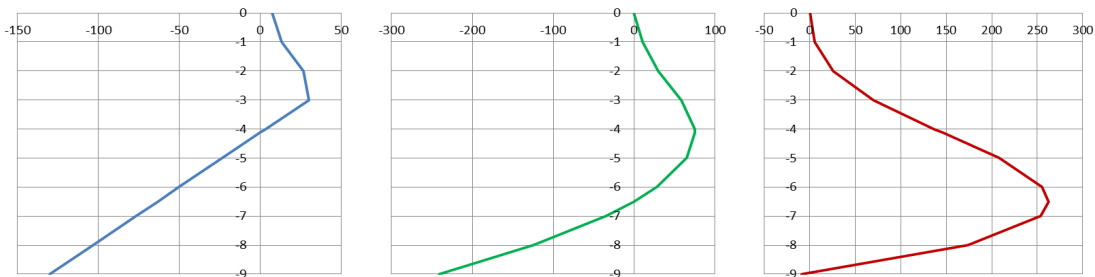
So, first the resulting stress diagram is drawn. This can be easily accomplished using Figure 39-10. The resulting horizontal stress can be found by just summarizing the horizontal soil stresses and the water pressures on both sides (active and passive) for every depth. For instance, at 1.00 m below the soil surface (right side), the total horizontal stress is  $0 + 13,33 = 13,33$  kN/m<sup>2</sup>. One metre lower, it is  $10 + 16,33 = 26,33$  kN/m<sup>2</sup>. Three metre below ground surface, the total horizontal stress is  $20 + 20 - 10 = 30$  kN/m<sup>2</sup>. The result can be seen in Table 39-5 (second column) and Figure 39-11 (left graph).

The shear force diagram, calculated in the same table, can be found by integrating the equation for total horizontal stress. This means that the area below the stress diagram equals the difference in the shear force diagram. At ground level, the shear force diagram starts with a value of 0 kN/m (because of Blums' schematisation), so, for instance at 1 metre below ground level, the value of the shear force diagram is  $0 + (7,33 + 13,33)/2 \cdot 1,0 = 10,33$  kN/m. This can be calculated for every slice of soil of 1,0 m. This has done a bit more precise to find the maximum shear force: this occurs where the total stress equals zero, which is at 4,125 m below ground level. An extra check here is that the shear force found at the toe of the wall (9 m below ground surface) should be the same as the value found for the substitute force  $Q$ , which luckily is the case.

The moment diagram can be found now by integrating the shear force diagram. The area below the shear force diagram is the change in moment diagram. Also here  $M = 0$  at ground level, so from there the  $M$ -line can be calculated downward. At 9 m below ground level,  $M$  should be 0, which is almost the case (small rounding-off error). The maximum moment appears where  $S = 0$ , at 6,505 m below ground level.

The resulting horizontal stresses, the shear forces and the moments are presented in Table 39-5 and Figure 39-11.

height	hor. stress	S-diagram	M-diagram
0,000	7,33	0,00	000
-1,000	13,33	10,33	5,17
-2,000	26,67	30,33	25,50
-3,000	30,00	58,67	70,00
-4,000	3,33	75,33	137,00
-4,125	0,00	75,54	146,43
-5,000	-23,33	65,33	208,06
-6,000	-50,00	28,67	255,06
-6,505	-63,47	0,02	262,30
-7,000	-76,67	-34,67	253,73
-8,000	-103,33	-124,67	174,06
-9,000	-130,00	-241,33	-8,94

Table 39-5 Resulting horizontal stresses [kN/m<sup>2</sup>], S-diagram [kN/m] and M-diagram [kNm/m]Figure 39-11 Resulting horizontal stresses [kN/m<sup>2</sup>], S-diagram [kN/m] and M-diagram [kNm/m]

The maximum moment in the sheetpile wall appears to be 262 kNm/m at a depth of 6,505 m below ground surface.

For those who like to solve this analytically, this is demonstrated here. There are four linear parts in the resulting horizontal stress development:

$$\begin{aligned}
 0 \leq z < 1,0: & \quad \sigma_{\text{hor, res}}(z) = 7\frac{1}{3} + 6 \cdot z \\
 1,0 \leq z < 2,0: & \quad \sigma_{\text{hor, res}}(z) = 13\frac{1}{3} + 13\frac{1}{3} \cdot (z-1) = 13\frac{1}{3} \cdot z \\
 2,0 \leq z < 3,0: & \quad \sigma_{\text{hor, res}}(z) = 26\frac{2}{3} + 3\frac{1}{3} \cdot (z-2) = 20 + 3\frac{1}{3} \cdot z \\
 3,0 \leq z < 9,0: & \quad \sigma_{\text{hor, res}}(z) = 30 - 26\frac{2}{3} \cdot (z-3) = 110 - 26\frac{2}{3} \cdot z
 \end{aligned}$$

Where  $z$  is the depth below ground level in [m].

The values for  $S$  can be found by integrating  $\sigma_{\text{hor, res}}(z)$ :  $S(z) = \int \sigma_{\text{hor, res}}(z) dz$ :

$$\begin{aligned}
 0 \leq z < 1,0: & \quad S(z) = \int (7\frac{1}{3} + 6 \cdot z) dz = 7\frac{1}{3} \cdot z + 3 \cdot z^2 \\
 1,0 \leq z < 2,0: & \quad S(z) = \int (13\frac{1}{3} \cdot z) dz = 3\frac{2}{3} + 6\frac{2}{3} \cdot z^2 \\
 2,0 \leq z < 3,0: & \quad S(z) = \int (20 + 3\frac{1}{3} \cdot z) dz = -16\frac{1}{3} + 20 \cdot z + 1\frac{2}{3} \cdot z^2 \\
 3,0 \leq z < 9,0: & \quad S(z) = \int (110 - 26\frac{2}{3} \cdot z) dz = -151\frac{1}{3} + 110 \cdot z - 13\frac{1}{3} \cdot z^2
 \end{aligned}$$

(The integral constants can be found by considering the highest level per range, for which the value of  $S$  is known, starting with  $S = 0$  at ground level.)

The same recipe can now be followed to find the expressions for  $M(z) = \int S(z) dz$ :

$$\begin{aligned}
 0 \leq z < 1,0: & \quad M(z) = \int (7\frac{1}{3} \cdot z + 3 \cdot z^2) dz = 3\frac{2}{3} \cdot z^2 + z^3 \\
 1,0 \leq z < 2,0: & \quad M(z) = \int (3\frac{2}{3} + 6\frac{2}{3} \cdot z^2) dz = -0,61 + 1,833 \cdot z^2 + 2,22 \cdot z^3 \\
 2,0 \leq z < 3,0: & \quad M(z) = \int (-16\frac{1}{3} + 20 \cdot z + 1\frac{2}{3} \cdot z^2) dz = 12,72 - 16\frac{1}{3} \cdot z + 10 \cdot z^2 + 0,556 \cdot z^3 \\
 3,0 \leq z < 9,0: & \quad M(z) = \int (-151\frac{1}{3} + 110 \cdot z - 13\frac{1}{3} \cdot z^2) dz = 147,72 - 151\frac{1}{3} \cdot z + 55 \cdot z^2 - 4\frac{4}{9} \cdot z^3
 \end{aligned}$$

The thus found values for  $M$  are slightly more accurate than those mentioned in Table 39-5, which is caused by the rather rough subdivision in slices of 1 m thick in the numerical calculation above. The analytically calculated maximum moment, however, is still about 262 kNm/m.

The section modulus of the sheet pile wall required to resist the maximum bending stresses is:

$$W_{\text{eff, y}} = \frac{M_{\text{max}}}{f_{y, d}} = \frac{262 \cdot 10^6}{235} = 1115 \cdot 10^3 \text{ mm}^3/\text{m} (= 1115 \text{ cm}^3/\text{m}) \text{ (for steel quality S235)}$$

Step 4. Choose a suitable sheetpile profile from the product specifications of the manufacturer.

20% should be added to  $t$  to compensate for the simplified schematisation:  $L_t = 1,20 \cdot t = 7,20$  m

A profile with a sufficient section modulus is Larssen 603, for which  $W_{eff,y} = 1200$  cm<sup>3</sup>/m > 1115 cm<sup>3</sup>/m (see Table 39-2).

Notice that the presence of a water mass at the passive side of the sheet pile wall works favourable for the strength of the sheet pile wall. Therefore one shall either assume a certain safe (= guaranteed!) water level at the passive side of the sheet pile or assume that no water is present at all above excavation level. In the elaborated example above it is assumed that the water is always present.

### Calculation of anchored sheet pile walls

If the design of cantilever sheet pile walls appears not to be stable, anchors could be applied as alternative to large profiles.

The mechanical schematisation of the anchored sheet pile structure as a beam on two supports, or on a support and a (partly) fixed end is a simplification of reality, but acceptable for a first conceptual design because it leads to conservative designs if the right safety factors are used. Figure 39-12 shows different schemes. If the wall has insufficient embedded depth, it will move/rotate towards the passive side, though translation of the anchor point is prevented (upper figure). This could be considered as a cantilever (*kraa-glijger*). If the sheet pile wall is elongated until equilibrium, it could be more or less considered as a beam on two supports (middle figure). If the wall becomes longer, a partly fixed end originates, which transforms into a fully fixed end at a certain depth, where the deflection angle is zero (lower figure). A further increase of the embedded depth does not lead to a change of the position of the fixed support and is needless.

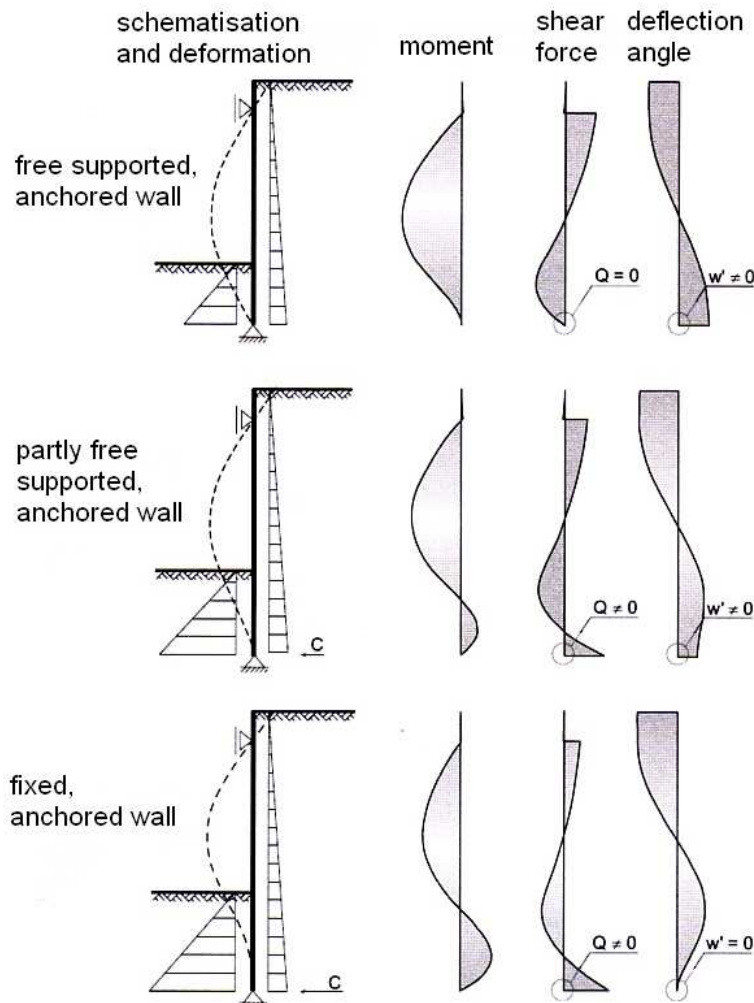


Figure 39-12 Mechanical schematisations of the sheet pile structure (from: ThyssenKrupp Spundwandhandbuch)

This paragraph gives two schematisations for the design of anchored sheet pile walls.

#### Simplified schematisation of anchored sheet pile walls

If anchors or struts are needed for the stability of a sheetpile wall, the computation method of the embedded depth differs from the method given for cantilever sheetpile walls. The wall is schematised as a beam on two free supports and it is assumed that the anchor provides the necessary resistance against rotation of the sheet pile instead of a clamping force. It is also assumed that the bending moment ( $M$ ) and the shear force ( $S$ ) at the top and the toe of the wall are zero.

Calculation steps of the embedded depth and anchor force per unit length:

Step 1: compute the equilibrium of moments around the anchor point  $\sum M_E = 0$  in order to determine the embedded depth.

Step 2: compute the strut or anchor force from the horizontal equilibrium  $\sum H = 0$ .

Step 3: compute the required section modulus ( $W_{eff,y}$ ).

Step 4: choose an appropriate sheet pile profile and length from the manufacturers information.

#### **Example calculation of required profile of an anchored sheetpile wall (simplified schematisation)**

In Figure 39-13 an overview is given of a sheet pile wall in homogeneous wet sand.

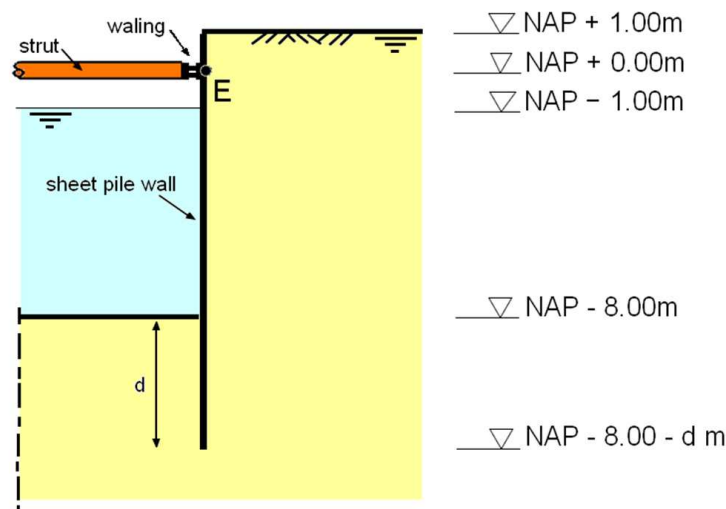


Figure 39-13 situation and soil profile.

#### **Given**

angle of internal friction of the sand  $\varphi = 30^\circ$

cohesion of the sand  $c = 0 \text{ kN/m}^2$

specific weight of the wet sand  $\gamma_{s,w} = 20 \text{ kN/m}^3$

wall friction for this smooth wall  $\delta = 0^\circ$

water and ground levels are indicated in the figure as well as the height of the strut.

#### **Question**

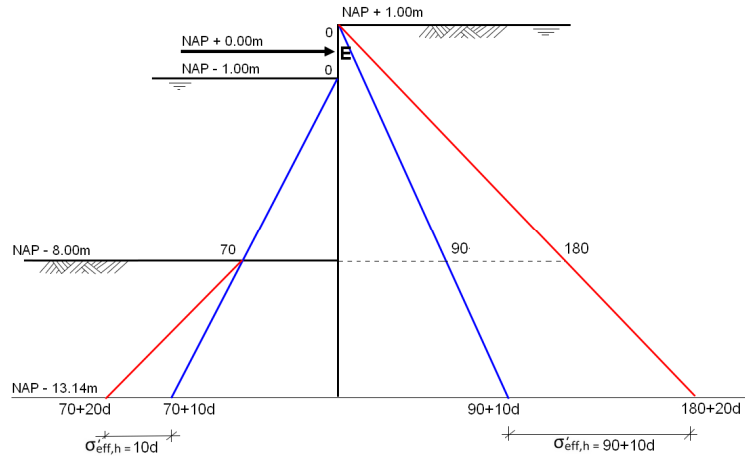
Calculate what sheetpile profile is needed to resist the loads in the given load situation. Choose a Hoesch profile with steel quality S235. There is no surcharge to be taken into account. Also the use of safety coefficients is refrained of in this example.

#### **Elaboration**

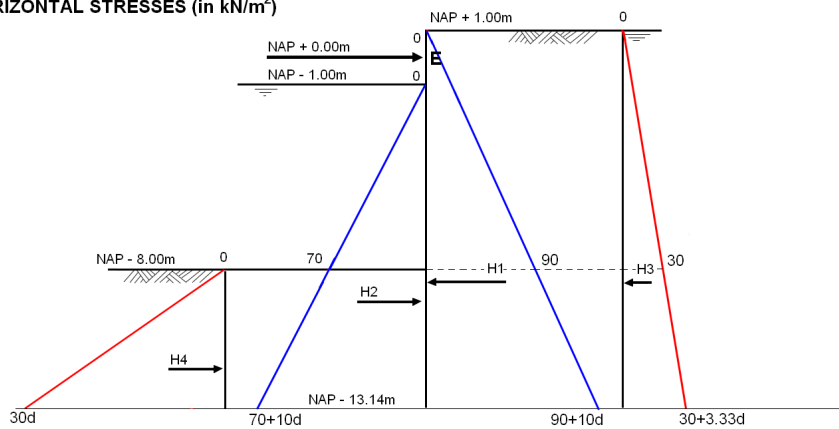
##### Step1. Calculate the embedded depth of the sheetpile wall

The first step is to calculate the embedded depth  $d$  of the sheet pile wall, by considering the equilibrium of moments around the anchor point (NAP + 0.00m). The vertical stresses are indicated below. The values at the lower/lowest levels are expressed as a function of  $d$ . The total soil stress and the water pressure are separately drawn, in order to be able to calculate the effective stress. The horizontal effective stresses are calculated by multiplying the effective vertical soil stresses with  $K_a = 0,33$  (active side) and  $K_p = 3,0$  (passive side). A value of  $\gamma_s = 20 \text{ kN/m}^3$  has been used everywhere, because the soil is wet on both sides in this (simplified) situation.

**VERTICAL STRESSES (in kN/m<sup>2</sup>)**



**HORIZONTAL STRESSES (in kN/m<sup>2</sup>)**



force:

$$\begin{aligned}
 H1 &= \frac{1}{2}(90+10d) \cdot (9+d) = 405 + 90d + 5d^2 \\
 H2 &= \frac{1}{2}(70+10d) \cdot (7+d) = 245 + 70d + 5d^2 \\
 H3 &= \frac{1}{2}(30+3.33d) \cdot (9+d) = 135 + 30d + 1.67d^2 \\
 H4 &= \frac{1}{2}(30d) = 15d^2
 \end{aligned}$$

arm:

$$\begin{aligned}
 a1 &= 5 + \frac{2}{3}d \\
 a2 &= 5\frac{2}{3} + \frac{2}{3}d \\
 a3 &= 5 + \frac{2}{3}d \\
 a4 &= 8 + \frac{2}{3}d
 \end{aligned}$$

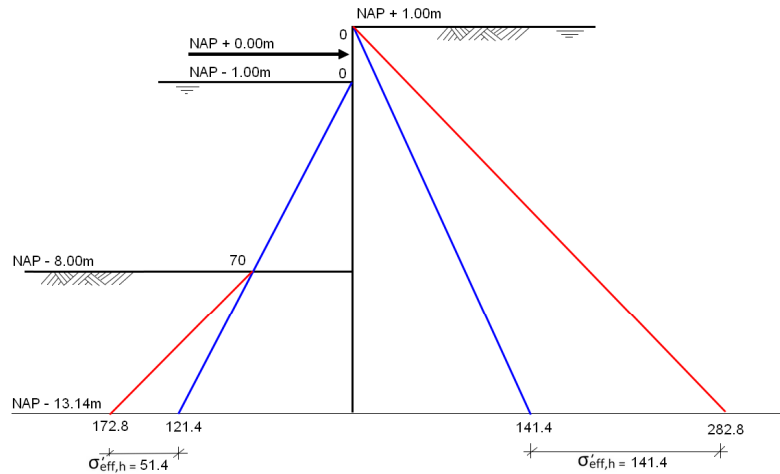
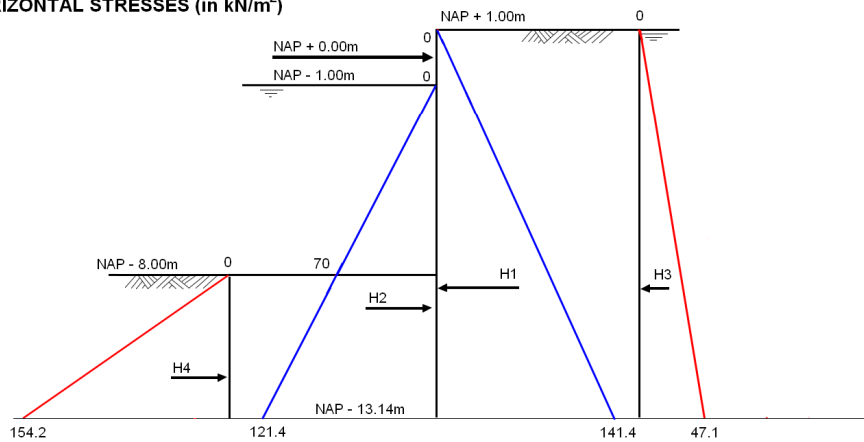
moment:

$M1_E = H1 \cdot a1 =$	2025	+ 720 d	+ 85 d <sup>2</sup>	+ 3,33 d <sup>3</sup>
$M2_E = H2 \cdot a2 =$	- 1388	- 560,3 d	- 75 d <sup>2</sup>	- 3,33 d <sup>3</sup>
$M3_E = H3 \cdot a3 =$	675	+ 240 d	+ 28,33 d <sup>2</sup>	+ 1,11 d <sup>3</sup>
$M4_E = H4 \cdot a4 =$			- 120 d <sup>2</sup>	- 10 d <sup>3</sup>
$\Sigma M =$	1312	+ 399,67 d	- 81,67 d <sup>2</sup>	- 8,89 d <sup>3</sup>

Equilibrium  $\Sigma M = 0$  is established for  $d = 5,14$  m.

Step 2. Calculate the required anchor force.

The stresses for  $d = 5,14$  m are indicated now below.

VERTICAL STRESSES (in kN/m<sup>2</sup>)HORIZONTAL STRESSES (in kN/m<sup>2</sup>)

Resulting horizontal forces:

Water:

$$H1 = 141,4/2 \times 14,14 = 999,7 \text{ kN/m'}$$

$$H2 = 121,4/2 \times 12,14 = 736,4 \text{ kN/m'}$$

Soil:

$$H3 = 47,3/2 \times 14,14 = 333,2 \text{ kN/m'}$$

$$H4 = 154,2/2 \times 5,14 = 396,3 \text{ kN/m'}$$

$$\Sigma H = 0 \rightarrow H_{strut} = H1 - H2 + H3 - H4 = 200 \text{ kN/m' } (\rightarrow)$$

Step 3. Calculate the required section modulus  $W_{eff,y}$ , choose a sheetpile profile:

The diagram of the resulting horizontal stresses can be found by summarizing the horizontal water pressures and horizontal effective soil stresses as given in the previous figure.

The shear force diagram is found by calculating the area under the resulting horizontal stresses diagram. The area of every slice equals the change in the shear stress diagram. (In other words: the shear stress is obtained by integrating the function for the resulting horizontal stresses). In the chosen schematisation, the shear stress diagram starts with 0 kN/m<sup>2</sup> (per m') at the soil surface.

The moment diagram is found by calculating the area under the shear stress diagram. The area per slice of the shear stress diagram equals the change in the moment diagram. The moment diagram starts with 0 kNm (per m') at the soil surface.

The M-diagram reaches its highest value where the value of the S-diagram is zero. This zero point can be calculated with the equation below (valid for  $2 < h < 9$  m and only for the situation in this example):

$$\frac{1}{2} \gamma_w (h-2)^2 + F_{strut} - \frac{1}{2} \gamma_w \cdot h^2 - \frac{1}{2} K_a \cdot h^2 \cdot (\gamma_{s,w} - \gamma_w) = 0 \rightarrow h = 6,95 \text{ m below ground level}$$

The point of zero shear force can also be found numerically by subdividing the soil into slices of 1 m and calculating the areas below the resulting horizontal stress diagram, which equals the change in the S-diagram line (which starts with  $S = 0$  at ground level). For instance, the total horizontal stress on the wall at NAP (1 m below ground level) is  $1.00 \cdot K_a (\gamma_{s,w} - \gamma_w) + 1.00 \gamma_w = 13,33 \text{ kN/m}^2$ . The value of the shear force in the wall at that point is  $\frac{1}{2} \cdot 13,3 \cdot 1,00 = 6,67 \text{ kN/m}$  (= the area below the resulting stress diagram over the highest 1 m). Because of the strut force, the shear force diagram then jumps to  $6,67 - 200 = -193,33 \text{ kN/m}$ . The shear diagram then follows a line to NAP - 5,95 m, where the shear stress is zero, then further to the right where it reaches a new (local) maximum and then it bends back because of the increasing passive stresses. This is a second degree function.

The moment diagram, a third degree function, can now be found by calculating the areas below the shear force diagram. These areas equal the changes in the moment diagram line. At ground level,  $M = 0$  because of the schematisation (free support). For the upper 1 m, this area is  $6,67 / 2 = 3,33 \text{ kNm/m}$ .

The values of the  $\sigma_h$ , S- and M-diagrams are given in the table below. This has been elaborated for slices of 1.00 m to obtain a rather precise result, see the following table and graphs.

depth level [m]	horizontal stress [kN/m]	S-diagram [kN/m]	M-diagram [kNm/m]
NAP + 1	0,00	0,00	0,00
NAP + 0	13,33	6,67	3,33
NAP + 0	13,33	-193,03	3,33
NAP - 1	26,67	-173,03	-179,70
NAP - 2	30,00	-144,70	-338,57
NAP - 3	33,33	-113,03	-467,43
NAP - 4	36,67	-78,03	-562,97
NAP - 5	40,00	-39,70	-621,83
NAP - 5.95	43,17	-0,20	-640,78
NAP - 6	43,33	1,97	-640,70
NAP - 7	46,67	46,97	-616,23
NAP - 8	50,00	95,30	-545,10
NAP - 9	23,33	131,97	-431,47
NAP - 9.875	0,00	142,17	-311,53
NAP - 10	-3,33	141,97	-293,77
NAP - 11	-30,00	123,22	-161,18
NAP - 12	-56,67	79,88	-59,63
NAP - 13	-83,33	12,00	-0,75
13.14	-87,07	0,00	0,00

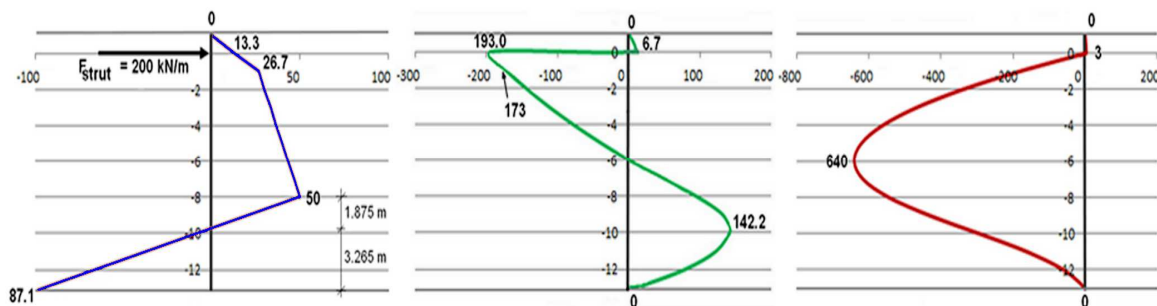
Table 39-6  $\sigma_h$ , S- and M-diagram

Figure 39-14 Resulting horizontal stress, shear force and moment diagrams

The maximum moment appears to be 641 kNm/m, at NAP - 5,95 m.

The required section modulus (*weerstandsmoment*) of the sheetpile profile then is:

$$W = \frac{M_{\max}}{f_{y,d}} = \frac{641 \cdot 10^3}{235} = 2728 \text{ m}^3/\text{m} = 2728 \cdot 10^3 \text{ mm}^3/\text{m}$$

Step 4: choose an appropriate sheet pile profile

According to the specifications of the manufacturer (Table 39-1), profile Hoesch 215 has a section modulus of  $3150 \times 10^3 \text{ mm}^3/\text{m}$ , which is a bit more than strictly required.

If the sheet pile wall is designed on the basis of the maximum bending moment there is no safety against failure. In order to increase the safety of the structure, often either a larger maximum bending moment is assumed than computed, or the passive ground pressure is reduced by using a conservative value for  $K_p$ .

#### Blum's schematisation of an anchored sheet pile wall

The schematisation of anchored sheetpile walls proposed by dr. Blum very much resembles his schematisation of cantilever sheetpile walls: The fixed end of the toe of the wall is replaced by a free support and a substitute force. In this case, however, the wall is considered to be flexible (deformable).

The loads on the sheet pile wall are schematized as shown on the right hand side of Figure 39-15.

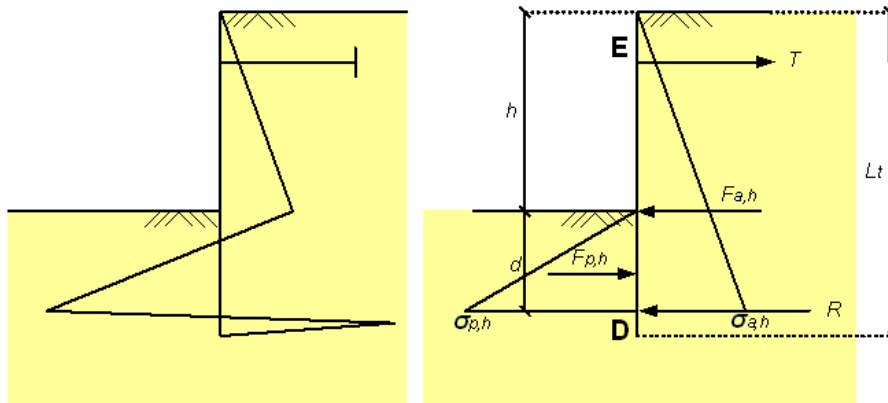


Figure 39-15 left: 'real' situation; right: Blum's schematisation.

In the above schematisation the substitute force  $R$  (= *Ersatzkraft*) is equivalent to the horizontal soil pressure at the lower part of the right hand side of the sheet pile wall. Furthermore it is assumed that the bending moment at the toe of the sheet pile is zero, but a shear force (of the magnitude  $R$ ) is allowed. To ensure that this shear force can develop, the actual length of the sheet piles should be longer than the sum of the retaining height and the embedded depth. Usually the computed embedded depth is increased by 20%.

The computation of the main sheetpile characteristics of anchored sheet pile walls differs from cantilever sheetpile walls, because now there are not two, but three unknown parameters: the embedded depth ( $d$ ), the anchor force ( $T$ ) and the substitute force ( $R$ ). They can be solved by considering the displacement at the anchor point, in addition to the horizontal equilibrium of forces, and the moment equilibrium. The displacement of the sheetpile wall at the anchor point is hindered by the anchors, so it equals zero.

Compared with the simplified method for anchored sheetpile walls, Blums' method will mostly lead to somewhat longer sheetpiles, but the required profiles will be lighter and also the displacements will be less. Hence the advantages of Blum's method, a lighter profile and smaller displacements, comes at the expense of a longer sheet pile wall.

The calculation of the embedded depth, anchor force and substitute force per unit length thus exists of the following steps:

- Step 1: compute the theoretical embedded depth ( $d$ ) using the condition that the horizontal displacement at the level of the anchor (point E) must be zero. Multiply this theoretical depth by 1,2 to compensate for the schematisation.
- Step 2: compute the equilibrium of moments around the toe of the sheet pile (point D) in order to determine the anchor force ( $T$ ).
- Step 3: compute the substitute force ( $R$ ), from the horizontal equilibrium  $\sum H=0$ .
- Step 4: compute the required section modulus ( $W_{eff,y}$ ).

### Example calculation of an anchored sheetpile wall using Blum's method

The situation and soil profile for this example are extremely simplified to avoid too complex computation, see Figure 39-16. It is assumed that the sheet pile wall is placed in a homogeneous dry soil (sand).

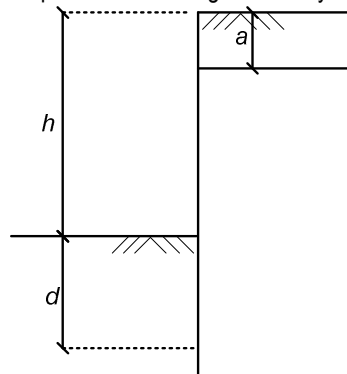


Figure 39-16 situation and soil profile.

#### Given

Active soil pressure coefficient ( $K_a$ )	$\frac{1}{3}$	[-]
Passive soil pressure coefficient ( $K_p$ )	3	[-]
Specific weight of dry sand ( $\gamma_d$ )	18	[kN/m <sup>3</sup> ]
Retaining height ( $h$ )	6	[m]
Depth of the anchor below ground level ( $a$ )	1	[m]
Cohesion ( $c$ )	0	[kN/m <sup>2</sup> ]
Wall friction for a smooth wall ( $\delta$ )	0	[°]

#### Asked

Calculate required section modulus and length of the sheetpile wall and choose a suitable Larssen profile with steel quality S235.

#### Elaboration

##### Step 1. Compute the embedded depth ( $d$ ) and the total length of the sheet piles ( $L_t$ )

For the computation of the horizontal displacement at the top of the sheet pile wall (which must be zero), the contribution of the three types of loading can best be considered separately, see figure below. The displacements are computed using the theory of bending beams, from applied mechanics.

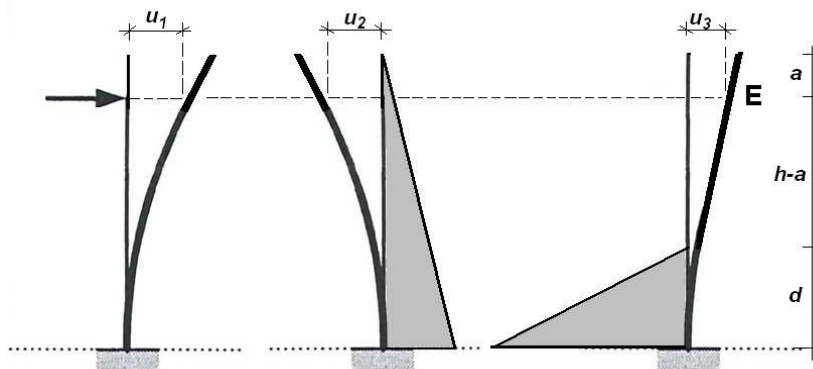


Figure 39-17 Displacement effects due to various loads.

The first loading case is the anchor force ( $T$ ), which leads to a horizontal displacement at the top of the sheet pile of:

$$u_1 = \frac{T \cdot (h+d-a)^3}{3 \cdot EI} + \frac{T \cdot (h+d-a)^2}{2 \cdot EI} \cdot a = \frac{T \cdot (h+d-a) \cdot (h+d-a)^2}{3 \cdot EI} + \frac{T \cdot (h+d-a) \cdot (h+d-a) \cdot a}{2 \cdot EI}$$

The first term in this expression indicates the displacement of the wall at the point of application of the anchor force, which can be found as a standard deflection formula (*vergeet-me-nietje*, see Section 3.1 of this Manual). The second term is the additional displacement of the wall above this point (over length  $a$ ) (*kwispeleffect*). For small angles  $\tan(\varphi) \approx \varphi$ , hence  $a \cdot \tan(\varphi) \approx a \cdot \varphi$

The loading as a result of the active soil pressure results in a horizontal displacement at the anchor point of:

$$u_2 = -\frac{q \cdot (h+d-a)^4}{30 \cdot EI} = -\frac{K_a \cdot \gamma_d \cdot (h+d-a)^5}{30 \cdot EI}$$

The loading as a result of the passive soil pressure results in a horizontal displacement at the anchor point of:

$$u_3 = \frac{q \cdot d^4}{30 \cdot EI} + \frac{q \cdot d^3}{24 \cdot EI} \cdot (h-a) = \frac{K_p \cdot \gamma_d \cdot d^5}{30 \cdot EI} + \frac{K_p \cdot \gamma_d \cdot d^4 \cdot (h-a)}{24 \cdot EI}$$

The first term in the expression indicates the displacement at the top of the load, the second term is the additional displacement of the wall above the top of the load.

The sum of these three displacements should be zero at the anchor point. After multiplication with  $\frac{EI}{K_p \cdot \gamma_d}$  and substituting

$T \cdot (h+d-a) = \frac{1}{6} \cdot K_a \cdot \gamma_d \cdot (h+d)^3 - \frac{1}{6} \cdot K_p \cdot \gamma_d \cdot d^3$  in the expression for  $u_1$  (which follows from an equilibrium of moments about the toe of the sheet pile), this results in a total displacement of:

$$u_1 + u_2 + u_3 = \frac{K_a \cdot (h+d)^3 \cdot (h+d-a)^2}{K_p \cdot 18} - \frac{d^3 \cdot (h+d-a)^2}{18} + \frac{K_a \cdot (h+d)^3 \cdot (h+d-a) \cdot a}{K_p \cdot 12} - \frac{d^3 \cdot (h+d-a) \cdot a}{12} - \frac{K_a \cdot (h+d-a)^5}{K_p \cdot 30} + \frac{d^5}{30} + \frac{d^4 \cdot (h-a)}{24} = 0$$

Because all variables are known except for  $d$ , this equation can be solved by substituting the other symbols with their values:

$$\frac{(6+d)^3 \cdot (5+d)^2}{162} - \frac{d^3 \cdot (5+d)^2}{18} + \frac{(6+d)^3 \cdot (5+d)}{108} - \frac{d^3 \cdot (5+d)}{12} - \frac{(5+d)^5}{270} + \frac{d^5}{30} + \frac{5 \cdot d^4}{24} = 0$$

It can now be iteratively computed that this equation is valid for  $d = 5.06$  m.

As was already mentioned earlier it is common practise to increase the embedded depth by 20% in order to provide some safety within the structure. The total length of the sheet piles then becomes:  $L_t = h + 1,2d = 6,00 + 1,2 \cdot 5,06 \approx 12,07$  m. According to the manufacturers of sheet pile elements, their delivered length can deviate +/- 0,20 m from the ordered length, so choose an overall-length of about 12,50 m.

**Step 2. Compute the anchor force ( $T$ ) per m<sup>1</sup>**

$$\sum M_D = 0 \rightarrow -F_{a,h} \cdot \frac{1}{3} \cdot (h+d) + F_{p,h} \cdot \frac{1}{3} \cdot d + T \cdot (h+d-a) = 0$$

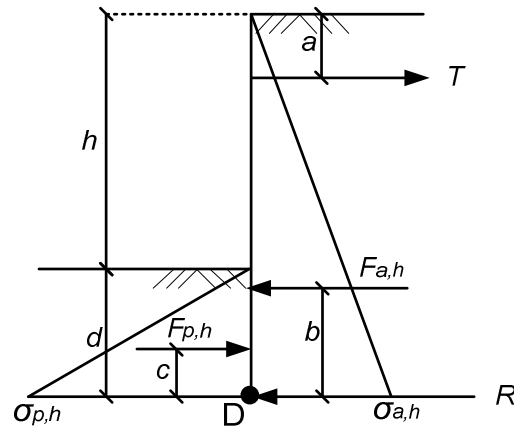


Figure 39-18 Forces working on the sheet pile wall.

$$\sigma_{p,h} = K_p \cdot \sigma_{p,eff,v} + \sigma_w = K_p \cdot \gamma_d \cdot d + 0$$

$$\sigma_{a,h} = K_a \cdot \sigma_{a,eff,v} + \sigma_w = K_a \cdot \gamma_d \cdot (h+d) + 0$$

$$F_{a,h} = \frac{1}{2} \cdot K_a \cdot \gamma_d \cdot (h+d)^2 \text{ and } F_{p,h} = \frac{1}{2} \cdot K_p \cdot \gamma_d \cdot d^2$$

$$b = \frac{1}{3} \cdot (h+d) \text{ and } c = \frac{1}{3} \cdot d$$

$$\sum M_D = 0 \Rightarrow -F_{a,h} \cdot \frac{1}{3} \cdot (h+d) + F_{p,h} \cdot \frac{1}{3} \cdot d + T \cdot (h+d-a) = 0$$

$$\Leftrightarrow T \cdot (h+d-a) = \frac{1}{6} \cdot K_a \cdot \gamma_d \cdot (h+d)^3 - \frac{1}{6} \cdot K_p \cdot \gamma_d \cdot d^3$$

$$\Leftrightarrow T = \frac{\frac{1}{6} \cdot K_a \cdot \gamma_d \cdot (h+d)^3 - \frac{1}{6} \cdot K_p \cdot \gamma_d \cdot d^3}{(h+d-a)} = \frac{\frac{1}{6} \cdot \frac{1}{3} \cdot 18 \cdot (6+5,06)^3 - \frac{1}{6} \cdot 3 \cdot 18 \cdot 5,06^3}{(6+5,06-1)} = 18,58 \text{ kN/m}$$

**Step 3. Compute the substitute force ( $R$ ) per m<sup>1</sup>**

$$\sum H = 0 \Rightarrow -F_{a,h} + F_{p,h} + T - R = 0$$

$$\Leftrightarrow R = -F_{a,h} + F_{p,h} + T$$

$$\Leftrightarrow R = -\frac{1}{2} \cdot K_a \cdot \gamma_d \cdot (h+d)^2 + \frac{1}{2} \cdot K_p \cdot \gamma_d \cdot d^2 + T$$

$$\Leftrightarrow R = -\frac{1}{2} \cdot \frac{1}{3} \cdot 18 \cdot (6+5,06)^2 + \frac{1}{2} \cdot 3 \cdot 18 \cdot 5,06^2 + 18,58 = -366,97 + 691,30 + 18,85 = 343,18 \text{ kN/m}$$

**Step 4. Compute the required section modulus ( $W_{eff,y}$ )**

The required section modulus can be found when the maximum bending moment in the wall and the yield stress of the steel are known. The yield stress is a material property which should be guaranteed by the manufacturer of the sheet piles (depending on the steel quality). The maximum bending moment can be computed with help of the diagrams of horizontal stress, the shear force diagram and moment diagram. The way of drawing these diagrams has been explained in the previous two examples, so only the result is presented here (Figure 39-19).

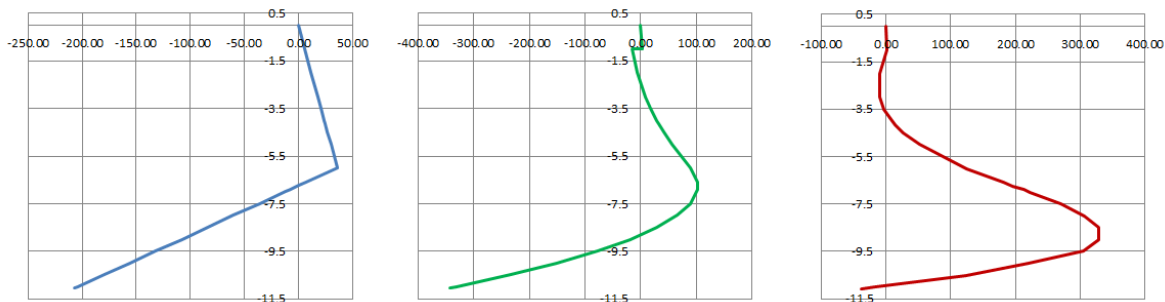


Figure 39-19 Resulting horizontal stress, shear force and moment diagrams

The maximum moment occurs where the shear force is zero. This is at 8,80 m below the ground surface, where  $M_{max} = 329,24$  kNm/m.

To check the calculation, two things can be done now:

1. Check if the value of the shear force diagram at  $d + h = 11,06$  m below soil surface equals the substitute force found in step 3 of the calculation.
2. Check if the value of the moment diagram is zero (or about zero) at  $d + h = 11,06$  m below soil surface.

#### Step 5. Choose a suitable profile.

The required section modulus (*weerstandsmoment*) of the sheetpile profile then is:

$$W = \frac{M_{max}}{f_{y,d}} = \frac{329,24 \cdot 10^3}{235} = 1401 \text{ m}^3/\text{m} = 1401 \cdot 10^3 \text{ mm}^3/\text{m} = 1401 \text{ cm}^3/\text{m}$$

According to Table 39-2 a Larssen 704 profile will suffice ( $W_y = 1600$  cm<sup>3</sup>/m). Again no factors of safety were used in this example!

Regards the relatively low anchor force, it is in a real design worthwhile to try whether a cantilever sheetpile wall would suffice here. Maybe the length and profile would increase, but it would save the costs (and trouble) of making anchors or a support framework.

### **Vertically loaded sheetpile walls**

Sheetpile walls can be exposed to vertical forces, originating from:

- self-weight of the sheetpile elements
- vertical component of resulting soil force (active + passive)
- vertical components of inclined anchors
- surcharge or vertical forces from superstructures
- possible other vertical forces acting on the wall

These forces have to be transferred to subsoil, which should have sufficient bearing capacity.

The vertical component of resulting soil force can be calculated according to:

$$F_v = F_h \cdot \tan(\delta)$$

where  $\delta$  represents the angle of wall friction (*wandwrijvingshoek*). This angle can be determined with help of tests on soil samples (direct shear stress test), but these tests are often difficult to carry out and the result is anyhow not very reliable. Therefore  $\delta$  is often related to the angle of internal friction ( $\varphi$ ) and also the coarseness of the soil. Eurocode 7 restricts  $\delta$  to  $2/3 \varphi'$  (for steel or concrete sheet piles in sand or gravel) and to  $\varphi$  for concrete cast in soil.

Based on long experience, Rijkswaterstaat found the following values for the angle of wall friction:

- |   |                         |
|---|-------------------------|
| - for gravel with $D_{50} > 8$ mm:      | $\delta = 0^\circ$      |
| - for coarse sand with $D_{50} > 2$ mm: | $\delta = 1/3 \varphi'$ |
| - for sand with $D_{50} < 2$ mm:        | $\delta = 2/3 \varphi'$ |
| - for loam                              | $\delta = 1/2 \varphi'$ |
| - for clay                              | $\delta = 1/3 \varphi'$ |

The direction of the wall friction respective to the wall is downward at the active side and upward at the passive side. In case of an external load on the sheetpile wall, these directions can revert.

The bearing capacity of the subsoil consists of two components:

- bearing capacity of the tip of the sheetpile elements
- bearing capacity of the wall friction of the sheetpile elements

According to CUR-publication 166 (*Handboek kademuren*), the calculation of the vertical bearing capacity can be done in analogy to the method for compression piles (see also Chapter 42 of this Manual):

$$F_{r, max} = F_{r, max, tip} + F_{r, max, wall}$$

and:

$$F_{r, max, tip} = A_{tip} \cdot p_{r, max, tip}$$

$$F_{r, max, wall} = 2 \cdot A_{wall} \cdot \int p_{r, max, wall} dz$$

where:

$F_{r, max, tip}$	[kN/m']	= bearing capacity of the tip
$F_{r, max, wall}$	[kN/m']	= shaft friction capacity
$A_{tip}$	[m <sup>2</sup> /m]	= cross-sectional area of the sheet pile wall
$A_{wall}$	[m <sup>2</sup> /m]	= wall area (one side of the wall)
$p_{r, max, tip}$	[kN/m <sup>2</sup> ]	= maximum tip resistance
$p_{r, max, wall}$	[kN/m <sup>2</sup> ]	= maximum wall friction

For the estimation of the maximum tip resistance  $p_{r, max, tip}$  and the maximum wall friction  $p_{r, max, wall}$ , reference is made to section 42.3.

For the calculation of the tip resistance of sheet pile walls, the following parameters should be used:

$\alpha_p = 1,0$ ;  $\beta = 1,0$ ;  $s = 0,62$ . The tip cross-sectional area can be computed with  $D_{eq} = \sqrt{\frac{4}{\pi} A_{tip}}$ .

If the average vertical load does not exceed 12.5 kN/m<sup>2</sup>, the vertical bearing capacity can be carried out separate from the horizontal equilibrium check. Otherwise, an interaction calculation should be carried out of vertical and horizontal forces. Usually finite element or spring models are used for these cases.

#### Note

- An eccentric vertical load will introduce a second order moment the wall, which should be taken into account.

## 39.2 Combi-walls

Combi-walls (*combiwanden*) are in fact reinforced sheet pile walls that consist of a combination of sheet piling and steel pipe piles. Usually a combi-wall section, see Figure 39-20, consists of two pipe piles with two to three Z-shaped sheet piles or one U-shaped sheet pile in between (The most commonly used configuration has two Z-sheet piles in between). The pipe piles are fitted with interlocks, thus providing a soil and water tight connection between the sheet piles and the pipe piles. The pipe piles have a far larger flexural rigidity ( $EI$ ) than the sheet piles and hence give the structure strength and stiffness. The sheet piles provide a watertight seal in between two pipe piles.



Figure 39-20 Cross-section, side-view and welded interlock of a combi-wall

An overview of combi-wall types is given in Figure 39-21.

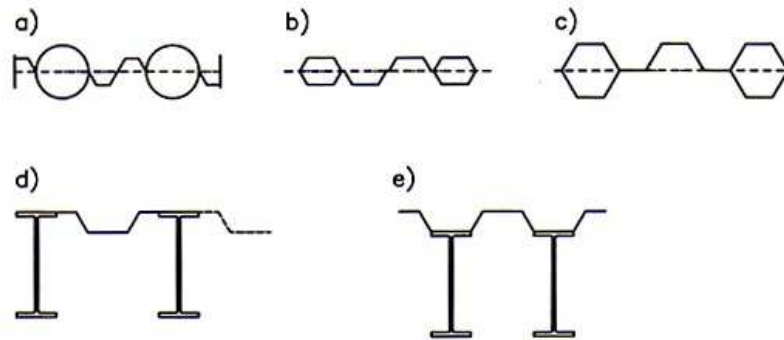


Figure 39-21 Types of combi-walls (from: Grundwerke in Beispielen)

The disadvantages of combi-walls are that the pipe piles make the wall much more expensive and that removing the pipe piles leaves a large hole, because the ground usually stays stuck within the tube (especially in cohesive ground layers).

Combi-walls are generally used for deep excavations. However as a result of the use of the pipe piles they can withstand larger loads than conventional sheet pile structures. Examples of the application of combi-walls are: underground car parks, quay walls and tunnel entrances. In quay walls the toe of sheet piles are often placed less deep than pipe piles. The customary external diameter of the steel pipe piles lies between about 800 and 2000 mm, the customary wall thickness lies between 10 and 20 mm.

As stated before, combi-walls have a far larger flexural rigidity. A combi-wall  $\varnothing 1620 \text{ mm} \times 19 \text{ mm} + 2 \text{ PU20}$  has an  $EI$  equal to  $2.28 \cdot 10^6 \text{ kNm}^2/\text{m}$ . That is almost 10 times as stiff as an AZ48! In this case the flexural rigidity of the PU20 sheet piling is almost negligible compared with that of the tubular pile.

It is easy to calculate the flexural rigidity of tubular piles. After all, for tubular profiles:

$$I_y = I_z = \frac{\pi(D^4 - d^4)}{64}$$

Where:

$I$	[m <sup>4</sup> /m]	=	area moment of inertia
$D$	[m]	=	outer diameter pipe pile
$t$	[m]	=	thickness tube wall = $(D - d)$
$d$	[m]	=	inner diameter pipe pile = $D - 2t$

For the Youngs' modulus one can use:

$$E_{\text{steel}} = 2,1 \cdot 10^5 \text{ N/mm}^2 (= 2.1 \cdot 10^8 \text{ kN/m}^2).$$

The bending stiffness (flexural rigidity)  $EI$  per metre combi-wall therefore mainly depends on the type of pipe pile and on the collective width of sheet piling between these tubular piles. The area moment of inertia ( $I$ ) of a sheet pile profiles can be found in Table 39-1, Table 39-2, Table 39-3 or in the manufacturers' fact sheet.

---

**Example calculation of the area moment of inertia of a combi-wall**
Given

A combi-wall consisting of: - steel pipe piles with a diameter of 1270 mm and a wall thickness of 16 mm;  
 - Hoesch 1705 sheet piles.

There are two sheet piles in between every two pipe piles.

Question

Compute the flexural rigidity of the combi-wall as a whole.

Elaboration

From Table 39-1:  $I_{sheetpile} = 30\,100\text{ cm}^4/\text{m}$  ( $= 30\,100 \cdot 10^4\text{ mm}^4/\text{m}$ ) and the width of the sheet piles is  $b = 575\text{ mm}$ .  
 The centre-to-centre distance of the pipe piles thus is  $1270/2 + 2 \cdot 575 + 1270/2 = 2420\text{ mm}$ .

$$I_{pipe\ pile} = \frac{\pi \cdot (1270^4 - 1238^4)}{64} = 12,392 \cdot 10^9\text{ mm}^4 \quad (= 1239\,200\text{ cm}^4)$$

$$I_{wall} = \frac{I_{pipe\ pile} + I_{sheetpile}}{ctc\text{-distance}} = \frac{12\,392 \cdot 10^6 + 301 \cdot 10^6}{2,420} = 524\,504 \cdot 10^4\text{ mm}^4/\text{m}$$

The computation shows that a combi-wall indeed has a much larger moment or inertia than a sheet pile wall ( $524\,504 \gg 30\,100\text{ cm}^4/\text{m}$ ), as was already expected. Note that the moment of inertia of the sheet pile profiles does barely contribute to the average flexural rigidity of the combi-wall.

---

**Note**

- *Combi-walls have to be checked for local buckling of the pile shaft.*

### 39.3 Diaphragm walls

The scarcity of space, especially in urban areas, has in recent years led to an increasing demand for underground structures. The required depth of these structures has increased over the years, and also stringent requirements regarding noise and vibration nuisance are imposed during construction. Furthermore often nearby adjacent properties are situated close to the building site, as a result of which the retaining walls should be very stiff in order to keep the deformation of the wall small. All in all diaphragm walls, also called slurry walls, (*diepwanden*) have become an indispensable alternative.

Especially for diaphragm walls the relationship between design and construction is important. Critical parts of the design and construction process are:

- the design of the reinforcement cage (good concrete flow ability and hence a large enough mesh width);
- control of the properties of both the concrete and bentonite;
- the process of de-sanding or exchanging the bentonite;
- the cleaning of the joints, if necessary;
- the process of casting the concrete.

#### **Design**

In this section only the basic outline of the design rules regarding diaphragm walls are treated. For more detailed information the reader is referred to the Handbook Sheetpile Structures (CUR 166, in Dutch), the Handbook Quay Walls (CUR 211, in English). CUR-report 76 gives design rules for diaphragm walls (in Dutch).

#### **Strength**

In essence the strength that a diaphragm wall needs is computed in a similar way as for sheet pile walls computations using Blum's method, see Section 39.1 of this Manual ("soil retaining walls"). However, there are some differences. First of all the bending stiffness ( $EI$ ) is rather different. As shown in the following computation the bending stiffness of a diaphragm wall is much larger than that of a very stiff sheet pile profile.

---

#### Example comparison bending stiffness of diaphragm wall and sheet pile

##### Given:

A sheet pile profile AZ48 with:

$$\begin{aligned} b &= 580 && [\text{mm}] \\ I &= 67\,090 \cdot 10^4 && [\text{mm}^4/\text{m}] \\ E &= 210\,000 && [\text{N}/\text{mm}^2] \end{aligned}$$

A diaphragm wall with:

$$\begin{aligned} b &= 1.00 && [\text{m}] \\ \ell &= 15.00 && [\text{m}] \\ I &= \frac{1}{12} \cdot b \cdot h^3 && [\text{mm}^4] \\ E &= 10\,000 && [\text{N}/\text{mm}^2] \end{aligned}$$

Please note that the Young's modulus used for the diaphragm is that of the cracked cross-section, see also Section 36.6 of this Manual: "Stiffness of a concrete structure". Also note that the Young's modulus for steel is 21 times larger than that of the cracked concrete.

Usually the panel width ( $b$ ) is in the order of 0,8-1,5 m, panel widths of 0,8, 1,0 and 1,2 m are most commonly used.

##### Elaboration:

The bending stiffness for 1 m sheet piles is:  $EI = 210\,000 \cdot 67\,090 \cdot 10^4 = 141 \cdot 10^{12} \text{ Nmm}^2 / \text{m}$

The bending stiffness for 1m diaphragm wall is:  $EI = 10\,000 \cdot \frac{1}{12} \cdot 1000 \cdot 1000^3 = 833 \cdot 10^{12} \text{ Nmm}^2 / \text{m}$

As expected the bending stiffness of the diaphragm wall is much larger than the bending stiffness of the sheet pile profile. This is a direct result of the fact that the area moment of inertia ( $I$ ) of the diaphragm wall is much larger.

---

As a result of the large bending stiffness of the diaphragm wall, the deformation at the top of the wall is very small, resulting in an equally very small deformation of the soil behind the wall. The horizontal passive soil pressure should therefore be calculated with a passive soil coefficient ( $K_p$ ) with an angle of internal friction of maximum  $\frac{2}{3}\phi \leq 20^\circ$ .

Another major difference with the computation of a sheet pile wall according to Blum's method is that after the initial computation, using Blum's method, the diaphragm wall has to be computed again using a simple spring model, e.g. DSheet. This is necessary because Blum's method gives a good initial estimation of the strength needed, but for a final design the computation with a simple spring model is necessary in order to establish the real occurring bending moments and shear forces, as these are slightly underestimated by Blum's method (in case of a diaphragm wall). Usually the diaphragm wall will turn out to be somewhat longer and heavier. The computed horizontal force and moment are used to determine the amount of reinforcement steel needed.

An additional benefit of using a computer model is that curved sliding planes can be used, which gives a more accurate representation of reality. For a hand calculation this is too complicated, so straight sliding planes are used then. This, however, leads to an overestimated strength, which is compensated by a reduction of the wall friction angle ( $\delta$ ). According to NEN 6740, table 4, the following values for the wall friction should be used in diaphragm computations:

Curved sliding planes: - in sand and clay:  $\delta/2$   
- in peat:  $\delta = 0$

Straight sliding planes: - in sand and clay:  $2/3 \delta$   
- in peat:  $\delta = 0$

#### Reinforcement and concrete cover

With respect to the computation regarding the required reinforcement, reference is made to Sections 36.5 and 36.6 of this Manual.

As a result of the way in which a diaphragm wall is constructed, some essential additional requirements have to be met with respect to the reinforcement cage:

- 1) due to the long panel length (6-8 m), usually two reinforcement cages are placed alongside (in top view). Since the forces are mostly directed perpendicular to the wall the cages are usually not coupled width-wise;
- 2) due to the large depth the reinforcement cages consist of parts of transportable lengths which are coupled on site before or during the lifting;
- 3) stiffness of the reinforcement cages is of minor importance because they are suspended vertically. Nevertheless, they should be stiff enough in order to be able to be transported and to prevent lasting deformations during the placement. Usually welded cages are used, in stead of twined cages (*gevlochten korven*);
- 4) the flow ability of the reinforcement cage has to meet high standards since the support fluid has to be displaced during the placement and because the concrete has to be poured continuously over a large height;
- 5) the concrete cover has to be at least 75 mm under normal conditions and at least 100 mm in case of weak soil layers, such as peat and clay;
- 6) the free space between the reinforcement cage and the grout float of the previous section must be at least 100 mm, but preferred is 200 mm. The distance between the bottom of the wall and the reinforcement cage must be at least 200 mm;
- 7) the minimum centre to centre distance between horizontal reinforcement bars amounts 200 mm, between vertical bars this distance is 100 mm;
- 8) the minimum distance between reinforcement cages within one panel must be at least 200 mm, but preferred is 400 mm.

The concrete used for diaphragm walls is usually C20/25 or C30/37 and the exposure classification is XC4, alternating wet and dry (see also Chapter 35 of this Manual). Additional requirements are:

- a high resistance against segregation (*ontmenging*);
- a good consistency (plastic behaviour) and maintaining sufficient consistency;
- a good coherence;
- certain self-compacting properties.

### Deformation

Both failure of the soil- and/or water retaining function of a diaphragm wall and the deformation of the wall are likely to lead to settlements of the soil behind the diaphragm wall. In order to prevent damage, the allowable deformations of the diaphragm wall and/or the adjacent land are limited. These limits are defined as an allowable combination of settlement, relative rotation ( $\beta$ ) and horizontal displacement ( $\epsilon_h$ ) that adjacent structures may undergo. In appendix H of NEN-EN 1997-1 recommendations are stated for the limit values for the deformation of normal, conventional structures. For many structures a maximum relative rotation of 1:500 is acceptable in order to prevent the occurrence of the serviceability limit state. The ultimate limit state occurs around a relative rotation of 1:150, see Table 39-7. The ratios mentioned apply to the sagging mode, see Figure 39-22. For a hogging mode (edge settling is larger than the part in between) the ratios mentioned should be halved.

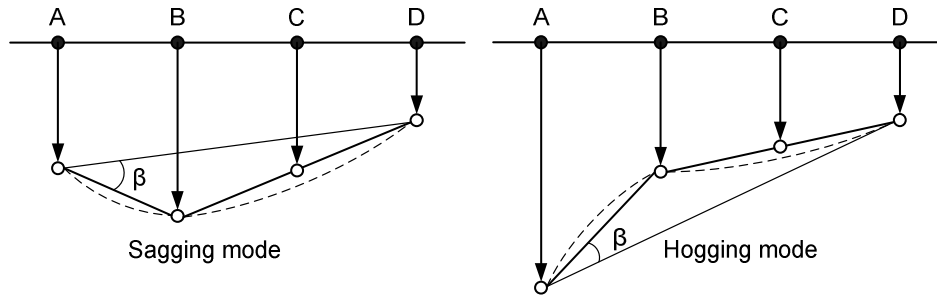


Figure 39-22 Structural deformation

Furthermore it is stated in the NEN-EN 1997-1 that for separate foundations under normal conditions a total settlement of maximum 50 mm is allowable. A larger settlement may be allowable provided that the relative rotation is limited and no problems with house connections and public utilities (*nutsvoorzieningen*) come into play.

Qualification	Limit state	Limit relative rotation ( $\beta$ )	
		Framing ( <i>skeletbouw</i> )	Masonry
Architectonic damage (cracks up to 5 mm)	SLS	1:300 (general)	1:600 (downward direction)
		1:600 (skyscrapers)	1:1200 (upward direction)
		1:1000 (warehouse)	
Structural damage (cracks 15-25 mm)	ULS	1:150	1:300 (downward direction)
			1:600 (upward direction)
Collapse	ULS	1:75	1:150 (downward direction)
			1:300 (upward direction)

Table 39-7 Allowable limits for the relative rotation

The above table is suitable for newly constructed structures. For an older structure, that is likely to have already undergone a differential settlement, stricter rules must be applied e.g. an allowable rotation that is 1.5 times smaller than otherwise (1:500 instead of 1:300).

In Figure 39-23 damage thresholds related to a combination of the relative rotation and the horizontal displacement are presented. In this figure, the relative rotation is the result of the differential settlement due to the self-weight of the structure and the horizontal displacements represent the influence of the nearby excavation.

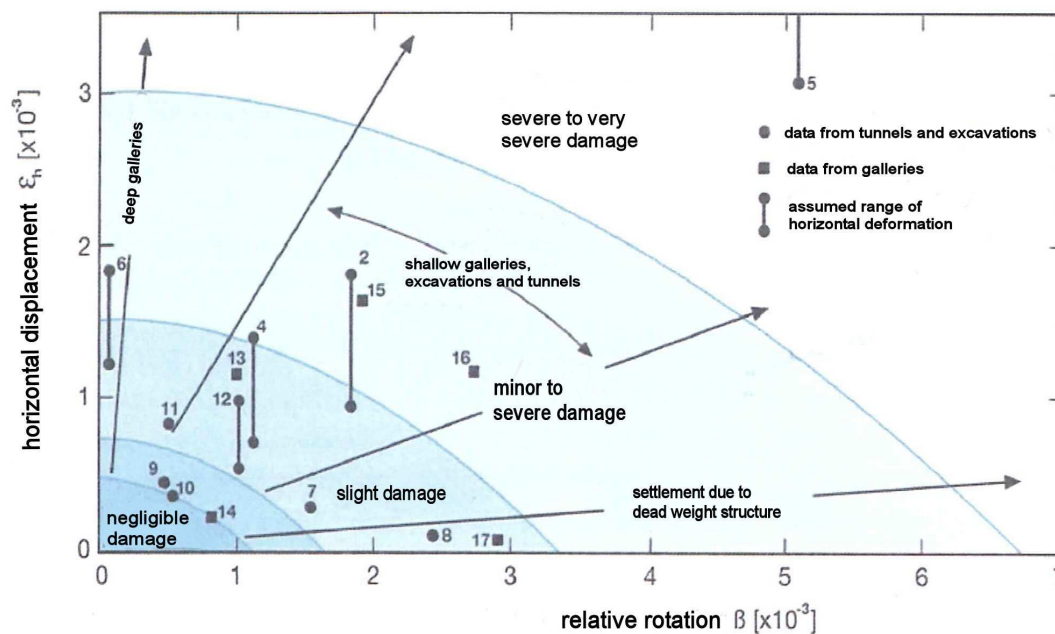


Figure 39-23 Damage thresholds of diaphragm walls

Limits for the horizontal displacement in the subsoil at the location of pile foundations are not found in literature. However during the design of the Willems railroad tunnel in Rotterdam a maximum horizontal displacement equal to 1/6 of the shaft diameter was allowed as a safe limit for prefabricated concrete piles. This limit value is related to the fact that in the case of a centric load on the pile no tensile stress occurs in the pile shaft as a result of eccentricity. For wooden foundation piles a horizontal displacement of 0.10 m was considered allowable.

**Water tightness**

In many cases diaphragm walls are used to enable dry excavation in a deep building pit. Often the lowest point of the wall is situated in an impermeable soil layer, but also underwater concrete can be used to close off the bottom of the building pit.

The under normal circumstances occurring amount of leakage water depends on the following environmental factors:

- permeability of the soil layers behind the diaphragm wall;
- water pressure present in these layers;
- quality of the diaphragm wall and the joints.

In order to be able to connect the usage of an underground space to the allowable amount of leakage water a classification is desired. A possible classification based on Austrian guidelines is presented in Table 39-8.

Classification	Description	Quantification water locking ability	Functionality
1	completely dry	-	specific goods storage
2	relative dry	damp stains acceptable up to 1‰ of the visible surface. Water trails up to 0,20 m	spaces for public use, storage
3	slightly damp	damp stains acceptable up to 1‰ of the visible surface. A few water trails are permitted	garages, infrastructural projects
4	damp	Maximum leakage per spot or per m <sup>1</sup> joint 0,2 l/h; and the average amount per m <sup>2</sup> wall 0,01 l/h	garages, infrastructural projects with additional measures
5	wet	Maximum leakage per spot or per m <sup>1</sup> joint 2 l/h; and the average amount per m <sup>2</sup> wall 1 l/h	-

Table 39-8 Classification regarding the amount of allowable leakage water.

Taking into account a high water table, which is customary in the western part of The Netherlands, and excavation depths for which the usage of a diaphragm wall is realistic, generally speaking the water pressure against the wall is 10 mwc or more. For a situation where aquifers are present behind the diaphragm wall it turns out that in practise only structures belonging to classes 4 and 5 are feasible. In case of water pressures exceeding 15 mwc only class 5 structures are feasible. The consequence of these findings is that usually a front wall (*voorzetwand*) must be constructed in front of the diaphragm wall.

### Construction

The construction stages of diaphragm walls are illustrated in Figure 39-24. First, the trench is excavated in panels with help of guiding beams and special rectangular diggers (stages 1 and 2). A standard panel has a width of 0,6 to 1,5 m and a length of 2,8 to 8,0 m. The depth can amount up to 30 m. As a rule of thumb the minimum dimensions of the guide walls have a height of 1,00 m and a width of 0,20 m. These guide wall dimensions are governed by the horizontal load (soil and equipment) and the changing fluid level in the trench during the excavation. The fluid level is not allowed to drop regularly beneath the guide walls as the fluid motion will erode the soil underneath the walls.

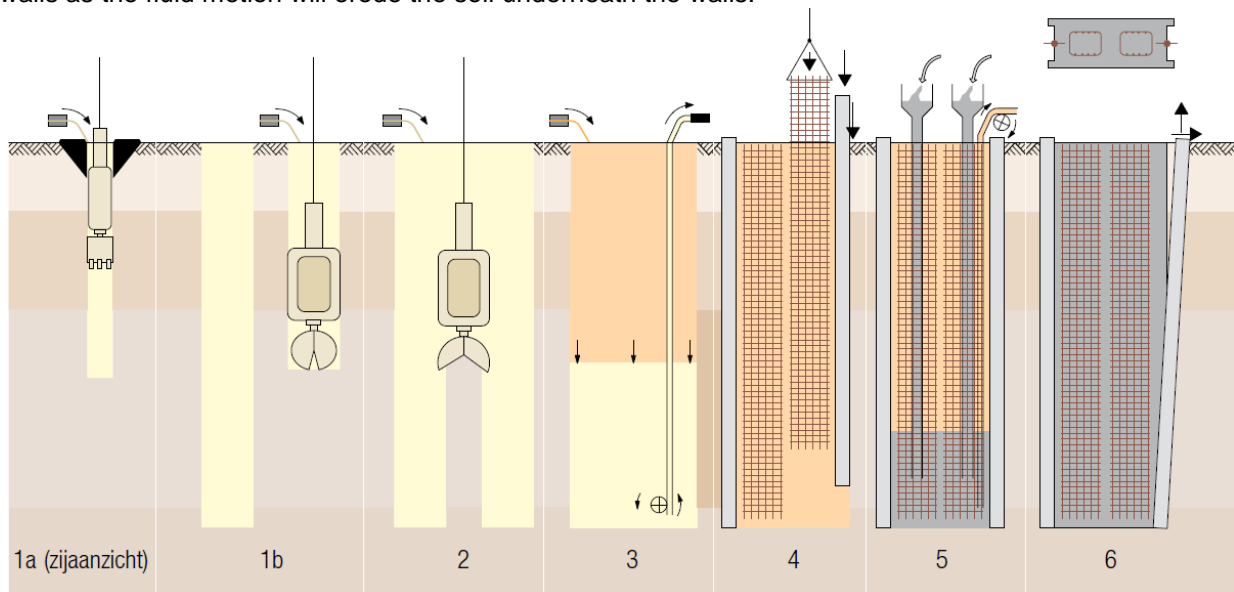


Figure 39-24 Construction stages of a diaphragm wall (from: <http://www.wtcb.be>)

The trench is filled with a support fluid (mostly bentonite) already during excavation to avoid collapse of the soil walls. So, the excavation takes place in the support fluid. The support fluid becomes mixed with soil falling down from the wall, so it is replaced by clean bentonite (stage 3) before the joints and the reinforcement cages are positioned (stage 4). Synthetic joint ribbons (*voegbanden*) are integrated in these joints so that they can be cast-in in the concrete.

Subsequently, concrete is cast with help of cast tubes (*stortbuizen*) (stage 5). Since the density of concrete is larger than that of the bentonite mixture and because the concrete mixture is pumped in the trench near the bottom, the bentonite mixture “floats” on top of the concrete and the surplus can be collected for re-use. There is some mixing, hence the upper 1 to 2 m concrete is of poor quality and must be removed (and eventually replaced) afterwards. Finally, the joints are removed, but the cast-in joint ribbons remain at their place so that they form a water-tight connection between the panels (stage 6).

### Leakage of the joints

If the diaphragm wall appears to contain soil or bentonite lumps adjacent to the joints, this will most probably lead to leakage. This can be repaired by attaching steel plates to the inside of the diaphragm walls and injecting PUR-foam behind the plates in the arisen gap. If the flow of the soil-water mixture through the gap is too strong to use this repair method, the gap can otherwise be blocked with a 'dam' consisting of clay or sand with a clay core, after which the soil behind the diaphragm wall is frozen by freeze lances. After the flow is stopped the temporary dam is removed and again steel plates are positioned over the weak spots. When this is done, the freeze lances can be removed.

### Trench stability

If no special measures are taken during excavation of a deep trench, it is very likely that the walls of the trench will collapse. In the case of diaphragm walls the trench is filled with a support fluid, usually a bentonite mixture, to enhance the stability of the trench walls.

One distinguishes between micro instability and macro instability of the trench walls, see Figure 39-25.

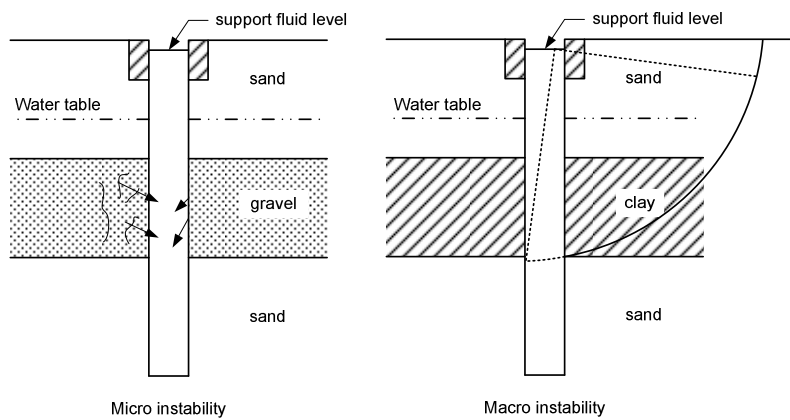


Figure 39-25 Micro and macro instability of trench walls

Micro-instability is a failure mechanism that only occurs in non-cohesive soils. It occurs when individual grains situated at the edge of the trench lose their stability and fall into the trench. Also the collapse of small sections of the trench walls is regarded as micro instability. The presence of support fluid in the trench can prevent micro instability. This will work if the support fluid does not move any more, in which case it will have a certain shear strength. The fluid that has infiltrated the grain skeleton of the soil will then stabilize the grains at the edge of the trench wall.

This yield stress (*zwichspanning*) can be computed as follows:

$$\tau_f \geq \frac{d_{10} \cdot \gamma'}{\tan(\varphi)},$$

where:

- $\tau_f$  [kN/m<sup>2</sup>] = yield stress
- $d_{10}$  [m] = grain diameter of the 10% fraction from the sieve curve of the soil
- $\gamma'$  [kN/m<sup>3</sup>] = effective volumetric weight of the support fluid
- $\varphi$  [°] = angle of internal friction of the soil

Note that the grain size is a very important parameter in determining the micro instability of a trench wall. In case the grain diameter is smaller than 0,2 mm or the layer thickness of the coarse material is smaller than 0.5 m micro instability can be disregarded.

Macro instability is failure due to the sliding of a large soil section. In order to prevent this failure mechanism the fluid pressure within the trench must be larger than the water pressure in the surrounding soil. This overpressure, however, does not have to be very large: According to DIN 4126 the hydrostatic bentonite mixture pressure must be 1.05 times larger than the hydrostatic water pressure at all depths. NEN-EN 1538 prescribes that the level of support fluid must be at least 1 m above the rise (*stijghoogte*) of the ground water in the layer under consideration. In general one strives to choose the support fluid level 2 m above the highest rise. Macro instability is often checked with a finite elements model (FEM), important for the computations is the fluctuating support fluid level as a result of the digging process (which may lead to erosion of the trench walls).

One should also be aware of the dynamic effects in the neighbouring area that can influence the trench stability, e.g. strong vibrations caused by the hammering down of piles or sheet piles.

Sequence of work and panel width

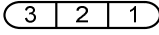
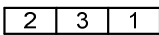
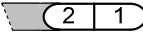
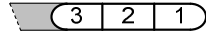
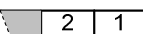
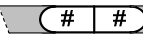
From an economical point of view it is recommended to make the panel width as large as possible. An additional advantage resulting from this is that the number of joints is as small as possible. It should nevertheless be kept in mind that in most cases trench stability and impact on the surroundings are the governing factors.

Important for the sequence in which the panels are dug are the shape of the panel, the type of joint (round or flat) between successive panels and the type of panel under construction.

One can distinguish the following panel types:

- start panels: do not connect to already constructed panels;
- follow up panels: connect to an existing panel at one side;
- end panels: connect to existing panels at both sides.

In the following table the different sequences of work are presented.

Panel type	Joint type	1 movement	2 movements	3 movements
Start	round	yes	no	yes 
	flat	yes	no	yes 
Follow	round	no	yes 	yes 
	flat	yes	yes 	yes 
End	round	yes	yes 	yes 
	flat	no	yes 	yes 

# sequence not relevant



3 movement sequence: between 2 start panels a end panel is constructed. So the sequence of work becomes: first A-C-E-G and then B-D-F

Table 39-9 applicability panel types and sequence of work

Usually one movement panels (*eengangspanelen*) are constructed in special situations, e.g. to limit the settlements of adjoining structures (higher trench stability!), or for logistic reasons (limitation of the amount of concrete needed to construct a panel, so less change on disruption of the pouring process) and as heavy foundation piles.

Types of joints between successive panels:

- joint pipe (*voegbuizen*);
- flat grout floats (*voegplanken*);
- permanent grout floats;
- Cascade joint.

## 39.4 References

Blum, H. *Einspannungsverhältnisse bei Bohlwerke*, 1931, Technische Hochschule Braunschweig.

Blum, H. *Beitrag zur Berechnung von Bohlwerken*. Die Bautechnik, 27 Jahrgang Heft 2 Februar 1950.

Blum, H. *Beitrag zur Berechnung von Bohlwerken unter Berücksichtigung der Wandverformung, insbesondere bei mit der Tiefe linear zunehmender Widerstandsziffer*. Berlin, 1951. Verlag von Wilhelm Ernst & Sohn.

Civieltechnisch Centrum Uitvoering Research en regelgeving (CUR), *CUR-publicatie 166: "Damwand-constructies"*, 5<sup>e</sup> druk, Gouda, 2008, CUR.

Civieltechnisch Centrum Uitvoering Research en regelgeving (CUR), *CUR/COB-rapport 231: "Handboek diepwanden – Ontwerp en uitvoering"*, 1<sup>e</sup> druk, Gouda, 2010, CURNET.

Civieltechnisch Centrum Uitvoering Research en regelgeving (CUR), *CUR-publicatie 211: "Handboek kademuren"*, Gouda, september 2005, Stichting CUR.

Nederlands Normalisatie instituut, *Eurocode 3: "Design of steel structures – Part 1-1: General rules for buildings"* (NEN-EN 1993-1-1), januari 2006, Nederlands Normalisatie instituut.

Nederlands Normalisatie instituut, *Eurocode 7: "Geotechnical design – Part 1: General rules"* (NEN-EN 1997-1), maart 2005, Nederlands Normalisatie instituut.

Verruijt, A., revised by S. van Baars, *Soil Mechanics*, Delft, 2005, VSSD.

### Websites:

[http://www.spoorzonedelft.nl/Het\\_project/Heden/Bouwtechniek\\_2](http://www.spoorzonedelft.nl/Het_project/Heden/Bouwtechniek_2)

<http://www.thyssenkrupp-bautechnik.com/products/sheet-piles/>

<http://sheetpiling.arcelormittal.com/>

## 40. Struts and wales

major revision : February 2011

Sheet pile walls are usually supported by struts (*stempels*) or anchors. The advantage of a support is that the embedded length of sheet piling doesn't need to be as long (less passive soil pressure) and heavy (smaller moment) compared to an unsupported wall, which saves money. Another advantage is that there is less settlement of the ground level behind the sheet piling. The disadvantages of supports are the higher costs and the possibility of obstruction during construction works.

As a rule, excavations of a couple of metres are carried out without supports, unless settlements behind the sheet piling are unacceptable, e.g. for buildings. Deeper excavations are normally spoken carried out with supports. Building site excavations can be supported in front of the sheet piling with struts. Support behind the sheet piling is possible by using anchors. The forces of the strut or anchor are usually not transferred to the sheet piling directly, but via wales (horizontal beams).

For the dimensioning of struts, see the following section; for wales see section 40.2 "Wales" and for anchors see Chapter 41 "Anchors".

### 40.1 Struts

Struts consist of steel profiles that can absorb axial compression forces (strut forces). These forces cause stress in the steel, which should not exceed the compression strength of the steel to avoid failure. Another possible way of failure is buckling. Buckling is possible both in the vertical and horizontal plane, therefore it should be resisted in both planes. That is the reason why circular pipes are often used for large spans and loads. For smaller spans and loads usually H-profiles are applied because they are less expensive and still sufficient against buckling.

So, struts should be checked on both strength and stability, which concerns their ultimate limit state (ULS). In theory, the deflection in the serviceability limit state (SLS) should also be checked, but experience has learned that this normally spoken is not necessary for the design of struts.

#### Strength check

The dominant load in struts is caused by the normal (axial) compression force in horizontal direction. The stress  $\sigma_c$  due to the combination of axial force and bending moments in two directions should not exceed the yield stress (*vloeispanning*) of the steel. The required unity check is as follows:

$$\frac{N_{Ed}}{A_{eff} \cdot f_y / \gamma_{M0}} + \frac{M_{y,Ed} + N_{Ed} \cdot e_{Ny}}{W_{eff,y,min} \cdot f_y / \gamma_{M0}} + \frac{M_{z,Ed} + N_{Ed} \cdot e_{Nz}}{W_{eff,z,min} \cdot f_y / \gamma_{M0}} \leq 1,0 \quad \text{where: } N_{Ed} = 1,5 \cdot N_{Rk}; \quad M_{i,Ed} = 1,5 \cdot M_{i,Rk}$$

Where the design shear force ( $V_{Ed}$ ) exceeds 50% of the plastic shear force ( $V_{pl,Rd}$ ), the cross-sectional design resistance to combinations of moment and axial force should be calculated using a reduced yield strength:

$$f_{red} = (1 - \rho) \cdot f_y$$

$$\text{for the shear area where } \rho = \left( \frac{2 \cdot V_{Ed}}{V_{pl,Rd}} - 1 \right)^2 \quad \text{and where: } V_{pl,Rd} = \frac{A_v (f_y / \sqrt{3})}{\gamma_{M0}}$$

The required unity check for the shear force is  $\frac{\tau_{Ed}}{f_y / (\sqrt{3} \gamma_{M0})} \leq 1,0$  and the local shear stress ( $\tau_{Ed}$ ) may be

$$\text{obtained from: } \tau_{Ed} = \frac{V_{Ed} \cdot S}{t \cdot l} = \frac{0,9 \cdot V_{Ed}}{t_w \cdot h}$$

where:

$N_{Ed}$	[N]	= design value of the compression force in the strut
$M_{y,Ed}$	[Nmm]	= design value for the bending moment in the strut about the y-y axis
$M_{z,Ed}$	[Nmm]	= design value for the bending moment in the strut about the z-z axis
$e_{Ny}$	[mm]	= eccentricity of the axial force in y-y direction
$e_{Nz}$	[mm]	= eccentricity of the axial force in z-z direction
The deflection of $e_{Ni}$ is taken explicitly into account, since it is causing a second order moment. Therefore it can remain included in the required unity check. $e_{N,i} = \frac{5}{384} \cdot \frac{q \cdot \ell^4}{EI} + \frac{1}{48} \cdot \frac{F_{Ed} \cdot \ell^3}{EI}$		
$F_{Ed}$	[N]	= design force of the load
$q$	[N/mm]	= uniformly distributed load
$E$	[N/mm <sup>2</sup> ]	= elastic modulus ( $E = 2,1 \cdot 10^5$ )
$I$	[mm <sup>4</sup> ]	= moment of area of the profile
$\ell$	[mm]	= length of the strut
$A_{eff}$	[mm <sup>2</sup> ]	= effective cross-sectional area of the member
For a cylindrical profile: $A_{eff} = \frac{\pi}{4} \cdot D^2 - \frac{\pi}{4} \cdot (D - 2 \cdot t)^2$		
$D$	[mm]	= diameter of the cylindrical profile
$t$	[mm]	= steel thickness
$f_y$	[N/mm <sup>2</sup> ]	= yield strength
$\gamma_{M0}$	[-]	= partial safety factor for resistance of cross-sections ( $\gamma_{M0} = 1,00$ )
$W_{eff,y,min}$	[mm <sup>3</sup> ]	= minimum section modulus (moment of resistance) in y-y direction
$W_{eff,z,min}$	[mm <sup>3</sup> ]	= minimum section modulus (moment of resistance) in z-z direction
$A_v$	[mm <sup>2</sup> ]	= projected shear area ( for a cylindrical profile $A_v = A_{eff}$ )
$S$	[mm <sup>4</sup> ]	= first moment of area

For calculating the moment of inertia  $I$  of cylindrical profiles see Section 39.2 "Combi-walls".

The moment in a strut is caused by a uniformly distributed load  $q$ , consisting of the self-weight and some dropped sand laying on the strut (about 1 kN/m'), and a concentrated load  $F_{Ed,grab}$  (10 kN) from a grab (*grijper*) that accidentally hits the strut in the middle and the second order moment:

$$M_{y,Ed} = \frac{1}{8} q \cdot \ell^2 + \frac{1}{4} F_{Ed,grab} \cdot \ell \quad (\text{The struts are considered to be hinge-supported.})$$

A second order effect due to the normal force in a deflected strut causes an additional moment in the strut ( $= N_{Ed} \cdot e_{Ny}$ ).

### Stability check

A strut is considered to be stable if the stress caused by normal force ( $\sigma_n$ ) and bending moment ( $\sigma_b$ ), including a second order effect introduced by initial bending of the strut, does not exceed the yield stress of the steel:

$$(\sigma_n + \sigma_b) \cdot \left( \frac{1}{1 - \frac{1}{\alpha_{cr}}} \right) \leq f_{y,d} \quad \text{where} \quad \alpha_{cr} = \frac{F_{cr}}{F_{Ed}} \quad \text{and} \quad F_{cr} = \frac{\pi^2 EI}{\ell^2}$$

$F_{cr}$  is the elastic critical buckling load (Euler force) for a global instability mode based on initial elastic stiffnesses and the design buckling load  $F_{Ed}$

It should also be checked that  $\frac{N_{Ed}}{N_{b,Rd}} \leq 1,0$  (unity check)

where:

$N_{Ed}$  [N] = design value of the compression force in the strut  
 $N_{b,Rd}$  [N] = design value for the buckling resistance of the compression member:

$$N_{b,Rd} = \frac{\chi \cdot A \cdot f_y}{\gamma_{M1}}$$

$\chi$  [-] = buckling factor (formerly indicated with  $\omega_{buc}$ )  
 $A$  [mm<sup>2</sup>] = cross-sectional area of the member  
 $f_y$  [N/mm<sup>2</sup>] = yield stress  
 $\gamma_{M1}$  [-] = partial safety factor for resistance to instability ( $\gamma_{M1} = 1,00$ )

The buckling factor  $\chi$  is a measure for the sensibility for buckling instability, and is dependent on the relative slenderness  $\bar{\lambda}$  of the profile. The relationship between the relative slenderness of a profile and its buckling factor is given by the instability curve (see the graph or the equation in part III, Section 37.3). For closed, hot formed tubular profiles, instability curve a is valid.

The relative slenderness is defined by:  $\bar{\lambda} = \sqrt{\frac{A \cdot f_y}{N_{cr}}} = \frac{L_{cr}}{i} \frac{1}{\lambda_1}$ ,

Where:

$\bar{\lambda}$  [-] = relative slenderness  
 $N_{cr}$  [N] = critical Euler load  
 $L_{cr}$  [mm] = the buckling length in the buckling plane considered  
 $i$  [mm] = radius of inertia

$\lambda_E$  [-] = Euler slenderness =  $\lambda_1 = \pi \cdot \sqrt{\frac{E}{f_y}} = 93,9 \cdot \varepsilon$

$\varepsilon$  [-] = strain

A third unity check deals with the ultimate limit state for the combination of flexural and lateral buckling (*knik en kip*):

$$\frac{N_{Ed}}{\chi \cdot N_{Rk} / \gamma_{M1}} + \frac{M_{y,Ed}}{\chi_{LT} \cdot M_{y,Rk} / \gamma_{M1}} \leq 1,0$$

Where:

$N_{Ed}$  [N] = design value for the compression force  
 $N_{Rk}$  [N] = characteristic value for resistance to compression for the critical cross-section  
 $M_{y,Ed}$  [Nmm] = design value for the bending moment in the strut about the y-y axis  
 $M_{y,Rk}$  [Nmm] = characteristic value of resistance to bending moments about the y-y axis  
 $\chi$  [-] = reduction factor (= buckling factor) (see Figure 36-1 on page 227)  
 $\chi_{LT}$  [-] = lateral-torsional reduction factor (see Section 36.5, page 229)

It is not necessary to check a cylindrical pipe strut on lateral buckling (*kippen*), because all the axes are equally strong. Therefore, the strut will sooner fail on vertical deformation than on lateral buckling. H-profiles should be checked separately on lateral buckling.

### Notes

- The strut (and also the sheet piling!) should be checked for fluctuating temperature loads during day and night.
- The construction site should be checked for strut failure, especially the zip effect, resulting from a strut being knocked out of position by a digger or crane.

For an example, see next section.

## 40.2 Wales

If the wales (*gordingen*) of a cofferdam are supported by struts, they usually exist of two H-beams placed against the wall, with the webs (*lijven*) horizontal, and the flanges (*flenzen*) one under the other. If the wales are supported by anchors, sometimes two U-profiles are used that are positioned opposite each other, with the end of the anchor in between.

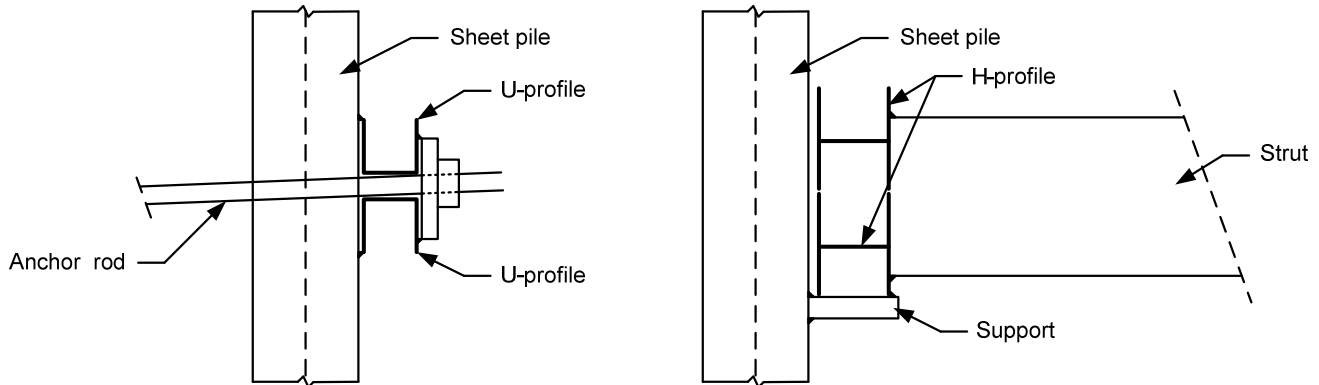


Figure 40-1: wales supported by anchors (left) and wales supported by struts (right).

The collar section of the H-beam will be the governing section of the entire cross-section. The combination of the normal, bending and shear stresses will be at its maximum here.

The stress due to the normal force  $F$  is  $\sigma_n = \frac{F}{A}$ , and is equally spread over the entire cross-section.

Stress caused by the bending moment can be calculated according to  $\sigma_b = \frac{M}{W}$ . The occurring bending moment is resisted mainly by the flanges. For a beam on two supports, the maximum moment in a bending beam is:  $M = \frac{1}{8} q \cdot \ell^2$  and for a beam on multiple supports:  $M = \frac{1}{12} q \cdot \ell^2$ . Furthermore the maximum

moment at the end of a beam on multiple supports is set in between these two values:  $M \approx \frac{1}{10} q \cdot \ell^2$ . This is a good estimate for the moment working on the wales in the corners of a building pit. The design of wales is therefore based on this moment.

Since it is assumed that the anchor force  $F_{\text{anchor}}$  is evenly spread across the sheet pile wall via the wales, the following applies:  $q = \frac{F_{\text{anchor}}}{\ell}$ . In which  $\ell$  is the distance between the anchors. The maximum bending

moment in the wale is therefore:  $M \approx \frac{1}{10} \cdot F_{\text{anchor}} \cdot \ell$

The maximum shear stress is located at the centre of the cross-section of the H-profile and thus mainly born by the web of the H-beam. Again the unity check is:

$$\frac{\tau_{Ed}}{f_y / (\sqrt{3} \cdot \gamma_{M0})} \leq 1,0 \quad \text{where } \tau_{Ed} \text{ may be obtained from: } \tau_{Ed} = \frac{V_{Ed} \cdot S}{t \cdot I} = \frac{0,9 \cdot V_{Ed}}{t_w \cdot h},$$

where:

$\tau_{Ed}$	[Nmm <sup>2</sup> ]	= local shear stress
$t_w$	[mm]	= nominal web thickness
$h$	[mm]	= height of the web

The combined stress at the collar section as a result of both the bending moment and shear force is determined from the stress distribution over the cross-section. Where the design shear force ( $V_{Ed}$ ) exceeds 50% of the plastic shear force ( $V_{pl,Rd}$ ), the design resistance of the cross-section to combinations of mo-

ment and axial force should be calculated using a reduced yield strength  $f_{red} = (1 - \rho) \cdot f_y$  for the shear area, where  $\rho = \left( \frac{2 \cdot V_{Ed}}{V_{pl,Rd}} - 1 \right)^2$ .

The required unity check for the ultimate limit state is as follows:

$$\frac{N_{Ed}}{A_{eff} \cdot f_y / \gamma_{M0}} + \frac{M_{y,Ed} + N_{Ed} \cdot e_{Ny}}{W_{eff,y,min} \cdot f_y / \gamma_{M0}} + \frac{M_{z,Ed} + N_{Ed} \cdot e_{Nz}}{W_{eff,z,min} \cdot f_y / \gamma_{M0}} \leq 1,0$$

Where:

$N_{Ed}$	[N]	=	design value of the compression force in the wale
$M_{y,Ed}$	[Nmm]	=	design value for the bending moment in the wale about the y-y axis
$M_{z,Ed}$	[Nmm]	=	design value for the bending moment in the wale about the z-z axis
$e_{Ny}$	[mm]	=	eccentricity of the axial force in y-y direction
$e_{Nz}$	[mm]	=	eccentricity of the axial force in z-z direction

The deflection of  $e_{Ni}$  is taken explicitly into account, since it is causing a second order moment. Therefore it can remain included in the required

$$\text{unity check: } e_{Ni} = \frac{5}{384} \cdot \frac{q \cdot \ell^4}{EI} + \frac{1}{48} \cdot \frac{F_{Ed} \cdot \ell^3}{EI}$$

$F_{Ed}$	[N]	=	design force of the load
$q$	[N/mm]	=	uniformly distributed load
$E$	[N/mm <sup>2</sup> ]	=	elastic modulus ( $E = 2,1 \cdot 10^5$ )
$I$	[mm <sup>4</sup> ]	=	moment of area of the profile
$\ell$	[mm]	=	length of the wale between successive anchors
$A_{eff}$	[mm <sup>2</sup> ]	=	effective cross-sectional area of the member
$f_y$	[N/mm <sup>2</sup> ]	=	yield strength
$\gamma_{M0}$	[-]	=	partial safety factor for resistance of cross-sections ( $\gamma_{M0} = 1,00$ )
$W_{eff,y,min}$	[mm <sup>3</sup> ]	=	minimum section modulus (moment of resistance) in y-y direction
$W_{eff,z,min}$	[mm <sup>3</sup> ]	=	minimum section modulus (moment of resistance) in z-z direction
$A_v$	[mm <sup>2</sup> ]	=	projected shear area ( for a cylindrical profile $A_v = A_{eff}$ )

The walings, being a beam on many supports (the struts), and being evenly supported by the sheet piling, will not be checked on stability (buckling).

### Example of a cofferdam: waling and struts

A building pit is designed with as much space for work and construction as possible. The number of struts between sheet piling should be minimised, as struts take up space and therefore limit the movement of equipment. A building pit and its parts are designed according to CUR 166 (sheet piling) and NEN 6740 (geotechnical engineering), see Chapter 39 "Soil retaining walls".

Design steps:

1. Situation description (drawing building pit)
2. Loads from soil pressure and sheet piling
3. Design and check struts
4. Design and check walings
5. Check welded connections
6. Calculate/design structural details (connections)

The installation of struts and walings is as follows:

1. Weld supports for the walings to the sheet piles
2. Place the walings upon the supports loosely, neatly along the sheet piles.
3. If necessary, place grout bags between waling and sheet pile in case of sheet pile misalignment
4. Measure and place the struts and braces, possibly tighten the waling and brace together
5. Welding is done during all activities

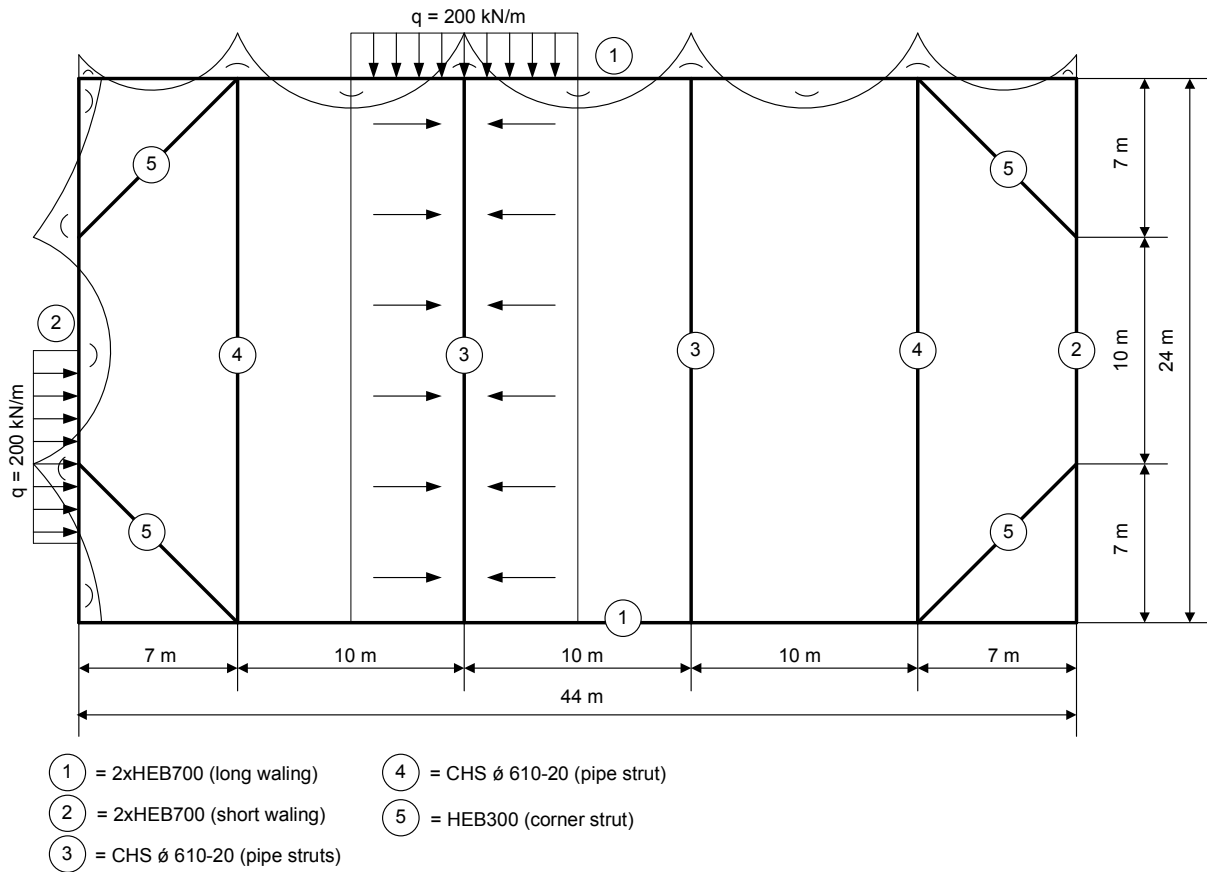


Figure 40-2: Building pit.

In this example, the soil pressure (anchor force) on the sheet pile and waling is estimated at 200 kN/m<sup>1</sup>. The struts are placed 10 m centre to centre. The load on the strut is  $q \cdot (2 \cdot \frac{1}{2} \ell) = q \cdot \ell$ . This causes a normal force. The load on the walings is equal to the soil pressure. The corners can be connected flexibly or rigidly.

Internal forces:

• Normal forces

Normal force in long walings:  
 $N = q \cdot \ell = 200 \cdot 12 = 2400 \text{ kN}$

Normal force in short walings:  
 $N = q \cdot \ell = 200 \cdot 3,5 = 700 \text{ kN}$

Normal force in pipe struts:  
 $N = q \cdot \ell = 200 \cdot 10 = 2000 \text{ kN}$

Normal force in outer pipe struts:  
 $N = q \cdot \ell = 200 \cdot 8,5 = 1700 \text{ kN}$

Normal force in H-beam strut:  
 $F = q \cdot \ell = 200 \cdot 8,5 = 1700 \text{ kN}$

$F_R = N = \sqrt{2} \cdot F_2 = 2404 \text{ kN}$

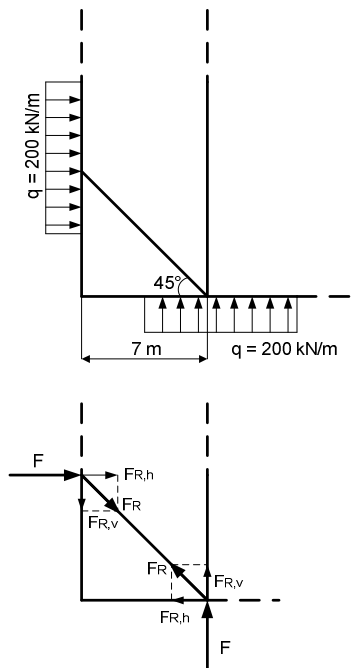


Figure 40-3: Normal force in corner strut.

- **Bending moments**

Bending moments in long waling:

$$M_{max,field} = 1/12 \cdot q \cdot \ell^2 = 1667 \text{ kNm (span } \ell = 10 \text{ m)}$$

$$M_{max,corner} = 1/10 \cdot q \cdot \ell^2 = 980 \text{ kNm (outer fields; span } \ell = 7 \text{ m)}$$

As the moment in the corner is relatively large, it is better to provide a support to the cantilever part (*uitkragend deel*) of the long waling with a bracing frame (*schoorstempel*)

Bending moments in short waling:

$$M_{max,field} = 1/12 \cdot q \cdot \ell^2 = 1667 \text{ kNm (span } \ell = 10 \text{ m)}$$

$$M_{max,corner} = 1/10 \cdot q \cdot \ell^2 = 980 \text{ kNm (outer fields; span } \ell = 7 \text{ m)}$$

Bending moment in the pipe strut:

The bending moment is caused by the dead weight of the pipe and a concentrated load of 10 kN, placed in the middle of the span of the strut. This load is an accidental load during construction of the structure within the building pit. An accidental move of a loaded crane, other machinery or personnel may cause this load on the strut.

$$M_{pipe\ strut} = 1/4 \cdot F \cdot \ell = 1/4 \cdot 10 \cdot 24 = 60 \text{ kNm}$$

Bending moment in corner strut:

$$M_{corner\ strut} = 1/4 \cdot F \cdot \ell = 1/4 \cdot 10 \cdot 9,9 = 25 \text{ kNm}$$

- **Shear forces**

Shear forces in the walings act in the plane of the bracing (horizontal shear), whereas shear forces in the struts act in vertical direction.

Shear forces in long waling:

$$V_{waling, field} = 1/2 \cdot q \cdot \ell = 1000 \text{ kN (span } \ell = 10 \text{ m)}$$

$$V_{waling, corner} = 1/2 \cdot q \cdot \ell = 700 \text{ kN (span } \ell = 7 \text{ m)}$$

Shear forces in short waling:

$$V_{waling, field} = 1/2 \cdot q \cdot \ell = 1000 \text{ kN (span } \ell = 10 \text{ m)}$$

$$V_{waling, corner} = 1/2 \cdot q \cdot \ell = 700 \text{ kN (span } \ell = 7 \text{ m)}$$

Shear forces in pipe strut:

$$V_{pipe\ strut} = 1/2 \cdot F = 5 \text{ kN}$$

Shear forces in corner strut:

$$V_{corner\ strut} = 1/2 \cdot F = 5 \text{ kN}$$

When computing the ultimate limit state, a safety factor of  $\gamma = 1,5$  shall be taken into account in the conceptual design.

Check of structural parts:

- **Long waling**

**Strength:**

$$N = 2400 \text{ kN}$$

$$M = 1667 \text{ kNm}$$

$$V = 1000 \text{ kN}$$

The normal forces are distributed over the entire cross-section. The bending moments are resisted by the flanges of the H-beam and the web of the H-beam takes the shear force load. The maximum values of the separate internal forces are checked, as is the governing combination of the internal forces at the collar section of the H-beam.

Properties of design estimate: HEB700 profile (S235):

$A_{eff}$	=	30638	[mm <sup>2</sup> ]
$h$	=	700	[mm]
$b$	=	300	[mm]
$t_w$	=	17 (web = lijf)	[mm]
$t_f$	=	32 mm (flange = flens)	[mm]
$G$	=	2,45	[N/mm]
$W_y$	=	$7340 \cdot 10^3$	[mm <sup>3</sup> ]
$W_z$	=	$963 \cdot 10^3$	[mm <sup>3</sup> ]

$$V_{pl,Rd} = \frac{A_v \cdot (f_y / \sqrt{3})}{\gamma_{M0}} = \frac{2 \cdot (h \cdot t_w) \cdot (f_y / \sqrt{3})}{\gamma_{M0}} = \frac{2 \cdot (700 \cdot 17) \cdot (235 / \sqrt{3})}{1.0} = 3229 \cdot 10^3 \text{ N}$$

Note that since two HEB700 profiles are used the total projected shear area ( $A_v$ ) is two times the projected shear area of the profile used.

The design shear force ( $V_{Ed}$ ) = 1000 kN, which is smaller than 50% of the plastic shear force ( $V_{pl,Rd}$ ), so one does not need to use a reduced yield strength ( $f_{red}$ ). The required unity check for the shear force is:

$$\frac{\tau_{Ed}}{f_y / (\sqrt{3} \cdot \gamma_{M0})} = \frac{\left( \frac{0,9 \cdot (1,5 \cdot 1000 \cdot 10^3)}{17 \cdot 700} \right)}{\frac{235}{(\sqrt{3} \cdot 1,0)}} = 0,836 \leq 1,0 \quad \text{where} \quad \tau_{Ed} = \frac{V_{Ed} \cdot S}{t \cdot I} = \frac{0,9 \cdot V_{Ed}}{t_w \cdot h} \Rightarrow \text{ok}$$

The required unity check for the ultimate limit state is as follows:

$$\frac{N_{Ed}}{A_{eff} \cdot f_y / \gamma_{M0}} + \frac{M_{y,Ed}}{W_{eff,y,min} \cdot f_y / \gamma_{M0}} \leq 1,0$$

$$\frac{1,5 \cdot 2400 \cdot 10^3}{(2 \cdot 30638) \cdot 235 / 1,0} + \frac{1,5 \cdot 1667 \cdot 10^6}{(2 \cdot 7340 \cdot 10^3) \cdot 235 / 1,0} = 0,97 \leq 1,0 \Rightarrow \text{ok}$$

#### • Short waling

##### Strength:

$N = 700 \text{ kN}$

$M = 1667 \text{ kNm}$

$V = 1000 \text{ kN}$

Properties of design estimate: HEB700 profile (S235):

$A_{eff}$	=	30638	[mm <sup>2</sup> ]
$h$	=	700	[mm]
$b$	=	300	[mm]
$t_w$	=	17	[mm]
$t_f$	=	32	[mm]
$G$	=	2,45	[N/mm]
$W_y$	=	$7340 \cdot 10^3$	[mm <sup>3</sup> ]
$W_z$	=	$963 \cdot 10^3$	[mm <sup>3</sup> ]

$$V_{pl,Rd} = \frac{A_v \cdot (f_y / \sqrt{3})}{\gamma_{M0}} = \frac{2 \cdot (h \cdot t_w) \cdot (f_y / \sqrt{3})}{\gamma_{M0}} = \frac{2 \cdot (700 \cdot 17) \cdot (235 / \sqrt{3})}{1.0} = 3229 \cdot 10^3 \text{ N}$$

Again 2 HEB700 profiles are used so the total projected shear area ( $A_v$ ) is two times the projected shear area of the profile used. Also the design shear stress is smaller than 50% of the plastic shear stress, so one does not have to use the reduced yield strength.

The required unity check for the shear force is:

$$\frac{\tau_{Ed}}{f_y / (\sqrt{3} \cdot \gamma_{M0})} = \frac{\left( \frac{0,9 \cdot (1,5 \cdot 1000 \cdot 10^3)}{17 \cdot 700} \right)}{\frac{235}{(\sqrt{3} \cdot 1,0)}} = 0,836 \leq 1,0 \quad \text{where} \quad \tau_{Ed} = \frac{V_{Ed} \cdot S}{t \cdot l} = \frac{0,9 \cdot V_{Ed}}{t_w \cdot h} \Rightarrow \text{ok}$$

And the required unity check for the ultimate limit state is again:

$$\frac{N_{Ed}}{A_{eff} \cdot f_y / \gamma_{M0}} + \frac{M_{y,Ed}}{W_{eff,y,min} \cdot f_y / \gamma_{M0}} \leq 1,0$$

$$\frac{1,5 \cdot 700 \cdot 10^3}{(2 \cdot 30638) \cdot 235 / 1,0} + \frac{1,5 \cdot 1667 \cdot 10^6}{(2 \cdot 7340 \cdot 10^3) \cdot 235 / 1,0} = 0,77 \leq 1,0 \Rightarrow \text{ok}$$

### • Pipe Strut Strength:

Properties of design estimate: profile S235 CHS  $\varnothing$  610-20

$A_{eff}$	=	37070	[mm <sup>2</sup> ]
$d_o$	=	610	[mm]
$d_i$	=	570	[mm]
$t$	=	20	[mm]
$G$	=	2.91	[N/mm]
$W_y = W_z$	=	$5295 \cdot 10^3$	[mm <sup>3</sup> ]
$i_y = i_z$	=	209	[mm]
$I_y = I_z$	=	$161,490 \cdot 10^4$	[mm <sup>4</sup> ]

$\ell = 24$  m (conservative value; actually  $\ell = 24 - 2 \cdot 0,7 = 22,6$  m)

steel weight:  $\rho = 7850$  kg/m<sup>3</sup> = 78,5 kN/m<sup>3</sup>

### Loads:

From the dead weight of the profile:

$$V_{dead\ weight} = 1/2 \cdot G \cdot \ell = 1/2 \cdot 2,91 \cdot 24 = 34,92 \text{ kN}$$

$$M_{dead\ weight} = 1/8 \cdot G \cdot \ell^2 = 209,52 \text{ kNm}$$

From the concentrated load (10 kN) in the middle of the strut:

$$V = 1/2 \cdot F = 5 \text{ kN}$$

$$M = 1/4 \cdot F \cdot \ell = 60 \text{ kNm}$$

Total:

$$V_{Ed} = 40 \text{ kN}$$

$$M_{y,Ed} = 270 \text{ kNm}$$

$$N = 2000 \text{ kN}$$

$$N_{outer} = 1700 \text{ kN}$$

$$V_{pl,Rd} = \frac{A_v \cdot (f_y / \sqrt{3})}{\gamma_{M0}} = \frac{37070 \cdot (235 / \sqrt{3})}{1,0} = 5030 \cdot 10^3 \text{ N}$$

Since the design value for the shear stress does not exceed 50% the plastic shear stress, one does not have to use the reduced yield strength. The required unity check results in:

$$\frac{\tau_{Ed}}{f_y / (\sqrt{3} \cdot \gamma_{M0})} = \frac{\left( \frac{0,9 \cdot (1,5 \cdot 40 \cdot 10^3)}{37070} \right)}{\frac{235}{(\sqrt{3} \cdot 1,0)}} = 0,011 \leq 1,0 \quad \text{where} \quad \tau_{Ed} = \frac{V_{Ed} \cdot S}{t \cdot l} = \frac{0,9 \cdot V_{Ed}}{A_{eff}} \Rightarrow \text{OK}$$

And the required unity check for the ultimate limit state is:

$$\frac{N_{Ed}}{A_{eff} \cdot f_y / \gamma_{M0}} + \frac{M_{y,Ed}}{W_{eff,y,min} \cdot f_y / \gamma_{M0}} \leq 1,0$$

For the outer pipe struts this results in:

$$\frac{1,5 \cdot 700 \cdot 10^3}{37070 \cdot 235 / 1,0} + \frac{1,5 \cdot 270 \cdot 10^6}{5295 \cdot 10^3 \cdot 235 / 1,0} = 0,46 \leq 1,0 \Rightarrow \text{ok}$$

For the other pipe struts this results in:

$$\frac{1,5 \cdot 2000 \cdot 10^3}{37070 \cdot 235 / 1,0} + \frac{1,5 \cdot 270 \cdot 10^6}{5295 \cdot 10^3 \cdot 235 / 1,0} = 0,67 \leq 1,0 \Rightarrow \text{ok}$$

### Stability (buckling):

For a closed hot formed tubular profile the instability curve a is valid (NEN 6770).

$\ell_{strut} = 24$  m (unsupported length)

buckling length factor for a hinged beam = 1.0

$L_{cr} = 24 \cdot 1,0 = 24$  m (buckling length)

$N_c = 2000$  kN (compression)

$$\varepsilon = \sqrt{\frac{235}{f_y}} = 1 \quad (f_y \text{ in N/mm}^2)$$

$$\lambda_1 = \pi \sqrt{\frac{E}{f_y}} = 93,9 \cdot \varepsilon = 93,9$$

$$\bar{\lambda} = \sqrt{\frac{A \cdot f_y}{N_{cr}}} = \frac{L_{cr}}{i} \cdot \frac{1}{\lambda_1} = \frac{24000}{209} \cdot \frac{1}{93,9} = 1,22$$

Buckling factor  $\chi = 0,52$  (figure 37-1 from chapter 36 "Steel")

$$F_{Euler} = F_{cr} = \frac{\pi^2 \cdot EI}{\ell_{buc}^2} = 5811 \cdot 10^3 \text{ N}$$

$$\sigma_b = \frac{M}{W} = \frac{1,5 \cdot 270 \cdot 10^6}{5295 \cdot 10^3} = 76 \text{ N/mm}^2$$

$$\sigma_n = \frac{N_{Ed}}{A} = \frac{1,5 \cdot 2000 \cdot 10^3}{37070} = 81 \text{ N/mm}^2$$

1<sup>st</sup> check: stress caused by the normal force in combination with the bending moment, including 2<sup>nd</sup> order effects:

$$(\sigma_n + \sigma_b) \cdot \left( \frac{1}{1 - \frac{1}{\alpha_{cr}}} \right) \leq f_{y,d}, \text{ where } \alpha_{cr} = \frac{F_{cr}}{F_{Ed}} = \frac{5811 \cdot 10^3}{2000 \cdot 10^3} = 2,91$$

$$(81 + 76) \cdot \left( \frac{1}{1 - \frac{1}{2,91}} \right) = 239 \leq 235 \rightarrow \text{not OK!}$$

So this profile does not meet the stability requirement!

Increasing the steel quality to S355 appears to be a sufficient solution for this problem.

$$\text{Unity check: } \frac{N_{Ed}}{N_{b,Rd}} = \frac{1,5 \cdot 2000 \cdot 10^3}{6843 \cdot 10^3} = 0,438 \leq 1,0$$

$$\text{where } N_{b,Rd} = \frac{\chi \cdot A \cdot f_y}{\gamma_{M1}} = \frac{0,52 \cdot 37070 \cdot 355}{1,0} = 6843 \cdot 10^3 \text{ N}$$

Closed circular sections have a high torsion resistance, therefore a torsion check is not expected to be necessary. Furthermore it is not necessary to perform a check on lateral buckling as a pipe is equally strong for all axis.

- **H-beam corner strut**

**Strength:**

Properties of design estimate: HEB300 profile (S235):

$A_{eff}$	=	14908	[mm <sup>2</sup> ]
$h$	=	300	[mm]
$b$	=	300	[mm]
$t_w$	=	11	[mm]
$t_f$	=	19	[mm]
$G$	=	1,19	[N/mm]
$W_y$	=	$1678 \cdot 10^3$	[mm <sup>3</sup> ]
$W_z$	=	$571 \cdot 10^3$	[mm <sup>3</sup> ]
$i_y$	=	130	[mm]
$i_z$	=	75	[mm]
$I_y$	=	$25166 \cdot 10^4$	[mm <sup>4</sup> ]
$I_z$	=	$8563 \cdot 10^4$	[mm <sup>4</sup> ]

$$\ell = \sqrt{7^2 + 7^2} = 9,9 \text{ m} \quad (\alpha = 45^\circ)$$

Loads:

From the dead weight of the profile:

$$V = 1/2 \cdot G \cdot \ell = 5,89 \text{ kN}$$

$$M = 1/8 \cdot G \cdot \ell^2 = 14,57 \text{ kNm}$$

From the concentrated load (10 kN) in the middle of the strut:

$$V = 1/2 \cdot F = 5 \text{ kN}$$

$$M = 1/4 \cdot F \cdot \ell = 24,75 \text{ kNm}$$

Total:

$$V_{Ed} = 10,90 \text{ kN}$$

$$M_{y,Ed} = 39,32 \text{ kNm}$$

$$N = 2404 \text{ kN}$$

$$V_{pl,Rd} = \frac{A_v \cdot (f_y / \sqrt{3})}{\gamma_{M0}} = \frac{(h \cdot t_w) \cdot (f_y / \sqrt{3})}{\gamma_{M0}} = \frac{(300 \cdot 11) \cdot (235 / \sqrt{3})}{1,0} = 448 \cdot 10^3 \text{ N}$$

The design shear stress is smaller than 50% of the plastic shear stress, so one does not have to use the reduced yield strength. The required unity check for the shear force is:

$$\frac{\tau_{Ed}}{f_y / (\sqrt{3} \cdot \gamma_{M0})} = \frac{\left( \frac{0,9 \cdot (1,5 \cdot 10,90 \cdot 10^3)}{11 \cdot 300} \right)}{\frac{235}{(\sqrt{3} \cdot 1,0)}} = 0,033 \leq 1,0 \quad \text{where} \quad \tau_{Ed} = \frac{V_{Ed} \cdot S}{t \cdot I} = \frac{0,9 \cdot V_{Ed}}{t_w \cdot h} \Rightarrow \text{ok}$$

And the required unity check for the ultimate limit state is:

$$\frac{N_{Ed}}{A_{eff} \cdot f_y / \gamma_{M0}} + \frac{M_{y,Ed}}{W_{eff,y,min} \cdot f_y / \gamma_{M0}} \leq 1,0$$

$$\frac{1,5 \cdot 2404 \cdot 10^3}{14908 \cdot 235 / 1,0} + \frac{1,5 \cdot 39,32 \cdot 10^6}{1678 \cdot 10^3 \cdot 235 / 1,0} = 1,18 \leq 1,0 \Rightarrow \text{not OK}$$

So this profile does not meet the strength requirement!

Increasing the steel quality to S355 appears to be a sufficient solution for this problem.

$$\frac{1,5 \cdot 2404 \cdot 10^3}{14908 \cdot 355/1,0} + \frac{1,5 \cdot 39,32 \cdot 10^6}{1678 \cdot 10^3 \cdot 355/1,0} = 0,78 \leq 1,0 \Rightarrow \text{ok}$$

**Stability (buckling):**

For a rolled hot formed HEB300 an instability curve b (y-y) or c(z-z) is valid (NEN 6770).

$$f_y = 355 \text{ N/mm}^2$$

$$l_{\text{strut}} = 9,9 \text{ m (unsupported length)}$$

Maximum buckling length factor for a beam = 0,8

$$L_{cr} = 9,9 \cdot 0,8 = 7,9 \text{ m (buckling length)}$$

$$N_c = 2404 \text{ kN (compression)}$$

$$\varepsilon = \sqrt{\frac{235}{f_y}} = 0,81 \text{ (} f_y \text{ in N/mm}^2 \text{)}$$

$$\lambda_1 = \pi \sqrt{\frac{E}{f_y}} = 93,9 \cdot \varepsilon = 76,1$$

$$\bar{\lambda} = \sqrt{\frac{A \cdot f_y}{N_{cr}}} = \frac{L_{cr}}{i} \frac{1}{\lambda_1} = \frac{7900}{130} \frac{1}{76,1} = 0,80$$

Buckling factor  $\chi = 0,67$  (figure 37-1 from chapter 36 "Steel")

$$F_{Euler} = F_{cr} = \frac{\pi^2 \cdot EI}{l_{\text{buc}}^2} = \frac{\pi^2 \cdot 210 \cdot 10^3 \cdot 25166 \cdot 10^4}{9900^2} = 5322 \cdot 10^3 \text{ N}$$

$$\sigma_n = \frac{N_{Ed}}{A} = \frac{1,5 \cdot 2404 \cdot 10^3}{14908} = 242 \text{ N/mm}^2$$

$$\sigma_b = \frac{M_{Ed}}{W} = \frac{1,5 \cdot 39,32 \cdot 10^6}{1678 \cdot 10^3} = 35 \text{ N/mm}^2$$

1<sup>st</sup> check: stress caused by the normal force in combination with the bending moment, including 2<sup>nd</sup> order effects:

$$(\sigma_n + \sigma_b) \cdot \left( \frac{1}{1 - \frac{1}{\alpha_{cr}}} \right) \leq f_{y,d}, \text{ where } \alpha_{cr} = \frac{F_{cr}}{F_{Ed}} = 5322 \cdot 10^3 / 2404 \cdot 10^3 = 2,21$$

$$(242 + 35) \cdot \left( \frac{1}{1 - \frac{1}{2,21}} \right) = 506 \not\leq 355 \text{ N/mm}^2 \rightarrow \text{not OK!}$$

Unity check: If  $N_{b,Rd} = \frac{\chi \cdot A \cdot f_y}{\gamma_{M1}} = \frac{0,67 \cdot 14908 \cdot 355}{1,0} = 3546 \cdot 10^3 \text{ N}$ , then

$$\frac{N_{Ed}}{N_{b,Rd}} = \frac{1,5 \cdot 2404 \cdot 10^3}{3546 \cdot 10^3} = 1,02 \not\leq 1,0 \rightarrow \text{also not OK!}$$

So this profile does not meet the stability requirement! One should choose a larger profile and redo the computation. The profile is not checked with regard to torsion forces, as that subject is outside the scope of this Manual.

**40.3 References**

Nederlands Normalisatie instituut, *Eurocode 3: "Design of steel structures – Part 1-1: General rules for buildings"* (NEN-EN 1993-1-1), januari 2006, Nederlands Normalisatie instituut.

Nederlands Normalisatie instituut, *Eurocode 3: "Design of steel structures – Part 1-5: Piling"* (NEN-EN 1993-1-5), februari 2008, Nederlands Normalisatie instituut.

## 41. Anchors

### 41.1 General

A soil retaining wall can be anchored in several ways. The most important anchor types are:

1. Grout anchors
2. Screw grout anchors (*schroefinjectiepaal*) and self-drilling anchors
3. Anchor piles
4. Continuous anchor walls (*doorgaande ankerwanden*) and anchor screens (*ankerschotten*)
5. Screw anchors

#### **Grout anchors**

A grout anchor consists of a cylindrical body of cement grout, created in the soil. It usually has a length between 4 and 20 metres and a diameter between 110 and 200 mm, depending on the diameter of the drill pipe used. The anchor is connected to the sheet piling by means of a steel rod or steel wire that is installed by driving or drilling a hollow drill pipe into the ground (see Figure 41-1, picture 1). Subsequently the steel rod or wire is inserted into the drill pipe (2) and the cement grout is injected under high pressure into the surrounding ground through the drill pipe while pulling back the pipe (3). When a grout body of sufficient length is created, the drill pipe is pulled out completely. When the cement of the grout body has hardened enough, the steel rod or wire is tightened up to 70-90% of the needed anchor force (4), after which the external load is exerted on the sheet piling. As a result of this pre-stressing of the steel rod or wire, most of the elastic strain is removed from the anchor. This thus limits the horizontal deformations of the soil retaining structure.

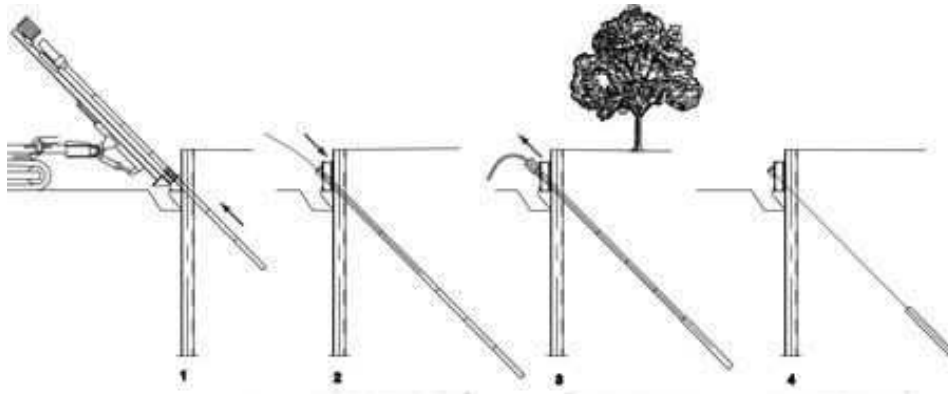


Figure 41-1 Installation of a grout anchor

The way in which the anchors are installed influences their yield strength. Usually one achieves higher tensile strengths using driven (*geheide*) anchors instead of drilled (*geboorde*) anchors. The anchors are installed under an angle of 25-45° to a depth where a sufficiently strong sand layer is present in order to form the grout body. Since the rods and wires are made of high quality steel with a relatively high allowable stress, their cross-section can be kept relatively small. Minor damage to a rod can therefore considerably decrease its cross-section area, which has large consequences for the reliability of an anchor. The maximum ultimate bearing capacity is around 3000 kN.

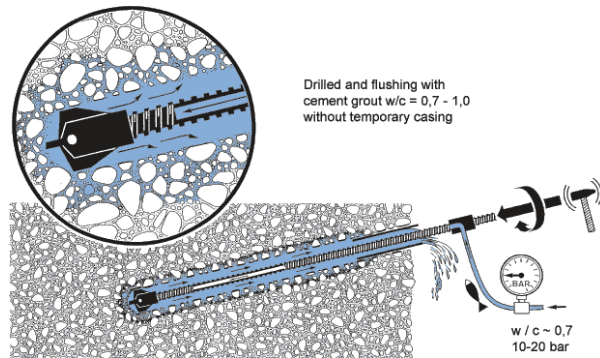
#### **Screwed grout anchors**

An anchor type derived from the grout anchor is the screw grout anchor, e.g. the *Leeuwanker*. This anchor type consists of a thick-walled tube with a spiral drill head welded onto the end. The grout body is formed by injecting grout through the drill head while installing the anchor. Compared to the grout anchors mentioned above the grout body is formed under relatively low pressure. The thick-walled pipe is made of normal quality steel, which means that the maximum allowable stresses in the tube are a lot less than for the high quality steel rods or wires in the grout anchors. The screw grout anchor, however, is a lot stiffer than the grout anchor.

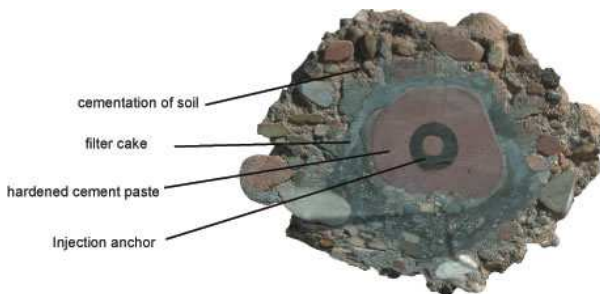
Another subtype of grout anchor that is often used nowadays is the self-drilling grout anchor, e.g. titan and jetmix anchors. The main advantage compared to the other grout anchors is that the system is cheaper to install (less laborious), but still has a large bearing capacity (1500-2000 kN). This anchor consists of a tube with thread (*schroefdraad*) and a drill head. These threads are formed much like the ribs on

a reinforcement bar and result in a higher bond friction with the grout body compared to standard drill steel. During installation the drill head is moved back and forth while at the meantime grout is being injected. In this way the soil is removed from the drill hole and replaced by the grout mixture. This results in a drill hole with a diameter between 150 and 200 mm. After reaching the planned position of the grout anchor, the grout pressure is increased and the drilling is continued until the thus created grout anchor has reached its required length. Note that the drill hole widens after increasing the pressure (Figure 41-2). After installation the tube serves as a draw bar (*trekelement*).

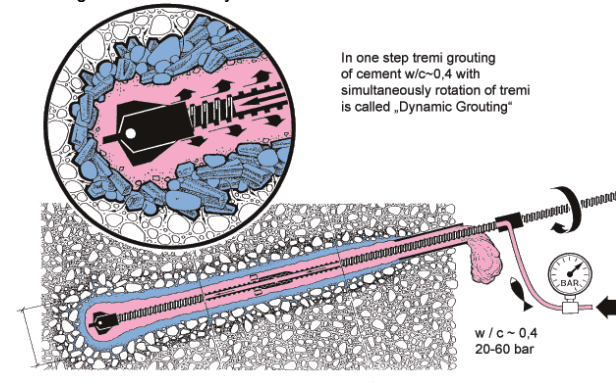
Drilling the drill hole



Cross-section of anchor body



Creating the anchor body



Drill tube

Figure 41-2 Installation of self-drilling grout anchor. (<http://www.ischebeck.de>)

### Anchor piles

Anchor piles are used when very large anchor forces are involved. Also this type of anchor transfers the load to the subsoil by means of friction. The presence of sand along the effective length of the pile is required. The effective length of the anchor pile is the part of the pile that is situated outside the active sliding zone behind the sheet piling, see Figure 41-3. Nearly all pile types that are suitable as vertical tension piles are also suitable as anchor piles. The strength of the anchoring pile is determined in the same way as for tension piles and the stability is checked by means of the clump criterion, see Section 43.3 of this manual.

An example of an anchor pile that is often used for heavy quay structures is the MV-pile (MV stands for *Müller Verfahren*, which is German for 'Müller method'). This type of pile consists of a steel H-beam which is coated with cement grout during installation. The cement grout coating can be applied in two ways, first by welding an enlarged foot at the end of the H-beam and second by welding steel strips on the outside of the flanges of the H-beam. In both cases the cement grout fills the cavities that are formed in the ground, thus forming the coating.

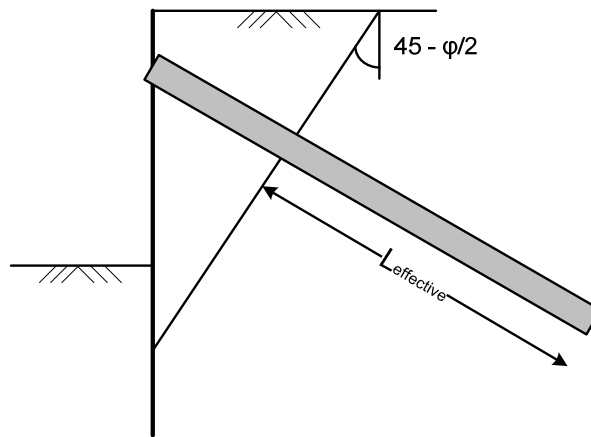


Figure 41-3 Effective length of an anchor pile.

### **Continuous anchor walls and anchor screens**

A continuous anchor wall and anchor screens can be used if there is:

- a reasonably strong and stiff top layer and fill.
- sufficient space to install the anchor wall and to excavate in order to install the tie rods.

As a rule, the advantage of anchor walls or anchor boards is that they are cheaper than other anchor systems. The disadvantage is that one must have sufficient space to dig trenches for the tie rods and to be able to drive the walls or boards into the ground.

### **Screw anchors**

Screw anchors consist of a steel tie rod with a diameter of approximately 30 mm width and at the end a steel screw blade of approximately 250 to 500 mm that is welded to the tie rod. To install the anchors only a small excavation behind the sheet piling is necessary. The anchors are installed using a vibrating drill. This type of anchors can be installed horizontally or at an angle. The maximum capacity is attained when the anchors are installed at a depth of approximately 12 times the diameter of the screw blade. When the depth over blade diameter ratio is increased further, the capacity of the anchor hardly increases. In case the depth over blade diameter ratio is smaller than 5, the capacity of the anchor will reduce rapidly. In general the bearing capacity of a screw anchor is rather small ( $< 75$  kN), therefore they are mainly used for campsheeting (*beschoeiingen*).

For all types of anchor structures the bearing capacity is extremely dependent on constructional aspects. To eliminate anchors with a small bearing capacity in an early stage, *each* anchor has to be tested before it is connected to the retaining structure. The magnitude of the test load is around the design load of the anchor force ( $F_{s,A;d}$ ).

## **41.2 Extreme tensile force**

### **Anchor wall and continuous anchor screen**

When regarding limit states in determining the ultimate resistance of anchor walls, one normally assumes straight slip planes according to Coulomb. These slip planes are shown schematically in Figure 41-4, along with the horizontal soil pressures working directly onto the both sides of the anchor screen. Generally one assumes slip planes that extend unto ground level. This situation corresponds with an anchor screen that extends till ground level. However this assumption only applies to anchor screens with a ratio of  $\frac{h_2}{h_1} \leq 1,5$ , since in such situations the ground above the anchor screen will slide in the same way as if the screen would extend all the way up to ground level. In other words the anchor screen is fully embedded.

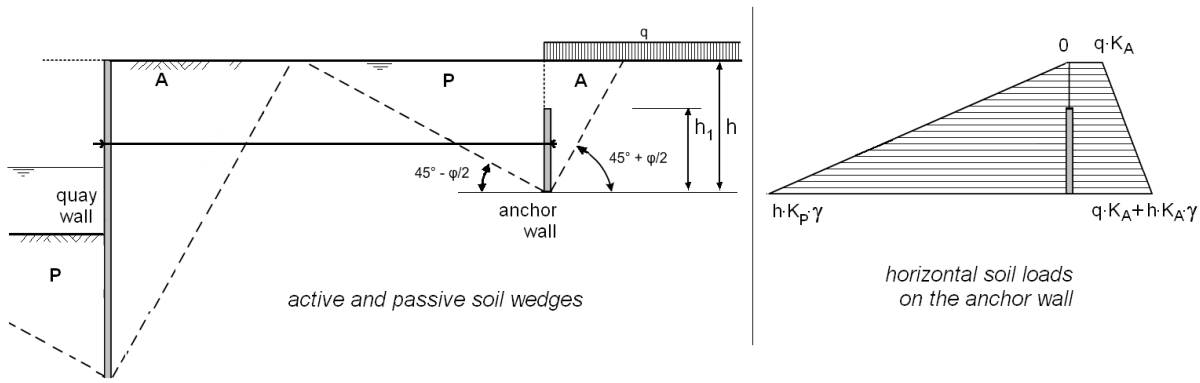


Figure 41-4 Unfavourable location of surcharge next to an anchor wall

Using Coulomb's theory and assuming that the anchor screen consists of steel rods connected to steel plates the maximum anchor force can be computed as follows:

$$F_{A;max;d} = K_p \cdot \frac{1}{2} \cdot \gamma' \cdot h^2 \cdot a - K_a \cdot \frac{1}{2} \cdot \gamma' \cdot h^2 \cdot a = (K_p - K_a) \cdot \frac{1}{2} \cdot \gamma' \cdot h^2 \cdot a$$

Where:

- $F_{A;max;d}$  [kN] = maximum anchor force the anchor screen can resist
- $K_p$  [-] = passive soil pressure coefficient
- $K_a$  [-] = active soil pressure coefficient
- $\gamma'$  [kN/m<sup>3</sup>] = effective volumetric weight of the soil (=  $\gamma_d$  or  $\gamma_s - \gamma_w$ )
- $h$  [m] = depth of the bottom tip of the anchor wall below ground surface
- $a$  [m] = centre-to-centre distance between the tie rods, with  $a \leq a_{max}$
- $a_{max}$  [m] = maximum centre to centre distance allowed between tie rods

In case a variable external load ( $q$ ) is present at ground level, see Figure 41-4, the most unfavourable situation is the presence of the load above the active slip plane of the anchor wall and the absence of the external load above the passive slip plane. The maximum anchor force is now computed as:

$$F_{A;max;d} = K_p \cdot \frac{1}{2} \cdot \gamma' \cdot h^2 \cdot a - K_a \cdot \frac{1}{2} \cdot \gamma' \cdot h^2 \cdot a - K_a \cdot q_d \cdot h \cdot a = (K_p - K_a) \cdot \frac{1}{2} \cdot \gamma' \cdot h^2 \cdot a - K_a \cdot q_d \cdot h \cdot a$$

where:

- $q_d$  [kN/m<sup>2</sup>] = design value of the external load

The design value for the maximum anchor force ( $F_{s;d}$ ) is determined as follows:

$$F_{s;d} = 1,1 \cdot F_{A;max;d}$$

In engineering practice a sheet pile wall is often anchored by a series of individual anchor boards spaced at certain distances. When regarding these anchor screens, the maximum anchor force can be computed in the same way as for a continuous anchor wall as long as the distance between the tie rods is not too large. For rectangular anchor boards the maximum distance between tie rods can be expressed as:

$$a_{max} = h_1 (\beta + \alpha - 1),$$

where:

- $a_{max}$  [m] = maximum centre to centre distance allowed between tie rods
- $h_1$  [m] = height of the anchor board
- $\alpha$  [-] = ratio between the height and width of the anchor screen:  $b/h_1$
- $\beta$  [-] = Buchholz's factor, according to Figure 41-5.

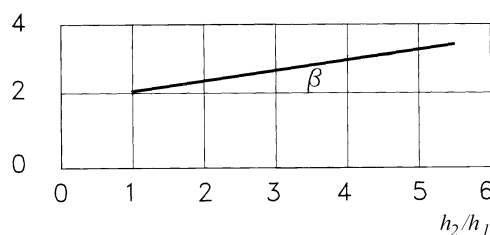


Figure 41-5 Buchholz's factor

If the centre to centre distance turns out to be larger than  $a_{max}$  then  $a_{max}$  is considered to be the total width of the ground slice that slips.

### Screw anchor

The way in which the ground around a screw anchor will fail depends both on the installation depth of the anchor and on the angle of the tie rod relative to horizontal.

If the depth over diameter ratio of a screw anchor is smaller than 5 ( $H / D \leq 5$ ), the anchor is considered to be shallow. This implies that the sliding planes reach unto ground level, see the upper anchor in Figure 41-6. In case of a deep anchor ( $H / D > 5$ ), the collapse pattern of the soil largely resembles that of the pattern around the tip of a compression pile, see the lower anchor in Figure 41-6.

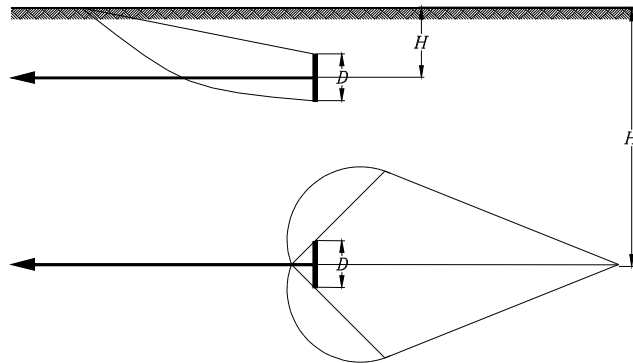


Figure 41-6 Collapse pattern around an anchor blade

Hergarden (1983) researched the maximum grip force of the anchor. For deep screw anchors in sandy ground he found a relationship between the maximum anchor force and the cone resistance in the area of influence of the anchor. This relationship reads as follows for sand:

$$F_{r;A;scr,min} = 0,4 \cdot A \cdot q_{c,avg} \geq F_{s;A;d}$$

Where:

$F_{r;A;scr,min}$	[kN]	=	minimum grip force of the screw anchor
$F_{s;A;d}$	[kN]	=	design value for the maximum anchor force the screw anchor can resist
$A$	[m <sup>2</sup> ]	=	area of the anchor blade
$q_{c,avg}$	[kPa]	=	average cone resistance in the area of influence (3·D above and beneath the anchor's axis)

In cohesive soils the relationship reads:

$$F_{r;A;scr,d} = 10 \cdot C_{u,d} \cdot A \geq F_{s;A;d}$$

Where:

$F_{r;A;scr,d}$	[kN]	=	design grip force of the screw anchor
$F_{s;A;d}$	[kN]	=	design value for the maximum anchor force the screw anchor can resist
$C_{u,d}$	[kPa]	=	design value for the undrained cohesion of the soil
$A$	[m <sup>2</sup> ]	=	area of the anchor blade

### Grout anchor

When determining the maximum strength of anchors, one usually assumes the values given in Figure 41-7.

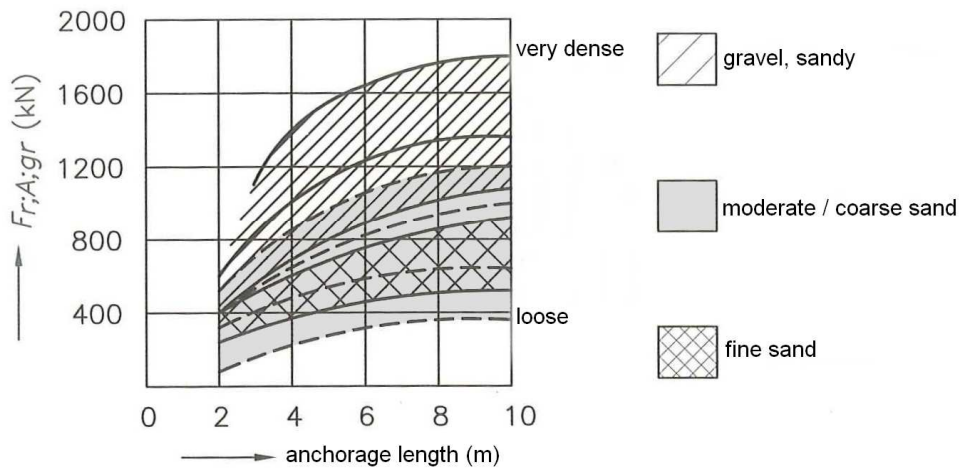


Figure 41-7 Maximum grip force for grout anchors with  $D_{\text{anchor}}$  is 100 - 150 mm and  $H \geq 4$  m.

The reader is referred to CUR report 166 for information regarding a more detailed design of grout anchors. All anchors have to be subjected to a test load equal to the design load ( $F_{s;A;d}$ ). The test results may lead to a lower safety factor, which in turn leads to the use of fewer anchors. One should be aware that over time the soil pressure, which is temporarily increased as a result of the installation of the grout anchors, will creep back to lower values (this holds in sand too). Since the test loads only have a short duration one tends to find too large values for the maximum anchor force ( $F_{A,max}$ ). Hence one should not simply use the test values found for determining the maximum grip force with Figure 41-7.

### Screw grout anchor

Screw grout anchors closely resemble auger piles (*avegaarpalen*), since no soil displacement occurs during construction of the pile. The minimum grip force and hence maximum anchoring force of the anchor is determined using:

$$F_{r;A;gr;min} = \alpha_t \cdot q_{c;gem} \cdot O \cdot L_A \geq F_{s;A;d}$$

where:

$F_{r;A;gr;min}$	[kN]	=	minimum grip force of the screw grout anchor
$F_{s;A;d}$	[kN]	=	design value for the maximum anchor force the screw grout anchor can resist
$\alpha_t$	[-]	=	pile class factor ( $\alpha_t = 0,011$ )
$q_{c;gem}$	[kPa]	=	average cone resistance along the embedded part of the anchor
$O$	[m]	=	average circumference of the embedded part of the anchor
$L_A$	[m]	=	length of the embedded part of the anchor

Again all anchors should be tested with a load equal to the design value for the maximum anchor force. This may lead to a lower safety factor, which in return leads to fewer anchors.

### 41.3 Strength of a tie rod

The design calculation of a sheet pile wall results in an anchor force per running meter, which has to be converted into an anchor force,  $F_A$ , per anchor. The design value used for the tensile force in a tie rod ( $F_{s;A;st;d}$ ) is found by increasing the design anchor force with an additional load factor:

$$F_{s;A;st;d} = F_{A;max;d} = \gamma_{f,b} \cdot F_{A;max} \quad \text{with: } \gamma_{f,b} = 1,25$$

Where:

$F_{s;A;st;d}$	[kN]	=	design value for the tensile force in the tie rod
$F_{A;max;d}$	[kN]	=	design value of the maximum anchor force
$F_{A;max}$	[kN]	=	maximum anchor force the anchor can resist
$\gamma_{f,b}$	[-]	=	load factor

The minimum cross-section of the tie rod is calculated using the maximum calculated force in the tie rod,  $F_{A;max;d}$ , according to:

$$F_{A;max;d} = \frac{A_s \cdot f_{br,d}}{\gamma_{m,a}} \quad \text{with: } \gamma_{m,a} = 1,4$$

Where:

$F_{A;max;d}$	[kN]	=	design value of the maximum anchor force
$A_s$	[m <sup>2</sup> ]	=	cross-section of the tie rod
$f_u$	[kPa]	=	tensile strength of steel (see Table 36-1)
$\gamma_{m,a}$	[-]	=	partial material factor

### 41.4 Total stability

One can distinguish three failure types for an anchored sheet pile wall:

- along a deep sliding plane;
- along a circular sliding plane;
- as a result of bursting of the bottom of the excavation pit, during construction of the anchor wall

See Figure 41-8.

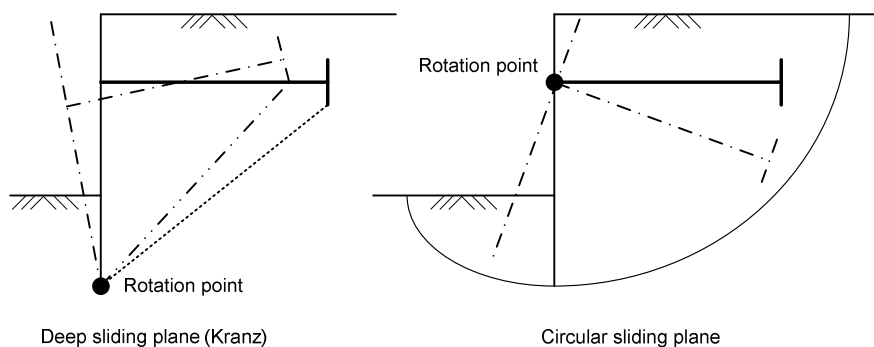


Figure 41-8 sliding planes

In the remainder of this section only the first failure mechanism will be discussed in detail, since checking for a circular slip plane is only required in specific circumstances such as short anchors and a small sheet pile length. Bursting of the bottom of an excavation pit occurs if the water pressure under an impermeable layer becomes too large compared to the layer thickness of the impermeable layer. This phenomenon is also called heave (*hydraulische grondbreuk*).

In case one keeps the areas of influence of the anchor plates, or other tension elements, and the sheet piling strictly separated, it is very unlikely that the whole structure consisting of sheet piling, anchor plates and soil will slide. The areas of influence are shown in Figure 41-9. As a rule of thumb there should always be a distance of at least 1 meter between the straight sliding planes at ground level (This is added safety!). If the distance between the sheet pile wall and the anchor becomes too small, the areas of influence intersect, see dashed lines in the figure below. This results in higher pressures at the active side of the retaining structure (here sheet pile wall), while the resistance of the anchor is reduced. That is the pressures at the passive side are lowered.

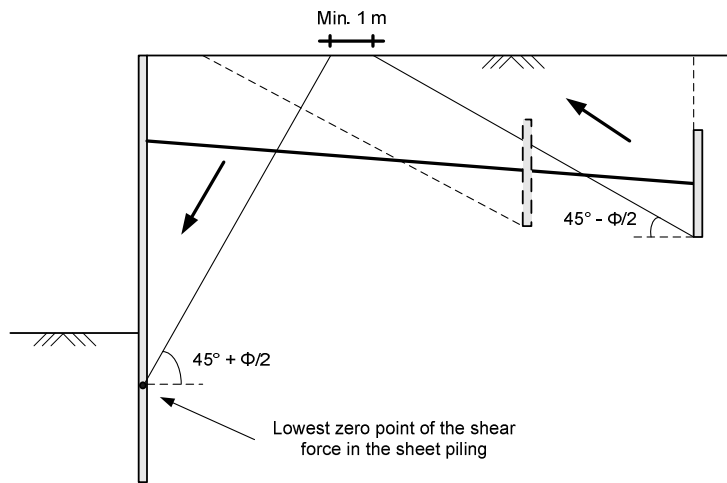


Figure 41-9 Areas of influence using straight slip planes (Coulomb).

Using the method of Kranz one can compute the required minimum distance between the anchor and the sheet pile wall. If this distance is too short a straight sliding plane will occur approximately between the point where the shear force in the sheet piling is zero and the bottom of the anchor plate. More specific, for free supported sheet piles and anchor screens the sliding plane will occur between the bottom of the sheet pile wall and the bottom of the anchor structure. For clamped sheet pile walls and anchor screens the sliding plane will occur between the lowest zero point of the shear force in the sheet pile wall and the bottom of the anchor structure.

In order to prove that the total stability is sufficient one should demonstrate that the design value of the maximum anchor force can be supported by the soil retained between the sheet pile walls and the anchor structure. This is done by regarding the balance of the soil body enclosed by ground level, the vertical planes just behind the sheet pile wall and just in front of the anchor structure and the assumed deep sliding plane, see Figure 41-10.

All the forces working directly on this soil body have to be taken into account when using this method. Forces working directly onto the retaining structure are already accounted for in the computation of the design value for the maximum anchor force. For example; if a bollard is situated in the ground behind the sheet pile wall, this force is working directly on the soil body regarded with Kranz's method. Thus it has to be accounted for. However if the bollard is connected to the sheet pile wall it has already been taken into account when computing the design value for the maximum anchor force. Therefore it is not considered in the Kranz method.

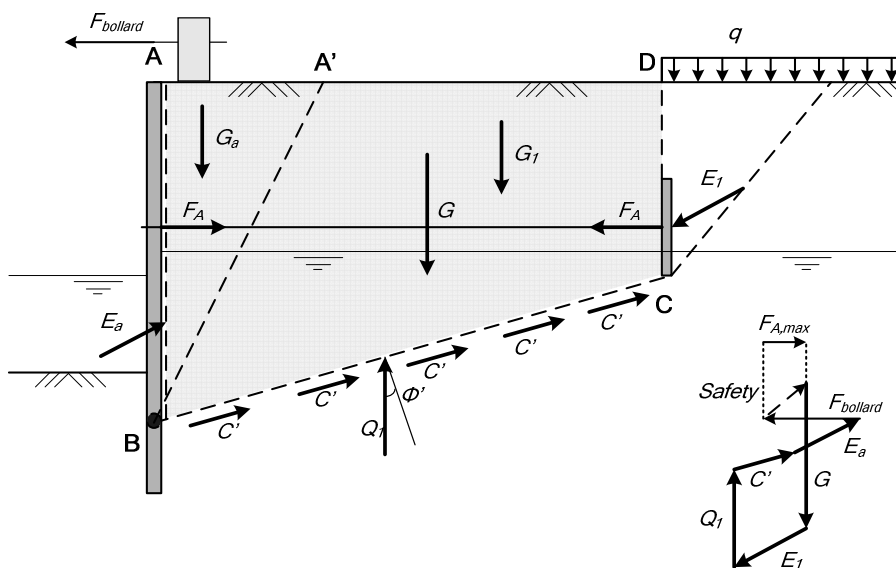


Figure 41-10 Computational scheme according to Kranz.

On the soil body ABCD (light shaded area in Figure 41-10) the following forces are working, which should balance each other:

$G$	[kN]	=	weight of the soil body ABCD
$E_a$	[kN]	=	force exerted on AB by the sliding active soil mass in case of failure. This force can be deduced from the active pressure on the sheet piling and the soil mass $G_a$ of the soil body AA' B working on the active sliding plane A'B.
$E_1$	[kN]	=	soil pressure exerted on the vertical through the anchor structure. In this force also the presence of a possible external load ( $q$ ) should be included.
$Q_1$	[kN]	=	force exerted on the plane BC, that in case of failure makes an angle ( $\varphi'$ ) with the normal on this plane.
$F_A$	[kN]	=	anchor force exerted on the soil body by the anchor structure, as computed in the sheet pile computation.
$F_{bollard}$	[kN]	=	bollard force, if present.
$c'$	[kN]	=	friction force as a result of cohesion, if present. This force works in the direction of plane AB.
$\varphi'$	[°]	=	angle of internal friction

In case the above forces do not balance each other, the soil body ABCD will slide along plane BC. As a result the direction of force  $Q_1$  is determined and the force polygon (*krachtenveelhoek*) can be drawn for the chosen distance between the sheet piling and the anchor structure, see Figure 41-10. Or one can determine the maximum allowable anchor force analytically.

Note that the presence of a horizontal groundwater table behind the sheet piling only affects the weight of the soil masses; there is no resulting horizontal water pressure. Water pressure as a result of a head difference is already included via the computed maximum anchor force as computed in the sheet pile computation. In case of a curved groundwater table behind the sheet piling one should include the influence of this curved groundwater table by including a resulting horizontal force caused by the difference in water pressure over the length of the anchor, see Figure 41-11.

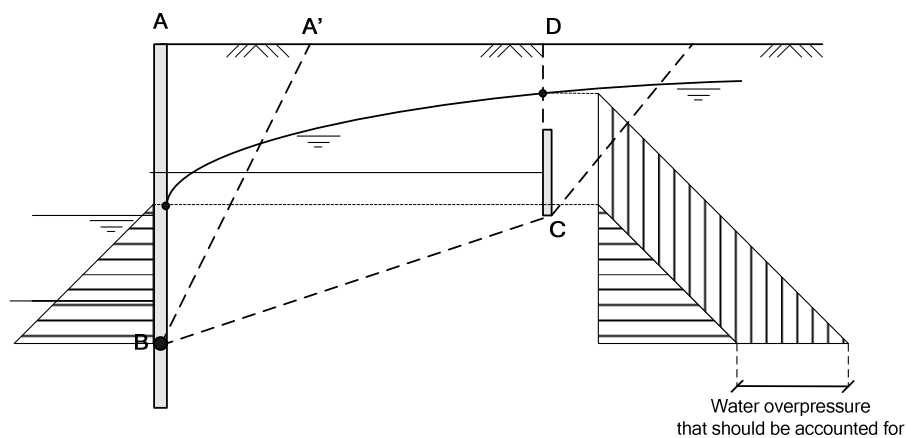


Figure 41-11 Influence of a curved groundwater table.

When after computation the maximum allowable anchor force is too large one can either increase the length of the anchor bar or increase the length of the sheet piles.

## 41.5 References

Civieltechnisch Centrum Uitvoering Research en regelgeving (CUR), *CUR-publicatie 166: "Damwand-constructies deel 1"*, 5<sup>e</sup> druk, Gouda, 2008, CUR.

Civieltechnisch Centrum Uitvoering Research en regelgeving (CUR), *CUR-publicatie 166: "Damwand-constructies deel 2"*, 5<sup>e</sup> druk, Gouda, 2008, CUR.

### Webpages:

<http://www.gebr-vanleeuwen.nl>

<http://www.ischebeck.de>

<http://www.jetmix.nl>

## 42. Compression piles

### 42.1 Strength, general

The ultimate bearing capacity of a compression pile is determined by both the tip bearing capacity and the shaft bearing capacity:

$$F_{r,max} = F_{r,max;tip} + F_{r,max;shaft}$$

where:

$$F_{r,max;tip} = A_{tip} \cdot p_{r,max;tip}$$

and:

$$F_{r,max;shaft} = O_{p,avg} \int_0^{\Delta L} p_{r,max;shaft} dz$$

in which:

$F_{r,max}$	[kN]	= maximum bearing force
$F_{r,max;tip}$	[kN]	= maximum tip resistance force
$F_{r,max;shaft}$	[kN]	= maximum shaft friction force
$A_{point}$	[m <sup>2</sup> ]	= surface area of the tip of the pile
$p_{r,max;tip}$	[kN/m <sup>2</sup> ]	= maximum tip resistance according to the sounding
$O_{p,avg}$	[m <sup>2</sup> ]	= circumference of the pile shaft
$\Delta L$	[m]	= length of the pile
$p_{r,max;shaft}$	[kN/m <sup>2</sup> ]	= maximum pile shaft friction according to the sounding

#### Notes

- In case prefab piles with enlarged feet are used,  $\Delta L$  may not be larger than the height of the enlarged foot  $H$  (see Figure 42-4).
- A reduced value of maximum tip resistance of 15 MPa is valid (see Figure 42-4).
- The net bearing capacity of the pile should be reduced with the value of negative shaft friction.

There are two methods to calculate the pile bearing capacity:

1. Prandtl and Meyerhof (only for preliminary design)
2. Koppejan (Dutch norm, so compulsory for final design)

### 42.2 Strength, Prandtl and Meyerhof

To calculate the tip bearing capacity, both Prandtl and Meyerhof assume a slip plane with a certain shape next to the foot of the pile. To determine the shaft bearing capacity one can simply total the maximum shear forces along the pile's surface.

#### Prandtl

The maximum tip resistance can be determined analogously to the bearing capacity of a shallow foundation, which is based on a slip plane according to Prandtl. This entails simply using the 2-dimensional solution for 3-dimensional collapse (conservative) and simply disregarding the shear strength, not the weight, of the soil above the foundation plane (conservative).

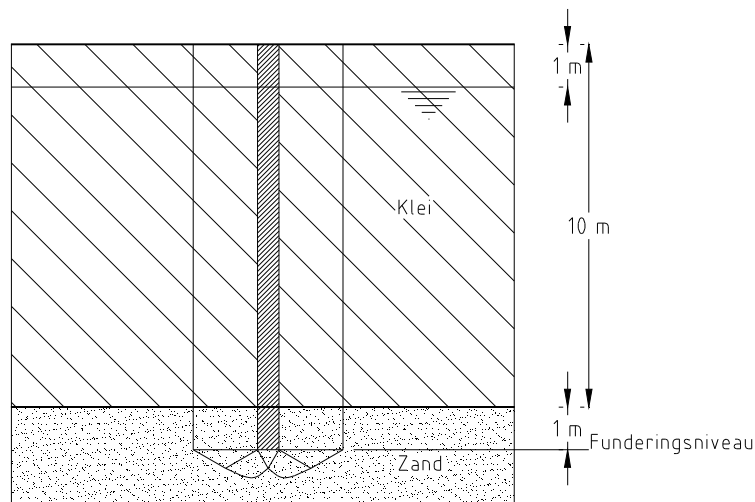


Figure 42-1 Slip planes under a pile according to Prandtl

In this case  $p_{r,max;tip}$  can be approached using  $\sigma'_{max,d}$  according to Part III, Section 32.2 "Soil, strength, Prandtl and Brinch Hansen". All this can be better explained using the following example. This example shows that the term  $0,5\gamma'_{e,d} B_{ef} N_{\gamma} s_{\gamma}$  is negligible relative to  $\sigma'_{v,z;0,d} N_q s_q$ . Therefore the tip resistance can most simply be calculated using:

$$p_{r,max;tip} = \sigma'_{v,z;0,d} N_q s_q$$

### Example

Given is a pile that is driven 11 metres into the ground according to Figure 42-1. The pile is in approximately 1 metre of sand; above the sand layer is 10 metres of clay. Groundwater level is 1 metre below ground level. The following data is given:

Sand:	$\phi = 40^\circ$
	$c = 0$
	$\gamma_{w,d} = 20 \text{ kN/m}^3$
Clay:	$\gamma_{w,d} = 15 \text{ kN/m}^3$
Pile dimensions:	$0,4 \times 0,4 \text{ m}^2$

According to Prandtl, because the cohesion is zero the maximum pressure below the tip of the pile will be:

$$p_{r,max;tip} = \sigma'_{v,z;0,d} N_q s_q i_q + 0,5\gamma'_{e,d} B_{ef} N_{\gamma} s_{\gamma} i_{\gamma}$$

According to part III Materials:  $N_q = 64$  and  $N_{\gamma} = 106$

The pile is only subjected to axial loads, so:  $i_q = i_{\gamma} = 1$

The shape factors can be derived from ( $B_{ef} = L_{ef}$ ):

$$s_q = 1 + \sin 40^\circ = 1,64 \quad s_{\gamma} = 1 - 0,3 = 0,7$$

The initial effective soil pressure is:

$$\sigma'_{v,z;0,d} = 10 \cdot 15 + 1 \cdot 20 - 10 \cdot 10 = 70 \text{ kN/m}^2$$

The maximum acceptable tip stress is:

$$\begin{aligned} p_{r,max;tip} &= 70 \cdot 64 \cdot 1,64 + 0,5 \cdot 10 \cdot 0,4 \cdot 106 \cdot 0,7 \\ &= 7,35 \cdot 10^3 + 0,15 \cdot 10^3 = 7,5 \cdot 10^3 \text{ kN/m}^2 \end{aligned}$$

So:  $0,5\gamma'_{e,d} B_{ef} N_{\gamma} s_{\gamma} \ll \sigma'_{v,z;0,d} N_q s_q$

### Meyerhof

Contrary to Prandtl, Meyerhof assumes that the slip plane developed below and beside the foundations, continues to above the foundation level. According to Meyerhof, one can differentiate between three basic cases (Figure 42.2), namely:

1. Surface foundations;
2. Transitional foundations;
3. Deep foundations.

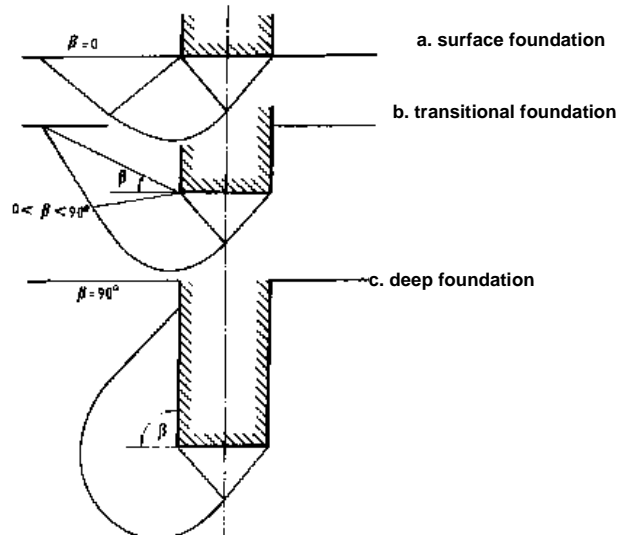


Figure 42-2 Basic cases according to Meyerhof

In his collapse analysis, besides normal stresses, Meyerhof also takes into account the shear stresses that could develop along the top of the slip plane and along the vertical part of the foundation element. This means Meyerhof's factors for the limit bearing capacity, especially in the case of high  $\phi$  values and relatively deep foundations are larger than Prandtl's. This leads to a more favourable, more economical design. The figure below shows the difference between Meyerhof and Prandtl for a foundation pile.

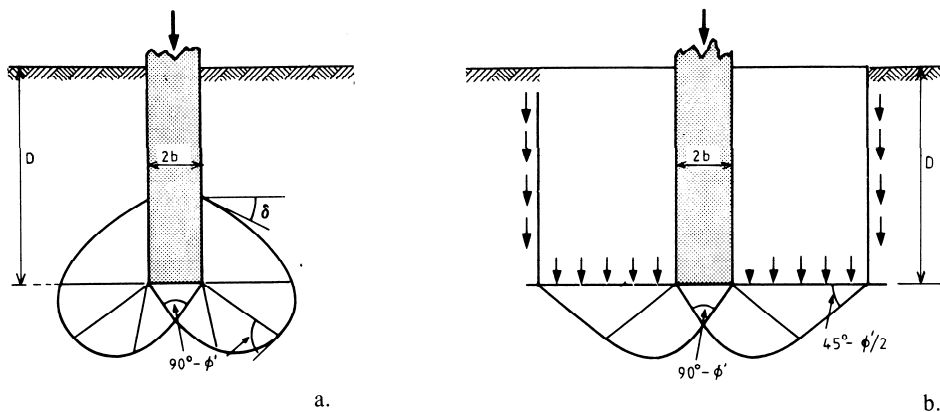


Figure 42-3 Slip planes according to Meyerhof (a) and Prandtl (b)

Figure 42-3 shows that according to Meyerhof, the ground properties above the foundation plane are also of importance when slip planes occur.

### Shaft bearing capacity

A simple method to estimate the shaft bearing capacity is to find the cumulative shear stress of all ground layers along the pile:

$$F_{shaft} = O_s \sum_n h \cdot \sigma'_v \cdot K \cdot \tan \delta$$

In the case of soil displacing piles (prefab driving piles) the ground is tensed horizontally, which means:  $K \geq K_0$ . In the case of drilled piles, one should assume  $K \leq K_0$ .

### 42.3 Strength, Koppejan (NEN 6743)

In the Netherlands, the bearing capacity of a pile is usually determined with soundings (Cone Penetration Tests). A sounding can be perceived as a model test, loading a compression pile beyond the state of collapse. Theoretically sounding entails determining the maximum tip resistance at every level in the ground. Because the size of the slip plane below and beside the pile or sounding cone depends on the dimensions of the foundation area, the cone resistance cannot be directly interpreted as the maximum tip resistance of a pile. Generally one assumes the slip plane continues to some 0,7 times the pile diameter below the pile and up to approximately 8 times the diameter above the foundation (Figure 42-1).

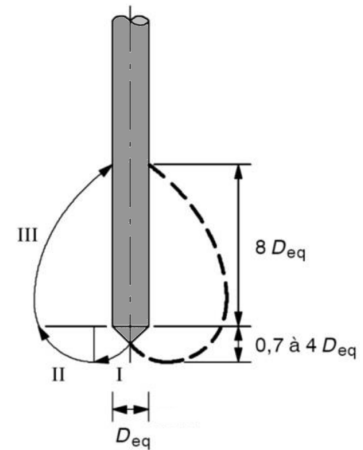


Figure 42-1 Definition of slip planes

#### Maximum tip resistance

In this case the maximum tip resistance can be derived from the sounding using:

$$p_{r,max;tip} = \frac{1}{2} \alpha_p \beta s \left( \frac{q_{c;I;avg} + q_{c;II;avg}}{2} + q_{c;III;avg} \right)$$

in which:

- $q_{c;I;avg}$  [MPa] = the average value of the cone resistances  $q_{c;z;corr}$  along section I, from the level of the tip of the pile to a level at least 0.7 times the equivalent centre line ( $D_{eq}$ ) and at most 4 times  $D_{eq}$  deeper. The bottom of section I must be selected between these boundaries so that  $p_{r,max;tip}$  is minimal;
- $q_{c;II;avg}$  [MPa] = the average value of the cone resistances  $q_{c;z;corr}$  along section II, from the bottom of section I to the level of the tip of the pile; the value of the cone resistance to be used in calculations may never exceed that of a lower level;
- $q_{c;III;avg}$  [MPa] = the average value of the cone resistances  $q_{c;z;corr}$  along section III, which runs up from the pile tip level to a level 8 times the equivalent centre line ( $D_{eq}$ ) above; as for section II the value used for the cone resistance may never exceed that of a lower level, starting with the value of cone resistance at the end of section II.
- In the case of auger piles (*avegaarpalen*), this section must start with a cone resistance equal to or less than 2 MPa, unless the sounding took place within 1 metre of the side of the pile after the pile was placed in the ground;

$D_{eq}$  [m] = equivalent pile tip diameter:

Round pile:  $D_{eq} = D$

Square/rectangular pile:  $D_{eq} = \sqrt{\frac{4}{\pi}} a \sqrt{b/a}$

$a$  = width of pile, shortest side

$b$  = width of pile, longest side (with  $a \leq b \leq 1,5a$ )

- $\alpha_p$  [-] = pile class factor according to Table 42-1. In NEN 9997-1 more or less similar values can be found, but they have to be multiplied by a factor 0,70 since 1-1-2016
- $\beta$  [-] = factor that takes into account the influence of the shape of the foot of the pile, determined using Figure 42-4 and Figure 42-5;
- $s$  [-] = factor that takes into account the influence of the shape of the cross-section of the foot of the pile, determined using Figure 42-6.

pile class / type	$\alpha_p$
<ul style="list-style-type: none"> <li>soil displacing placement methods                             <ul style="list-style-type: none"> <li>- driven piles</li> <li>- driven piles, formed in the soil</li> <li>- screwed piles, formed in the ground</li> <li>- prefabricated screwed piles</li> </ul> </li> </ul>	1,0
	1,0
	0,9
	0,8
<ul style="list-style-type: none"> <li>piles with little soil displacement, such as steel profiles and open steel tubes</li> </ul>	1,0
<ul style="list-style-type: none"> <li>piles made with soil removal                             <ul style="list-style-type: none"> <li>- auger piles</li> <li>- drilled piles</li> <li>- pulsated piles</li> </ul> </li> </ul>	0,8
	0,5
	0,5
	0,5

Table 42-1 Values of the pile class factor  $\alpha_p$

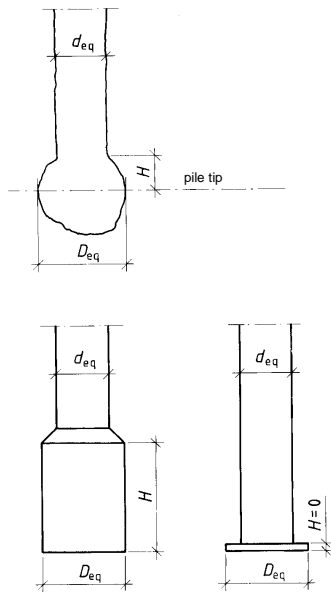


Figure 42-4 Shape of the foot of the pile

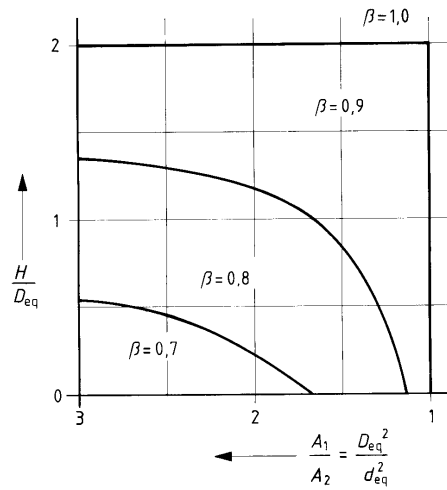


Figure 42-5 Factor for the shape of the foot of the pile  $\beta$

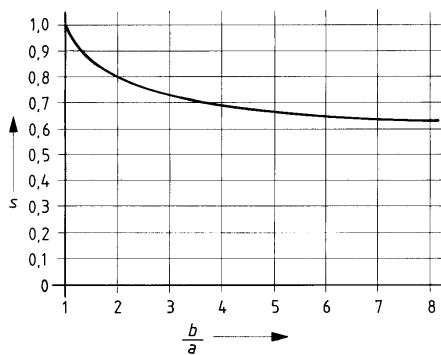
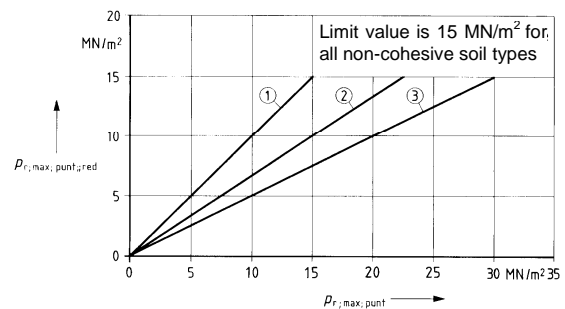


Figure 42-6 Values of s



1. sand and gravel  $OCR \leq 2$
2. sand and gravel  $2 < OCR \leq 4$
3. sand and gravel  $OCR > 4$

OCR = degree of overconsolidation

Figure 42-7 Value of the maximum tip resistance in sand and gravel

**Maximum pile shaft friction**

The maximum pile shaft friction derived from the sounding is:

$$p_{r,max;shaft;z} = \alpha_s q_{c;z;a}$$

in which:

- $p_{r,max;shaft;z}$  [MPa] = maximum pile shaft friction at depth  $z$ ;  
 $\alpha_s$  [-] = factor that takes into account the influence of the method of pile installation. Table 42-2 applies for fine to coarse sand. An additional reduction factor of 0,75 applies for extremely coarse sand. For gravel this reduction factor is 0,50. For clay, silt or peat, Table 42-3 should be used.  
 $q_{c;z;a}$  [MPa] = cone resistance, whereby the peaks in the sounding diagram with values larger than 15 MN/m<sup>2</sup> are removed if these values occur over sections of at least 1 metre and otherwise at values of 12 MN/m<sup>2</sup>.

Pile class / type	$\alpha_s$
<ul style="list-style-type: none"> <li>• <b>ground displacing placement methods:</b> <ul style="list-style-type: none"> <li>- driven smooth prefab concrete pile and steel tube pile with closed tip</li> <li>- pile made in the soil, whereby the concrete column presses directly onto the ground and the tube was driven back out of the ground</li> <li>- in the case of a tube removed by vibration</li> <li>- tapered wooden pile</li> <li>- screwed piles               <ul style="list-style-type: none"> <li>with grout injection or grout mix</li> <li>without grout</li> </ul> </li> </ul> </li> <li>• <b>piles with little ground displacement</b> <ul style="list-style-type: none"> <li>- steel profiles</li> </ul> </li> <li>• <b>piles made with ground removal</b> <ul style="list-style-type: none"> <li>- auger piles</li> <li>- drilled piles</li> <li>- pulsated piles</li> </ul> </li> </ul>	<p>0,010</p> <p>0,0014</p> <p>0,0012</p> <p>0,0012</p> <p>0,009</p> <p>0,006</p> <p>0,0075</p> <p>0,006</p> <p>0,006</p> <p>0,005</p>

Table 42-2 Maximum values of  $\alpha_s$  in sand and in sand containing gravel

ground type	relative depth $z/D$	$\alpha_s$
clay/silt : $q_c \leq 1\text{Mpa}$	$5 < z/D < 20$	0,025
clay /silt : $q_c \geq 1\text{Mpa}$	$z/D \geq 20$	0,055
clay /silt : $q_c > 1\text{Mpa}$	not applicable	0,035
peat	not applicable	0

Table 42-3 Values of  $\alpha_s$  for clay, silt or peat

**Notes**

- The shaft friction factor is in fact the same as the friction value of a CPT-sounding test as mentioned in Part III, Chapter 31 'Determination soil type'. The only difference is that for  $\alpha_s$  one does not use an average, but for safety's sake, a lower limit value.
- In the case of peat one assumes no frictional strength because it is not certain that the shear stress doesn't relax to zero due to the creep of the peat.

**Maximum negative shaft friction**

The effective bearing capacity of the pile is not only determined by the shaft bearing capacity and the tip bearing capacity, but also by the negative shaft friction, which influences the capacity unfavourably. The ground (only in the case of ground settlements!) can hang onto the pile. This causes a downward shaft friction force at the top of the pile. For the calculation of the negative shaft friction, refer to the example calculation of a prefab concrete pile on the following page.

**Note**

For groups of piles the following applies: The negative shaft friction per pile can never be larger than the total weight of the settling ground divided by the number of piles. The weight of the weak ground per pile is therefore an upper limit for the calculation of the negative shaft friction ( $\gamma_{m;g} = 1,0$  !).

### Example according to NEN 6743

To illustrate how to calculate the bearing capacity of a pile, the following example is of a prefab concrete pile at the point of sounding test S12396. The pile's dimensions are 160 x 160 mm<sup>2</sup>. The following table describes the soil layer composition. The *italic* values can be calculated from the previous (given) layer thicknesses and ground weights. The sounding is given in Figure 43-8.

Layer	Top [m NAP]	Thickness (h) [m]	$\gamma_{\text{sat}}$ [kN/m <sup>3</sup> ]	$\sigma'_{v,\text{rep}}$ [kPa]	$\sigma'_{v,\text{avg}}$ [kPa]	$h^* \sigma'_{v,\text{avg}}$ [m kN/m]
Peat (MV)	-4,61	0,6	10,3	<i>0,0</i>	<i>0,1</i>	<i>0,1</i>
Clay, sandy	-5,2	1,6	17,0	<i>0,2</i>	<i>5,8</i>	<i>9,3</i>
Peat deep	-6,8	1,5	11,1	<i>11,4</i>	<i>12,2</i>	<i>18,3</i>
Clay	-8,3	1,5	14,7	<i>13,0</i>	<i>16,6</i>	<i>24,8</i>
Sand loose	-9,8	7,4	18,9	<i>20,1</i>	-	-
Sand deep	-17,2	3,8	20,0	-	-	-

Table 42-1 Layer thickness and soil weight

S12396

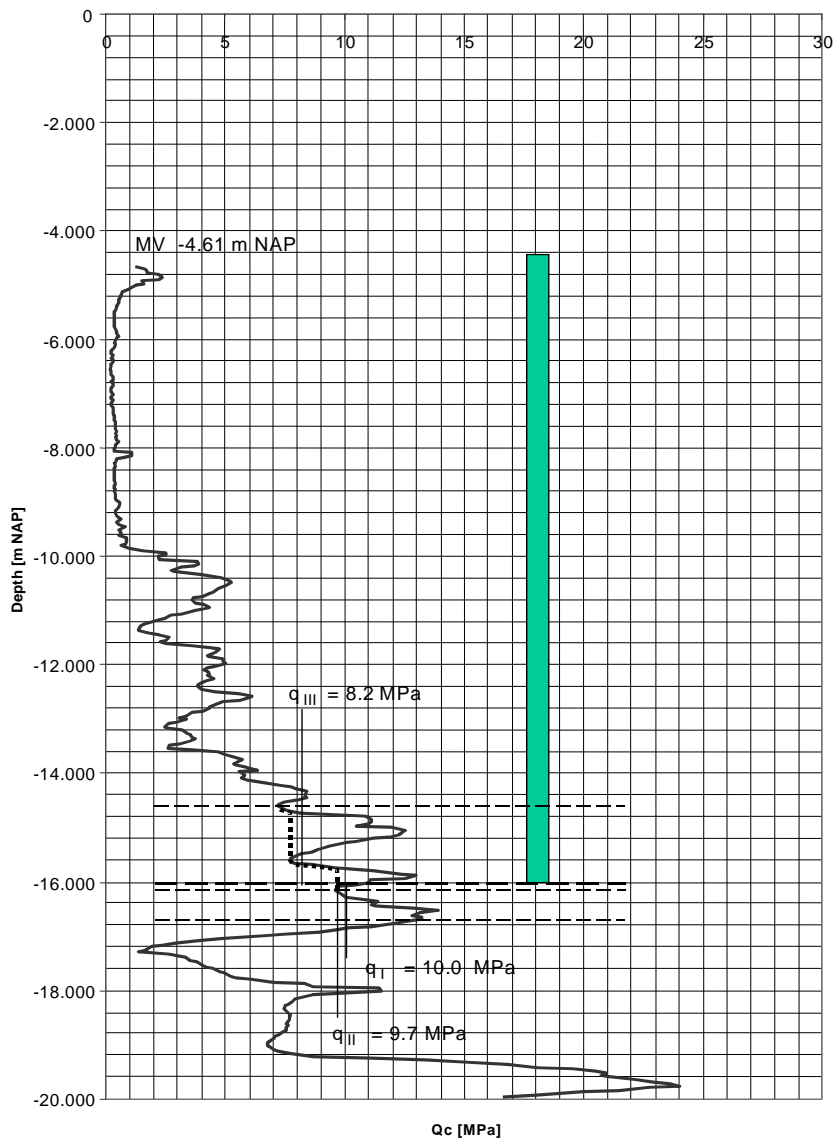


Figure 42-8 Sounding

The negative shaft friction is calculated as follows:

$$F_{s,nk,rep} = O_s \sum_n h \cdot \sigma'_{v,avg} \cdot K_{0,rep} \cdot \tan \delta_{rep}$$

in which:

$$\sum_n h \cdot \sigma'_{v,avg} = 0,1 + 9,3 + 18,3 + 24,8 = 52,5 \text{ kN/m}$$

$$K_{0,rep} \cdot \tan \delta_{rep} \geq 0,25 \quad (\text{somewhat conservative, but saves a lot of calculation})$$

Substitution gives:

$$F_{s,nk,rep} = (4 \cdot 0,16) \cdot 52,5 \cdot 0,25 = 8,4 \text{ kN}$$

The normally-shaped ( $s = 1,0$ ), square ( $\beta = 1$ ) and driven ( $\alpha_p = 1,0$ ) piles are driven to NAP  $-16,0$  m. One then finds (see Figure 42-8 Sounding):

$$q_I = 10,0 \text{ MPa and } q_{II} = 9,7 \text{ MPa and } q_{III} = 8,2 \text{ MPa}$$

hence:

$$p_{r,max;tip} = s \alpha_p \beta \frac{q_I + q_{II} + q_{III}}{2} = 9,0 \text{ MPa}$$

The tip bearing capacity is:

$$F_{r,max;tip} = A_{tip} p_{r,max;tip} = 0,16^2 \cdot 9,0 = 231 \text{ kN}$$

The shaft friction develops in "Sand, loose" layer. Between NAP  $-10$  m and NAP  $-16$  m one finds per metre an average  $q_c$  of respectively 4 MPa, 3 MPa, 4,5 MPa, 4 MPa, 8,5 MPa and 9,5 MPa (see Figure 42-8 Sounding). This leads to an average  $q_c$  of 5,6 MPa.

$$F_{r,max;shaft} = O_{tip} \int_0^{\Delta L} (\alpha_s q_c) dz = 4 \cdot 0,16 \cdot 0,010 \cdot 5,6 \cdot (16,0 - 9,8) = 222 \text{ kN}$$

The load bearing capacity of the pile consists of the bearing capacities of the tip and of the shaft:

$$F_{r,max;d} = F_{r,max;tip} + F_{r,max;shaft} = 231 + 222 = 453 \text{ kN}$$

In the case of a relatively flexible foundation plate ( $M=1$ ) and with 4 sounding tests per area ( $N=4$ ) one applies a sounding factor of:  $\xi = 0,80$ .

The material factor (method factor) is:  $\gamma_{m;b} = 1,25$

With these factors the maximum load bearing capacity of the pile becomes:

$$F_{r,found;max;d} = \frac{\xi}{\gamma_{m;b}} F_{r,max;d} = 290 \text{ kN}$$

After the subtraction of the negative shaft friction, the pile can carry the following load:

$$F_{r,found;all;d} = F_{r,found;max;d} - 1,0 \cdot F_{s,nk} = 282 \text{ kN}$$

## 42.4 Stiffness

As a rule of thumb, calculation programmes often use a pile length of  $2\ell$  instead of  $\ell$ . This provides a fairly good estimate of the stiffness of the pile and the soil together.

It is more accurate to divide the pile settlement into two parts:

1. The shortening of the pile
2. The settlement of the tip of the pile

The calculation method for the pile settlement under a load has been normalised (see NEN 6743) and needs to be calculated according to this norm for the final design. The principle of this norm is described briefly below.

**Pile shortening**

The shortening of the pile  $\Delta\ell$  can be estimated using:

$$\sigma = E\varepsilon$$

with:

$$\sigma = \frac{F}{A}$$

$$\varepsilon = \frac{\Delta\ell}{\ell}$$

in which:

$F$  [kN] = load on the pile

$\ell$  [m] = representative pile length

The representative pile length is shorter than the true pile length because the load on the pile is already partly absorbed by the shaft friction, which reduces the compression stress and therefore also the strain in the pile. See the following table for the Youngs' moduli of several pile materials.

Material	$E$ -value
Concrete	$20 \cdot 10^6$ kN/m <sup>2</sup>
Steel	$200 \cdot 10^6$ kN/m <sup>2</sup>
Wood	$15 \cdot 10^6$ kN/m <sup>2</sup>

Table 42-2 Youngs' moduli

**Pile tip settlement**

For a preliminary design one can assume a rough estimate of the pile tip settlement.

The settlement of the pile tip largely depends on the proportion between the true pile load and the maximum acceptable load on the pile. Due to the coefficients of safety, there is a ratio of about 1.5 between these two. In this case the tip settlement of a ground displacing pile (prefab concrete) is:

$$w_{tip} \approx 2\% \text{ to } 3\% \cdot D_{eq}$$

The tip settlement of drilled and auger piles is roughly twice as large because the ground has not been compressed as for driven prefab concrete piles, but has even been made looser by the drilling. A temporary excavation (deep building site excavation or drill tunnel) near the pile tip will cause relaxation of the soil, a drop of the value of  $q_c$  and a serious increase of the pile tip settlement.

For a more accurate description, refer to: NEN 6743 "Berekeningsmethoden voor funderingen op palen, drukpalen" (Calculation methods for foundations on piles, compression piles).

## 43. Tension piles

Major revision: February 2011

In some cases, resulting loads will cause structures to lift, if the present piles are not able to bear the tension forces. For quay walls founded on piles and similar structures, a number of piles will normally spoken be subjected to tension forces where the soil pressure exerts a horizontal force on the structure. Other examples of structures that may need tension piles are the access ramps of tunnels, parts of infrastructure like a railroad that are situated partially deeper than the surrounding ground water level, pump cellars etc. In such cases one needs to compute the maximum admissible tension force, which is the subject of this chapter.

A foundation pile that is subjected to a tension force will generate shear stresses along the shaft. Since the tip is not loaded, tip resistance should not be taken into account when calculating the strength. Note that during the construction phase a tension pile can be exposed to compression forces (due to the lowering of the ground water table by well-pointing (*bronbemaling*)). In other cases, e.g. a lock chamber (*sluis-kolk*), well-pointing results in the opposite situation. When the chamber is in use, a compression load is exerted on the piles. The same chamber, when it is in maintenance and therefore empty, can be subjected to a buoyancy force under its floor, causing a tensile load on the foundation piles. In order to determine the shaft friction it seems logical to use the friction chart (*wrijvingsgrafiek*) of a sounding. This, however, is not possible without restrictions since the friction as a result of tension is less than the friction due to compression, see Figure 43-1. This reduction of the shear stress is a result of the fact that in case of compression the vertical soil pressure increases around the mantle of the sounding pipe which leads to an increased shaft friction, while in case of tension the vertical soil pressure decreases.

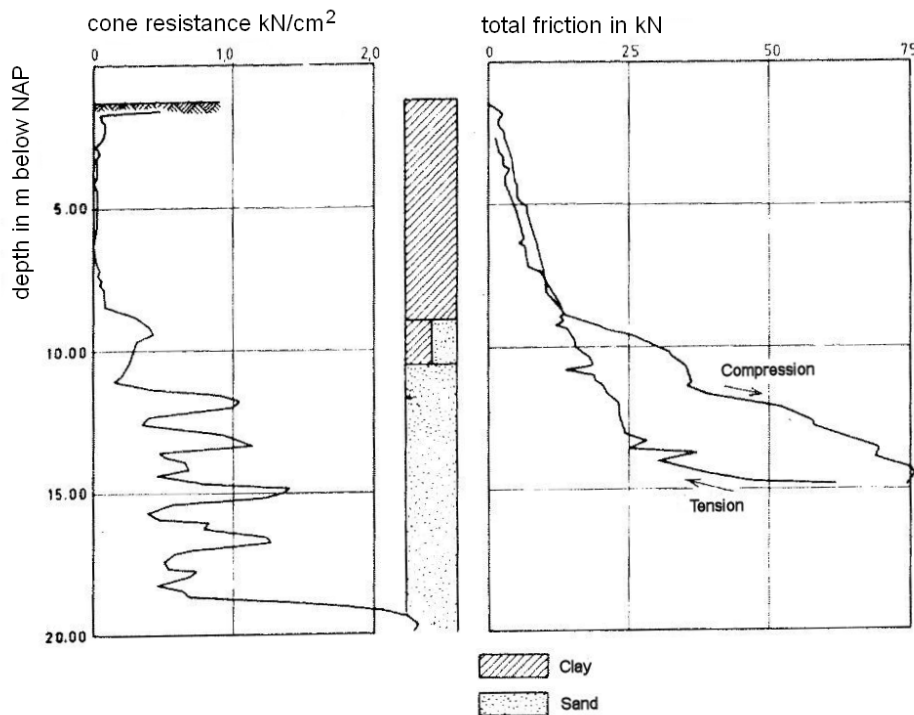


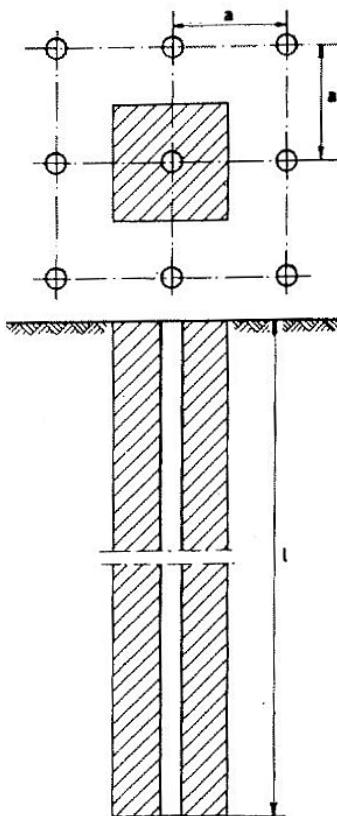
Figure 43-1 friction chart of a sounding illustrating the difference between pressing and pulling of the sounding pipe.

As can be seen in the figure above there is not much difference in the clay layer, but there is a significant difference visible in the sand layer.

### 43.1 Strength, general

The strength calculation of tension piles resembles that of compression piles. There are, however, some differences that should be kept in mind:

1. Tension piles only generate strength as a result of shaft friction, not tip resistance;
2. Tension piles have smaller coefficients for shaft friction than compression piles;
3. Tension piles are most commonly used in excavated construction sites to withstand the buoyancy force underneath the structure after construction. As a result of the excavation of the construction site, the soil pressure is reduced due to a weight reduction. Hence the effective soil pressure is also reduced and thus the value of  $q_c$  and the friction force on the pile are reduced;
4. Due to the tensile force exerted by the tension piles, the vertical effective soil pressure is reduced and as a result also the value of  $q_c$ , see Figure 43-1;
5. Not only should a single pile be tested for possible slip, but also a group of piles should be tested as the piles may influence each other in a unfavourable way. If the piles are placed in a group, the zones from which each pile receives its strength may overlap thus reducing the strength of each pile. This is checked with the clump weight (*kluitgewicht*) criterion, which states that the tensile force of a pile can never be larger than the weight of the soil that is, on average, present between the piles, see also Figure 43-2;
6. The safety factors used in the computation are larger than in case of compression piles. This is a result of the fact that inaccuracies in determining the shaft friction are larger than when determining the tip resistance. These inaccuracies are enhanced further as a result of the effect described in statement 4;
7. The dead-weight of the pile, usually the underwater weight, has a positive effect on the strength of the tension pile.



As a result of statements 1-6 the tensile capacity of a pile is much less than the compression capacity of a pile. No standards exist for the computation of tension piles. Usually the rules according to the CUR-report 2001-4 "Design rules for tension piles" are used, but they are disputable.

Particularly for very large tension forces grout anchors are used instead of tension piles. For this the reader is referred to Section 41.2 "Extreme tensile force, grout anchor" of this manual.

In the remainder of this chapter the method for computing the strength of a single tensile pile is described, after which the method for checking the clump criterion is explained in order to establish whether a group of piles is stable or not.

Figure 43-2 Maximum occurring friction in pile groups

### 43.2 Strength, CUR-report 2001-4

For the computation of the strength of a tension pile many influences have to be taken into account. For instance the reduction of the shaft friction due to reduction of the vertical effective soil pressure as a result of the exerted tensile force and the excavation works. This leads to a complex computation method. Hence, in general, the strength of tension piles is computed using a computer programme that determines the maximum shaft friction of the pile. In order to be able to make a first estimate of the tensile force that a tension pile can resist, the  $q_c$ -method is explained in this manual. Other methods are the slip method and the method according to Begemann. The most important reason for choosing the  $q_c$ -method is that it does not include the soil-pressure-coefficient ( $K$ ) and the angle of internal friction ( $\varphi$ ) of the soil, since these parameters are difficult to determine and therefore often empirical values.

The maximum tensile force that a pile can resist without slipping is computed with the following equation:

$$F_{r,tension,d} = \int_{z=0}^L q_{c,z,d} \cdot f_1 \cdot f_2 \cdot O_{p,mean} \cdot \alpha_t dz \quad (44.1)$$

Where:

$F_{r,tension,d}$	[kN]	=	design value for the tensile strength of the soil
$q_{c,z,d}$	[kN/m <sup>2</sup> ]	=	design value of the cone resistance at depth z
$f_1$	[-]	=	pile installation factor ( $f_1 \geq 1$ )
$f_2$	[-]	=	cone resistance reduction factor ( $f_2 \leq 1$ )
$O_{p,mean}$	[m]	=	average circumference of the pile shaft
$\alpha_t$	[-]	=	pile class factor ( <i>paalklasse factor</i> )
$L$	[m]	=	length over which shaft friction is computed
$z$	[m]	=	depth

In order to be able to compute the maximum tensile strength with the formula presented above, one should first compute the different parameters. This is explained in the remainder of this paragraph.

#### Cone resistance

The design value for the cone resistance is determined per soil layer, using the following equation:

$$q_{c,z,d} = \frac{q_{c,z,rep}}{\gamma_{m,b,4} \cdot \gamma_{m,var,qc}} \quad \text{where } q_{c,z,rep} = \xi \cdot q_{c,z,max} \quad (44.2)$$

Where:

$q_{c,z,d}$	[MN/m <sup>2</sup> ]	=	design value for the cone resistance at depth z
$q_{c,z,rep}$	[MN/m <sup>2</sup> ]	=	representative value for the cone resistance at depth z
$q_{c,z,max}$	[MN/m <sup>2</sup> ]	=	value of the cone resistance at depth z in the sounding <sup>1</sup>
$\xi$	[-]	=	factor dependent on the number of performed soundings, the number of piles and the stiffness of the construction (see Table 43-1)
$\gamma_{m,b,4}$	[-]	=	material factor for tension piles (= 1,4)
$\gamma_{m,var,qc}$	[-]	=	material factor for variable loads (=1,0)

<sup>1</sup> If the cone resistance in the sounding exceeds 12 MPa the value of 12 MPa should be used, unless the layer for which the cone resistance is exceeding 12 MPa is at least one meter thick. In that case the cone resistance of the sounding can be used with a maximum of 15 MPa.

If an excavation takes place after the soundings were made or there is over-consolidation of the soil, the design value for the cone resistance has to be corrected for the reduction in cone resistance that is caused by these processes. In case of an excavation this is done as follows:

- Piles driven after excavation or with a high vibration level:

$$q_{c,z,exca,max} = q_{c,z,max} \cdot \frac{\sigma'_{v,z,exca}}{\sigma'_{v,z,0}} \quad \text{where } q_{c,z,max} \leq 12 \text{ or } 15 \text{ MPa} \quad (44.3)$$

Where:

$q_{c,z,exca,max}$	[MN/m <sup>2</sup> ]	=	corrected cone resistance at depth z after excavation
$q_{c,z,max}$	[MN/m <sup>2</sup> ]	=	value of the cone resistance at depth z in the sounding
$\sigma'_{v,z,exca}$	[kN/m <sup>2</sup> ]	=	vertical effective soil pressure at depth z after excavation
$\sigma'_{v,z,0}$	[kN/m <sup>2</sup> ]	=	vertical effective soil pressure at depth z before excavation

- Piles driven before excavation or with very low vibration level:

$$q_{c,z,exca,max} = q_{c,z,max} \cdot \sqrt{\frac{\sigma_{v,z,exca}}{\sigma_{v,z,0}}} \quad \text{where } q_{c,z,max} \leq 12 \text{ or } 15 \text{ MPa} \quad (44.4)$$

If the corrected cone resistance is computed with equations (44.3) and (44.4), equation (44.2) should be used to determine the design value of the cone resistance at depth z by replacing  $q_{c,z,max}$  with  $q_{c,z,exca,max}$ .

- In case of over consolidated soil and the piles are driven using vibrations the cone resistance is corrected using the following equations:

$$q_{c,z,nc,max} = q_{c,z,max} \cdot \sqrt{\frac{1}{OCR}} \quad \text{where } q_{c,z,max} \leq 12 \text{ or } 15 \text{ MPa} \quad (44.5)$$

Where:

$q_{c,z,nc,max}$	[MN/m <sup>2</sup> ]	=	cone resistance at depth z corrected for over consolidation
$q_{c,z,max}$	[MN/m <sup>2</sup> ]	=	value of the cone resistance at depth z in the sounding
OCR	[-]	=	factor expressing the degree of over-consolidation

Again the design value of the cone resistance at depth z is computed using equation (44.2), now replacing  $q_{c,z,max}$  with  $q_{c,z,nc,max}$ .

**Material factor for variable loads ( $\gamma_m$ )**

Alternating loading, meaning alternately a compression force and a tensile force or a large tensile force and a small tensile force, on a structure leads often to the normative loading situation. In Figure 43-3 the test results of a tensile test (*trekproef*) with alternating loading are showed. As one can see, the effect of the alternating loading is that the pile head will rise when a large tensile force is exerted and will lower again when the tensile force is reduced. Alternating loading, however, will cause a gradually rise of the pile head, which is called creep. Tension piles are very sensitive for creep, which is therefore the most common shortcoming of this type of piles.

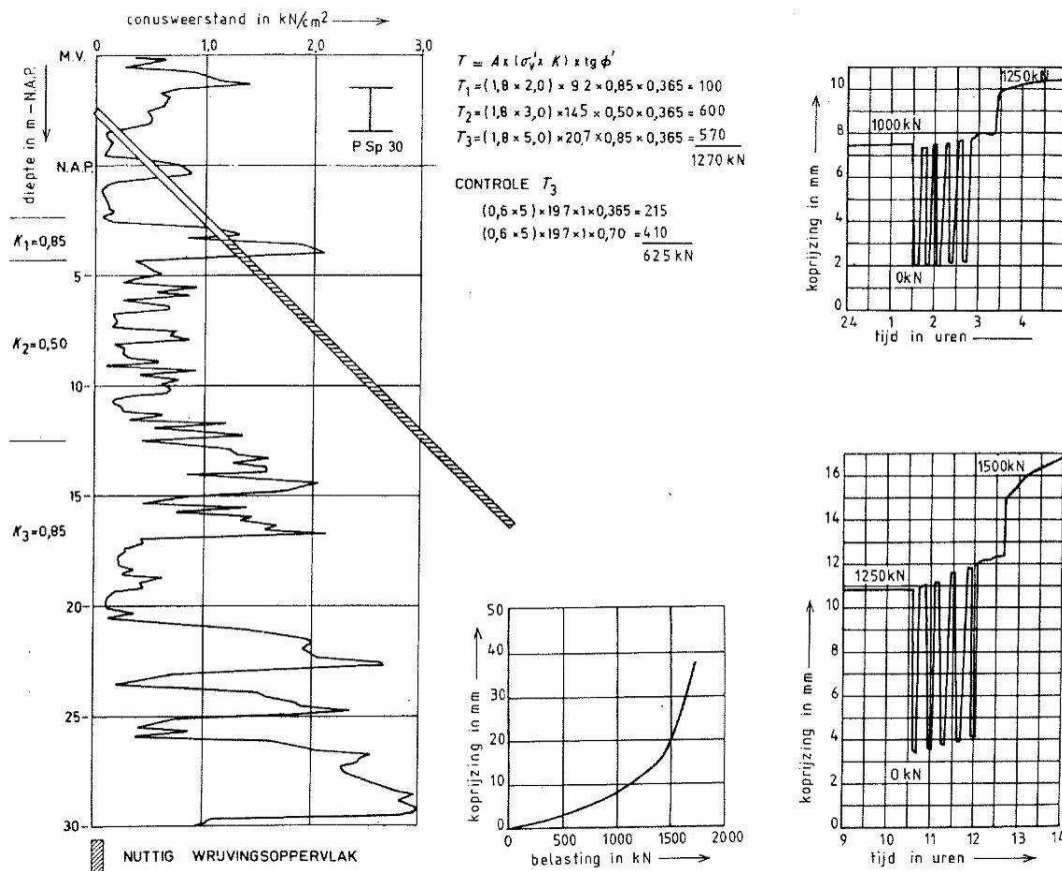


Figure 43-3 Results of a test load on a prefabricated concrete pile (tension)

The effects of alternating loading are taken into account with the material factor for variable loads, which is a function of the maximum and minimum force exerted on the tension pile, see the figure below. In case of tension the force has a positive value; in case of compression the force is assumed to be negative. The maximum value of the material factor for variable loads is 1.5.

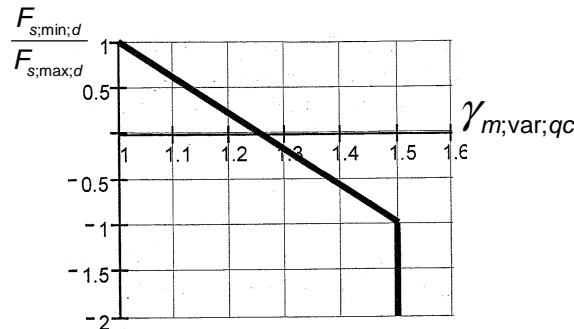


Figure 43-4 Material factor for variable loads.

The corresponding equation reads:

$$\gamma_{m,var,qc} = 1,0 + 0,25 \cdot \frac{F_{s,max,d} - F_{s,min,d}}{F_{s,max,d}} \quad \text{where } \gamma_{m,var,qc} \leq 1,5 \quad (44.6)$$

Where:

$\gamma_{m,var,qc}$	[-]	=	material factor for variable loads
$F_{s,max,d}$	[kN]	=	maximum design value of the exerted force
$F_{s,min,d}$	[kN]	=	minimum design value of the exerted force

#### *Influence of the number of soundings and installed piles*

The influence of the number of performed soundings, the number of installed piles and the stiffness of the construction is expressed by the factor  $\xi$ . Table 43-1 is used to determine this factor.

M	N						
	1	2	3	4	5	10	>10
1	0,75	0,78	0,79	0,80	0,81	0,82	0,83
2	0,78	0,81	0,83	0,83	0,84	0,86	0,87
3-10	0,81	0,84	0,86	0,87	0,87	0,89	0,90
>10	0,82	0,86	0,87	0,88	0,89	0,91	0,92

Table 43-1 Values for  $\xi$ .

Where:

M	[-]	=	number of piles installed underneath a structure
N	[-]	=	number of performed Standard Penetration Tests (SPT)

#### **Pile installation factor ( $f_1$ )**

When piles are driven into the ground the soil is compressed under the tip and along the shaft. As a result the soil becomes stiffer, hence the cone resistance increases. The stiffening of the soil is taken into account via the pile installation factor ( $f_1$ ). In case of a single pile the pile installation factor is 1.0, the same holds when a soil exploration is performed after the installation of the pile(s). Note that one may take this effect into account only for ground displacing installing methods.

$$q_{c,z,1} = f_1 \cdot q_{c,z,d} \quad (44.7)$$

Where:

$q_{c,z,1}$	[MN/m <sup>2</sup> ]	=	corrected design value for the cone resistance after pile installation
$q_{c,z,d}$	[MN/m <sup>2</sup> ]	=	design value for the cone resistance before pile installation
$f_1$	[-]	=	pile installation factor

Note that equation (44.7) already is integrated in equation (44.1).

The pile installation factor can be computed as follows:

$$f_1 = e^{3 \cdot \Delta R_e} \quad \text{where} \quad \Delta R_e = \frac{\sum_1^n \Delta e}{(e_{\max} - e_{\min})} \quad (44.8)$$

$$\text{and} \quad \sum_1^n \Delta e = -\frac{r-6}{5,5} \cdot \frac{1+e_0}{50} \quad \text{and} \quad R_e = 0,34 \cdot \ln \left( \frac{q_{c,z}}{61 \cdot (\sigma'_{v,z,0})^{0,71}} \right) \quad (44.9), (44.10)$$

Where:

$f_1$	[-]	=	pile installation factor
$R_e$	[-]	=	initial value of the relative density of the soil
$\Delta R_e$	[-]	=	increase of the relative density of the soil as a result of pile installation
$\Delta e$	[-]	=	decrease of the void ratio within a radius of $6 D_{eq}$ <sup>1)</sup> of the pile
$e_{\max}$	[-]	=	maximum void ratio of the soil (0,80 in NL)
$e_{\min}$	[-]	=	minimum void ratio of the soil (0,40 in NL)
$e_0$	[-]	=	initial void ratio of the soil.
$n$	[-]	=	number of piles within a radius of $6 D_{eq}$
$r$	[-]	=	distance, expressed in $D_{eq}$ , from an arbitrary pile to the pile that is regarded <sup>2)</sup>
$q_{c,z}$	[kN/m <sup>2</sup> ]	=	initial value of for the cone resistance
$\sigma'_{v,z,0}$	[kN/m <sup>2</sup> ]	=	initial value of the effective stress at depth z

<sup>1)</sup>  $D_{eq} = 1,13 \cdot D_{\square}$ , so for a pile 400x400 mm  $D_{eq} = 1,13 \times 400 = 452$  mm.

<sup>2)</sup> When  $r > 6$ , the pile will not be effected by the other pile(s), therefore the maximum value for  $r = 6$ .

This parameter enables one, in combination with equation (44.9), to distinguish between centre piles, edge piles and corner piles.

In Figure 43-5 the relative density of soil is given as a function of the cone resistance for different effective stresses. The influence area of a pile with respect to the increase of the relative density is a cylindrical area with a maximum radius of  $6 D_{eq}$ .

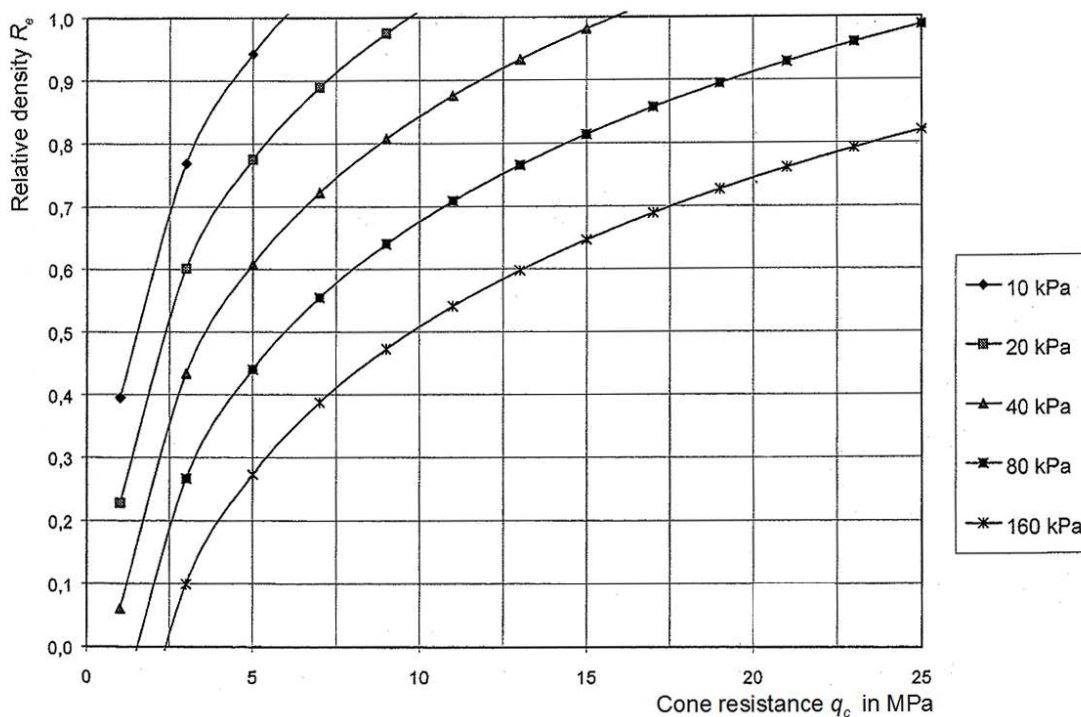


Figure 43-5 Relative density as a function of the cone resistance for different effective stresses.

If one uses a pile installation factor that is larger than one, one should perform a standard penetration test after installation in order to check whether the effective soil pressure indeed has increased or not. In the latter case it is not allowed to use a value larger than 1 for the pile installation factor. In sand the pile installation factor may be larger than one, in clay it is always one.

**Cone resistance reduction factor ( $f_2$ )**

The tensile load on a pile group reduces the effective soil pressure in the soil layers from which a single pile receives its tensile strength. Since for piles placed in a group these zones may overlap, the strength of each pile is thus reduced even more. This reduction is taken into account by applying a reduction factor  $f_2$  to the cone resistance. In case of a single pile the reduction factor  $f_2$  has a value of 1.0. The value of the cone resistance reduction factor is always one for clay, in sand the value may become less than one.

The reduction of the effective soil pressure is taken into account by dividing the soil along the length of the pile into layers of for example 0.5 metres thick. The factor  $f_2$  is subsequently computed per layer using the following equation:

$$f_{2,i} = \frac{-M_i + \sqrt{M_i^2 + (2 \cdot \sigma'_{v,z,d,0,i} + \gamma'_{d,i} \cdot d_i) \cdot \left( 2 \cdot \sigma'_{v,z,d,0,i} + \gamma'_{d,i} \cdot d_i - 2 \cdot \sum_{n=0}^{i-1} T_{d,n} \right)}}{2 \cdot \sigma'_{v,z,d,0,i} + \gamma'_{d,i} \cdot d_i} \quad (44.11)$$

$$\text{With: } M_i = \frac{f_{1,i} \cdot O_{p,i} \cdot \alpha_t \cdot q_{c,z,d,i} \cdot 1000 \cdot d_i}{A} \quad \text{and} \quad T_{d,i} = M_i \cdot f_{2,i} \quad (44.12), (44.13)$$

Where:

$f_{2,i}$	[-]	= cone resistance reduction factor for layer $i$
$M_i$	[kN/m <sup>2</sup> ]	= reduction of the vertical effective soil pressure in layer $i$
$\sigma'_{v,z,d,0,i}$	[kN/m <sup>2</sup> ]	= vertical effective soil pressure on top of layer $i$
$\gamma'_{d,i}$	[kN/m <sup>3</sup> ]	= design value of the effective volumetric weight of the soil in layer $i$
$d_i$	[m]	= thickness of layer $i$
$T_{d,i}$	[kN/m <sup>2</sup> ]	= maximum possible friction between the pile and the soil
$f_{1,i}$	[-]	= pile installation factor for layer $i$
$O_{p,i}$	[m]	= average circumference of the pile in layer $i$
$\alpha_t$	[-]	= pile class factor as indicated in Table 43-2 or Table 43-3
$q_{c,z,d,i}$	[MN/m <sup>2</sup> ]	= average cone resistance in layer $i$
$A$	[m <sup>2</sup> ]	= influence surface area of the pile

The vertical effective soil pressure can be computed using the design value of the volumetric mass of the soil:

$$\sigma'_{v,z,d,0,i} = \sum_{n=0}^{i-1} \gamma'_{d,n} \cdot d_n \quad \text{Above the water table: } \gamma'_d = \frac{\gamma}{\gamma_{m,g}} \quad (44.14)$$

$$\text{Beneath the water table: } \gamma'_d = \frac{\gamma}{\gamma_{m,g}} - \gamma_{water}$$

Where:

$\sigma'_{v,z,d,0,i}$	[kN/m <sup>2</sup> ]	= vertical effective soil pressure on top of layer $i$
$\gamma'_{d,i}$	[kN/m <sup>3</sup> ]	= design value of the effective volumetric weight of the soil in layer $i$
$d_i$	[m]	= thickness of layer $i$
$\gamma_{m,g}$	[-]	= material factor for the weight of the soil
$\gamma_w$	[kN/m <sup>3</sup> ]	= volumetric weight of water

The material factor for the weight of the soil ( $\gamma_{m,g}$ ) is to be taken 1,0 if the weight of the soil works favourable on the pile's maximum admissible tension force and 1,1 if the weight of the soil works unfavourable on the pile's maximum admissible tension force. As a result the material factor for the weight of the soil will be 1,0 from ground level to the excavation level and 1,1 beneath the excavation level.

**Useful friction area of the pile shaft ( $O_{p,mean}$ )**

When a tensile force is exerted on a foundation pile deformation of the soil occurs (in the direction of the pile axis), causing a friction force along the pile shaft. The magnitude of this friction force depends, among other things, on the amount of deformation. The deformation process depends on the soil type, e.g. small deformations in sand and large deformations in clay. Since the soil structure consists of several layers with a different deformation process not all layers contribute to the useful friction area of the pile shaft. In Figure 43-3 the useful friction area is shaded.

When determining the useful friction area of the pile shaft one should keep the following aspects in mind:

1. As long as the subsoil consists of relative homogeneous sand, the circumference of the pile shaft over the whole length of the pile is considered to be part of the useful friction area;
2. If the upper layers consist of clay or peat with a relative homogeneous sand layer beneath these layers, only the contact surface area pile/sand is considered to be the useful friction area;
3. If the subsoil consists of two (or more) qualitatively different types of sand (density and composition) the whole contact surface area pile/sand is regarded as useful friction area. However one should also account for the fact that:
  - when the deformation is so small in the qualitatively poorer sand layer(s) only part of the shear stresses will be developed;
  - when the deformation is so large in the qualitatively good sand layer(s) only the residual shear stresses will occur (12 or 15 MPa);
4. When in a certain section of the subsoil (thin) clay layers occur one should account for the consequences of possible consolidation (as a result of the driving or the occurrence of a tensile force), such as relaxation or the deformation of the sand layers.

### **Pile class factor ( $\alpha_t$ )**

The pile class factor ( $\alpha_t$ ) takes a correction into account for the shape of the pile head and the soil type in which the pile is driven. The magnitude of the pile class factor depends on the roughness of the shaft and the installing method. In Table 43-2 the pile class factors are given for piles driven in sand and sand containing gravel, whereas Table 43-3 shows the pile class factors for clay and silt.

Pile class/type	$\alpha_t$
<ul style="list-style-type: none"> <li>• Ground displacing installing methods:               <ul style="list-style-type: none"> <li>○ driven smooth prefab concrete pile and steel tube pile with closed tip<sup>1)</sup></li> <li>○ pile made in the soil, whereby the concrete column directly presses onto the ground and the tube is driven back (<i>teruggeheid</i>) out of the soil<sup>2)</sup></li> <li>○ ditto, in case the tube is removed by vibration</li> <li>○ tapered wooden pile</li> </ul> </li> <li>• Screwed piles:               <ul style="list-style-type: none"> <li>○ with grout injection or mixing</li> </ul> </li> </ul>	0,007 0,012 0,010 0,012 0,009
<ul style="list-style-type: none"> <li>• Piles with little ground displacement:               <ul style="list-style-type: none"> <li>○ driven steel profiles</li> </ul> </li> </ul>	0,004
<ul style="list-style-type: none"> <li>• Soil removing piles:               <ul style="list-style-type: none"> <li>○ drilled piles (and auger piles)</li> </ul> </li> </ul>	0,0045
<sup>1)</sup> The base of a tube pile with a closed tip shall not exceed 10 mm beyond the tube protruding. <sup>2)</sup> For this type of pile the diameter of the base may in principle be 30-50 mm larger than the outside diameter of the casing.	

Table 43-2 Maximum values for the pile class factor in sand and sand containing gravel

Soil type	Relative depth $z/D_{eq}$	$\alpha_t$
Clay/silt: $q_c \leq 1$ Mpa	$0 < z/D_{eq} < 20$	0,02
Clay/silt: $q_c \leq 1$ Mpa	$z/D_{eq} > 20$	0,025
Clay/silt: $q_c > 1$ Mpa	not applicable	0,025

Table 43-3 Maximum values for the pile class factor in clay and silt

### 43.3 Clump criterion

Not only should one check whether the tension pile will fail due to sliding and whether it can be pulled "clean" out of the ground. One should also verify if a pile, including the surrounding soil, cannot be pulled out of the ground. This is achieved by verifying that the clump criterion is met. The clump criterion states that the tensile force on a pile can never be larger than the average weight of the ground that is situated around a pile or, for a group of piles, the average weight of the ground situated around a pile between the other piles.

The clump criterion is computed using the following equation:

$$F_{clump} = F_{r,tension,max,d} = (V_{cone} + V_{cylinder}) \cdot \gamma'_d \quad (44.15)$$

Where:

$F_{clump}$	[kN]	=	maximum tensile force the soil can absorb
$F_{r,tension,max,d}$	[kN]	=	maximum tensile force the soil can absorb
$V_{cone}$	[m <sup>3</sup> ]	=	volume of the conical soil volume at the tip of the pile
$V_{cylinder}$	[m <sup>3</sup> ]	=	volume of the schematically cylinder-shaped soil volume along the other part of the pile shaft
$\gamma'_d$	[kN/m <sup>3</sup> ]	=	design value for the effective specific weight of the soil

Since the soil can absorb a tensile load only once, it is not allowed for the zones to overlap. The maximum influence area of a pile is a cylindrical area with a radius of  $3 D_{eq}$ .

In order to be able to determine the volumes of the cone and cylinder in equation (44.15), the top angle should be known. This angle depends on the pile type and the position of a pile within the pile group. As a result of the influence of other piles the top angle of piles within a group will be larger than for piles along the edge of the group, see also Table 43-4. This means that the shape of the clump around the pile is asymmetric for edge piles, at the outer edge the top angle is smaller and therefore the volume of the clump is larger than at the inner side of the edge pile due to the influence of the other piles (larger top angle).

Pile type	Half top angle of piles within a group or the inner side of edge piles [°]	Half top angle of the outer side of edge piles [°]
Ground displacing installing methods	45	30
Piles with little ground displacement	$2/3 \varphi'$	$1/2 \varphi'$
Soil removing piles	$2/3 \varphi'$	$1/2 \varphi'$

( $\varphi'$  = angle of internal friction of the soil at the pile tip)

Table 43-4 Top angle used for determining the clump volume

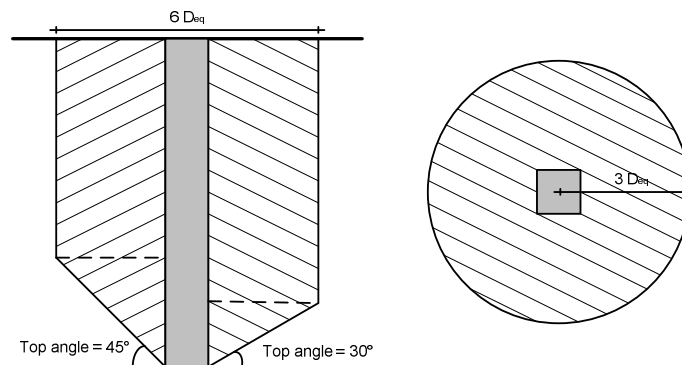


Figure 43-6 Clump volume of tension piles

As said, clumps around piles cannot overlap, so if the centre-to-centre distance of the piles is less than the maximum clump diameter  $6 D_{eq}$  (Figure 43-7), the clumps will be smaller than a cylinder around the pile with diameter  $6 D_{eq}$ . Therefore, the shape of these clumps will actually be less round (partly straight planes). The clump will even be completely box-shaped if the centre-to-centre distance is small enough ( $< 6/\sqrt{2} \cdot D_{eq}$ ). In this last case, the part of the clump at the tip of the pile has a truncated pyramid shape.

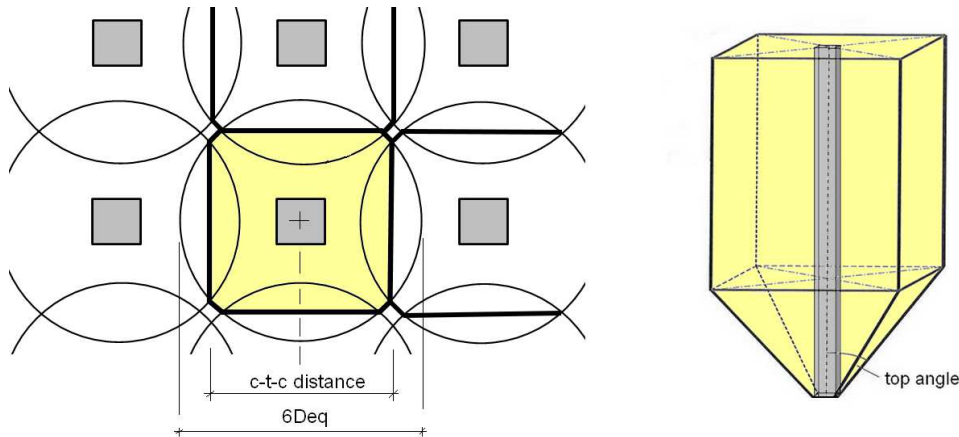


Figure 43-7 Different clump shape for dense pile groups

### Self-weight of the pile

Since the self-weight of a tension pile is working favourably for its strength it may be taken into account as follows:

$$W_{pile,d} = V_{pile} \cdot \gamma'_{pile,d} \quad \text{where} \quad \gamma'_{pile,d} = \frac{\gamma_{pile}}{\gamma_{m,g}} - \gamma_{water} \quad (44.16)$$

Where:

$W_{pile,d}$	[kN]	= design value of the pile's self-weight
$V_{pile}$	[m <sup>3</sup> ]	= pile volume (see Section 3.2 for the volumes of cones and pyramids)
$\gamma'_{pile,d}$	[kN/m <sup>3</sup> ]	= design value for the effective volumetric weight of the pile
$\gamma_{pile}$	[kN/m <sup>3</sup> ]	= volumetric weight of the pile
$\gamma_{m,g}$	[-]	= material factor for the pile weight (1,1)
$\gamma_{water}$	[kN/m <sup>3</sup> ]	= volumetric weight of water

The design value for the dead weight of the pile can be added to the maximum design value for the tensile force of the soil computed according to equation (44.1).

### 43.4 Edge piles

Particularly around an open access road to a tunnel, edge piles sometimes have larger tensile loads than the other piles. In this case, to determine the tensile load capacity, one must take into account:

- Limited reduction of the sounding resistance along the edge of the excavated building site due to the excavations.
- Group action based on the average pile tensile forces in a cross-section and thus not based on the tension in the edge piles themselves.
- Possible horizontal forces in sheet piling next to the pile.

### 43.5 Stiffness

This manual does not go into the description of the stiffness/flexural behaviour of tension piles. If grout anchors are used they must be stressed after they have been placed, so that the subsoil does not float on the groundwater but builds up effective soil pressure and thereby responds more stiffly.

### Example calculation maximum design value for the tensile resistance of the soil

#### Given:

Pile type: driven smooth prefab concrete pile  
 Shaft size: 450 x 450 mm ( $D_{eq} = 0,508$  m)  
 Pile length: 18 m (pile tip level NAP - 24,00 m)  
 Number of penetration tests: 4  
 Heart-to-heart distance: x- direction = y-direction = 2,00 m  
 Loading: static tensile load ( $\gamma_{var} = 1,0$ )  
 Ground level: NAP -0,70 m  
 Excavation level: NAP -6,00 m  
 Upper level sand layer: NAP -15,00 m  
 The effective vertical soil pressure at this level is originally (before excavation) 102,6 kN/m<sup>2</sup>.  
 The effective weight of the excavated soil is 54,1 kN/m<sup>2</sup>.

In this example the effect of the clay layers will not be taken into account, see Figure 43-8.

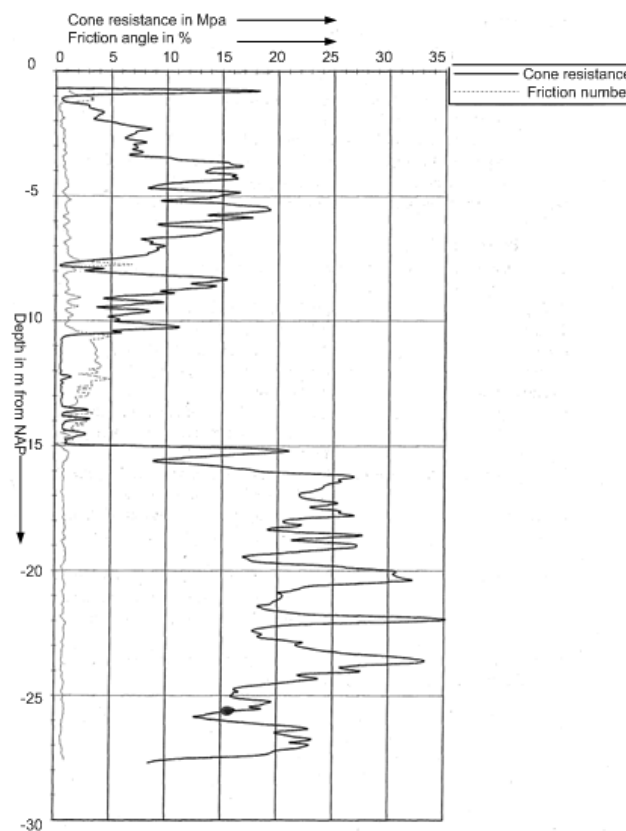


Figure 43-8 Sounding graph at the project site

#### Question

What is the maximum tensile strength of a single pile and what is the tensile strength for a pile in the centre of a pile group?

#### Answer

First the values for some parameters have to be determined. Since the number of performed penetration tests is 4, the factor depending on the number of performed soundings ( $\xi$ ) amounts to 0,80 for a single pile (Table 43-1). The pile class factor ( $\alpha_t$ ) is 0,007 (Table 43-3). Furthermore, the material factor for tensile piles ( $\gamma_{m,b4}$ ) is 1,4.

#### Single pile:

In Table 43-5 an overview of the computation is given for the sounding presented in Figure 43-8. From the table it follows that the maximum design value for the tensile force of the soil amounts to 796 kN.

Depth of layer [m relative to NAP]	$q_{c,z}$ [MPa]	$q_{c,z;exca;i}$ [MPa]	$q_{c,z;d;i}$ [MPa]	$q_{r,z;d;i}$ [kPa]	$F_{r;tension;d;i}$ [kN]	$F_{r;tension;d}$ <sup>1)</sup> [kN]
-16	15	8,1	4,6	32	58	58
-17	24	12,0	6,9	48	86	145
-18	24	12,0	6,9	48	86	232
-19	23	12,0	6,9	48	86	319
-20	22	12,0	6,9	48	86	406
-21	26	15,0	8,6	60	108	514
-22	23	15,0	8,6	60	108	622
-23	20	12,0	6,9	48	86	709
-24	26	12,0	6,9	48	86	796

<sup>1)</sup> The dead weight of the pile is not taken into account.

Table 43-5 Design value for the tensile force for a single pile

Pile in the centre of a pile group:

The computation starts with the determination of the pile installation factor ( $f_1$ ), which is now larger than 1,0. In Table 43-6 an overview of the computation is given. Furthermore it is assumed that  $e_{max} - e_{min} = 0,4$ . Within the influence area of  $6D_{eq} \times 6D_{eq}$  of the pile under consideration there are 8 other tension piles present, 4 with a heart-to-heart distance of 2 m and 4 with a heart-to-hearth distance of  $2,8 \text{ m} (= 2\sqrt{2} \text{ m})$ .

Depth on layer [m NAP]	$q_{c,z}$ [MPa]	$q_{c,z;exca;i}$ <sup>1)</sup> [MPa]	$\gamma'_i$ [kN/m <sup>3</sup> ]	$\sigma'_{v,z;i}$ during penetration [kPa]	$R_{e,i}$ [-]	$e_{0,i}$ [-]	$\Delta e_i$ <sup>2)</sup> [-]	$e_{1,i}$ [-]	$\Delta R_{e,i}$ [-]	$f_{1,i}$ [-]
-16	15	8,1	10,0	117,6	0,72	0,41	-0,0511	0,361	0,128	1,47
-17	24	13,8	10,0	127,6	0,86	0,36	-0,0491	0,307	0,123	1,44
-18	24	14,6	10,0	137,6	0,84	0,36	-0,0493	0,314	0,123	1,45
-19	23	14,6	10,0	147,6	0,81	0,38	-0,0498	0,326	0,124	1,45
-20	22	14,4	10,0	157,6	0,78	0,39	-0,0502	0,338	0,126	1,46
-21	26	17,6	10,0	167,6	0,82	0,37	-0,0496	0,321	0,124	1,45
-22	23	16,0	10,0	177,6	0,77	0,39	-0,0504	0,343	0,126	1,46
-23	20	14,2	10,0	187,6	0,71	0,42	-0,0513	0,366	0,128	1,47
-24	26	18,9	10,0	197,6	0,78	0,39	-0,0502	0,337	0,125	1,46

<sup>1)</sup> In the calculation of  $f_1$  the value for  $q_{c,z;exca;i}$  is not limited by 12 or 15 MPa  
<sup>2)</sup> In the calculation of  $f_1$  is  $\sigma'_{v,z;i}$  used, this is the effective stress in the middle of a layer i.

Table 43-6 Determination of the pile installation factor per layer

Also the cone resistance reduction factor ( $f_2$ ) has to be computed which is smaller than 1.0, the results are presented in Table 43-7. Again the pile under consideration has an influence area of  $6D_{eq} \times 6D_{eq}$ . The top angle is assumed to be  $45^\circ$ .

Depth layer [m + NAP]	$q_{c,z;d;i}$ [MPa]	$M_i$ [kPa]	$\gamma'_{d;i}$ [kN/m <sup>3</sup> ]	$\sigma'_{v,z;d;i}$ [kPa]	$f_{1,i}$ [-]	$T_{i-1}$ [kPa]	$\sum T_{i-1}$ [kN]	$f_{2,i}$ [-]	$F_{r,tension,d}$ [kN] <sup>1)</sup>	$F_{r,tension,max,d}$ [kN] <sup>1) 2)</sup>
-15	-	-	-	-	-	-	0,0	-	-	-
-16	4,6	22,52	8,2	47,7	1,47	18,2	18,2	0,81	69	182
-17	6,9	32,87	8,2	55,9	1,44	19,9	38,0	0,60	144	213
-18	6,9	32,93	8,2	64,1	1,45	15,3	53,4	0,47	203	244
-19	6,9	33,05	8,2	72,3	1,45	12,3	65,7	0,37	250	275
-20	6,9	33,16	8,2	80,5	1,46	10,4	76,2	0,31	289	306
-21	8,6	41,26	8,2	88,6	1,45	10,5	86,7	0,26	329	337
-22	8,6	41,51	8,2	96,8	1,46	9,2	95,9	0,22	364	369
-23	6,9	33,43	8,2	105,0	1,47	7,6	103,5	0,23	393	400
-24	6,9	33,15	8,2	113,2	1,46	7,6	111,1	0,23	422	431

<sup>1)</sup> The dead weight of the pile is excluded in the computation.  
<sup>2)</sup>  $F_{r,tension,max;d}$  represents the design value for the clump weight.

Table 43-7 Determination of the cone resistance reduction factor per layer

The computed design value of the maximum tensile load ( $F_{r,tension,d}$ ) the pile can resist amounts to 422 kN. The computed clump criterion results in a value of 431 kN. Since this is higher than the design value for the maximum tensile load, the maximum tensile load is representative for the total strength of the pile.

---

### 43.6 References

Civieltechnisch Centrum Uitvoering Research en regelgeving, *Cur-rapport 2001-4: "Ontwerpregels voor trekpalen"*, Gouda, juni 2001, Curnet.

Keverling Buisman, A.S., *Grondmechanica*, Delft, 1944, Waltman.

Verruijt, A., revised by S. van Baars, *Soil Mechanics*, Delft, 2005, VSSD.

## 44. Laterally loaded piles

improved: February 2016

### 44.1 Introduction

The forces on the foundation of buildings predominantly work in vertical direction. In general, the use of only vertical foundation piles will suffice for buildings. Hydraulic structures, on the contrary, frequently have to resist very considerable horizontal (= lateral) forces, besides the vertical forces. Think of horizontal soil and water pressures behind a soil retaining structure, mooring and berthing forces on a jetty or quay wall, etc. A deep foundation with only vertical piles is generally not suited to for resisting the large horizontal forces and the overturning moment accompanying these forces. Therefore, the deep foundation of a hydraulic structure is often a combination of vertical piles and piles driven under an angle to the vertical. These piles are called 'raking piles' or 'batter piles' (*schoorpalen*).

Irrespective of the type of structure and the type of pile, vertical or batter, the horizontal load has to be transferred into deeper soil layers where enough horizontal bearing capacity can be provided.

### 44.2 Blum: pile theory

A commonly used method to compute the required embedded depth (*inheidiepte*) needed to provide enough passive soil resistance to lateral loads, is Blum's method (*Die Bautechnik*, Heft 5, 1932). Blum used the following assumptions for his theory:

- 1) the embedded part of the foundation pile is regarded as an elastically supported beam;
- 2) the soil response is perfectly plastic;
- 3) the soil reaction on the deeper part of the pile is substituted by a concentrated force known as the *Ersatzkraft* ( $R_3$ ), see Figure 44-2;
- 4) for stiffness considerations the pile is thought to have a fixed support at the depth were the concentrated force  $R_3$  is acting on the pile.

Ad 2: It is assumed that the elastic range of the soil is extremely small. As soon as there is a displacement ( $u$ ) the soil response is either immediately at its maximum (passive,  $\sigma_{h,max}$ ) or minimum (active,  $\sigma_{h,min}$ ). Hence the stiffness of the soil is assumed to be very large. It is to be expected that the displacements as a result of the load will be somewhat underestimated (see Figure 44 1).

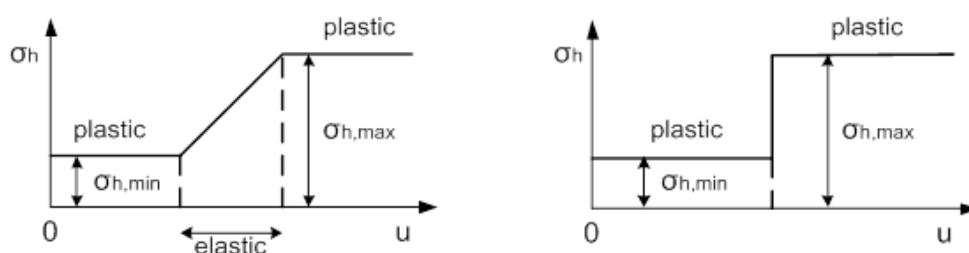


Figure 44-1 On the left: elasto-plastic soil response. On the right: perfectly plastic soil response.

Ad 3: The basic idea is that the pile is displaced towards the right by the applied force, except at the lower end where a displacement towards the left occurs because the pile rotates around a point somewhere above its deepest point. The soil reaction towards the left is replaced by the concentrated force ( $R_3$ ) generally known as *Ersatzkraft* (German for substitute force), see Figure 44 2.

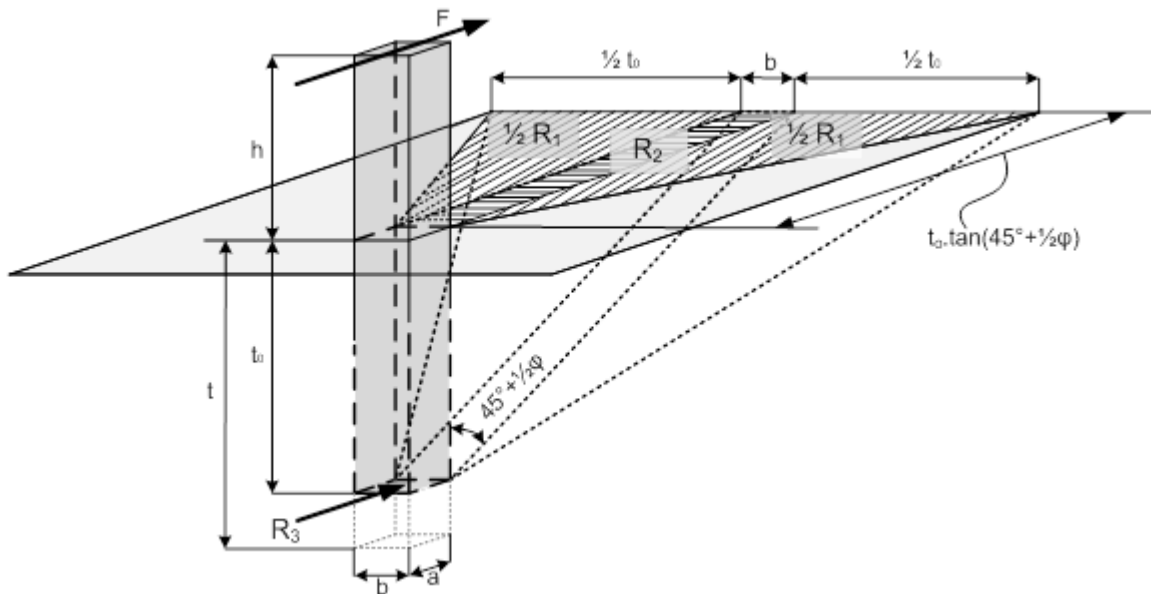


Figure 44-2 Schematic representation of the shearing soil wedge behind a laterally loaded pile.

where:

$F$	[kN]	=	load
$R_1$	[kN]	=	resultant force of the soil wedges on both sides next to the soil wedge directly behind the pile (two half pyramids)
$R_2$	[kN]	=	resultant force of the soil wedge directly behind the pile (a triangle with width $b$ )
$R_3$	[kN]	=	substitute force ('Ersatzkraft')
$a$	[m]	=	width of the pile in the direction of the load
$b$	[m]	=	width of the pile perpendicular to the load
$h$	[m]	=	length of the unsupported part of the pile
$t_0$	[m]	=	theoretical embedded depth
$t$	[m]	=	practical embedded depth $t = 1,2 \cdot t_0$
$\varphi$	[°]	=	angle of internal friction

**Strength**

The maximum load the soil wedge behind the pile is able to resist can be computed by taking the sum of the moments at depth  $t_0$  below bed level, in this way the concentrated force  $R_3$  does not enter into the equations (see Figure 44-3).

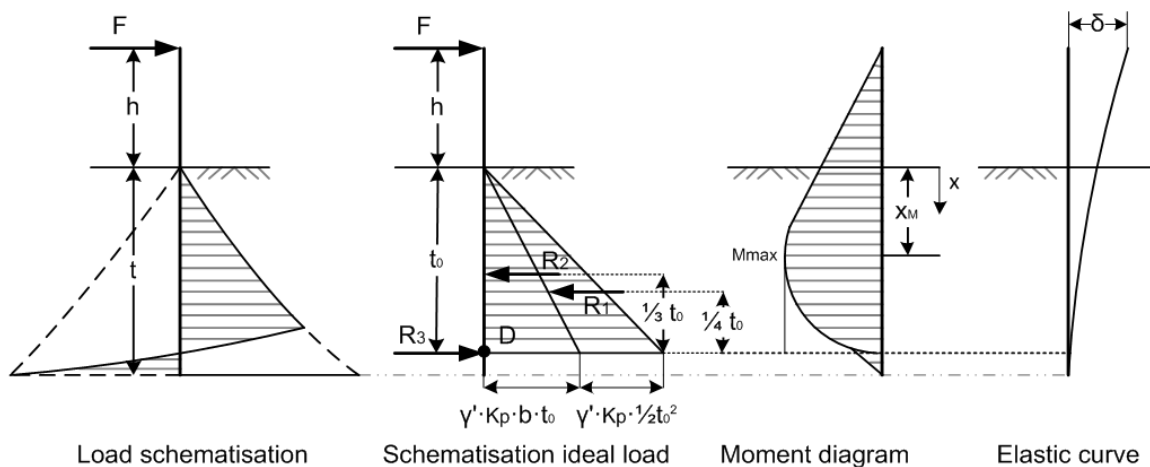


Figure 44-3 Blum's schematization

$$\begin{aligned}
\sum M_D &= 0 \\
-F_{max} \cdot (t_0 + h) + R_1 \cdot \frac{1}{4} \cdot t_0 + R_2 \cdot \frac{1}{3} \cdot t_0 &= 0 \\
F_{max} \cdot (t_0 + h) &= \left(\frac{1}{6} \cdot \gamma' \cdot K_p \cdot t_0^3\right) \cdot \frac{1}{4} \cdot t_0 + \left(\frac{1}{2} \cdot \gamma' \cdot K_p \cdot b \cdot t_0^2\right) \cdot \frac{1}{3} \cdot t_0 \\
F_{max} \cdot (t_0 + h) &= \frac{1}{24} \cdot \gamma' \cdot K_p \cdot t_0^4 + \frac{1}{6} \cdot \gamma' \cdot K_p \cdot b \cdot t_0^3 \\
F_{max} &= \gamma' \cdot K_p \cdot \frac{t_0^3}{24} \cdot \frac{t_0 + 4 \cdot b}{t_0 + h}
\end{aligned} \tag{44-1}$$

where:

$F_{max}$	[kN]	= maximum load that can be resisted
$R_1$	[kN]	= resulting force of soil at either side of the pile
$R_2$	[kN]	= resulting force of soil directly behind the pile
$b$	[m]	= width of the pile perpendicular to the load
$h$	[m]	= length of the unsupported part of the pile
$t_0$	[m]	= theoretical embedded depth
$K_p$	[-]	= passive soil pressure coefficient
$\gamma'$	[kN/m <sup>3</sup> ]	= effective volumetric weight ( $\gamma_s - \gamma_w$ )
$\delta$	[°]	= (pile) wall friction; generally $\delta = -\frac{2}{3}\phi$

$$K_{p,h,\sigma} = \frac{\cos^2(\phi - \alpha)}{\cos^2(\alpha) \left(1 - \sqrt{\frac{\sin(\phi - \delta)\sin(\phi + \beta)}{\cos(\alpha - \delta)\cos(\alpha + \beta)}}\right)^2} \quad \text{with } \alpha = \beta = 0$$

Because all (shear) forces are known, the moment diagram can be determined, using the following equation:

$$M_x = F \cdot (h + x) - \gamma' \cdot K_p \cdot (x + 4 \cdot b) \cdot \frac{x^3}{24} \tag{44-2}$$

where:

$M_x$	[kNm]	= moment at depth $x$
$F$	[kN]	= load
$x$	[m]	= distance below bed level

The maximum moment  $M_{max}$  occurs at depth  $X_m$ , where  $\frac{\delta M}{\delta x} = 0$ . This depth is found by solving the following equation iteratively:

$$x_M^2 \cdot (x_M + 3 \cdot b) = \frac{t_0^3}{4} \cdot \frac{t_0 + 4 \cdot b}{t_0 + h} \tag{44-3}$$

### Notes

1. The soil resistance only depends on the angle of internal friction and the volumetric weight of the soil. Almost always the effective (submerged) weight of the soil has to be used in combination with  $\delta = -\frac{2}{3}\phi$ , to calculate the  $K_p$ , and arrive at the lateral bearing capacity.

2. In case of an impact load (stootbelasting) the load duration is short; in cohesive soils there is quite a possibility that the groundwater does not have time to flow out of the soil wedge behind the foundation pile or flow into the soil in front of the pile. For that reason Blum proposes to use the volumetric weight of saturated soil ( $\gamma_s$ ), however in combination with  $\delta = 0$  to calculate the  $K_p$ .

3. For the strength considerations in the above, the position of the fixed support of the pile is at a distance  $X_M$  below ground level.

### Stiffness

When loaded in a direction perpendicular to its axis, a foundation pile will bend. The displacement of the part of the pile embedded in soil results in a passive resisting force. The graph of the bending moments in the pile, according to Blum's strength considerations, shows a curved development, see Figure 44-4. The pile could also be modelled as a cantilevering beam with concentrated load (horizontal). For this last schematization the bending moment diagram and the formula for the maximum displacement are well known:

$$\delta = \frac{F \cdot L_i^3}{3EI} \quad (44-4)$$

where  $EI$  is the stiffness of the cantilever; in this case, the pile stiffness.

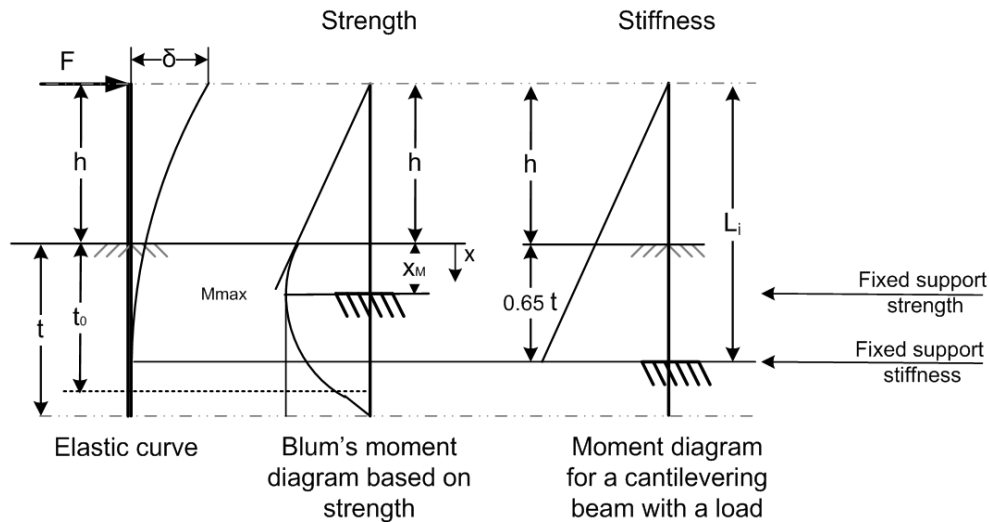


Figure 44-4 Moment diagrams for laterally loaded piles

Equating the statical moments of both moment diagrams, Blum found the following expression for the displacement of the pile head as a result of a lateral load  $F$ :

$$\delta = \frac{F \cdot (h + 0,65 \cdot t)^3}{3EI} \quad (44-5)$$

where:

$\delta$	[m]	= displacement of the pile head
$F$	[N]	= load
$h$	[m]	= length of the unsupported part
$t$	[m]	= practical embedded depth
$E$	[N/m <sup>2</sup> ]	= Young's modulus of the pile material
$I$	[m <sup>4</sup> ]	= moment of inertia of the pile
$L_i$	[m]	= $h + 0,65 \cdot t$

Hence the overall pile stiffness, the spring stiffness  $k$  of the pile, which includes a contribution of both soil and pile material, when the maximum load is acting, can be estimated as follows:

$$k_{pile} = \frac{F_{max}}{\delta} = \frac{3EI}{(h + 0,65 \cdot t)^3} \quad (44-6)$$

As long as the soil can be schematized as one layer, Blum's schematization results in a reasonable approximation of the maximum absorbable lateral load on a foundation pile. However when the soil profile consists of multiple layers, then the displacements better be analysed using a finite element model or an elasto-plastic spring model. In the latter case the foundation pile will be schematized as a beam on an elastic bed. For subgrade moduli ( $k$ -values) of the soil (*beddingsconstanten van grond*) the reader is referred to Section 33.5 of this Manual.

### 44.3 References

Blum, H., *Die Bautechnik*, Heft 5, 1932.

N.V. Houthandel v/h G. Alberts Lzn. & Co., *Het ontwerpen, berekenen en vergelijken van ducdalven in tropisch hout en staal*, Middelburg, september 1957.

Veen, van der, C., Horvat, E., Kooperen, van, S.H., *Grondmechanica met beginselen van de funderingstechniek*, Waltman, Delft, oktober 1981.

Verruijt, A., *Laterally loaded pile*, March 29, 1999.

## 45. Pile groups

The previous chapters gave calculation methods for the determination of the pile load. The choice of method depends on the schematisation of the structure. Figure 45-1 is a flow chart to determine which calculation method to use. It is always possible to use a method shown to the right of the calculation method selected with the flow chart.

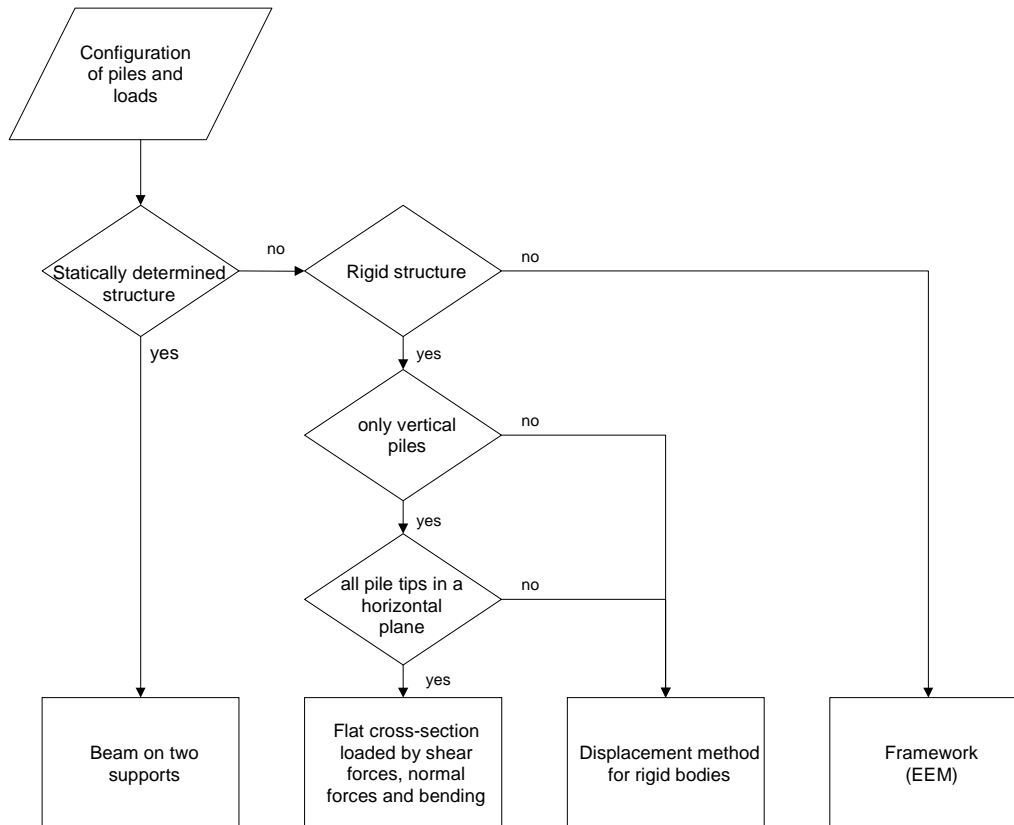


Figure 45-1 Flow chart for the determination of a calculation method

A common problem in structural hydraulic engineering is group of horizontally loaded piles. The example determines whether a jetty can absorb the mooring energy.

### Example calculation of the horizontal force on a pile due to ship collision with a jetty

#### Given

Details of the jetty:

- The deck-pile connection can be considered a hinge
- Linear spring stiffness of rubber fender  $k = 100 \text{ kN/m}$
- Square wooden piles  $0,25 \times 0,25 \text{ m}^2$
- Wood type: Azobé with  $E = 17000 \text{ N/mm}^2$
- Fictitious length of fixed-end  $10 \text{ m}$

Details of the fishing boats:

- length  $L = 24 \text{ m}$
- width  $W = 6 \text{ m}$
- draught  $D = 4 \text{ m}$
- block coefficient  $C_b = 0.7$

Collision in point A:

- Mooring speed  $\perp$  jetty  $= 0,5 \text{ m/s}$
- Distance centre of mass of boat to point of collision  $= 12 \text{ m}$
- Approach angle  $\gamma = 60^\circ$
- $\rho_{\text{water}} = 1000 \text{ kg/m}^3$

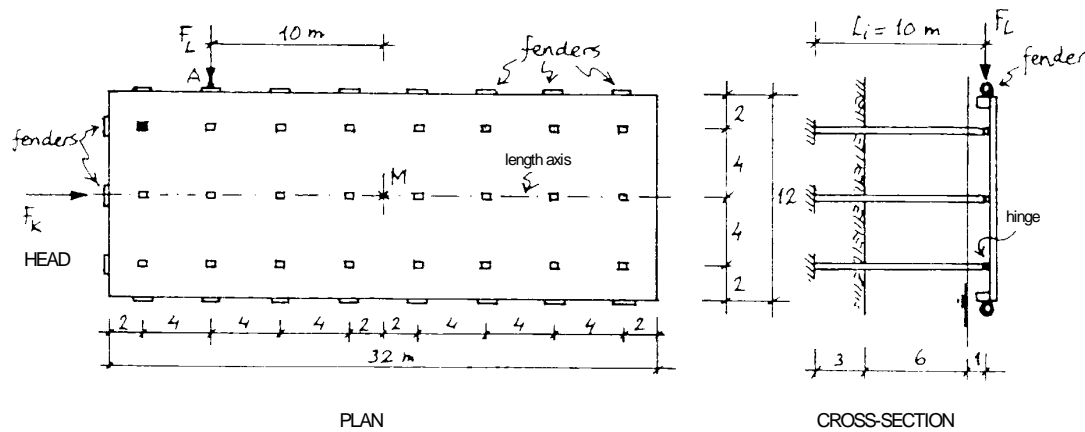


Figure 45-2 Overview and dimensions of jetty

**Asked**

Calculate the acting horizontal force on the outer pile.

**Elaboration**

To determine the mooring energy, see Part II, Loads, Mooring:

$$m_s = \rho C_b L W D = 1 \cdot 0.7 \cdot 24 \cdot 6 \cdot 4 = 403 \text{ tonnes}$$

$$m_w = \rho L \frac{1}{4} \pi D^2 = 1 \cdot 24 \cdot \frac{1}{4} \cdot \pi \cdot 4^2 = 300 \text{ tonnes}$$

$$k = (0.19 C_b + 0.11) L = (0.19 \cdot 0.7 + 0.11) \cdot 24 = 5.8 \text{ m}$$

$$C_E = \frac{k^2 + r^2 \cos^2(\gamma)}{k^2 + r^2} = \frac{5.8^2 + 12^2 \cos^2(60^\circ)}{5.8^2 + 12^2} = 0.39$$

$$C_s = 1$$

$$C_c = 1$$

$$E_{kin} = \frac{1}{2} (m_s + m_w) v_s^2 C_E C_s C_c = \frac{1}{2} (403 + 300) 0.5^2 \cdot 0.39 \cdot 1 \cdot 1 = 34 \text{ kNm}$$

The spring stiffness of one pile is:

$$k_{1 \text{ pile}} = \frac{3EI}{L_i^3} = \frac{3 \cdot 17 \cdot 10^6 \cdot 1 / 12 \cdot 0.25 \cdot 0.25^3}{10^3} = 16.6 \text{ kN/m}$$

For all piles:

$$k_{\text{all piles}} = n k_{1 \text{ pile}} = 24 \cdot 16.6 = 400 \text{ kN/m}$$

The polar moment of inertia of the pile plan is:

$$I_p = \sum k_{\text{pile } i} (x_i^2 + y_i^2) = k_{1 \text{ pile}} \{ 6 \cdot (2^2 + 6^2 + 10^2 + 14^2) + 16 \cdot (4^2) \} = 38000 \text{ kNm}$$

The spring stiffness of the jetty is:

$$\frac{1}{k_{\text{jetty}}} = \frac{1}{k_{\text{all piles}}} + \frac{e^2}{I_p} = \frac{1}{400} + \frac{10^2}{38000} \Rightarrow k_{\text{jetty}} = 195 \text{ kN/m}$$

The spring stiffness of the jetty and fender together is therefore:

$$\frac{1}{k_{\text{total}}} = \frac{1}{k_{\text{jetty}}} + \frac{1}{k_{\text{fender}}} = \frac{1}{195} + \frac{1}{100} \Rightarrow k_{\text{total}} = 66 \text{ kN/m}$$

The maximum impact force is:

$$F_{st} = k \Delta x = \sqrt{2k E_{kin, \text{max}}} = \sqrt{2 \cdot 66 \cdot 34} = 67 \text{ kN}$$

Accordingly, the displacement of the jetty + fender is very large:

$$\Delta x = \frac{F_{st}}{k} = \frac{67}{66} = 1.02 \text{ m}$$

The horizontal force against the outer pile is found with:

$$F_y = \frac{F_{st}}{n} + \frac{F_{st} e a_y}{I_p} = \frac{67}{24} + \frac{67 \cdot 10 \cdot 14}{38\,000} = 2,78 + 0,25 = 3.03 \text{ kN}$$

$$F_x = \frac{F_{st} e a_x}{I_p} = \frac{67 \cdot 10 \cdot 4}{38\,000} = 0,07 \text{ kN}$$

$$F = \sqrt{F_y^2 + F_x^2} = 3,03 \text{ kN}$$

For this force two matters must be verified:

- Does the moment ( $M = F l_i = 29 \text{ kN}$ ) in the pile cause a stress ( $\frac{M}{W} = \sigma = 11 \text{ MPa}$ ) larger than the acceptable (tensile and) compression stress for Azobé ( $\sigma_{pressure} = 20 \text{ MPa}$ )? Answer: no!
- Is the horizontal force on the pile too large for the passive resistance of the group around the pile? See Chapter 44.

If the force appears to be too large for the passive strength of the ground, one can opt for a fender with inferior spring stiffness.

---

## 46. Underwater concrete floor

### 46.1 General

Underwater concrete is usually not reinforced. In exceptional cases, reinforced underwater concrete could be considered, but this is problematic regards construction. However, if it is reinforced, it can be considered structural concrete, for which one needs to take larger tolerances concerning the shape, the dimensions and the quality of the concrete into account. Loads on reinforced underwater concrete are usually transmitted by bending and shear forces.

Non-reinforced concrete transmits its loads different from reinforced concrete, as non-reinforced concrete cannot take tensile forces. Hence, as a rule, more concrete is required in case of non-reinforced concrete. On the other hand, one does not need to place reinforcement cages under water.

The forces in a non-reinforced underwater concrete floor can be compared to those in masonry arches. Between the floor supports (piles and sheet piling), pressure arches are created, which transmit the loads to the supports.

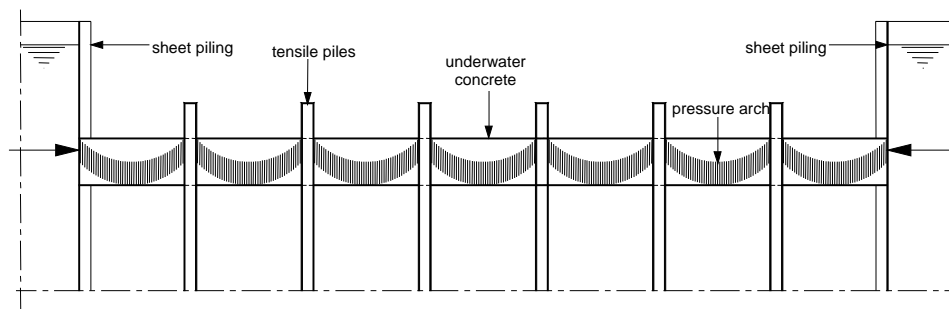


Figure 46-1 Pressure arches in underwater concrete

An arched structure owes its strength to so-called arch thrust. This arch thrust is a horizontal reaction force in the support (see Figure 46-1 and Figure 46-2). The arch thrust makes an equilibrium with the strutting force in the floor, which originates from the sheet piling.

The non-reinforced concrete floor can also be compared with a pre-stressed floor. In this case the strutting forces can be considered pre-stressing forces in the floor. Because the floor is subjected to a compression load, the non-reinforced concrete is able to absorb moments without the presence of tensile stresses.

The non-reinforced concrete floor can therefore be schematised as a number of arches between the supports and as a plate that is pre-stressed in two directions with supports in a number of points and lines.

At the supports, however, the reaction force has to be transmitted by a shear force between the concrete and the pile. If steel piles are used, the concrete is usually well attached to the pile, however, if the shape of the pile encourages the creation of gravel pockets or soil enclosures, one cannot simply depend on the attachment. Clean contact areas are of large importance for a good attachment. If prefab concrete piles are used, the top metres of the sides of those piles are often given ribs to improve the join.

### 46.2 Limit states

There are three ultimate limit states that apply for an underwater concrete floor:

1. Floatation of the floor
2. Fracture of the floor
3. Fracture of the join between the floor and the tension piles

### **Floatation of the floor**

In the case of this ultimate limit state; one must consider the equilibrium of the floor. The downward forces are:

- the weight of the floor
- the weight of the piles and anchors, plus the attached clump weight (weight of the soil under water that is pulled up by the piles) or the maximum friction along the pile shaft

The upwards forces are:

- the upwards groundwater pressure under the floor
- the effective soil pressure under the floor (loads caused by swell of lower clay and peat layers)

### **Fracture of the floor**

Fracture of the floor is possible when the ultimate bearing capacity of the arch is exceeded. The determination of the ultimate bearing capacity of the arch created in the underwater concrete floor is not simple because the geometry of the arch is not set beforehand. To determine the maximum bearing capacity one often assumes an arch with a height of 75% of the floor thickness and with a thickness of 10% of the floor thickness. Generally, this limit state is not normative for the thickness of the underwater concrete.

### **Fracture of the join between the floor and the tension piles**

A fracture of the join between the floor and the pile is possible if the maximum acceptable shear stress along the piles is exceeded.

To describe this limit state one cannot simply use the limit state "Punch" of TGB 1990 for columns punching through floors, because there is no firm attachment to the reinforcement steel. A safe approach is to only consider the transfer of forces from the floor to the pile in the contact areas between the pile and the underwater concrete.

In the case of a steel pile the force from the floor is transferred in the entire contact area, assuming a good attachment of the pile and the concrete. The slide plane in the concrete is assumed to be the smallest envelope around the pile.

In the case of prefabricated concrete piles, one usually assumes that the shear force in the floor is transferred to the pile along the ribbed sides of the pile.

The limit state involved assumes that the calculation value of the occurring shear force in the mentioned slide planes equals the maximum acceptable shear force in the underwater concrete.

## **46.3 2-D Arch effect**

The shape and height of the pressure arches depend on the type of load and the arch thrust that occur.

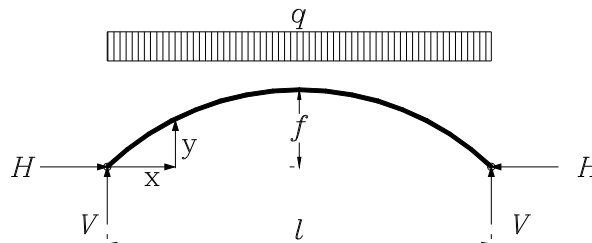


Figure 46-2 Schematisation of a pressure arch

Before we look more closely at the (3-D) arch that is created between the supports, the general distribution of forces in a two-dimensional arch is considered first.

The value of the arch thrust can be found by considering the balance of moments in the centre. The vertical reaction force and the uniform distributed load to the left of the centre cause an anticlockwise moment equal to  $1/8 q l^2$ . The arch thrust in the left support causes a clockwise moment equal to  $H \cdot f$ .

The balance of moments leads to:

$$H = \frac{q l^2}{8 f} \quad \text{or} \quad f = \frac{q l^2}{8 H}$$

The optimum shape of an arch with a uniform distributed load is derived from the balance of moments for every point on the arch:

$$H y = \frac{1}{2} q x (l - x)$$

The position of the median of a pure pressure arch, loaded by an equally spread load is:

$$y = \frac{qx(l-x)}{2H}$$

For a horizontal non-reinforced concrete beam, in which a uniform distributed load leads to a pressure arch, the height of the arch is determined by the point of application of the horizontal arch thrust and the centroid of the stress diagram in the middle of the beam. The shape of the stress diagram depends on the deformations in the cross-section of the beam and on the  $\delta$ - $\epsilon$  diagram of concrete. Figure 46-3 shows a number of possible stress diagrams.

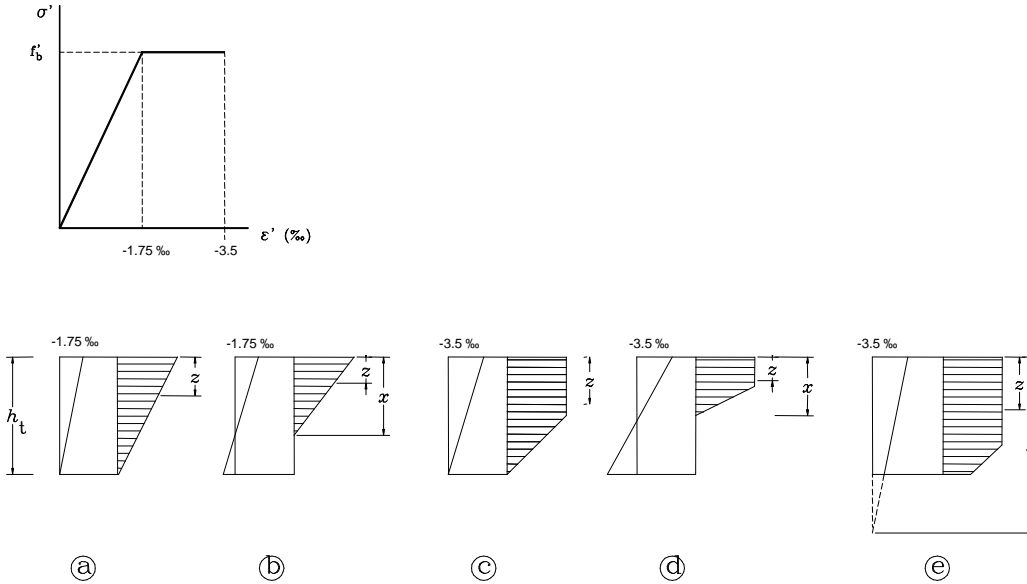


Figure 46-3 Centroid of the pressure arch in concrete, dependent on the deformation

The position of the line of action of the horizontal arch thrust depends, amongst others factors, on the way the pressure is applied to the side of the beam. In this case the position of the line of action depends on the angle of rotation of the plane on which the force acts. For an underwater concrete floor in an excavated building site, this angle of rotation occurs when the wall and floor deflect after the water has been removed from the site.

### 46.4 3-D Dome effect

The previous section only discussed the arch. In an underwater concrete floor with tension piles, pressure arches will occur between the piles in different directions. Between these pressure arches, the load is also transferred by means of arches. Between four piles the arches will form an inverted dome. Figure 46-4 schematically shows the main load bearing structure, drawn in thick lines.

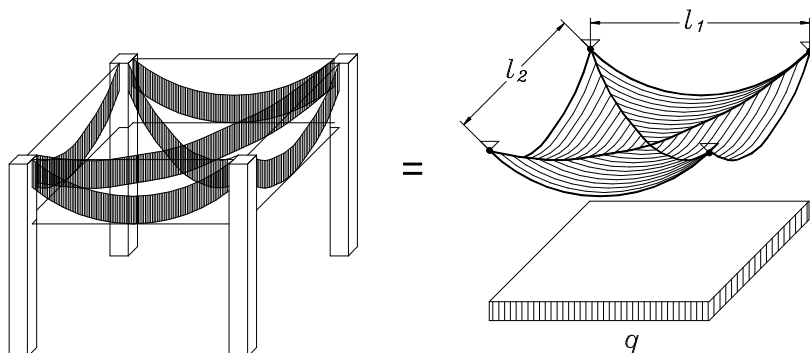


Figure 46-4 Dome effect between four piles

The horizontal arch thrusts on the dome can be calculated by considering the balance of moments around a horizontal axis through the centre of the dome.

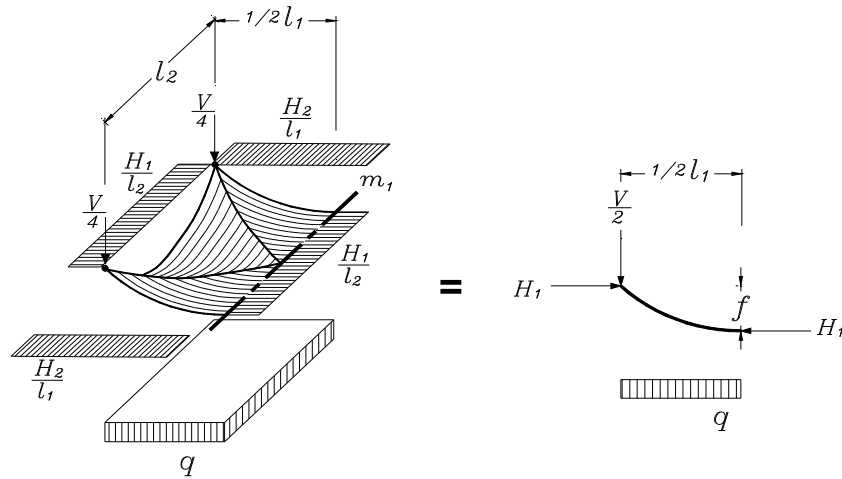


Figure 46-5 Balance of moments around an axis through the centre

The equilibrium leads to:  $H_1 = \frac{q l_2 l_1^2}{8f}$  and  $H_2 = \frac{q l_1 l_2^2}{8f}$

Consequently:  $\frac{H_1}{H_2} = \frac{l_1}{l_2}$

The vertical reaction force is:  $\frac{V}{4} = \frac{q l_1 l_2}{4}$

### 46.5 Transfer of forces to piles

The reaction force that the piles have to provide is transferred from the floor to the pile through the contact area between the floor and pile.

For a clean steel pile, the steel and concrete attach like reinforcement steel attaches to concrete. Next to the pile, the load is transferred to the underwater concrete floor by means of shear stress (see Figure 46-6).

For a smooth prefab concrete pile, the attachment between the underwater concrete and the pile is inferior. For this reason prefab piles usually have ribs along the top few metres, to ensure a certain amount of catch resistance.

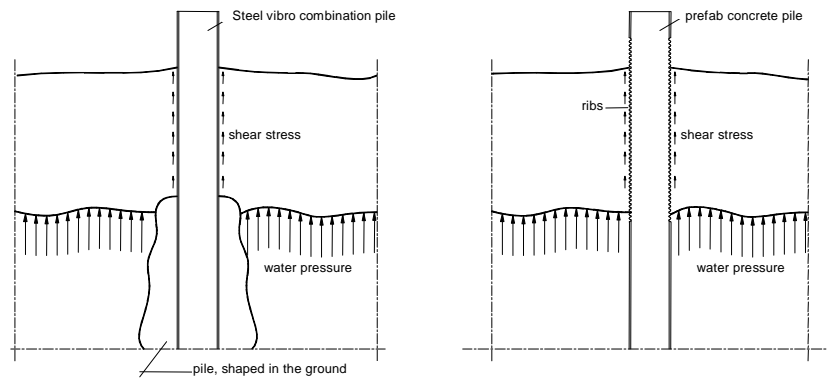


Figure 46-6 Shear stress along a pile shaft

The underwater concrete floor is loaded by the upward water pressure less its own weight. The floor transfers the load to the piles. A test calculation will have to decide whether the thickness determined practically is sufficient. An example of such a calculation follows.

---

**Example calculation of bending stress in concrete floor**
Given

Starting values:

thickness of floor: 1,50 m

concrete quality: B 22.5

piles: 0,40 m, c-c. 3,05 m (in both directions)

groundwater pressure underneath floor: 100 kN/m<sup>2</sup>

Calculated value for the load in the limit state of collapse:

$$q = 1.7 \cdot (100 - 1.5 \cdot 23) = 111.35 \text{ kN/m}^2$$

(N.B.  $\gamma = 1.2$  for dead weight and 1.5 for water pressure lead to a lower  $q$ ; see also VB 1974/1984, article A 401.2.2).

Along the circumference plane of the pile (this is the least favourable shear plane due to the join between old and new concrete) the shear force is:

$$T_d = 3.05^2 \cdot 111.35 = 1035.8 \text{ kN}$$

$$\tau_d = \frac{1035.8}{4 \cdot 0.4 \cdot 1.5} = 431.6 \text{ kN/m}^2 < \tau_1$$

$$\sigma_1 = 0.5 \cdot f_b = 675 \text{ kN/m}^2 \text{ (} f_b \text{ is the calculation value of the tensile strength of concrete)}$$

The concrete can therefore transfer the shear force. Note that in the case of underwater concrete this deviates from VB 1974/1984, in which part D states that non-reinforced concrete cannot take on shear forces unless a normal compression force is present. Instead, the shear force calculations given in part E (reinforced concrete) are used.

The bending moment in the underwater concrete is initially set at:

$$\frac{1}{10} \cdot q \cdot l^2 = 103.6 \text{ kNm/m}^1$$

$$\sigma_b = \frac{103.6}{\frac{1}{6} \cdot 1 \cdot 1.5^2} = 276.3 \text{ kPa}$$

276,3 < 0,7 ·  $f_b$  (= 910 kN/m<sup>2</sup>) and is therefore acceptable (VB 1974/1984, art. D 503.5).

In reality the moment is smaller because it is a mushroom slab spanning two directions. In the final check one must also review the moment and normal compression force, caused by the sheet piling supports on the floor.

In use the pile will be subjected to a tensile force of  $3.05^2 \cdot (100 - 1.5 \cdot 23) = 609 \text{ kN}$  and must therefore be sufficiently pre-stressed. The limit tensile force  $T$  of a pile equals the sum of the local shaft resistances. See Section 43 "Tension piles".

---

## 47. Dewatering

Major revision: February 2008

This chapter first covers dewatering in general. Subsequently, it shows how (theoretical) designs are made. Finally, it will give some examples.

For comprehensibility of the dewatering mechanism, one should distinguish between two types of aquifers (*waterhoudende grondlagen*):

- An "unconfined aquifer" is an underground layer of porous material with a free groundwater level (*niet-afgesloten grondlaag met freatisch water*).
- In a "confined aquifer" the groundwater is trapped between impermeable ground layers (*afgesloten grondlaag met spanningswater*). The water level usually rises above the top of the aquifer, in which case the well is called an artesian well (artesian water, *overspannen water*). Sometimes the water level is below the top of the aquifer (*onderspannen water*).

### 47.1 General

#### Dewatering methods

Theoretically two methods of dewatering are possible:

- open dewatering, where drainage trenches along the foot of a slope carry the water to wells. From there the water is removed from the construction site using dirty-water pumps (Figure 47-1). Dewatering in the open is only possible for small water level reductions in impermeable soil types (at most 4 to 5 metres in clay).

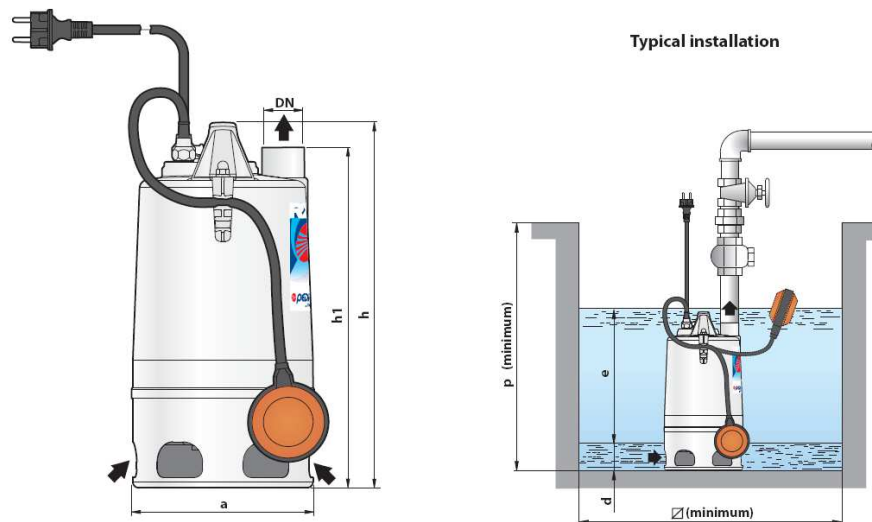


Figure 47-1 Dirty-water pump (from [www.pedrollo.co.uk/](http://www.pedrollo.co.uk/))

- wellpoint drainage (*bronbemaling*), for which the following systems can be distinguished (see Figure 47-2):
  - vacuum drainage with closed wells, where flexible pipes connect the riser (*stijgbuis*) of every well to a header (= suction pipe, *zuigbuis*). The underpressure in the header is created using centrifugal or plunger pumps.
  - vacuum drainage with open wells. The system is the same as the vacuum drainage mentioned above, though here each well has a draw pipe (*haalbuis*) suspended in it. The advantage over the system mentioned above is that the water level in the wells can be reduced maximally, provided the draw pipes are long enough.

Because the underpressure can never be more than atmospheric pressure (1 atm = 101 kPa  $\approx$  10 m column of water), the water level reduction that can be achieved by means of vacuum drainage is rarely more than 5 to 6 metres. Vacuum drainage in deep excavations must therefore be carried out in stages. The method is applicable to a range of soil types, from silty to fine sand sills. The yield per well is approximately 1,5 to 2,0 m<sup>3</sup>/hour.

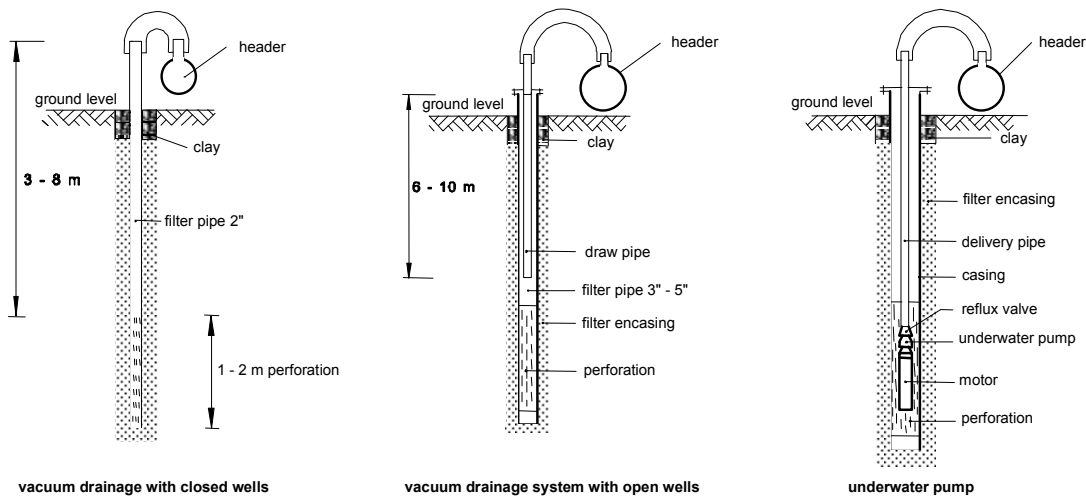


Figure 47-2 Types of wellpoint drainage

- a pumping system with underwater pumps, in which a pump is placed in every well (*perspomp*).

Underwater pumps are suspended in the groundwater and force up the water mainly through compression instead of suction. Thus the limit of the suction head (*zuighoogte*) is not relevant and large groundwater level reductions can be realised. This makes this type of pump attractive for the construction of hydraulic engineering works. The installation is more reliable than a vacuum drainage system, in which air leaks can lead to problems (air suction in one well can stop the water yield of all other wells connected to the same pump). One must ensure that the pump is suspended at sufficient depth to prevent it from falling dry. Underwater pumps are used in soil types ranging from fine sand to coarse gravel. The capacity of the pumps varies between 5 and 250 m<sup>3</sup>/hour. In hydraulic engineering pumps with capacities between 40 and 120 m<sup>3</sup>/hour are usually employed.

### **Dewatering problems**

A pump system (e.g. consisting of wells with underwater pumps) can start to function less efficiently or even fail entirely due to a number of reasons. Causes could include:

- electricity failure (power station, transformer station, cables etc.)
- mechanical or electrical defects of the pump(s)
- breakage, tearing and leakage of the pipes
- blocked pipes (for instance due to iron oxide deposits) and/or filters encasings (*filteromstoringen*) and blocked perforations in the casings (see Figure 47-3).
- air in the drainage pipes or suction of air via the pumps. The air can accumulate in high points of a non-level discharge pipe, increasing the resistance.



Figure 47-3 Blocked pipe used during construction of the Haringvliet discharge sluice in the building pit

Reduced efficiency or even failure can have the following consequences:

- in an unconfined aquifer:  
the excavation can be partly or entirely flooded, which will lead to a work delay and possibly to damaged equipment, certainly as regards electrical or electronic items.
- in a confined aquifer:  
as for an unconfined aquifer, but also bursting open of the bottom of the excavation, in case of an aquitard (*slechtdoorlatende laag*) or impermeable aquifer. This can cause disturbance of the foundation soil of the structure under construction. For an explanation of the bursting open of a clay layer, see CTB2410 (Waterbouwkunde), section 3.7.3 "Opbarsten".

Depending on the extent of the possible damage, measures must be taken such as placing emergency generators, which partially or fully take over the power supply in case of power failure, and double cables on the building site. The examples above are based on the assumption that the building site uses power from the national grid. However, if the building site is in an isolated location, it can be worthwhile to use generators for the daily power supply. In this case one could also consider backup generators.

Depending on the extent of the possible damage and on the duration of the drainage, the following matters will also be necessary:

- regular inspection
- preventive maintenance
- monitoring operations
- emergency procedures for calamities, etc.

Particularly the last two points depend largely on the situation. In small projects stagnation of the drainage needs not be very grave (though disruption of the foundation base is also serious in these projects). However, in large projects it can be beneficial to register certain parameters continuously and to sound alarms and trigger certain procedures automatically when certain limits are exceeded. Limits that could be exceeded are the groundwater level measured in a well (upper limit), and the minimum drainage discharge (lower limit). The alarm can be sounded in a permanently staffed area, in somebody's home, close to the site and with an occupant who is on guard duty outside normal working hours or by phone. Procedures that can be initiated automatically include starting emergency generators if the grid fails.

### **Trouble for the surroundings**

Often a building pit (with slopes and a dewatering system) leads to lower building costs than a coffer dam, even if one includes the possible damage to the surroundings. Disadvantages of the building pit construction method can be the consequences of dewatering on the surroundings and the large use of space (the slopes require a lot more space than is necessary for the completed structure, which can cause problems in built-up areas and if the new structure is to be built next to an existing structure). Very often dewatering causes no damage at all or only limited damage.

In agricultural areas, dewatering dehydrates soil, thereby ruining crops. Nature reserves and recreational areas can also suffer badly from a lowered groundwater level. Sometimes the surface layer will "retain" sufficient amounts of precipitation to counter the effect of the lowered groundwater level. Furthermore, precipitation wells for agriculture and horticulture can dry up.

Another important point is the possible settlement as a result of the temporary lowering of the groundwater level. This causes an increase of the effective soil pressure (see part II Loads, Soil, Groundwater). In soil types that are susceptible to this, it will lead to compression of the soil and settlement of the ground level, as well as to an increase of negative shaft resistance on piles. If houses or buildings settle evenly across the whole of their foundation, this does not have to result in damages. It can be worse if settlements are uneven for one building. The breaking of unfounded sewer pipes and cables at the point where they connect to a house or building on a pile foundation is not uncommon. Wooden piles can start to decay above groundwater level.

Even settlements of the ground level in agricultural areas are not a problem as long as the water level in the ditches can be adjusted accordingly. In old agricultural areas with considerable differences in ditch levels this adjustment is not always possible, because lowering of the ground level could lead to a decrease of the distance between groundwater and ground level, which can result in a permanent reduction of crop productivity (however, if the distance between ground water and ground level was too high, productivity could be increased). Uneven settlements can be a nuisance for sowing and harvesting. Drains can get an unfavourable slope.

In water extraction areas dewatering is usually forbidden, because, as a rule, drainage water is pumped out to open water and is therefore lost. Return pumping can offer a solution: the water pumped out of the site is returned to the ground through injection wells, at some distance from the building site. During the construction of the tunnel under the Dordtse Kil, for example, a large amount of drainage water was supplied directly to the water works. The water was taken from a soil layer that was normally not used for drinking water extraction, but with sufficient quality. The extraction from deeper layers could be reduced during the construction of the tunnel.

Sometimes the water acquired by means of drainage is of bad quality and may not be discharged into open water. Drained water in coastal areas and deep polders can be salty, which could cause open water to become brackish (this was a problem for the construction of the Schiphol tunnel near Amsterdam). In that case separate discharge is required to protect agriculture, horticulture or livestock industry. Moreover, people in the past few years have become aware that groundwater flow (however slow) can lead to unwanted diffusion of harmful substances from toxic waste dumps.

Once again: these problems can occur although they often don't. If damages occur they will have to be compensated by the construction company. Good observation (groundwater levels, height measurements, descriptions of buildings and crops) before, during and after dewatering is necessary to identify the damages. Photos can be used to describe houses and buildings. In fact, in the Netherlands this is prescribed: an independent committee makes an estimate of the expected damage. Constructors generally buy off the risk.

## 47.2 Design

Groundwater can be divided into two types: groundwater in an unconfined aquifer and groundwater in a confined aquifer. In an unconfined aquifer the flow profile equals the piezometric height. The groundwater level is therefore free. In a confined aquifer the flow profile is determined by an impermeable layer. A badly sealed layer that leaks, is called a semi-confined aquifer. The water level can be above or below the top of the aquifer (*overspannen of onderspannen water*).

### Unconfined aquifer

A drainage well will affect the phreatic surface in a certain volume of permeable soil around it. The phreatic surface drops gradually until a stationary situation is achieved. In an ideal situation, the affected soil body has a cylindrical shape with radius  $R$ , see Figure 47-1. The subsoil is impermeable, in contrary to the soil that surrounds the soil body.

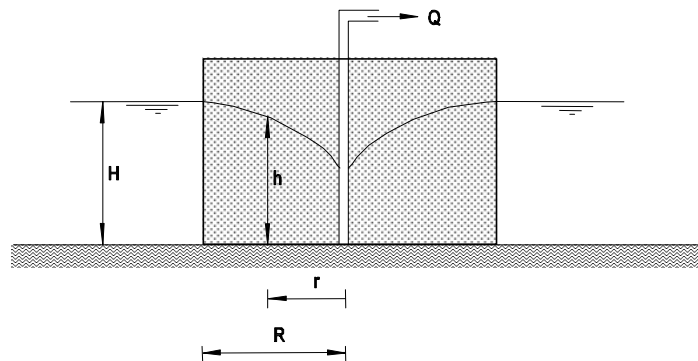


Figure 47-1 Dewatering of groundwater in an unconfined aquifer in a cylindrical soil body

The discharge of the well depends on the slope of the groundwater level and the permeability of the soil, which is expressed in Darcy's law:

$$q = k \cdot i$$

in which:

$$\begin{aligned}
 q \quad [\text{m}^3/\text{s}/\text{m}^2 = \text{m}/\text{s}] &= \text{specific discharge in the soil body} \\
 k \quad [\text{m}/\text{s}] &= \text{coefficient of permeability (see Table 47-2)} \\
 i \quad [-] &= \text{slope} = \frac{dh}{dr}
 \end{aligned}$$

For the total discharge  $Q$ , we can write  $Q = q \cdot F$  [ $\text{m}^3/\text{s}$ ], where  $F$  is the circumference area of the soil body:  $F = \pi \cdot d \cdot h = \pi \cdot 2r \cdot h$  [ $\text{m}^2$ ].

For the well this means:

$$Q = k \cdot i \cdot F = k \cdot \frac{dh}{dr} \cdot 2\pi r h$$

or

$$2h dh = \frac{Q}{\pi k} \frac{dr}{r}, \text{ so:}$$

$$2 \int h dh = \frac{Q}{\pi k} \int \frac{1}{r} dr,$$

where the solution is:  $h^2 = \frac{Q}{\pi k} \ln r + C$

If  $r = R$  (and  $h = H$ ) then:  $H^2 = \frac{Q}{\pi k} \ln R + C$

If we subtract the equations from one another:

$$H^2 - h^2 = \frac{Q}{\pi k} (\ln R - \ln r) = -\frac{Q}{\pi k} \cdot \ln\left(\frac{r}{R}\right)$$

In practice it is customary to determine the maximum allowable water level first, to avoid that water will enter the building pit. The phreatic water level should be at least 0.50 m below the pit floor. (This applies to all places on the construction site to avoid problems with saturated soil, freezing and the accumulation of rainwater; see Section 4.1 ('Construction Pit') of the general lecture notes of the course "Hydraulic Structures 1"). Knowing this, the value of the acceptable groundwater height  $h$  can be affixed. With  $h$ , the required total discharge can be calculated if we rewrite the previous equation:

$$Q = -\frac{\pi k (H^2 - h^2)}{\ln\left(\frac{r}{R}\right)}$$

### **Confined aquifer**

Similarly, we can derive the following relation for the groundwater in a confined artesian aquifer, in the permeable layer shown in Figure 47-2:

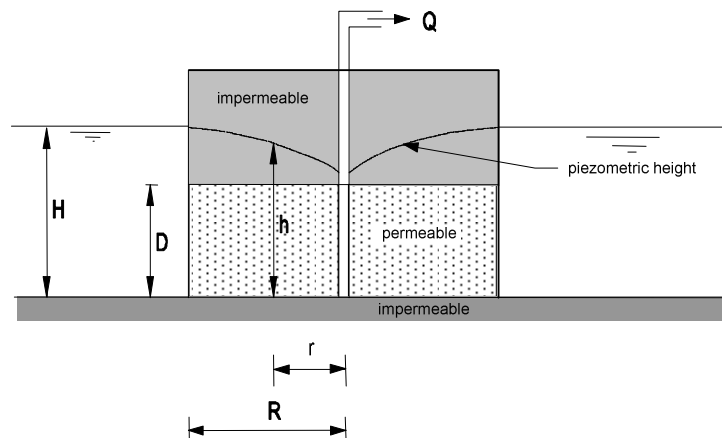


Figure 47-2 Dewatering of confined aquifer in a cylindrical soil body (artesian well)

$$Q = k \cdot 2\pi r \cdot D \cdot \frac{dh}{dr} \rightarrow dh = \frac{Q}{2\pi k r D} dr \rightarrow \int dh = \frac{Q}{2\pi k D} \int \frac{1}{r} dr \rightarrow h = \frac{Q}{2\pi k D} \ln r + C,$$

$$\text{and also: } H = \frac{Q}{2\pi k D} \ln R + C$$

$$\text{Subtraction yields: } H - h = -\frac{Q}{2\pi k D} \ln\left(\frac{r}{R}\right),$$

$$\text{from which the discharge can be derived: } Q = -\frac{2\pi k D (H - h)}{\ln\left(\frac{r}{R}\right)}$$

This equation can be used when the maximum allowed piezometric height  $h$  has been determined with respect to the bursting open criterion (an impermeable layer should not burst open because of too high water pressure from the layer underneath).

### **Semi-confined aquifer**

Usually the sealing layer is not entirely impermeable and the water is in a semi-confined aquifer. Figure 6-14 shows a common profile: two very permeable layers separated by an almost impermeable layer of clay with thickness  $d$ . We assume that any withdrawal of water from the bottom layer does not cause a reduction of the groundwater level in the top layer (for instance, this is realised by polder ditches in the top layer). This means that the bottom layer is fed by the top layer through the layer of clay.

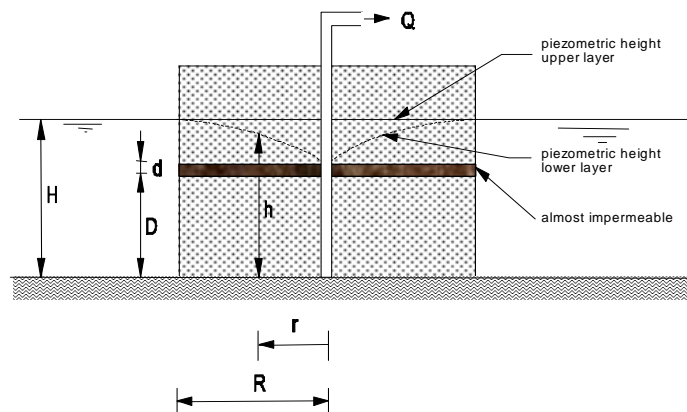


Figure 47-3 Dewatering of semi-confined aquifer in a cylindrical soil body

According to Darcy, this supply  $q$  equals

$$q = k' \cdot i = k' \cdot \frac{H - h}{d}$$

per unit of area, in which  $k'$  is the vertical coefficient of permeability of the layer of clay. In this situation the following relation can be derived (see also lecture notes *Soil Mechanics* by Verruijt / Van Baars):

$$H - h = -\frac{Q}{2\pi k D} K_0(r/\lambda)$$

in which:

$K_0(r/\lambda)$  = a modified Bessel-function of the first type, order zero.

(see following table, or see lecture notes *Soil Mechanics*; appendix A, or see Abramowitz & Stegun: 'Handbook of mathematical functions').

$\lambda$  = the leakage factor =  $\sqrt{k D C}$  [-]

$C$  = the resistance of the clay layer =  $\frac{d}{k'}$  [s] or [d]

$r/\lambda$	0,1	0,5	1,0	1,5	2,0	2,5	3,0	4,0
$K_0(r/\lambda)$	2,43	0,92	0,42	0,21	0,11	0,062	0,035	0,011

Table 47-1 Values for the Bessel function

### **Schematization effects**

The formulas above have all been derived for so-called perfect wells, i.e. their filters run along the full height of the layer from which water is extracted. This will not always be the case. In an unconfined aquifer the following applies: If the bottom of the well does not coincide with an impermeable layer the formula for unconfined aquifer is still used, as it has been shown that the water beneath the bottom of the well hardly participates in the flow (i.e. assume that the impermeable layer does not extend beyond the bottom of the well). If the impermeable layer is very deep, Sichardt advises us to increase the calculated discharge by 20%.

The formulas have been derived for a cylindrical volume of soil, not an everyday situation. In reality the excavated site that needs to be dewatered is usually on land.  $R$  is understood to be the distance from the well to a point where the groundwater level reduction approaches zero. For small dewatering systems,  $R$  is sometimes approximated with Sichardt's empirical formula:

$$R = 3000 (H - h) \sqrt{k} \quad (\text{units in metres and seconds}).$$

For a first rough estimation, the following table gives an overview of order of magnitude of the permeability  $k$ , it is certainly is not absolute:

Soil type	$k$ [m/s]
gravel	$10^{-2}$
coarse sand	$10^{-3}$
moderately coarse to moderately fine sand	$10^{-3}$ to $10^{-4}$
fine sand	$10^{-4}$ to $10^{-5}$
clay	$10^{-9}$ to $10^{-11}$

Table 47-2 Permeability

For large scale dewatering one uses experience or pump tests. The influence of a "wrong" estimate of  $R$  on the discharge calculation is limited by the use of the natural logarithm of  $r/R$ .

The formulas are derived for one well in the centre. In practice a number of wells will be placed around the building site. In this case the principle of superposition applies, i.e. the water level reduction in any one point is the sum of the reductions caused by each individual well. In an unconfined aquifer this is not the case, as this requires the superposition of the differences of the squares of  $H$  and  $h$ .

The formulas are derived for a stationary situation. Other formulas apply for the preceding non-stationary phases. However, dewatering systems are usually designed for the stationary situation, though it is important to start pumping well in time because it takes some time to reach the stationary situation (and the desired situation). Furthermore, the pump system needs to have sufficient overcapacity to deal with precipitation (a greater reduction of the groundwater level than technically necessary can create a buffer for extreme rainfall) and the possible failure of one of the pumps.

Certain parameters, such as the coefficient of permeability  $k$ , can be found by carrying out laboratory tests on undisturbed samples. However, they are usually not representative for the extensive area in which the groundwater flow occurs. It is therefore desirable, if not indispensable, to carry out a pump test; a dewatering well surrounded by a number of measuring wells. The pump test can determine parameters such as the coefficient of transmissibility  $kD$  (usually in  $\text{m}^2/\text{day}$ ) and the leakage factor  $\lambda$  ([m]).

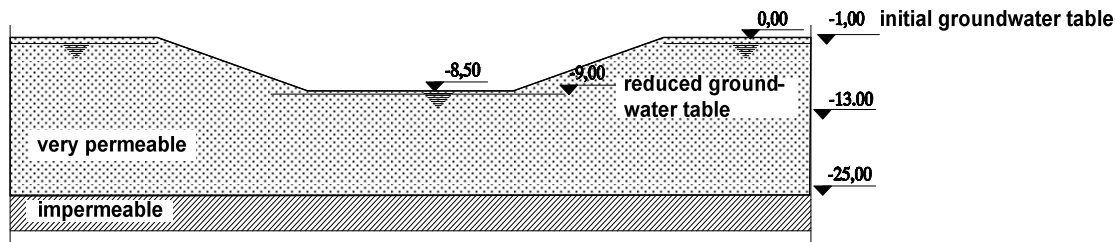
**Example unconfined aquifer**

Figure 47-4 Situation first mathematical example

Consider an excavated building site which measures  $50 \cdot 100 \text{ m}^2$  and which is located in a 25 m thick layer of very permeable soil found, in turn, on an impermeable layer. The groundwater table is 1 metre below ground level ( $H = 24 \text{ m}$ ). At the site we want to reduce the groundwater level by 8 metres ( $h = 16 \text{ m}$ ), so to 0,5 m below the bottom of the site. For the soil:  $k = 5 \cdot 10^{-4} \text{ m/s}$  applies.

We schematise the rectangular site (diagonal = 112 m) as a circle with a radius of 56 m and imagine replacing the drainage wells, which are really placed along the sides of the rectangular site, by one single large well in the middle of the circle (strictly speaking this is only justifiable if the real wells are divided evenly around the circumference of a circle).

We estimate  $R$  to be 1000 m and then find:  $24^2 - 16^2 = -\frac{Q}{\pi \cdot 5 \cdot 10^{-4}} \ln \frac{56}{1000}$

This results in:  $Q = 0,174 \text{ m}^3/\text{s}$  or  $628 \text{ m}^3/\text{h}$ . This means 16 underwater pumps, each of  $40 \text{ m}^3/\text{hour}$ . These drainage wells are projected around the site (they will be installed from ground level outside the excavated site) and are to be spread evenly round the circumference. Subsequently one has to check whether the groundwater level is at least 0,50 m below the bottom of the excavation everywhere on the site.

If that is not the case one has to see into a different distribution of the pumps (or possibly different pump capacities). This will also be necessary if the groundwater table has been reduced too much. Some spare capacity is welcome in case of the failure of one of the pumps, etc.

What influence does the choice of radius have?

If we use Sichardt's empirical formula, which is only used for small drainages and is certainly not valid here, we find a radius  $R = 537 \text{ m}$ , from which we derive a discharge  $Q = 800 \text{ m}^3/\text{h}$  (27.4% more than with a radius  $R = 1000 \text{ m}$ ). For a radius  $R = 2000 \text{ m}$  the discharge becomes  $Q = 506 \text{ m}^3/\text{h}$  (19,4% less). In other words, the discharge is relatively insensitive to the size of the radius, which was nearly halved and doubled in the above.

**Influence of supply borders**

Building sites as a rule are close to waterways (rivers, canals), which are to take on the hydraulic engineering work some time later. This waterway can act as a supply for the construction pit. The water level in the waterway ( $H$ ) will not be affected by the dewatering, so the piezometric height at this supply border remains the same. Mathematically this can be approximated by introducing a fictitious "mirror well" (i.e., a supply) on the same distance from the waterway as the construction pit, but on the opposite side of the waterway (see Figure 47-5).

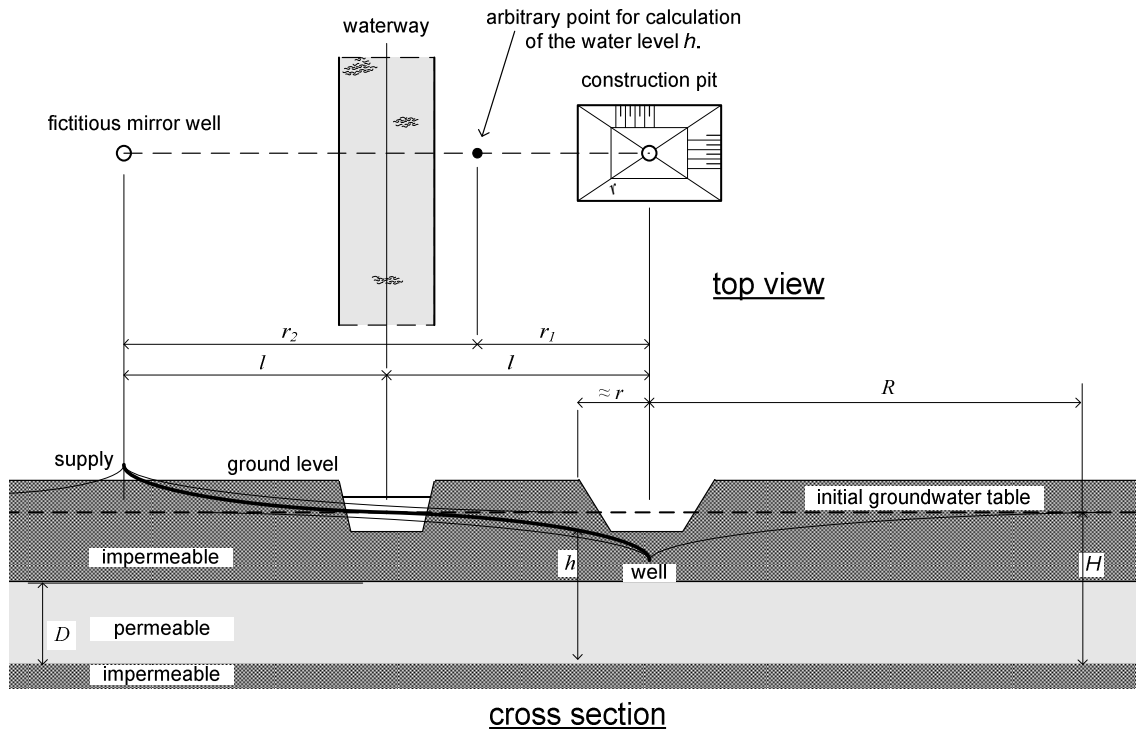


Figure 47-5 Schematisation of the mirror well principle

So, draw a line from the dewatering well perpendicular to the supply border and project an injection well on the opposite side of the border, which injects as much water as the first well discharges, on this line. By making the distances to the border ( $l$ ) the same, the piezometric height remains the same along the border line (middle of the waterway), provided it is straight, so  $(h_2 + h_1)/2 = H$ . The reduction of the water level caused by the drainage well is compensated by the injection of water in the other well. With both of these wells one can calculate the water level at any point on the side of the drainage well.

In case of a confined aquifer the following applies to a given point on the line between the well and the fictitious injection well:

$$h = H + \sum_{j=1}^n \frac{Q}{2\pi kD} \ln\left(\frac{r_j}{R}\right) = H + \frac{Q}{2\pi kD} \ln\left(\frac{r_1}{R}\right) - \frac{Q}{2\pi kD} \ln\left(\frac{r_2}{R}\right)$$

(derived from the formula for  $n$  wells).

Given that the distance from the drainage well -and hence also from the injection well- to the border is  $l$ , and expressing  $r_1$  and  $r_2$  in  $r$  ( $r_1 = r$  and  $r_2 = 2l - r$ ) this equation reads:

$$h = H + \frac{Q}{2\pi kD} \ln\left(\frac{r}{R}\right) - \frac{Q}{2\pi kD} \ln\left(\frac{2l-r}{R}\right) = H + \frac{Q}{2\pi kD} \ln\left(\frac{r}{2l-R}\right)$$

from which can be derived:

$$H - h = -\frac{Q}{2\pi kD} \left( \ln\frac{r}{R} - \ln\frac{2l-r}{R} \right)$$

For an unconfined aquifer the formula is:

$$H^2 - h^2 = -\frac{Q}{\pi k} \left( \ln\frac{r}{R} - \ln\frac{2l-r}{R} \right)$$

Note that the supply border normally is not perfect. In wide, deep rivers (e.g. the Nieuwe Maas at Pernis near Rotterdam, measuring approximately 600 m by 13 m) the influence of the dewatering system on one side was still detectable on the other side. A layer of silt on the riverbed creates a large entry resistance,

which means the river does not qualify as a perfect supplying border: no reduction of the piezometric height at the border as a result of dewatering. In that case the border should really be moved, from the waterway to further inland, on the fictitious injection side. If the river has just been dredged, the layer of silt will have been removed and the river can act as a perfect supplying border.

### Example confined aquifer with supplying border

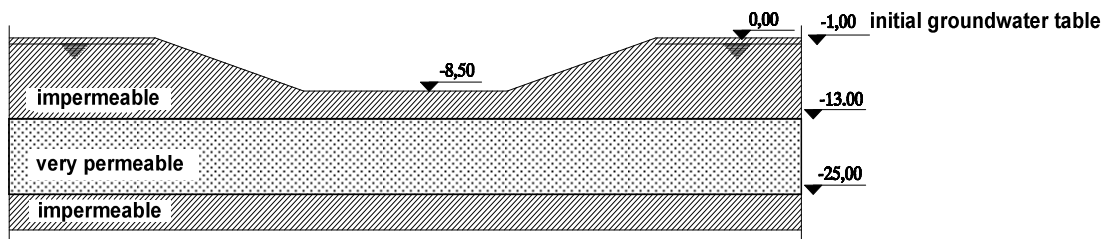


Figure 47-6 Situation second mathematical example

Assume the composition of the soil is different. The top 13 metres are impermeable, whilst the soil below remains unchanged and the piezometric height is - 1.00 m.

The underside of this impermeable layer is subject to an upward water pressure of 120 kN/m<sup>2</sup>. After the excavation a layer of only 4.5 m remains above the -13 m mark. For a volumetric weight is 16 kN/m<sup>3</sup> this leaves a downward pressure of 72 kN/m<sup>2</sup>, too little to find an equilibrium, which will lead to the bottom bursting open. If we want to include a safety factor of 1.2, the upward pressure may not exceed 72/1.2 = 60 kN/m<sup>2</sup>. In other words: the piezometric height must be reduced by 6 m. The thickness of the water-containing layer is  $D = 25 - 13 = 12$  m. Because this layer is a perfectly confined aquifer, we use the following formula:

$$6 = -\frac{Q}{2\pi \cdot 5 \cdot 10^{-4} \cdot 12} \ln \frac{56}{1000}$$

This gives:  $Q = 0,078$  m<sup>3</sup>/s or 283 m<sup>3</sup>/h.

If eight underwater pumps of 40 m<sup>3</sup>/hour each are projected around the site, again, one must check whether the piezometric height is reduced by at least 6 metres everywhere below the excavated area.

What would change if there was a "supplying border", 300 metres from the centre of the site? (this should be a deep river because it should make direct contact with permeable aquifer, which starts at -13 m)

The following approximation:

$$6 = -\frac{Q}{2\pi \cdot 5 \cdot 10^{-4} \cdot 12} \left( \ln \frac{56}{1000} - \ln \frac{2 \cdot 300 - 56}{1000} \right) \text{ results in: } Q = 0,099 \text{ m}^3/\text{s or } 358 \text{ m}^3/\text{h.}$$

If one does not add at least 2 underwater pumps, there is a risk that the site bottom will burst open. (One underwater pump is not enough, because it leaves insufficient spare capacity for precipitation, etc.)

## 48. Gates

There are many different types of closure mechanisms, namely:

- flat gate
- vertical lift gate
- drop gate
- sliding gate
- mitre gate
- single gate
- shutter weir
- visor dam
- radial gate
- sector gate
- inflatable dam

This chapter, however, only covers the action of forces in the following types:

- flat gate
- mitre gate
- radial gate
- sector gate
- arc

### 48.1 Flat gate

A flat gate (*vlakke schuif of deur*) transfers the load onto its rabbeted stops. These rabbeted stops can be positioned both on the sides and on the top and bottom. If rabbeted stops are only positioned on the sides, the total load must be transferred horizontally. This horizontal transfer of load can be accomplished using various systems. The flat sluice can, for instance, be equipped with vertical girders that transfer the load a number of horizontal rails, which, in turn, transfer the load to the supports. It is also possible to mainly use rails that transfer the load to the supports in one go. The use of rails and/or vertical girders depends highly on the shape of the gate or sluice and the position of the rabbeted stops.

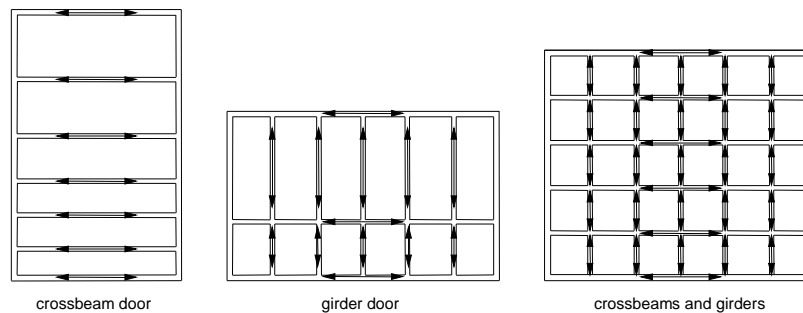


Figure 48-1 Principle support system with rails and girders

The rails and girders can be constructed as a solid web girder, a Vierendeel girder, a box girder or a truss (see also Figure 48-2). For small span girders (= c-c distance of horizontal rails), one can also use a so-called trough girder.

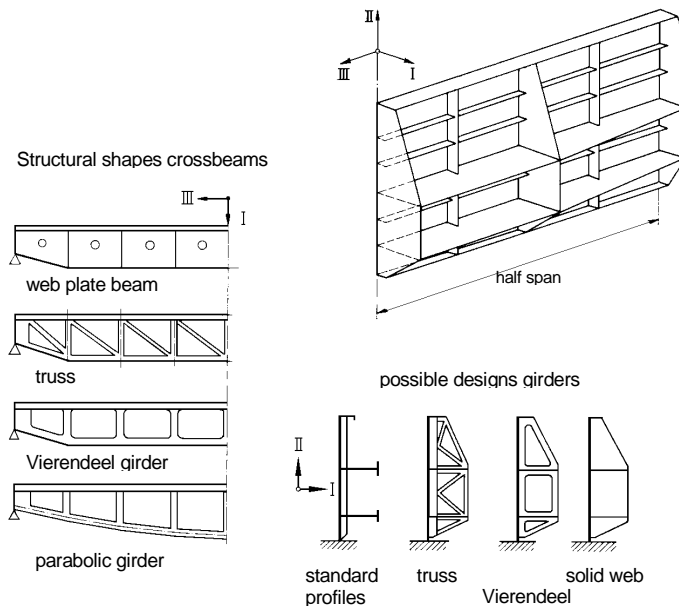


Figure 48-2 Some possible structural shapes of a gate or sluice on double supports

The vertical girders outside of a gate that rest on the rabbeted stops are known as “posts”.

If the gate also transfers load to a sill and/or an upper rabbeted stop, the use of rails and girders is obvious. The transfer of loads and the forces and moments in the girders and rails of such a gate can be calculated by schematising the structure as a beam grid. In such a calculation the torsional rigidity of the profile must be estimated correctly, because this can have an important effect on the spread of the load. Particularly when applying box girder profiles or plates on two sides, this is of large importance.

An alternative to a gate with rails and girders is a gate with plates on both sides, where the rails and girders are plates that keep the main plates together and create a rigid profile. This structure is used in particular for sliding gates. The forces and moments in such a gate can be calculated using the three dimensional finite elements method, where the gate is modelled with plates and discs.

A gate with plates on two sides has reasonable to large torsional rigidity. The result of this is that, in the case of hinged supports on the sides and top and/or bottom of the gate, the gate will want to curl inwards and will therefore start to leak. For this reason such a method of load transfer is avoided or is combined with measures in the bottom rabbeted stops to counter the curling. Such a measure could be to insert a jack in the gate, which fixes the corner of the gate. However, the edges of the structure have to be very stiff to ensure that it is fully waterproof.

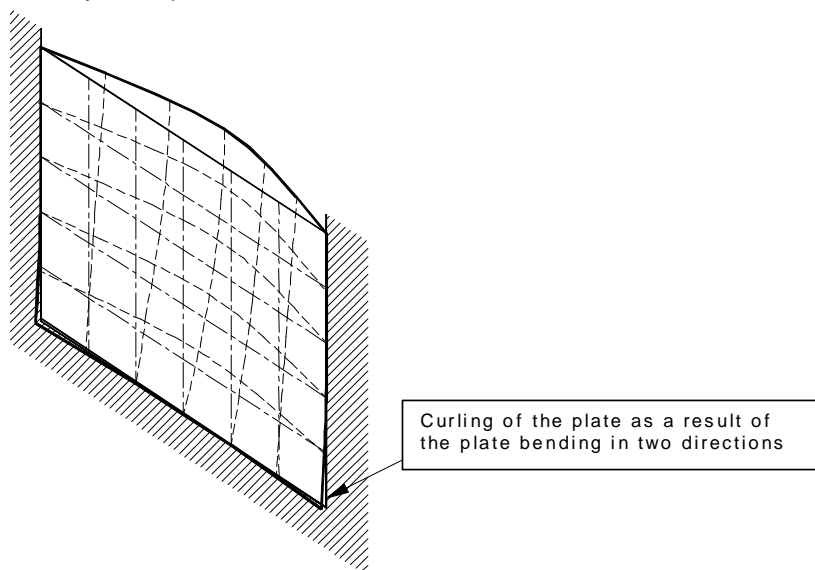


Figure 48-3 Curling of a gate or sluice supported on three sides

The supports of the sluice can be single points or linear. For single point supports it seems obvious that the supports should be positioned at the ends of the rails and girders. For linear supports, the posts need

to be sufficiently stiff to be able to spread the load from the girders over the entire rabbeted stop. The same applies for a structure, supported on three or four sides, for the top and bottom rails.

## 48.2 Mitre gate

In mitre gates the load is transferred to the side rabbeted stops of the gate. The bottom rail is generally not considered as a support, because torsional moments will occur in the gate. Both outer vertical girders of the mitre gate are called posts ("har"s, after the old Dutch word for hinge). The girder nearest the rotational axis is called the rear post, whilst the girder at the loose end of the gate is called the front post. If the gate is closed, the support of both vertical girders can be uniformly distributed or concentrated in two or more points.

For an even spread transfer of the load at the rear post, it is necessary that there is some give in both points of rotation. The lower hinge usually has a little give, because the pivot would otherwise have to be set infinitely accurately, relative to the vertical rabbeted stop strip. The upper hinge needs more give, because, during closure, the gate can be pushed against the rabbeted stop in the sluice wall by the water pressure. If there is no give available in the upper hinge, the reaction forces will have to be supplied by both hinges. In this case, too, a small amount of give is allowed in the bottom hinge in order to be able to lower the pivot socket over the pivot when the gate is put in place.

First, the gate is considered in its closed position, subjected to a load caused by the water pressure, due to the head over the gate. This situation is shown in Figure 48-4. By regarding the mitre gate as a triple hinge truss, symmetry considerations dictate that the forces in the contact point between the front posts have to be in equilibrium i.e. equally large but aimed in opposite directions, perpendicular to the sluice axis.

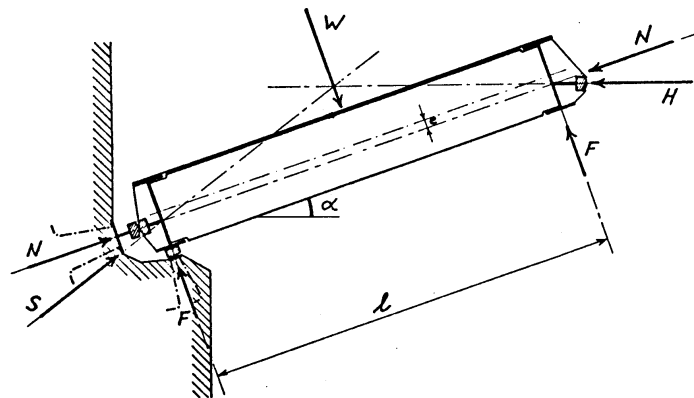


Figure 48-4 Forces and reactions on a closed gate

The reaction force  $S$  can be resolved in a force parallel to the gate ( $N$ ) and a force perpendicular to the gate ( $F$ ). These reaction forces can be denoted as a function of the resulting force from the water  $W$  and the angle  $\alpha$  between the gate doors and the sluice axis (see Figure 48-4).

$$S = H = \frac{W}{2 \cdot \sin \alpha}$$

$$F = \frac{1}{2} W$$

$$N = \frac{W}{2 \cdot \tan \alpha}$$

were:  $S$  [kN] = reaction force of the sluice head  
 $H$  [kN] = force from the other door (perpendicular to the length axis of the sluice or lock)  
 $W$  [kN] = resulting hydrostatic force on the door  
 $\alpha$  [°] = angle between the gate door and the length axis of the sluice or lock

From the formulas one can deduct that if the angle  $\alpha$  is small, the reaction force is very large. This advocates a large angle  $\alpha$ . However, if angle  $\alpha$  is large, the gate doors become longer and hence the load ( $W$ ) becomes larger. Furthermore, longer gate doors would mean heavier gate doors as well as longer gate chambers and lock heads. For economic reasons, one often usually chooses a ratio of  $\tan \alpha = 1:3$ .

The way the reaction forces  $S$  and  $H$  are provided depends strongly on the choice of supports along the vertical sides. One could opt for a uniformly distributed load transmission or a load transmission with support points.

**Uniformly distributed load transfer**

As mentioned earlier, a uniformly distributed load transfer, requires a certain amount of give in both hinges. The transfer of load at the lock head then takes place according to the linear loads  $N$  and  $F$ . Due to structural considerations, one also opts for a uniformly distributed load transfer at the front post, there in the direction of  $H$ . In this case, an adjustable gate is selected, in order to approximate a uniformly distributed load as well as possible.

**Load transfer via point supports**

To transfer the loads via point supports there may not be any give in the top hinge. At the rear post, the hinges provide the reaction forces, which point in the direction of  $S$ . Two supports are also made in the front post. It seems obvious to make two heavy horizontal rails between the four supports and to transfer the load on the plates to these rails via girders (girder gate). For the height of these rails, an optimum between the moments in the girders and in the rear post is sought (see Figure 48-5).

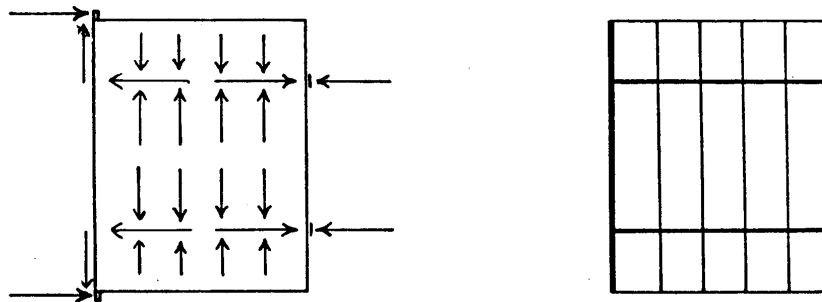
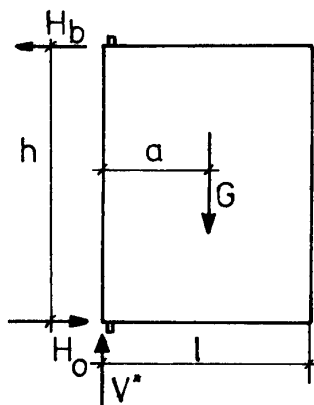


Figure 48-5 Internal transfer of forces in the girder gate

Nowadays, the latter solution is employed often. Setting vertical rabbeted stop plains (for  $N$  and  $F$ ) at the rear post, which has to carry the load as evenly as possible, is very difficult. However, according to the solution given in Figure 48-5 only two points have to be positioned accurately. Moreover, techniques have been developed to equip the top hinge with ball bearings that tolerate barely any give and that can absorb large forces.

Another load situation occurs when the door is open, in which case the hinges only need to be able to take on the self-weight of the gate. The vertical load, the self-weight of the gate, is nearly always taken on by the lower hinge. The moment that is thus created results in a tensile force in the upper hinge and a compression load in the lower hinge (see Figure 48-6).



$$\begin{aligned} \sum V &= 0 \rightarrow V^* = G \\ \sum H &= 0 \rightarrow H_b = H_o \\ \sum M &= 0 \rightarrow H_b \cdot h = G \cdot a \\ &\text{of } H_b = H_o = G \cdot a/h \\ a &= \frac{1}{2} l \end{aligned}$$

Figure 48-6 Balance of forces for an open gate

As the length of the gate increases, the gate is more and more inclined to start to sag (*zakken*) at the loose end, due to its self-weight, so-called tilting. This problem especially affects wooden adjustable gates. This is because they are not very rigid. Tilting can be avoided by creating rigid triangles. Starting from the hinges one can create a triangle by placing a compression bar.

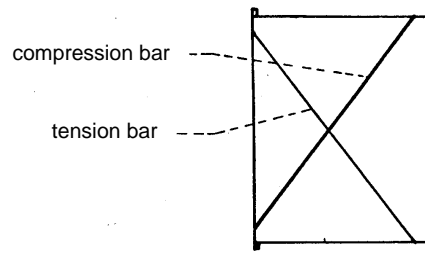


Figure 48-7 Diagonal compression and tension bar

Further structural measures include placing a tension bar and applying planks in the direction of the compression bar.

Steel mitre gates can be made sufficiently structurally stiff, hence the tilting problem is no longer relevant.

### 48.3 Water pressure on radial gates

See also Chapter 9 of part II of this manual for hydrostatic loads.

One distinguishes between radial lock gates with horizontal and vertical axes.

#### Radial gate with a horizontal axis

Figure 48-8 gives an example of a radial lock gate with a horizontal axis. The moving parts are not included. Basically, the radial lock gate consists of a gate, which can be built up out of beams and girders with plates on the high water side, and an arm that transfers the forces on the gate to the hinge. It is important that the curves of the gate correspond to a circle and the hinge is placed in the middle of this circle.

The transfer of the loads on the gate is completely dependent on the type of load. Hence, such the (partially immersed) self-weight of the structure is carried by both the sill and the hinges, but the load caused by the water pressure is taken on entirely by the hinges.

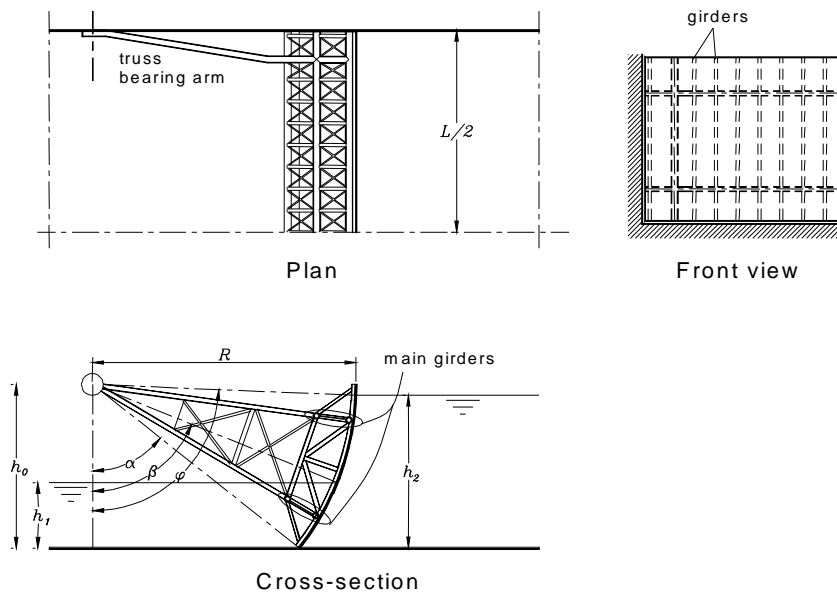


Figure 48-8 Radial gate with a horizontal axis

A special transfer of load to the hinge occurs if the gate is equipped with watertight plates on two sides, or if the rear side of the gate is not circular. Figure 48-9 gives an example of such a gate. The horizontal component of the load remains the same but the vertical component is anomalous and is wholly determined by the lift force of the hatched areas shown in Figure 48-9. In this case, the resultant of the water pressure does not pass through the hinge. However, the resultant can be resolved into a force through the hinge (water pressure, high water side) and a force in another direction (water pressure, low water side). In the calculations it is sometimes also useful to combine the water pressure on the side of the low water level with a part of the self-weight, so this combined load also passes through the gate's hinge.

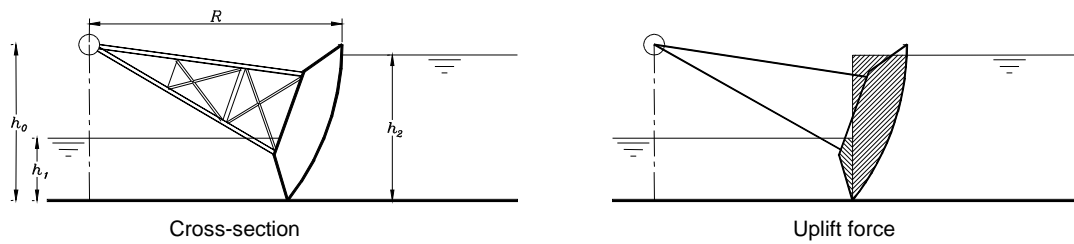


Figure 48-9 Radial gate with water proof plating on both sides

To calculate the load on the gate with the line of action through the hinge, the structure can be schematised as a two-dimensional framework.

Depending on the shape of the arms and the way the arms are attached to the gate, a force parallel to the hinge axis is applied to the hinge, as well as a force perpendicular to its axis. Figure 48-10 shows this for a structure in which the gate is hinged to the truss arms. The line of action of the resultant load on the axis of the hinge passes through two structural hinges. In the case of a small angle between the arms and the perpendicular of the axis and a load perpendicular to the gate, this results in a small force parallel to the axis. The downside of the given structure is that it is not stable for a load parallel to the gate. Such a load can occur if the gate is open and there is a side wind. That is why such a system requires guidance equipment for the gate that offers sufficient lateral support to guarantee stability.

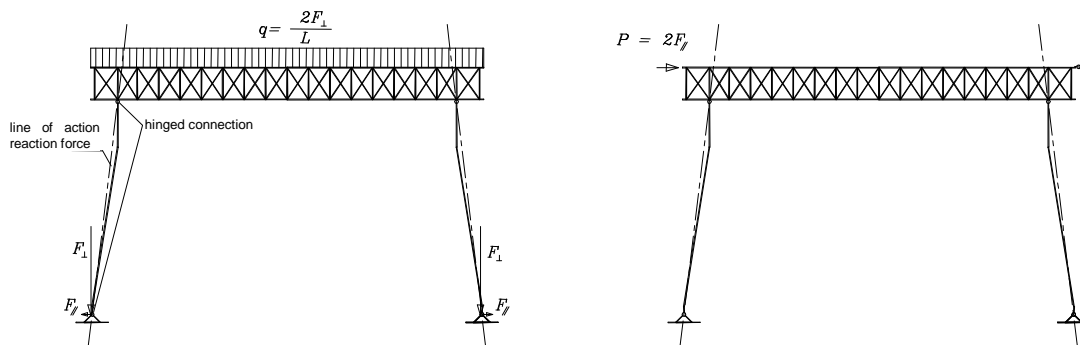


Figure 48-10 Force parallel to the axis of the hinge in the case of hinged arms

If the truss arms are fixed to the gate (not hinged), one creates a stable system in the shape of a portal frame (see Figure 48-11). In this case, for a load  $q$  perpendicular to the axis, the force  $F_{||}$  parallel to the axis of the hinge will be larger than with hinged arms. This parallel force is caused by the deflection of the radial gate. This generates an outwards rotation of the arms, which is prevented in the hinges.

The relationship between the forces perpendicular and parallel to the axis of the hinge depends on the stiffness of the truss arm and the gate. The stiffer the arms, the larger the load parallel to the axis. The theoretical maximum parallel load caused by a load perpendicular to the wall is:

$$F_{||} = \frac{L}{4R} F_{\perp}$$

However, this can only occur with infinitely stiff truss arms.

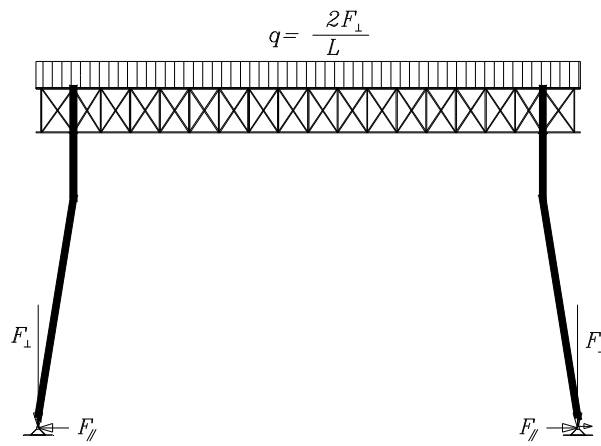


Figure 48-11 Force parallel to the axis of the hinge in the case of fixed arms

**Radial gate with a vertical axis**

In the case of a radial gate with a vertical axis, the gate is curved in the horizontal plane to an arc with a centre that coincides with the position of the hinge. Thus the resultant of the water pressure load goes precisely through the hinge in the horizontal plane. The direction of the resultant depends on the lengthwise profile of the gate. This is apparent in Figure 48-12, which shows two different profiles.

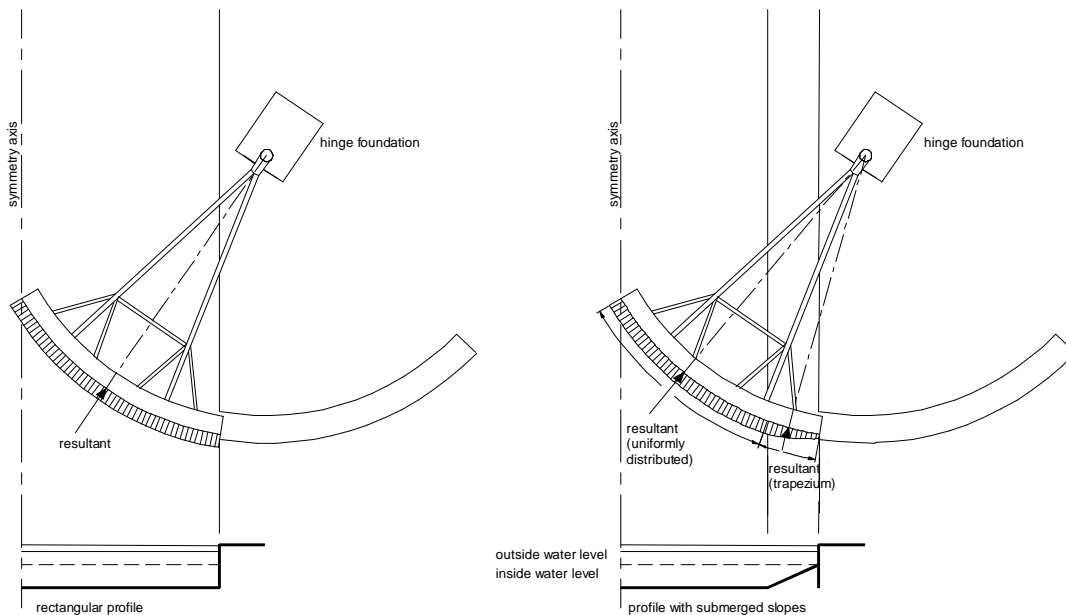


Figure 48-12 Direction of the resultant water pressure on a radial gate with a vertical axis

In the vertical plane, the direction and the position of the resultant of the water pressure depends on the shape of the gate in the vertical cross-section. Figure 48-13 shows a number of possible cross-sections and the forces on the gate per metre. The position of the seal with the bottom is an important detail which determines the size of the upward force.

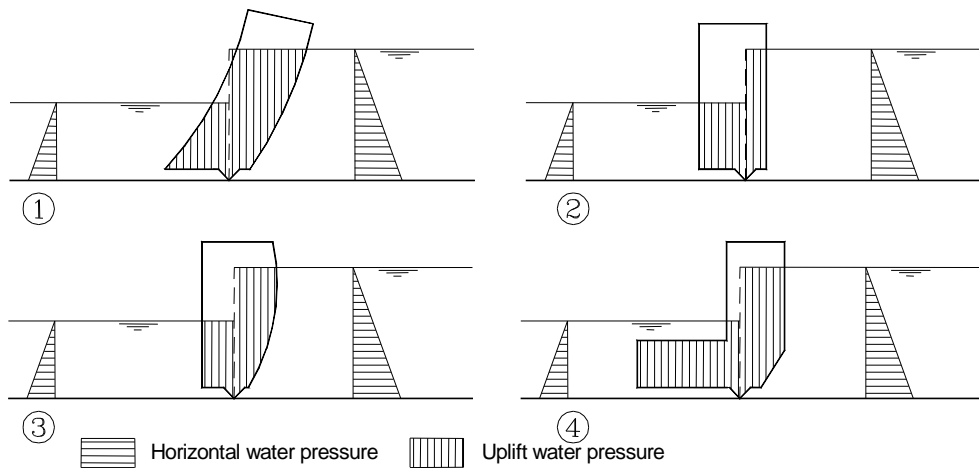


Figure 48-13 Loads dependent on the shape of the gate

A force with a line of action that does not go through the hinge can be replaced with a force through the hinge plus a moment. An example of this is given in Figure 48-14. The moment is taken on by the system as for a beam on two supports.

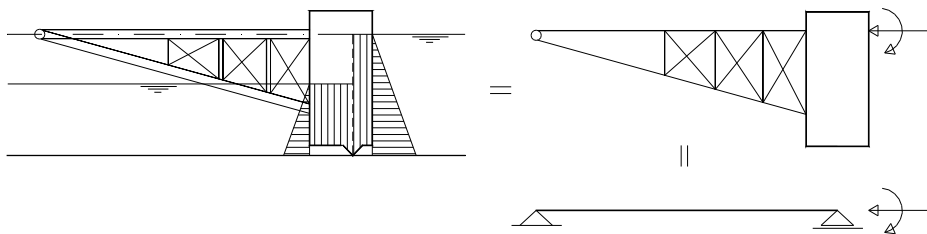


Figure 48-14 Schematisation of the load from the gate on the arms

### 48.4 Water pressure on sector gates

The sector gate transfers its loads directly to the sill. The line of action of the resultant of the water pressure on the plates on the side of the high water level goes through the hinge. The water pressure on the plates on the side of the low water level causes a moment relative to the hinge. This moment is in equilibrium with the moment on the hinge as a result of the self-weight of the gate and the possible reaction force created by a rabbeted stop.

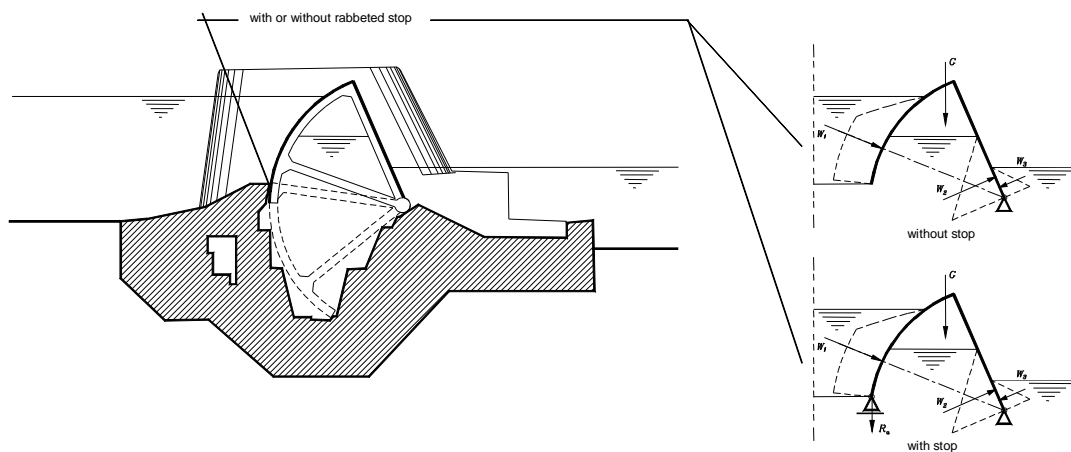


Figure 48-15 Action of forces in a sector gate

If, on the low water side, the gate is not only subject to hydrostatic loads, but also to dynamic loads such as waves, one will always opt to include a rabbeted stop for the gate. The water level in the gate is then kept high enough to ensure that there is always a force present in the rabbeted stop.

Waves on the high water side do not influence the position of the gate, because the resultant water pressure goes through the hinge.

### 48.5 Water pressure on arcs

Arcs that are subjected to a load on all sides (fluid or gas pressure) do not develop any shear stresses or moments, only normal forces. One can make use of this property to optimise the use of materials. Concrete, for instance, will be used in a compression arc (dam) and steel will be used in a tension arc (visor dam).

The transfer of load in an arc is relatively simple because the direction of the forces in the supports is known; these naturally follow the tangent of the circle. This is shown in Figure 48-16.

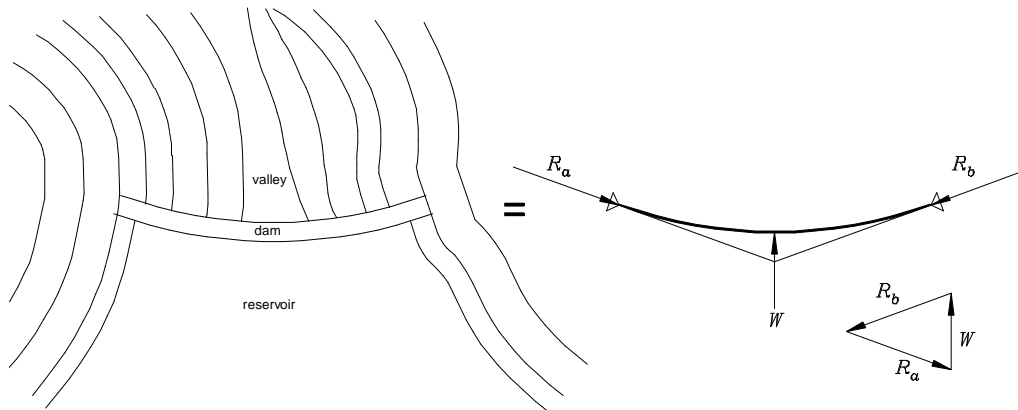


Figure 48-16 Load transfer in a circular arc

## 49. The height of flood defences

New chapter: February 2016

### 49.1 Design philosophy of flood defences

The required height of a flood defence (or the crest height (*kruinhoogte*) of dikes) is determined in such a way that the structure reduces the amount of water entering the hinterland to acceptable quantities. This implies that the flood defence is high enough, but also sufficiently strong and stable. The performance of a flood defence is usually expressed by its reliability, which is the probability that the flood defence fulfils its function<sup>3</sup>. The required reliability of a flood defence should be such that it complies with an acceptable risk of flooding of the hinterland<sup>4</sup>.

The settling of the acceptable flood risk level (safety level) is based on answering the question 'how safe is safe enough', because 100% safety cannot be achieved. Three criteria can be distinguished in settling this safety level:

- Economic risk: the investments in flood protection should balance the therewith obtained risk reduction;
- Individual risk: the probability that a human being, residing at one location during one year, will die because of a flood;
- Societal or group risk: the probability that a number of people, residing at one location during one year, will die because of a flood.

The most severe of these criteria should determine the safety level (if affordable). In the Netherlands, the target safety level is stipulated in the Water Act of 2009 (*Waterwet*).

Once the allowable risk level has been determined, the corresponding maximum allowable probability of flooding of the hinterland can be found. This flood probability can then be related to the maximum failure probability of the flood defence, which in its turn is related to a normative extreme water level with a certain exceedance probability (see Section 13.3). In the traditional design approach, Dutch flood defences are primarily designed to resist this normative water level. Therefore, the height of a dike is the basic design parameter. Other properties, like the geometry (shape) and materials, are then designed to provide the flood defence with sufficient stability<sup>5</sup>. This chapter explains how to determine the height of flood defences. Other design principles are treated in the lecture notes of course CIE5314 'Flood defences'.

### 49.2 Determination of the retaining height of a flood defence

In general, the required height of a flood defence is mainly determined by the following two components:

- Normative high water level NHW (*maatgevende hoogwaterstand MHW*)
- Maximum allowable discharge of wave overtopping or overflow

The normative high water level is officially determined for a limited number of locations, so local circumstances can deviate from this. Circumstances can also change over time, so temporal effects should also be taken into account, depending on the reference period for which the flood defence is evaluated. Figure 49-1 depicts the components that determine the height of a flood defence. These components are explained in the following paragraphs. It should be determined per location what components are relevant.

<sup>3</sup> Reliability is complementary to failure probability.

<sup>4</sup> Flood risk is defined as the probability of flooding multiplied by the consequences of a flood.

<sup>5</sup> In 2017, the policy will change to a failure probability approach, where the probabilities of failure per mechanism and per flood defence section are combined into an over-all failure probability per dike trajectory. This implies that the probability of failure due to, for example, piping, erosion or macro-instability will have to be determined as well. This chapter explains the traditional overload per dike section approach, as described in several guidelines and technical reports of the Dutch Technical Advisory Committee for Flood Defences (TAW). The method of calculating over-all failure probabilities is taught in MSc-courses of the Hydraulic Engineering track, which will be better understandable when the old approach is known.

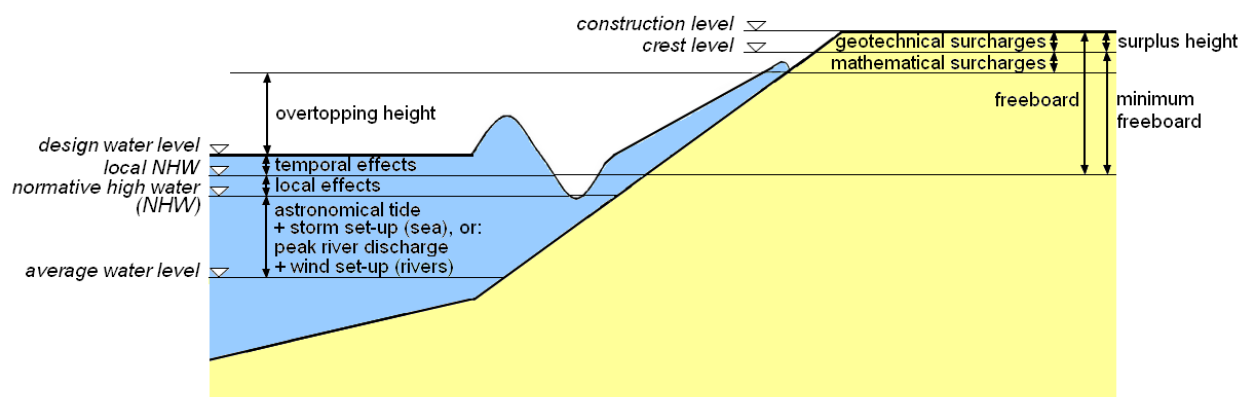


Figure 49-1 Determination of the construction level of a dike

### **Normative high water level**

The normative high water level (NHW) along the coast is determined at locations where measurements have been carried out for many years, which have been extrapolated to rare circumstances. The normative high water level is found by relating the water levels to acceptable exceedance probabilities (see also Section 13.3). Along rivers, the normative high water level is determined at locations where the river discharge has been calculated. The thus determined critical water level along coasts and rivers is the **assessment level (toetspeil)**, as listed in the book *Hydraulische Randvoorwaarden* (Hydraulic Boundary Conditions) of *Rijkswaterstaat*. This book is used to evaluate the reliability of existing flood defences.

#### NHW along the coast

The measurements along the coast include:

- astronomical tides,
- wind set-up, including a possible funnel effect (*trechtereffect*).

Water level changes along the coast by astronomical tides are explained in Section 13.1 of this Manual. Wind fields can head up the water in shallow seas, deltas, closed-off creeks and lakes because of friction between wind and the water surface (Section 13.2). Wind set-up is usually included in the estimate of the normative high water level by using the peak-over-threshold method. If the wind blows in a direction where the water surface becomes narrower, the water level will be pushed up even more. This additional set-up is called the 'funnel effect'.

#### NHW along rivers

The governing water level along river dikes can be based on the design river discharge for the location where it enters the Netherlands (like Lobith for the Rhine) and then making a discharge computation for locations further downstream. The levels in the lower rivers (*benedenrivieren*) are influenced by both river discharge and tidal influences from sea. Control objects like weirs and discharge sluices can influence the water level in lower and upper rivers (*bovenrivieren*), so these effects have to be taken into account as well.

### **Local normative high water level**

Circumstances can deviate locally from the NHW-values mentioned in the *Hydraulische Randvoorwaarden*. Local effects should therefore be added to the formal normative high water level:

- **Local wind set-up.** The normative high water level includes the effect of wind set-up, but this has only been estimated for certain measurement points along the coast. So, if there is local wind set-up that is not included in the normative water level, this effect should be added.
- **Shower gusts and shower oscillations.** Shower gusts are single elevations of the sea water level caused by atmospheric depressions. Gusts are generated when a storm with low air pressure approaches the coast, thus building up an increasingly large wave. The duration of a gust can vary between a couple of minutes and more than one hour. The shower gust elevation along the Dutch coast can be up to 0,50 m, or even more, but it is not very likely that this coincides with extreme water levels, so usually only a reduced effect of shower gusts is taken into account. This reduced value depends on the height needed to reduce wave run-up to acceptable amounts. The maximum value is 0,30 m along the Dutch coast, and only 0,05 m 20 km landward (TAW, 1989). The Dutch guide on lake and sea dikes (TAW, 1999a) has adopted these values.

If shower gusts appear in a more or less regular series, the phenomenon is called 'shower oscillations'. In Dutch waters, the gust effect dominates the effect of shower oscillations. Therefore, it is as-

sumed that the effect of the latter is discounted in the contribution of the shower gust (TAW, Grondslagen voor Waterkeren, 1989).

Because of the presence of the Hartelkering and the Maeslantkering, shower gusts and shower oscillations have become much less relevant behind these barriers. The Dutch committee on flood defence (TAW) therefore recommended neglecting these effects behind the barriers, until further research has been carried out (TAW, TR Ontwerpbelastingen voor het Rivierengebied, 2007).

- **Seiches** are oscillatory elevations of the water level in a basin enclosed on three sides, for instance a sheltered harbour. They are caused by oscillations of the (sea) water level outside the basin, particularly by shower oscillations with periods ranging from a couple of minutes to an hour. Typical periods of seiches are between 10 and 120 minutes. Because of the presence of the Hartelkering and the Maeslantkering, the importance of seiches has become much less relevant behind these barriers, like shower gusts and shower oscillation.
- **Tidal resonance.** Tidal waves in estuaries, bays or river mouths can possibly be reflected. Interference of the reflected wave with the incoming wave will then lead to an increase of the water level, which has to be taken into account when determining the height of a flood defence.

### **Design water level (ontwerpwaterstand)**

The design water level is based upon the local normative high water level, but temporal effects should also be included to comply with the requirements at the end of the design lifetime of the flood defence. Local normative high water levels are namely determined for assessment purposes, with a reference period of a few years<sup>6</sup>, whereas the reference period (design life time) of flood defences usually is 50 years (for dikes if they can be easily adapted) or 100 years (for engineering works) (TAW Leidraad Kunstwerken, 2003).

The main temporal effects are:

- **High water rise (sea level rise and increase of river discharges).** An increase of the average temperature causes thermal expansion of the ocean water, resulting in a water level elevation. The melting of ice masses on land (flowing into the oceans) has only a relative small effect on the sea water level. It is also believed that the rivers will be influenced by climate change, because the highest and lowest river discharges will become more extreme, due to more fluctuations of rainfall over land.
- **Land subsidence.** Geological processes and gas and oil extraction result in a general sinking of deeper ground layers. The rate of subsidence varies per location in the Netherlands. Outside the Netherlands, these deeper layers can also gradually rise, dependent on the geological history of that area.

The combined effect of (absolute) sea level rise and land subsidence is indicated as 'relative sea level rise'. The average trend observed in the Netherlands since 1900 is 0,19 m/century (Dillingh, 2008) and a deviation from this trend has not yet been observed. Forecast models, however, come with a wide range of results, up to 2 metre per century (and even more) in the very near future. It is the task of engineers to find a way to deal to cope with these alternatives, ranging from adaptive to robust design strategies.

### **Crest level (kruinhoogte, dijktafelhoogte)**

The crest level of a flood defence is primarily based on the design water level (for design purposes) or the local normative high water level (for assessment purposes)<sup>7</sup>, but it includes an additional height to reduce wave overtopping discharges to acceptable amounts. Furthermore, some mathematical surcharges have to be added.

These effects that have to be included when determining the crest level are:

- **Wave-overtopping height (overslaghoogte).** This height is required to limit wave overtopping to acceptable amounts (Section 17.2). This mainly applies to coastal defences and flood defences along the lower rivers. For the upper rivers, where there is no tidal influence, overflow is usually more critical than overtopping. The height needed to reduce wave overtopping is known as the 'overtopping height'.
- **Mathematical surcharges:**
  - **Length effect.** The failure probability of a long dike is higher than the failure probability of a short dike because of partial correlation or independence between different cross-sections and/or structural elements. An additional height compensates this effect.

<sup>6</sup> The reference period should preferably equal the return period of the assessments. For the third nationwide assessment of primary flood defences 2006-2011, this was five years. This return period has increased to twelve years (*Wet van 15 mei 2013 tot wijziging van de Waterwet*).

<sup>7</sup> The required crest level can be calculated for assessment or design purposes. For design, the wave overtopping height and the mathematical surcharges should be added to the design high water level. For assessment purposes, they should be added to the local NHW level, leaving out the temporal effects that are not relevant for this.

- **Deterministic design surcharge.** For dunes, there is a compensation for not applying a full probabilistic design method, to account for uncertainties in profile measurements. This corresponds to an additional height of 2/3 of the decimating height<sup>8</sup> (TAW, *TR Ontwerpbelastingen voor het Riviereengebied*, 2007).
- **Robustness surcharge (*robuustheidstoeslag*).** For uncertainties regarding changes in the estimation of water levels, changes in prescribed calculation principles and changes in strength criteria, a robustness surcharge is used as compensation (TAW, *TR Ontwerpbelastingen voor het Riviereengebied*, 2007). The aim of adding this surcharge is to cope with eventual setbacks during the lifetime of a structure.

Two main types of robustness uncertainties can be distinguished:

- Technical uncertainties:
  - magnitude of discharges
  - modelling uncertainties (water levels and wave parameters)
  - climate change scenario uncertainties
  - statistical uncertainties in load parameters
- Policy uncertainties

The Dutch TAW-guidelines do not prescribe statistical and policy uncertainties, because a useful estimation could not be made. For the Design Toolkit 2014 (*Ontwerpinstrumentarium 2014*) a robustness surcharge of 0,30 m (for rivers) up to 0,70 m (for the Ketelmeer) is recommended to account for modelling uncertainties (Rijkswaterstaat, *Handreiking ontwerpen met overstromingskansen*, 2014).

### **Construction level (*aanleghoogte*)**

For the design of flood defences, the following surcharges for geotechnical effects have to be taken into account to find the initial construction level (if applicable):

- **Settlement.** Soil gradually settles because of extra loading, namely by the weight of the dike. This has to be compensated by a surplus height. Compaction can occur in the subsoil (*zetting*) and the embankment itself (*klink*). The rate of compaction depends on the development of the consolidation in time, which indicates how much water has already been expelled. In the Netherlands, mainly two methods are used in engineering practice: Koppejan (modified) or Terzaghi/Bjerrum (Section 34.2). For a very rough indication, when no data is available, as a rule of thumb, a value of 10% settlement could be used for clay, or 5% if the clay is carefully applied and densified. For sand, a value of 5% could be used, but if it is well compacted, settlement of sand can be neglected.
- **Local subsidence.** If local land subsidence can be expected that is not yet included in the design water level, it should be added here. This can for instance be caused by extraction of mineral resources (natural gas or oil) or water from the subsoil.
- **Earthquake surcharge.** Earthquakes induced by seismic movements and by extraction of natural resources can cause deformation of dikes, next to subsoil subsidence. This could cause additional lowering of the crest by compaction of the dike core, squeezing of softened soil (*zijdelings wegpersen van verweekte grond*), or macro-instability induced by an earthquake (rotational slip of the slope). Usually, advanced calculation methods are used to compute the magnitude of these effects and research is still in progress. These calculation methods are not included in this Manual.

The height needed to compensate settlement and local subsidence is called 'surplus height' (*overhoogte*).

### **Freeboard**

Freeboard<sup>9</sup> is not uniformly defined, so the exact definition varies per guideline. The freeboard is more or less defined as the difference between construction level and (local) assessment level (for assessment purposes) or between construction level and design water level (for design purposes).

Often, a minimum value of 0,50 m is prescribed for the freeboard. This minimum freeboard applies to the crest level, not the construction level!

<sup>8</sup> The 'decimating height' (*decimeringshoogte*) is the difference in water level between two points that differ with a factor 10 in exceedance probability (see the graph in Figure 13-6, where the decimating height equals about 0,70 m).

<sup>9</sup> Freeboard = *waakhoogte* in Dutch, which is sometimes erroneously translated into English as *wake height and back into Dutch as vrijboord*, which has a completely different meaning! In Dutch, *waakhoogte* is also known as *kruinhoogtemarge*, as proposed in *Voorschrift Toetsen op Veiligheid voor de tweede toetsronde 2001 - 2006*.

**Notes**

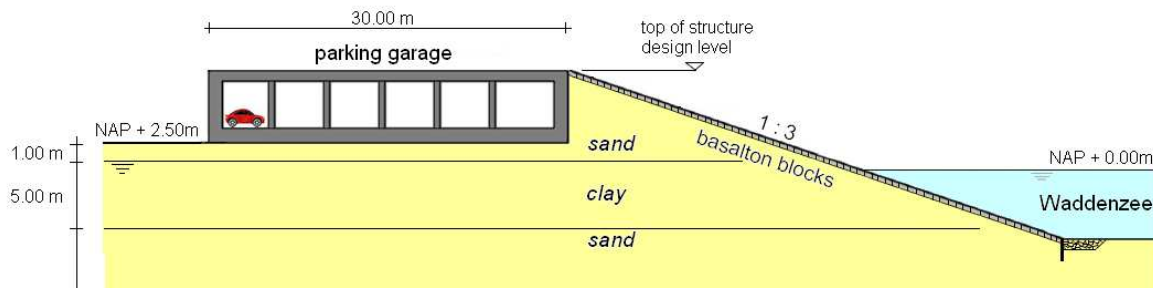
1. Just to give an idea about the magnitude of the surcharges: For the new Scheveningen boulevard, the following surcharges were taken into account for a design life time of 100 years: 0,30 m for the length effect, extra wind set-up due to more severe storms: 0,40 m, higher shower oscillations also due to more severe storms: 0,10 m. Water Board Rivierenland uses a robustness surcharge of 0,30 m for their primary river dikes (unless a probabilistic model is used for calculation) (TAW, 1999a).
2. The indicated local effects as well as the wave height, wind set-up and peak river discharge can also increase over time, mainly due to climate change. For lake dikes, a wave height elevation of 45% of the expected high water level rise has been taken into account (for a reference period of 100 years). Pay attention to these changes too when determining the design crest height!

**Example retaining height of a flood defence**

(Based on the exam of April, 2014)

**Given:**

A dike along a small town in West Friesland, bordering the Waddenzee, needs to be heightened because it is not up to the required standard for primary flood defences. To improve the flood defence and the urban quality of the town, the idea is to construct a 120 m long and 30 m wide parking garage into the dike, see the simplified cross-section in the Figure below. Only the right-hand part of the parking garage replaces a part of the original dike.



From NAP + 2,50 m downward, the soil consists of a top layer of 1,00 m middle fine sand, a 5,00 m thick clay layer and then a sand layer that reaches quite deep, with the same properties of the upper layer.

	Soil properties						
	$\gamma$ [kN/m <sup>3</sup> ]	$\gamma_{sat}$ [kN/m <sup>3</sup> ]	$\varphi$ [degrees]	$c'$ [kPa]	$q_{c,average}$ [MPa]	$C'_p$ [-]	$C'_s$ [-]
Both sand layers	18	21	30	-	15	-	-
Clay layer	-	15	22.5	15	3	18	120

The ground water level behind the dike is at NAP + 1,50 m.

The dike protects dike ring area no. 12, which means that the dike should resist the loads related to a water level that will not be exceeded more often than once per 4000 years on average (according to the appendix to the Water Act). Because water levels (including astronomical tide + wind set-up) have been measured for a long time, the water level belonging to an exceedance frequency (overschrijdingsfrequentie) of 1/4000 year<sup>-1</sup> can be calculated. The measured water levels and average exceedance frequencies are usually plotted in a graph like the well-known graph for Hook of Holland, as can be found in Figure 13-6 of this Manual. Our West Frisian location, obviously, is different, so the indicated water levels in the Hook of Holland graph do not correspond to our location. Based on a statistical analysis on water level measurements, two points on the line for our location are known:

1.  $f = 1/100 \text{ year}^{-1}$      $h = \text{NAP} + 3,55 \text{ m}$
2.  $f = 1/1000 \text{ year}^{-1}$      $h = \text{NAP} + 4,10 \text{ m}$

The relation between  $f$  and  $h$  is assumed exponential:  $f(h) = e^{-\left(\frac{h-A}{B}\right)}$

Where:

$f(h)$  : average frequency of the water level  $h$  being exceeded [year<sup>-1</sup>]

$A, B$  : constants

Question A

Calculate the normative high water level corresponding to an average exceedance frequency of 1/4000 per year. (Solve this analytically)

Question B

The wind set-up at our location does not differ from the measurement station and there are no seiches or tidal resonances along our flood defence.

The average sea water level at present is NAP + 0,00 m. During the 100 year design life time of the combined garage-dike structure, the sea level is expected to rise 0,40 m due to climate change. Future shower gusts cause an additional (temporary) rise of the water level of 0,37 m.

Calculate the design water level.

Question C

The European Overtopping Manual gives maximum values of overtopping discharges (as mentioned in Chapter 17 of this Manual) and distinguishes between structural safety (Table 17-1) and usability (Table 17-2). The crest and rear side of our multifunctional flood defence are well protected by the concrete structure of the parking garage and the pavement behind it. Regarding hindrance for pedestrians, it is decided that the road behind the garage will have to be closed-off for pedestrians during severe storms. Measures should be taken to prevent water to enter the garage from the rear side (by closing off the entrance). This will occur only very rarely, so could be considered acceptable. Therefore, during a design storm, only well-shod and protected staff should be able to walk directly behind the garage.

What overtopping discharge [ $\ell/s/m$ ] is governing for the design?

Question D

The significant wave height  $H_s$  at present is 2,20 m, but at the end of the design life an increase of 0,20 m is expected due to more severe storms (climate change). The governing peak wave period then is  $T_p = 5,56$  s. Assume perpendicular wave attack.

Calculate the required overtopping height [m] according to the European Overtopping Manual, needed to restrict the overtopping discharge to the acceptable amount determined in Question C.

Question E

The responsible water board (*waterschap*) has indicated that the surcharge for the length-effect, deterministic design and robustness surcharge together can be assumed to be 0,60 m.

Calculate the required design height (crest level) of the parking garage (top of structure at the end of the design lifetime).

Answer A

Formulate the constant A as an expression with variables  $f_1$  and  $h_1$  and constant B:

$$f_1 = e^{-\left(\frac{h_1 - A}{B}\right)} \Leftrightarrow \ln(f_1) = \ln\left(e^{-\left(\frac{h_1 - A}{B}\right)}\right) = -\frac{h_1 - A}{B} \Rightarrow A = B \cdot \ln(f_1) + h_1$$

Substitute the expression of A in  $\ln(f_2)$  to find an expression for B that is independent of constant A:

$$f_2 = e^{-\left(\frac{h_2 - A}{B}\right)} \Leftrightarrow \ln(f_2) = -\frac{h_2 - A}{B} = \frac{B \cdot \ln(f_1) + h_1 - h_2}{B} \Rightarrow B = \frac{h_1 - h_2}{\ln(f_2) - \ln(f_1)}$$

Substituting the values for  $h_1$ ,  $h_2$ ,  $f_1$  and  $f_2$  results in the value of B:

$$B = \frac{3,55 - 4,10}{\ln(1/1000) - \ln(1/100)} = 0,239 \Rightarrow A = B \cdot \ln(f_1) + h_1 = 0,239 \cdot \ln(1/100) + 3,55 = 2,449$$

Now, for any third point on the line, the normative high water level  $h_3$  can be computed, given its frequency  $f_3$ :

$$h_3 = A - B \cdot \ln(f_3) \rightarrow h_3 = 2,449 - 0,239 \cdot \ln(1/4000) = 4,43 \text{ m (above NAP)}$$

Answer B

The design water level is based on the normative high water level and includes local and temporal effects:

- normative high water = NAP + 4,43 m
- local wind set-up = 0,00 m
- shower gusts = 0,37 m
- seiches = 0,00 m
- tidal resonance = 0,00 m
- relative sea level rise = 0,40 m
- design water level = NAP + 5,20 m

Answer C

The mean overtopping discharge regarding the structural integrity of the flood defence (crest and rear slope) is 50 to 200  $\ell/s/m$  (see Table 17-1 of the Manual). The pedestrian requirement of 1 to 10  $\ell/s/m$  (Table 17-2) is more critical, thus governing for design. For this example we continue with 10  $\ell/s/m$ .

Answer D

Use the principal equation from the European Overtopping Manual for flood defences with a slope (see Section 17.2 of this Manual):

$$\frac{q}{\sqrt{g \cdot H_{m0}^3}} = a \cdot e^{\left(\frac{-b R_c}{H_{m0}}\right)} \Leftrightarrow R_c = -\frac{H_{m0}}{b} \cdot \ln\left(\frac{q}{a\sqrt{gH_{m0}^3}}\right)$$

$\alpha$  = angle of the slope with the horizontal  $\rightarrow \tan(\alpha) = 1:3$

$$T_{m-1,0} \approx 0,9 \cdot T_p = 0,9 \cdot 5,56 = 5,0 \text{ s}$$

$$\xi_{m-1,0} = \frac{\tan \alpha}{\sqrt{H_s / (1,56 \cdot T_{m-1,0}^2)}} = \frac{1/3}{\sqrt{2,40 / (1,56 \cdot 5,0^2)}} = 1,34$$

- $\gamma_b$  = 1 (no berm)
- $\gamma_f$  = 0,95 (same as for concrete blocks, block mats)
- $\gamma_\beta$  = 1,0 (perpendicular wave attack:  $\beta = 0^\circ$ )
- $\gamma_v$  = 1,0 (no vertical wall on top of the crest)
- $q$  = 10  $\ell/s/m = 0,010 \text{ m}^3/s/m$  (see answer C)

$$a = \frac{0,067}{\sqrt{\tan \alpha}} \cdot \gamma_b \cdot \xi_{m-1,0} = \frac{0,067}{\sqrt{1/3}} \cdot 1 \cdot 1,34 = 0,156$$

$$b = \frac{4,3}{\xi_{m-1,0} \cdot \gamma_b \cdot \gamma_f \cdot \gamma_\beta \cdot \gamma_v} = \frac{4,3}{1,34 \cdot 1,0 \cdot 0,95 \cdot 1,0 \cdot 1,0} = 3,38$$

$$R_c = -\frac{H_{m0}}{b} \cdot \ln\left(\frac{q}{a\sqrt{gH_{m0}^3}}\right) = -\frac{2,40}{3,38} \cdot \ln\left(\frac{0,010}{0,156 \sqrt{10 \cdot 2,4^3}}\right) = 3,70 \text{ m}$$

Answer E

The crest level of the multifunctional flood defence equals the design water level plus the overtopping height and mathematical surcharges:

- design water level = NAP + 5,20 m
- overtopping height = 3,70 m
- mathematical surcharges = 0,60 m
- crest level = NAP + 9,50 m

The freeboard then is  $(\text{NAP} + 9,50) - (\text{NAP} + 4,80) = 4,70 \text{ m}$ , which is more than the minimum required 0,50 m.

### 49.3 Literature

Dilingh, D. (2008). Zeespiegelstijging langs de Nederlandse kust. Personal correspondence. Deltares.

Ministerie van Verkeer en Waterstaat (2007). Hydraulische Randvoorwaarden primaire waterkeringen voor de derde toetsronde 2006-2011 (HR 2006). Ministerie van Verkeer en Waterstaat.

Rijkswaterstaat (2014a). Achtergrondrapport ontwerpinstrumentarium.

Rijkswaterstaat (2014b). Handreiking ontwerpen met overstromingskansen.

TAW (1998). Grondslagen voor waterkeren. Balkema uitgevers BV.

TAW (1985). Leidraad voor het ontwerpen van rivierdijken. Deel 1 - bovenrivierengebied. Staatsuitgeverij 's-Gravenhage.

TAW (1985). Leidraad voor het ontwerpen van rivierdijken. Deel 2 - benedenrivierengebied. Staatsuitgeverij 's-Gravenhage.

TAW (1999). Leidraad zee- en meerdijken. Staatsuitgeverij 's-Gravenhage.

TAW (2003). Leidraad kunstwerken. Rijkswaterstaat, Dienst Weg- en Waterbouwkunde.

TAW (2007). Technisch Rapport Ontwerpbelastingen voor het Rivierengebied.

Visschedijk, M.A.T., P. Meijers, R van der Meij, E.H. Chbab, G.A.M. Kruse, Zuada Coelho, D.S. Nugroho, C.M. Wesselius, W.J. de Lange and G.A. van den Ham (Deltares) (2014). Groningse kades en dijken bij geïnduceerde aardbevingen. Globale analyse van sterkte en benodigde maatregelen.